# The Loma Prieta, California, Earthquake of October 17, 1989—Liquefaction

U.S. GEOLOGICAL SURVEY PROFESSIONAL PAPER 1551-B

# AVAILABILITY OF BOOKS AND MAPS OF THE U.S. GEOLOGICAL SURVEY

Instructions on ordering publications of the U.S. Geological Survey, along with prices of the last offerings, are given in the current-year issues of the monthly catalog "New Publications of the U.S. Geological Survey." Prices of available U.S. Geological Survey publications released prior to the current year are listed in the most recent annual "Price and Availability List." Publications that may be listed in various U.S. Geological Survey catalogs (**see back inside cover**) but not listed in the most recent annual "Price and Availability List" may no longer be available.

Reports released through the NTIS may be obtained by writing to the National Technical Information Service, U.S. Department of Commerce, Springfield, VA 22161; please include NTIS report number with inquiry.

Order U.S. Geological Survey publications **by mail** or **over the counter** from the offices listed below.

## BY MAIL

### Books

Professional Papers, Bulletins, Water-Supply Papers, Techniques of Water-Resources Investigations, Circulars, publications of general interest (such as leaflets, pamphlets, booklets), single copies of Earthquakes & Volcanoes, Preliminary Determination of Epicenters, and some miscellaneous reports, including some of the foregoing series that have gone out of print at the Superintendent of Documents, are obtainable by mail from

**U.S. Geological Survey, Information Services**
**Box 25286, Federal Center**
**Denver, CO 80225**

Subscriptions to periodicals (Earthquakes & Volcanoes and Preliminary Determination of Epicenters) can be obtained ONLY from the

**Superintendent of Documents**
**Government Printing Office**
**Washington, DC 20402**

(Check or money order must be payable to Superintendent of Documents.)

### Maps

For maps, address mail orders to

**U.S. Geological Survey, Information Services**
**Box 25286, Federal Center**
**Denver, CO 80225**

Residents of Alaska may order maps from

**U.S. Geological Survey, Earth Science Information Center**
**4230 University Dr., Rm. 101**
**Anchorage, AK 99508–4664**

## OVER THE COUNTER

### Books and Maps

Books and maps of the U.S. Geological Survey are available over the counter at the following U.S. Geological Survey offices, all of which are authorized agents of the Superintendent of Documents.

- **ANCHORAGE, Alaska**–Rm. 101, 4230 University Dr.
- **LAKEWOOD, Colorado**–Federal Center, Bldg. 810
- **MENLO PARK, California**–Bldg. 3, Rm. 3128, 345 Middlefield Rd.
- **RESTON, Virginia**–USGS National Center, Rm. 1C402, 12201 Sunrise Valley Dr.
- **SALT LAKE CITY, Utah**–Federal Bldg., Rm. 8105, 125 South State St.
- **SPOKANE, Washington**–U.S. Post Office Bldg., Rm. 135, West 904 Riverside Ave.
- **WASHINGTON, D.C.**–Main Interior Bldg., Rm. 2650, 18th and C Sts., NW.

### Maps Only

Maps may be purchased over the counter at the following U.S. Geological Survey offices:

- **ROLLA, Missouri**–1400 Independence Rd.

# The Loma Prieta, California, Earthquake of October 17, 1989—Liquefaction

THOMAS L. HOLZER, *Editor*

STRONG GROUND MOTION AND GROUND FAILURE
THOMAS L. HOLZER, *Coordinator*

**U.S. GEOLOGICAL SURVEY PROFESSIONAL PAPER 1551-B**

*Prepared in cooperation with the National Science Foundation*



UNITED STATES GOVERNMENT PRINTING OFFICE, WASHINGTON : 1998

**DEPARTMENT OF THE INTERIOR**

**BRUCE BABBITT,** *Secretary*

**U.S. GEOLOGICAL SURVEY**

**MARK SCHAFER,** *Acting Director*



Manuscript approved for publication
December 19, 1997

Library of Congress catalog-card No. 92-32287

For sale by the
U.S. Geological Survey
Information Services
Box 25286
Federal Center
Denver, CO 80225

## CONTENTS

## PLATES

STRONG GROUND MOTION AND GROUND FAILURE

# INTRODUCTION

By Thomas L. Holzer,
U.S. Geological Survey

## CONTENTS



## INTRODUCTION

The 1989 Loma Prieta earthquake both reconfirmed the vulnerability of areas in the San Francisco-Monterey Bay region (fig. 1) to liquefaction and provided an opportunity to test methodologies for predicting liquefaction that have been developed since the mid-1970's. This vulnerability is documented in the chapter edited by O'Rourke (1992) and by the investigators in this chapter who describe case histories of liquefaction damage and warn us about the potential for even greater damage from liquefaction if an earthquake similar to the 1989 Loma Prieta earthquake, but located closer to their study sites, were to occur.

Demonstration of liquefaction problems is not new. The investigation of the great 1906 San Francisco earthquake (Lawson, 1908) documented extensive permanent ground deformation in fills that had been placed along the shoreline of the city of San Francisco and in the loose, sandy deposits of the major streams of the San Francisco-Monterey Bay region. Moreover, Lawson's report included descriptions from the earthquakes of 1865 and 1868 that clearly document liquefaction in some of these same fills and deposits. Despite these observations, much of the fill that was placed into San Francisco Bay after 1906 was sited without concern for its seismic stability. Thus, the bad news is that liquefaction damage caused by the 1989 Loma Prieta earthquake is one more reminder of the seismic hazard posed by the many loose sandy fills around the margins of San Francisco Bay and the natural deposits that underlie our stream valleys.

The postearthquake investigations described here document that we have reliable methods to predict at both local and regional scales the susceptibility of sites to liquefaction. The simplified procedure for site-specific prediction (Seed and others, 1983), which is widely used in modern engineering practice, worked well at sites where it was applied. Predictive regional maps based on state-of-the-art mapping techniques (Youd and Perkins, 1978) in northern Monterey and southern Santa Cruz Counties were generally successful in anticipating which areas were or were not vulnerable to liquefaction. Equally reassuring was the performance of sites where liquefaction problems were anticipated and the underlying soil was improved to increase its liquefaction resistance. None of these sites failed in 1989. Thus, the good news is that methods are in hand to predict and to mitigate liquefaction hazards.

## CASE HISTORIES

Of the 12 papers in this chapter, 9 include case histories of liquefaction. Investigations ranged from small areas to broad regions. They document detailed aspects of the 133 liquefaction occurrences compiled at 1:100,000 scale by Tinsley and others (this chapter) (fig. 1). An important aspect of the mapped compilation is that damaging liquefaction occurred at a greater distance from the seismic source zone than is normally observed. The greatest distance from the epicenter of the earthquake at which liquefaction occurred was 121 km, in the tidal flats of Bolinas Lagoon. The most distant significant damage from liquefaction occurred along an arc approximately 98 km from the epicenter or 84 km from the end of the seismic source zone, in hydraulic fills placed into San Francisco Bay: in the Marina District, on Treasure Island, and along the Oakland-Berkeley shoreline. Minor damage occurred in Richmond, 92 km from the seismic source zone (fig. 1). This 84-km distance is greater than that predicted by Youd and Perkin's (1978) correlation of the maximum distance to which liquefaction is observed with earthquake magnitude, but is less than that predicted by Keefer's (1984) correlation (fig. 2).

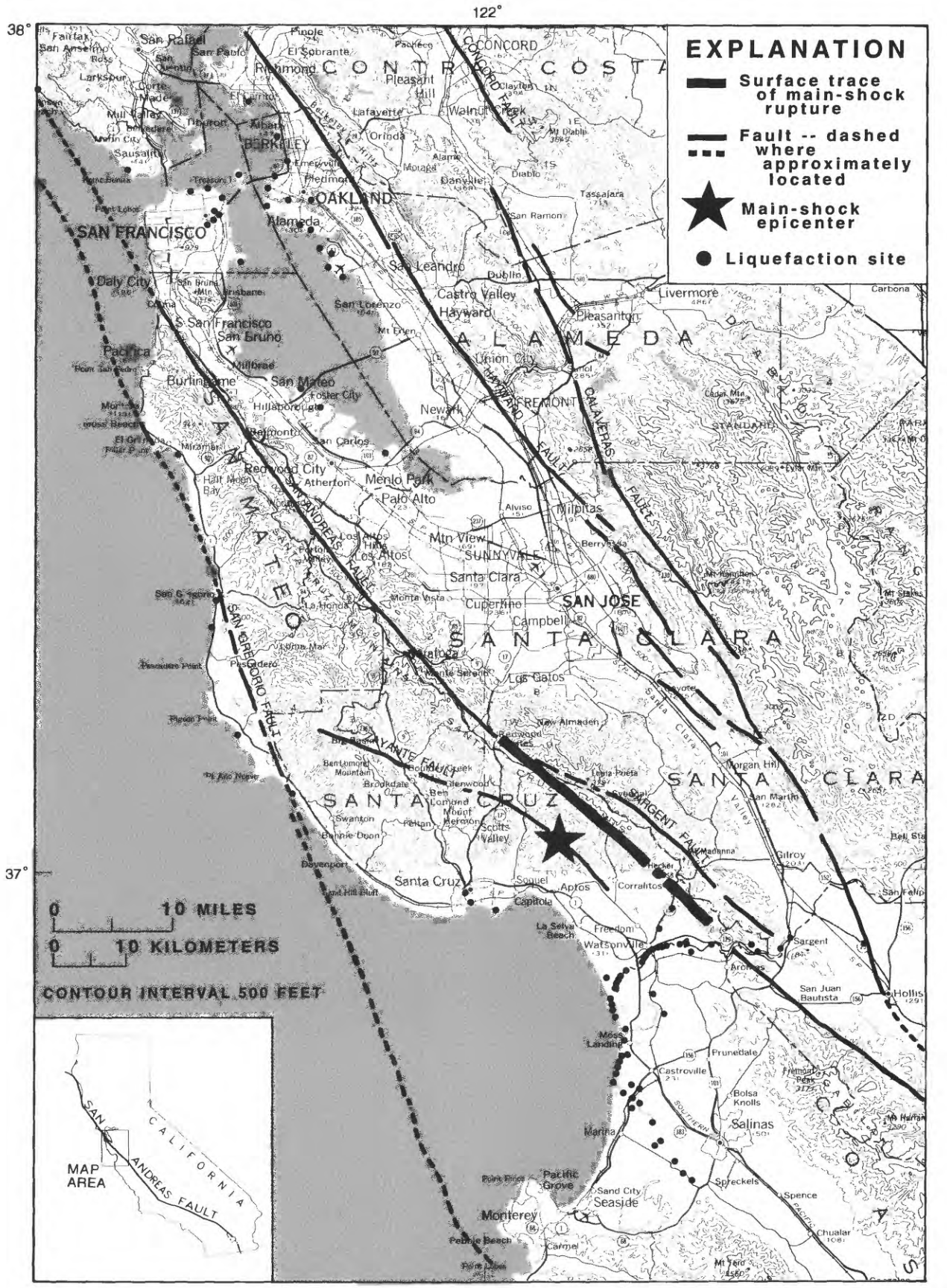


Figure 1.—San Francisco-Monterey Bay region, showing locations of sand boils, lateral spreads, and significant ground settlements associated with liquefaction caused by 1989 Loma Prieta earthquake (adapted from pls. 2 and 3).

Most of these distant occurrences of liquefaction are believed to be where significant local amplification of ground motion was caused by underlying soft sediment (Borcherdt and Glassmoyer, 1994). In addition, path effects involving reinforcing reflections of seismic waves bouncing off the Moho (Sommerville and others, 1994) and directivity—a phenomenon by which amplitudes of seismic waves are higher in the direction of rupture (Campbell, in press)—may have caused larger ground motion than is normally observed at these epicentral distances.

These observations have implications for liquefaction-potential mapping that relies on empirical observations of the relation between the maximum distance to damaging liquefaction and earthquake magnitude. For example, mapping techniques based on this approach should consider possible ground-motion amplification. Local site effects, in particular, may be important because sites underlain by liquefiable soils commonly are also underlain by geologically young deposits with the potential to amplify seismic waves. The problem of amplification adds a challenging complexity to liquefaction-potential mapping because ground motions can be amplified by multiple mechanisms (Joyner and Boore, 1988).

Seven of the case histories in this chapter address the stability of the tens of millions of cubic meters of fills that have been placed into San Francisco Bay since 1845 to reclaim more than 40 $km^2$ of tidal and submerged land. These case histories describe liquefaction and subsurface investigations of loose, sandy parts of these fills in the bay near and in San Francisco and Oakland: (1) Chameau and others (this chapter) investigated the San Francisco waterfront from the Embarcadero to Hunters Point; (2) Pease and O'Rourke (this chapter) studied subsurface conditions in the Mission District and South of Market area of San Francisco; (3) Kayen and others (this chapter) investigated the east bay from Richmond to Oakland; and (4) Power and others (this chapter), Bennett (this chapter), and Hryciw and others (this chapter) investigated Treasure Island. In addition, Rollins and McHood (this chapter), Bennett (1990), O'Rourke and others (1992), and Taylor and others (1992) described the liquefaction and geotechnical properties of the fills in the Marina District. These investigators confirm that the areas of liquefaction in 1989 were underlain predominantly by loose sandy fills, much of which was hydraulically placed. Bennett (1990 and this chapter) correlated sand boils with fill units in the Marina District and on Treasure Island and confirmed the conclusions, based on measurements of penetration resistance, about which parts of the fill liquefied. Power and others (this chapter), who investigated local variations of liquefaction resistance in the fill of Treasure Island, conclude that liquefaction was not uniformly distributed in the fill and that sand boils vented only in areas where liquefied layers were within 3 m of the land surface. Chameau and others (this chapter) report evidence that some loose fills which liquefied during the earthquake may have been densified by it and therefore may be more resistant to liquefaction in future earthquakes.

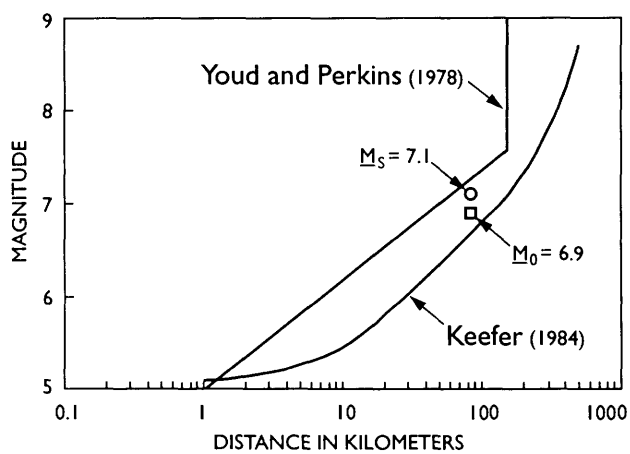


Figure 2.—Earthquake magnitude versus maximum distance to damaging liquefaction from seismic source zone of 1989 Loma Prieta earthquake. Correlations by Youd and Perkins (1978) and Keefer (1984) use surface-wave magnitude ($M_S$) and moment magnitude ($M_0$), respectively.

Dupré and Tinsley (this chapter), Tinsley and Dupré (1992), and Tinsley and others (this chapter) comprehensively document liquefaction and ground failure in natural deposits of the Monterey Bay region. Liquefaction occurred mainly in late Holocene fluvial and estuarine deposits along the Pajaro, Salinas, and San Lorenzo Rivers, as well as along estuaries and spits in the Moss Landing area. Of the 47 lateral spreads documented by Tinsley and Dupré (1992), 79 percent were in fluvial point-bar and channel-deposit facies. Comparison of the liquefaction sites in 1989 with those in 1906 described by Lawson (1908) and Youd and Hoose (1978) clearly illustrates that liquefaction is a recurrent problem in areas underlain by loose sandy material. An interesting aspect to repeated liquefaction at some localities was that the recurrence involved new and different deposits. A trench at a liquefaction site near the Salinas River revealed that flooding since 1906 had locally eroded the sediment which liquefied in 1906 and deposited new sediment which liquefied in 1989 (J.D. Sims, written commun., 1993).

Mejia (this chapter) describes liquefaction at the Moss Landing Marine Laboratory on Monterey Bay. Approximately 1.4 m of lateral spreading occurred at Moss Landing where it had been previously described during the 1906 San Francisco earthquake. The subsurface exploration described by Mejia indicates that a buried beach deposit at a depth ranging from 3.0 to 6.1 m beneath the laboratory liquefied. He also reports field evidence for liquefaction of a clayey silt with a <5μm fraction of 24 percent.

Sims and Garvin (this chapter) investigated a report of repeated liquefaction at the same site, Soda Lake, from both the main shock and two aftershocks. Their

investigation may help interpret the seismic significance of paleoliquefaction features, evidence of liquefaction that is preserved in the stratigraphic record. Paleoliquefaction is widely used to infer strong shaking from prehistoric earthquakes in other regions of the United States where faults are poorly expressed at the land surface. Sims and Garvin found that approximately 70 percent of the sand boils from the first aftershock coincided with those generated by the main shock and that sand boils from the second aftershock were restricted to only a few of the larger sand boils associated with the main shock. Structural and stratigraphic relations between sand boils formed during the main shock and aftershocks were similar to relations observed in sand boils associated with earthquakes that were decades or centuries apart.

An ominous concern expressed by most of the authors in this chapter is the continuing vulnerability of these liquefiable deposits to future earthquakes. These investigators are particularly concerned about the hydraulic fills that have been placed into San Francisco Bay on which industrial or residential development has occurred. Although much of the hydraulic fill in the bay was placed after 1906, the date of the latest major earthquake to strongly shake the San Francisco Bay region, some fills in the bay are older and have been shaken and liquefied repeatedly even before the 1989 Loma Prieta earthquake. Liquefaction and ground failures during earthquakes in 1865, 1868, and 1906 have been insufficient to force resolution of this hazard. These investigators propose that a moderate to large earthquake on the Hayward fault, Rodgers Creek fault, or the peninsula segment of the San Andreas fault would cause much more serious liquefaction and greater ground deformation in the San Francisco Bay region than did the 1989 Loma Prieta earthquake.

Table 1. *Losses associated with liquefaction in the San Francisco and Monterey Bay regions*

[Types of ground deformation: bc, bearing-capacity failure; ls, lateral spreading; s, settlement]

| Area/facility | Type of ground deformation | Loss (Millions of dollars) |
|---|---|---|
| San Francisco: | | |
| Marina District | s,bc,ls | 27.2 |
| Mission District and South of Market | s | 2.8 |
| Port of San Francisco | s | 3.6 |
| Treasure Island and Hunters Point | s,ls | 4.2 |
| Oakland: | | |
| Bay Bridge Toll Plaza | ls | 2.5 |
| Oakland Airport | ls | 4.0 |
| Port of Oakland | ls,s | 38.3 |
| Alameda: | | |
| Alameda Naval Air Station | ls | 2.2 |
| Bay Farm Island | ls | 2.8 |
| Santa Cruz | bc | 1.2 |
| Moss Landing Marine Laboratory | ls | 8.0 |
| Flood control levees, Pajaro and Salinas Rivers | bc, ls | 2.5 |
| **TOTAL** | | **99.2** |

## COSTS AND CAUSES OF DAMAGE

Property loss caused by liquefaction during the 1989 Loma Prieta earthquake was at least $99 million (table 1). This estimate, which was compiled by individually contacting public officials and engineers involved in repair, probably represents at least 80 percent of the total property damage from liquefaction. The largest losses, $41.9 million, involved the port facilities in Oakland and San Francisco. Damage to lifelines was the second most costly loss, amounting to more than $23 million, of which $17 million was the cost of repairing the gas pipeline system in the Marina District. The largest uncertainty in the liquefaction-loss estimate is the cause of damage to buildings in the Marina District. Although buildings were substantially damaged in the part of the district where liquefaction occurred, investigators have attributed most of this damage, including collapsed corner apartments, to ground shaking (Harris and Egan, 1992). Total losses to buildings in the area affected by liquefaction was $35 million (C. Taylor, written commun., 1993), and I arbitrarily attributed 20 percent of this loss to liquefaction. Although it is impractical in the compilation of property losses to assign losses to the specific type of ground deformation associated with liquefaction, damage clearly was associated with several types of permanent ground deformation, including lateral spreading, settlement caused by postliquefaction consolidation, and bearing-capacity failure.

Although direct losses from liquefaction were small relative to the total $5.9 billion in property loss caused by the 1989 earthquake (Holzer, 1994), it is important to note that liquefaction can also cause substantial indirect property loss by fire. The conflagration after the 1906 San Francisco earthquake, which completely destroyed 492 city blocks (U.S. Geological Survey, 1907), remains the greatest single fire loss in U.S. history. The fire spread virtually unchecked because liquefaction-induced ground deformation ruptured critical pipelines and cut off water supply to the burned area (Scawthorn and O'Rourke, 1989). Catastrophic destruction by fire may have been narrowly

averted in 1989 when liquefaction-induced ground deformation ruptured water mains that served the underground supply to the Marina District (O'Rourke and others, 1992). If the fire in this district at Divisadero and Beach Streets had spread to one or two blocks, building losses would have been several times larger than those actually sustained. The importance of liquefaction with respect to water-pipeline systems and its potential impact on fire damage should not be underestimated; it continues to be a significant source of seismic risk throughout the San Francisco Bay region.

Lateral spreading caused the most costly loss, $8 million, with the destruction of the Moss Landing Marine Laboratory. This was only one of many spectacular and damaging lateral spreads in the Monterey Bay area where kilometer-long spreading with displacements greater than 1 m occurred primarily in agricultural areas (Dupré and Tinsley, this chapter; Holzer and others, 1994; Tinsley and others, this chapter). Damage to other civil works in the Monterey Bay region was modest. Two railroad bridges, the Southern Pacific Railroad bridge crossing the Salinas River near Neponset, and a short bridge across the Pajaro River 0.4 km south of Main Street in Watsonville (fig. 1), were deformed by lateral spreads, as were flood-control levees and small buildings along the Pajaro River. Lateral spreading typically occurred within 150 m of channel margins. Some failures occurred along the margins of abandoned channels filled with organic-rich sediment where the free face was less than 1 m high but where the compressible material filling the channel readily accommodated the laterally displaced mass. Lateral displacements, based on cumulative crack opening, ranged from a few millimeters to as much as 2 m; vertical displacements were generally less than 0.3 m. Failure zones locally could be followed for distances as long as 2 km.

Patterns of ground cracks in the fills of San Francisco Bay generally were inchoate, prompting some investigators to speculate that the duration of ground shaking was too short to cause major lateral spreading and systematic ground cracking. For example, a complex pattern of north-south and east-west ground cracks formed within a northwest-trending zone in the parking lot of Winfield Scott School in the Marina District (Bennett, 1990). Aggregate displacements were large—230 mm of east-west compression and 150 mm of north-south extension—but their relation to areal deformation in the Marina District was unclear. Near the shoreward margins of the fills, ground cracks generally were more systematically oriented. Taylor and others (1992) documented 600 mm of northward displacement across east-west cracks caused by the damaging bayward lateral spreading at the St. Francis Yacht Club in the Marina District. Power and others (this chapter) infer about 300 mm of bayward lateral displacement on the east side of Treasure Island. Ground cracking associated with lateral spreading on the island was generally concentrated within a zone that extended only about 60 m from the perimeter of the island. These observations suggest that progressive failure in the fills was initiating which could have led to greater lateral displacements involving large areas if the strong motion had persisted.

The correlation of damaged underground utilities with areas of differential settlements associated with postliquefaction consolidation is one of the more important observations of the postearthquake investigation. Bennett (1990) and Power and others (this chapter) documented settlements as large as 143 mm by comparing preearthquake and postearthquake leveling surveys of bench marks in the Marina District and on Treasure Island, respectively. Major damage to buried utilities occurred in the area of settlement in the Marina District. Approximately 2.7 km of water mains in the Municipal Water Supply System required replacement; the 123 pipeline repairs in the Marina District were approximately 3 times the number of repairs elsewhere in San Francisco. O'Rourke and others (1992) concluded—on the basis of the concentration of the pipe failures around the edges of the fill, the types of failure, and the inverse correlation of damage with pipe diameter—that there was a strong link between damage to pipelines in the Marina District and soil deformation associated with postliquefaction consolidation. Power and others similarly concluded about the pipeline failures on Treasure Island, where 44 pipeline, including 28 freshwater line, breaks were documented. Many of these breaks occurred in the central part of the island, where liquefaction without lateral spreading occurred. In general, damage to buried utilities from settlements was restricted to areas where the settlements were greater than approximately 40 mm.

Bearing-capacity failures and associated differential settlements also caused major damage. Approximately 4.8 km of flood-control levees along the Pajaro, Salinas, and San Lorenzo Rivers were damaged predominantly by bearing-capacity failures when levees settled differentially into underlying liquefied material. Settlements larger than 0.5 m were observed. At eight localities, lateral spreading contributed to the damage to the levees. Levee repairs cost about $2.5 million. At least 12 single-family residences in the Marina District settled by as much as 150 mm by punching through the overburden into the underlying liquefied hydraulic fill (Bennett, 1990). Power and others (this chapter) observed damage caused by differential settlements of buildings on Treasure Island that were built on shallow foundations.

An intriguing, but inadequately documented, phenomenon, owing to its belated recognition, was postearthquake deformation across lateral spreads. Tinsley and others (this chapter) document such deformation on Treasure Island (loc. 3, pl. 2) and in Santa Cruz (loc. 52, pl. 2). Neither site, however, was sufficiently studied to determine the cause of the postearthquake deformation.

## EVALUATION OF PREDICTIVE METHODS

One of the most reassuring results of postearthquake investigations was the reliability of predictive methods for both site-specific and regional studies of liquefaction potential. In addition, the earthquake provided an opportunity to test both proposed methods for quantitatively predicting such effects as settlement and lateral spreading and recently developed new field techniques for assessing liquefaction potential.

The simplified procedure of Seed and others (1983), which is based on a correlation of cyclic-stress ratio and standard-penetration-test (SPT) blowcounts, proved highly reliable. The case histories for the east bay (Kayen and others, this chapter), Treasure Island (Power and others, this chapter), the Marina District (Bennett, 1990; O'Rourke and others, 1992), Moss Landing (Mejia, this chapter), and Watsonville (Holzer and others, 1994) all demonstrate that Seed and others' procedure reliably predicted both the occurrence and nonoccurrence of liquefaction during the 1989 Loma Prieta earthquake. Kayen and others (this chapter) also successfully used correlations of SPT blow counts with Arias intensity to predict liquefaction in the east bay. Power and others provide an unusually detailed examination of the three-dimensional variation in liquefaction susceptibility of the hydraulic fill composing Treasure Island.

Several of the case histories in this chapter explore the use of cone-penetration testing (CPT) and shear-wave-velocity measurements to evaluate liquefaction potential. CPT-based methods potentially offer greater stratigraphic resolution for assessing the liquefaction potential at a specific site because they are based on continuous measurements of penetration resistance. Kayen and others (this chapter), who performed CPT's at five sites in the east bay, concluded that the correlations between tip resistance and cyclic-stress ratios proposed by Robertson and Campanella (1985), Shibata and Teparaksa (1988), and Mitchell and Tseng (1990) accurately predicted field performance. Chameau and others (this chapter) based their study of the performance of fills along the San Francisco waterfront on CPT measurements. Hryciw and others (this chapter) also found good agreement on Treasure Island between field performance and the predictions of CPT-based methods; however, their results in Santa Cruz were less conclusive, possibly owing to local stratigraphic complexities. Both Kayen and others and Hryciw and others also sought to correlate field performance with shear-wave-velocity measurements. Kayen and others propose a new liquefaction boundary based on the correlation of shear-wave velocity and cyclic-stress ratio at liquefaction sites in the east bay.

Hryciw and others (this chapter) and Charlie and others (this chapter) applied new field techniques to evaluate liquefaction potential. Hryciw and others used a flat-plate dilatometer on Treasure Island and in Santa Cruz and verified published liquefaction criteria for cyclic-stress ratios ranging from 0.1 to 0.2. At the higher cyclic-stress ratios inferred in Santa Cruz, predictions of liquefaction at sites without surface manifestations may have compromised by other factors such as depth and thickness of the liquefiable layer. Charlie and others tested the Colorado State University piezovane™, a shear vane capable of measuring pore-pressure response during shearing, in three lateral spreads explored by Bennett and Tinsley (1995) in the Monterey Bay region. The piezovane identified contractive sands, which presumably have a potential for flow failure and lateral spreading, at all three sites.

Power and others (this chapter), Rollins and McHood (this chapter), and O'Rourke and others (1992) compared observed and predicted postliquefaction consolidation. The results are mixed. In general, state-of-the-art predictive techniques tend to overestimate the amount of settlement, particularly in hydraulic fills. The problem is primarily caused by the fines contents of the fills, and they propose corrective approaches.

Several investigators evaluated both empirical and analytical techniques for predicting horizontal displacements associated with lateral spreading. Pease and O'Rourke (this chapter) statistically correlate displacements that occurred during the 1906 San Francisco earthquake with both the submerged thickness of liquefiable material and ground slope within two areas in San Francisco. They conclude that thickness is the best single predictor of displacement: Displacements were approximately 30 percent of the submerged thickness. Power and others (this chapter) and Mejia (this chapter) used sliding-block models to infer residual strengths that are consistent with the displacements observed in 1989; these models permit predictions of ground displacements for stronger earthquakes—results that are sobering. Thus, displacements of 1.2 to 3 m are predicted for earthquakes closer to Treasure Island, in contrast to the 0.3 m observed during the 1989 Loma Prieta earthquake. Holzer and others (1994) showed that observed horizontal displacements at a large lateral spread near Watsonville in the Monterey Bay region were less than displacements predicted by empirical methods.

The mapping technique of Youd and Perkins (1978), which was developed for regional assessments of liquefaction potential, worked well in the areas where it had been applied. Preearthquake regional mapping of liquefaction potential was highly successful in predicting the distribution of liquefaction in parts of the Monterey Bay region (Dupré and Tinsley, this chapter). All of the major occurrences of liquefaction were in areas previously mapped as having a high to very high liquefaction suscep-

tibility. Large areas mapped in this category that did not fail reflected the absence of sand-rich facies, which had not been recognized by surficial-materials and geomorphic mapping.

## ASSESSMENT OF GROUND IMPROVEMENTS

The 1989 Loma Prieta earthquake provided an opportunity to evaluate the field performance under seismic loading conditions of soil that has been modified to increase its liquefaction resistance. Mitchell and Wentz (this chapter) compiled information on the performance of 12 sites with ground improvements in both the San Francisco-Monterey Bay region, including 5 sites on Treasure Island that are also described by Power and others (this chapter). Ground-improvement methods included vibration to densify the soil, installation of compaction piles to densify and strengthen the soil, and grouting to strengthen the soil. All but one site was underlain by nonengineered fill, mostly hydraulically placed. At all 12 sites, Mitchell and Wentz found little or no damage to either improved ground or associated facilities or structures. In many places, adjacent unimproved ground showed evidence of liquefaction. At all but two sites in Santa Cruz, levels of ground shaking were substantially below design values, and so the earthquake did not provide a definitive test of the ground improvement. Nevertheless, Mitchell and Wentz conclude that ground improvement is an effective method for mitigation of liquefaction risk.

## CONCLUDING REMARKS

The 1989 earthquake reminds us once again of the hazard to residential and industrial development posed by both the loose sandy fills that have been placed into San Francisco Bay and the natural deposits that underlie stream valleys. Abundant geotechnical data indicate that much material beneath these areas is susceptible to liquefaction, as does the recurrent liquefaction in earthquakes in 1865, 1868, 1906, and now in 1989. The 1989 Loma Prieta earthquake also reminds us that damaging ground deformation from liquefaction is multifaceted. Horizontal displacements associated with lateral spreading can tear structures apart, as occurred with the $8-million loss of the Moss Landing Marine Laboratory; postliquefaction consolidation can cause settlements that are associated with damage to underground utilities, as in the Marina District, where 123 water-main breaks occurred; and bearing capacity failures can devastate structures by causing them to settle differentially into underlying liquefied material, as did the 4.8 km of flood-control levees along the major rivers of the Monterey Bay region. Nonetheless, state-of-the-art techniques can predict problems both regionally and at specific sites: Liquefaction-potential maps were successful in anticipating areas of liquefaction and site-specific data were consistent with field observations of liquefaction. In addition, favorable experience in 1989 with the performance of improved ground suggests that we now have techniques to mitigate the hazard posed by liquefaction at problematic sites.

## REFERENCES CITED

Bennett, M.J., 1990, Ground deformation and liquefaction of soil in the Marina District, chap. D *of* Effects of the Loma Prieta earthquake on the Marina District, San Francisco, California: U.S. Geological Survey Open-File Report 90–253, p. D1–D36.

Bennett, M.J., and Tinsley, J.C., III, 1995, Geotechnical data from surface and subsurface samples outside of and within liquefaction-related ground failures caused by the October 17, 1989, Loma Prieta earthquake, Santa Cruz and Monterey Counties, California: U.S. Geological Survey Open-File Report 95–663, 358 p.

Borcherdt, R.D., and Glassmoyer, Gary, 1994, Influences of local geology on strong and weak ground motions recorded in the San Francisco Bay region and their implications for site-specific building code provisions, in Borcherdt, R.D., ed., The Loma Prieta, California, earthquake of October 17, 1989—strong ground motion: U.S. Geological Survey Professional Paper 1551–A, p. A77–A108.

Campbell, K.W., in press, Empirical analysis of peak horizontal acceleration, peak horizontal velocity and modified Mercalli intensity, *in* Holzer, T.L., ed., The Loma Prieta, California, earthquake of October 17, 1989—earth structures and engineering characterization of ground motion: U.S. Geological Survey Professional Paper 1552–D.

Dupré, W.R., and Tinsley, J.C., 1980, Maps showing geology and liquefaction potential of northern Monterey and southern Santa Cruz Counties, California: U.S. Geological Survey Miscellaneous Field Studies Map MF–1199, scale 1:62,500, 2 sheets.

Harris, S.K., and Egan, J.A., 1992, Effects of ground conditions on the damage to four-story corner apartment buildings, *in* O'Rourke, T.D., ed., The Loma Prieta, California, earthquake of October 17, 1989—Marina District: U.S. Geological Survey Professional Paper 1551–F, p. F181–F194.

Holzer, T.L., 1994, Loma Prieta damage largely attributed to enhanced ground shaking: Eos (American Geophysical Union Transactions), v. 75, no. 26, p. 299–301.

Holzer, T.L., Tinsley, J.C., III, Bennett, M.J., and Mueller, C.S., 1994, Observed and predicted ground deformation—Miller Farm lateral spread, Watsonville, California: Buffalo, N.Y., National Center for Earthquake Engineering Research Technical Report NCEER–94–0026, p. 79–99.

Joyner, W.B., and Boore, D.M., 1988, Measurement, characterization, and prediction of strong ground motion, *in* Von Thun, J.L., ed., Proceedings: Earthquake Engineering and Soil Dynamics II—recent advances in ground-motion evaluation: American Society of Civil Engineers Geotechnical Special Publication 20, p. 43–102.

Keefer, D.K., 1984, Landslides caused by earthquakes: Geological Society of America Bulletin, v. 95, no. 4, p. 406–421.

Lawson, A.D., chairman, 1908, The California earthquake of April 18, 1906; report of the State Earthquake Investigation Commission: Carnegie Institution of Washington publication 87, 2 v.

Mitchell, J.K., and Tseng, D.J., 1990, Assessment of liquefaction potential by cone penetration resistance, *in* Duncan, J.M., ed., H. Bolton Seed Symposium: Vancouver, British Columbia, Canada, BiTech, v. 2, p. 335–350.

O'Rourke, T.D., ed., 1992, The Loma Prieta, California, earthquake of October 17, 1989—Marina District: U.S. Geological Survey Professional Paper 1551–F, p. F1–F215.

O'Rourke, T.D., Pease, J.W., and Stewart, H.E., 1992, Lifeline performance and ground deformation during the earthquake, in O'Rourke, T.D., ed., The Loma Prieta, California, earthquake of October 17, 1989—Marina District: U.S. Geological Survey Professional Paper 1551–F, p. F155–F180.

Robertson, P.K., and Campanella, R.G., 1985, Liquefaction potential of sands using the CPT: Journal of Geotechnical Engineering, v. 111, no. 3, p. 384–403.

Scawthorn, C.R., and O'Rourke, T.D., 1989, Effects of ground failure on water supply and fire following earthquake: Buffalo, N.Y., National Center for Earthquake Engineering Research Technical Report NCEER–89–0032, p. 16–35.

Seed, H.B., Idriss, I.M., and Arango, Ignacio, 1983, Evaluation of liquefaction potential using field performance data: Journal of Geotechnical Engineering, v. 109, no. 3, p. 458–482.

Shibata, Toru, and Teparaksa, Wanchai, 1988, Evaluation of liquefaction potential of soil using cone penetration tests: Soil and Foundations, v. 28, no. 2, p. 49–60.

Sommerville, P.G., Smith, N.F., and Graves, R.W., 1994, Effect of critical reflections from the Moho on the attenuation of strong motion, *in* Borcherdt, R.D., ed., The Loma Prieta, California, earthquake of October 17, 1989—strong ground motion: U.S. Geological Survey Professional Paper 1551–A, p. A67–A75.

Taylor, H.T., Cameron, J.T., Vahdani, S., and Yap, H., 1992, Behavior of seawalls and shoreline during the earthquake, *in* O'Rourke, T.D., ed., The Loma Prieta, California, earthquake of October 17, 1989—Marina District: U.S. Geological Survey Professional Paper 1551–F, p. F141–F154.

Tinsley, J.C., and Dupré, W.R., 1992, Liquefaction hazard mapping, depositional facies, and lateral spreading ground failure in the Monterey Bay area during the 10/17/89 Loma Prieta earthquake: Buffalo, N.Y., National Center for Earthquake Engineering Research Technical Report NCEER–92–0019, p. 71–85.

U.S. Geological Survey, 1907, The San Francisco earthquake and fire of April 18, 1906, and their effects on structures and structural materials: Bulletin 324, 170 p.

Youd, T.L., and Hoose, S.N., 1978, Historic ground failures in northern California triggered by earthquakes: U.S. Geological Survey Professional Paper 993, 177 p.

Youd, T.L., and Perkins, D.M., 1978, Mapping liquefaction-induced ground failure potential: American Society of Civil Engineers, Proceedings, Geotechnical Engineering Division Journal, v. 104, no. 4, p. 433–446.

THE LOMA PRIETA, CALIFORNIA, EARTHQUAKE OF OCTOBER 17, 1989:
LIQUEFACTION

STRONG GROUND MOTION AND GROUND FAILURE

# LIQUEFACTION CHARACTERISTICS OF SAN FRANCISCO BAYSHORE FILLS

By Jean-Lou A. Chameau, G. Wayne Clough, and J. David Frost,
Georgia Institute of Technology; and
Fernando A.M. Reyna,
Universidad Católica de Córdoba, Argentina

## CONTENTS



ABSTRACT

After the 1989 Loma Prieta earthquake, we initiated a study to evaluate the liquefaction potential of fill soils in San Francisco. We conducted field investigations at several sites along the San Francisco waterfront where preearthquake data were available and (or) the field performance during the earthquake was well documented. From the interpretation of cone-penetration-test data, several areas with dune sand fills appear to have densified. Preearthquake data indicate that these fill sands were in a loose to medium-dense state before the earthquake. Although several steps in this interpretation require assumptions, the liquefaction assessments for Loma Prieta-type conditions correlate well with the observed performance of the different sites. We show that the damage at several sites would be severe during a postulated $M$=7.5 event occurring close to San Francisco and that many other sites would be affected to a lesser degree. Even engineered fills may be susceptible to some distress because of zones of looser material at shallow depths.

## INTRODUCTION

After the earthquake, we initiated a study to evaluate the liquefaction characteristics of fill soils in San Francisco. The first part of our study involved a 5-day field investigation in March 1990 to conduct piezocone tests along the Embarcadero (fig. 1) from Piers 7 to 33. In addition, we collected and reviewed field data available from other sources. This particular section of the Embarcadero was selected because of a preearthquake study at the same site (Clough and Chameau, 1979, 1983) in which detailed investigations had been conducted at Telegraph Hill (site 2, fig. 1), along the Embarcadero between North Point and Francisco Streets, and at Yerba Buena Cove (site 3, fig. 1) between Greenwich and Filbert Streets. At a third location (site 4, fig. 1), along the Embarcadero between Vallejo and Broadway Streets, a sand boil about 2 m (7 ft) in diameter was observed after the earthquake.

We conducted another field investigation in August 1990 at additional sites along the San Francisco waterfront: at Pier 45 (site 1, fig. 1), Pier 80 (site 5), Pier 94 (site 6), and Hunters Point Naval Base (site 7). Our selection of these sites was based on one or more of the following criteria: (1) well-documented performance of the site during the earthquake, (2) existence of preearthquake data, and (3) importance of the facility. In combination with the Embarcadero sites, the data base covers a range of fill types (from dumped in place to engineered) and observed performance during the earthquake (from major lateral spreading and liquefaction at site 1 to no observable liquefaction at sites 5 and 6). This second part of our study included piezocone tests, seismic cone-penetration tests (SCPT's), pushed-and-driven dilatometer tests (DMT's), and standard penetration tests (SPT's). In addition, several samples of fill and bay mud were collected.

Our work concentrated on the interpretation and use of SCPT's, with special attention to the data from sites 2 and 3 (fig. 1) because of the opportunity to compare our data with the preearthquake data of Clough and Chameau (1983). A similar evaluation is possible for Hunters Point Naval Base (site 7) because preearthquake CPT data are available (Ng and others, 1988).

Reyna (1991) examined the levels of ground acceleration at the various sites through total- and effective-stress analyses based on one-dimensional wave propagation, using the computer programs *SHAKE* and *DESRA*. Ground-motion records from the earthquake were obtained at stations installed by the California Strong Motion Instrumentation Program of the California Division of Mines and Geology and at other stations monitored by the U.S. Geological Survey.

## GENERAL DESCRIPTION OF FILL SITES

### THE EMBARCADERO

The San Francisco waterfront was built between 1850 and 1920 by randomly dumping fills into San Francisco Bay. These fills, as much as 15 m (50 ft) thick, consist primarily of dune sand, rock fragments, bay mud, and construction debris. During the late 1970's, the seismic response of these fills was evaluated, particularly in two areas known to have sustained different levels of ground motion in the 1906 San Francisco earthquake: (1) Yerba Buena Cove (site 3, fig. 1), which showed evidence of large ground motion and liquefaction; and (2) Telegraph Hill (site 2, fig. 1), which showed evidence of only small ground motion. This earlier study (Clough and Chameau, 1983) involved a historical review of waterfront construction, field testing and sampling, laboratory testing, and geotechnical analysis. Of importance to the present study is that SCPT's were conducted at both sites 2 and 3 (Clough and Chameau, 1979). Large zones of uniform dune-sand fill (mean grain diameter $D_{50}$=0.28 mm; coefficient of uniformity Cu=1.50) identified at site 3 explained the ground failures in that area associated with the 1906 San Francisco earthquake, as well as with the 1868 Hayward earthquake. It was postulated from analytical studies that an $M$=7 event with an epicenter close to San Francisco (within 16 km) could bring the loosest zones of the dune-sand fill (that is, at 4.5–7.6-m [15–25 ft] depth) to a state of zero effective stress with limited permanent displacement. At site 2, the dune-sand fills were found to

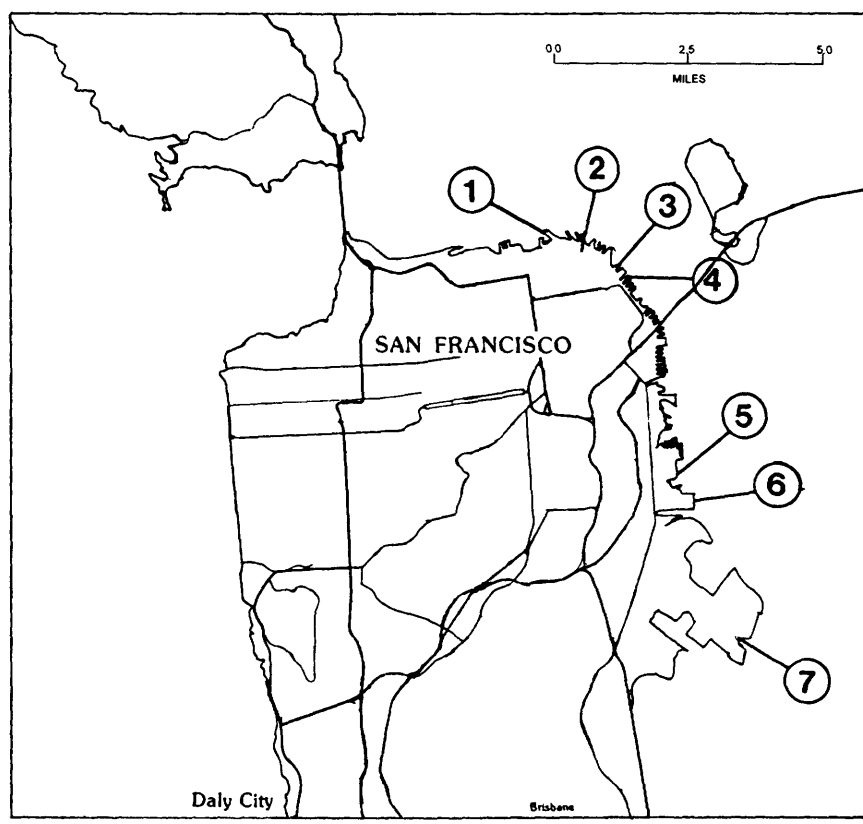


Figure 1.—San Francisco, showing locations of fill sites investigated in this study: 1, Pier 45; 2, Telegraph Hill; 3, Yerba Buena Cove; 4, Broadway; 5, Pier 80; 6, Pier 94; 7, Hunters Point. Dots, locations of cone-penetration tests.

be denser and so were not expected to show substantial ground failures during $M$=7.0 to 7.5 events.

Clough and Chameau (1979) did not report on any field experiments at site 4 (fig. 1), although that site was included in their soil profiles: one borehole south of Broadway showed a thick layer of dune-sand fill between 4.5- and 14-m (15–46 ft) depth. One sand boil was observed just north of Broadway after the 1989 Loma Prieta earthquake, and evidence of ground displacement and settlement was observed south of Broadway, under the Embarcadero Freeway.

Site 1 (fig. 1) was not part of that earlier field investigation, and only limited data are available on the site from other studies. Nevertheless, this site was included in our field investigation because of the major displacements and sand boils that were observed there after the earthquake. Large longitudinal cracks extended the length of Pier 45. The ground-water table at the Embarcadero sites is generally 1.5 to 2.4 m (5–8 ft) below the ground surface.

### PIERS 80 AND 94

Sites 5 and 6 (fig. 1) were selected for study because their facilities are vital to the economy of San Francisco, and the fills on which they are founded are controlled and (or) engineered hydraulic fills, thus allowing a comparison with the dumped-in-place random fills found elsewhere along the margins of San Francisco Bay. The upper 3 m (10 ft) of these fill deposits consist of fine to coarse sand, with some gravel, silt, and a few thin clayey beds. The upper part of the fill is underlain by a layer of fine to medium sand ($D_{50}$=0.27 mm, Cu=1.6), which is of concern with regard to liquefaction. The thickness of this sand layer varies widely, and the depth to bay mud ranges from 9 to 21 m (30–70 ft). The ground-water table at Piers 80 and 94 is about 2.4 m (8 ft) below the ground surface.

### HUNTERS POINT

Preearthquake geotechnical information for part of site 7 (fig. 1) was available from a study on single piles and pile groups by Ng and others (1988). The site is a fill area at Hunters Point Naval Base, located north of Candlestick Park in San Francisco Bay. The site was built during the 1940's by constructing cellular cofferdams that were hydraulically filled with sand. The hydraulic fill is 13 to 15 m (43–50 ft) deep, overlying a fractured serpentine bedrock. In the upper part of the fill (1–1.5-m [3–4.5 ft] depth), the sand is mixed with coarse particles (max 150 mm diam); below this upper layer, the sand is clean and poorly graded ($D_{50}$=0.29 mm, Cu=1.8). The ground-water table is approximately 2.5 m (8 ft) below the ground surface.

In addition to performing SCPT's and DMT's in this area, our study included CPT soundings within three other cofferdam cells that sustained extensive lateral displacements and settlements during the earthquake; one of these cells collapsed. Additional details on the performance of the cofferdam cells and fill soils at Hunters Point were reported by Frost and others (1993).

## CONE-PENETRATION TESTING ALONG THE EMBARCADERO

### PREVIOUS DATA

The SCPT's were conducted with a mechanical Begemann-type cone; three tests were performed at each of sites 2 and 3 (fig. 1). The results from various holes in the dune-sand zones within a given area were generally consistent except for test 5 at site 2, where cobbles or bricks were encountered. Similar problems arose for several soundings during our study, indicating the randomness of the fills. In the dune sand, friction ratios were relatively constant with depth (approx 2 percent), indicating a clean sand, in agreement with numerous grain-size analyses of the sands at both sites that showed them to be nearly identical and classifiable as poorly graded to uniform clean sands.

In spite of the similarity of index properties of the sands at sites 2 and 3 (fig. 1), the tip resistances differed substantially. At site 3, the tip resistance increased slightly from 4- to 6-m (13–20 ft) depth, decreased from 6- to 8-m (20–26 ft) depth, and then increased again, whereas at site 2 it was about the same as at site 3 down to 4-m (13 ft) depth but then increased continuously throughout the profile (Clough and Chameau, 1979). We note that the decrease in tip resistance with depth at site 3 correlated well with reduced blowcounts determined from SPT's.

Using the tip resistances, we estimated relative densities ($D_r$ values) for the sands, using the procedure of Schmertmann (1976). Our results indicate that the $D_r$ value at site 3 (fig. 1) ranges from 40 to 50 percent from 4- to 6-m (13–20 ft) depth, decreases to 30 to 35 percent from 6- to 8-m (20–26 ft) depth, and increases to only 40 percent at the bottom of the sand layer, whereas at site 2 it ranges from 50 to 70 percent from 4- to 5.5-m (13–17 ft) depth and is relatively constant (60 percent) from 5.5- to 9-m (17–27 ft) depth. On the basis of the CPT results, supplemented with SPT and laboratory data, we conclude that the dune-sand zones in the old Yerba Buena Cove area contain a low-density zone which is susceptible to liquefaction. This conclusion correlates well with the large ground motions observed in this area during the 1906 San

Francisco earthquake. North of the cove, the low-density zones in the dune sands were not penetrated, and $D_r$ values appeared to be about 60 percent.

## MECHANICAL VERSUS ELECTRICAL CONE RESISTANCE

The CPT data in the present study were measured with an electrical friction cone penetrometer. We recognized that measurements of the tip resistance, as well as the friction ratio, are influenced by the shape of the cone and differences in the test procedure. Therefore, we conducted a detailed review of previous investigations and existing data on this topic as part of our study. The results are summarized in figure 2.

The plot in figure 2 was originally based on the work of Schmertmann (1976, 1978), who compiled data from several sources and plotted the ratio of the tip resistance measured by the mechanical cone (Delft type advanced incrementally) to that measured by the Fugro electrical cone as a function of the mechanical tip resistance, $q_c$. Schmertmann's (1976, 1978) data were updated in this study, using the data of Bennett and others (1981) and Reyna (1990) for the Heber Road site in the Imperial Valley, southern California.

The trends originally observed by Schmertmann (1978) are confirmed in figure 2 and quantified by a hyperbolic regression curve. For $q_c$<5 MPa (52 tons/ft$^2$), the mechanical tip resistance is larger than the electrical tip resistance. For $q_c$=2.5 to 5 MPa (26–52 tons/ft$^2$), the mechanical/electrical ratio ranges from 1.0 to 1.50 and averages 1.10 (based on the regression curve). These ratios were obtained for soils containing a small amount of fines (5–10 weight percent), and larger ratios may be applicable for finer materials, as suggested in figure 2 for low $q_c$ values. For $q_c$>5 MPa (52 tons/ft$^2$), the mechanical tip resistance is generally less than the electrical tip resistance; their ratio ranges from about 0.75 to 1.0 and averages 0.85.

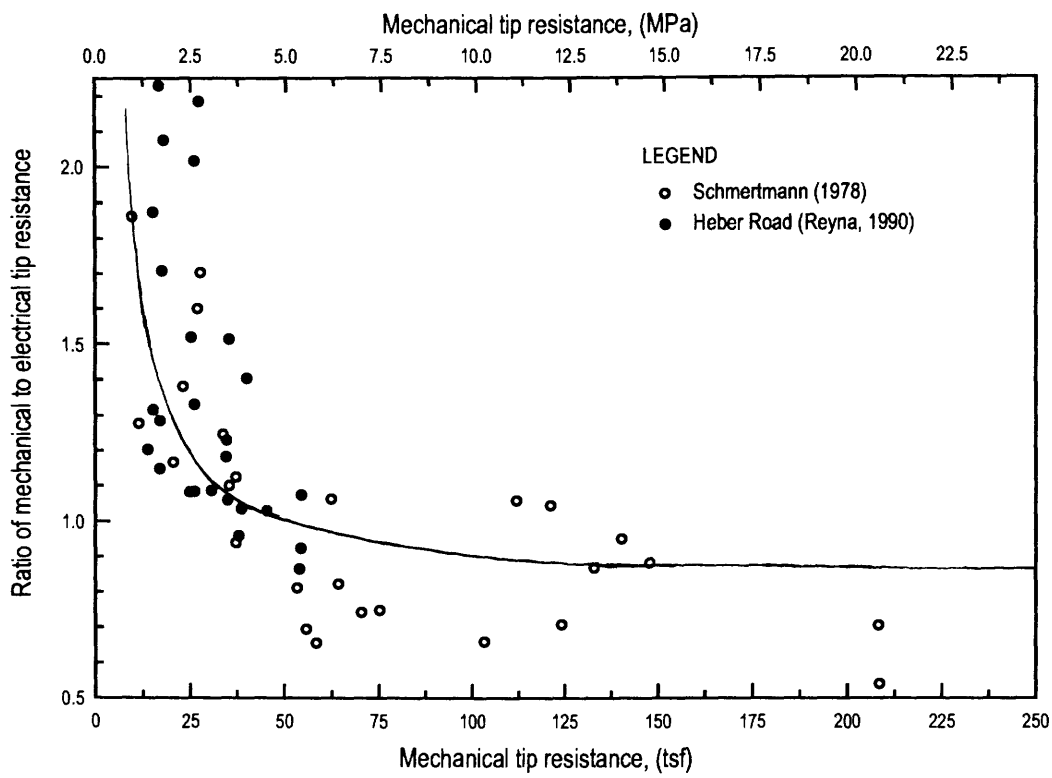


Figure 2.—Ratio of mechanical to electrical tip resistance versus mechanical resistance measured in soils by cone-penetration testing.

## COMPARISON OF PREEARTHQUAKE AND POSTEARTHQUAKE DATA

The cone soundings at sites 2 and 3 (figs. 1, 3) were conducted on property where there is no commercial development, and so these sites have remained essentially undisturbed since the original work in 1979–83. No utility-related construction has been done in the area since that time. Data from the upper 4 m (13 ft) of the soundings, representing the sand used to backfill the preaugered hole in the rubbly fill, are omitted in figure 3; only the data in the dune sand and underlying bay mud are presented.

Considering average $q_c$ values in the dune sand, the tip resistances that we measured at site 3 (fig. 1) are significantly larger than those measured by Clough and Chameau (1983). For depths of 5.5 to 8 m (18–27 ft) that were identified as the most critical by Clough and Chameau (1979, 1983), the average increase in $q_c$ value is about 40 percent. At site 2, the observed increased in $q_c$ value is less, about 10 to 15 percent.

Although the data plotted in figure 3 were not corrected for the differences between mechanical and electrical tip resistances, on the basis of the data plotted in figure 2, a correction would reinforce the above findings. For the mechanical data at site 3 (fig. 1) with $q_c$~3 to 5 MPa (31–52 tons/ft$^2$), the ratio of mechanical to electrical tip resistance would be greater than 1.0, typically 1.10 to 1.20. Thus, if the data of Clough and Chameau (1979) were corrected to equivalent electrical measurements, they would appear to be at least 10 percent lower (that is, would move to the left in figure 3), and so the increase in tip resistance at site 3 would even be larger than reported above. The reverse would be true, however, for site 2, where the mechanical tip resistances are approximately 6 to 8 MPa (63–84 tons/ft$^2$). For such $q_c$ values, the correction factor would be less than 1.0 (approx 0.80–0.90), thus shifting the data of Clough and Chameau (1979) to the right and essentially eliminating any difference between preearthquake and postearthquake results.

In summary, comparison of our field measurements along the Embarcadero with those by Clough and Chameau (1979, 1983) shows that tip resistance increased significantly in the loose sand at site 3 (fig. 1) but little, if any, in the denser material at site 2. To further illustrate these changes, we calculated $D_r$ values (fig. 4), using the procedures of Schmertmann (1976) and Jamiolkowski and others (1988). The procedure of Jamiolkowski and others was selected because it is representative of controlled experimental studies that were unavailable when Clough and Chameau's (1979, 1983) studies were conducted. The differences in $D_r$ value calculated by the two predictive techniques are typical of the variations observed in other sands. For example, the procedure of Schmertmann predicts larger $D_r$ values in the upper part of the soil profile at site 3 and smaller $D_r$ values in the pocket of loose sand than does the procedures of Jamiolkowski and others. Regardless of the data-reduction procedure used, however, figure 4 shows that the amount of densification indicated is significant at site 3. The procedure of Jamiolkowski and others predicts that at 6- to 9-m (20–30 ft) depth the $D_r$ value increases from about 35 to 40 to more than 50 percent, whereas at site 2 it changes only negligibly. As discussed above, if corrections were applied to the mechanical data, the trends of $D_r$ value would simply be reinforced (that is, an increase at site 3, no change at site 2).

## CONE-PENETRATION TESTING AT HUNTERS POINT

Differences between preearthquake and postearthquake CPT data were also observed at site 7 (fig. 1). We noted that only electrical cones were used at this site, and so there is no question as to the effects of differences in equipment. The average CPT resistances measured at the site at three different times are summarized in figure 5: (1) before driving piles (1985), (2) after driving piles (1986), and (3) after the 1989 Loma Prieta earthquake (1990). The average CPT tip resistances measured in August 1990 are significantly larger than at either of the earlier times over a wide range of depths. These differences evidently reflect changes in the $D_r$ value (fig. 6). From 5- to 11-m (16–37 ft) depth, $D_r$ values range from 35 to 50 percent on the basis of the 1986 data, and from 60 to 75 percent on the basis of the 1990 data.

For practical geotechnical applications, an average $q_c$ value over some depth interval or soil layer of interest is generally more useful than discrete values. Therefore, to fully appreciate the importance of the data plotted in figures 5 and 6, average $q_c$ values are summarized in table 1 for depth intervals of 1.0 m (3 ft). These averages show that although the increase in $q_c$ value from 1986 to 1990 was negligible from 3- to 5-m (10–16.4 ft) depth, it ranged from 30 to 70 percent at 5- to 11-m (16.4–36 ft) depth. This result does not imply, however, that any single measurement made in 1990 would always be higher than one obtained earlier. Significant randomness is always present in soil data, as indicated by the coefficients of variation listed in table 1. There is statistical overlap between the 1986 and 1990 data, but on average the $q_c$ values significantly increased. A comparison of preearthquake and postearthquake SPT, DMT, and shear-wave-velocity data at site 7 (fig. 1) leads to the same conclusion as reported by Frost and others (1993).

In summary, the CPT data at site 7 (fig. 1) support the observations at site 3: that is, the $q_c$ values and, thus, the $D_r$ values measured in fill sands after the 1989 Loma Prieta earthquake are larger than those measured before

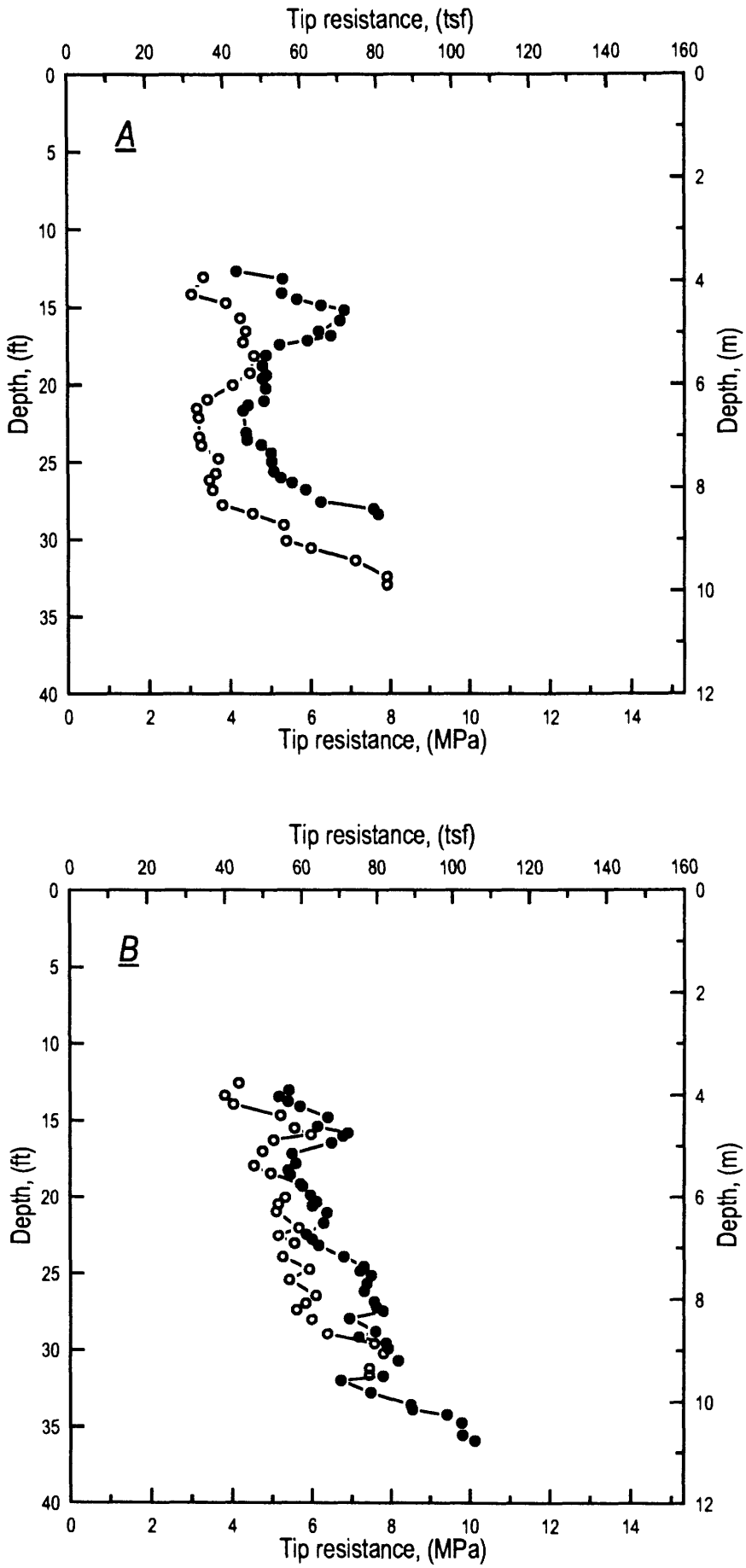


Figure 3.—Average mechanical tip resistance (circles; from Clough and Chameau, 1979) and average electrical tip resistance (dots) versus depth at sites 2 (*A*) and 3 (*B*) (see fig. 1 for locations).

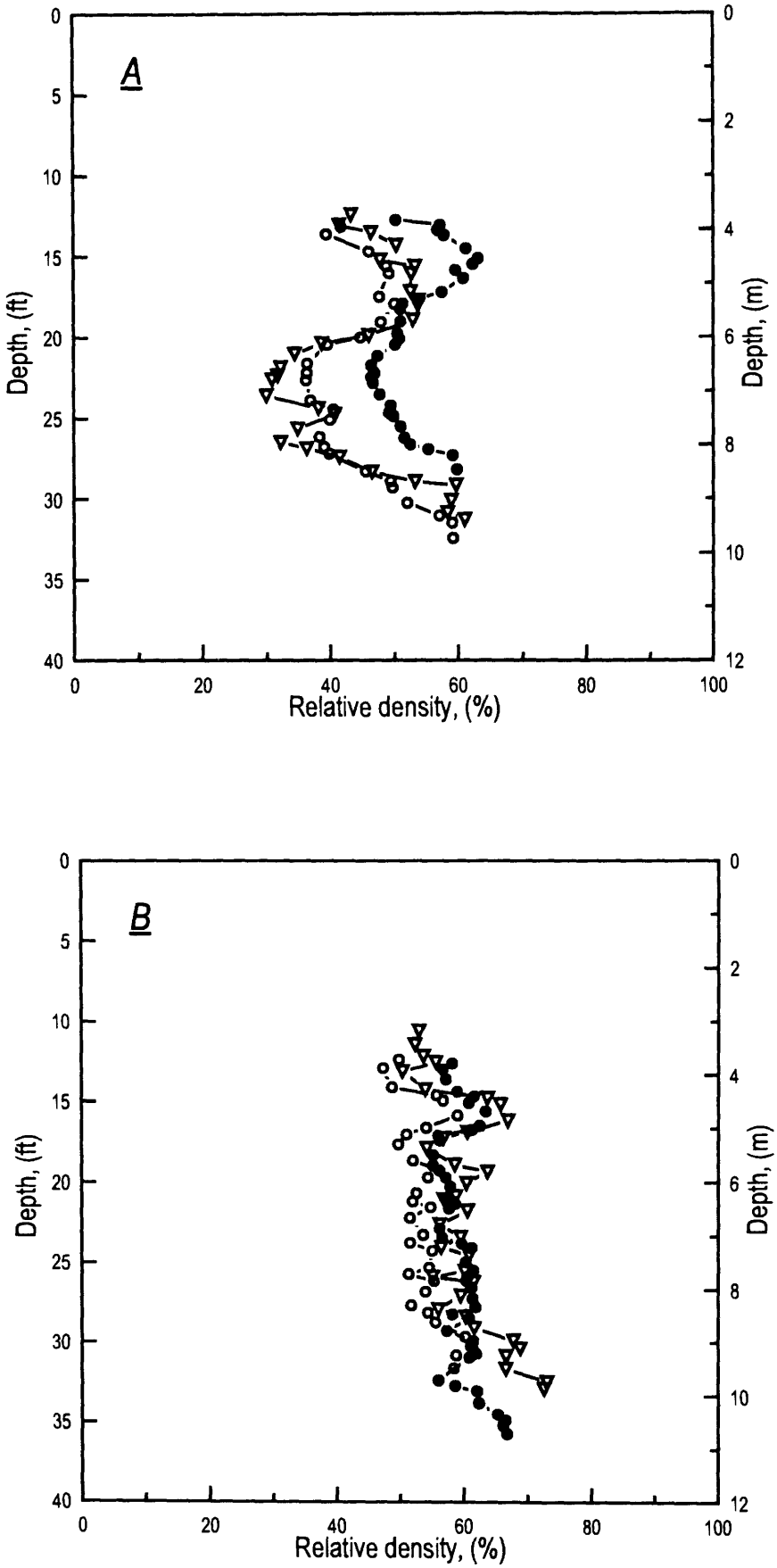


Figure 4.—Average relative soil density versus depth at sites 2 (*A*) and 3 (*B*) (see fig. 1 for locations). Circles, data of Clough and Chameau (1979); dots, this study; triangles, data of Clough and Chameau (1979), reduced using procedures of Schmertmann (1976).

the earthquake. In the denser material at site 2, the changes in $q_c$ and $D_r$ values were negligible.

## RELATIVE LIQUEFACTION POTENTIAL OF FILL SOILS

### INTERPRETATIVE FRAMEWORK

Interpretation of CPT data allows a comparison of the relative liquefaction hazards at different sites underlain by fills in San Francisco. We use the method illustrated in figure 7 because it provides a convenient and logical means to update earlier studies of the fills. This method involves comparing the actual $D_r$ value at a given depth with that below which liquefaction is predicted to occur during an earthquake. The inplace $D_r$ value of a soil can be deduced from CPT data, whereas the critical $D_r$ value—that is, the $D_r$ value below which liquefaction occurs—is determined from the results of one-dimensional wave-propagation analyses and undrained cyclic triaxial tests on dune sand. The three curves in figure 7 corresponded to scenarios involving earthquakes of $M$=7, 7.5, and 8.0 with 10, 20, and 30 strong-motion cycles, respectively. Figure 7 suggests the following conclusions: (1) At site 3 (fig. 1), the soil between 6- and 8-m (20–26 ft) depth is highly susceptible to liquefaction; liquefaction is predicted even for an $M$=7 event with 10 strong-motion cycles. (2) The soils at site 2 are more uniform than those at site 3 and more resistant to liquefaction; however, both sites would be susceptible to ground motion in a catastrophic event. We note that slightly different numbers of strong-motion cycles—for example, 15 and 26—for $M$=7.5 and 8 events (Seed and Idriss, 1983) reinforce these conclusions with regard to the relative safety of 2 and 3.

### LIQUEFACTION POTENTIAL IN A LOMA PRIETA-TYPE EVENT

Clough and Chameau's (1983) study of sites 2 and 3 (fig. 1) can be reevaluated in the light of our data, and the method extended to the other sites. First, we take advantage of ground-motion records (Diamond, Rincon, Telegraph Hill, fig. 1) to estimate the $D_r$ value below which liquefaction would occur in a Loma Prieta-type event; these records show peak ground accelerations of 0.08 to 0.12 $g$. We conducted a series of one-dimensional wave-propagation analyses with these records for sites 2 through 4. Using best estimates of soil parameters deduced from the field tests (CPT data and shear-wave-velocity mea-

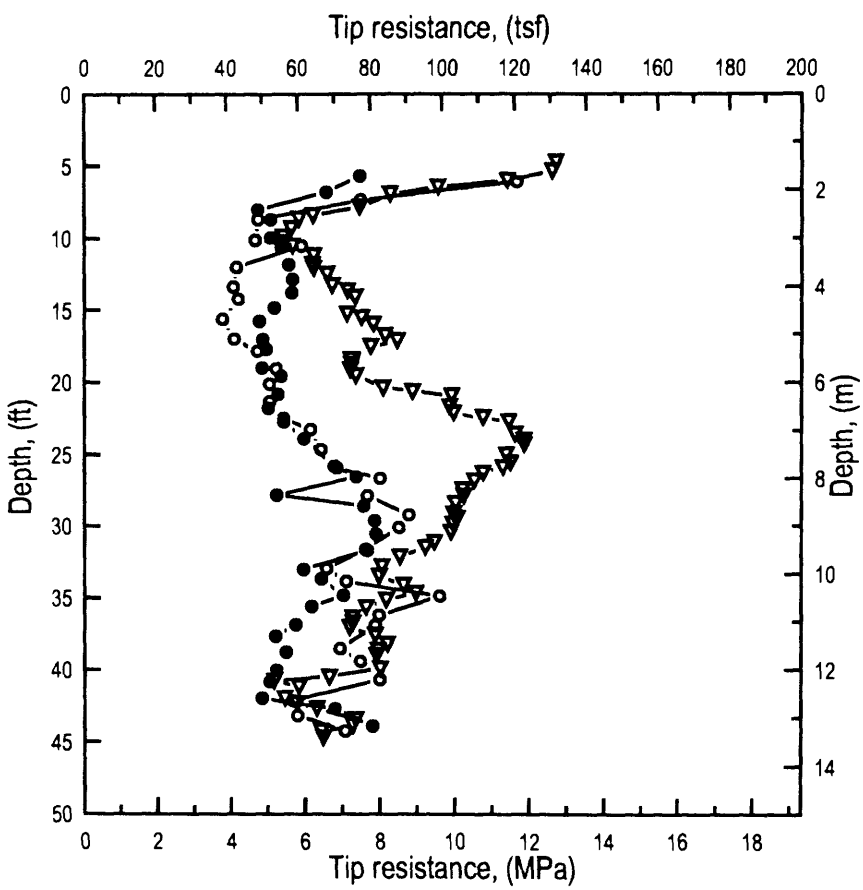


Figure 5.—Average tip resistance versus depth at site 7 (fig. 1). Triangles, data in 1985 before driving piles; circles, data in 1986 after driving piles; dots, data in 1990 after 1989 Loma Prieta earthquake.

surements) and typical modulus-reduction curves (Seed and Idriss, 1970; Sun and others, 1988; Vucetic and Dobry, 1991), the computed peak ground accelerations for these three Embarcadero sites range from 0.15 to 0.20 *g* (Reyna, 1991), which is within the range reported for other soft-soil sites in the San Francisco Bay region (Idriss, 1990). These records, as well as computed time histories, show numbers of equivalent strong-motion cycles for liquefaction analysis of approximately 3 to 4, using the procedure of Seed and others (1975). Combining these parameters with data from cyclic triaxial tests on reconstituted specimens of dune sand (Clough and Chameau, 1979) leads to estimates of a critical $D_r$ value of 38±3 percent, below which liquefaction would occur at 5- to 9-m (16–30 ft) depth in a Loma Prieta-type event (hatched area, fig. 7). This result shows that, on the basis of preearthquake CPT and density data, a safety margin exists for site 2, whereas the actual $D_r$ values at site 3 are within or below the critical range at 6- to 8-m (20–27 ft) depth. We recognize that although tests on reconstituted samples do not incorporate the influence of fabric, aging, and all aspects of stress history, the conclusions noted above, which are based on evaluations performed with these tests, are consistent with observations during reconnaissance on the day after the earthquake: There was no sign of ground displacement across from Piers 33 and 35 (site 2), whereas several longitudinal cracks (fig. 8) were observed in the vicinity of Piers 19 and 23 (site 3).

The assumptions and limitations in the above estimates of the critical $D_r$ value in the dune sand require further investigation, such as effective-stress analyses and cyclic torsional-shear tests. Nevertheless, our estimates appear reasonable enough to allow a comparison of the relative liquefaction hazards for each of the study sites. Average $D_r$ values deduced from CPT data are plotted versus depth at the seven sites in figure 9. For sites 3 and 7 (fig. 1), curves are shown for both preearthquake and postearthquake data; for site 7, a curve (HPL) is also shown for the area where extensive liquefaction damage occurred in 1989. The peak ground accelerations at sites 5 through 7 were similar to those along the Embarcadero, on the basis of several records obtained in the vicinity of the different sites and one-dimensional wave-propagation analyses of these sites.

Using average $D_r$ values to compare relative liquefaction potential may not be the best criterion because the process of liquefaction can be expected to initiate in the area of lowest resistance within a soil mass. Thus, a more realistic assessment may be obtained with lower-bound values at each site, as illustrated in figure 10.

The liquefaction performance of the seven sites can be assessed by inspection of figures 9 and 10:

1. Sites 1 and 7 (fig. 1) appear to be the most susceptible to liquefaction, as confirmed by their performance in 1989: Both sites sustained very large displacements, with collapse of a cofferdam cell at site 7. The profiles

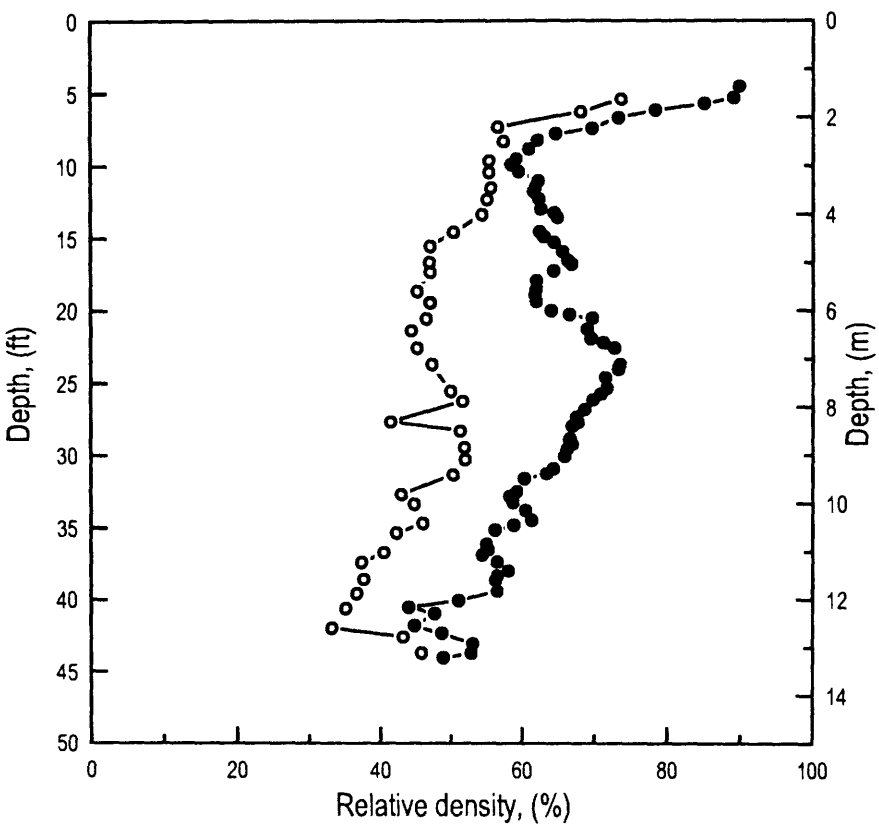


Figure 6.—Average relative soil density versus depth at site 7 (fig. 1). Dots, data in 1986 after driving piles; circles, data in 1990 after 1989 Loma Prieta earthquake.

Table 1.—*Average cone-penetration resistance for selected depth intervals at Hunters Point site (7, fig. 1)*

| Depth interval (m) | Preearthquake CPT data | | Postearthquake CPT data | |
|---|---|---|---|---|
| | Average (MPa) | Coefficient of variation (percent) | Average (MPa) | Coefficient of variation (percent) |
| 3–4 | 6.5 | 35 | 6.8 | 42 |
| 4–5 | 5.7 | 22 | 5.9 | 32 |
| 5–6 | 5.2 | 32 | 7.2 | 25 |
| 6–7 | 4.9 | 20 | 7.7 | 32 |
| 7–8 | 5.1 | 22 | 9.2 | 33 |
| 8–9 | 6.3 | 14 | 11.4 | 23 |
| 9–10 | 6.9 | 27 | 10.4 | 29 |
| 10–11 | 7.6 | 17 | 9.2 | 30 |

at these two sites show low $D_r$ values at shallow depths (3–4 m [10–13 ft]), and the low-density zones extend deeper there than at the other sites (for example, to 9–14-m [30–46 ft] depth in borehole HPL–16, fig. 10). The preearthquake $D_r$ values are not well defined at these two sites. Although we can postulate that they were low, it is difficult to assess whether they were higher or lower after the earthquake. The lateral displacements may have been large enough for the soil mass to be in a looser state after the earthquake. Nevertheless, this scenario is unlikely at site 7 for the cells that did not collapse because the sheet-pile walls restricted lateral movements, and the site now shows 15 to 22 cm (6 to 9 in.) of vertical displacement. Therefore, the present $D_r$ values at site 7 almost certainly are higher than before the earthquake (that is, preearthquake $D_r$ values fall to the left of the critical zone in figs. 9 and 10).

2. Sites 3 and 4 represent borderline conditions, and some liquefaction would be expected, in agreement with the ground cracks and fissures observed at site 3 and the small sand boil at site 4. This sand boil appears to have originated at shallow depth (approx 4 m [13 ft]), near a minimum in the $D_r$ curve. As noted above, postearthquake data show an increase in $D_r$ value at site 3, and so this site is safer now than before the earthquake. A similar increase in $D_r$ value probably also occurred at site 4.
3. Site 2 and the main part of site 7 should not be susceptible to liquefaction in a Loma Prieta-type event.
4. The engineered fills at sites 5 and 6 are generally denser than most of the hydraulic fills, and their safety margin with respect to the critical $D_r$ value agrees with their good performance during the earthquake. Nevertheless, we note that even these engineered fills can include pockets of loose sand. An example is the low tip resistance and $D_r$ values measured at 4.5- to 6-m (15–20 ft) depth in one borehole (P94–6, fig. 10) at site 6.

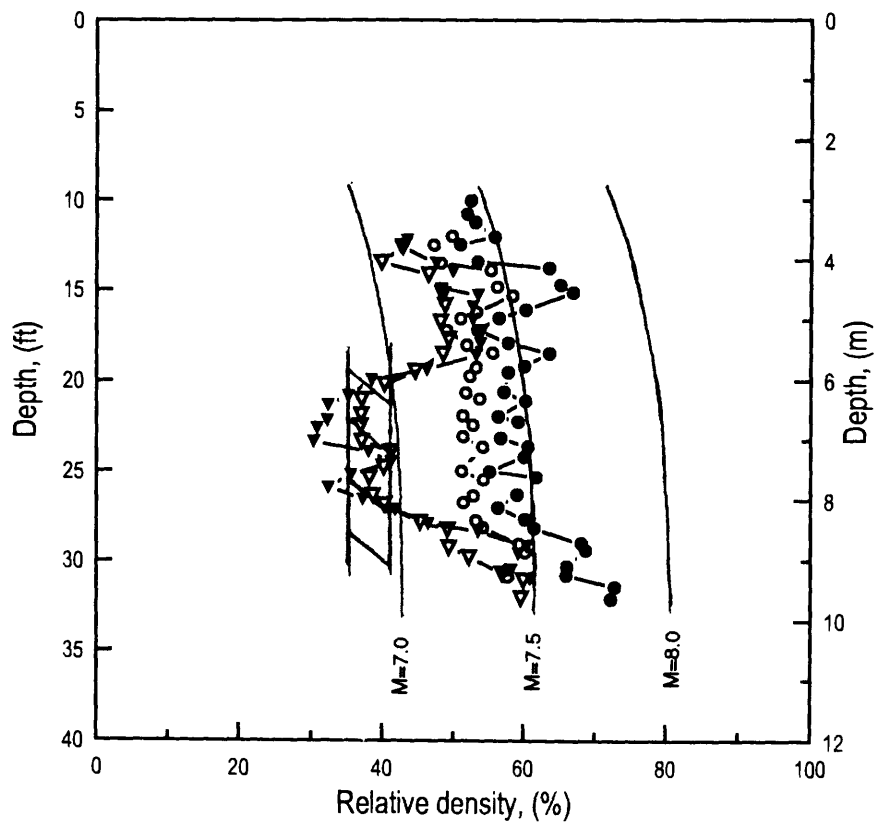


Figure 7.—Average relative soil density ($D_r$) versus depth at sites 2 (open symbols) and 3 (solid symbols) (see fig. 1 for locations), showing range of critical $D_r$ values for evaluating liquefaction potential in a Loma Prieta-type event (hatched area). Circles, data of Jamiolkowski (1988); triangles, data of Schmertmann (1978). Curves show $D_r$ thresholds below which liquefaction is predicted to occur in earthquakes of $M$=7.0, 7.5, and 8.0, using data of Clough and Chameau (1979). Modified from Clough and Chameau (1983).

## LIQUEFACTION POTENTIAL IN A LARGER EVENT

The relative resistance to liquefaction of the different fills under conditions estimated for a Loma Prieta-type event is illustrated in figures 7, 9, and 10. More important to the San Francisco waterfront, however, is the relative performance of these fills in a more severe event. A qualitative evaluation of this performance can be attempted for an $M$=7.5 earthquake with a fault rupture occurring in the vicinity of San Francisco. The critical $D_r$ value below which liquefaction would be likely is estimated to range from 55 to 60 percent, on the basis of cyclic-strength data available for the dune sand (Clough and Chameau, 1979). Because the difference between the actual and critical $D_r$ values is an index of the liquefaction susceptibility of the various sites (fig. 1), a comparison of this range (55–60 percent) with the $D_r$ values plotted in figures 7, 9, and 10 leads to the following conclusions: (1) such sites as 1 and 7 would sustain major damage in such an event; (2) some liquefaction would certainly occur at such sites as 2, 3, and 4, with deformations likely to be more significant than in 1989, although these deformations would probably be less than those observed during the 1906 earthquake, given the increase in $D_r$ values noted at sites 2 and 3; and (3) site 7 and the engineered fills, such as at sites 5 and 6, should perform well, although they could certainly undergo some liquefaction because of low-density zones (for example, at 3.5–5-m [11.5–16.4 ft] depth at site 5 and at 10–13-m [33–43 ft] depth at site 7).

Figure 8.—Typical ground crack observed across from Pier 23 at site 3 (fig. 1). Photograph taken October 19, 1989.

## LIQUEFACTION RESISTANCE

The data plotted in figures 7, 9, and 10 rely on an assessment of a critical $D_r$ value that, in turn, relies on laboratory experiments on the dune sand; however, these data are supported by a direct correlation with measured tip resistances (fig. 11). As for any correlation between soil indices and physical behavior, some uncertainty exists in such a relation. The demarcation lines (curves, fig. 11) emphasize this uncertainty: They are based on an interpretation of previous studies (Ishihara, 1985; Robertson and Campanella, 1985; Seed and de Alba, 1986) for sand with small fines content (less than 5 percent) and uniform to poorly graded grain-size distribution, with a $D_{50}$ value of 0.25 to 0.30 mm (that is, over the range applicable to the dune sand).

The data plotted in figure 11 correspond to tip resistances at selected depths at the Embarcadero sites (1–4, fig. 1). For example, the data for site 3 represent tip resistances of about 4.6 MPa (48 tons/ft$^2$) over a depth range of 7 to 8 m (23–26 ft). This $q_c$ value, which is a lower bound of the average $q_c$ profile at this site, is representative of a wide zone of the dune sand (that is, 5.0–8.0-m [16–26 ft] depth, fig. 3). The same rationale was used in the selection of representative $q_c$ values at the other sites. Inspection of figure 11 confirms the expected behavior of the Embarcadero sites, as discussed above (figs. 9, 10), from worst at site 1 to best at site 2.

Existing correlations to evaluate liquefaction susceptibility based on inplace tests (for example, fig. 11) rely mostly on data that were recorded after major events (that is, inplace tests, such as SPT's and CPT's, conducted after an earthquake at sites that did or did not liquefy). Comparison of preearthquake and postearthquake data at sites 3 and 7 (fig. 1) shows a significant increase in tip resistances at sites where only limited deformation occurred during earthquake loading. This phenomenon has probably been observed during other historical events that form the basis of the present data base, and so the question of reliability is raised. On the basis of the simple arguments that (1) the postearthquake state of sites where large displacements and ground failures occurred may not be improved relative to their original (loose) condition,

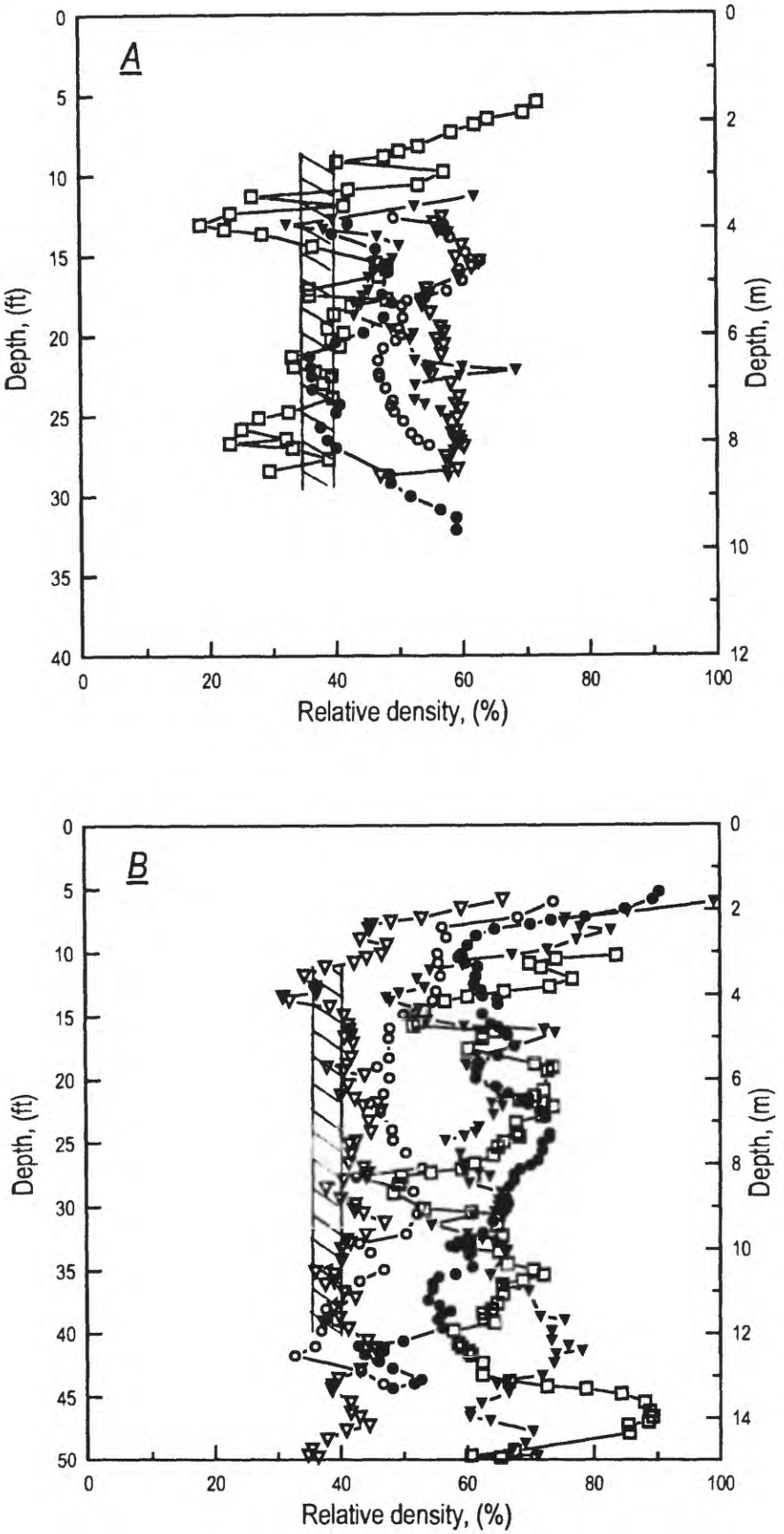


Figure 9.—Average relative soil density ($D_r$) versus depth at sites 1 through 4 (*A*) and 5 through 7 (*B*), showing range of critical $D_r$ values for evaluating liquefaction potential in a Loma Prieta-type event (hatched area). *A*, Data from Embarcadero sites: dots, site 1; circles, site 2; squares, site 3 (from Clough and Chameau (1979); open triangles, site 3 (this study); solid triangles, site 4. *B*, Data from Hunters Point: open triangles, site 5; solid triangles, site 6; dots, site 7 in 1986 after driving piles; circles, site 7 in 1990 after the earthquake; squares, area at site 7 where extensive liquefaction damage occurred.

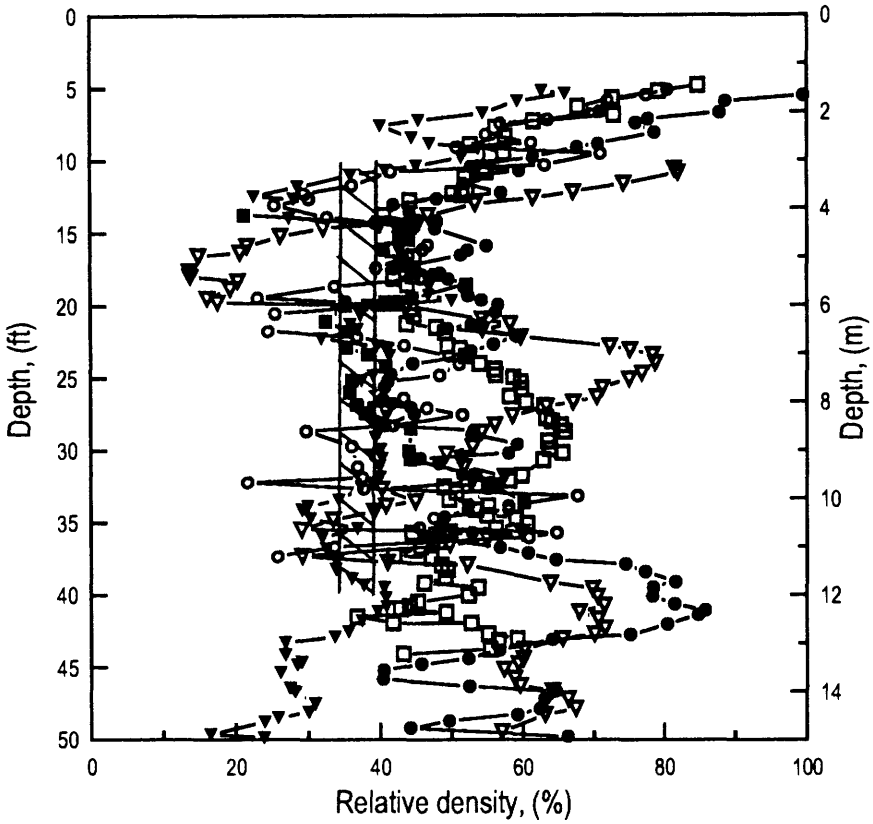


Figure 10.—Average relative soil density ($D_r$) versus depth at sites on bayshore fill (see fig. 1 for locations), showing range of critical $D_r$ values for evaluating liquefaction potential in a Loma Prieta-type event (hatched area). Circles, data from site 1 (borehole P45–8); solid squares, data from site 3 (borehole YBC–1; from Clough and Chameau, 1979); dots, data from site 5 (borehole P80–7); open triangles, data from site 6 (borehole P95–6); open squares, data from site 7 (borehole HP–103; from Jamiolkowski, 1988); solid triangles, data from area at site 7 where extensive liquefaction damage occurred (borehole HPL–16).

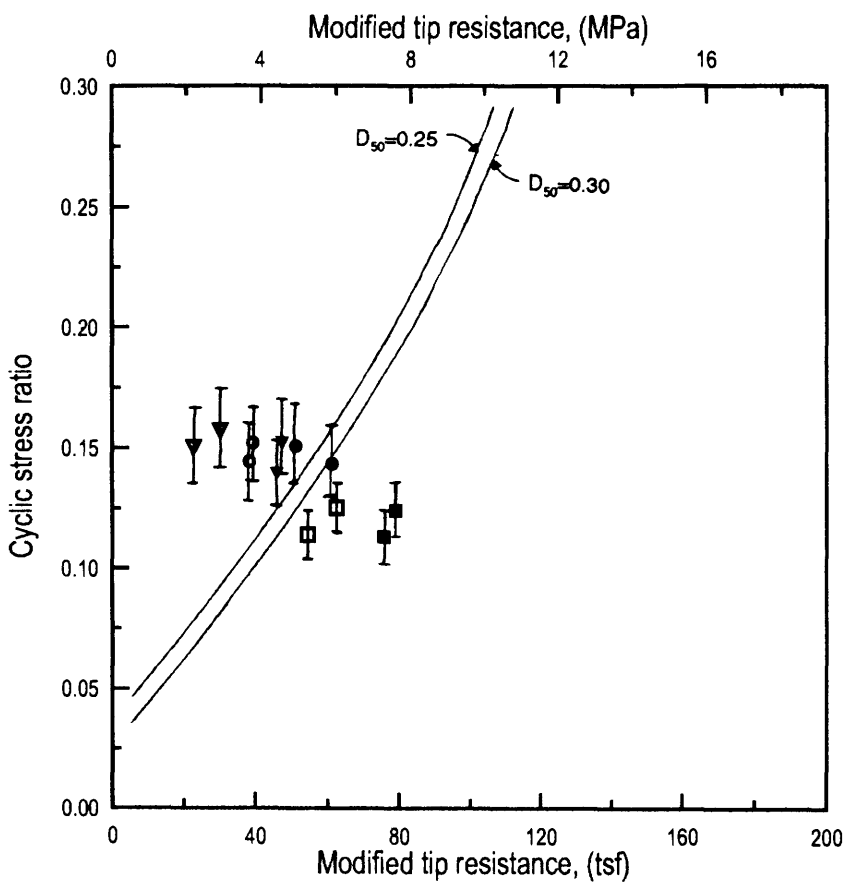


Figure 11.—Cyclic stress ratio versus modified tip resistance measured by cone-penetration testing at Embarcadero sites (see fig. 1 for locations) over depth ranges 3–4 m (A), 4–5 m (B), 5–6 m (C), 6–7 m (D), and 7–8 m (E). Solid triangles, site 1; open squares, site 2 (from Clough and Chameau, 1979); open triangles, site 2 (this study); dots, site 3 (from Clough and Chameau, 1979); open triangles, site 2 (this study); dots, site 3 (from Clough and Chameau, 1979); circles, site 3 (this study); solid squares, site 4. Error bars show range of estimated peak ground acceleration from 1989 Loma Prieta earthquake. Two curves show predicted liquefaction potential in a Loma Prieta-type event for fills with different mean grain diameter ($D_{50}$, in millimeters).

and that (2) dense to very dense sites show few changes, we could tentatively postulate that the demarcation lines presently used in engineering practice may be too conservative. For example, a site similar to site 3 would be considered in a borderline to unsafe condition, although its characteristics could improve during earthquake loading as long as a state of large deformation is not reached.

We note that our results also confirm the need for further research on the effect of cyclic-strain history on the liquefaction potential of sands. This research is critical because, for example, sands with essentially the same $D_r$ value have been shown to exhibit diverse cyclic undrained behavior as a function of their earlier cyclic-strain history. In fact, some studies have shown that cyclic prestraining involving relatively large shear strains creates a particle packing which, though dense, may be more susceptible to pore-pressure buildup under undrained cyclic loading (for example, Finn and others, 1970; Ishihara and Okada, 1982; Suzuki and Toki, 1984; Alarcon and others, 1989). Thus, although increased $D_r$ values are viewed favorably in this paper, laboratory experiments need to be conducted on the dune sand of San Francisco fills to provide a fuller and more reliable assessment of their expected behavior in future earthquakes.

To quantitatively assess the relative liquefaction susceptibility of the various sites, probabilistic analyses need to be conducted based on the concept of the liquefaction-potential index (for example, Chameau and Clough, 1983; Iwasaki, 1986; Shinozuka, 1990), which allows for a variation in tip resistance with depth and includes a subjective weighting function reflecting the liquefaction damage to manmade structures as a function of the depth and extension of the liquefied zone, as illustrated in figure 12.

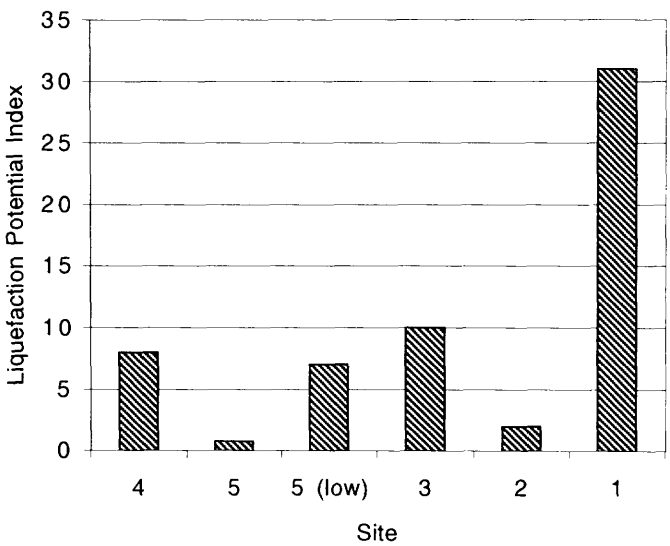


Figure 12.—Liquefaction-potential index for peak ground acceleration of 0.20 *g* at selected sites on bayshore fill, based on data plotted in figure 11.

From an evaluation of 85 sites in Japan, Iwasaki (1986) concluded that the following relative liquefaction risks can be attached to the liquefaction-potential index: 0 to 5, low; 5 to 15, high; >15, very high. Figure 12 clearly illustrates the different risks at the various sites. For example, site 1 (fig. 1) is much more at risk than the other sites, and the difference between sites 2 and 3 also is quite significant. Furthermore, although site 5 clearly has a very low risk, on the basis of average CPT data, one zone there (5 low) with lower tip resistances is as likely to liquefy as site 3. Additional evaluations being pursued using this approach to extend Iwasaki's data base should ultimately provide an efficient risk assessment for designers and decisionmakers in the San Francisco Bay region.

## SUMMARY AND CONCLUSIONS

The development of the San Francisco waterfront involved the placement of more than 18 million $m^3$ (20 million $yd^3$) of fill during the period 1845–1920. These fills have been a source of problems over the years in terms of both long-term subsidence and ground motion during earthquakes. Significant permanent displacements occurred in the 1979 Hayward earthquake, and lateral displacements as large as 1.8 m (6 ft) were reported in the 1906 San Francisco earthquake. The most widely publicized problems in the 1989 Loma Prieta earthquake were reported in the Marina District (O'Rourke, 1992). Surveys made shortly after this earthquake along the Embarcadero showed evidence of lateral spreading at several sites and settlements of 7 to 20 cm (3–8 in.) in some areas next to the piers, as well as in the Financial District. The goal of our study was to combine information from field investigation, laboratory experiments, and numerical analyses in an overall assessment of the expected behavior of these fills under adverse seismic events. Our motivation lies in the need to provide San Francisco and nearby communities with research results that have direct value in the planning of new facilities or remedial measures for existing facilities. Efforts have concentrated on field investigation, and useful conclusions can be drawn on the basis of SCPT's performed at seven sites along the San Francisco waterfront (fig. 1).

1. From field data obtained before and after the 1989 Loma Prieta earthquake, some densification apparently occurred at site 3 as a result of the earthquake. From the standpoint of $q_c$ and $D_r$ values, the dune sand in this area may now be in a state more similar to that at site 2; that is, the differences observed in 1979–83 have been significantly reduced. Similar observations were made for site 7. The dune sand was in a loose to medium-dense state in both these areas before the earthquake.

2. The increase in $q_c$ and $D_r$ values noted above is applicable to such areas as sites 3 and 7, where the dune sand in the fills was in a loose to medium-dense state. Sand layers initially in a denser state do not exhibit such an increase. For example, the change in $D_r$ value at site 2 was negligible relative to that at site 3. At sites where the fills were in a looser state before the earthquake, such as at site 1, large lateral displacements occurred during the earthquake, and the sites are still considered to be highly susceptible to liquefaction.
3. The relative $q_c$ and $D_r$ values at sites 1, 2, 3, and 4 agree with field observations at these sites of ground failure, no cracks, cracks and minor lateral displacement, and sand boils, respectively. Similar conclusions apply to the relative performance of the fills at sites 5 through 7. These results are supported by (a) comparison of critical $D_r$ values to inplace values estimated from CPT data and (b) direct use of CPT data to assess liquefaction resistance.
4. Fills presently in a state similar to those at sites that liquefied during the earthquake (for example, site 1 and one area at site 7) will be highly susceptible to liquefaction again in a postulated $M$=7.5 earthquake close to San Francisco. In such an event, liquefaction would probably occur in numerous places along the waterfront where the dune sands presently have $D_r$ values in the range 50–60 percent, such as at sites 2 through 4; however, the resulting displacements would be limited.
5. The controlled hydraulic fills, such as those underlying sites 5 and 6, are generally in a safer condition than the random hydraulic fills; however, even these controlled fills would become unstable in a large earthquake, owing to zones of looser material at shallow depths.
6. The unique opportunity to compare well-documented preearthquake and postearthquake information provided by the 1989 Loma Prieta earthquake is leading to conclusions regarding (a) evaluation of liquefaction susceptibility based on inplace tests and (b) the importance of cyclic prestraining on subsequent undrained cyclic shear.

## ACKNOWLEDGMENTS

This research was supported by U.S. National Science Foundation grants BCS–9002866 and BCS–9003473. We thank Jimmy Martin, Grigg Mullen, and Carmen Polito of the Virginia Polytechnic Institute and State University, and Leon Botham, Terry Sullivan, and Kevin Sutterer, formerly of Purdue University, for their assistance with the fieldwork. The SCPT's were conducted in collaboration with the engineering and technical staff of Earth Technology Corp., including Ed Kavazanjian and Geoff Martin. Special thanks are due to Demi Koutsoftas of Dames & Moore, who shared his knowledge of the soils in the San Francisco Bay region and provided access to reports on site conditions. Others who aided our field investigations include Steve Dickerson of the University of California, Berkeley, Victor Yew of the San Francisco Port Authority, and Rick Swanstrom of the San Francisco Clean Water Project.

## REFERENCES CITED

Alarcon-Guzman, Adolfo, Chameau, J.-L., Leonards, G.A., and Frost, J.D., 1989, Shear modulus and cyclic undrained behavior of sands: Soils and Foundations, v. 29, no. 4, p. 105–119.

Bennett, M.J., Youd, T.L., Harp, E.L., and Wieczorek, G.F., 1981, Subsurface investigation of liquefaction, Imperial Valley earthquake, California, October 15, 1979: U.S. Geological Survey Open-File Report 81–502, 87 p.

Chameau, J.-L., and Clough, G.W., 1983, Probabilistic pore pressure analysis for seismic loading: Journal of Geotechnical Engineering, v. 109, no. 4, p. 507–524.

Clough, G.W., and Chameau, J.-L., 1979, A study of the behavior of the San Francisco waterfront fills during seismic loading: Stanford, Calif., Stanford University Report 35.

———1983, Seismic response of San Francisco waterfront fills: Journal of Geotechnical Engineering, v. 109, no. 4, p. 491–506.

Finn, W.D.L., Bransby, P.L., and Pickering, D.J., 1970, Effect of strain history on liquefaction of sand: American Society of Civil Engineering Proceedings, Journal of Soil Mechanics and Foundations Division, v. 96, no. SM6, p. 1917–1934.

Frost, J.D., Reyna, F.A.M, Chameau, J.-L., and Karanikolas, P., 1993, Performance of fill soils during the Loma Prieta earthquake: International Conference on Case Histories in Geotechnical Engineering, 3d, St. Louis, Mo., Proceedings, v. 1, p. 541–546.

Idriss, I.M., 1990, Response of soft soil sites during earthquakes, *in* Duncan, J.M., ed., H. Bolton Seed Memorial Symposium: Berkeley, Calif., BiTech, v. 2, p. 273–289.

Ishihara, Kenji, 1985, Stability of natural deposits during earthquakes: International Conference on Soil Mechanics and Foundation Engineering, 11th, San Francisco, 1985, Proceedings, v. 1, p. 321–376.

Ishihara, Kenji, and Okada, Shigeru, 1982, Effects of large preshearing on cyclic behavior of sand: Soils and Foundations, v. 22, no. 3, p. 109–125.

Iwasaki, Toshio, 1986, Soil liquefaction studies in Japan; state of the art: Soil Dynamics and Earthquake Engineering, v. 5, no. 1, p. 1–68.

Jamiolkowski, M., Ghionna, v., Lancellotta, R., and Pasqualini, E., 1988, New correlations of penetration test for design practice: International Symposium on Penetration Testing, Orlando, Fla., 1988, Proceedings, v. , p. 263–296.

Ng, E., Briaud, J.L., and Tucker, L.M., 1988, Pile foundations; the behavior of piles in cohesionless soils: U.S. Federal Highway Administration Report FHWA–RD–88–081, 2 v.

O'Rourke, T.D., ed., The Loma Prieta, California, earthquake of October 17, 1989—Marina District: U.S. Geological Survey Professional Paper 1551–F, p. F1–F215.

Reyna, F.A.M., 1990, Field investigation and liquefaction potential in the Imperial Valley: Geotechnical Report 90/1, 230 p.

———1991, In situ tests for liquefaction potential evaluation—application to California data including data from the 1989 Loma Prieta earthquake: Lafayette, Ind., Purdue University, Ph.D. thesis, 502 p.

Robertson, P.K., and Campanella, R.G., 1985, Liquefaction potential of

sands using the CPT: Journal of Geotechnical Engineering, v. 111, no. 3, p. 384–403.

Schmertmann, J.H., 1976, Pilot field and laboratory study of the feasibility of using the Wissa-type piezometer probe to identify the liquefaction potential of saturated fine sands: Vicksburg, Miss., U.S. Army Corps of Engineers, Waterways Experiment Station Report DACW–39–76–M–6646.

Seed, H.B., and de Alba, Pedro, 1986, The use of SPT tests for evaluating the liquefaction resistance of sands in situ: American Society of Civil Engineers, Geotechnical Engineering Division Specialty Conference, Blacksburg, Va., 1986, Proceedings, p. 281–302.

Seed, H.B., and Idriss, I.M., 1970, Soil moduli and damping factors for dynamic response analysis: Berkeley, University of California, Earthquake Engineering Research Center Report UCB/EERC–70/10, 48 p.

———1983, Evaluation of liquefaction potential using field performance data: Journal of Geotechnical Engineering, v. 109, no. 3, p. 458–482.

Seed, H.B., Idriss, I.M., Makdisi, F.I., and Banerjee, N.G., 1975, Representation of irregular stress time histories by equivalent uniform stress series in liquefaction analysis: Berkeley, University of California, Earthquake Engineering Research Center Report EERC 75–29.

Shinozuka, Masanobu, 1990, Crude oil transmission study—probabilistic models for liquefaction: NCEER Bulletin, p. 3–8.

Sun, J.I., Golesorkhi, Ramin, and Seed, H.B., 1988, Dynamic moduli and damping ratios for cohesive soils: Berkeley, University of California, Earthquake Engineering Research Center Report UCB/EERC–88/15, 42 p.

Suzuki, Teruyuki, and Toki, Shosuke, 1984, Effects of preshearing on liquefaction characteristics of saturated sand subjected to cyclic loading: Soils and Foundations, v. 24, no. 2, p. 16–28.

Vucetic, Mladen, and Dobry, Ricardo, 1991, Effect of soil plasticity on cyclic response: Journal of Geotechnical Engineering, v. 117, no. 1, p. 89–107.

STRONG GROUND MOTION AND GROUND FAILURE

# LIQUEFACTION HAZARDS IN THE MISSION DISTRICT AND SOUTH OF MARKET AREA, SAN FRANCISCO

By Jonathan W. Pease, Dames & Moore, Inc.; and
Thomas D. O'Rourke, Cornell University

## CONTENTS



ABSTRACT

This paper provides a detailed assessment of subsurface conditions in the Mission District and South of Market area of San Francisco. Recurrence of liquefaction and lifeline damage in both of these areas during the 1906 San Francisco and 1989 Loma Prieta earthquakes has important implications for seismic-hazard mitigation in San Francisco and provides case-study information useful for investigating and characterizing urban liquefaction in other U.S. communities.

We undertook a site-investigation program in the Mission District and South of Market area in conjunction with the collection and analysis of hundreds of existing borehole records, historical evidence of earthquake damage, and observations of pipeline repairs. This paper summarizes the results of our investigations and presents a synthesis of subsurface data. We evaluate pipeline and building damage during the 1906 and 1989 earthquakes in relation to mapped ground deformations, soil deposits, and ground-water levels. Earthquake damage to pipelines was extensive throughout the liquefaction areas, either in the zones of deepest submerged artificial fill or along the boundaries of submerged fill where ground cracks and severe differential movements occurred. Review of 1906 data in the South of Market area provides unmistakable evidence of ground oscillation, or severe transient deformation, in addition to permanent displacement associated with lateral spreading and subsidence. The maximum lateral displacement is shown to correlate reasonably well with the thickness of submerged fill.

Submerged-fill thickness appears to be the most significant factor affecting ground subsidence and permanent lateral displacements in the study areas. We present hazard maps that show the liquefaction susceptibility in the study areas for an event similar in magnitude to the 1906 earthquake. These maps also provide a means to evaluate the liquefaction susceptibility for smaller events.

## INTRODUCTION

In both 1906 and 1989, San Francisco was shaken by a major earthquake during which soil liquefaction was a major factor in loss of life and damage to buildings and infrastructure. Disruption of the water supply in 1906, caused primarily by liquefaction, resulted in the worst single fire loss in U.S. history, in which about 500 city blocks were destroyed by the conflagration (Gilbert and others, 1907). Catastrophic fire was narrowly averted after the 1989 Loma Prieta earthquake, despite failure of water-supply systems due to liquefaction-induced ground deformations (for example, O'Rourke and others, 1992a; Scawthorn and others, 1992).

As shown in figure 1, soil liquefaction occurred in five principal areas in San Francisco in 1906 and 1989. The

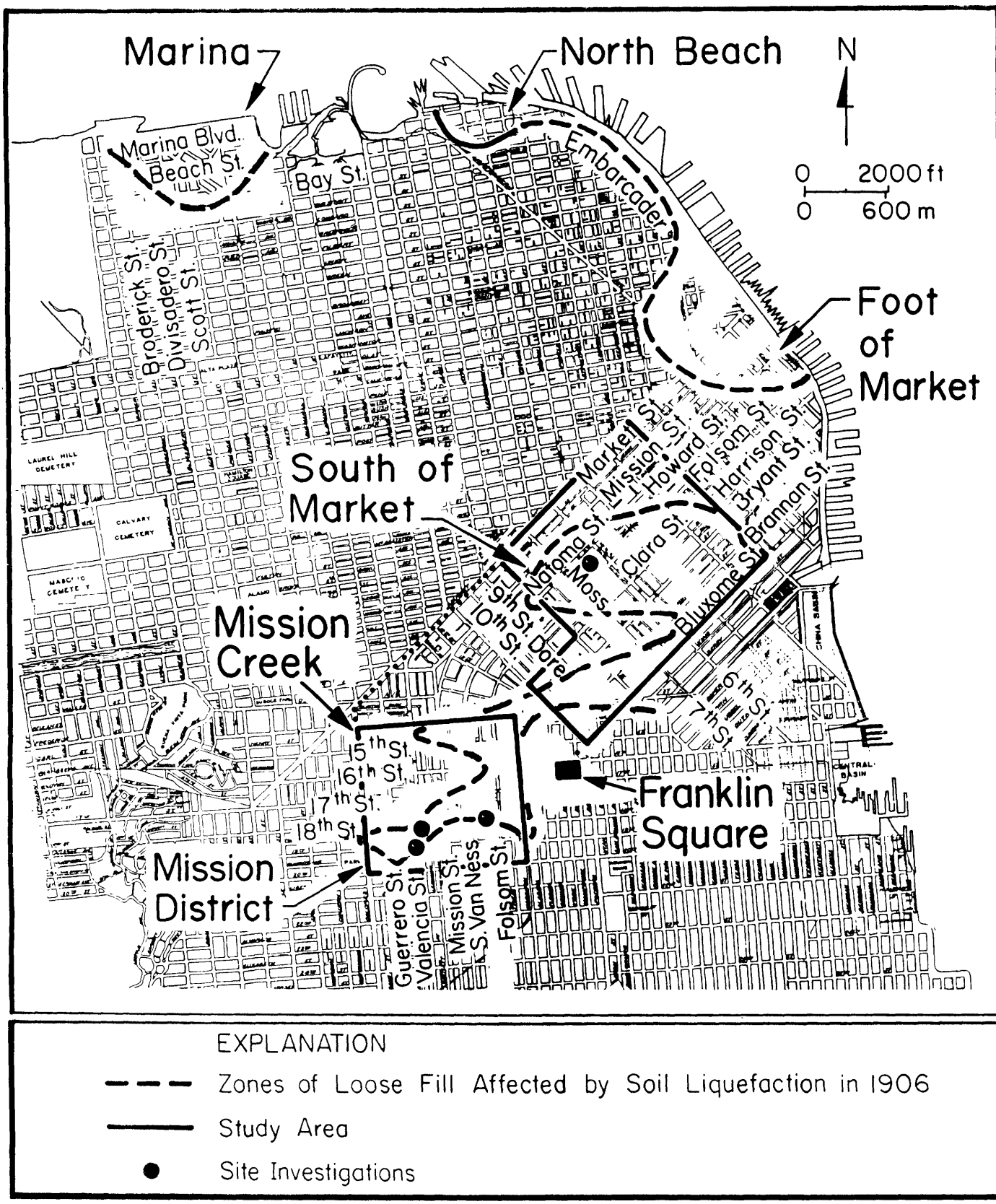


Figure 1.—San Francisco, showing locations of principal areas of soil liquefaction in 1906 and 1989, study areas of this paper, and site investigations.

area of most intense liquefaction-induced damage in 1989, the Marina District, was discussed in detail by O'Rourke (1992) and O'Rourke and others (1991, 1992). In 1989, liquefaction damage also was severe in the Mission District and South of Market area. Of special interest is that liquefaction during the 1989 Loma Prieta earthquake caused damage, including disruption of water-supply pipelines, in the same general places in the Mission District and South of Market area as those documented in the 1906 San Francisco earthquake. Recurrence of liquefaction and lifeline damage in the same areas during two different earthquakes has important implications for hazard mitigation in San Francisco and, at the same time, provides an opportunity to test modeling and prediction capabilities for the types of ground failure and deformation caused by liquefaction.

Because of substantial gaps in our knowledge of subsurface conditions and their relation to previous seismic damage, we undertook a site-investigation program in the Mission District and South of Market area in conjunction with the collection and analysis of hundreds of existing borehole records, historical evidence of earthquake damage, and observations of pipeline repairs (Pease and O'Rourke, 1993). This paper summarizes the results of our investigations and presents a synthesis of subsurface data. We constructed maps of potentially liquefiable deposits from the subsurface data base and, by inference, from geology and historical geography; we compare these maps with damage patterns in the 1906 and 1989 earthquakes. By integrating the subsurface data and historical evidence of damage, we present liquefaction-susceptibility maps as a basis for improved engineering and planning in San Francisco.

## SITE INVESTIGATIONS

We investigated four sites in San Francisco in 1991, using an integrated program of conventional borehole-sampling procedures, standard penetration tests (SPT's), cone-penetration tests (CPT's), and seismic-velocity measurements (Pease and O'Rourke, 1993). The conventional boreholes included SPT measurements, piston-tube samples of Holocene bay mud, and split-spoon sampling for soil classification. Temporary open-cased piezometers were established in several places to confirm depth to water table in the fill. The CPT soundings allowed a continuous and detailed assessment of soil lenses and the variation in inplace density of sands that was complementary to and independent from SPT measurements. Both the SPT's and CPT's conformed closely to accepted testing procedures and practices (American Society for Testing and Materials, 1991a, c). Special cone-penetration equipment was used at three sites to obtain downhole shear-wave-velocity profiles for seismic evaluation (O'Rourke and others, 1992b).

The locations of three of the sites are shown in figure 2*A*, with the modern street grid in the Mission District superimposed on the topography as mapped by the U.S. Coast Survey (1853). The 1853 topographic features help delineate the previous course of Upper Mission Creek (see section below entitled "Mission District Study Area") and point out areas of previous marshes and tidal flats. The three sites are at Mission Playground, Valencia Street between 18th and 19th Streets, and Shotwell Street between 17th and 18th Streets. The location of the fourth site, on Howard Street, with respect to former Sullivan Marsh and the present street grid in the South of Market area is shown in figure 2*B*.

Except where noted otherwise, all elevations in this report refer to the San Francisco City Datum (SFCD), the standard reference elevation for municipal and engineering surveys in San Francisco, which is 2.6 m higher than mean sea level (Brown and others, 1932). Soils are identified on the basis of the Unified Soil Classification (American Society for Testing and Materials, 1991b).

### MISSION PLAYGROUND SITE

We investigated a site in the Mission District adjacent to 19th Street on a lawn at the north end of Mission Playground, a neighborhood park operated by the San Francisco Department of Parks and Recreation. The ground surface is at 12.5 m elevation. The locations of boreholes and CPT soundings and a soil profile are shown in figures 3*A* and 3*B*, respectively.

We had considerable difficulty in the top 2.5 m of exploration, owing to masonry rubble mixed in with the artificial fill. A 4-m-deep pit dug to retrieve broken equipment penetrated a brick foundation wall 6 m from the streetline of 19th Street and approximately 1.5 m south of the line of CPT soundings. This wall is a remnant of the Youth's Directory, a four-story brick bearing-wall structure that was destroyed in the 1906 San Francisco earthquake and fire (Lawson, 1908). The face of the wall is approximately 1.5 m closer to 19th Street than the distance shown on an insurance map (Sanborn Ferris Map Co., 1899). This offset is comparable to the 1.8 m of lateral spreading on 19th Street in historical accounts and photographs. No significant damage occurred at this site in the 1989 Loma Prieta earthquake.

Sand fill with negligible cohesion or fines (grain size, less than 0.075 mm diam) content was penetrated below the brick foundation to 8.5-m depth. The ground-water level was at 5.5-m depth, and the sand is loose to medium dense, indicating that 3 m of fill was saturated and thus liquefiable. The bottom of the fill is at 4.0-m elevation, or 5.8 m above high-tide level. The cross section in figure

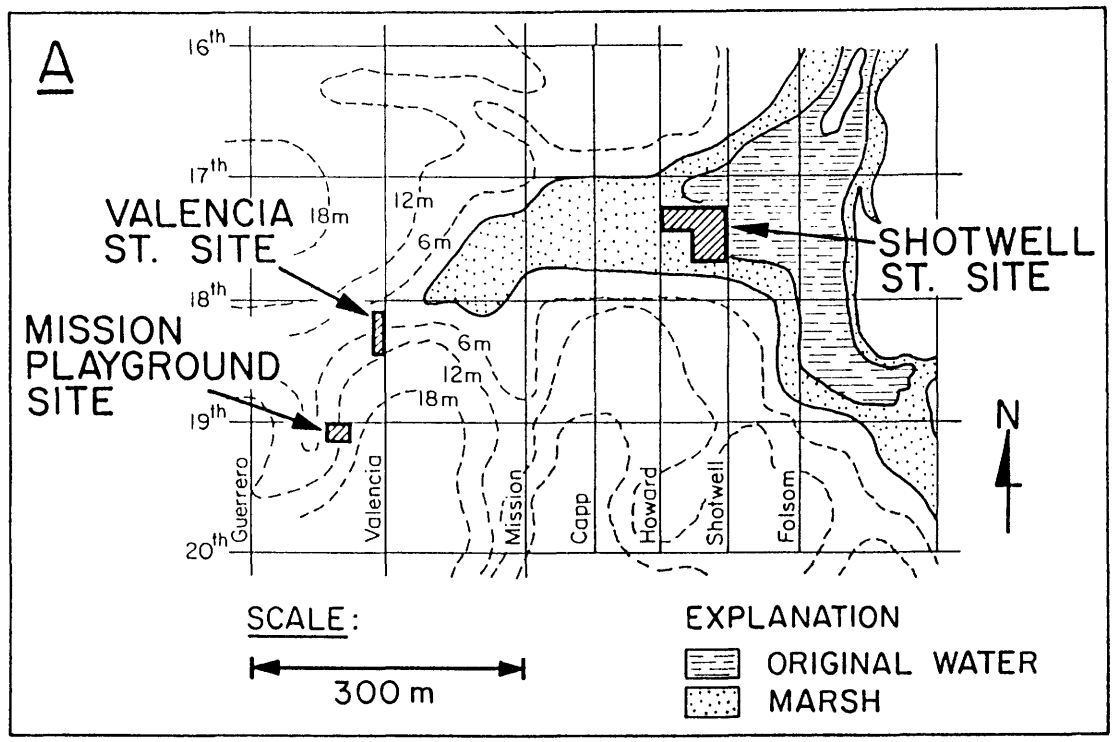


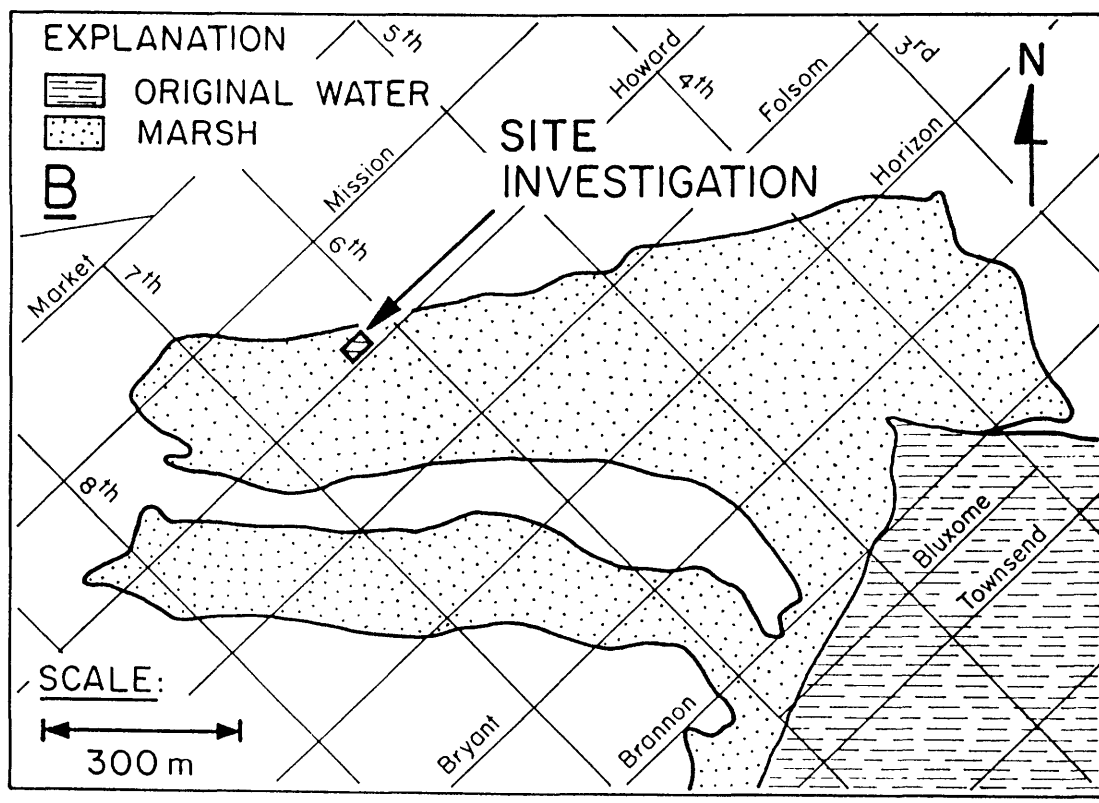


Figure 2.—Study areas in San Francisco, showing locations of site investigations with respect to modern street grid and former marshes and tidal flats in the Mission District (*A*) and South of Market area (*B*) (see fig. 1 for locations). Topography from U.S. Coast Survey (1853); contour interval, 6 m.

3*B*, which is parallel to the modern slope and perpendicular to the preexisting valley, shows no obvious changes in the thickness or elevation of the deposit boundaries. The underlying deposit of gray low-plasticity clay, which includes gray subrounded gravel and is above sea level, is most likely of alluvial origin. Bedrock is at 34-m depth, below 22 m of dense orange-brown plastic clays that appear to be weathered colluvial soils.

## VALENCIA STREET SITE

We investigated a site in the Mission District on the west side of Valencia Street between 18th and 19th Streets. Valencia Street has a 1.9-percent gradient downhill toward the north, and the site was located at about 10.5-m elevation. The locations of boreholes and CPT soundings and a soil profile are shown in figures 4*A* and 4*B*, respectively. This site is at the location of the Valencia Street Hotel, which collapsed catastrophically in the 1906 San Francisco earthquake (Derleth, 1906; Hansen and Condon, 1989). The hotel site is currently occupied by a two-story unreinforced-masonry garage. No major damage occurred to this building in 1989, although 3-mm-wide diagonal cracks were observed in its north wall. It is not known whether these cracks resulted from the earthquake.

The top 1.5 m of artificial fill is poorly graded (well sorted) sand, silt, and debris, including small pieces of masonry, vitrified-clay pipe, and fragments of glass. Deeper fills are poorly graded fine sand, containing 3 to 6 percent fines, to 10.4-m depth. The bottom of the fill is at -0.1-m elevation, or 1.75 m above high-tide level. The ground-water level was not measured directly but was interpolated from adjacent boreholes to be at 2.7-m depth. Approximately 6.0 to 7.7 m of liquefiable fill underlie the site. Underlying natural soils are lean silty clays with a few traces of subangular gravel, probably Holocene in age.

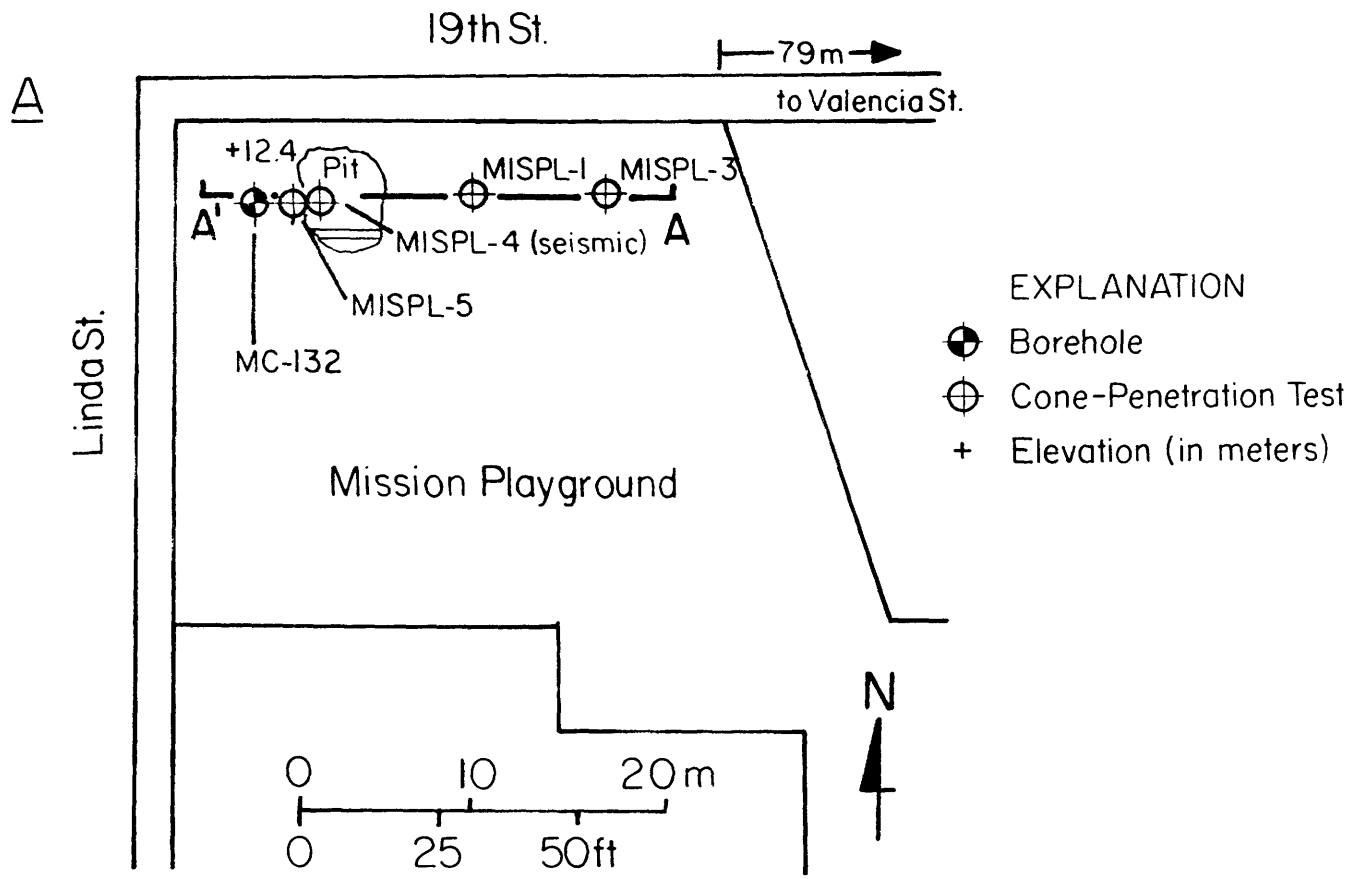


Figure 3.—Schematic map (*A*) and cross section (*B*) of Mission Playground site (fig. 1), showing locations of boreholes, cone-penetration tests (CPT's), and soil profile. Soil profile is 19 m long. Depths on cross section are in meters. CPT measurements: $q_c$, tip resistance (in megapascals); FR, friction ratio (in percent). Soils are identified by symbols in Unified Soil Classification (American Society for Testing and Materials, 1991b): CH, high-plasticity clay; CL, low-plasticity clay; SC, clayey sand; SM, silty sand; SP, poorly graded sand. LL, liquid limit; PL, plastic limit; w, natural-water content (in percent).

## SHOTWELL STREET SITE

We investigated a site in the Mission District in vacant lots on the west side of Shotwell Street between 17th and 18th Streets. Two- to three-story wood-frame houses had existed at these sites before 1989, but they were damaged by liquefaction during the 1906 earthquake and subsequently removed. Earthquake damage at this site is discussed in more detail in the following subsections. The locations of boreholes and CPT soundings and a soil profile are shown in figures 5*A* and 5*B*, respectively.

The existing grade of the lots at the time of our investigation was at about 2.0-m elevation. The upper 0.9 m of sandy fill had been removed, replaced, and compacted with a vibratory roller in 1990. The soil profile (fig. 5*B*) shows a considerable increase in tip resistance above 2- to 3-m depth, probably owing to surface compaction. The fill averages 5.5 m in depth across the site, slightly decreasing in thickness toward the south. As at the other sites, the fill is clean, poorly graded, fine sand containing less than 2 percent fines. The bottom of the fill is at -2.4-m elevation, slightly above mean sea level and within the tidal zone. In several shallow wells, ground-water levels ranged from 0.61 to 1.14 m in depth. Ignoring the increase in density of the soil due to compaction, about 5 m of liquefiable soil probably existed beneath the site at the time of the 1989 earthquake.

The fill overlies Holocene bay mud, which consists of high-plasticity silt containing some peat and organic matter. The silt is normally consolidated, with a natural-water content of 90 to 100 percent, close to the plastic limit of the material. The base of the bay mud slopes at a gradient of approximately 6 percent toward the north along the cross section, following the slope of the former ravine at this site. The underlying unit is layered, yellow-brown, stiff sandy clay of probable alluvial origin. Natural soils, consisting of alternating estuarine and subaerial Pleistocene deposits, extend to weathered bedrock at 56-m depth.

## HOWARD STREET SITE

We investigated a site in the South of Market area in a parking lot on the northwest side of Howard Street be-

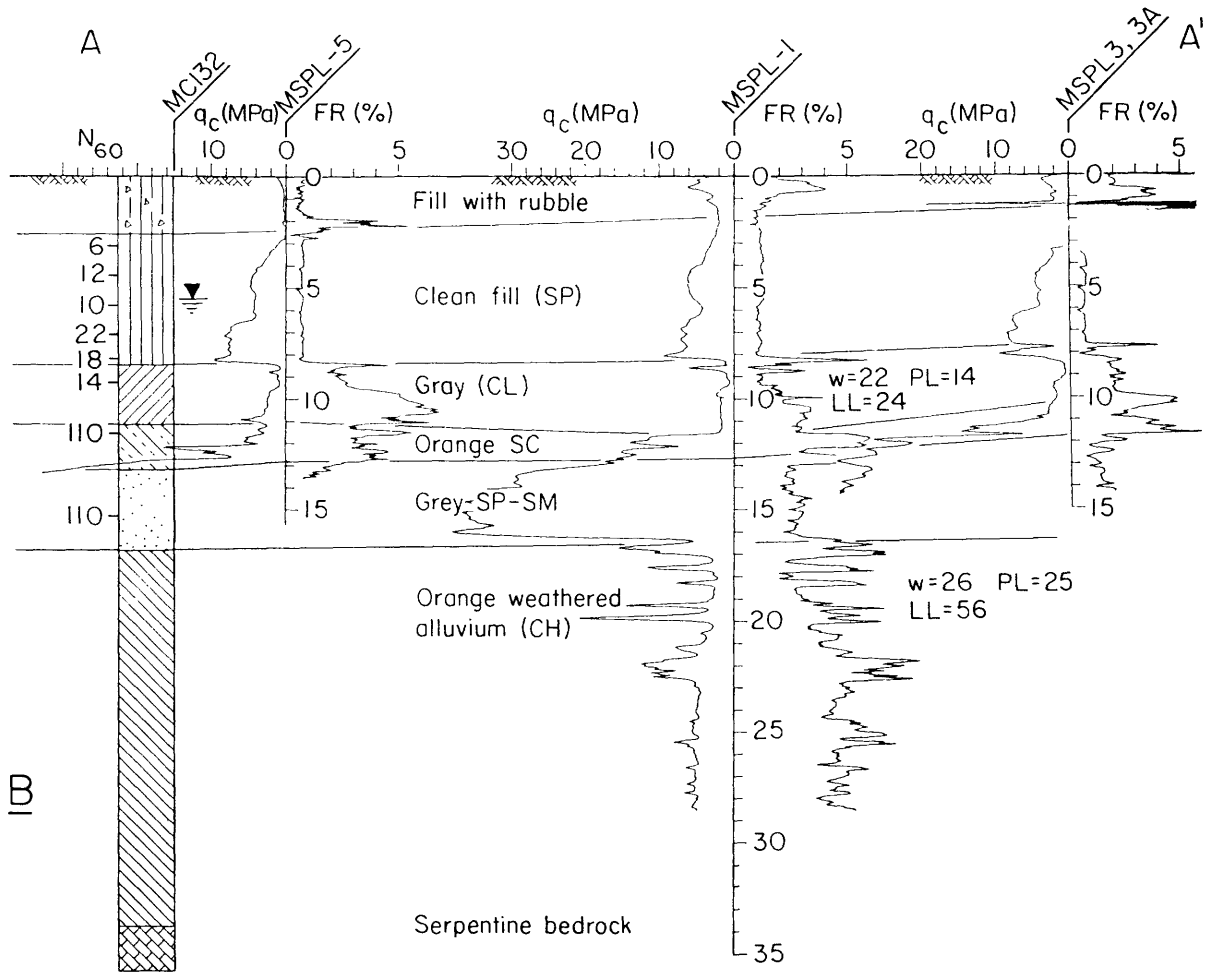


Figure 3.—Continued.

tween 6th and 7th Streets, near the north boundary of a former marsh (fig. 2*B*). Extensive wavelike deformations of the ground were observed near this site after the 1906 San Francisco earthquake. The locations of boreholes and CPT soundings and a soil profile are shown in figures 6*A* and 6*B*, respectively.

The site is approximately level, at 3.7-m elevation. The fill ranges from 4 to 6.5 m in depth, increasing in depth toward the south. The top approximately 1 m of fill consists of easily penetrable sand, gravel, and rubble. The fill below the surface layer is poorly graded sand containing less than 2 percent fines. The fill at this site appears to be somewhat denser than those at the Mission District sites, on the basis of blowcounts and CPT logs. The water table is at 2.7-m depth. There is a liquefiable layer 1 to 3 m thick at this location.

Underlying the fill is a fibrous-matted peat layer, as much as 3.3 m thick. The surface of this peat layer (base

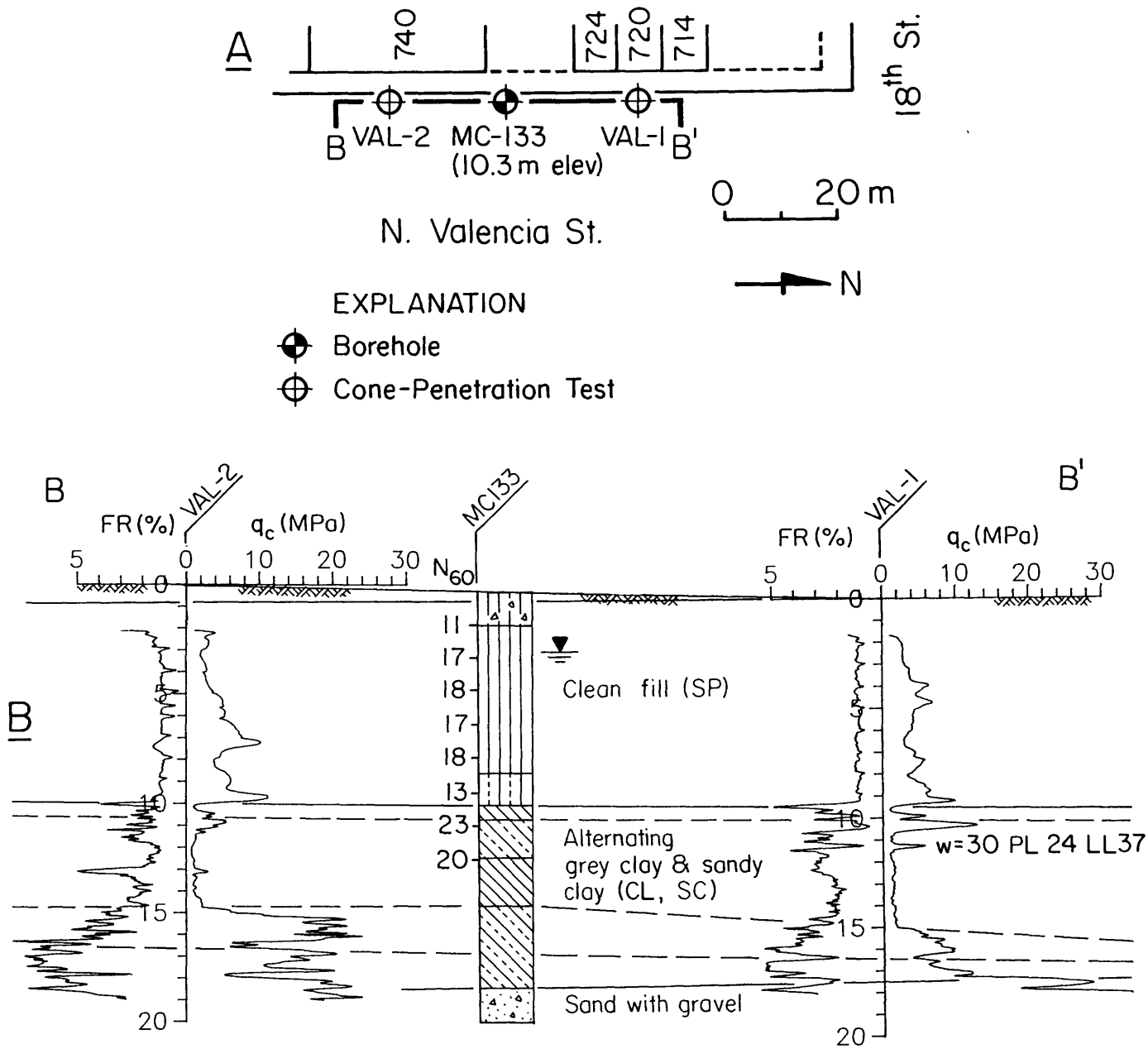


Figure 4.—Schematic map (*A*) and cross section (*B*) of Valencia Street site (fig. 1), showing locations of boreholes, cone-penetration tests (CPT's), and soil profile. Soil profile is approximately 55 m long. Depths on cross section are in meters. CPT measurements: $q_c$, tip resistance (in megapascals); FR, friction ratio (in percent); $N_{60}$, standard-penetration-test blowcount (in blows per foot). Soils are identified by symbols in Unified Soil Classification (American Society for Testing and Materials, 1991b): CL, low-plasticity clay; SC, clayey sand; SP, poorly graded sand. LL, liquid limit; PL, plastic limit; w, natural-water content (in percent).

of fill) ranges from -2.8 to 0 m in elevation, or from 1.8 m above to 0.2 m below high-tide level. The underlying Holocene bay mud is as thin as 3 m at one CPT sounding. Bay mud under the site is silty and sandy, with a low plasticity and a natural-water content of 20 percent, and includes mica flakes and shell fragments. As at the Shotwell Street site, alternating estuarine and subaerial Pleistocene deposits extend to bedrock at 62-m depth.

## DATA-COLLECTION AND MAPPING PROCEDURES

Two data bases of 146 and 306 boreholes, CPT soundings, and surface excavations were collected to evaluate subsurface conditions in the Mission District and South of Market area, respectively. The age and quality of the records range from well logs predating 1913 to modern geotechnical investigations conducted after the 1989 Loma Prieta earthquake. These data were summarized by Pease and O'Rourke (1993), including identification of the original report or source, location of exploration, and subsurface data.

Subsurface records were located and mapped with respect to a rectangular coordinate system based on the street grid for each area. Elevations were interpreted for the top and bottom of each subsurface record, the ground-water table, and the boundaries of artificial fill, Holocene bay mud, Pleistocene clay, and bedrock. Contour maps were drawn to show the variations in elevation of the ground surface and bedrock, thickness of Holocene bay mud, and depths of the water table, fill, and submerged fill.

The contour maps in this paper were generated with the computer program *Surfer* from Golden Software of Golden, Colo. The program uses an algorithm known as kriging to perform a statistical evaluation of randomly spaced data and construct an evenly spaced grid of data with minimal estimation variance (Ripley, 1987). Surfaces are represented and stored in the computer by using the abstraction of a rectangular grid of data from which contour lines can be plotted. Data from two grids can also be manipulated mathematically to produce a third grid, providing an easy means to superimpose different surfaces.

The average surface area per borehole in the Mission District and South of Market area, calculated by dividing each area by the number of boreholes and CPT soundings,

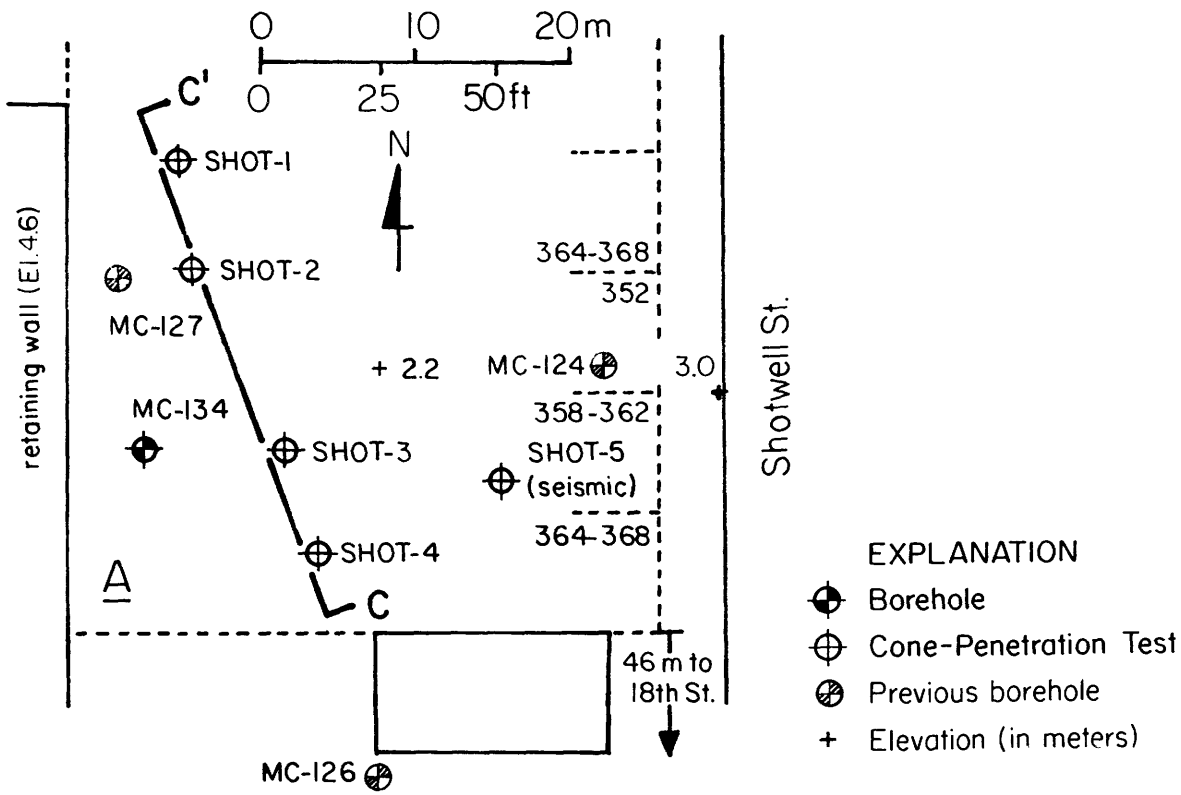


Figure 5.—Schematic map (*A*) and cross section (*B*) of Shotwell Street site (fig. 1), showing locations of boreholes, cone-penetration tests (CPT's), and soil profile. Soil profile is approximately 30 m long. Depths on cross section are in meters. CPT measurements: qc, tip resistance (in megapascals); FR, friction ratio (in percent); $N_{60}$, standard-penetration-test blowcount (in blows per foot). Soils are identified by symbols in Unified Soil Classification (American Society for Testing and Materials, 1991b): CH, high-plasticity clay; CL, low-plasticity clay; SM, silty sand; SP, poorly graded sand. LL, liquid limit; PL, plastic limit; w, natural-water content (in percent).

is 8,500 to 9,500 $m^2$, equivalent to explorations at 90-m spacing. Exploration density is not uniform; the spacing of data was closer in some areas and farther apart in others. The dimensions of the contouring grids were set so that gridpoint spacing was 30 to 40 m, thus taking advantage of sites where closely spaced data were available.

Two primary sources of geographic and topographic information for San Francisco before urbanization are maps by the U.S. Coast Survey (1853, 1857). In these maps, parts of which are reproduced in figures 7 and 16, marshes, shallow alluvial surfaces, ravine slopes, and bedrock surfaces all show characteristic gradients, lengths of slope, and wavelength between repetition of gully and stream-canyon features. These features are consistent over lengths of 100 m to several hundred meters, and slopes and stream gradients can be interpolated with fewer data. Accordingly, the boundaries of fill over major buried alluvial and estuarine features can be successfully mapped, given the available spacing of explorations and choice of grid size. In contrast, the former eolian features in San Francisco include ridges less than 100 m wide, with slope heights of 30 m or less. With boreholes at 90-m spacings, individual ridges or valleys could lie between explorations. The varying size and shape of dune ridges and depressions in the eolian landscape makes the interpolation of overlying-fill thickness difficult.

Owing to limitations of space, only selected maps most relevant to the discussion of liquefaction and liquefaction site response are presented in this paper. Pease and O'Rourke (1993) presented comprehensive geotechnical characterizations of both study areas derived from the subsurface data bases. Their maps show bedrock, Holocene bay mud, fill, and water-table depths. On the basis of their report, in the following sections we present maps illustrating submerged-fill thickness, fill characteristics, and surface slope, chosen as most informative in evaluating liquefaction site response.

## MISSION DISTRICT STUDY AREA

We defined a study area of 1.2 $km^2$ in the Mission District within the 36-block area bounded by Harrison, Dolores, 14th, and 20th Streets (fig. 7). "Mission Creek" refers to a former north-south-trending estuary in the Mission District between Folsom and Harrison Streets from

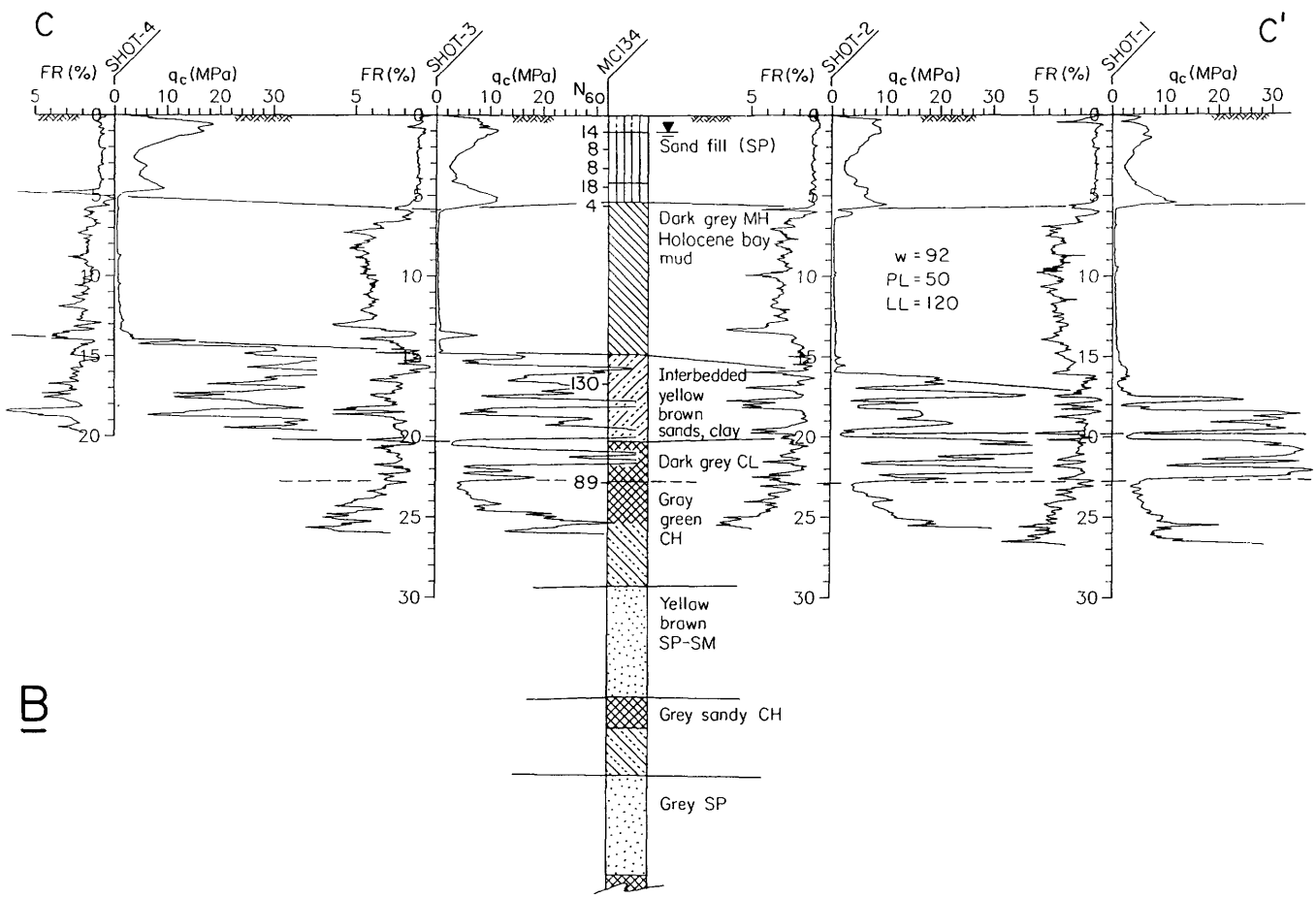


Figure 5.—Continued.

15th to 22nd Streets that connected to Mission Bay through the South of Market area (see fig. 16). A major branch of Mission Creek flowed eastward between 17th and 19th Streets, where it joined the estuary. Thus, in this paper we refer to the estuary and valley to the east of Shotwell Street as "Lower Mission Creek," and the stream and ravine to the west of Shotwell Street as "Upper Mission Creek." A third filled area of less significance is a shallow east-west-trending valley in the vicinity of 14th Street. The Mission District was rapidly urbanized between 1860 and 1890 as the city of San Francisco expanded. Ravines and estuaries in the study area were filled during this period, resulting in deposits of loose, cohesionless fine sand that are susceptible to liquefaction.

Much of the Mission District was urbanized by 1875, with completion of fills over much of Upper and Lower Mission Creek. By 1876, streets had been graded to near their present elevations, and brick and wooden sewers had been constructed. Only a narrow (less than 30 m wide) channel remained in Lower Mission Creek, confined by fill, between Folsom and Harrison Streets (Humphreys, 1876). No surface drainage remained by 1906 in either Upper or Lower Mission Creek, owing to extensive filling and urbanization.

## LIQUEFIABLE THICKNESS

We use submerged thickness of artificial fills to represent the thickness of liquefiable deposits. On the basis of studies of tip resistance, natural sands are recognized to be considerably denser than historical fills with similar grain-size characteristics in the study area (Roth and Kavazanjian, 1984) and elsewhere in San Francisco (Pease and others, 1992). These studies also indicate that sand fills are moderately to highly susceptible to liquefaction, whereas natural sands typically are insusceptible, owing to their relatively high inplace density.

Liquefiable deposits were identified by means of SPT and CPT data, where available. Because valid SPT and CPT data are available for only a few locations, extrapolation and judgment are required to delineate the boundaries of liquefiable soil throughout the study areas. We assumed that loose, relatively clean (less than 20 percent fines), sandy fills would be susceptible to liquefaction. The depth and areal extent of these materials were estimated from both SPT and CPT data.

The thickness of submerged fill was calculated by subtracting the elevation of the base of the fill from that of the water table. Seasonal and yearly fluctuations in ground-

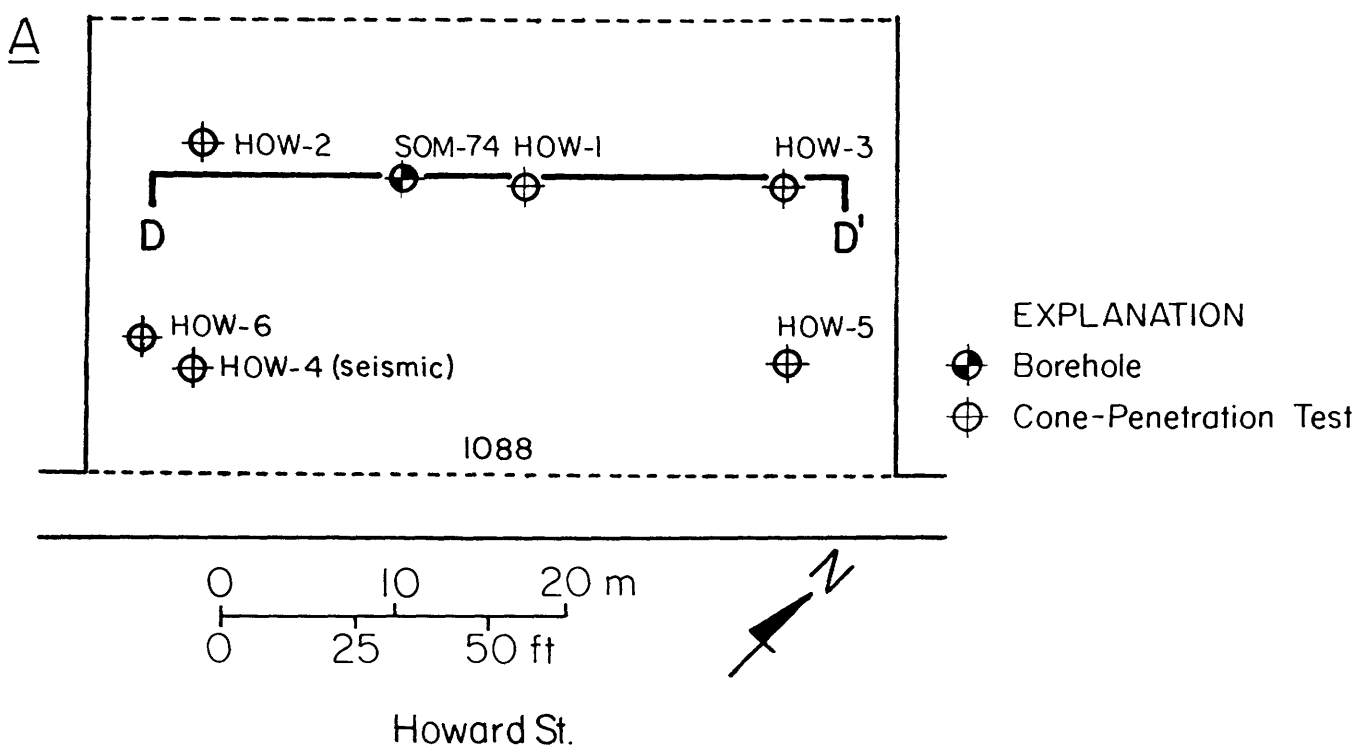


Figure 6.—Schematic map (*A*) and cross section (*B*) of Howard Street site (fig. 1), showing locations of boreholes, cone-penetration tests (CPT's), and soil profile. Soil profile is approximately 34 m long. Depths on cross section are in meters. CPT measurements: $q_c$, tip resistance (in megapascals); FR, friction ratio (in percent); $N_{60}$, standard-penetration-test blowcount (in blows per foot). Soils are identified by symbols in Unified Soil Classification (American Society for Testing and Materials, 1991b): CH, high-plasticity clay; CL, low-plasticity clay; SM, silty sand; SP, poorly graded sand. LL, liquid limit; PL, plastic limit; w, natural-water content (in percent).

water level could not be analyzed from the available data, and near-surface ground-water levels were assumed not to be influenced significantly by pumping in either 1906 or 1989. The elevation of the base of the fill similarly was evaluated on the basis of interpretations of subsurface records. Where historical maps indicate that a site was previously bay or marsh, the base of the fill typically is determined as the surface of Holocene bay mud or marsh deposits in boreholes or CPT soundings. Where fills are underlain by materials of similar consistency, determination of the base of the fill requires judgment based on density, soil type, soil color, and interpretation of the drilling log. Relative changes in tip resistance from both SPT and CPT data provided the most reliable method of determining the boundary between fill and natural sand. Submerged-fill thickness in the Mission District is mapped in figure 8.

Liquefaction is likely to be most severe in thick layers of submerged fill. In figure 8, 4 to 8 m of submerged fill was observed at both Valencia and Shotwell Streets in former Upper Mission Creek, only 2 to 3 m under Mission Street near 18th Street, and as much as 4 m in former estuarine areas of Lower Mission Creek. A shallow lens of submerged fill was also noted near the 14th Street valley.

Because liquefiable thickness in the Mission District and South of Market area is determined on the basis of submerged deposits, it follows that the depth to ground water represents the thickness of overlying nonliquefiable soils. In Upper Mission Creek in the Mission District, unsaturated surface fills may be 2 to 6 m thick; in Lower Mission Creek, liquefiable zones are capped with only 1 to 3 m of unsaturated cover. Along the 14th Street valley, pockets of liquefiable fill are overlain by 5 to 6 m of partially saturated fill. The thickness of nonliquefiable deposits has been shown to influence liquefaction-induced ground deformation and the presence of sand boils (Ishihara, 1985).

## FILL CHARACTERISTICS

Soil types in the Mission District are classified with respect to liquefaction susceptibility in figure 9. Highly liquefiable soils are present along the axis of Upper Mis-

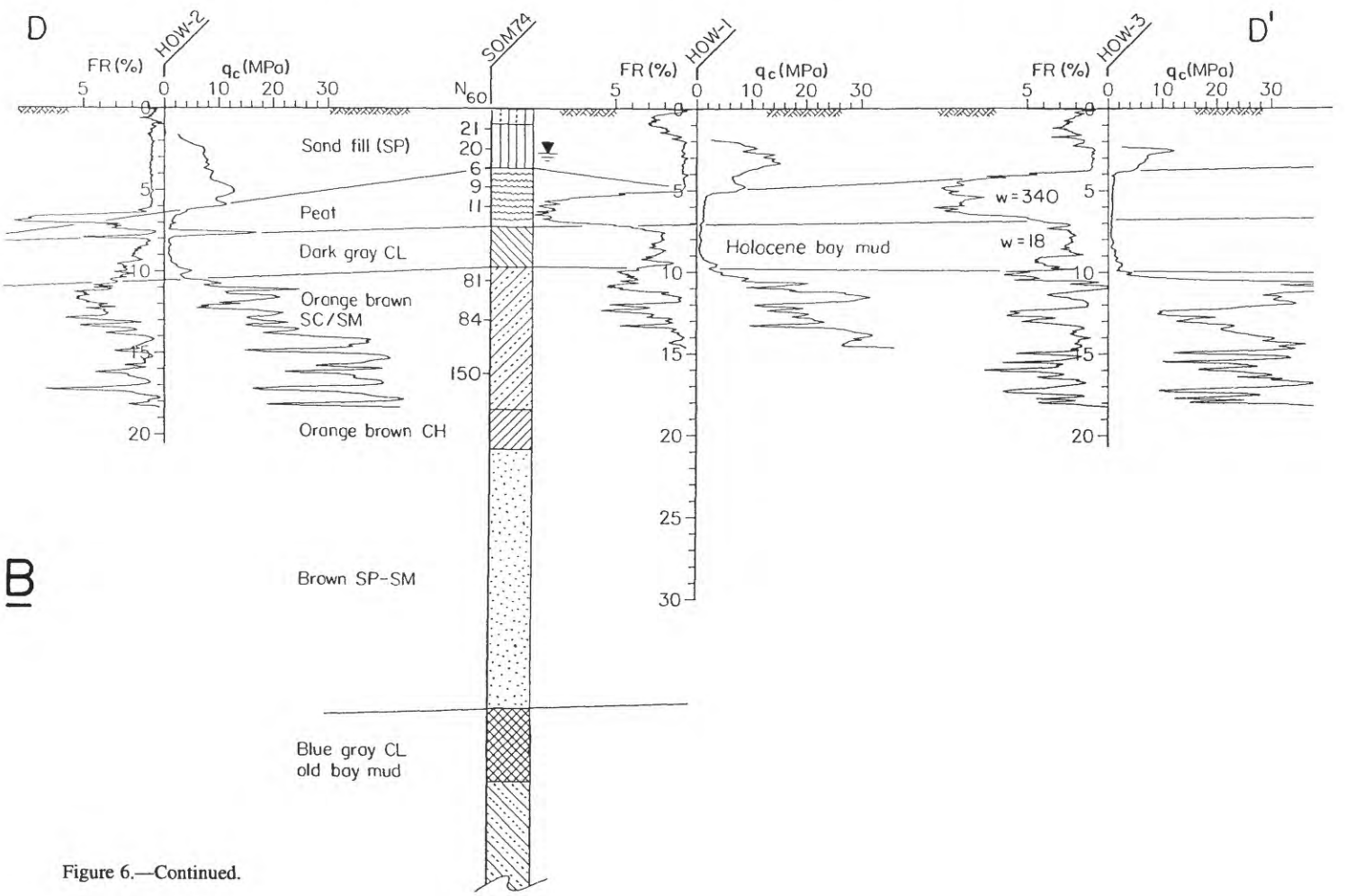


Figure 6.—Continued.

sion Creek. Poorly graded, fine- to medium-grained, clean sand fill, highly susceptible to liquefaction, was penetrated in boreholes as far east as 18th and Folsom Streets. The extensive, clean, poorly graded sands in Upper Mission Creek almost certainly were derived from dune sands. The submerged fill is generally uniform and homogeneous throughout.

In Lower Mission Creek, increasingly silty and clayey fills were penetrated below the water table. Several boreholes indicate no liquefiable fill. The fill appears to be more heterogeneous. Rubble or debris layers were noted, as were some loose sand layers. Lower Mission Creek was filled at approximately the same time as Upper Mission Creek, though apparently with borrow material from a different origin. Because of its proximity to a former dune field, some dune-sand fills are probably present in the area north of 16th Street. The submerged fills near 14th and Valencia Streets are brown or orange sandy clay or silt, although poorly graded clean sand was penetrated at the base of two boreholes. As in Lower Mission Creek, fill near the water table appears to be heterogeneous and may include layers of liquefiable sand.

## TOPOGRAPHY

Current surface contours in the Mission District are mapped in figure 10. The ground surface in the study area has gradients toward the east of 2.5 percent or less; steeper slopes occur along bedrock spurs at 20th and Dolores Streets and at 14th and Dolores Streets. Between 17th and 19th Streets, the former Upper Mission Creek ravine is shown by the looping of contours between Dolores and Valencia Streets; below Valencia Street, this ravine is not apparent. Along 18th Street from Valencia Street to South Van Ness Avenue, the typical gradient of the filled ravine is 1.1 percent. Uphill, from Valencia to Guerrero Streets, the gradient of 18th Street decreases to 0.6 percent. The area of Lower Mission Creek in the vicinity of Folsom Street between 14th and 18th Streets is nearly flat.

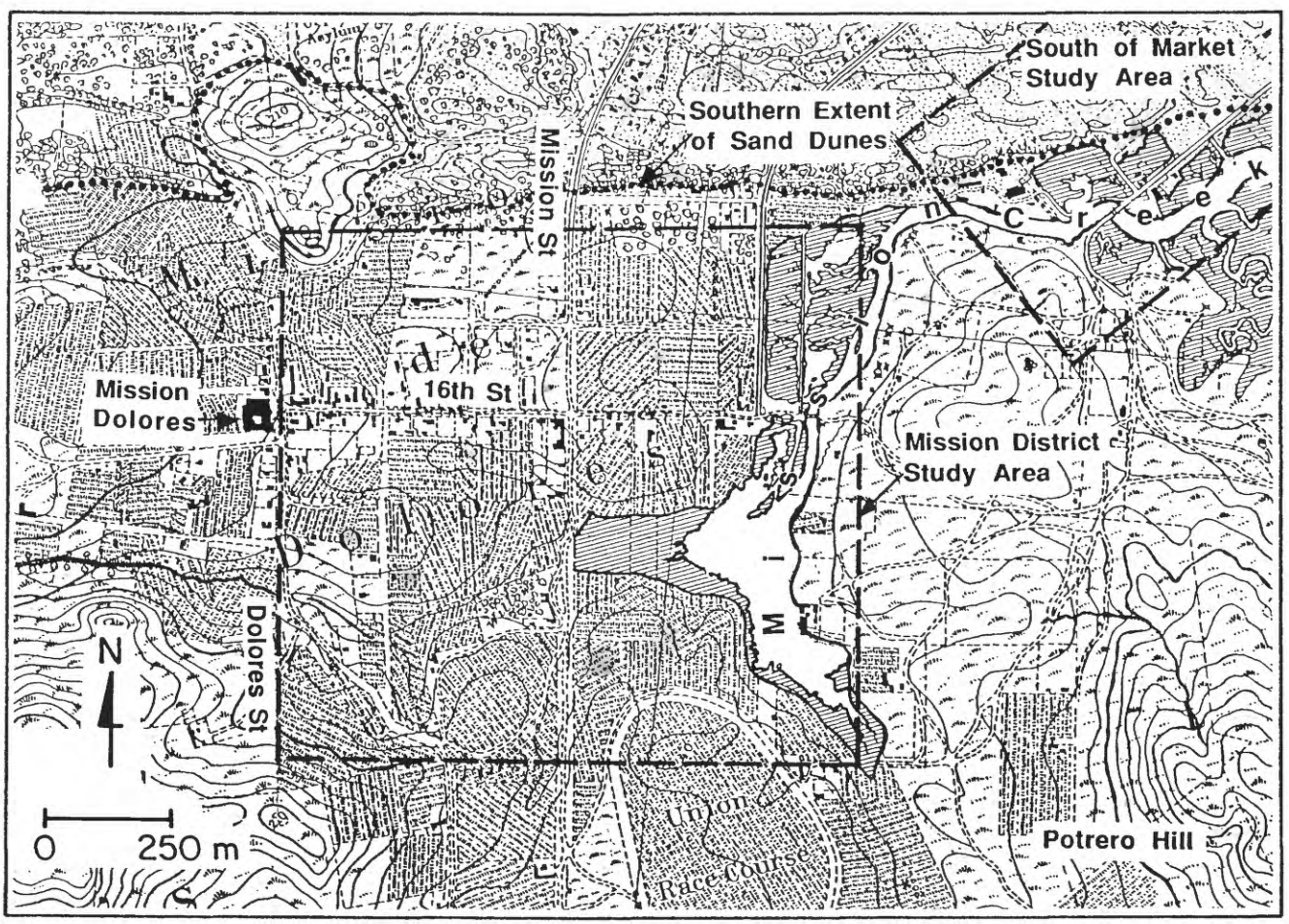


Figure 7.—Part of U.S. Coast Survey (1857) map of San Francisco (see fig. 1 for location), showing boundaries of Mission District and South of Market study areas (dashed), alignments of modern streets, south edge of former dune field (dotted), and predevelopment topographic contours (measured above mean sea level; interval, 6 m). Diagonal-lined areas, marshes. Stippled areas probably correspond to sandy ground; other-textured areas indicate trees or brush that have grown on and stabilized many dunes.

## LIQUEFACTION IN THE 1906 SAN FRANCISCO EARTHQUAKE

Ground deformations and liquefaction features observed in the Mission District after the 1906 San Francisco earthquake are mapped in figure 11. A striking feature of figure 11 is the occurrence of lateral spreading in areas with about 2 m or more of submerged fill. A major lateral spread is centered on Valencia Street, where the submerged fill is more than 6 m thick. The ground under Valencia Street spread eastward and slightly northward down the center of a former ravine, with maximum lateral displacements of 1.8 m to 2.4 m and a settlement of 1.5 m. A second lateral spread occurred between Capp Street and South Van Ness Avenue, where a maximum lateral movement of 1.2 m was measured. The submerged fill is more than 2 m thick in this area, increasing toward the east. Maximum lateral movement and settlement of 0.3 m occurred over a width of 120 m across Mission Street between these two areas. Given the relatively small movement on Mission Street, the lateral spreading in Upper Mission Creek may not have developed as continuous movement. It may have occurred as two or more discontinuous areas of displacement where the submerged fill is thickest.

Nearly all liquefaction features were confined within the predicted zones of submerged fill. Compressional, extensional, or lateral offsets were conspicuous at the edges of zones where the submerged fill is from 1 to 4 m thick. Buckled curbs, major extension cracks, and distortion of pavements were conspicuous on 18th Street between Mission and Folsom Streets on the south side of the liquefaction zone. Cracks were widest near Folsom Street, where the submerged fill is as much as 4 m thick. The offsets appear to be concentrated at the boundaries of lateral spreads, where soils on one side were constrained and on the other side were subjected to either permanent or transient deformations.

Settlement, lateral spreading, and damage to water mains and sewers occurred on 14th Street between Valencia Street

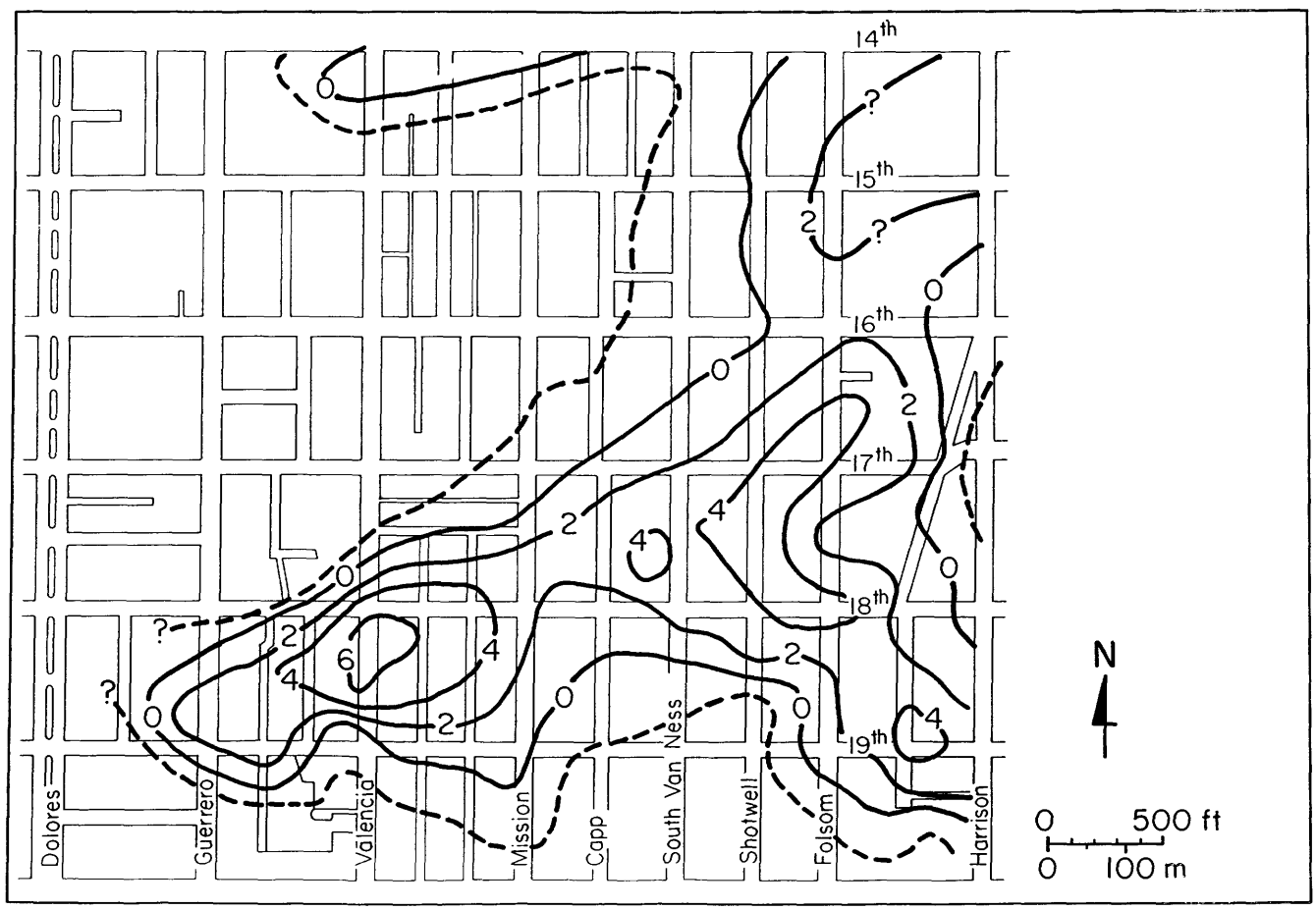


Figure 8.—Mission District study area, showing thickness of submerged fill (solid contours; interval, 2 m). 0-m contour, which indicates where elevation of water table is at base of fill, represents a theoretical boundary between regions where liquefaction can and cannot occur. Upper-bound contour (dashed), which delimits area where ground-water level is within 2 m of base of fill, is proposed as a reasonable limit on maximum extent of potential hazard in case of nonuniform changes in fill thickness or unpredictable variations in ground-water level.

and South Van Ness Avenue, where there is also a layer of submerged fill (Derleth, 1906; Schussler, 1906). Cripple walls of buildings were extensively damaged and foundations cracked on Folsom and Treat Streets for two or three blocks south of 18th Street (Lawson, 1908), in an area that approximately coincides with the limits of submerged fill in the southern branch of Mission Creek (fig. 1).

Damage to the water-supply and sewer system in the Mission District from the 1906 San Francisco earthquake is mapped in figure 12. A total of 50 water-main breaks (dots, fig. 12) were reported, 80 percent of which occurred in the zone of submerged fill. Two areas of multiple breaks occurred on trunklines across the zone of submerged fill at Valencia and Harrison Streets. Between Valencia and Harrison Streets, breaks were less concentrated and generally located toward the margins, rather than the centers, of the submerged-fill zone. In many places, breaks corresponded to the locations of scarps and offsets shown in figure 11. Some breaks occurred near the upper-bound contour (dashed) in figure 8, suggesting that some breaks may have resulted from liquefaction influenced by higher ground-water levels in spring 1906 than those indicated by subsurface records collected in this study.

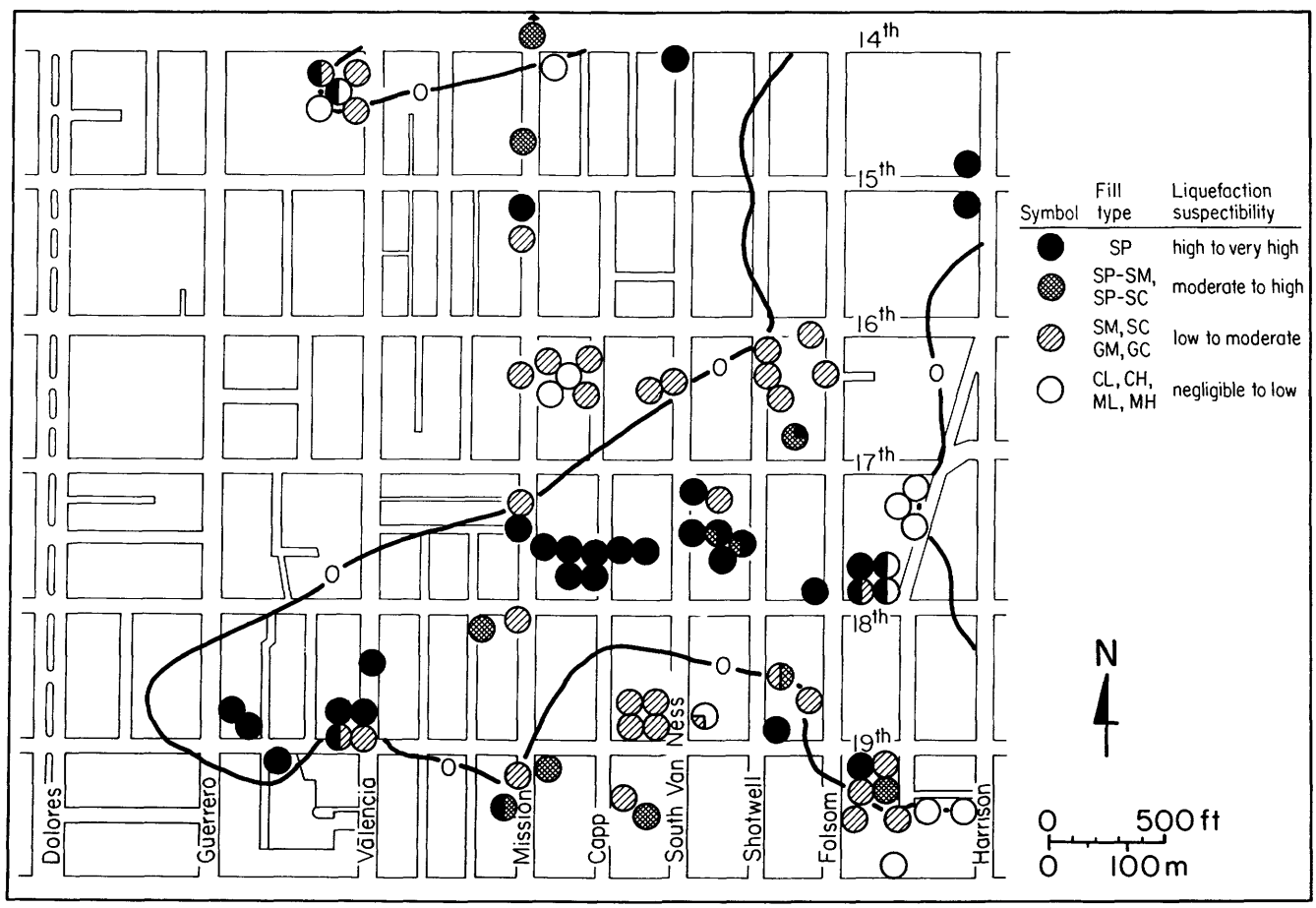


Figure 9.—Mission District study area, showing soil characteristics and liquefaction susceptibility of submerged fill. 0-m contour marks boundary between areas of submerged fill and unsaturated fill, as shown in figure 8. Shaded circles indicate classification of fills based on data from boreholes or cone-penetration-test soundings at each location. Where submerged fill occurs (within bounded area), shading indicates only soil types below water table; where there is no submerged fill below water table or borehole terminated above water table, shading indicates only soil type closest to base of fill. Soils are identified by symbols in Unified Soil Classification (American Society for Testing and Materials, 1991b): CH, high-plasticity clay; CL, low-plasticity clay; GC, clayey gravel; GM, silty gravel; MH, high-plasticity silt; ML, low-plasticity silt; SC, clayey sand; SM, silty sand; SP, poorly graded sand. Clays and silts consist of materials of which more than 50 weight percent passes a No. 200 sieve. Proportion of circle with a particular shading reflects approximate proportion of corresponding soil type below water table at that location. In general, liquefaction susceptibility of soils containing 20 to 50 weight percent fines is considered to be low, and that of fairly clean soils containing less than 20 weight percent fines to be moderate. This classification is considered valid for San Francisco soils on the basis of observations that the fines in these soils (particles smaller than 0.075 mm) are typically clay minerals and that relatively few soil samples contain much low-plasticity or cohesionless silt. Although soils containing more than 20 weight percent fines have been observed to liquefy during earthquakes, such occurrences have been confined to regions where low-plasticity silts are a common constituent of fines (Cao and Law, 1991).

## LIQUEFACTION IN THE 1989 LOMA PRIETA EARTHQUAKE

In the 1989 Loma Prieta earthquake, liquefaction in the Mission District resulted in light to moderate damage associated with sand boils, settlement, pavement cracking, and strong ground shaking, which was limited to Lower Mission Creek. The most significant damage occurred between South Van Ness Avenue and Shotwell, 17th, and 18th Streets, as described below. Damage on both sides of Shotwell Street included sand boils, building settlement, tilting, and structural damage. Liquefaction-induced damage in this area extended to Folsom Street between 17th and 18th Streets, where settlement and sand boils were observed.

Elsewhere in the Lower Mission Creek area, minor ground deformations were evident. Sand boils were observed in front of Victorian frame buildings on the north side of 15th Street, about 30 m west of Folsom Street, where minor tilting and differential settlements occurred in these structures. Sidewalks were buckled to the east of the corner of Folsom and 15th Streets, apparently owing to east-west compression. Differential settlement and minor street cracking were observed on 14th Street between Folsom and Harrison Streets. Street cracks in the Mission District commonly paralleled the centerline and may represent minor ground movements due to settlement adjacent to pile-supported sewers (Seed and others, 1991).

Two pipeline breaks occurred in the Mission District in the 1989 earthquake: A 150-mm-diameter Municipal Water Supply System pipe was broken near Shotwell and 18th Street, and a hydrant connection for the Auxiliary Water Supply System was broken at 18th and Folsom Streets.

No liquefaction features were observed west of South Van Ness Avenue, suggesting that liquefaction was absent in Upper Mission Creek. A possible explanation may be that the liquefaction in San Francisco in 1989 was limited to areas overlying Holocene bay mud, which produced site-amplification effects. However, soft Holocene

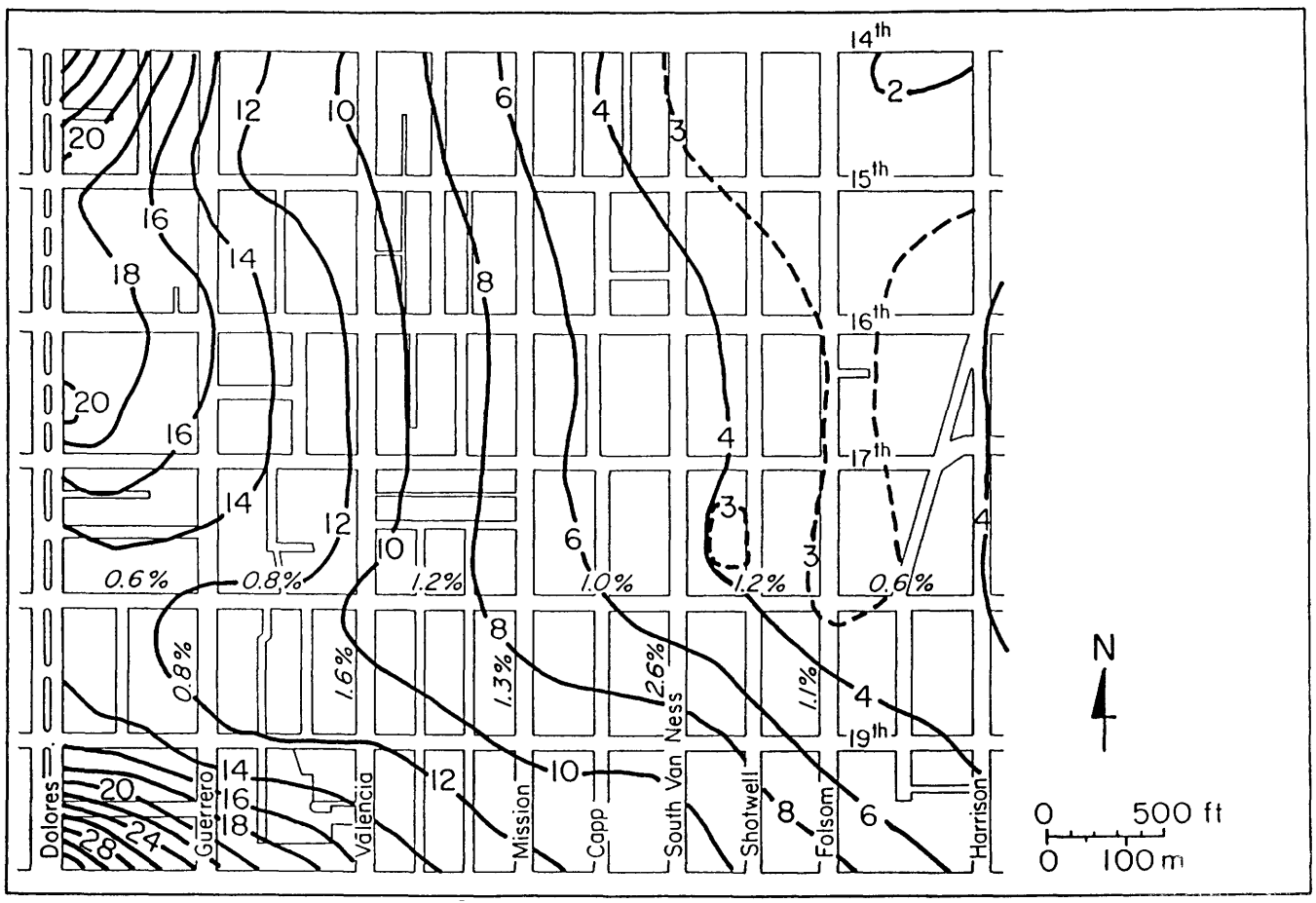


Figure 10.—Mission District study area, showing surface elevation (solid contours; interval, 2 m) and intermediate contour (dashed) relative to San Francisco City Datum. Contours are based on survey data from major street intersections at approximately 190-m spacing collected by San Francisco Department of Public Works in 1973 and 1991. Italic numbers, average street gradient (in percent).

bay mud, as much as 11 m thick, extends as far as one block westward of South Van Ness Avenue in Upper Mission Creek. Furthermore, a study by O'Rourke and others (1992b) suggested that Holocene bay mud at Shotwell Street and Holocene alluvial clay at Valencia Street, as studied by deep soil profiles, produced similar levels of site amplification, although significant liquefaction effects were confined principally to the Shotwell Street site. Deeper ground-water levels in Upper Mission Creek would have resulted in greater confining stresses, thereby increasing the threshold level of ground motions required for liquefaction. Greater confining stresses, in combination with a larger thickness of nonliquefiable soil near the surface probably contributed to greater resistance to liquefaction, as well as to reduced opportunities for its expression on the ground surface.

## SOUTH VAN NESS AVENUE AND SHOTWELL STREET

The most severe liquefaction-induced damage in the Mission District from the 1989 Loma Prieta earthquake occurred on the block bounded by South Van Ness Avenue and Shotwell, 17th, and 18th Streets. This block was spared by the fire in 1906, and numerous buildings have survived both earthquakes. A photograph taken after the 1906 earthquake (fig. 13) provides a background against which to examine the damage in 1989. Damage on this block in the 1906 and 1989 earthquakes is summarized in figure 14.

Maximum lateral movement of approximately 1.2 m occurred perpendicular to South Van Ness Avenue in the 1906 earthquake, and extension cracks were observed on

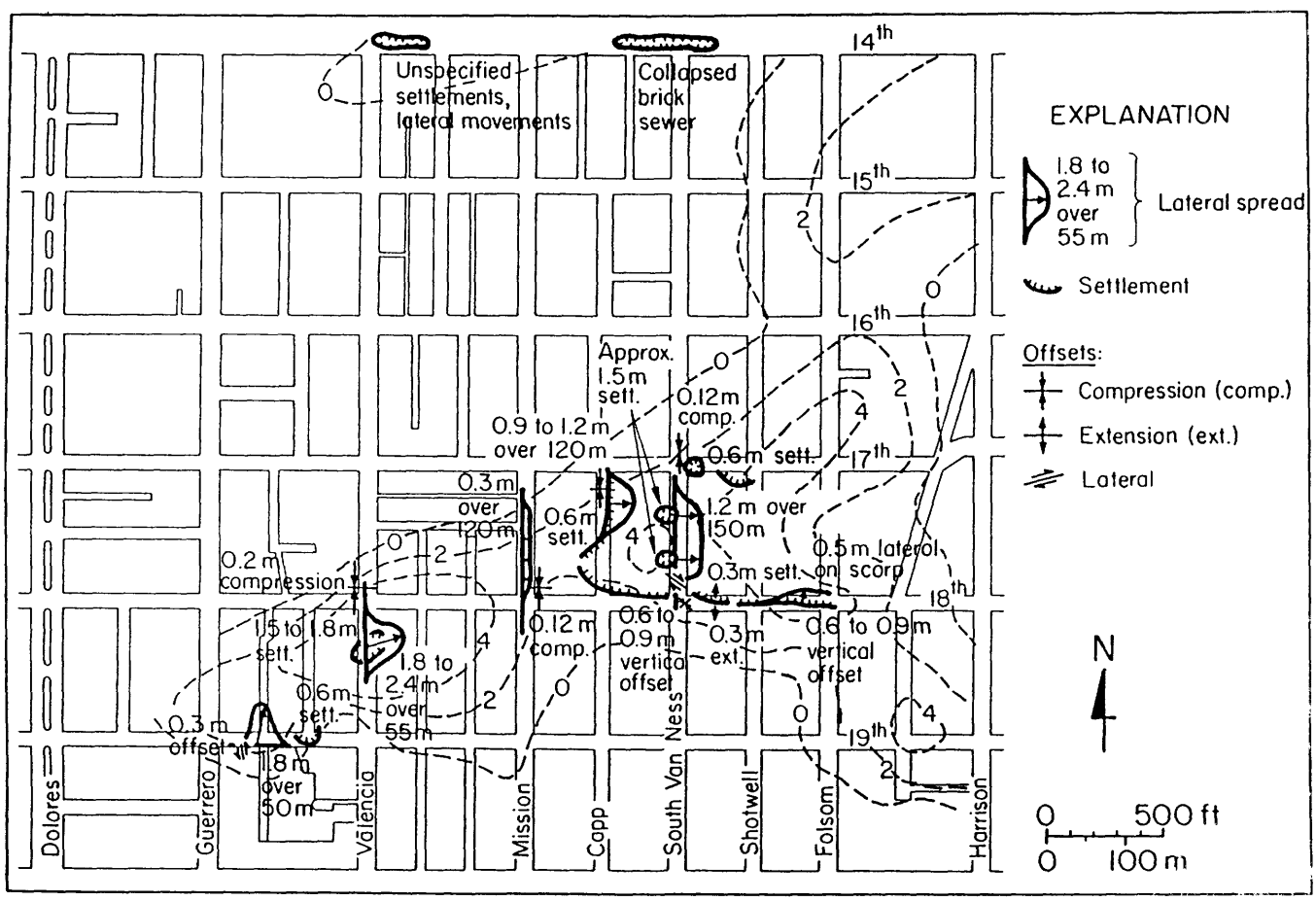


Figure 11.—Mission District study area, showing thickness of submerged fill (dashed contours; interval, 2 m) and locations of lateral spreading, differential settlement, and offsets in 1906 San Francisco earthquake. Hachures, which point toward area of settlement, may indicate either gradual subsidence or an abrupt scarp. Absence of historical data in a given area may indicate that only relatively minor damage occurred there in comparison with documented areas. From O'Rourke and others (1992a).

Folsom Street (fig. 14*A*). The worst building damage was on South Van Ness Avenue, in the vicinity of two of the cripplewall failures mentioned in the preceding subsections, decreasing toward both ends of the block. Seven to nine Victorian houses on Shotwell Street probably survived the 1906 earthquake and were still standing in 1989. Except for architectural finishes, these nine buildings have the same plan dimensions as those shown on insurance maps (Sanborn Ferris Map Co., 1899). The house at 334 Shotwell Street was reported by tenants to have been built between 1894 and 1896. Modern insurance records indicate that this and six other of these buildings have no listed date of construction, suggesting that records were missing or destroyed in the earthquake.

Damage on the same block in the 1989 earthquake is shown in figure 14*B*. Ground cracks as much as 20 mm wide were observed after the earthquake along the centerline of South Van Ness Avenue. Some cracks appeared to be fresh at the time of our site investigation, but farther toward 18th Street we observed asphalt patching, suggesting repairs at this location before the earthquake. Earthquake-induced cracking and 70 mm of settlement of the sidewalk and steps with respect to the buildings were observed on the east side of South Van Ness Avenue.

The building at 655–695 South Van Ness Avenue is a one- to two-story concrete-frame structure, the back columns of which are supported on a 2.4-m-high by 61-m-long retaining wall that overlooks the back of the Shotwell Street lots. Postearthquake observations indicate that whereas the south end of this wall remained vertical, its north end rotated outward at the base 3.5°, resulting in 150 to 200 mm of lateral movement. Cracking and damage, minimal at the south end of the wall, increased in intensity toward the north. The northernmost bay of the

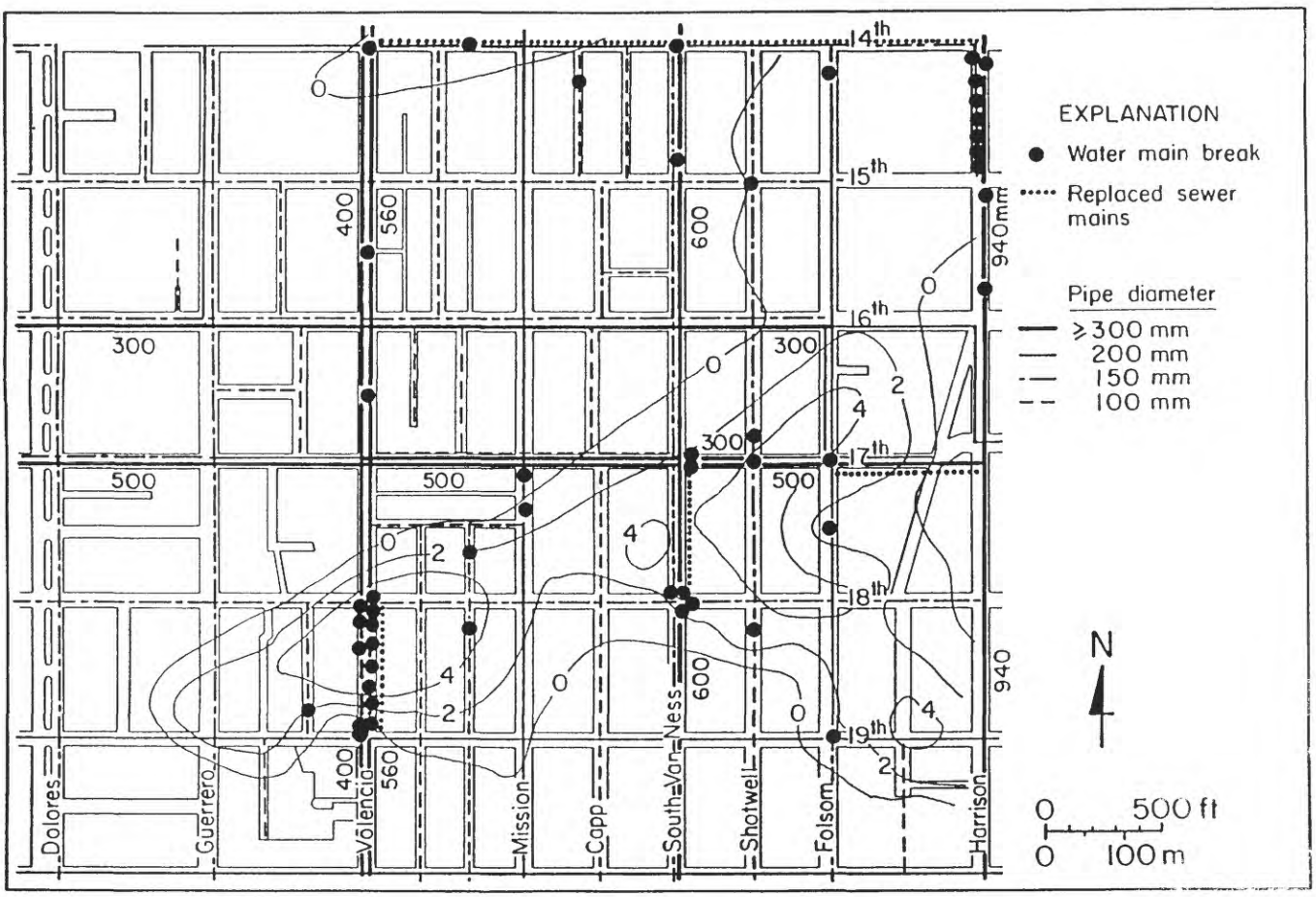


Figure 12.—Mission District, showing thickness of submerged fill (contour interval, 2 m), diameters of pipes, locations of water-supply pipelines, and locations of broken water mains and replaced sewer mains from 1906 San Francisco earthquake reported as of July 1906. Broken water mains were reported by the Spring Valley Water Co. (Schussler, 1906; Manson, 1908). In some places where pipelines cross or run parallel, it is uncertain which pipes were broken; for example, more than one break occurred on South Van Ness Avenue at 17th and 18th Streets (Manson, 1908), and multiple breaks may have occurred elsewhere as well. Locations of replaced sewer mains are based on repairs reported by the City of San Francisco (Schussler, 1906).

structure, at 655 South Van Ness Avenue, was subsequently torn down. Distortion of fences in back yards on Shotwell Street indicate that 200 to 400 mm of differential vertical movement occurred 4 to 15 m from the base of the retaining wall. An unreinforced-concrete slab 15 m from the base of the wall was buckled in an east-west direction.

In the 1989 earthquake, houses on Shotwell Street were moderately to heavily damaged. Several buildings on this block settled differentially and sustained considerable structural distortion. Tilting of the buildings was by approximately 2°–3°. Buckling of a concrete slab behind one house resulted in distortion of the back porch, built on isolated footings. Sand boils were observed in back yards and between buildings. Six of these buildings were subsequently demolished.

Although the severity of damage near South Van Ness Avenue was substantially less in 1989 than in 1906, the patterns of damage are similar and are related to liquefiable thickness. Lateral spreading in 1906 and lateral movements in 1989 occurred where the submerged fill is more than 2 m thick. Severely damaged and collapsed houses in 1906 and damaged structures in 1989 generally were located in areas underlain by approximately 4 m of submerged fill.

A cross section of the present ground surface between 17th and 18th Streets is shown in figure 15. The average gradient between South Van Ness Avenue and Folsom Street between 17th and 18th Streets is 1.2 percent. However, a 2.4-m-high retaining wall divides the block between South Van Ness Avenue and Shotwell Street. This retaining wall and the surcharge associated with approximately 2.4 m of soil appear to have locally influenced ground deformation. As previously mentioned, vertical and lateral surface movements were greatest in 1989 near the base of the north end of this wall. Moreover, Himmelwright (1906) observed that the back ends of several houses on South Van Ness Avenue dropped 3 m after the 1906 earthquake. Apparently, this 2 to 3 m of differential height of soil affected ground deformation between South Van Ness Avenue and Shotwell Street during both earthquakes.

As shown in figure 15, the gradient from Shotwell Street to Folsom Street is only 0.5 percent. A gradient of 0.5 percent has been reported as the approximate lower limit for lateral spreading (U.S. National Research Council, 1985). Gradients across Shotwell Street and to the east toward Folsom Street are negligible, suggesting that lateral spreading would not have occurred here in 1906 despite the presence of thick liquefiable fills.

Figure 13.—Buildings on east side of South Van Ness Avenue between 17th and 18th Streets after 1906 San Francisco earthquake and fire. Stars denote structures still standing in 1993. Two buildings to left of center sustained cripplewall failure and were shifted to left (northward) off their foundations. As a result of these failures, they are tilted to right and away from street. Rubble from another building that collapsed into an adjacent vacant lot is visible in center. View from Capp and 18th Streets (see fig. 9 for location).

## SOUTH OF MARKET STUDY AREA

We defined a study area of 2.2 $km^2$ in the South of Market area, bounded by Market and Townsend Streets between Third and Eighth Streets, and by Harrison and Division Streets between Eighth and 11th Streets (fig. 16). The city of San Francisco expanded into this district from the 1850's to the 1870's as it rapidly outgrew its original settlement in Yerba Buena Cove. The study area includes two major lateral spreads in the 1906 earthquake: former Sullivan Marsh and the channel of Lower Mission Creek near Dore Street (fig. 16). Both of these areas were tidal lands, artificially filled with soil from adjacent sand dunes. Liquefaction-induced damage was concentrated in the same zones after the 1989 earthquake.

Sullivan Marsh, the most conspicuous feature in the South of Market area before development, occupied about 70 ha, or half of all the marsh areas adjacent to Mission Bay. The surface of this marsh typically consisted of 1 m to several meters of soft, highly compressible peat that was noted to "sustain a small house or a loaded wagon, though a man, swinging himself from side to side, could give it a perceptible shiver" (Hittel, 1878).

Adjacent to Sullivan Marsh, to the north and south, were extensive sand dunes, typically 12 to 15 m high. Interdune hollows and depressions were marshy or peaty, and the map by the U.S. Coast Survey (1857) shows ponds in several of the depressions. Several sand dunes, as much as 24 m high, are mapped in figure 16, typically with a base near sea level in the adjacent hollows. A low sand ridge divides Sullivan Marsh into a northern section and a smaller southern section. South of Sullivan Marsh, the channel of Mission Creek is adjacent to the low serpen-

tine ridge of Potrero Hill (fig. 7) at Franklin Square (fig. 1). Soundings in Mission Bay, on the southeast edge of the study area, show an average depth below mean lower low water of 0.3 m, or an elevation of about 3.8 m.

## LIQUEFIABLE THICKNESS

We evaluated the extent and thickness of liquefiable deposits in the South of Market area by the same method-

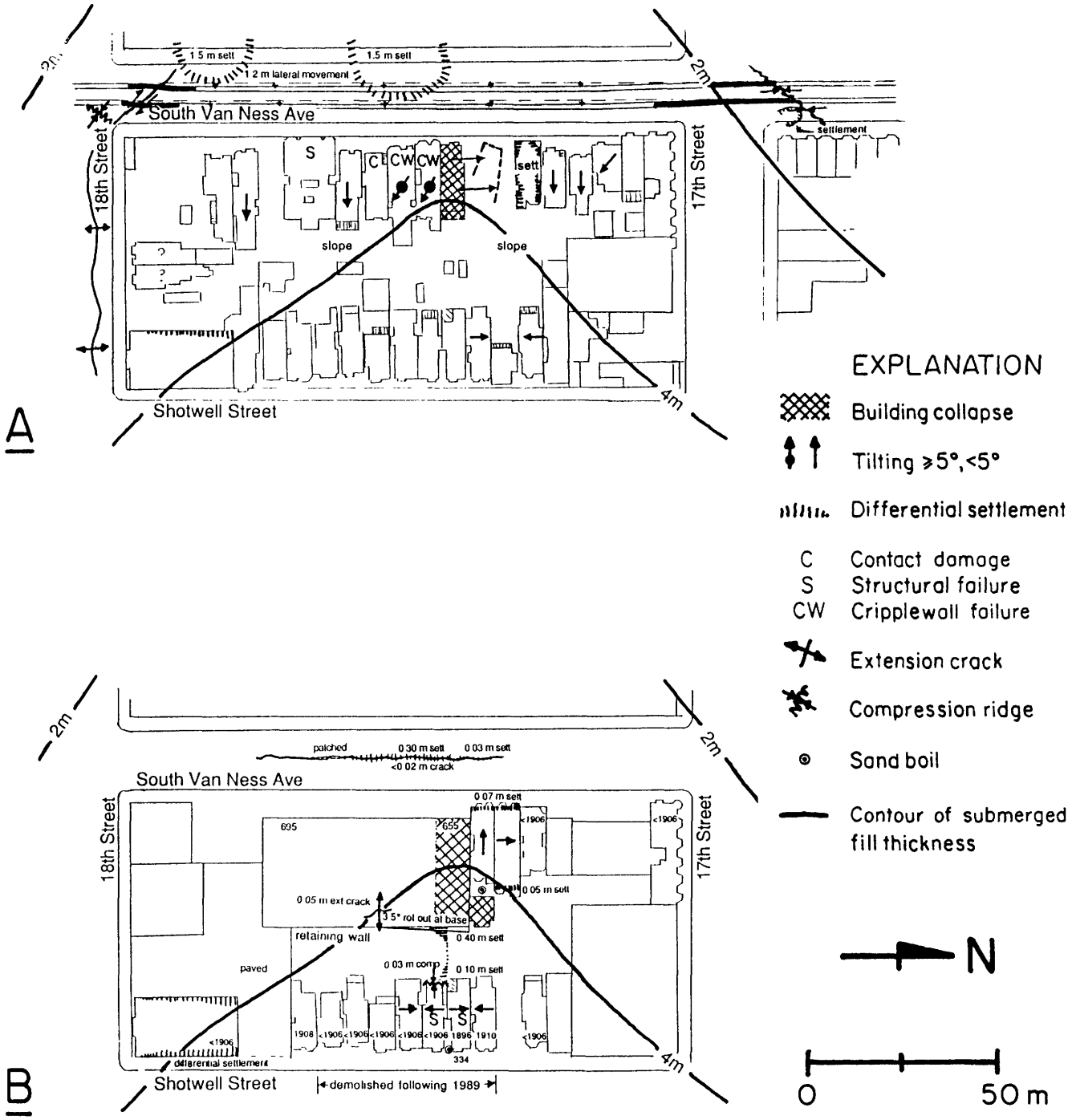


Figure 14.—Ground deformation and building damage from liquefaction in 1906 San Francisco (*A*) and 1989 Loma Prieta (*B*) earthquakes in block bounded by South Van Ness Avenue and Shotwell, 17th, and 18th Streets. Outlines of buildings not visible in photographs are queried or omitted for clarity. Where no symbol appears, damage cannot be inferred from photographs, but building should not be interpreted as undamaged. Length of lines indicates severity of differential settlement. Contact damage ("pounding"), damage caused by impact with an adjacent structure during earthquake shaking; shear distortion, structural failure of one or more upper stories; cripplewall failure, collapse or shifting of framing between foundation and first floor. Dashed outline, postearthquake position of collapsed building. For simplicity, lateral spreading is indicated only by relative dislocation of streetcar tracks on South Van Ness Avenue.

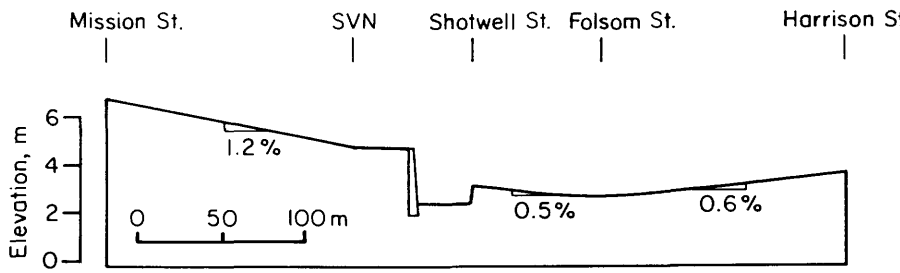


Figure 15.—Profile of ground surface north of 18th Street from Mission to Harrison Street, showing surface elevation and gradient (in percent), including retaining wall between South Van Ness Avenue (SVN) and Shotwell Street.

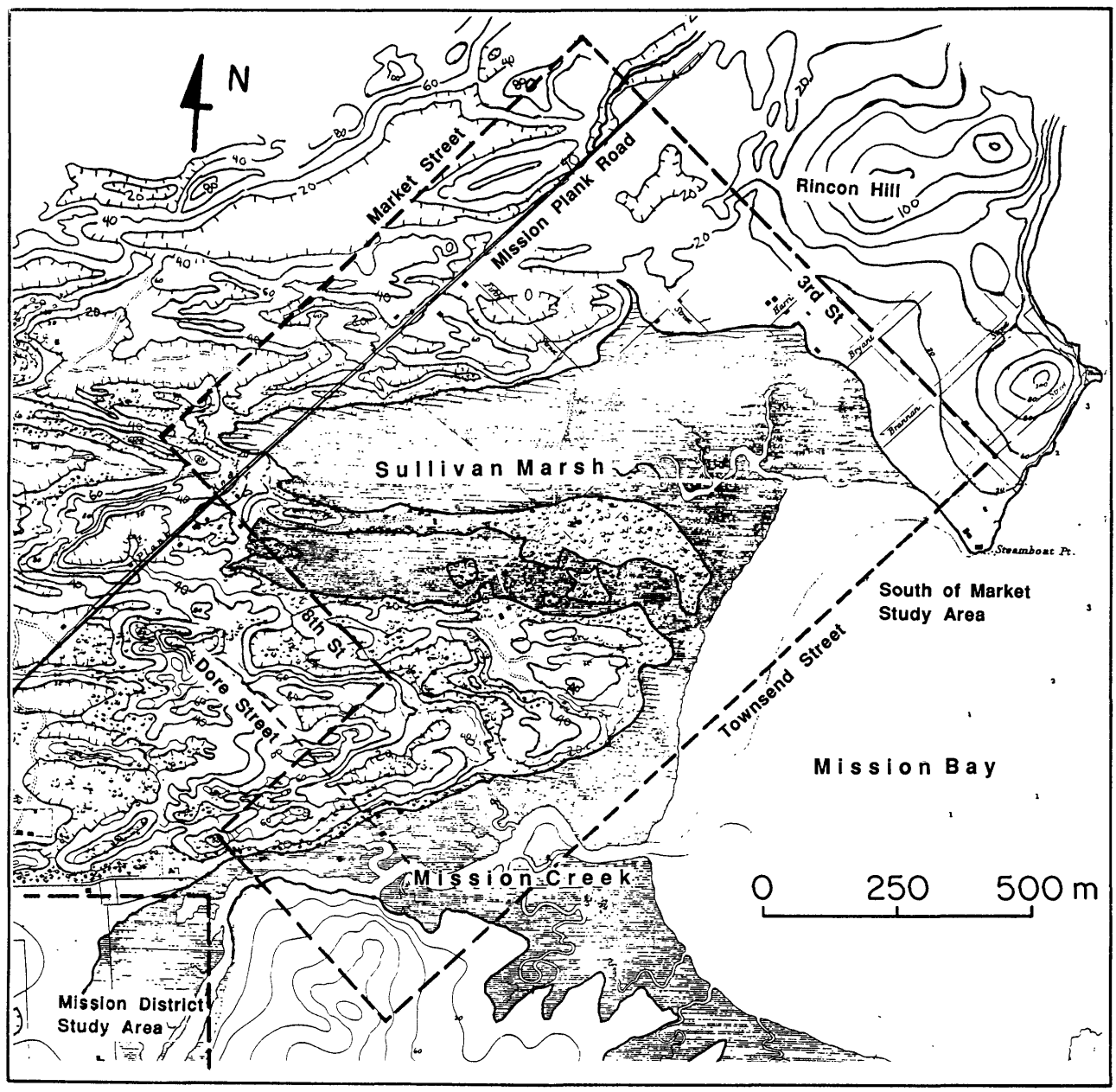


Figure 16.—Part of U.S. Coast Survey (1853) map of San Francisco, showing boundaries of South of Market study area, alignment of modern streets (dashed), locations of bay and marsh areas, and predevelopment topographic contours (measured above mean sea level; interval, 6 m). Contour lines and boundaries of marsh are darkened to accentuate topographic features; hachures are added to contours to clarify downslope direction in complete or partial depressions. Physical and cultural features in north corner of map are omitted for clarity.

ologies as those described for the Mission District. In the South of Market area, fills containing rubble near the surface are commonly underlain by thicker layers of clean sand fill containing little or no debris. Accordingly, the absence of debris does not always indicate natural soil. As in the Mission District, CPT and SPT data indicating changes in density provided the most reliable method of observing the boundary between fill and natural sand. Liquefiable thickness is evaluated as the thickness of submerged fill, obtained by subtracting the elevation of the base of the fill from the water-table elevation. The thickness of submerged fill in the South of Market area is mapped in figure 17.

As shown in figure 17, approximately 6 m of saturated loose fill occurs at 7th Street from Mission Street to Howard Street. Submerged fill also is more than 4 m thick along Mission Creek at Dore and Brannan Streets, Fifth and Harrison Streets, and Sixth and Townsend Streets. These areas overlie buried narrow Holocene bay-mud-filled ravines, as much as 30 m deep, with natural-water contents of 50 to 100 percent, such that additional fill may have been added as major ground settlement occurred because of consolidation. The submerged fill is at least 2 m thick throughout the former marsh area.

Outside the main filled zones, isolated thin layers of submerged fill occur. Within the former dune field, interdune depressions extend close to the water table. One such depression is shown in figure 17 at Howard and Third Streets, and submerged fill more than 2 m thick at Seventh and Market Streets. As noted in the section above entitled "Data Collection and Mapping Procedures," the available subsurface data base may be too coarse to accurately characterize the fill geometry and, thus, the submerged-fill thickness in the former dune landscape of the South of Market area. The occurrence of submerged fill in this area (fig. 17) can be confirmed by individual bore-

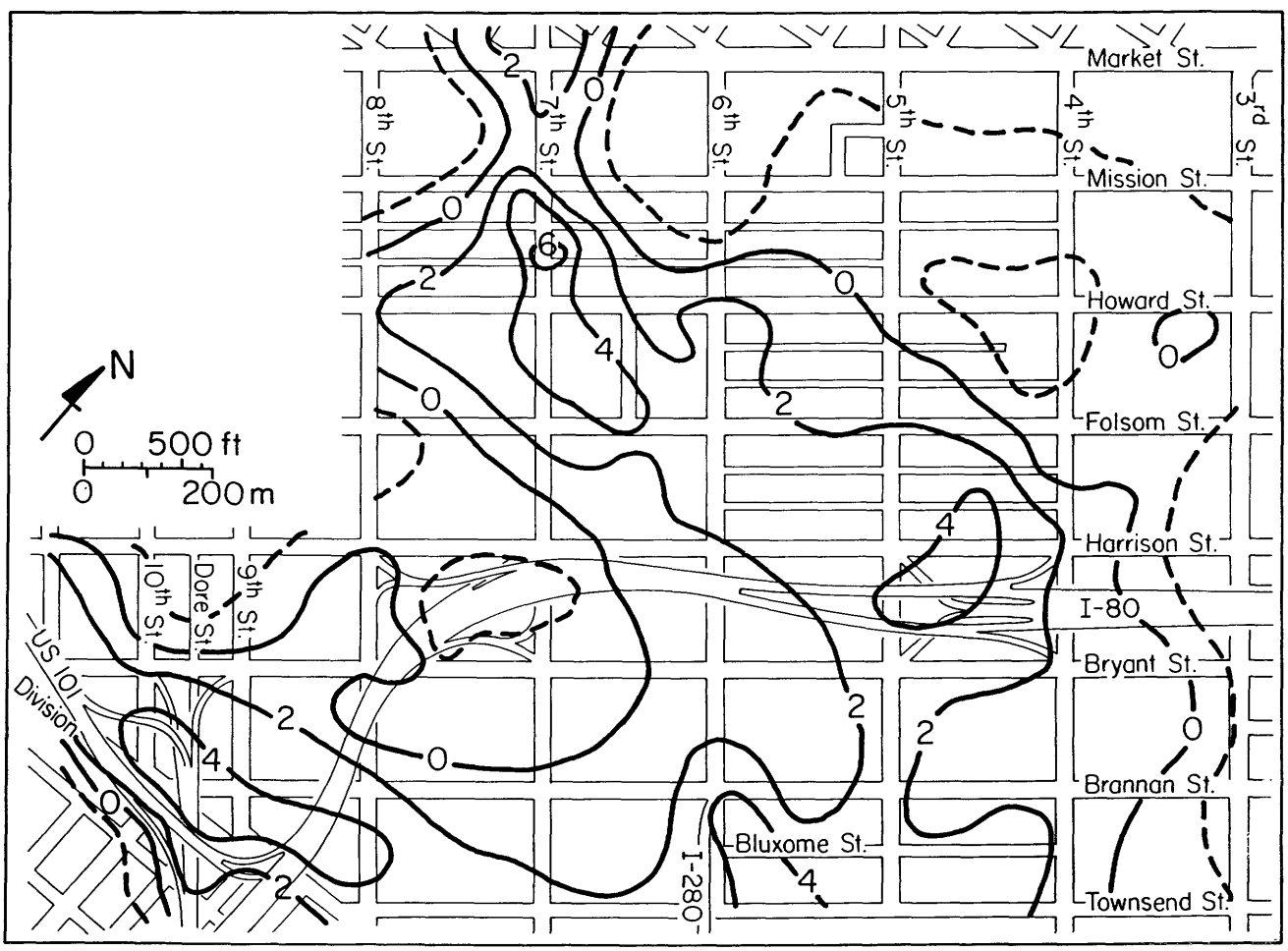


Figure 17.—South of Market study area, showing thickness of submerged fill (solid contours; interval, 2 m). 0-m contour, which indicates where elevation of water table is at base of fill, represents a theoretical boundary between regions where liquefaction can and cannot occur. Upper-bound contour (dashed), which delimits area where ground-water level is within 2 m of base of fill, is proposed as a reasonable limit on maximum extent of potential hazard in case of nonuniform changes in fill thickness or unpredictable variations in ground-water level.

holes in which both water level and fill depth are measured; however, localized areas of both submerged fill and buried dunes may exist that are not identified by the available records.

The ground-water level represents the thickness of nonliquefiable soils overlying liquefiable deposits. In the South of Market area, submerged fills in former Sullivan Marsh and in Lower Mission Creek are overlain by less than 2 m of overlying soil. Near Mission and Howard Streets, the surface layer is 4 to 6 m thick. Isolated areas of loose saturated fill, which may exist in the former dune fields near Market Street, are overlain by 4 to 8 m of unsaturated soils.

## FILL CHARACTERISTICS

Soil types in the South of Market area are classified with respect to liquefaction susceptibility in figure 18.

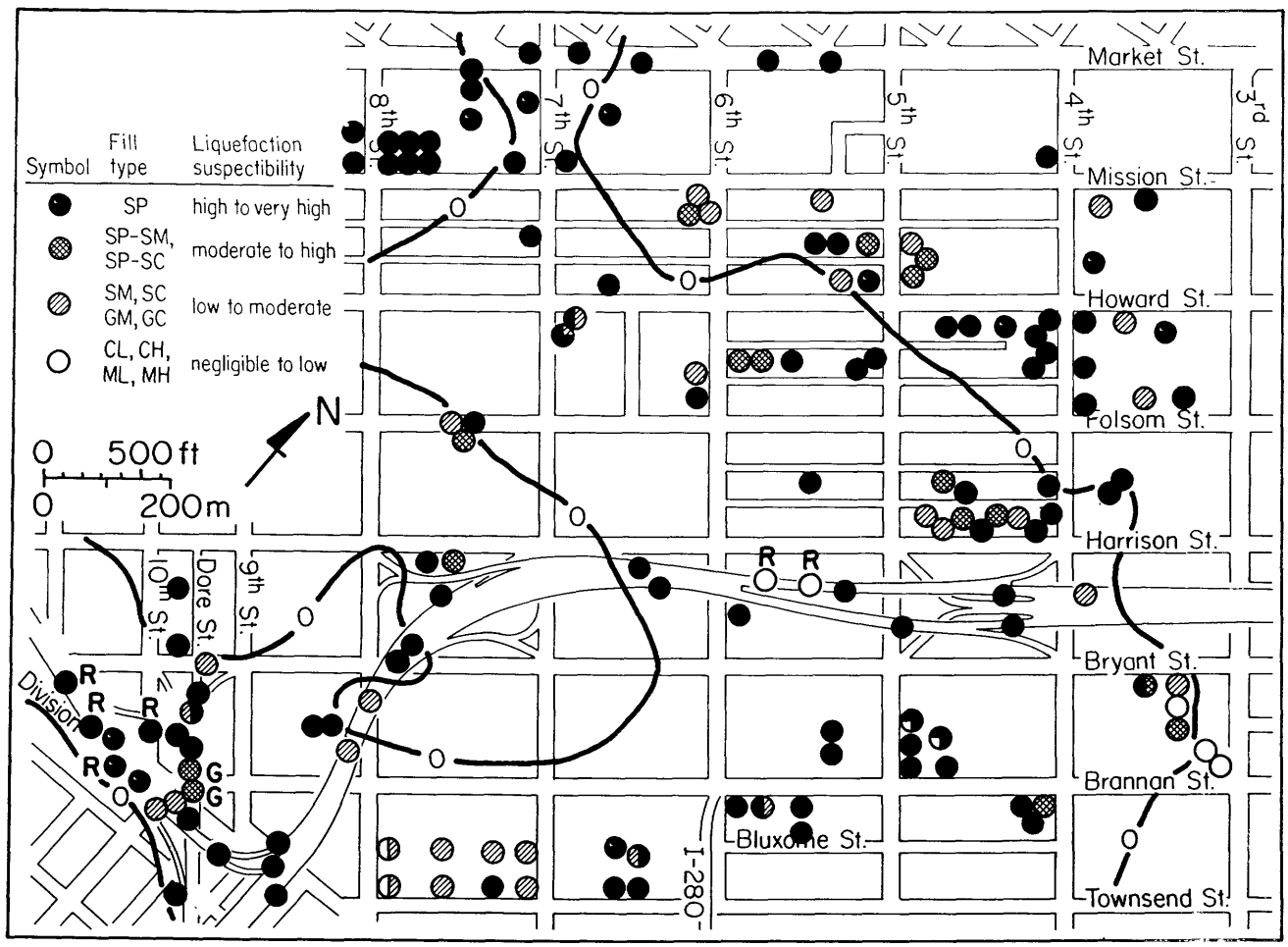


Figure 18.—South of Market study area, showing soil characteristics and liquefaction susceptibility of submerged fill. 0-m contour marks boundary between areas of submerged fill and unsaturated fill, as shown in figure 17. Shaded circles indicate classification of fills based on data from boreholes or cone-penetration-test soundings at each location. Boreholes that penetrated a significant amount of rubble (R) or gravel (G) are so denoted because presence of these materials may influence liquefaction susceptibility. Where submerged fill occurs (within bounded area), shading indicates only soil types below water table; where there is no submerged fill below water table or borehole terminated above water table, shading indicates only soil type closest to base of fill. Soils are identified by symbols in Unified Soil Classification (American Society for Testing and Materials, 1991b): CH, high-plasticity clay; CL, low-plasticity clay; GC, clayey gravel; GM, silty gravel; MH, low-plasticity silt; ML, high-plasticity silt; SC, clayey sand; SM, silty sand; SP, poorly graded sand. Clays and silts consist of materials of which more than 50 weight percent passes a No. 200 sieve. Proportion of circle with a particular shading reflects approximate proportion of corresponding soil type below water table at that location. In general, liquefaction susceptibility of soils containing 20 to 50 weight percent fines is considered to be low, and that of fairly clean soils containing less than 20 weight percent fines to be moderate. This classification is considered valid for San Francisco soils on the basis of the observation that the fines in these soils (particles smaller than 0.075 mm) are typically clay minerals and relatively few soil samples contain much low-plasticity or cohesionless silt. Although soils containing more than 20 weight percent fines have been observed to liquefy during earthquakes, such occurrences have been confined to regions where low-plasticity silts are a common constituent of fines (Cao and Law, 1991).

Poorly graded (well sorted) fine sand without a significant amount of silt or clay was penetrated in about 70 percent of the boreholes through submerged fill. Only two sites show clay fill with a negligible to low liquefaction susceptibility: on Townsend Street between Seventh and Eighth Streets, and between Bryant and Brannan Streets near Third Street. The Third Street site is adjacent to borrow areas on Rincon Hill and Steamboat Point (fig. 16). The site between Seventh and Eighth Streets on the north side of Townsend Street, which formerly was a railroad yard, may be representative of fills typically placed in Mission Bay. Fill containing significant amounts of rubble below the water table was penetrated between Harrison and Bryant Streets, and in former Mission Creek near Division Street. Extensive gravel was also penetrated in the vicinity of Dore Street.

## TOPOGRAPHY

Current surface contours in the South of Market area are mapped in figure 19. Low elevations of the ground surface occur in the areas of made ground over previous marshes, relative to the ground surface over previous sand ridges. Except for the bedrock spur of Potrero Hill (fig. 7), at Franklin Square in the south corner of the study area (fig. 1), the total relief in the study area is 12 m. Contours indicate that the South of Market area has shallow gradients averaging 1 percent from northwest to southeast. A relatively steep gradient of 2.3 percent occurs between Mission and Howard Streets on Seventh Street, and of 3.2 percent between Mission and Howard Streets on Sixth Street. From Third to Fifth Streets, similar gradients occur on the north side of the former marsh, outside

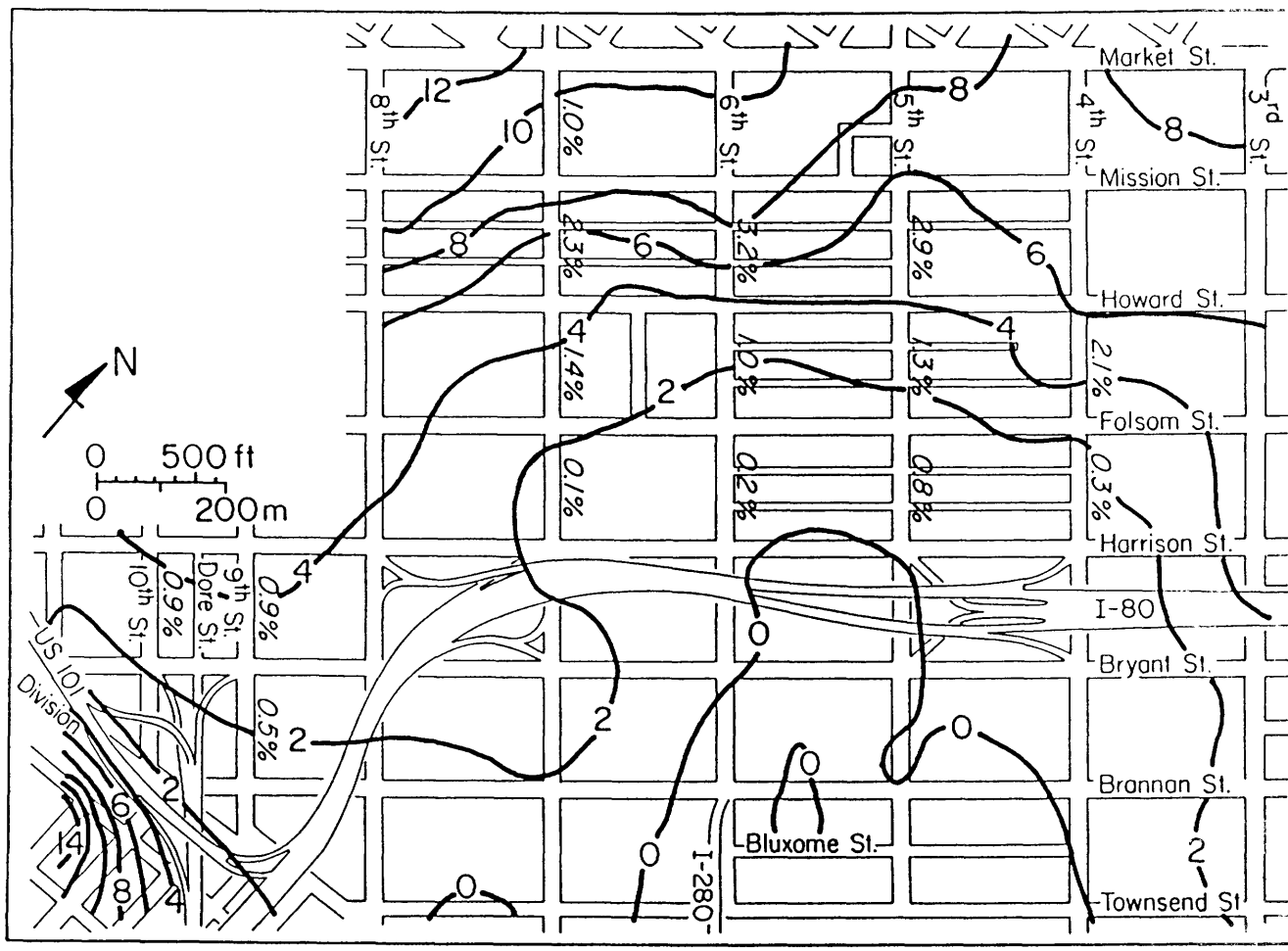


Figure 19.—South of Market study area, showing surface elevation (solid contours; interval, 2 m) and intermediate contour (dashed) relative to San Francisco City Datum. Contours are based on survey data from major street intersections at approximately 190-m spacing collected by San Francisco Department of Public Works between 1985 and 1991. Italic numbers, average street gradient (in percent).

the submerged-fill zone. Between Howard and Folsom Streets, some gradients are approximately 1 percent. Between Folsom and Townsend Streets in the former Sullivan Marsh, surface gradients are negligible. Local gradients may be steeper over parts of a block to obtain the average gradients listed above. For example, on Dore Street, surface gradients are about 0.5 percent between Bryant and Brannan Streets, but closer to 1.0 percent near the north end of the block.

On the basis of a comparison of historical and current topographic maps and an evaluation of photographed earthquake settlement, O'Rourke and others (1992a) concluded that combined subsidence and regrading in the South of Market area after the 1906 San Francisco earthquake did not result in changes of local street elevation of more than 0.3 to 0.5 m. We note that several sites overlie deep clay-filled Wisconsin-age ravines in the South of Market area which have subsided appreciably. Settlement rates of 50 to 70 mm/yr were measured between 1902 and 1904 over these buried features (Lawson, 1908), and 1- to 2-m settlements of post-1906 construction in the same areas were reported by Wahrhaftig (1966). Nevertheless, current regional slopes are believed to be representative of the 1906 gradients because of (1) the narrow width of thick Holocene bay-mud deposits, limited to buried ravines, resulting in highly localized rather than regional settlements; and (2) the agreement of elevations of survey monuments at major street intersections in the 1910's, 1920's, and 1930's within 200 to 300 mm of current elevations of similar survey points. Where major subsidence did occur, regrading was performed on city streets to match the elevations of adjacent areas, thereby maintaining the approximate street gradients.

## LIQUEFACTION IN THE 1906 SAN FRANCISCO EARTHQUAKE

Ground deformations and liquefaction features observed in the South of Market area after the 1906 San Francisco earthquake are mapped in figure 20. Schussler (1906) reported that lateral spreads, offsets, and wavelike deformation were common throughout this area. Lawson (1908) reported settlements ranging from a few millimeters to 900 mm or more throughout former Sullivan Marsh.

Lateral displacement of 1.5 to 2.4 m was observed nearly parallel to Seventh Street between Mission and Howard Streets (Reynolds, 1906). The northernmost extent of ground failure, near the U.S. Post Office at Seventh and Mission Streets, was well documented by contemporary photographs. Maximum eastward displacement of 1.5 m and settlement of 1.5 m were noted at that corner. Submerged fill under this block is as much as 6 m thick, and the gradient of the street is 2.3 percent. Lateral displacement of streets by 0.9 to 1.8 m eastward was typical farther east in Sullivan Marsh. The exact magnitudes and locations of displacements within these blocks typically were not reported and so cannot be related to submerged-fill thickness.

Between Bryant and Brannan, Ninth, and 10th Streets, lateral spreading occurred with as much as 2.4-m displacement. Distinct scarp-bound blocks were associated with lateral spreading on Dore and Ninth Streets, where displacements were distinguished by numerous vertical scarps that gave the appearance of wavelike deformation, with amplitudes of differential settlement as high as 1.8 m.

Ground deformations were less severe southeast of Brannan Street in filled areas of former Mission Bay. Gradients in this area are negligible. Lawson (1908) noted that the differences in fill materials underlying this area may have resulted in less damage.

In several places, both compressional and extensional offsets were superimposed. Kurtz (1906) described a streetcar track at Fourth and Bryant Streets where rails were buckled from 60 to 150 mm of shortening in compression but then translated back to their original position, leaving a 150-mm gap in the joints at the same location. In front of the U.S. Post Office at Seventh and Mission Streets, a 1-m-high compression ridge formed adjacent to settlement of a similar magnitude, parallel to cracks indicating more than 1 m of lateral extension. At Brannan and Ninth Streets, a 0.3-m-high compression ridge marked the edge of the Dore Street subsidence zone, but settlement of 300 mm occurred immediately adjacent to the buckled pavement. The occurrence of compressional features adjacent to zones of permanent extensional displacement is possible only if the compression is related to transient effects, such as would occur during ground oscillation.

Damage to the water-supply and sewer systems in the South of Market area from the 1906 San Francisco earthquake is mapped in figure 21. A total of 79 pipeline breaks (dots, fig. 21) were reported in the South of Market area; of these breaks, 85 percent occurred in areas of submerged fill or immediately adjacent to the zero-fill-thickness contour. Breakage was extensive on pipelines crossing former Sullivan Marsh on Mission and Howard Streets. In contrast, pipeline breaks in former Sullivan Marsh south of Howard Street tended to be concentrated at the margins, rather than in the center, of the zone of lateral spreading. Except on 11th Street, pipeline breaks in Lower Mission Creek also were concentrated along the edges of this zone.

## MISSION AND MARKET STREETS

A remarkable aerial photograph of the area between Market and Howard Streets (fig. 22) clearly shows the

wavelike deformation of streets and sidewalks, buckled curbs, vertical scarps, and numerous sand boils.

On the basis of maps by the U.S. Coast Survey (1853, 1857), the blocks adjacent to Market Street are mapped in figure 23 to show the existence of deep fill where historical surface topography may intersect the current groundwater level. Elevation of the base of fill is determined from analysis of the contours shown in figure 16. Groundwater levels were determined from the data base for the South of Market area and eight locations north of Market Street.

In the South of Market area, figure 23 agrees substantially with figure 17 on the locations of zones of submerged fill in former Sullivan Marsh but also indicates other small, deep fill areas. North of Market Street, the broadest depressions were observed under the Civic Center between Fulton, Golden Gate, Polk, and Market Streets and between Turk, Ellis, Jones, and Market Streets. Excluding former Sullivan Marsh, localized deep fill accounts for about 15 percent of the area mapped in figure 23. From 0 to 1 m of submerged fill was penetrated in boreholes at Leavenworth and McAllister Streets and also 30 m northeast of Van Ness Avenue and Fell Street.

Of the 32 pipeline breaks near Market Street that were located outside former Sullivan Marsh, 16, or 50 percent, occurred in or adjacent to the zones of deep fill (shaded areas, fig. 23). Deep, loose fills may pose a seismic hazard due to consolidation and settlement in response to prolonged shaking. Moreover, subsurface evidence suggests that submerged fills were present at sites near Market Street, and so liquefaction could also have affected ground movement in these areas. These submerged fills are probably no more than 2 m thick and are overlain by 4 to 10 m of unsaturated fill that would have substantially damped and restricted any movement of the liquefiable layer.

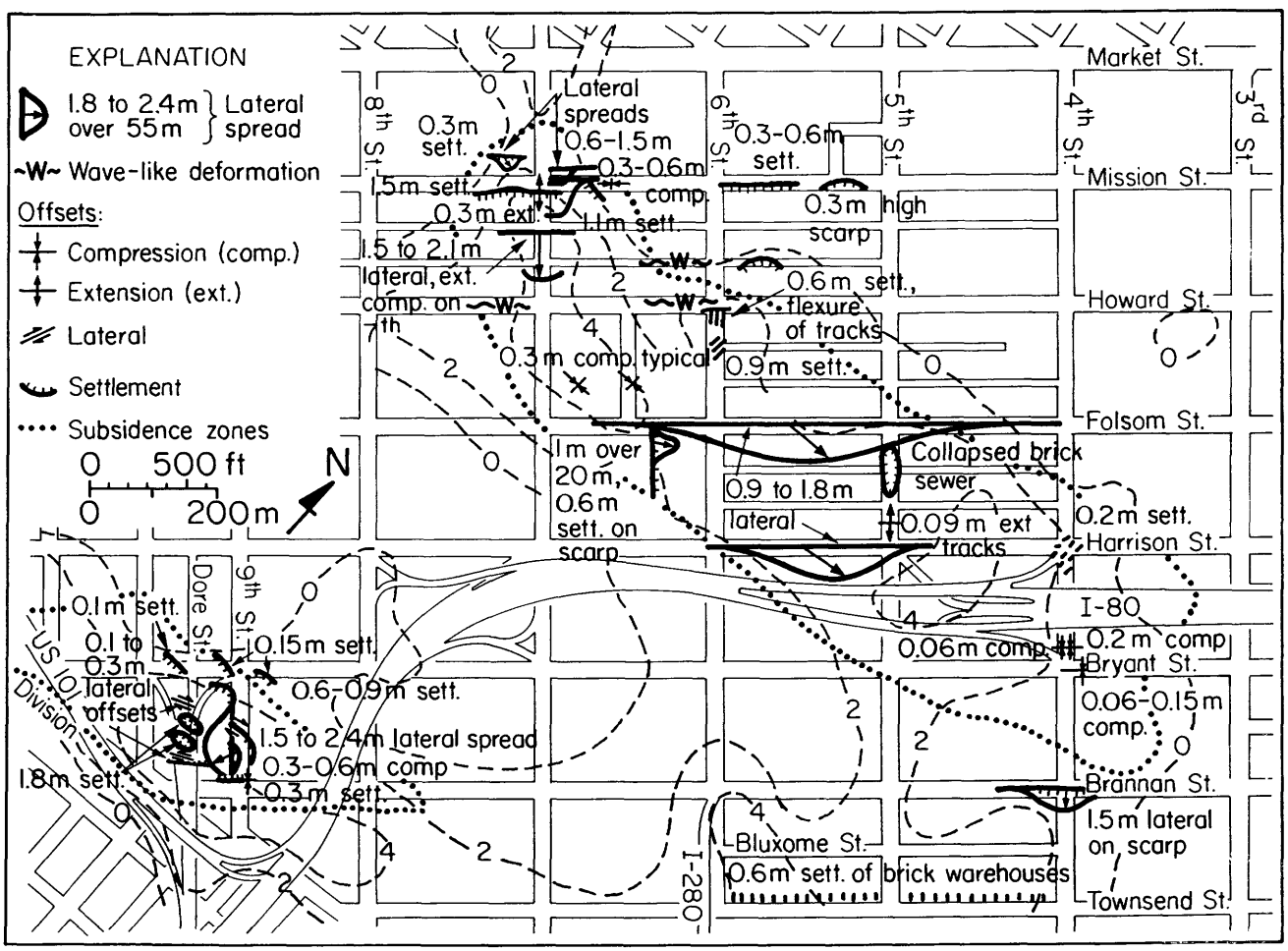


Figure 20.—South of Market study area, showing thickness of submerged fill (dashed contours; interval, 2 m) and locations of lateral spreading, differential settlement, and offsets in 1906 San Francisco earthquake. Hachures, which point toward area of settlement, may indicate either gradual subsidence or an abrupt scarp. Dotted outline denotes major subsidence zones reported by Schussler (1906). From O'Rourke and others (1992a).

## LIQUEFACTION IN THE 1989 LOMA PRIETA EARTHQUAKE

During the 1989 Loma Prieta earthquake, liquefaction resulted in moderate to severe damage associated with sand boils, settlement, pavement damage, strong ground shaking, and pipeline breaks in the South of Market area, as summarized in figure 24. Cracks, 10 to 30 mm wide, and differential settlement were observed down the centerline of Seventh Street between Mission and Folsom Streets. Settlement was noted as far north as the corner of the U.S. Post Office on Mission Street, where large settlements had occurred in 1906. Large differential settlements of 300 to 500 mm were observed adjacent to buildings on Seventh Street just north of Howard Street. Rupture of a 300-mm-diameter water main may have contributed to the damage in this area. Extensional cracks were also observed in Sixth Street between Folsom and Harrison Streets. Multiple compression ridges buckled street pavements and sidewalks along Russ Street approximately 30 to 60 m north of Folsom Street. Beneath the west curb of Sixth Street at Townsend Street, ground settled sharply 400 to 500 mm adjacent to a 2-m-diameter pile-supported concrete sewer.

About 300 mm of localized subsidence and several cracks were observed in a parking lot on Dore Street approximately 30 m northwest of Bryant Street, at the approximate north limit of major lateral spreading in this area in 1906. The sidewalk near the northeast corner of Bryant and Dore Streets was buckled, and a water-service connection was ruptured. Both the buckled pavements and extension cracks paralleled the north boundary of a zone of submerged fill.

Accurate settlements were obtained from elevation surveys by the San Francisco Department of Public Works between 1981 and 1985, and repeated between 1990 and

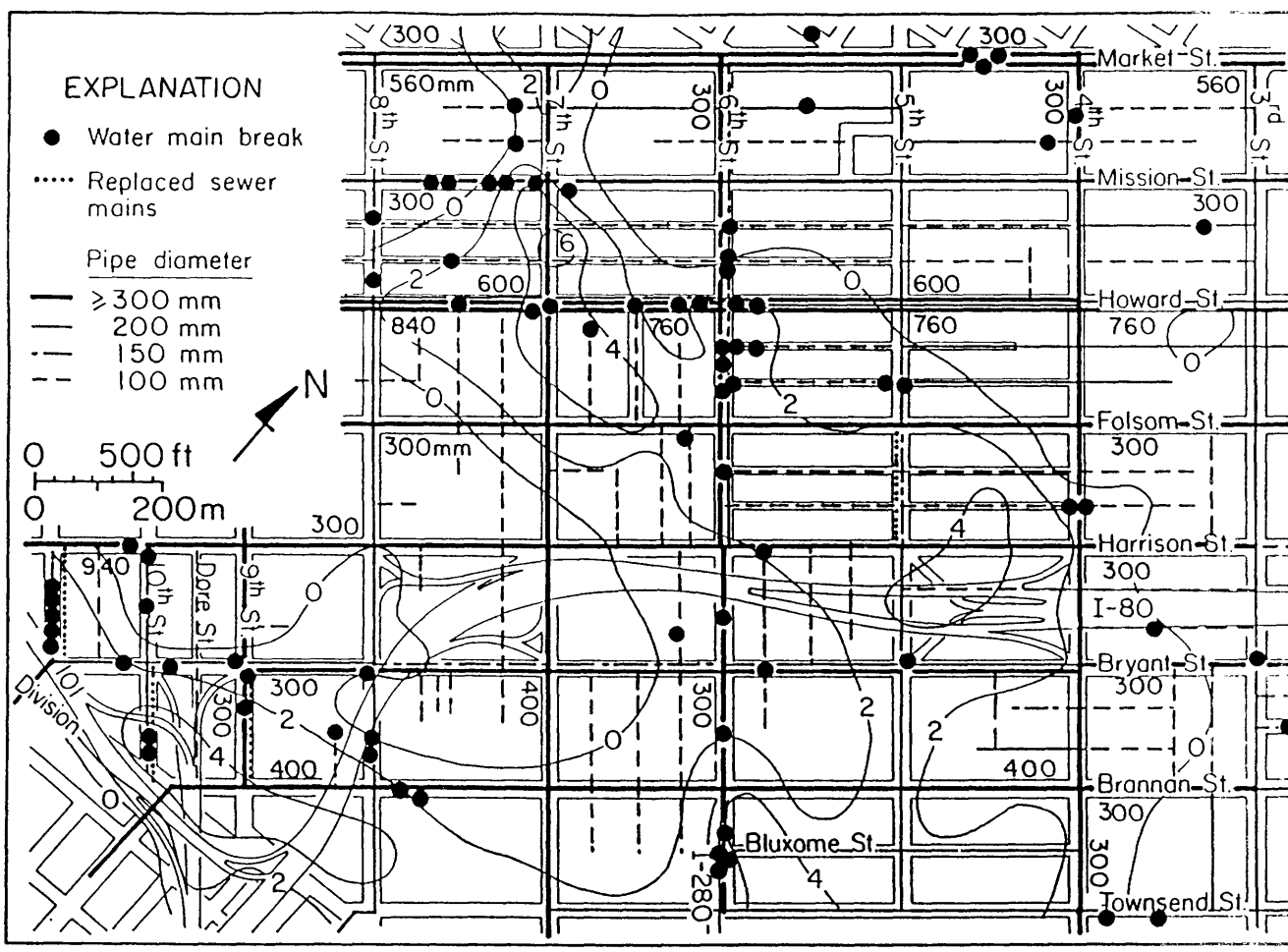


Figure 21.—South of Market area, showing thickness of submerged fill (contour interval, 2 m), diameters of pipes, locations of water-supply pipelines, and broken water mains and replaced sewer mains from 1906 San Francisco earthquake reported as of July 1906. Broken water mains were reported by the Spring Valley Water Co. (Schussler, 1906; Manson, 1908). Multiple breaks may have occurred at marked locations. Locations of replaced sewer mains are based on repairs reported by the City of San Francisco (Schussler, 1906).

1992. Typical survey monuments are provided at major intersections on curbs, sidewalks, sewer catch basins, and fire hydrants. Some settlement is likely to have occurred because of secondary settlement of Holocene bay mud, but no correction for this settlement is made in figure 24. The trend in settlements along these streets corresponds

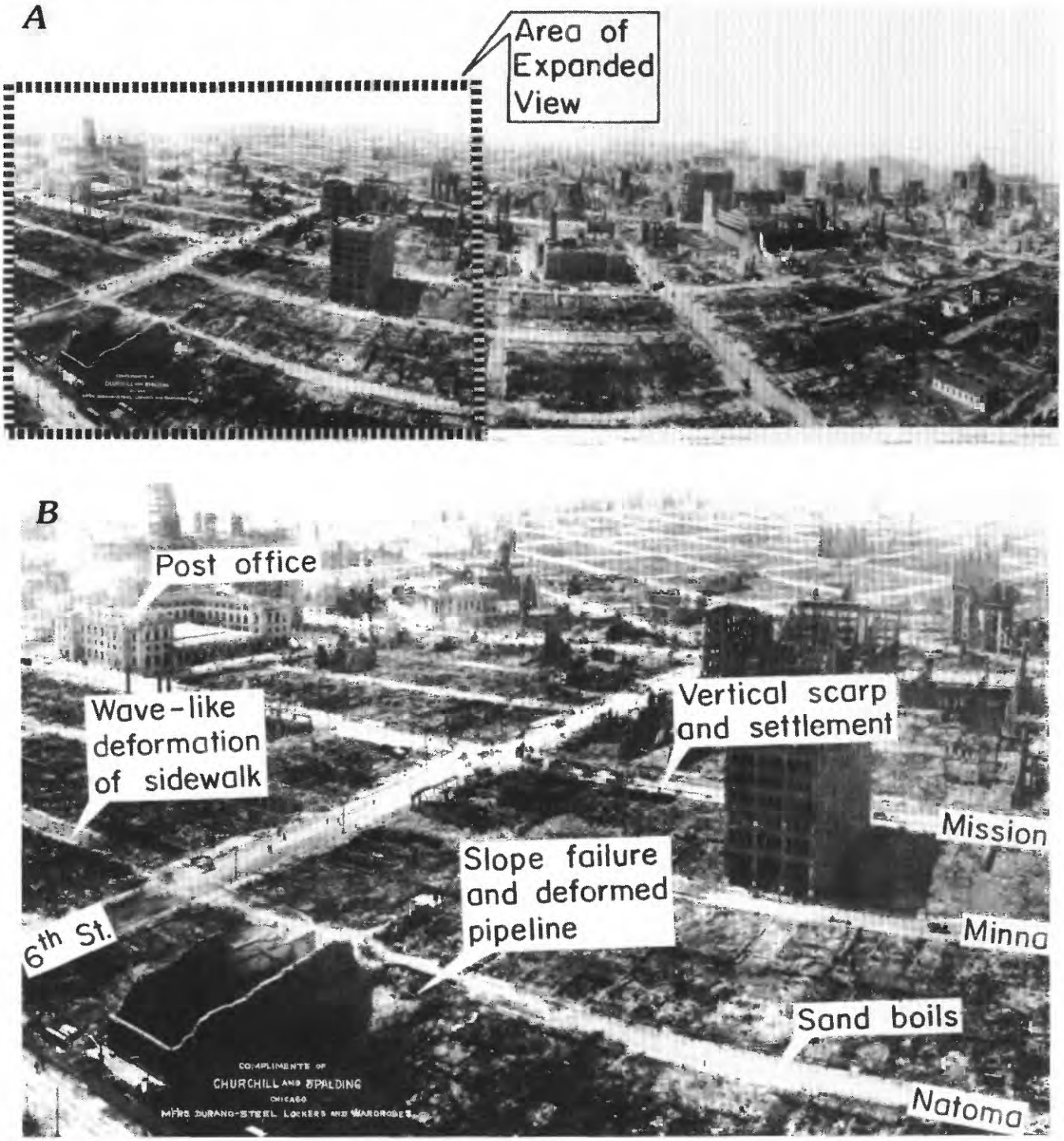


Figure 22.—Part of panorama of San Francisco after 1906 earthquake and fire (*A*), showing liquefaction-induced ground deformations in devastated area bounded approximately by Mission, Fifth, Seventh, and Natoma Streets (*B*). Between Sixth and Seventh Streets, ground deformation falls within zone of submerged fill overlying former marsh. Extension cracks, vertical scarps, and settlement monoclines were photographed on Mission Street. At south corner of Post Office, which was built on isolated grillage footings as deep as 6 m below surface, Lawson (1906) reported 40 to 120 mm of settlement adjacent to an area in which ground settled 600 mm. Ruined dome of City Hall, which was severely damaged and lost much of its facing in earthquake, is visible behind Post Office. Photograph by G.R. Laurence, using a patented system of kites and wires to carry a panoramic camera 250 m above ground (Bronson, 1959); center of view in figure 22*A* is approximately southeastward.

closely to changes in liquefiable thickness. Settlements of more than 80 mm were measured at Seventh and Howard Streets and at Sixth and Townsend Streets, where the submerged fill is more than 4 m thick. Settlements of 10 to 20 mm are seen in areas of 0- to 2-m-thick submerged fill, including Mission Creek on Division Street. No settlement occurred on Seventh Street at Harrison and Bryant Streets, where the fill boundary is higher than the groundwater level.

In the South of Market area, 14 repairs in the Municipal Water Supply System were reported. Except for the break on Sixth Street near Market Street, all of these breaks lie in the submerged-fill zone as outlined from subsurface mapping; the anomalous break near Market Street may be explained by the submerged fill delineated in figure 23.

Including a hydrant break at Sixth and Bluxome Streets that resulted from falling masonry, all four breaks in the Auxiliary Water Supply System in the South of Market area occurred in submerged-fill zones. The most serious damage to this system was due to a broken 300-mm-diameter water main on Seventh Street between Mission and Howard Streets. Flow through this one break helped to empty one of the two reservoirs supplying the Auxiliary Water Supply System in approximately 30 to 40 minutes (O'Rourke and others, 1991).

Liquefaction in the South of Market area recurred in 1989 in the same places as in 1906. Observed damage in 1989 was generally in areas underlain by more than 2 m of submerged fill. In 1989, as in 1906, the most severe damage occurred in the vicinity of Seventh Street between Mission and Howard Streets. Similar centers of pipeline damage were on Sixth Street near Market Street, on Sixth Street near Bluxome Street, at Eighth and Bryant Streets, and at Brannan and Dore Streets, all in areas of deep submerged fill. The close correlation between type and relative severity of damage in both earthquakes suggests that these sites are especially prone to liquefaction and associated damage.

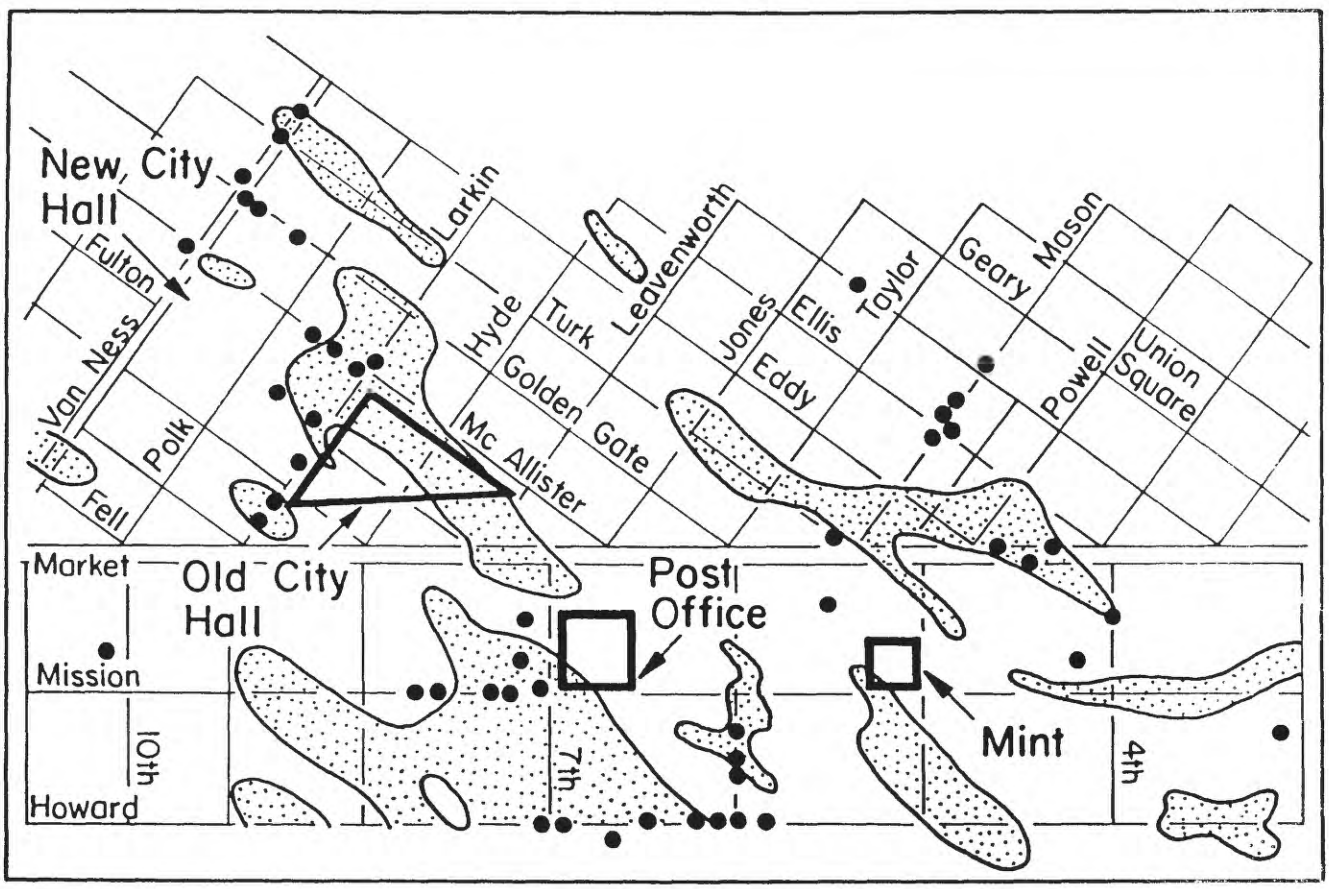


Figure 23.—Vicinity of Market Street between Third and 11th Streets, showing locations of zones of probable submerged fill (stippled areas), based on interpretation of historical topography (U.S. Coast Survey, 1853, 1857), and broken water mains (dots). South half of map overlaps with area of figures 17 through 21, 24, and 27.

# IMPLICATIONS FOR ENGINEERING AND PLANNING

## MAGNITUDE OF LATERAL DISPLACEMENT

Correlations between the magnitude of horizontal surface displacement associated with lateral spreading and various topographic, geologic, and soil factors have been investigated previously (for example, Hamada and others, 1986; Bartlett and Youd, 1992). Hamada and others correlated horizontal movement with several different parameters, including thickness and depth of liquefiable layer, gradient of ground surface, gradient of base of liquefiable layer, and soil factors indicating relative susceptibility to liquefaction. They reported that the best correlation involved the thickness of the liquefiable layer. Subsequent publications by Hamada (1992a, b) have substantiated these initial assessment and have indicated that, for data from the 1964 Niigata and 1983 Nihonkai-Chubu earthquakes, the thickness of the liquefiable layer is the most significant parameter which correlates with magnitude of lateral movement. Hamada (1992a, b) reported that correlations involving surface slope and gradient of the base of the liquefiable layer do not result in a statistically meaningful basis for empirical prediction of lateral displacement.

Bartlett and Youd (1992) studied lateral displacements in various U.S. and Japanese earthquakes; most of their data were from the 1964 Niigata and 1983 Nihonkai-Chubu earthquakes. They performed multiple linear-regression analyses on the assembled data base, using a stepwise procedure, to search for parameters with the highest degree of correlation with magnitude of lateral movement. They identified two general conditions associated with (1) the presence of a free face, such as a wall or embankment slope; and (2) the absence of a free face, which they called a ground-slope condition. They found that lateral

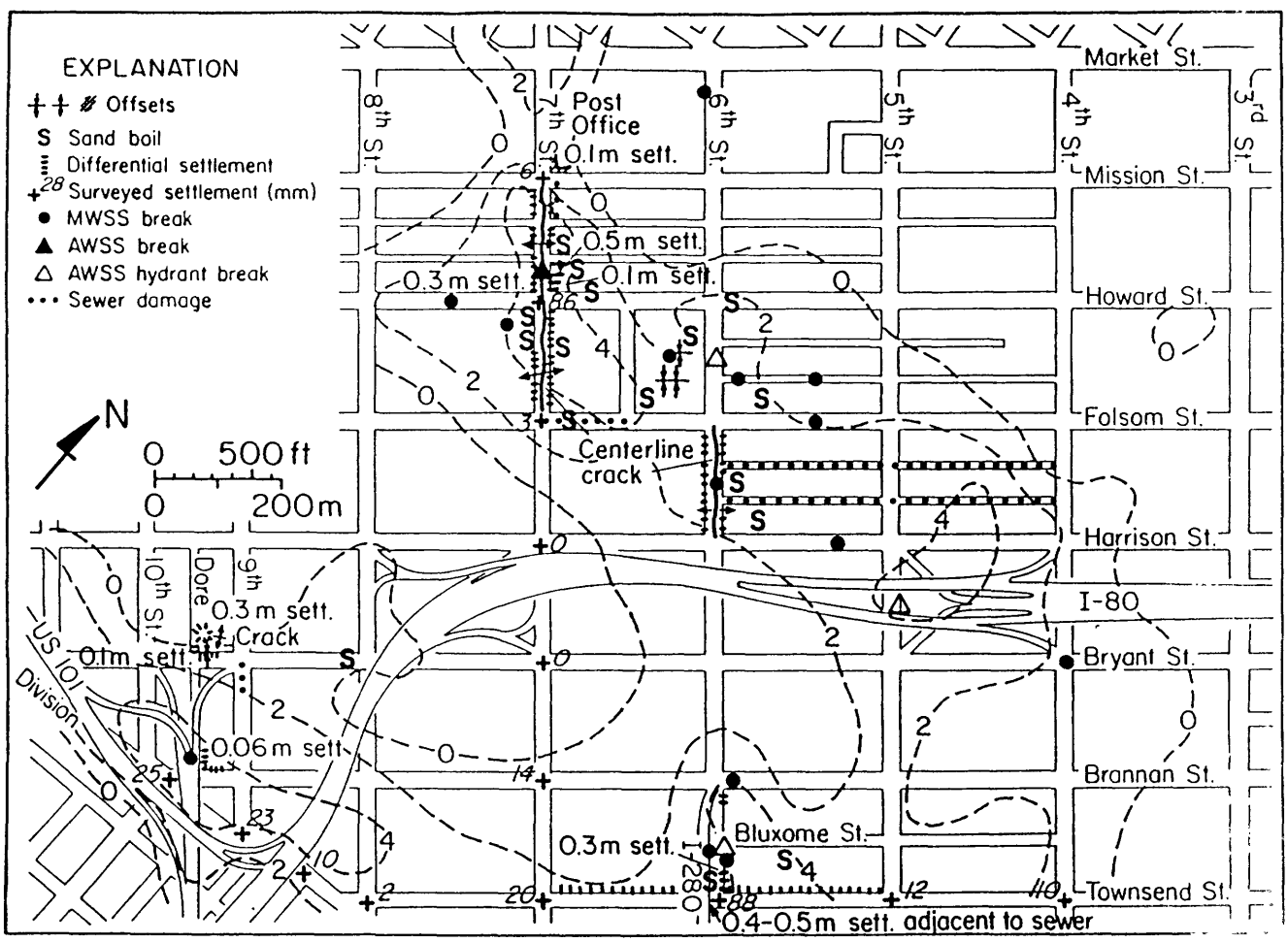


Figure 24.—South of Market area, showing thickness of submerged fill (dashed contours; interval, 2 m) and locations of lateral spreading, differential settlement, offsets, and broken water main (dots) in 1989 Loma Prieta earthquake. Surveyed settlements are differential settlements measured by the City of San Francisco between 1985 and 1991. Locations of sand boils and sewer damage from Harding Lawson Associates, Dames & Moore, Kennedy/Jenks/Chilton, and EQE Engineering (1991). AWSS, Auxiliary Water Supply System; MWSS, Municipal Water Supply System.

movement showed the highest degree of correlation with either distance from a free face or surface gradient for the free face and ground-slope condition, respectively.

The observed lateral movement, surface gradient, estimated slope of the base of submerged fill, submerged-fill thickness, and surface-layer thickness at 15 locations in the two study areas in 1906 are summarized in table 1. Where a range of values is presented in figures 11 and 20, the average maximum displacement is listed. Subsurface parameters were determined at the location of maximum displacement of each lateral spread. Surface gradient and slope of the base of fill are averages evaluated from computerized surfaces over a 60- to 90-m horizontal distance.

As shown in figure 25*A*, a reasonable fit exists for the plot of lateral ground displacement versus submerged-fill thickness. About half the variation in displacement data is explainable by the thickness of liquefiable soils ($r^2$=0.50). Lateral displacement is about 30 percent of the thickness of submerged fill, and most data are bounded by ratios corresponding to 15 to 45 percent of submerged-fill thickness.

Surface gradient as a function of lateral ground displacement is plotted in figure 25*B*. Consistent with observations by the U.S. National Research Council (1985), surface slopes of lateral-spread zones range from 0.5 to 2.5 percent. The best linear fit of the data has $r^2$=0.25, which represents a poor correlation for explaining the variation in observations. Single-variable and multiple linear regressions involving surface-layer thickness did not improve the coefficient of determination achieved by regression with only the thickness of liquefiable fill.

Some of the variations in figure 25*B* could be due to the fact that current street gradients differ from those in 1906, or that local gradients are not reflected in the street grid. We do not believe, however, that these sources of variation have strongly influenced the statistical trends. We noted local deviations, such as the abrupt elevation change at the rear of buildings on South Van Ness Avenue between 17th and 18th Streets.

The data of Hamada (1992a, b) indicate that lateral spreads in Japan average 125 percent of liquefied thickness, about 4 times greater than the displacement at San Francisco sites plotted in figure 25*A*. The models of Bartlett and Youd (1992), who included data from the Mission District and South of Market area in their study, significantly overpredict lateral displacement in 1906 by a factor of 5 to 10.

It is unclear which conditions have contributed to the significantly smaller magnitude of lateral spreading in San Francisco than that observed elsewhere. Most of the sites evaluated by Hamada and others (1986) and Bartlett and Youd (1992) are primarily in alluvium or other natural deposits. In contrast, liquefaction in San Francisco occurred in sandy fills, which may have soil characteristics or geometric features that differ from those of natural deposits. Bartlett and Youd suggested that the three-dimensional geometry of filled channels may have been a factor in reducing displacements. Many liquefiable deposits in the Mission District and South of Market area are only about a block wide, a feature that may have limited displacement due to lateral resistance along the boundaries of filled channels, and that may have resulted in nonuniform and somewhat-discontinuous patterns of both horizontal and vertical movement. In contrast, liquefiable soils at sites in Niigata, Japan (for example, Hamada, 1992a), are more widely distributed because of their alluvial origin, an observation that may explain both more persistent liquefaction features and greater magnitude of deformation. Finally, because case studies involve unique seismic events, characteristics of the 1906 ground mo-

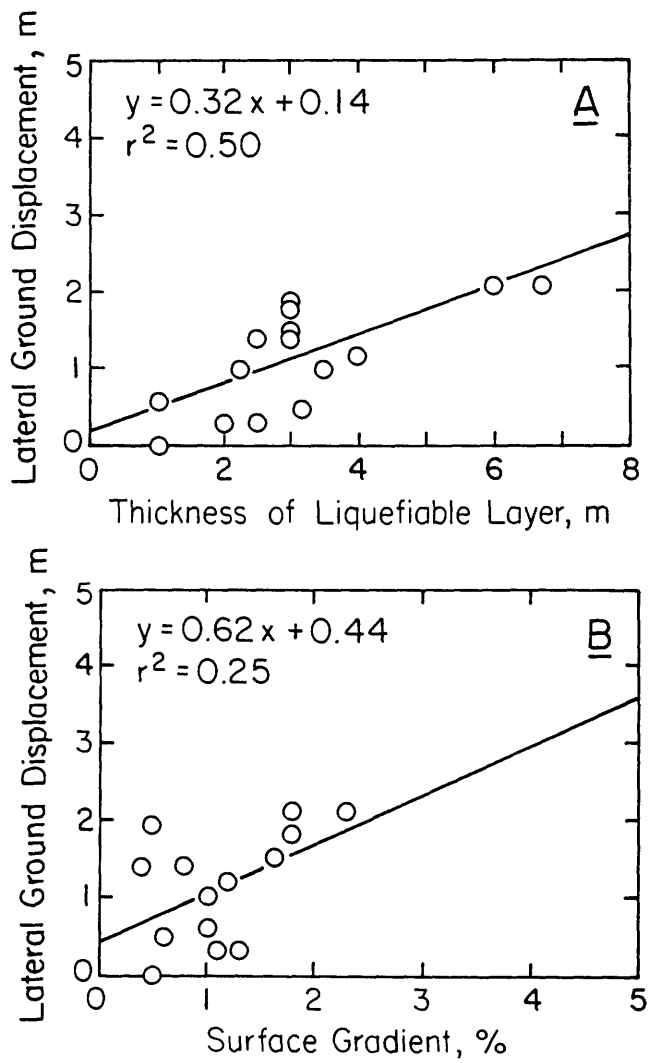


Figure 25.—Linear regressions of thickness of liquefiable layer (*A*) and surface gradient (*B*) versus lateral ground displacement in 1906 San Francisco earthquake.

tions in San Francisco, which are poorly documented, may have affected the site response for lateral spreading in our study.

The uncertainty in each of the mapped ground-water and fill elevations is estimated at ±0.5 m for most of the areas in figures 8 and 17, corresponding to a 95-percent-confidence level. The uncertainty in the submerged-fill thickness, which combines variations in ground-water and fill elevations, is ±0.7 m. Considerable uncertainty exists in estimates of fill thickness at the locations of former dune topography shown in figure 16. As explained previously, the average borehole spacing is equivalent to the widths of previous dunes and depressions, thus contributing to a considerably higher uncertainty in fill thickness at these locations that is difficult to quantify.

The data listed in table 1 are generally more certain than the contours mapped in figures 8 and 17, owing to borehole data that were obtained at many sites of lateral spreading. Submerged-fill and surface-fill data listed in table 1 from the Mission District have an estimated uncertainty of ±0.5 m or less, whereas those from the South of Market area have an estimated uncertainty of ±0.7 m. Surface gradients at most sites are believed to be accurate to within ±1 percent, and the slope of the base of fill, depending on location, at best to within ±1–3 percent.

The water table was evaluated from records obtained under a range of seasonal recharge and discharge conditions. Accordingly, the mapped ground-water levels should be representative of average ground-water conditions. Seasonal fluctuations in ground-water level will be small for sites at low elevation where sea level exerts a strong influence along filled marshes and bays, whereas for slope and upland areas, which correspond to sand dunes, borders of marshes and bays, and the margins of submerged fill, recharge will have a greater effect. Limited evidence suggests that ground-water level can fluctuate by ±1 m at higher elevations in the study areas (Pease and O'Rourke, 1993). The combination of uncertainty and potential for ground-water-level variations provides a rationale for using an upper-bound contour, 2 m above the mapped submerged-fill zones, as the maximum lateral extent of liquefiable ground.

## LIQUEFACTION-SUSCEPTIBILITY MAPS

A remarkably consistent spatial correlation exists between the zones of thickest liquefiable fill and the areas of most severe damage in the 1906 and 1989 earthquakes. Recognizing the close correlation between the thickness of liquefiable fill and the potential severity of such damage, we present liquefaction-susceptibility maps of the Mission District and South of Market area in figures 26*A* and 26*B*, respectively. In each of these figures, the thickness of submerged fill is used as the primary index for identifying potential areas of liquefaction-induced damage. For an event similar in magnitude to the 1906 San Francisco earthquake, the range of maximum lateral displacement that is possible for areas with varying thicknesses of liquefiable fill is keyed to the different patterns. Thus, liquefiable thickness provides a means to predict the magnitude of permanent lateral displacement. Manifestations of other liquefaction features, including subsidence, sand boils, ground deformations, and pavement offsets, also are likely to be found in these areas in proportion to the severity of permanent lateral deformation, and so they are related to liquefiable thickness. For example, the magnitudes of major scarps, ground deformations, and offsets at the edges of zones of deep submerged fill result from the magnitude of relative displacement between the liquefaction zone and adjacent nonliquefiable zones.

The limits of the liquefaction zone in the Mission District shown in figure 26*A* approximately coincide with the delineations of liquefaction zones in previous studies (for example, Youd and Hoose, 1978; O'Rourke and others, 1992a). In contrast, the upper bound of the liquefaction zone in the South of Market area shown in figure 26*B* includes dune depression fills that were not recognized in previous studies and that may increase the extent of the potential hazard.

Damage in the study areas after the 1989 Loma Prieta earthquake was not observed where unsaturated fill above the water table was more than 3 m thick. The thickness of unsaturated fill in the Mission District and South of Market area appears to have influenced liquefaction susceptibility during the 1989 Loma Prieta earthquake.

In the course of our study, we identified other factors that reduce the liquefaction susceptibility in areas of submerged fill. Specifically, any hazard assessment must include consideration of the fines content and plasticity of fill materials. In particular, figure 26 shows that severe liquefaction is unlikely in the vicinity of 19th Street between Folsom and Harrison Streets, despite the presence of submerged fill more than 2 to 4 m thick. Boreholes in this area indicate that the fill has a relatively high fines content, which substantially reduces its liquefaction susceptibility. Similarly, the hazard in other areas may be low because of fill characteristics. Figures 9 and 18 can be used to make preliminary estimates of soil types and their influence on liquefaction susceptibility. We advise caution, however, because liquefiable-sand pockets and seams may occur in the predominantly fine grained fill. Figure 26, supplemented by figures 9 and 18, would best be used to delineate hazards in a general way for planning purposes, whereas site-specific investigations would be needed to provide detailed information for engineering and design decisions.

Table 1.—*Summary of 1906 observations of lateral spreading in the Mission District and South of Market area, with data on the geometry of fills*

[$H_1$, thickness of nonliquefiable surface layer; $H_2$, thickness of liquefiable deposit]

| Location | Lateral movement (m) | Surface slope (pct) | Slope of base of fill (pct) | $H_2$ (m) | $H_1$ (m) |
|---|---|---|---|---|---|
| 19th Street at Mission Playground. | 1.8 | 1.8 | 5.0 | 3.0 | 5.5 |
| Valencia at 18th to 19th Streets. | 2.1 | 1.8 | 1.8 | 6.8 | 3.0 |
| Mission Street at 17th to 18th Streets. | .3 | 1.1 | .5 | 2.0 | 3.5 |
| Capp Street at 17th to 18th Streets. | 1.0 | 1.0 | .8 | 3.5 | 4.3 |
| South Van Ness Avenue at 17th to 18th Streets. | 1.2 | 1.2 | 1.2 | 4.0 | 3.2 |
| 18th Street at South Van Ness Avenue to Shotwell Street. | .3 | 1.3 | 6.0 | 2.5 | 2.5 |
| 18th Street at Shotwell to Folsom Streets. | .5 | .6 | 3.0 | 3.2 | 2.5 |
| Ninth Street at Bryant to Brannan Streets. | 1.9 | .5 | 1.8 | 3.0 | 2.5 |
| Seventh Street at Market to Mission Streets. | .6 | 1.0 | 6.0 | 1.0 | 4.5 |
| Mission and 7th Streets | 1.5 | 1.7 | 6.0 | 3.0 | 4.0 |
| Seventh Street at Mission to Howard Streets. | 2.1 | 2.3 | 6.0 | 6.0 | 3.7 |
| Columbia Street at Folsom Street. | 1.0 | 1.0 | 1.5 | 2.3 | 2.0 |
| Columbia Street at Harrison Street. | .0 | .5 | 1.5 | 1.0 | 2.0 |
| Folsom Street at 5th to 6th Streets. | 1.4 | .8 | 1.8 | 2.5 | 2.0 |
| Harrison Street at 5th to 6th Streets. | 1.4 | .4 | .5 | 3.0 | 1.5 |

## CONCLUDING REMARKS

From 1850 to 1870, urbanization considerably altered the topography of the Mission District and South of Market area by removal of sand ridges and filling of low-lying areas. The use of artificial fill to reclaim Holocene marsh, tidal-flat, and bay areas resulted in thick fill profiles below ground-water levels.

The submerged fills in both study areas are typically 2 to 4 m thick, in some places as much as 8 m thick. Zones of greatest submerged-fill thickness are limited to areas of one or two city blocks. Fills in the Mission District and South of Market area consist primarily of poorly graded dune sand with negligible silt or clay content that are highly susceptible to liquefaction. Submerged fills in Lower Mission Creek in the Mission District consist of a heterogeneous mixture of clay, silt, rubble, and sand layers, in which liquefaction-induced damage may be concentrated where pockets of sand fill are present.

Historical patterns of liquefaction-induced damage are consistent with the thickness of submerged fill: The largest lateral spreads occurred at sites with the thickest submerged fill. Numerous cracks, compression ridges, and offsets of pavements were conspicuous at sites on the

boundaries of submerged-fill zones. Earthquake damage to pipelines was extensive throughout the liquefaction areas, either in zones of deepest submerged fill or along the boundaries of submerged-fill zones where offsets and cracks occurred. The 1906 data in the South of Market area provide evidence of ground oscillation, or severe transient deformation, in addition to permanent displacements associated with subsidence and lateral spreading. The observed damage in 1906 and 1989 in the Mission District and South of Market area provides unmistakable evidence of the recurrence of liquefaction and the potential for liquefaction-induced ground failure in the event of a future major earthquake in the San Francisco Bay region.

Submerged-fill thickness appears to be the most significant factor affecting subsidence and lateral spreading caused by liquefaction. On the basis of the thicknesses of liquefiable fill and of the nonliquefiable surface layer, we have mapped liquefaction susceptibility in the Mission District and South of Market area for an event similar in magnitude to the 1906 San Francisco earthquake, as well as for smaller events. The thickness of liquefiable fill or natural-sand deposits is easily adapted to Geographical Information Systems (GIS) and thus is a useful parameter for assessing urban hazards, microzoning for seismic-hazard reduction, and planning for optimal lifeline performance during an earthquake.

## ACKNOWLEDGMENTS

This research was supported by the U.S. Geological Survey under contracts 14–08–0001–G2128 and 14–34–93–G2332. Data collected and analyses performed under project 922302, sponsored by the National Center for

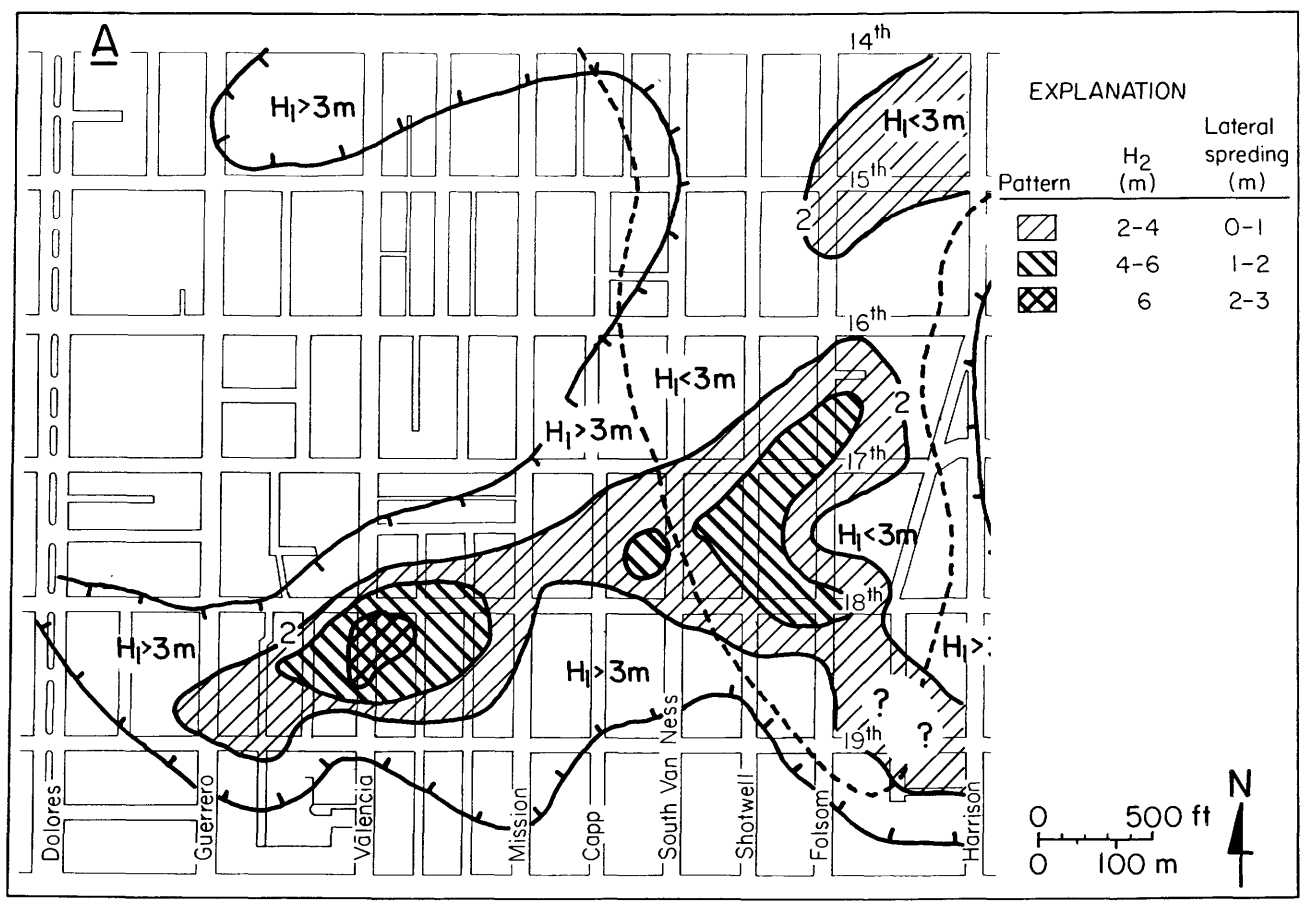


Figure 26.—Liquefaction-susceptibility maps of the Mission District (*A*) and South of Market area (*B*), showing areas of highest potential for damage from lateral spreading, based on submerged-fill thickness. $H_1$, thickness of nonliquefiable surface layer; $H_2$, thickness of liquefiable deposit. Upper-bound contour (dashed), which delimits area where ground-water level is within 2 m of base of fill, is proposed as a reasonable limit on maximum extent of potential hazard in case of nonuniform changes in fill thickness or unpredictable variations in ground-water level. Patterned areas, where $H_2$>2 m, are associated with estimates of expected lateral spreading for an event similar in magnitude to 1906 San Francisco earthquake. Dashed line, contour of $H_1$=3 m; in areas where $H_1$<3 m, liquefaction-induced damage is more likely to be observed during smaller events, such as 1989 Loma Prieta earthquake. In figure 26*A*, fill in area of 19th Street between Folsom and Harrison Streets contains much clay, which reduces its liquefaction susceptibility.

Earthquake Engineering Research, Buffalo, N.Y., also were used in this study. We thank R. Darragh and D.C. Koutsoftas of Dames & Moore, who provided resources, including the use of Dames & Moore's geotechnical laboratory in San Francisco; and H. Taylor, S. Vahdani, and G. Wray of Harding Lawson Associates, who were of major assistance in our site-investigation program. We are grateful to these and numerous other individuals, including C. Ng and J. Grech of the San Francisco Department of Public Works, for their help in assembling geotechnical data for the subsurface data base. We appreciate the help of A. Avcisoy, who drafted the illustrations, and L. McCall, who typed the manuscript.

## REFERENCES CITED

American Society for Testing and Materials, 1991a, Standard method for penetration test and split-barrel sampling of soils (D–1586–84), *in* Annual book of standards: Philadelphia, v. 4.08, p. 232–239.

———1991b, Standard test method for classification of soils for engineering purposes (D–2487–90), *in* Annual book of standards: Philadelphia, v. 4.08, p. 309–319.

———1991c, Standard test method for deep, quasi-static, cone and friction cone penetration tests of soil (D–3441–86) *in* Annual book of standards: Philadelphia, v. 4.08, p. 439–444.

Bartlett, S.F., and Youd, T.L., 1992, Empirical prediction of lateral spread displacement, *in* Japan-U.S. Workshop on Earthquake Resistant Design of Lifeline Facilities and Countermeasures for Soil Liquefaction, 4th, Honolulu, 1992, Proceedings: Buffalo, N.Y., National Center for Earthquake Engineering Research Technical Report NCEER–92–0019, v. 1, p. 351–365.

Bronson, William, 1959, The earth shook, the sky burned: Garden City, N.Y., Doubleday, 192 p.

Brown, A.A., Forbes, Hyde, Nishkian, L.H., Owens, M.J., and White, F.G., 1932, Subsidence and the foundation problem in San Francisco: San Francisco, American Society of Civil Engineers, San Francisco Section, 32 p.

Cao, Y.L., and Law, K.T., 1991, Energy approach for liquefaction of sandy and clayey silts: International Conference on Recent Advances in Geotechnical Earthquake Engineering and Soil Dynamics, 2d, St. Louis, Mo., 1991, Proceedings, v. 1, p. 491–497.

Derleth, C.J., 1906, Some effects of the San Francisco earthquake on waterworks, streets, sewers, car tracks, and buildings: Engineering News, v. 55, no. 20, p. 548–554.

Gilbert, G.K., Humphrey, R.L., Sewell, J.S., and Soule, Frank, 1907, The San Francisco earthquake and fire of April 18, 1906, and their effects on structures and structural materials: U.S. Geological Survey Bulletin 324, 170 p.

Hamada, Masanori, 1992a, Large ground deformations and their effects on lifelines, 1964 Niigata earthquake: Buffalo, N.Y., National Center for Earthquake Engineering Research Technical Report NCEER–92–0001, p. 3–1 to 3–123.

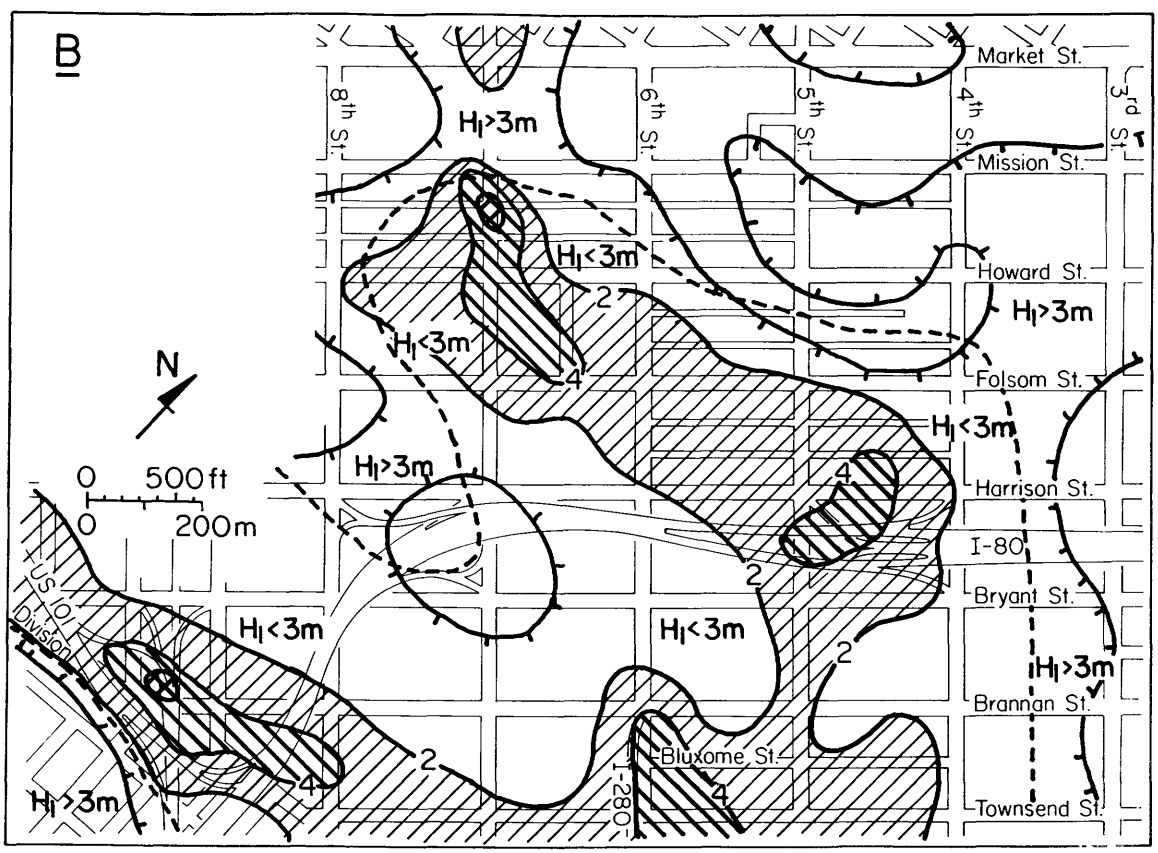


Figure 26.—Continued.

———1992b, Large ground deformations and their effects on lifelines, 1983 Nihonkai-Chubu earthquake: Buffalo, N.Y., National Center for Earthquake Engineering Research Technical Report NCEER–92–0001, p. 4–1 to 4–85.

Hamada, Masanori, Yasuda, Susumu, Isoyama, Ryuji, Emoto, Katsutushi, 1986, Study on liquefaction-induced ground displacements: Tokyo, Association for the Development of Earthquake Prediction, 87 p.

Hansen, Gladys, and Condon, Emmet, 1989, Denial of disaster; the untold story and photographs of the San Francisco earthquake and fire of 1906: San Francisco, Cameron and Co., 160 p.

Harding Lawson Associates, Dames & Moore, Kennedy/Jenks/Chilton, and EQE Engineering, 1991, Liquefaction study: Mission District and Sullivan Marsh area, San Francisco, California: report prepared for City and County of San Francisco, 144 p.

Himmelwright, A.L.A., 1906, The San Francisco earthquake and fire; a brief history of the disaster: New York, Roebling Construction Co., 125 p.

Hittel, J.S., 1878, A history of San Francisco and incidentally of the State of California: San Francisco, A.L. Bancroft, 498 p.

Humphreys, W.P., 1876, Atlas of the City and County of San Francisco: San Francisco, 6 sheets.

Ishihara, Kenji, 1985, Stability of natural soil deposits during earthquakes: International Conference on Soil Mechanics and Foundation Engineering, 11th, San Francisco, 1985, Proceedings, v. 1, p. 321–376.

Kurtz, C.M., 1906, The effect of the earthquake on street car tracks in San Francisco: Engineering News, v. 55, no. 20, p. 554.

Lawson, A.C., chairman, 1908, The California earthquake of April 18, 1906; report of the State Earthquake Investigation Commission: Carnegie Institution of Washington Publication 87, 2 v.

Manson, Marsden, 1908, Reports on an auxiliary water supply system for fire protection for San Francisco, California: San Francisco Board of Public Works, 173 p.

O'Rourke, T.D., ed., 1992, The Loma Prieta, California, earthquake of October 17, 1989—Marina District: U.S. Geological Survey Professional Paper 1551–F, p. F1–F215.

O'Rourke, T.D., Beaujon, P.A., and Scawthorn, C.R., 1992a, Large ground deformations and their effects on lifeline facilities; 1906 San Francisco earthquake: Buffalo, N.Y., National Center for Earthquake Engineering Research Technical Report NCEER–92–0002, 175 p.

O'Rourke, T.D., Gowdy, T.E., Stewart, H.E., and Pease, J.W., 1991, Lifeline and geotechnical aspects of the 1989 Loma Prieta earthquake: International Conference on Recent Advances in Geotechnical Earthquake Engineering and Soil Dynamics, 2d, St. Louis, Mo., 1991, Proceedings, v. 2, p. 1601–1612.

O'Rourke, T.D., Meyersohn, W.D., Stewart, H.E., Pease, J.W., and Miyajima, M., 1992b, Site response and soil liquefaction in San Francisco during the Loma Prieta earthquake, *in* Japan-U.S. Workshop on Earthquake Resistant Design of Lifeline Facilities and Countermeasures for Soil Liquefaction, 4th, Honolulu, 1992, Proceedings: Buffalo, N.Y., National Center for Earthquake Engineering Research Technical Report NCEER–92–0019, v. 1, p. 53–70.

O'Rourke, T.D., and Pease, J.W., 1992, Large ground deformations and their effects on lifeline facilities; 1989 Loma Prieta earthquake: Buffalo, N.Y., National Center for Earthquake Engineering Research Technical Report NCEER–92–0002, p. 5–1 to 5–85.

Pease, J.W., and O'Rourke, T.D., 1993, Liquefaction hazards of the Mission District and South of Market area, San Francisco, California: Ithaca, N.Y., Cornell University, 194 p.

Pease, J.W., O'Rourke, T.D., and Stewart, H.E., 1992, Post-liquefaction consolidation and lifeline damage in the Marina District after the 1989 Loma Prieta earthquake, *in* Japan-U.S. Workshop on Earthquake Resistant Design of Lifeline Facilities and Countermeasures for Soil Liquefaction, 4th, Honolulu, 1992, Proceedings: Buffalo, N.Y., National Center for Earthquake Engineering Research Technical Report NCEER–92–0019, v. 1, p. 395–412.

Reynolds, L.E., 1906, How electricity was served to consumers and street car lines by the San Francisco Gas and Electric Co. after the fire: Pacific Coast Gas Association Annual Meeting, 14th, San Francisco, 1906, Proceedings, p. 365–373.

Ripley, B.D., 1987, Spatial statistics: New York, John Wiley and Sons, 252 p.

Roth, R.A., and Kavazanjian, E.J., 1984, Liquefaction susceptibility mapping for San Francisco, California: Association of Engineering Geologists Bulletin, v. 21, no. 4, p. 459–478.

Sanborn Ferris Map Co., 1899 [1905], Insurance maps, San Francisco, California: New York, v. 1–4.

Scawthorn, C.R., Porter, K.A., and Blackburn, F.T., 1992, Performance of emergency-response services after the earthquake *in* O'Rourke, T.D., ed., The Loma Prieta, California, earthquake of October 17, 1989—Marina District: U.S. Geological Survey Professional Paper 1551–F, p. F195–F215.

Schussler, Hermann, 1906, The water supply of San Francisco, California, before, during and after the earthquake of April 18th, 1906, and the subsequent conflagration: New York, Martin B. Brown, 103 p.

Seed, R.B., Dickenson, S.E., and Riemer, M.F., 1991, Liquefaction of soils in the 1989 Loma Prieta earthquake: International Conference on Recent Advances in Geotechnical Earthquake Engineering and Soil Dynamics, 2d, St. Louis, Mo., 1991, Proceedings, v. 2, p. 1575–1586.

U.S. Coast Survey, 1853, City of San Francisco and its vicinity, California: Washington, D.C., scale 1:10,000.

———1857, City of San Francisco and its vicinity, California: Washington, D.C., scale 1:10,000.

U.S. National Research Council, 1985, Liquefaction of soils during earthquakes: Washington, D.C., National Academy Press, 240 p.

Wahrhaftig, Clyde, 1966, A walker's guide to the geology of San Francisco: Mineral Information Service, v. 19, no. 11, p. S.1–S.29.

Youd, T.L., and Hoose, S.N., 1978, Historic ground failures in northern California triggered by earthquakes: U.S. Geological Survey Professional Paper 993, 177 p.

STRONG GROUND MOTION AND GROUND FAILURE

# SOIL LIQUEFACTION IN THE EAST BAY DURING THE EARTHQUAKE

By Robert E. Kayen, U.S. Geological Survey;
James K. Mitchell, Virginia Polytechnic Institute and State University;
Raymond B. Seed, University of California, Berkeley; and
Shin'ya Nishio, Shimizu Corp.

## CONTENTS



ABSTRACT

Uncompacted artificial-fill deposits on the east side of San Francisco Bay underwent moderate to severe levels of soil liquefaction during the 1989 Loma Prieta earthquake. Typical of all these sites, which represent occurrences of liquefaction-induced damage farthest from the rupture zone, are low cone-penetration-test (CPT) and standard-penetration-test (SPT) resistances in zones of cohesionless silty and sandy hydraulic fill. Along the east-bay shoreline, these fill deposits overlie soft cohesive Holocene sediment, and more deeply buried Pleistocene estuarine sediment and alluvium, that strongly amplified local bedrock motions. The most noteworthy damage occurred at the Port of Richmond, San Francisco-Oakland Bay Bridge Toll Plaza, Port of Oakland, Alameda Naval Air Station, Bay Farm Island, and Oakland International Airport. Postearthquake investigations at five study sites using SPT's and seismic CPT's provide a basis for evaluation of the cyclic-stress-ratio- and Arias intensity-based methodologies for assessment of liquefaction susceptibility.

We found that for both SPT and CPT field data, these methods performed well at identifying liquefiable layers.

## INTRODUCTION

The 1989 Loma Prieta earthquake ($M_S$=7.1) occurred when a segment of the San Andreas fault northeast of Santa Cruz, Calif., ruptured over a length of approximately 45 km (Borcherdt, 1994; Spudich, 1996). The epicenter was located at lat 37.037° N., long 121.883° W. The earthquake hypocenter, which was located at 18-km depth, during the next 8 to 10 s ruptured bilaterally for approximately 20 km northward and 20 km southward. The rupture propagated toward the Earth's surface, up to a depth of approximately 5 to 7 km. This paper describes soil liquefaction, ground deformations, and associated liquefaction damages in artificial-fill deposits on the east-bay shoreline from Oakland International Airport to the Port of Richmond in response to the earthquake, and presents the results of our postearthquake studies at five study sites near the east-bay shoreline: (1) the Port of Richmond, (2) the San Francisco-Oakland Bay Bridge Toll Plaza, (3) the Port of Oakland's Marine Container Terminal at Seventh Street, (4) Bay Farm Island and Harbor Bay Plaza, and (5) Oakland International Airport (fig. 1).

Peak horizontal accelerations at sites underlain by rock and stiff alluvium in the east bay generally ranged from 0.08 to 0.12 *g*, but amplification due to the presence of soft, deep cohesive-soil deposits underlying artificial fills produced peak accelerations from 0.11 to 0.29 *g* at strong-motion-recording stations located on these fills. Peak accelerations near most of our study sites (see fig. 1) can be estimated from strong-motion records obtained near the east-bay shoreline. On the basis of available strong-motion data (Shakal and others, 1989; Kayen and others, 1992), the peak horizontal accelerations on bayshore fills in the vicinity of Oakland International Airport and Bay Farm Island were apparently about 0.27 *g*, and at the San Francisco-Oakland Bay Bridge Toll Plaza and the Port of Oakland's Marine Container Terminal at Seventh Street probably about 0.28 to 0.29 *g*. Arias intensities, integrated from the strong-motion records, ranged from 0.8 m/s at

Oakland International Airport, Bay Farm Island, and Alameda Naval Air Station to 1.71 m/s at the Port of Oakland's Marine Container Terminal at Seventh Street and the San Francisco-Oakland Bay Bridge Toll Plaza.

At the Port of Richmond, the most northerly study site, no nearby strong-motion recordings were obtained for sites with similar soil conditions. Approximately 2 km to the north, however, a peak horizontal acceleration of 0.13 *g* on the south component was recorded at Richmond's City Hall. We used this record, from California Division of Mines and Geology's California Strong Motion Instrumentation Program (CSMIP) strong-motion-recording

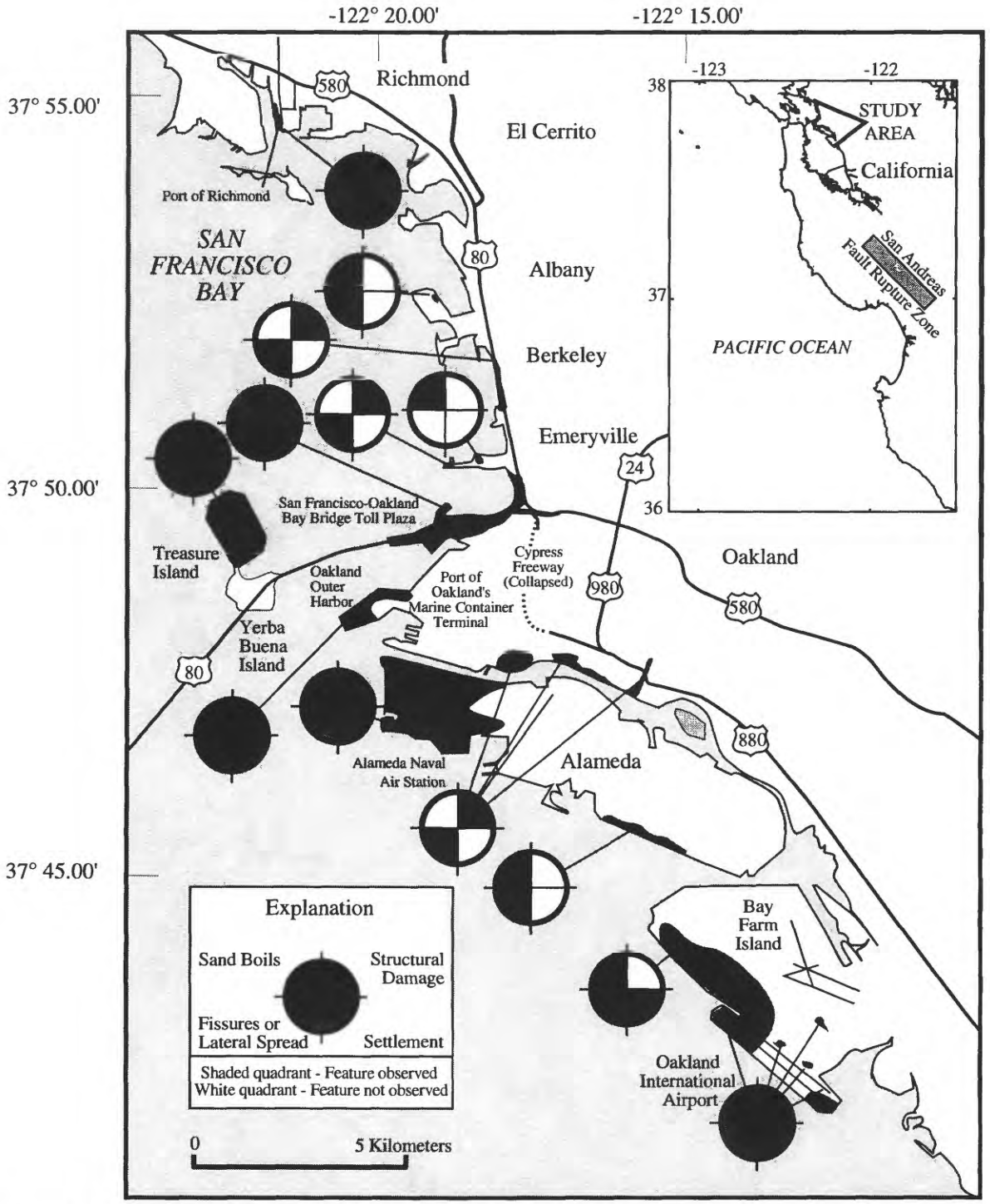


Figure 1.—San Francisco east-bay shoreline, showing locations of sites where liquefaction-induced damage occurred from 1989 Loma Prieta earthquake and of study sites where soil investigations were performed.

station 58505, to model the site response at the Port of Richmond study site, where soft, deep cohesive-soil deposits underlie artificial fill, by means of one-dimensional equivalent-linear seismic site-response analyses, using the computer program *SHAKE90* (a modified version of the computer program *SHAKE*; Schnabel and others, 1972). These results indicate that peak horizontal accelerations at the Port of Richmond were probably about 0.18 *g*. Synthetic seismograms from the *SHAKE90* analysis were integrated, and we estimate the Arias intensity at the Port of Richmond site to be approximately 0.6 to 0.7 m/s.

## INPLACE TESTING METHODS

Standard penetration tests (SPT) were performed in shallow 10-cm (4 in.)-diameter uncased rotary-wash boreholes drilled with CME model 450 and 750 drill rigs, following the guidelines of the American Society for Testing and Materials (1984). SPT-energy calibrations, using the stress-wave method (Farrar, 1991), were made on a CME model 450 drill rig to adjust the field-measured standard penetration resistance, $N$, to a normalized 60-percent-hammer-efficiency blowcount, $(N_1)_{60}$.

The electronic cone-penetration tests (CPT's) followed the procedures of the American Society for Testing and Materials (1986a). Liquefaction analyses were made by using the methods of Robertson and Campanella (1985), Robertson (1986, 1990), Shibata and Teparaksa (1988), and Mitchell and Tseng (1990). The cone apparatus used has a standard cross-sectional area of 10 $cm^2$ and a standard 60° apex tip. A pore-pressure transducer and a porous stone were mounted directly behind the cone, followed by a standard 150-$cm^2$-area friction sleeve. Mounted above the sleeve is a single-component accelerometer that was used to measure the velocities of shear waves ($V_s$) propagating vertically from the ground surface down to the cone tip. Shear-wave measurements were made by using the seismic-CPT method of Robertson and others (1986).

The friction ratio, FR, is calculated as the measured sleeve friction, $f_s$, normalized by the overburden-stress-corrected tip resistance, $(q_c\text{-}\sigma'_{vo})$ (Wroth, 1984),

$$FR = \frac{fs}{q_c - \sigma_{vo}} \times 100; \quad (1)$$

and the pore-pressure ratio, $B_q$, is calculated as the measured deviation of pore pressure from hydrostatic normalized by the overburden-stress-corrected cone-tip resistance (Wroth, 1984),

$$B_q = \frac{u - u_o}{q_c - \sigma_{vo}}, \quad (2)$$

where $q_c$ is the cone penetration tip resistance, $\sigma_{vo}$ is the total overburden stress, $u$ is the measured pore-water pressure, and $u_o$ is the hydrostatic pressure at the same depth.

## PORT OF RICHMOND

Soil liquefaction occurred at a study site in the western part of Richmond Inner Harbor, as shown in figure 2. The area that liquefied is a zone approximately 75 m wide and 300 m long at the foot of Harbor Way Road (10th Street). Approximately 85 km north of the Loma Prieta rupture zone, this site represents the most distant point from the zone of energy release to undergo soil liquefaction sufficient to damage structures. Much of the land at the edges of the Richmond Inner Harbor had been created by placement of uncompacted sandy hydraulic fill. The liquefaction zone overlies deposits of soft bay mud, which are underlain, in turn, by deeper deposits of stiffer, overconsolidated noncohesive and cohesive soils that naturally fill a deep fluvial channel at the west end of the harbor. Thus, the deposits at this site are thicker than those of the Richmond Inner Harbor to the east, and these thicker deposits amplified the level of ground motion at this site and so contributed to the observed soil liquefaction (Seed and others, 1990). The study site runs along the west wall of the former Ford Motor Co. Plant (now closed) and westward across an undeveloped field. Four large and a dozen smaller sand boils vented fine sand and silty sand from the underlying fill (fig. 3). In addition, minor settlements of approximately 2 to 8 cm and lateral spreading of similar magnitude occurred at the edge of the harbor adjacent to a small pile-supported dock at the Tweed Towing/Maas Boats facility. Ground settlement and minor lateral spreading, both of as much as 8 to 10 cm, were observed at the dock of Tweed Towing. The abandoned warehouse adjacent to the study site, an unreinforced-masonry structure, was considerably damaged during the earthquake. The absence of damage to several other similar masonry structures in the Richmond Inner Harbor area may indicate that the Ford Plant area sustained unusually high localized levels of ground shaking, owing to the underlying alluvial-channel deposits.

Near the end of the main shock, Liela Tweed, proprietor of Tweed Towing, exited the structure adjacent to the dock and observed, first, the collapse of the south wall of the Ford Motor Co. Plant and the shattering of windows along the west wall, and then the active issuing of water and sand from the ground in the places shown in figure 4. She noted that active seepage from these sand boils continued for as long as 24 hours. SPT and CPT data from the site indicate that a surficial deposit of tan-brown silty clay, 1.8 to 4.1 m thick, that overlies the liquefiable sandy hydraulic fill at this site probably served as a drainage barrier preventing more rapid venting of excess pore pressures.

## PENETRATION TEST LOGS

The locations of three boreholes (POR–2 through POR–4) drilled in the open space north of the Tweed Towing building are shown in figure 2. The first borehole, POR–1, was abandoned after a computer malfunction. SPT's were performed in shallow boreholes adjacent to each CPT. The logs of the boreholes drilled at the Port of Richmond study site (figs. 2) are similar and are characterized in the upper part of the section by an oxidized, tan-brown crusted silty sand to 0.8-m depth; oxidized tan-brown silty sand to 1.8-m depth; and oxidized, tan-brown sandy clay to reduced sandy clay to 4.1-m depth (fig. 4). The water table was approximately at a depth of 2.5-m during sampling. This section has low $q_c$ values (approx 1–3 MPa), FR values greater than 3 percent, minor pore-pressure generation, and $N$ values ranging from 1 to 6 blows/ft.

Below this section, at 4.1- to 7.8-m depth, is a hydraulic-fill layer of olive-gray fine-silty sand containing shell fragments. This layer almost certainly was responsible for

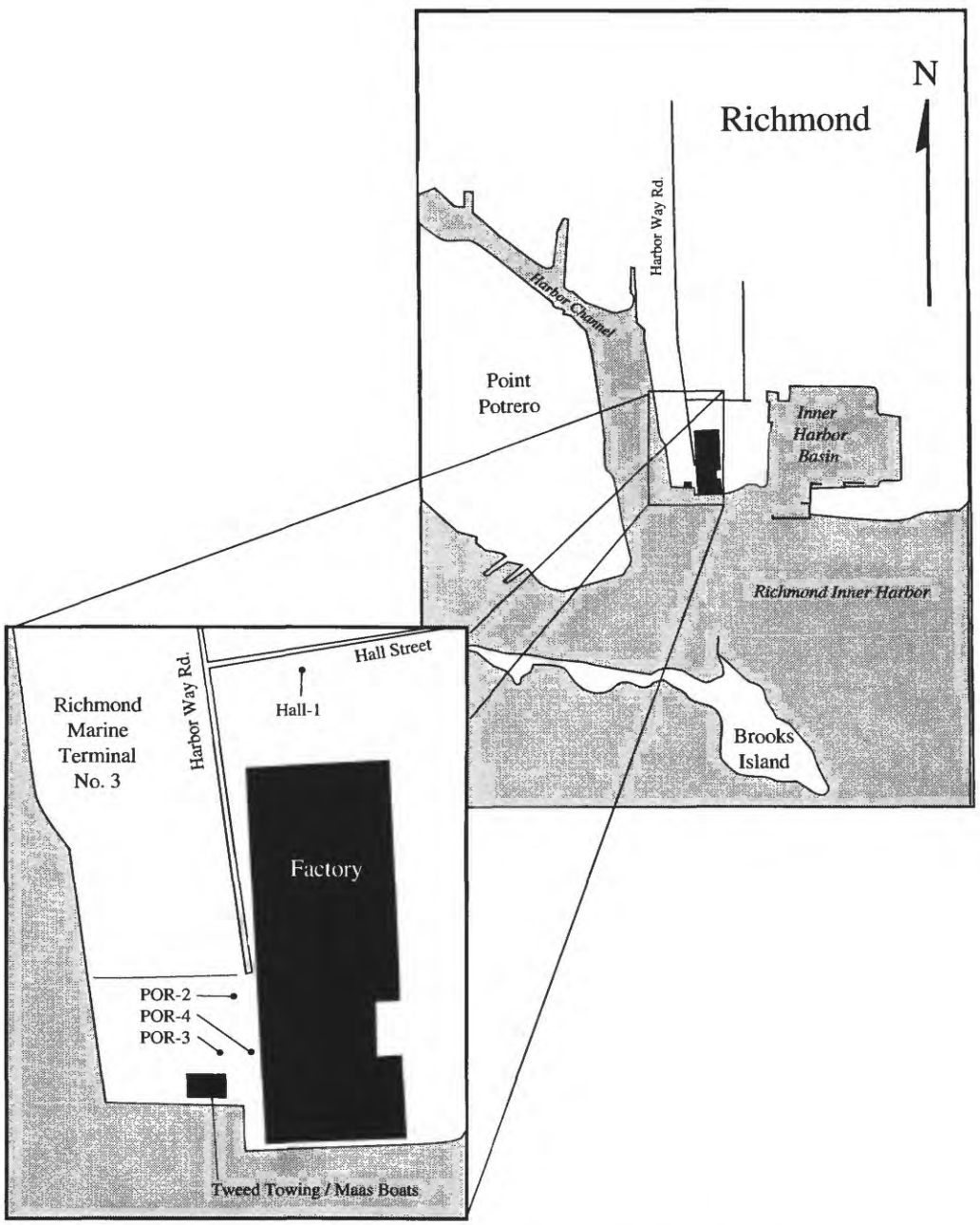


Figure 2.—Port of Richmond and Inner Harbor Basin, showing locations of boreholes (dots).

the observed liquefaction at the surface, and surface sand-boil material is identical to SPT samples of this layer. This layer has extremely low $q_c$ values (1–3 MPa), average FR values of 0.3 to 1.0 percent, and minor pore-pressure generation during cone penetration, and $N$ values of 2 to 11 blows/ft but typically 2 to 5 blows/ft when

Figure 3.—Sand boils on undeveloped land at end of Harbor Way Road in the Port of Richmond.

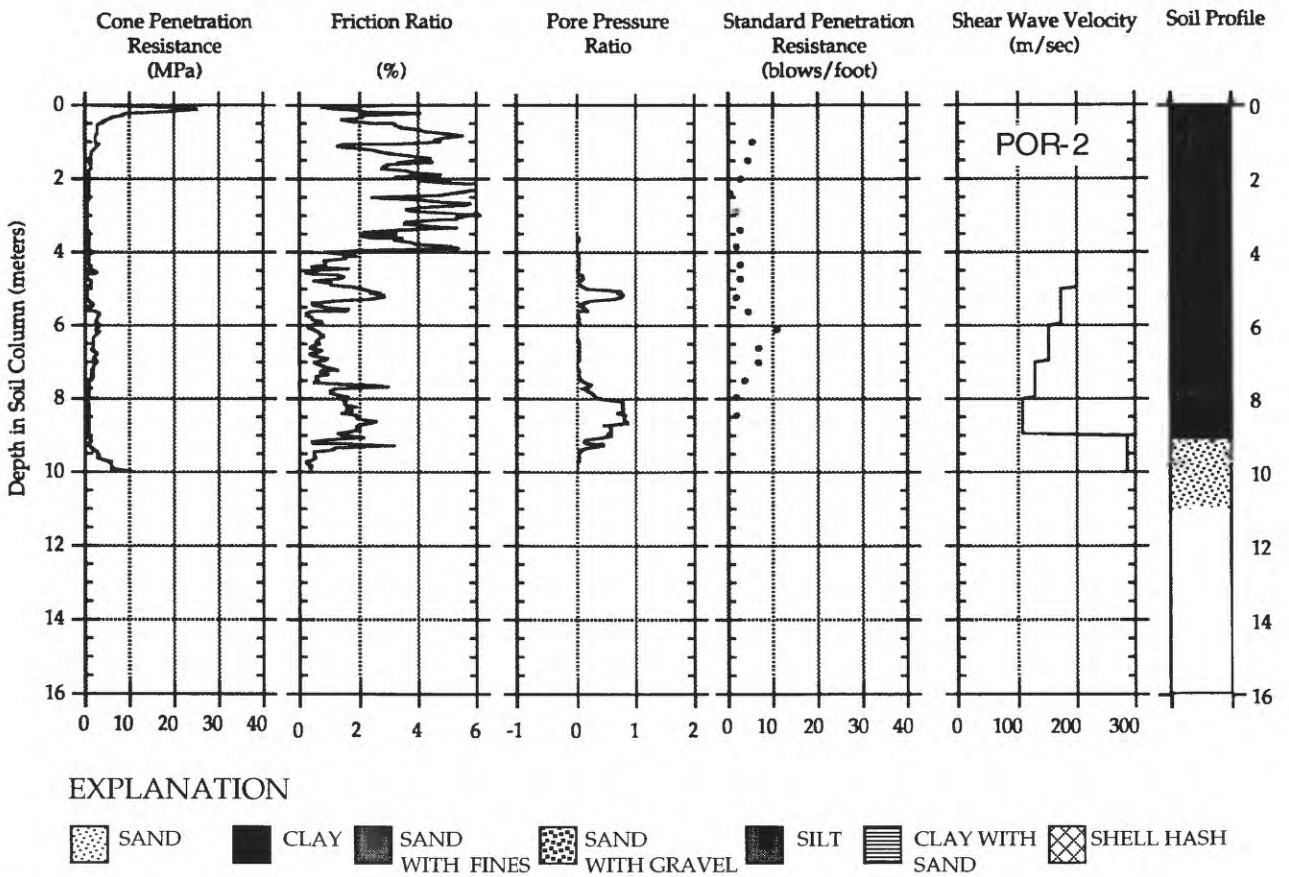


Figure 4.—Log of borehole POR–2 in fill deposits at Port of Richmond study site (see fig. 2 for locations).

evaluating all three borehole logs. $V_s$ values in this layer typically range from 140 to 170 m/s. Below this layer is a thin deposit of soft bay mud to 9.5-m depth, underlain by dense sand deposits. Detailed descriptions of the borehole logs from all the study sites, including those discussed herein, were presented by Kayen and others (1992), Kayen (1993), and Mitchell and others (1994).

## SAN FRANCISCO-OAKLAND BAY BRIDGE TOLL PLAZA

The San Francisco-Oakland Bay Bridge mole (peninsula-approach fill), immediately south of Emeryville (figs. 1, 5), was extensively damaged by soil liquefaction.

Appreciable settlement (max 40 cm) occurred over most of the mole. In some places, differential settlements produced an uneven, hummocky surface with permanent "waves" as large as 15 cm in amplitude. Lateral spreading also was significant along most of the fill, causing numerous longitudinal fissures in the pavement parallel to the fill edges. Many of these fissures exuded fine sand and silty sand, and numerous additional sand boils erupted along the median strip of the roadway, as well as off the shoulders of the roadway in undeveloped land at the bay's edge. The fissures opened to widths of approximately 7 to 8 cm and exhibited maximum differential vertical offsets of 3 to 5 cm (fig. 6). Liquefaction-induced settlement adjacent to the east side of the Toll Plaza administration building is shown in figure 7. The building itself, which is pile supported, was not seriously damaged by liquefaction, although settlement of the surrounding fill hindered access to the building and affected buried utilities.

Settlements of the mole and the elevated structures of Interstate Highway 580 and West Grand Avenue were severe, resulting, at each site, in pavement collapse and open fissures, as much as 0.3 m wide, at the soil-structure interface. The approach mole also settled below the bridge- and ramp-structure road level by as much a 0.5 m. The fissures and uneven pavement surface interrupted ground transportation in the interchange areas after the earthquake. Soil liquefaction was also observed adjacent to the piers of elevated-highway distribution structures (fig. 8)

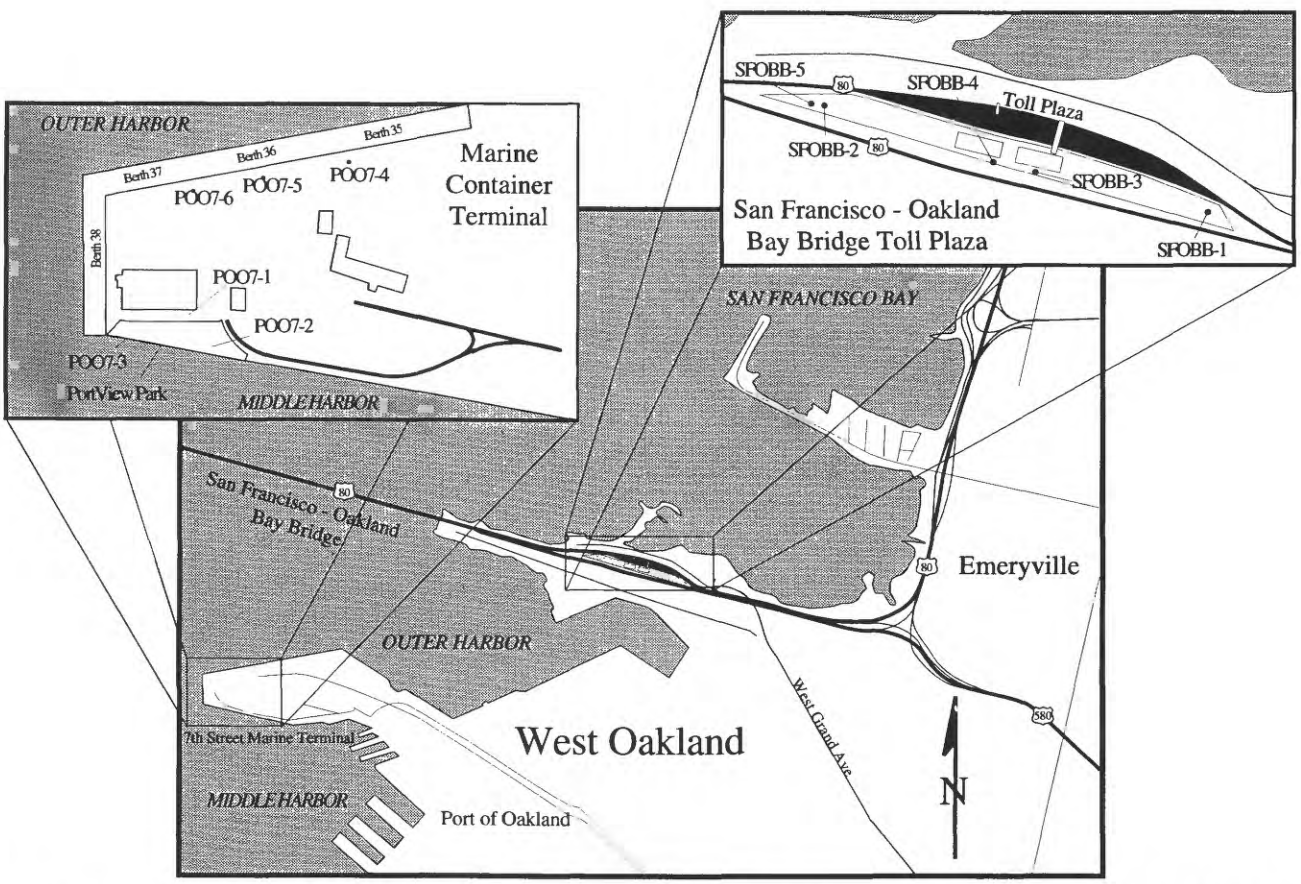


Figure 5.—Emeryville-Oakland shoreline, showing locations of boreholes (dots) near San Francisco-Oakland Bay Bridge Toll Plaza and Port of Oakland's Marine Container Terminal at Seventh Street.

## PENETRATION TEST LOGS

The logs of five boreholes drilled at the San Francisco-Oakland Bay Bridge Toll Plaza study site suggest a more complex stratigraphy than at the Richmond testing site. Five sets of logs were taken at places along the median strip and open space between the eastbound and westbound lanes of Interstate Highway 80, as shown in figure 5. Sand boils, lateral spreading, or settlement was observed in each place, as discussed below.

The log of borehole SFOBB–1 (fig. 9) was taken at the easternmost end of the Toll Plaza parking lot. This log indicates essentially no piezocone pore-pressure generation during cone penetration until bay mud was reached at 15-m depth. The log is marked by a moderately dense surface crust between 0- and 2.8-m depth, followed by an apparently interbedded sequence of cohesionless silty sand and cohesive clay to 4.5-m depth, as noted by the local variations in FR and $q_c$ values. The water table during sampling was in the upper part of the section at approximately 2-m depth. Between 4.5- and 7.5-m lies cohesionless material with low $q_c$ values averaging 5 MPa and $N$ values of typically 5 to 17 blows/ft, with a maximum $N$ value of 28 blows/ft at 5.2-m and a minimum $N$ value of 0


Figure 6.—Fissure in pavement caused by settlement in rightmost eastbound lane of Interstate Highway 80 west of San Francisco-Oakland Bay Bridge Toll Plaza administration building (visible in distance).

Figure 7.—Settlement at the east side of the San Francisco-Oakland Bay Bridge Toll Plaza administration building.


Figure 8.—Sand boils beneath elevated West Grand Avenue distribution structure adjacent to Interstate Highway 80 east of San Francisco Oakland Bay Bridge Toll Plaza.

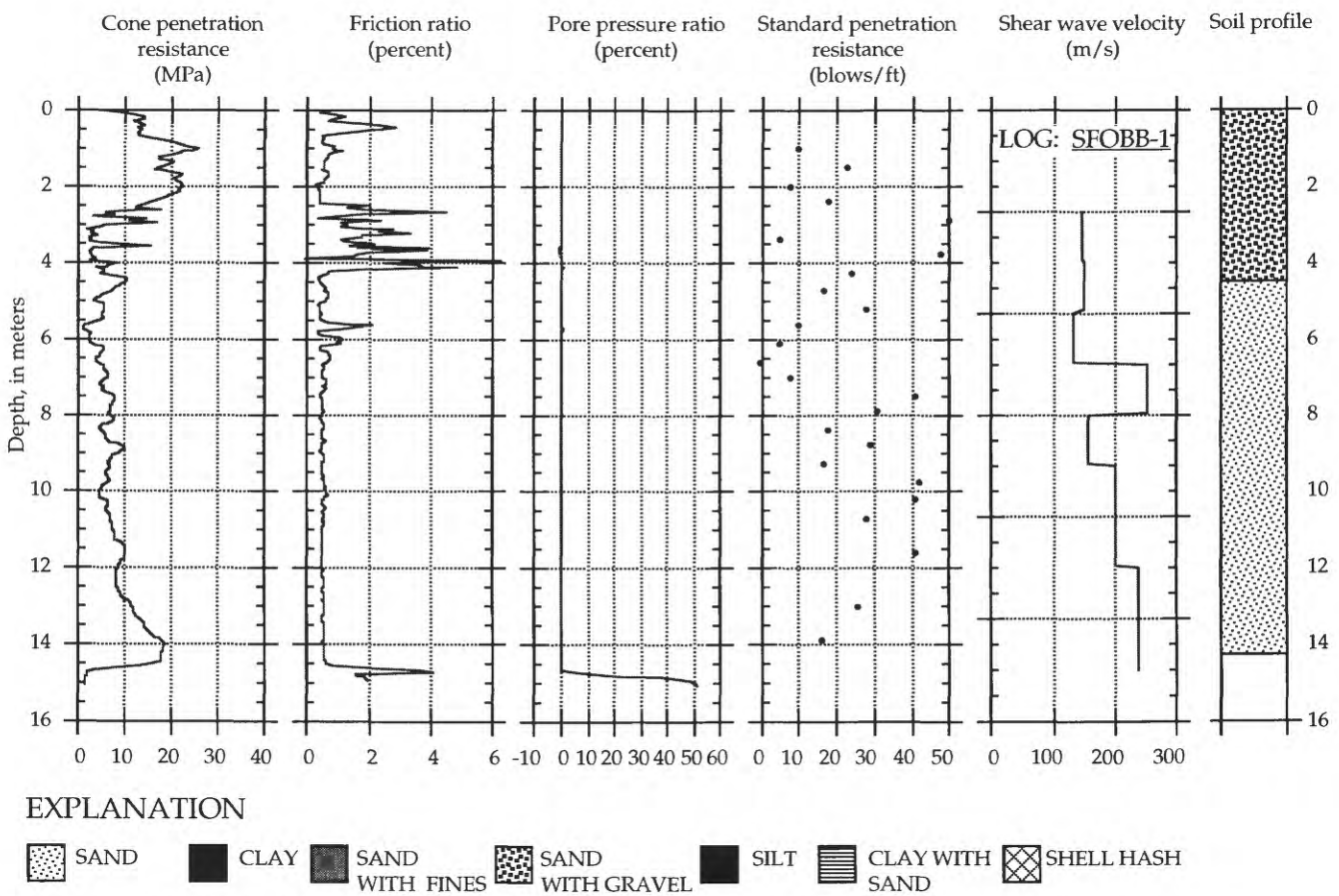


Figure 9.—Log of borehole SFOBB–1 on east shoreline of San Francisco-Oakland Bay Bridge mole (see fig. 5 for location).

blows/ft (drill rod and hammer sank under their own weight) at 6.6-m depth. This layer appears to have been responsible for the observed liquefaction, on the basis of both inplace testing and correlation with surface sand-boil material.

The logs of two boreholes, SFOBB–3 and SFOBB–4 (see Mitchell and others, 1994), drilled in the central part of the median strip directly south of the Toll Plaza and maintenance buildings, show similar soil profiles. The upper 4-m sections of these two logs suggest moderately loose sand ($q_c$=5–15 MPa) interbedded with finer materials. Below, there is a somewhat-uniform, more sand rich deposit to 8-m, with $q_c$ values of typically 4 to 15 MPa. This layer appears to be the principal liquefied layer. No SPT measurements were made at boreholes SFOBB–3 and SFOBB–4.

The logs of two boreholes, SFOBB–2 and SFOBB–5 (log of SFOBB–5 is shown in fig. 10), in a wooded area at the west end of the median strip show gravelly sand to 6-m depth beneath a dense crust. From 6- to 8.5-m depth is a layer of silty and sandy soil, with $q_c$ values of 5 to 10 MPa and $N$ values of 7 to 19 blows/ft, within which liquefaction apparently occurred.

## PORT OF OAKLAND

Immediately south of the San Francisco-Oakland Bay Bridge, soil liquefaction caused considerable damage to marine-container facilities at several places in the Port of Oakland, adjacent to the Oakland Outer Harbor, as shown in figure 1. Much of the extreme western part of the area near the Oakland shoreline, south of the mole, is filled land underlain by a relatively thin layer of soft, normally consolidated Holocene marine clay (bay mud). These shallow surficial units are, in turn, underlain by upwards of 180 m of stiffer Pleistocene glacial and interglacial deposits.

Most of the surface fills at the Port of Oakland were hydraulically placed to sea level, above which a combination of hydraulic and dumped fill was placed. After placement of the unimproved hydraulic fill, a relatively thick asphalt-cement pavement was laid in many of the terminal areas to support heavy vehicles and shipping containers. As shown in figure 1, three general areas encompassing four major terminals owned by the Port of Oakland were significantly damaged by soil liquefaction during the earthquake: (1) the Marine Container Terminal at Seventh

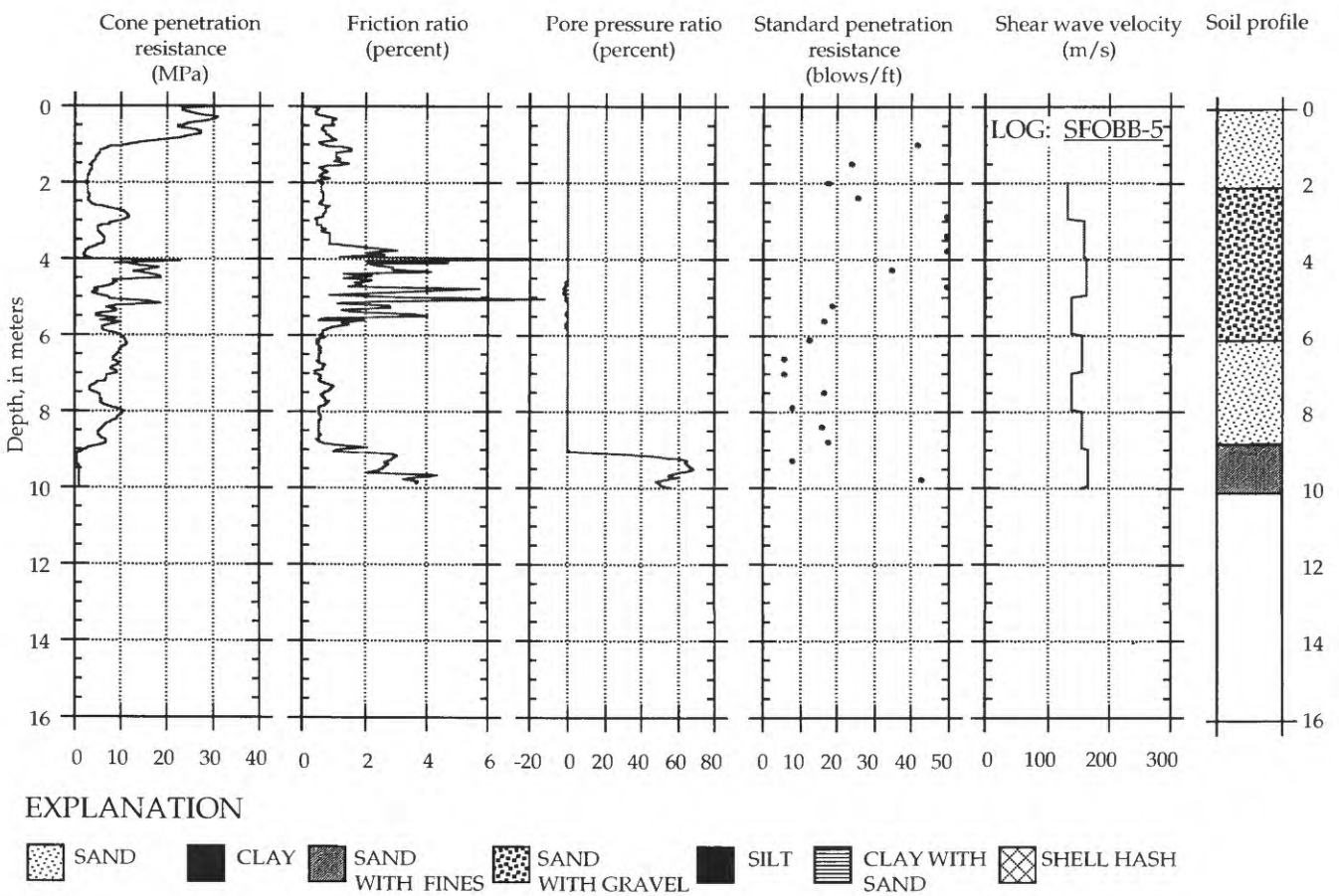


Figure 10.—Log of borehole SFOBB–5 on east shoreline of San Francisco-Oakland Bay Bridge mole (see fig. 5 for location).

Street; (2) the Matson Terminal, directly east of the Marine Container Terminal at Seventh Street; (3) the American Presidents Line (APL) Terminal at Middle Harbor; and (4) the Howard Terminal, farther east along the Oakland Inner Harbor, north of the Alameda (figs. 1, 5).

All of these terminals have pile-supported concrete wharves at the loading-dock edge of the terminal fill. At the Howard Terminal, these piles extend through a rock dike that serves as the perimeter containment for hydraulic fill inboard of the wharves. At the Marine Container Terminal at Seventh Street and at the Matson Terminal, the piles extend through rock fill that overlies a base of hydraulic sand fill. The hydraulic fills consist primarily of fine dredged sand and silty sand.

The most severe liquefaction-induced damage to port facilities occurred at the Marine Container Terminal. Liquefaction of the hydraulic fill resulted in settlement, lateral spreading, and cracking of the pavement over large areas of the terminal. Maximum settlements of the paved container yards inboard of the wharves were about 0.3 m. Several large cranes along the edge of the fill traverse laterally along the wharves on heavy rails. The outboard pile supported rail did not settle appreciably. The inboard crane rail, however, which was supported on fill throughout the entire terminal, underwent differential settlement, making several of the loading cranes and, thus, the dock facility inoperable after the earthquake. The Matson Terminal was able to continue limited operations because both its outboard and inboard crane rails were founded on a pile-supported concrete wharf deck.

Two of the large cranes operating along the north edge of the Marine Container Terminal at Berths 35 and 36 are shown in figure 11. A closeup of the pavement damage and approximately 0.15 m of settlement beneath the crane nearest to the camera in figure 11 is shown in figure 12. The observed settlement, which occurred in the vicinity of the inboard crane rail (fig. 16), resulted in severe distress to the crane system. In fact, one crane jumped the inboard rail at this site. Similar cracks and fissures occurred along much of the terminal. A 10-m-diameter, 0.3-m-high sand boil in the paved container yard south of the C.F.S. Building (now removed) near Berth 38 is shown in figure 13.

In addition to settlement and lateral spreading, as well as associated pavement damage and related mobility problems for the large cranes, damage occurred at the tops of several piles supporting the wharves in this area, as shown in figure 18. A cross section through the north edge of the Marine Container Terminal is shown in figure 19. Damage to battered piles, which occurred at the tops of a single row of inboard and outboard batters, consisted primarily of tensile failures.

As a result of widespread damage to the battered piles, they have been replaced by the Port of Oakland with vertical piles that are designed to provide lateral flexibility during earthquake loading. The pile-supported wharf deck has also been extended inboard, with additional vertical piles to provide improved support for the inboard crane rails. Stone columns were installed through the sand dike fill to limit deformations of the dike during future earthquakes.

At the south end of Berth 38, liquefaction-related features were observed in (now closed) Port View Park, located at the west end of Seventh Street (fig. 5). Lateral spreading and failure of the southern perimeter dike, with lateral movements toward the bay of several meters, were

Figure 11.—Wharf of Port of Oakland's Marine Container Terminal at Seventh Street (viewed from Berth 37), showing shipping-container cranes, damaged pavement, and extruded sand.

observed, although an area inboard of the dike near borehole POO7–3 had no surface manifestations of liquefaction. It may be that a thin seam of sand at approximately 6.5-m depth in borehole POO7–3 liquefied and that lateral displacement bayward of the site, and the opening of fissures, relieved excess pore-water pressures.

The Howard and APL Terminals differ in their design from the Marine Container Terminal in that (1) fill-containment dikes at the Howard Terminal are composed entirely of rock, and at the APL Terminal entirely of sand; (2) both the inboard and outboard crane rails are pile supported; and (3) all the piles supporting the wharves and the crane rails at the Howard Terminal are vertical or nearly vertical (max batter, 1:12). Liquefaction of the hydraulic fill caused appreciable settlements (max 30 cm) over large areas of the Howard and APL Terminals. Although pavement was damaged at the edges of the wharves and in the inboard container yards, there was no apparent damage to piles or adverse movements of the crane rails.

### PENETRATION TEST LOGS

Two of the six logs of six boreholes drilled at the Port of Oakland study site (figs. 1, 5) near the Marine Container Terminal at Seventh Street are shown in figure 14 and 15. Detailed description of the Port of Oakland borehole logs, including those discussed here, were presented by Kayen (1993) and Mitchell and others (1994). Three SPT's were performed near the southwest corner of the fill area near Berth 38 and Port View Park, and six CPT soundings near the north side of the facility near Berths 36 and 37. We note that evidence of liquefaction of the subbase material appears to have extended across much of the entire western part of the Marine Container Terminal, as evidenced by settlement, sand boils, and tension cracking of the asphalt. The study sites were selected for ease of access, not because of the severity of liquefaction damage, except at borehole POO7–3, where liquefaction was not observed. These sites typically have a resistant surface layer in the upper 3 to 4 m, with $q_c$ values typically 25 to 35 MPa and $N$ values of 25 to 36 blows/ft. The water table within this layer averages approximately 2- to 2.3-m depth and fluctuates with tidal action. Below this surface layer, the fill consists of looser deposits of fine marine sand with $q_c$ values of 5 to 15 MPa and $N$ values of 10 to 25 blows/ft. Liquefaction appears to have occurred in the materials between 4- and 8-m depth in borehole POO7–2, on the basis of correlations of SPT samples with surface sand-boil material recovered. Borehole POO7–3 is characterized by $q_c$ values greater than 10 MPa and $N$ values greater than 21 for the entire submerged soil profile, except for a muddy-sand unit between 5- and 7-m depth.

## ALAMEDA NAVAL AIR STATION AND THE ALAMEDA

Soil liquefaction occurred over large areas of Alameda Naval Air Station (ANAS), immediately south of the Port of Oakland, as shown in figure 1. Numerous, commonly large sand boils, settlements, and lateral spreads occurred over a large area at the west end of ANAS. The airfield's

Figure 12.—Closeup of damaged pavement near boreholes POO7–5 and POO7–6 at Port of Oakland Berths 36 and 37 (see fig. 5 for locations), showing differential settlement, open fissures, and lateral spreading.

Figure 13.—Sand boil near borehole POO7–1 at Port of Oakland Berth 38 and Port View Park (see fig. 5 for locations).

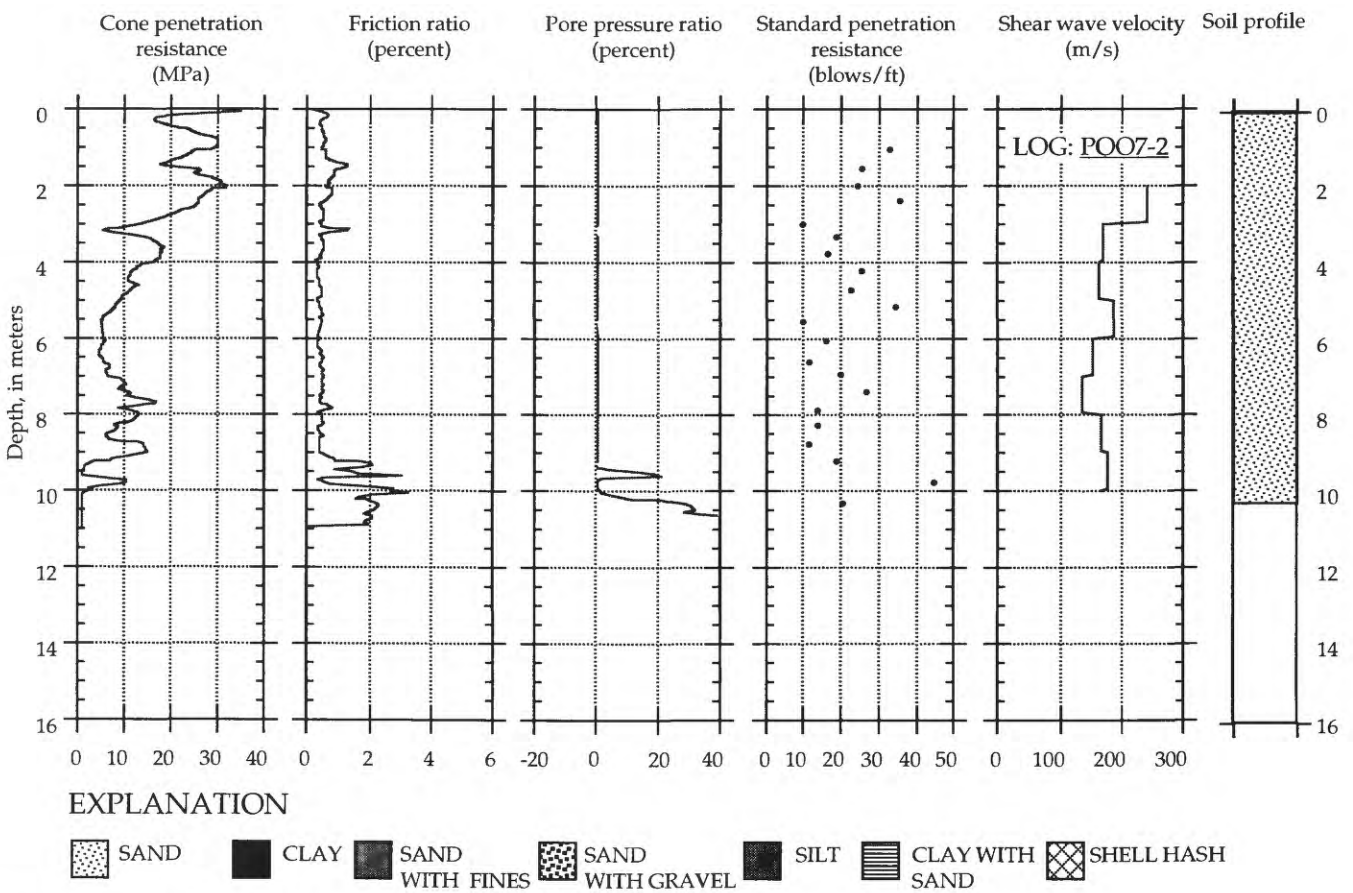


Figure 14.—Log of borehole POO7–2 in fill deposits at Port of Oakland (see fig. 5 for location).

two runways and two taxiways were significantly damaged and inoperable after the earthquake. A large sand boil and vent on the taxiway of the two runways at ANAS is shown in figure 16. Pavement damage consisted of heaving, settlement, and minor lateral spreading, resulting in separation at joints. Maximum crack and joint openings were about 10 cm, and maximum vertical offsets were approximately 5 cm.

As at many of the sites discussed above, the western part of ANAS is built on hydraulic fill, underlain at shallow depths by soft bay mud, and at greater depths by older, stiffer soil units. Settlements of as much as 30 cm occurred over much of the west end of the ANAS; however, little liquefaction occurred to the east in the area occupied by base-operations buildings. A few structures were lightly damaged in the eastern part of ANAS as a result of relatively modest foundation movements, but most buildings were undamaged. Minor settlements and ground displacements in some places resulted in separation of exterior steps and cracking of concrete sidewalks. In addition, several sewer-line and waterline breaks occurred in this area.

Scattered evidence of liquefaction, as evidenced by sand boils, minor settlements, and minor lateral spreading, occurred in several places along the west coast of the Alameda outside ANAS. These ground deformations caused minor cracking of pavements and ruptured many pipelines but caused no serious damage to structures. A typical example of the minor ground deformations in this area is shown in figure 17. No inplace testing was performed either at ANAS or on the Alameda as part of our studies.

## BAY FARM ISLAND AND HARBOR BAY PLAZA

At Bay Farm Island, immediately north of Oakland International Airport (figure 1, 18), considerable liquefaction occurred at the northwest corner and at points along the west edge of the fill (fig. 19).

Most of the western part of Bay Farm Island consists of sandy hydraulic fill, underlain by bay mud and deeper,

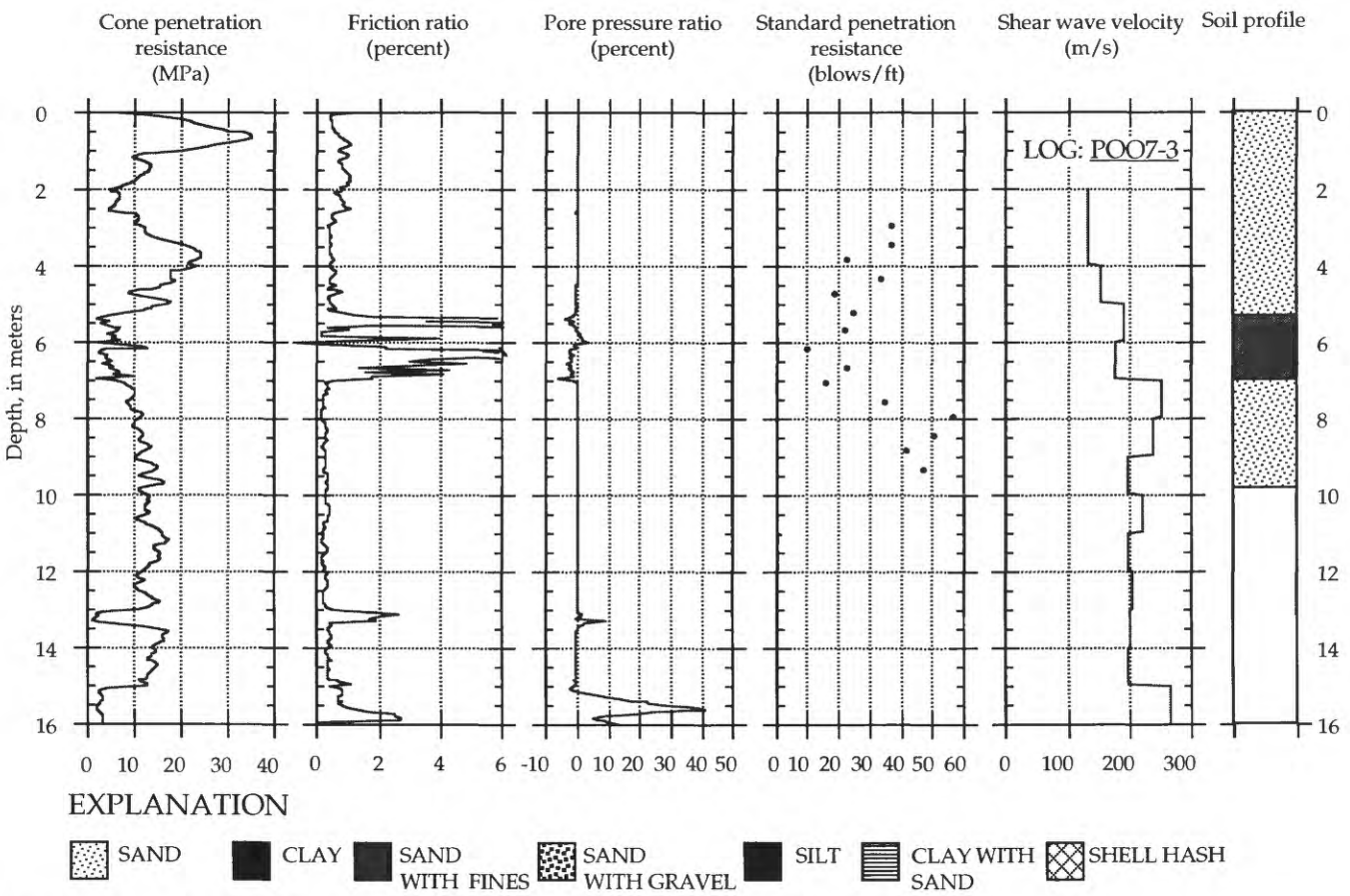


Figure 15.—Log of borehole POO7–3 in fill deposits at Port of Oakland (see fig. 5 for location).

stiffer alluvium. Soil liquefaction in the northern part of the island was largely confined to undeveloped, artificially filled land in the areas on the south side of Bay Farm Slough, northwest of the intersection of Aughinbaugh Way and Mecartney Road (fig. 18). This area, which served as our study site, is presently undergoing residential development. Much of the rest of the island had already been developed for lightweight residential housing and light commercial use.

Fill in the perimeter dike was densified by dynamic compaction. Densification appears to have successfully prevented soil liquefaction of the western-perimeter dike during the earthquake. In contrast, in an area of unimproved fill, damage to roadway and parking-lot pavements occurred at the Harbor Bay Plaza business park (fig. 18). Numerous sand boils, many relatively large (more than 3 m in diameter), erupted in this area (fig. 20).

Figure 16.—Liquefaction-induced damage to taxiway pavement at Alameda Naval Air Station.


Figure 17.—Minor settlement and buckling of pavement at southwest edge of the Alameda (fig. 1).

## PENETRATION TEST LOGS

The logs of one of the three boreholes drilled at the Bay Farm Island study sites (figs. 1, 18) are shown in figure 21. These logs suggest a complex stratigraphy of relatively thin (less than 1 m thick) interbeds of sand and finer material. A total of 20 CPT logs were also taken at the liquefaction site northwest of the intersection of Aughinbaugh Way and Mecartney Road to observe any changes in strength over time; a representative log is shown in figure 21. These logs indicate a noncohesive layer of sand and silty sand at 2- to 3-m, with $q_c$ values of typically 2 to 16 MPa and $N$ values of 8 to 18 blows/ft. The water table is within this layer between 1.5- and 2-m depth. Below this layer, to approximately 6.5-m depth, is a set of finer interlayered deposits with decreasing $q_c$ values and elevated $B_q$ and FR values. Below 6.5-m depth, silty sand with a low $q_c$ value defines the rest of the logged soil column. Liquefaction probably occurred in the fine sand and silty sand at 2- to 3-m depth, on the basis of correlation of sand-boil materials with recovered samples.

CPT and SPT logs were taken along the improved perimeter dike, which did not liquefy during the earthquake. At the elevated dike structure, the water table is some-

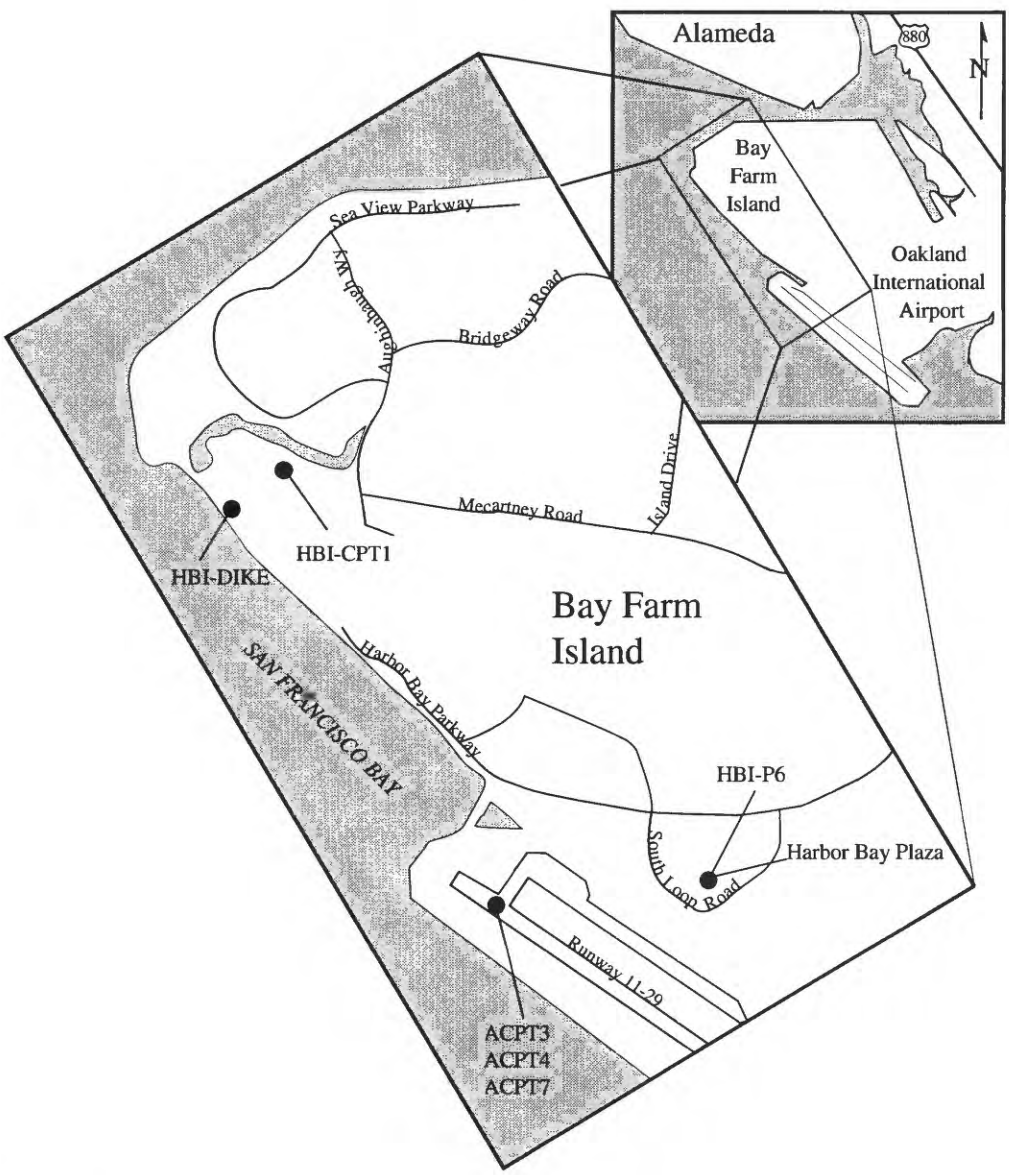


Figure 18.—Northern part of Oakland International Airport and Bay Farm Island, showing locations of boreholes (dots).

what deeper in the soil profile at 2.5-m depth. However, within the sandy deposits at 2.5- to 7-m depth, $q_c$ values are noticeably higher, ranging from 10 to 35 MPa, and $N$ values range from 29 to 58 blows/ft.

At the Harbor Bay Plaza business park, we performed tests in a parking area on South Loop Road. The soil at the site consists of fine hydraulic fill sand with low $q_c$ values to 4-m depth, below which are interbedded layers of bay mud and sand. Liquefaction almost certainly occurred at 2- to 4-m depth in the soil profile.

## OAKLAND INTERNATIONAL AIRPORT

Immediately south of Bay Farm Island, soil liquefaction caused considerable damage to the main jet runway (11–29) at Oakland International Airport (figs. 1, 18). Additional evidence of liquefaction, including sand boils, settlement, and lateral spreads, occurred over wide areas of airport fill to the north, south, and east of the damaged runway section. As shown in figure 18, the main runway is located at the southwest edge of the airport.

Figure 19.—Sand boils west of Aughinbaugh Way near borehole HBI–CPT1 on Bay Farm Island (see fig. 18 for locations).

Figure 20.—Sand boil near Harbor Bay Plaza on west side of Bay Farm Island.

Much of the runway and inboard taxiway area is built on loose sandy fill underlain at shallow depths by soft bay mud and at greater depths by older, stiffer sedimentary deposits. The perimeters of the airport fill have dikes to prevent inundation during unusually high tides and storms.

Extensive soil liquefaction occurred in the western section of the airport fill, damaging the northwestern 900 m of the 3,000-m-long main runway. In addition, the adjacent taxiway pavement also was heavily damaged (fig. 22). At the northwest end of the main runway (left side, fig. 22), sand boils and cracks appeared in the pavement (figs. 23, 24). These cracks were as much as 30 cm wide, with vertical offsets of as much as 15 cm. Most of the runway damage was repaired within 4 weeks, and as a result, the airport was able to resume essentially full operations with a shortened operational runway 2,700 m long on November 20, 1989.

Settlement and lateral spreading occurred in several places in the surrounding perimeter dikes at the west end of the runway fill. The maximum observed levee settlement of the perimeter dikes was approximately 0.5 to 0.7 m, and lateral deformations were similar in magnitude. Liquefaction-induced ground deformations also damaged an undeveloped area of fill to the north and northeast of the main runway. Sand boils and major fissures caused by lateral spreading in this area are shown in figure 30. Liquefaction was also observed near the main terminal buildings, which are supported on deeper foundations and were not significantly damaged, although settlements of as much as 8 cm were observed in several places in the surrounding soils. In addition, a below-ground tramway, which allows service vehicles carrying passengers' luggage to pass under part of one of the main terminal buildings, filled to a depth of 2 m with exuded sand and water, as shown in figure 25.

## PENETRATION TEST LOGS

The log of one of the three boreholes drilled at the OIA study site along the north end of runway 11–29 (fig. 18) are shown in figure 26. Additional SPT boreholes and CPT soundings were located in this area as part of ongoing geotechnical investigations directed toward evaluating and, if necessary and feasible, improving conditions

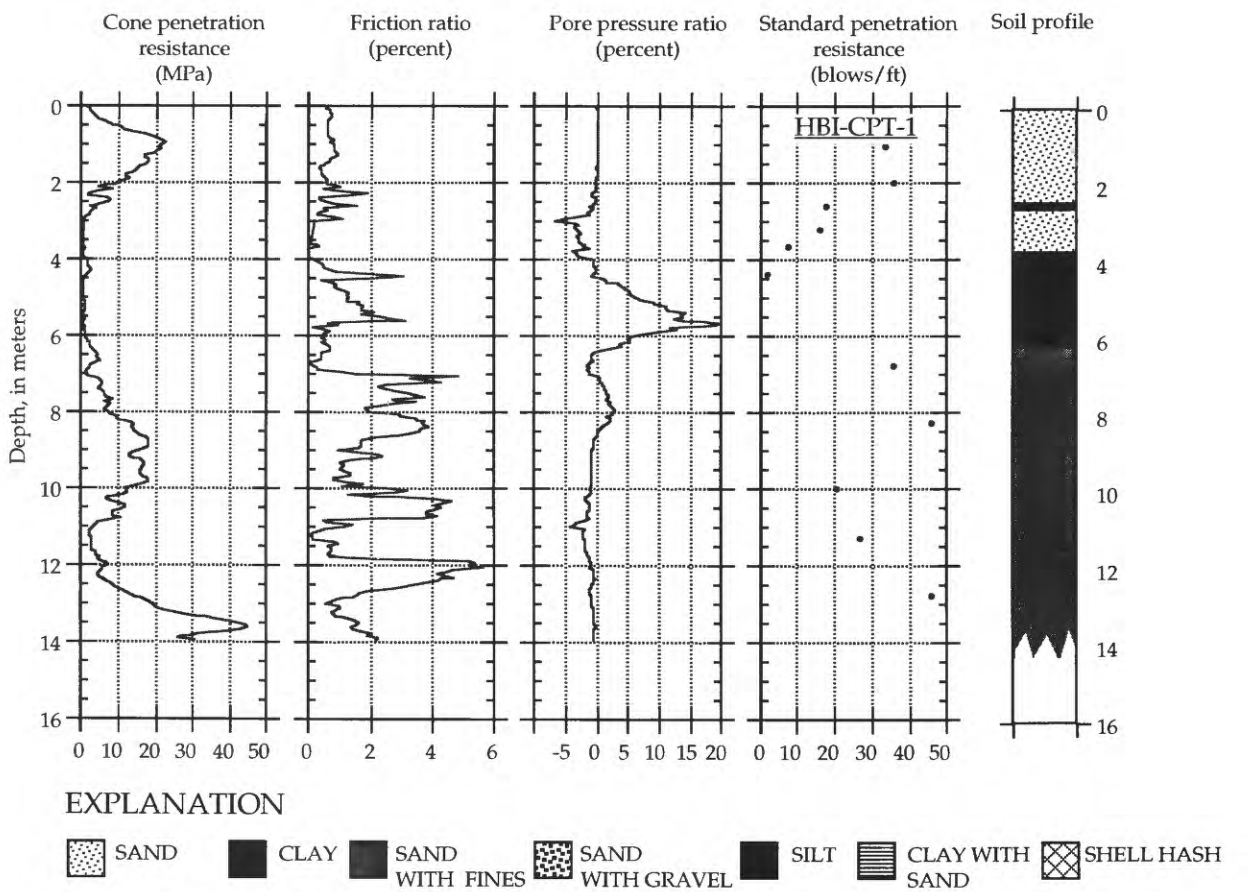


Figure 21.—Log of borehole HBI–CPT1 in fill deposits at Bay Farm Island study site (see fig. 18 for location).

along the runways to ensure operability in the wake of a future earthquake.

As shown in figure 26, a modest surficial crust is present between 0- and 2-m depth, where the water table was penetrated. From 2- to 4.5–5.8-m depth, depending on the borehole, is an extremely loose deposit of fine-sand hydraulic fill that almost certainly was responsible for the observed liquefaction and lateral spreading. $q_c$ values within this deposit range from 2 to 14 MPa, and $N$ values from 1 and 4 blows/ft. The material in this layer correlates with sand-boil material observed at the surface. Below this deposit, young bay mud with a low $q_c$ value defines the rest of the soil profile.

## DISCUSSION

We compared the observed liquefaction behavior of east-bay fills with the liquefaction potential of the study sites, as measured by $q_c$ and $N$ values. To remove the influence of effective overburden stress on the field penetration-resistance measurements so that we may evaluate the liq-

Figure 22.—Northwest end of main runway (bottom) and adjacent taxiway (top) at Oakland International Airport (fig. 1). Photograph taken October 18, 1989.

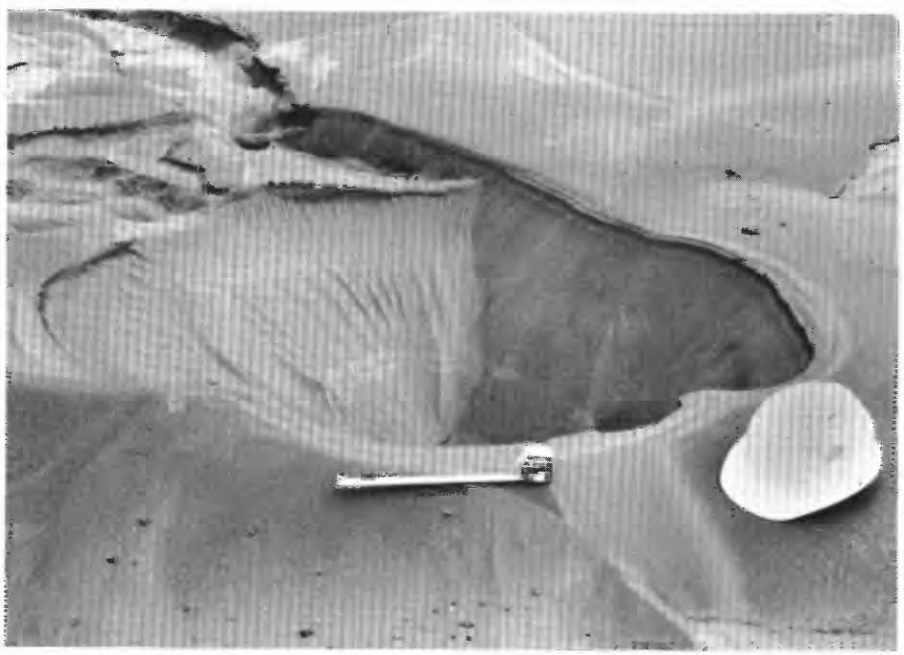

Figure 23.—Large sand boil near north end of main runway at Oakland International Airport (fig. 1).

Figure 24.—Fissures, sand boils, and grabens associated with lateral spreading near northwest end of main runway at Oakland International Airport. Photograph courtesy of B.A. Vallerga.

Figure 25.—Below-grade tramway, filled with as much as 1.8 m of extruded sand, at Oakland International Airport Terminal Building. Photograph courtesy of B.A. Vallerga.

uefaction potential of soil in a manner that is independent of soil depth, we normalized the field measurements to values at a corresponding reference vertical effective stress of 1 atm. For example, $N$ values can be normalized to a reference effective overburden stress of 1 atm ($\sigma'_{vo}$=0.096 MPa) by correcting for overburden effects on penetration resistance, using the relation of Seed and Idriss (1971)

$$N_1 = C_n N. \tag{3}$$

We found that the overburden-stress-correction factor, $C_n$, can be reasonably expressed as

$$C_n = \frac{2.2}{1.2 + \left(\frac{\sigma'_{vo}}{\sigma'_{ref}}\right)}, \tag{4}$$

where $N_1$ is the overburden-stress-corrected standard penetration resistance, $\sigma'_{vo}$ is the effective overburden stress, and $\sigma'_{ref}$ is a reference stress of 1 atm. Likewise, to evaluate $q_c$ values at a common reference stress, we adjust the measured $q_c$ values as follows:

$$q_{c1} = C_q q_c. \tag{5}$$

We found that $C_q$ can be reasonably expressed as

$$C_q = \frac{1.8}{0.8 + \left(\frac{\sigma'_{vo}}{\sigma'_{ref}}\right)}, \tag{6}$$

The $N$ values were also adjusted to account for the efficiency of the SPT hammer system and the effects of sampler configuration. A standard SPT hammer efficiency of 60-percent energy transmission to the drill rod and sampler was adopted by Seed and others (1984). The actual

SPT hammer efficiency of the drill rig used (a model CME–450) during most of the testing at east-bay sites was less than 60 percent. We used a Binary Instruments model 102 calibrator to determine the actual efficiency by stress-wave energy measurement (American Society for Testing and Materials, 1986b) and corrected the $N_1$ measurements according to the recommendations of Farrar (1991; J.A. Farrar, oral commun., 1992). We also accounted for the influence of a split-spoon sampler that did not have a constant inside diameter of 5.50 cm (sampler configured to permit the use of internal sample liners and the liners were omitted) by increasing the recorded blowcounts by 10 to 20 percent for low and high $N$ values, respectively (Seed and others, 1984).

Liquefiable layers at the Toll Plaza, Port of Oakland, Bay Farm Island, and Oakland International Airport study sites can be characterized as clean sand with a mean grain diameter ($D_{50}$) of at least 0.25 mm and a fines content of less than 5 percent. The liquefiable layer at the Port of Richmond study site has a $D_{50}$ value of approximately 0.06 to 0.07 mm and a fines content (<0.074 mm) of more than 35 percent. Silty sands, like those at the Port of Richmond study site, with the same liquefaction resistance as that of a corresponding reference "clean sand," are typically observed to have distinctly lower measured penetration-resistance values. Seed and others (1984) presented boundary curves that effectively convert penetration-resistance values of silty sands to those of clean sands containing no fines, and defined an SPT fines-content correction factor (Seed and de Alba, 1986):

$$(N_{1,f_c})_{\text{clean-sand equivalent}} = (N_1)_{\text{silty sand measured}} + \Delta N_1. \quad (7)$$

where $\Delta N_1$, the fines-content correction factor, is a function of the fines content, FC (in percent). According to the guidelines presented in a consensus statement from the NCEER Workshop on Evaluation of Liquefaction Resistance, held January 4–5, 1996, in Salt Lake City, Utah, we used the following equations for correcting the SPT values of low-plasticity silty sands to equivalent values for clean sand

$$\Delta N_1 = \begin{pmatrix} \text{FC} \le 5\%: & 0 \\ 5\% < \text{FC} < 35\%: & (\text{FC} - 5)(7/30) \\ \text{FC} \ge 35\%: & 7 \end{pmatrix}. \quad (8)$$

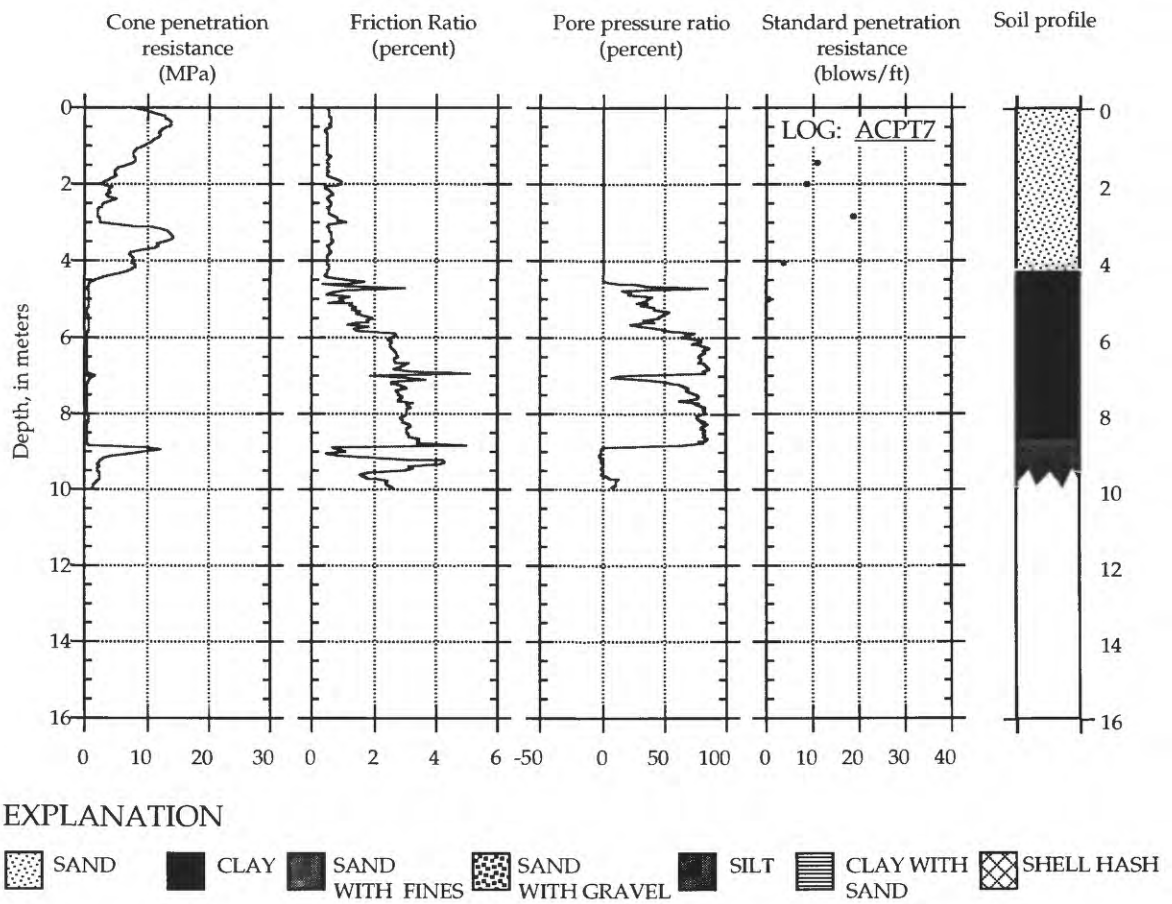


Figure 26.—Log of borehole ACPT7 in fill deposits at Oakland International Airport study site (see fig. 2 for location).

We applied this correction factor to the SPT data at the Port of Richmond study site.

We used two approaches to assess the intensity of seismic shaking at the study sites. The first approach used the conventional cyclic-stress-ratio (CSR) method of Seed and others (1984), and the second approach used a new method based on the Arias intensity of ground motion recorded near the study sites (Kayen and Mitchell, in press). The first method utilizes a uniform CSR to represent the complex and irregular earthquake-induced stress-time history. This equivalent series of cyclic loads of uniform amplitude is expressed as follows (Seed and Idriss, 1982):

$$\mathrm{CSR} = 0.65 \frac{a_{\max}}{g} \frac{\sigma_{vo}}{\sigma'_{vo}} r_d, \quad (9)$$

where $a_{max}$ is the peak ground acceleration, $g$ is the gravitational acceleration (981 cm/s$^2$), $\sigma_{vo}$ is the total overburden stress, $\sigma'_{vo}$ is the effective overburden stress, and $r_d$ is a depth-reduction factor, which can be estimated in the upper 10 m of the soil column by the following relation:

$$r_d = 1 - 0.012z, \quad (10)$$

where $z$ is the depth (in meters) (Kayen and others, 1992).

The second approach utilizes a quantitative measure of earthquake shaking intensity termed the Arias intensity (Arias, 1970), which is the sum of the energy per unit weight absorbed by an evenly spaced population of idealized undamped simple oscillators in response to the earthquake motion. For the two horizontal components of motion, the Arias intensity, $I_h$, is calculated as

$$I_h = I_{xx} + I_{yy} = \frac{\pi}{2g}\int_0^{t_0} a_x^2(t)dt + \frac{\pi}{2g}\int_0^{t_0} a_y^2(t)dt, \quad (11)$$

where $I_{xx}$ and $I_{yy}$ are the intensities measured in the $x$- and $y$-directions, respectively, in response to transient motions in the $x$- and $y$-directions; $g$ is the acceleration due to gravity; $t_0$ is the duration of earthquake shaking; and $a_x(t)$ is the transient acceleration. The Arias intensity integral has the dimensional units of $L/T$.

To assess the soil-liquefaction potential, the advantages in using Arias intensity over peak ground acceleration (PGA), as used in the CSR method, are that (1) Arias intensity is derived from the acceleration records of both horizontal components of motion over the entire duration of motion, whereas PGA utilizes a single arbitrarily selected value; and (2) Arias intensity incorporates the intensity of motions over the full range of recorded frequency, whereas PGA is commonly associated with high-frequency motion. Furthermore, the breakdown of soil structure that results in liquefaction depends fundamentally more on input energy than on a single level of acceleration (Liang and others, 1995).

As in the case of PGA, we find that $I_h$ typically decreases with depth in the soil column. To assess the soil-liquefaction potential, we need to know the $I_h$ profile within the soil column. We estimated the decrease in $I_h$ with depth through a parametric analysis of synthetic accelerograms based on shear-modulus representations of soil columns at our east-bay study sites. Synthetic seismograms were generated for the surface and depth nodes of soil-column input files with the ground-response computer-program *SHAKE90* (modified version of program presented by Schnabel and others, 1972). Using *SHAKE90*, strong-motion records from eight earthquakes were propagated through a soil column representing loose sandy fill ($V_s$=150 m/s) overlying cohesive soil with shear-wave-velocity profiles representative of known San Francisco bayshore sites (Sun and others, 1989; Kayen, 1993). Each profile was underlain by an elastic base-rock material with a shear wave velocity of 2,500 m/s. Output synthetic acceleration-time histories for layer nodes at depth in the model soil profiles were integrated to calculate $I_h$ and then normalized by the respective $I_h$ at the surface. This normalization process allows us to evaluate the depth dependency of $I_h$ over a broad range of earthquake and site conditions by collapsing the profiles to a common reference value (unity) at the ground surface. We define an Arias intensity depth-of-burial-reduction parameter, $r_b$, as the ratio of the buried to the surface cumulative Arias intensity:

$$r_b = \frac{I_{h\ (\mathrm{depth})}}{I_{h\ (\mathrm{surface})}}. \quad (12)$$

The $r_b$ parameter, which is analogous to $r_d$ (Seed and Idriss, 1982), can be calculated from either one- or two-component horizontal Arias intensity. The mean±1$\sigma$ responses calculated from the suite of *SHAKE* runs are plotted in figure 27. The mean $r_b$ value decreases somewhat linearly from 1.0 to a value of 0.58 at 6-m depth and then to 0.46 at 10-m depth; $r_b$ remains essentially constant below 10-m depth. We calculated the Arias intensity within the soil column, $I_{hb}$, as the product of $I_h$ measured from recorded seismograms in the east bay and $r_b$ estimated from the *SHAKE90* study.

$$I_{hb} = I_h r_b. \quad (13)$$

In our study, we associate CSR and $I_{hb}$ profiles with the liquefaction field-performance data $(N_1)_{60}$ and $q_{c1}$ from our study sites. The CSR and $I_{hb}$ values used in the analyses of critical soil layers at the east-bay study sites (fig. 1) are summarized in table 1. Two SPT boundary-curve sets for the assessment of soil-liquefaction potential based on $I_{hb}$ (Kayen and Mitchell, in press) and CSR (Seed and others, 1984) for soils with low-plasticity fines content of less than 5 percent are shown in figure 28. The CSR by itself does not account for earthquake magnitude and du-

ration, and so magnitude-correction factors must be applied to CSR values to scale for the severity of earthquake shaking. This approach results in a suite of magnitude-dependent boundary curves. Several magnitude-correction-factor curves for CSR have been proposed (Seed and Idriss, 1982 ; Ambraseys, 1988; Arango, 1996). The Arias intensity incorporates magnitude, frequency, and earthquake-shaking-duration elements of strong motion and thus needs no magnitude-correction factors.

The $I_{hb}$ and CSR values at the liquefaction boundary in figure 28 represent the minimum threshold seismic intensity ($I_{hb,l}$ and $CSR_l$, respectively) required to induce liquefaction in soil with a given $(N_1)_{60}$ or $q_{cl}$ value. We compared $I_{hb,l}$ and $CSR_l$ with the corresponding seismic-shaking-intensity function induced by the earthquake, using equations for Arias intensity at depth ($I_{hb,eq}$) and cyclic-stress ratio ($CSR_{eq}$), to determine profiles of factor of safety against liquefaction. The Arias intensity-based factor of safety $F_{Ihb}$ against liquefaction occurrence is defined as the ratio of the Arias intensity required to cause liquefaction to the Arias intensity imparted by the earthquake:

$$F_{Ihb} = \frac{I_{hb,l}}{I_{hb,eq}}. \quad (14)$$

This Arias intensity-based factor of safety is analogous to that defined by Seed and others on the basis of cyclic-stress ratio ($F_{CSR}$).

We converted the *N* profiles from figures 4, 9, 10, 14, 15, 21, and 26 into factor-of-safety profiles for both $F_{CSR}$ and $F_{Ihb}$ in figure 29, on the basis of the calculated CSR and $I_{hb}$ values for the study sites. At the Port of Richmond study site, the $F_{Ihb}$ and $F_{CSR}$ profiles accurately identify the liquefaction zone between 4- and 5-m depth in profile POR–1. At borehole POR–Hall St. (log not shown), both profiles accurately indicate no liquefaction. Profiles of $F_{CSR}$ and $F_{Ihb}$ for the San Francisco-Oakland Bay Bridge study site correctly indicate that liquefaction occurred principally between approximately 5.5- and 7.5-m depth at borehole SFOBB–1 and between 6.0- and 9.0-m depth at borehole SFOBB–5, on the basis of field observations. The profiles for borehole POO7–2 are in agreement and identify the zone of liquefaction between 5- and 8-m depth, and borehole POO7–3 indicates thin seams of loose potentially liquefiable material at 6.5- and

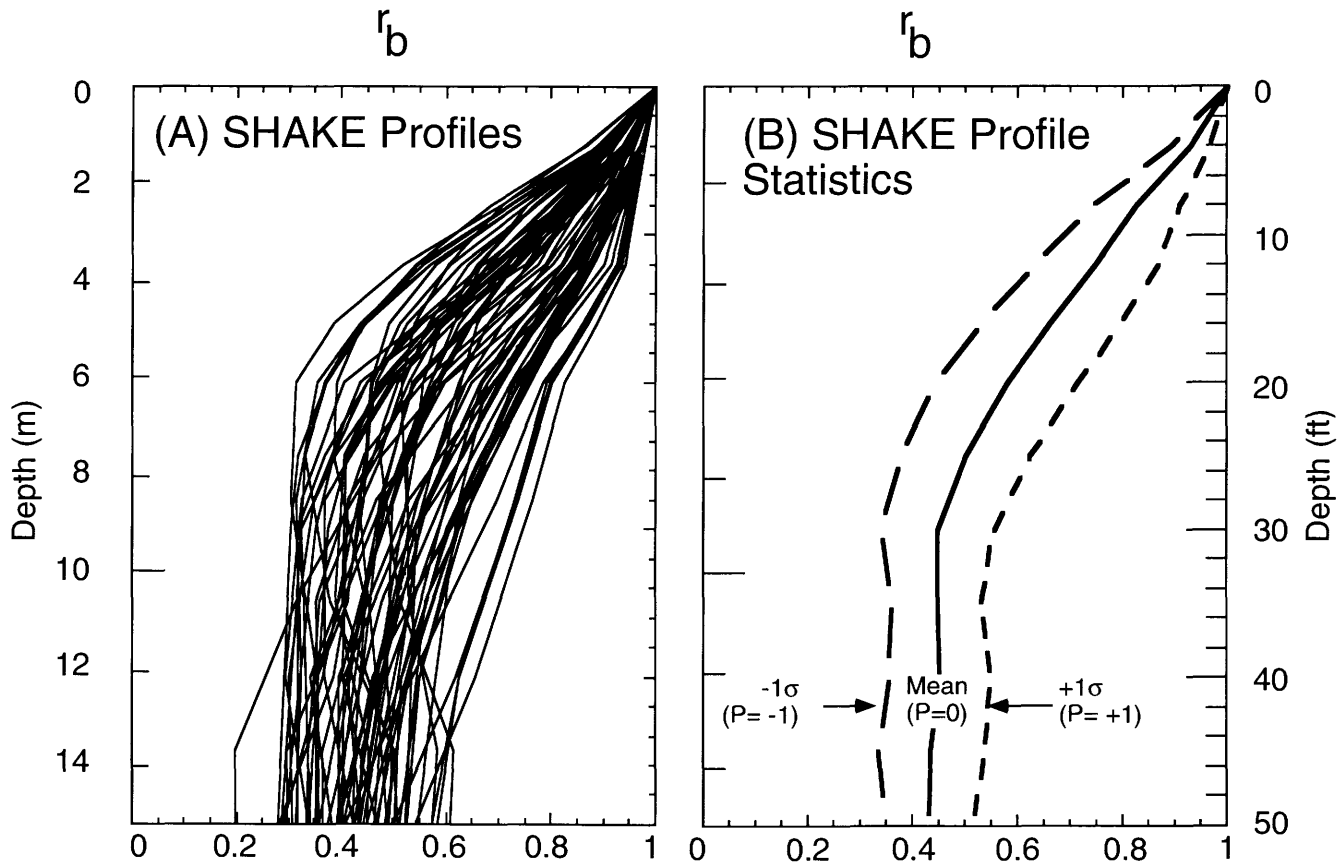


Figure 27.—Profiles of Arias intensity depth-of-burial-reduction parameter versus depth (*A*) and mean±1σ curves (*B*), modeled using ground-response program *SHAKE*.

Table 1.—*Representative values of parameters used in liquefaction-susceptibility analyses for critical soil layers at east-bay study sites*

[See figures 1 through 4 for locations of boreholes. $I_h$, Arias intensity at the surface; PGA, peak ground acceleration; CSR, cyclic-stress ratio; $I_{hb}$, Arias intensity within the soil column; $(N_1)_{60}$, normalized 60-percent-hammer-efficiency blowcount; $(N_1)_{60,fc}$, fines-content corrected normalized standard penetration resistance; $q_{c1}$, normalized cone-penetration resistance; FC, fines content. S.F., San Francisco]

| Site | Case | Seismogram | $I_h$ (m/s) | PGA (g) | CSR | Depth (m) | $I_{hb}$ (m/s) | $(N_1)_{60}$ | $(N_1)_{60,fc}$ | $q_{c1}$ (MPa) | FC (pct) | Liquefaction |
|---|---|---|---|---|---|---|---|---|---|---|---|---|
| S.F.-Oakland Bay Bridge 1 | 3 | Oakland Outer Harbor | 1.71 | 0.29 | 0.25 | 7 | 0.99 | 10 | 11.2 | 8 | 10 | Yes |
| S.F.-Oakland Bay Bridge 2 | 4 | Oakland Outer Harbor | 1.71 | .29 | .26 | 7.5 | .96 | 12 | 13.2 | 11 | 10 | Yes |
| S.F.-Oakland Bay Bridge 3 | 5 | Oakland Outer Harbor | 1.71 | .29 | .26 | 7 | .99 | --- | --- | 9 | 10 | Yes |
| S.F.-Oakland Bay Bridge 4 | 6 | Oakland Outer Harbor | 1.71 | .29 | .26 | 7 | .99 | --- | --- | 5 | 10 | Yes |
| S.F.-Oakland Bay Bridge 5 | 7 | Oakland Outer Harbor | 1.71 | .29 | .26 | 7 | .99 | 10 | 11.2 | 9 | 10 | Yes |
| Treasure Island | 71 | Treasure Island | .54 | .18 | .17 | 6 | .34 | 5 | 5.0 | --- | 5 | Yes |
| Port of Oakland, Seventh St. 1 | 8 | Oakland Outer Harbor | 1.71 | .29 | .23 | 6.5 | 1.03 | --- | --- | 12 | 5 | Yes |
| Port of Oakland, Seventh St. 2 | 9 | Oakland Outer Harbor | 1.71 | .29 | .23 | 6 | 1.00 | 15 | 15.0 | 9 | 2 | Yes |
| Port of Oakland, Seventh St. 3 | 10 | Oakland Outer Harbor | 1.71 | .29 | .22 | 6–7 | .99 | 18 | 18.0 | 7 | 2 | Yes |
| Port of Oakland, Seventh St. 4 | 11 | Oakland Outer Harbor | 1.71 | .29 | .24 | 9 | .88 | 37 | 37.0 | 17 | 5 | No |
| Port of Oakland, Seventh St. 5 | 12 | Oakland Outer Harbor | 1.71 | .29 | .22 | 5 | 1.15 | --- | --- | 12 | 5 | Yes |
| Port of Oakland, Seventh St. 6 | 13 | Oakland Outer Harbor | 1.71 | .29 | .22 | 5.5 | 1.10 | --- | --- | 10 | 5 | Yes |
| Bay Farm Island-Lagoon (CPT1) | 14 | Alameda NAS | .8 | .27 | .23 | 3-4 | .60 | 16.9 | 16.9 | 7 | 2 | Yes |
| Bay Farm Island-S. Loop Rd. | 15 | Alameda NAS | .8 | .27 | .23 | 3-4 | .60 | 15 | 15.0 | 12 | 5 | Yes |
| Bay Farm Island, improved dike | 16 | Alameda NAS | .8 | .27 | .22 | 3-4 | .60 | 38 | 38.0 | 35 | 5 | No |
| Port of Richmond | 82 | City Hall, Richmond/*SHAKE* | .7 | .18 | .17 | 6 | .44 | 5 | 12.0 | 1 | 35 | Yes |
| Port of Richmond | 83 | City Hall, Richmond/*SHAKE* | .7 | .18 | .17 | 6 | .44 | 3 | 10.0 | 1.3 | 35 | Yes |
| Port of Richmond | 84 | City Hall, Richmond/*SHAKE* | .7 | .18 | .17 | 6 | .44 | 3 | 10.0 | 2 | 35 | Yes |
| Oakland International Airport 3 | 17 | Alameda NAS | .8 | .27 | .23 | 2-4 | .58 | 3 | 3.0 | 10 | 5 | Yes |
| Oakland International Airport 4 | 18 | Alameda NAS | .8 | .27 | .23 | 2-4 | .58 | 9 | 9.0 | 5 | 5 | Yes |
| Oakland International Airport 7 | 19 | Alameda NAS | .8 | .27 | .23 | 2-4 | .58 | 12 | 12.0 | 10 | 5 | Yes |

7.5-m depth, but otherwise no liquefaction susceptibility. Likewise, at Bay Farm Island, both methods accurately predict no liquefaction at the improved dike and liquefaction at 3.5- to 4.5-m depth at profile HBI–CPT1; and at Oakland International Airport, both methods predict liquefaction in a zone between approximately 2- and 5-m depth.

The CPT data used to construct the plot of $I_{hb}$ versus $q_{c1}$ in figure 30*A* are almost exclusively from the Loma Prieta data set. $q_{c1}$ is plotted against CSR in figure 30*B* with respect to the boundary curves proposed by Robertson and Campanella (1985), Seed and de Alba (1986), Shibata and Teparaksa (1988), and Mitchell and Tseng (1990). The boundary curves proposed by Robertson and Campanella (1985) and Seed and de Alba (1986) are based on $q_c/N$ ratios rather than direct field investigations of liquefaction test sites. The method of Shibata and Teparaksa (1988) is based on a limited data set of direct measurements at liquefaction sites for earthquakes in Japan, China, and the United States. Mitchell and Tseng (1990) proposed boundary curves developed from the $q_c$-$D_r$ (relative density)-CSR relation at a given effective confining stress, which are based on cavity-expansion theory and cone-chamber test results.

The data points for sandy-fill deposits in the east bay observed to have liquefied plot on or to the left of the boundary curves proposed by Robertson and Campanella (1985), Shibata and Teparaksa (1988), and Mitchell and Tseng (1990) for medium sand. The dense layers at borehole POO7–3 and the Bay Farm Island dike (fig. 24), which are not believed to have liquefied, plot to the right of all the boundary curves. One boundary curve proposed by Seed and de Alba (1986) did not fully capture the observed occurrences of liquefaction for several soil layers and appears to be somewhat unconservative. The boundary curve for $D_{50}$=0.05 mm proposed by Shibata and Teparaksa (1988) falls to the left of the data points for the Port of Richmond study site and appears to be somewhat unconservative for fine-sand material.

## CONCLUSIONS

Extensive soil liquefaction occurred during the 1989 Loma Prieta earthquake in uncompacted artificial-fill deposits of the east bay from Oakland International Airport to the Port of Richmond, from 65 to 85 km from the north end of the rupture zone. We present the results of studies at five sites near the east-bay shoreline: the Port of Richmond, San Francisco-Oakland Bay Bridge Toll Plaza, the Port of Oakland's Marine Container Facility at Seventh Street, Bay Farm Island and Harbor Bay Plaza, and Oakland International Airport. Typical of all these sites are extremely low to low $N$ and $q_c$ values in layers of cohesionless hydraulic fill that overlie deep, primarily cohesive soil deposits. Two factors, low density (as reflected by low penetration resistance) and amplification of seismic shaking by the underlying soils, combined to give the sites a relatively high liquefaction susceptibility.

Comparing the CSR- and Arias intensity-based methods for assessing soil-liquefaction potential, we found that when using SPT data, the two methods agree in predict-

ing the occurrence or nonoccurrence of liquefaction in soils layers at our study sites during the earthquake. The CPT data allow for an evaluation of liquefaction susceptibility using various proposed CSR-based boundary curves. We found that the proposed boundary curves of Robertson and Campanella (1985), Shibata and Teparaksa (1988), and Mitchell and Tseng (1990) did well in distinguishing liquefiable from nonliquefiable soils at our study sites, whereas the boundary curve proposed by Seed and de Alba (1986) appears to be somewhat unconservative. Field data from the Loma Prieta study sites allow us to construct an Arias intensity/cone-penetration-resistance boundary for assessment of soil-liquefaction potential.

## ACKNOWLEDGMENTS

This research was supported the U.S. Geological Survey and an unrestricted gift to the University of California, Berkeley, from the Institute of Technology, Shimizu Corp., Japan. We thank Angela Lodge (University of California, Berkeley) and Roberto Coutinho (Universidade Federal de Pernambuco, Brazil) for their participation in the collection of field data. John Egan and Larry Scheibel (Geomatrix Consultants, Inc.) generously contributed data for several of the east-bay study sites.

## REFERENCES CITED

Ambraseys, N.N., 1988, Engineering seismology: Earthquake Engineering & Structural Dynamics, v. 17, no. 1, p. 1–105.

American Society for Testing and Materials, 1984, Standard method for penetration test and split-barrel sampling of soils: Annual Book of ASTM standards, sec. 4, v. 04.08, D1586–84.

———1986a, Standard method for quasi-static, cone and friction cone penetration test of soil, Annual Book of ASTM standards, Section 4, Volume 04.08, D3441–86.

———1986b, Standard test method for stress wave energy measurement for dynamic penetrometer testing systems: Annual Book of ASTM Standards, sec. 4, v. 04.08, D4633–86, p. 943–946.

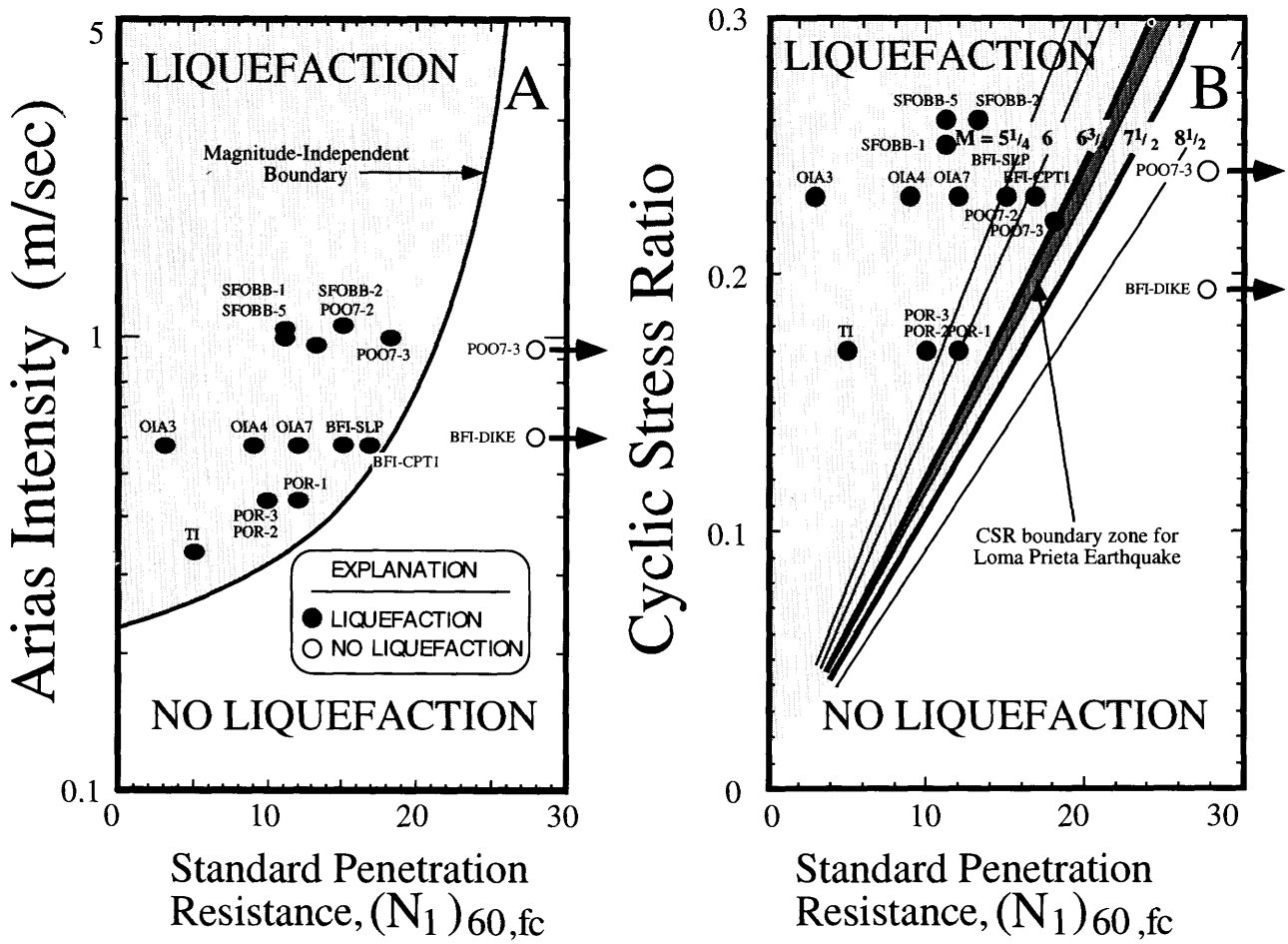


Figure 28.—Assessment of soil-liquefaction potential from Arias intensity versus cyclic-stress-ratio method. *A*, Arias intensity within soil column versus normalized 60-percent-hammer-efficiency blowcount for sites in the United States and Japan, with fines-content correction to equivalent "clean sand." *B*, Cyclic-stress ratio versus normalized 60-percent-hammer-efficiency blowcount for Loma Prieta study sites.

Arango, Ignacio, 1996, Magnitude scaling factors for soil liquefaction evaluations: Journal of Geotechnical Engineering, v. 122, no. 11, p. 929–936.

Borcherdt, R.D. *ed.*, 1994, The Loma Prieta, California, earthquake of October 17, 1989—strong ground motion: U.S. Geological Survey Professional Paper 1551–A, p. A1–A272.

Campanella, R.G., and Robertson, P.K., 1982, State-of-the-art in in-situ testing of soils; developments since 1978: Engineering Foundation Conference on Updating Subsurface Sampling of Soils and Rocks and Their In-Situ Testing, Santa Barbara, Calif., 1982, Proceedings, p. 1–23.

Farrar, J.A., 1991, Field energy measurements of standard penetration testing: Denver, University of Colorado, M.S. thesis, 400 p.

Hardin, B.O., and Drnevich, V.P., 1972, Shear modulus and damping of soils; measurement and parameter effects: American Society of Civil Engineers Proceedings, Soil Mechanics and Foundations Division Journal, v. 98, no. SM6, p. 603–624.

Kayen, R.E., 1993, Accelerogram-energy approach for prediction of earthquake-induced ground liquefaction: Berkeley, University of California, Ph.D. thesis, 289 p.

Kayen, R.E., Mitchell, J.K., Lodge, A.G., Seed, R.B., Nishio, Shin'ya, and Coutinho, Roberto, 1992, Evaluation of SPT-, CPT-, and shear wave-based methods for liquefaction potential assessment using Loma Prieta data, *in* Hamada, Masanori, and O'Rourke, T.D., eds., Proceedings of the Fourth Japan-U.S. Workshop on Earthquake Resistant Design of Lifeline Facilities and Countermeasures for Soil Liquefaction: Buffalo, N.Y., National Center for Earthquake Research Technical Report NCEER–92–0019, v. 1, p. 177–204.

Kayen, R.E., Mitchell, J.K., and Holzer, T.L., 1994, Ground motion characteristics and their relation to soil liquefaction at the Wildlife Liquefaction Array, Imperial Valley, California, *in* O'Rourke, T.D., and Hamada, Masanori, eds., Proceedings of the Fifth U.S.-Japan Workshop on Earthquake Resistant Design of Lifeline Facilities and Countermeasures for Soil Liquefaction: Buffalo, N.Y., National Center for Earthquake Research Technical Report NCEER–94–0026, p. 267–283.

Kayen, R.E., and Mitchell, J.K., 1997, Assessment of liquefaction potential during earthquakes by Arias intensity: Journal of Geotechnical and Geoenvironmental Engineering, ASCE, v. 123, no. 12.

Liang, Liqun, Figueroa, J.L., and Saada, A.S., 1995, Liquefaction under random loading; unit energy approach: Journal of Geotechnical Engineering, v. 121, no. 11, p. 776–781.

Mitchell, J.K., and Tseng, D.-J., 1990, Assessment of liquefaction potential by cone penetration resistance, *in* Duncan, J.M., ed., H. Bolton Seed Memorial Symposium: Berkeley, Calif., BiTech, v. 2, p. 335–350.

Mitchell, J.K., Lodge, A.L., Coutinho, R.Q., Kayen, R.E., Seed, R.B., Nishio, Shin'ya, and Stokoe, K.H., II, 1994, Insitu test results from four Loma Prieta earthquake liquefaction sites; SPT, CPT, DMT and shear wave velocity: Berkeley, University of California, Earthquake Engineering Research Center Report UCB/EERC–94/04, 179 p.

Robertson, P.K., 1986, In situ testing and its application to foundation engineering: Canadian Geotechnical Journal, v. 23, no. 4, p. 573–594.

———1990, Soil classification using the cone penetration test: Cana-

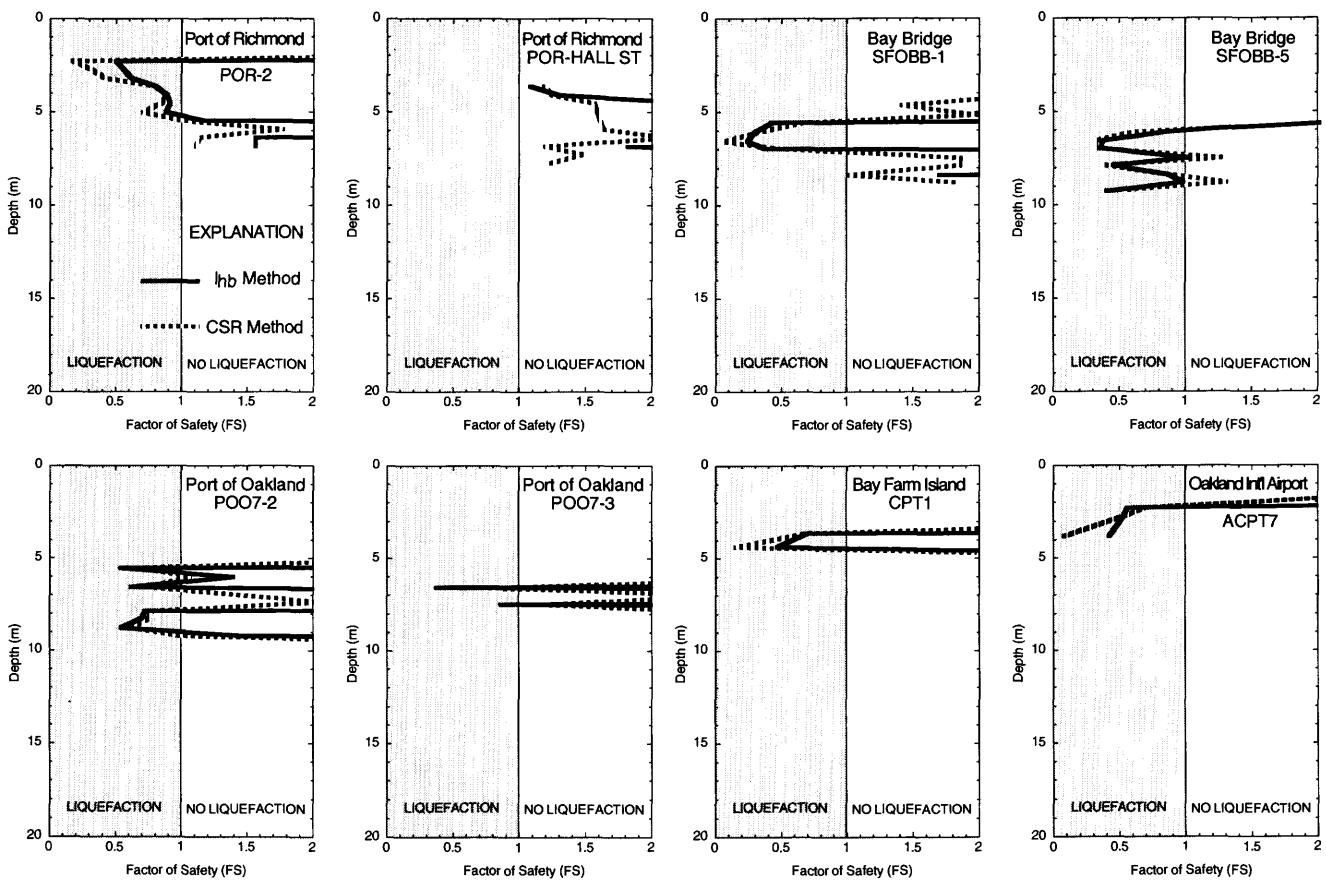


Figure 29.—Comparison of factor of safety against liquefaction (FS£1.0 = liquefaction; FS>1.0 = no liquefaction) for study sites on east side of San Francisco Bay, using Arias intensity and cyclic-stress-ratio methods.

dian Geotechnical Journal, v. 27, no. 1, p. 151–158.
Robertson, P.K. and Campanella, R.G., 1985, Liquefaction of sands using the CPT: American Society of Civil Engineers Proceedings, Geotechnical Engineering Division Journal, v. 111, no. GT3, p. 384–403.
Robertson, P.K., Campanella, R.G., Gillespie, Don, and Rice, A., 1986, Seismic CPT to measure in situ shear wave velocity: Journal of Geotechnical Engineering, v. 112, no. 8, p. 791–803.
Schnabel, P.B., Lysmer, John, and Seed, H.B., 1972, SHAKE; a computer program for earthquake response analysis of horizontally layered sites: Berkeley, University of California, Earthquake Engineering Research Center Report UCB/EERC–72/12.
Seed, H.B., and de Alba, Pedro, 1986, Use of SPT and CPT tests for evaluating the liquefaction resistance of sands, in Clemence, S.P. ed., Use of in-situ tests in geotechnical engineering: New York, American Society of Civil Engineers, p. 281–302.
Seed, H.B., and Idriss, I.M., 1971, Simplified procedure for evaluating soil liquefaction potential: American Society of Civil Engineers Proceedings, Soil Mechanics and Foundations Division Journal, v. 97, no. SM9, p. 1249–1273.
———1982, Ground motions and soil liquefaction during earthquakes: Berkeley, University of California, Earthquake Engineering Research Institute, 139 p.
Seed, H.B., Idriss, I.M., and Arango, Ignacio, 1983, Evaluation of liquefaction potential using field performance data: Journal of Geotechnical Engineering, v. 109, no. 3, p. 458–482.
Seed, H.B., Tokimatsu, Kohji, Harder, L.H., and Chung, R.M., 1984, The influence of SPT procedures in soil liquefaction evaluations: Berkeley, University of California, Earthquake Engineering Research Center Report 84–15, 50 p.
Seed, R.B., Dickenson, S.E., Reimer, M.F., Bray, J.D., Sitar, Nicholas, Mitchell, J.K., Idriss, I.M., Kayen, R.E., Kropp, Alan, Harder, L.F., Jr., and Power, M.S., 1990, Preliminary report on the principal geotechnical aspects of the October 17, 1989 Loma Prieta earthquake: Berkeley, University of California, Earthquake Engineering Research Center Report UCB/EERC–90/05, 137 p.
Shakal, A.F., Huang, M.J., Reichle, Michael, Ventura, C.E., Cao, T.Q., Sherbourne, R.W., Savage, M.K., Darragh, R.B., and Petersen, C.P., 1989, CSMIP strong-motion records from the Santa Cruz Mountains (Loma Prieta), California earthquake of 17 October 1989: California Division of Mines and Geology, Office of Strong Motion Studies Report OSMS 89–06, 196 p.
Shibata, Toru, and Teparaksa, Wanchai,1988, Evaluation of liquefaction potentials of soils using cone penetration tests: Soils and Foundations, v. 28, no. 2, p. 49–60.
Spudich, Paul, ed., 1996, The Loma Prieta, California, earthquake of October 17, 1989—main-shock characteristics: U.S. Geological Survey Professional Paper 1550–A, p. A1–A297.
Wroth, C.P., 1984, The interpretation of in situ soil tests: Géotechnique, v. 34, no. 4, p. 449–489.

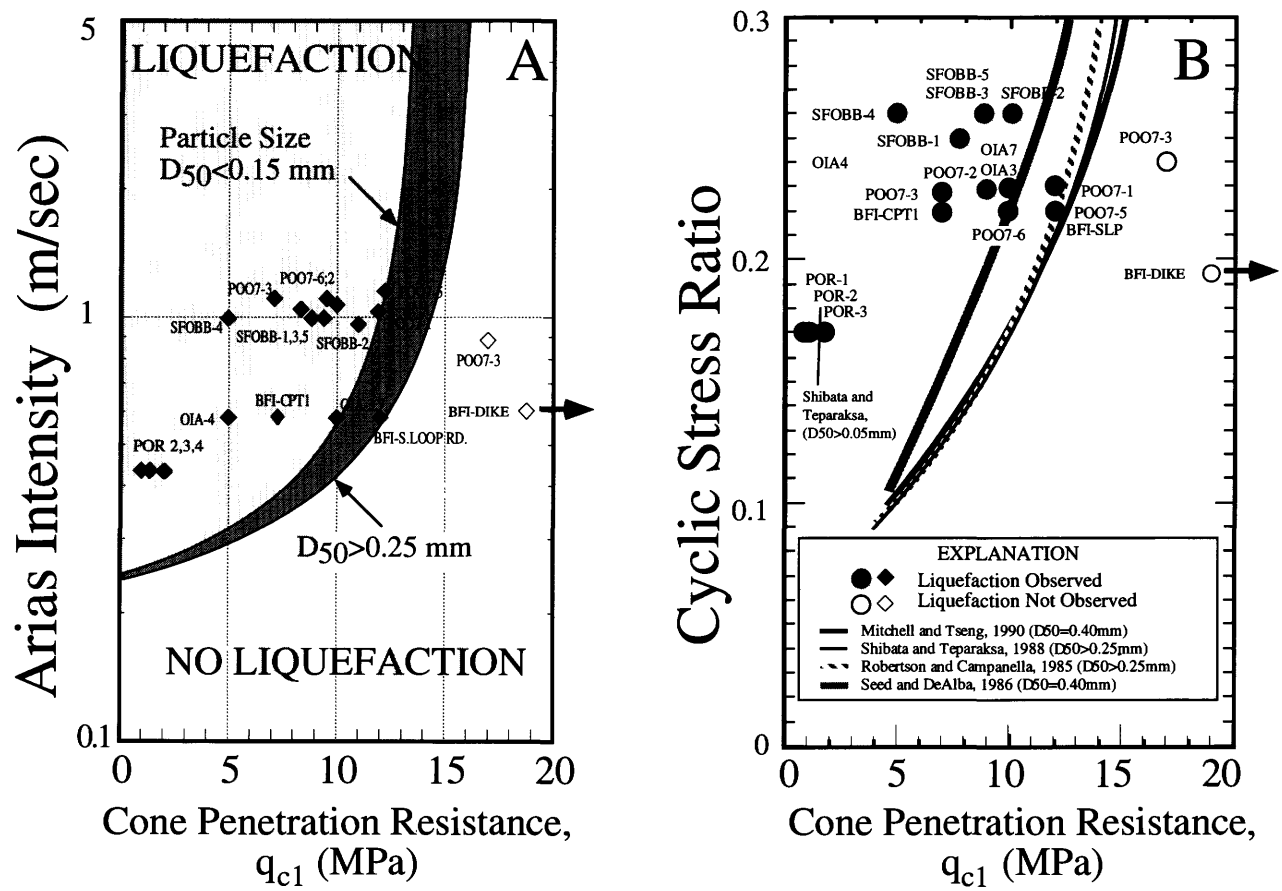


Figure 30.—Assessment of soil-liquefaction potential from Arias intensity versus cyclic-stress-ratio method, showing plots of Arias intensity within soil column (*A*) and cyclic-stress ratio (*B*) versus normalized cone-penetration resistance for Loma Prieta study sites listed in table 1.

STRONG GROUND MOTION AND GROUND FAILURE

# ANALYSIS OF LIQUEFACTION-INDUCED DAMAGE ON TREASURE ISLAND

By Maurice S. Power and John A. Egan, Geomatrix Consultants;
Scott E. Shewbridge, Scott Shewbridge Associates; and
John deBecker and J. Richard Faris,
U.S. Navy, Naval Facilities Engineering Command, Western Division

## CONTENTS



ABSTRACT

During the 1989 Loma Prieta earthquake, liquefaction occurred in hydraulically placed sand fill on Treasure Island, a manmade island in San Francisco Bay. Comparison of preearthquake and postearthquake survey data, mapping of ground cracks, and other postearthquake observations established that the island settled and spread laterally several inches during the earthquake. Locally, settlements as great as 2 ft were documented. Damage to the U.S. Naval Station buildings on the island was generally minor, but some buildings were moderately damaged, particularly in lateral-spreading zones near the island's perimeter. Utilities were extensively damaged.

The recorded level of ground shaking on the island, the occurrence of liquefaction, and the magnitude of liquefaction-induced compaction settlements were reasonably consistent with postearthquake analyses using state-of-the-art methods. Residual strengths for the liquefied sand were inferred from backanalyses of observed lateral-spreading displacements. During future earthquakes that could be larger and (or) closer to Treasure Island than the 1989 Loma Prieta earthquake, the potential for ground failure on the island is much higher than in 1989. The liquefaction hazard, which is the chief ground-failure hazard on the island, could be effectively mitigated by creating a ground-stabilized buttressing area near the island's edge.

## INTRODUCTION

The U.S. Naval Station on Treasure Island (fig. 1) is located on a manmade island that was created during the mid-1930's by hydraulically placing sand fill over soft sedimentary deposits in San Francisco Bay. During the 1989 Loma Prieta earthquake, the sand fill composing the island liquefied. As a result, small amounts of lateral spreading (generally less than 1 ft of horizontal movement) occurred around the island's perimeter, and the interior of the island subsided several inches. The U.S. Navy conducted a study (Geomatrix Consultants, 1990a, b) to investigate the island's behavior during the earthquake, as well as to evaluate its expected behavior during future earthquakes that could occur closer to Treasure Island and (or) be larger than the 1989 Loma Prieta earthquake. This paper focuses on aspects of that study which describe the observed behavior of the island during this earthquake,

and compares the observations with predictions made by using current analytical methods and correlations.

## CONSTRUCTION HISTORY

Accounts of Treasure Island's construction provide an important initial picture of geotechnical conditions on the island. In an effort to collect information about the creation of Treasure Island, we consulted many potential sources, including U.S. Army Corps of Engineers records stored at the National Archives and Records Center in San Bruno, Calif.; files of the U.S. Navy's Naval Facilities Engineering Command, Western Division, in San Bruno; the historical archives of the Bancroft Library at the University of California, Berkeley, and of the San Francisco Public Library; television stations KQED and KRON documentary program files; and the geotechnical

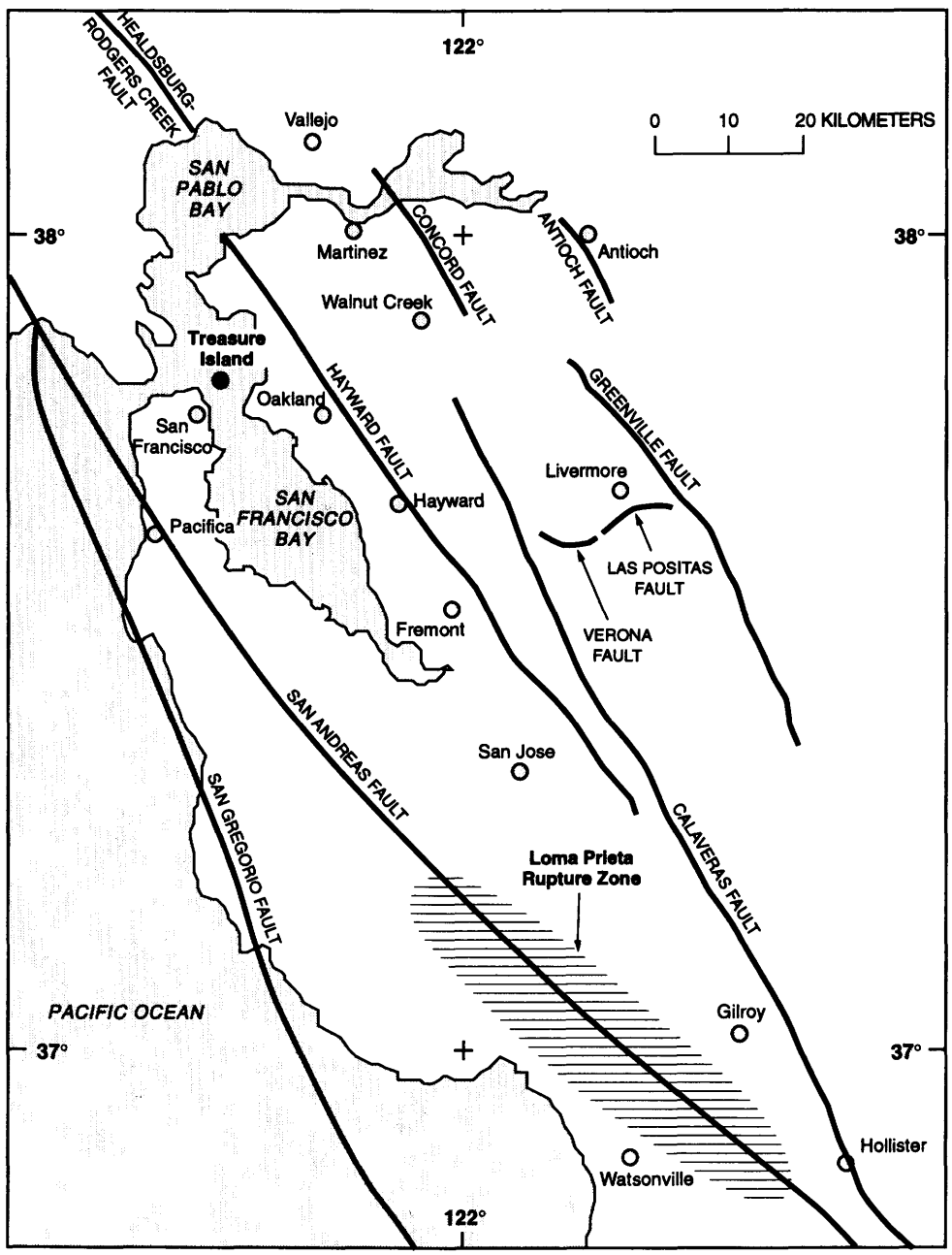


Figure 1.—San Francisco Bay region, showing location of Treasure Island in relation to active faults and rupture zone of 1989 Loma Prieta earthquake.

literature. From these sources, we obtained written documents, photographs, and plans that report on various aspects of Treasure Island's filling history. These records mostly addressed the perimeter-dike construction, the dredging equipment, fill-material borrow sources and the type and quantity of materials handled, and the general sequence of filling for the island. Little information is available, however, regarding such details as where and what type of fill material (or from what borrow source(s)) was placed in the island during the filling operation; thus, the possible spatial variation of material characteristics within the island fill cannot be defined from these historical records. Nonetheless, these accounts of the island's construction have been valuable in helping us evaluate the expected performance of Treasure Island and its facilities during future strong earthquake ground shaking, on the basis of the performance of similar hydraulically placed fills during large earthquakes. Accounts of the construction of Treasure Island reported by the Engineering News-Record (1937, 1938), Lee (1969), and Hagwood (1980) provide the basis for our summary of the island-filling operation presented below.

Treasure Island was originally conceived of as a midbay airport facility. The concept quickly evolved into a site for celebration of the completion of the Golden Gate and San Francisco-Oakland Bay Bridges, which took the form of the 1939 Golden Gate International Exposition. The shape and dimensions of the island (approx 5,500 ft long by 3,400 ft wide) were dictated by requirements for the airport that was still planned to replace the exposition after its closure. More than 29 million $yd^3$ of dredged material, mostly sand, was handled during filling operations that began in February 1936 and were completed in August 1937. Approximately 21 million $yd^3$ remained in place to create the 397-acre-area island over the shallow Yerba Buena Shoals north of Yerba Buena Island; the rest was lost to wind erosion, settlement, and washing away of fines during deposition. The bay bottom of the shoals area ranged in elevation from 2 to 26 ft below mean lower low water (MLLW) across the island footprint. Approximately 75 percent of the bay bottom in this area was composed of sand, and soft clay was exposed over the rest of the site. Bay-bottom conditions before island construction, including the approximate limits of the sand and clay bottom sediment, are mapped in figure 2.

Treasure Island was constructed under the direction of the U.S. Army Corps of Engineers by hydraulically placing the fill materials with pipeline (suction), hopper, and clamshell dredging equipment. In areas where the bay bottom was below 6 ft MLLW, a bed of hydraulic sand fill was placed to raise the bottom to this elevation. Next, along the island's perimeter, a low mound of rock was placed on either the native soil or fill materials to act as a retaining dike for subsequently placed sand fill. Fill material was pumped or deposited in place until it approximately reached the top of this low rock mound; another low rock mound was then placed on the previously constructed rock dike, and filling operations continued. This process was repeated until the surface of the fill reached approximately 13 ft above MLLW. The rock dikes were not constructed to surround the entire island concurrently but progressed outward as fill was deposited, starting at the southwest corner of the island and working their way around the west, south, and east toward the north. On the north and west sides of the island, these dikes also acted as backing for a uniformly riprapped slope. This construction method resulted in an island configuration of hydraulically placed sand fill retained by a relatively thin rock face founded on either native shoal materials or hydraulically placed fill. Cross sections of the original perimeter-dike configuration are shown in figure 3.

The perimeter dike failed during construction near the north end of the east dike: A 500-ft-long section of the dike settled 10 to 14 ft. This area was stabilized by flattening the slope and placing a bed of "heavy" sand beyond the toe of the dike to act as a counterweight (Lee, 1969). As a result of this failure, the north seawall was modified by excavating a trench approximately 400 ft wide by 30 to 40 ft deep along the seawall, backfilling the trench with coarse sand, and then constructing the initial rock dike on that bed of sand. The approximate location of the excavated area is shown in figure 3.

Dredged material for the filling operation was obtained from various borrow sources within San Francisco Bay, as mapped in figure 4. Material obtained from borrow areas immediately south, east, and north of the island's footprint was a blue silty, fine sand. A yellow, well-graded, fine to medium sand was obtained from an east-bay borrow area about 3,000 ft east of the island (Lee, 1969). Coarse sand and gravel were hauled to the site in hopper dredges from the Presidio, Alcatraz, and Knox Shoals.

A low weir was installed near the center of the north seawall to allow water from the hydraulic dredges and soft mud to escape as the filling proceeded from south to north. A mud wave formed, however, and soft mud became trapped within the island perimeter. A small dredge was set up inside the seawall and excavated 6 to 12 ft into this mud. This small dredge continued to excavate mud as it was pushed up by the filling operations.

Several projects to protect the riprapped face of the perimeter dikes have been undertaken since the original construction, resulting in the placement of additional rock facing and, in local areas, widening of the perimeter dikes. Where these dikes have been widened, the composition of additional dike materials is presently unknown. Siltation has also resulted in the deposition of materials outside of the perimeter dikes, and erosion has apparently removed

some shoal sand materials outside of the perimeter dikes at the northwest corner of the island.

## SUBSURFACE CONDITIONS

We investigated the subsurface conditions on Treasure Island both by compiling preexisting geotechnical information and by conducting supplementary subsurface explorations around the perimeter of the island. The preexisting geotechnical information consisted of geotechnical reports and accompanying borehole logs and laboratory-test data in U.S. Navy files. We compiled data from 182 boreholes drilled during 31 previous geotechnical studies for various Treasure Island facilities. The locations of these boreholes are shown in figure 5.

The supplementary exploration program included 12 onshore boreholes, 7 offshore boreholes, and 36 onshore cone-penetration tests (CPT's); the locations of boreholes and CPT probes are shown in figure 5. Laboratory tests were conducted on samples recovered from boreholes, including particle-size analyses, liquid- and plastic-limit determinations, water-content and dry-density tests, consolidation tests, and both unconsolidated undrained (UU) and consolidated undrained (CU) triaxial tests. Field data and (or) laboratory-test data contained in borehole logs and geotechnical reports that were pertinent to the present study were compiled into a computerized data base

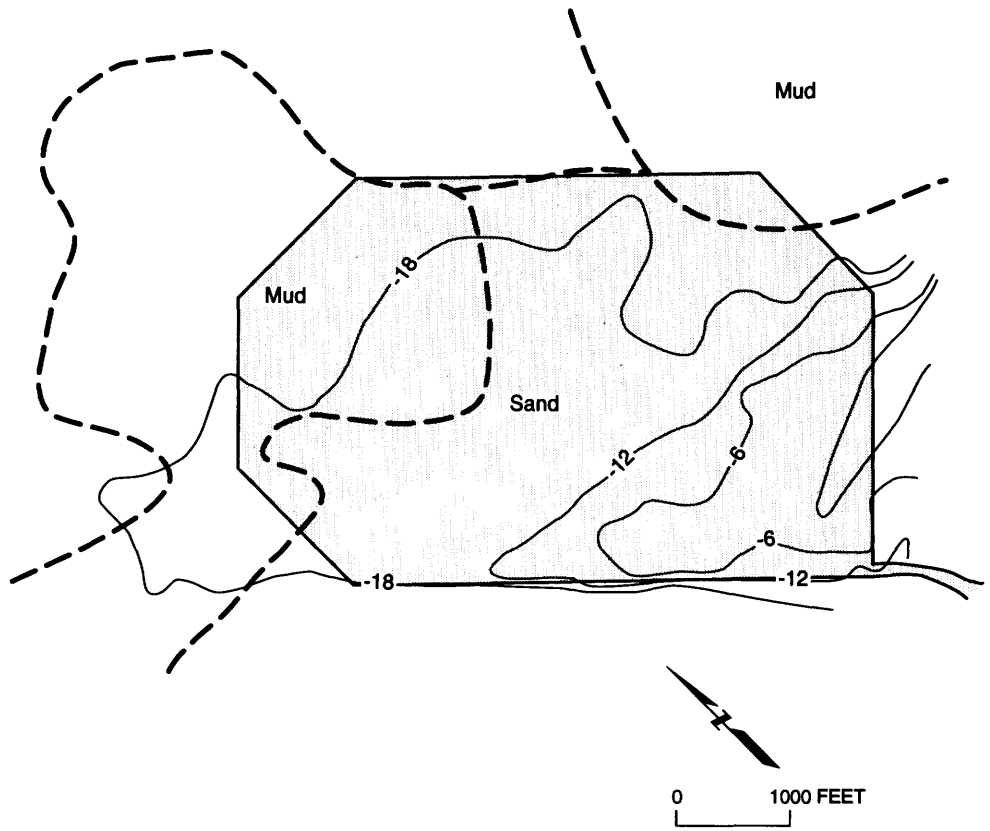


Figure 2.—Sketch map of Treasure Island (shaded area), showing preconstruction conditions and contours of original bay bottom. From Lee (1969).

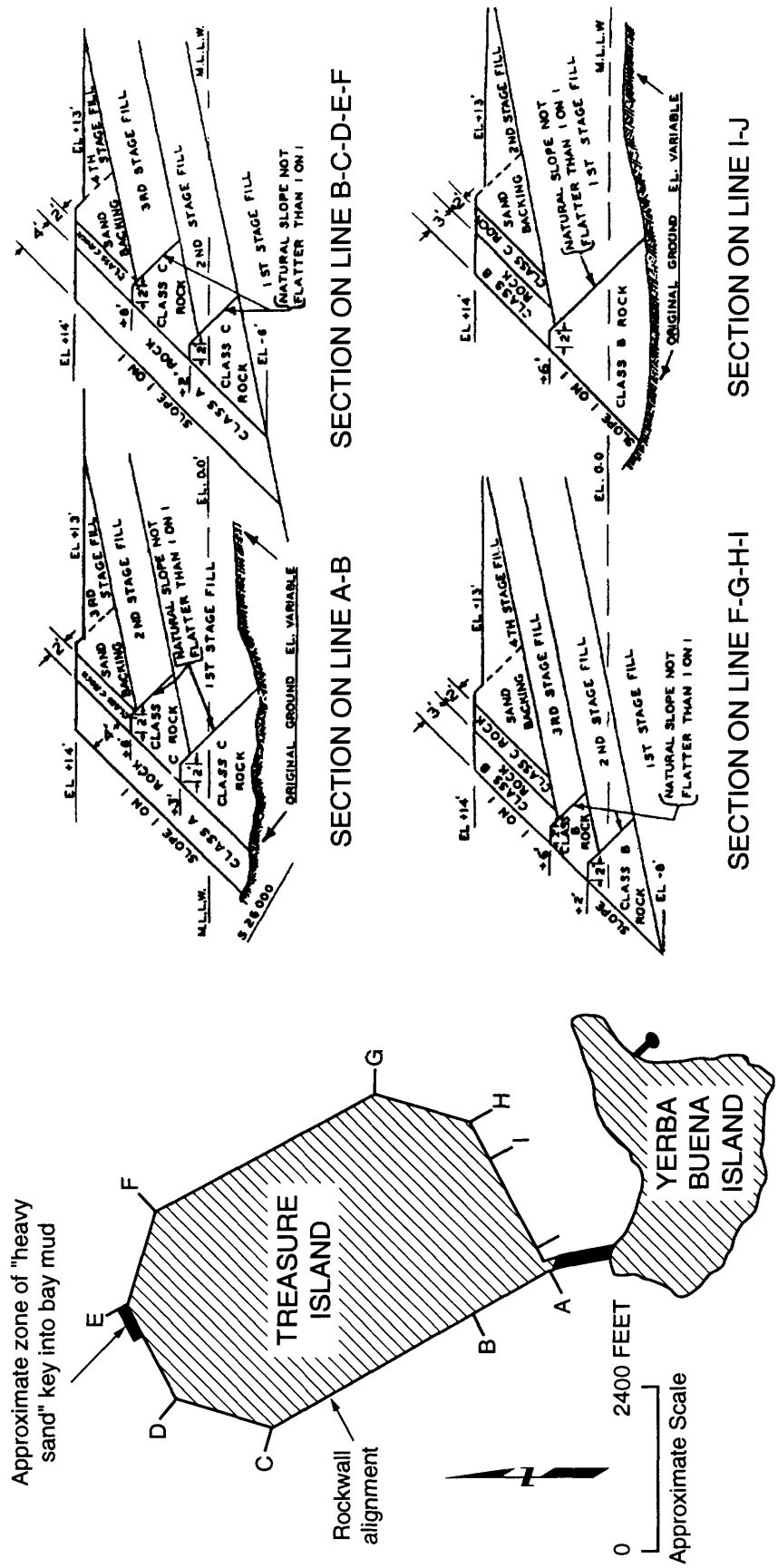


Figure 3.—Treasure Island and Yerba Buena Island, showing configuration of original perimeter dikes as mapped by U.S. Engineers Office, San Francisco, in March 1936 (from Hagwood, 1980).

(Geomatrix Consultants, 1990a) containing data for more than 2,000 sample locations.

## GENERAL STRATIGRAPHIC CONDITIONS

Treasure Island is relatively flat. The top of the perimeter dikes range in elevation from 10.5 to 16 ft above MLLW, and the island's interior ground surface ranges in elevation from about 6.5 to 14.5 ft above MLLW.

Subsurface materials penetrated in the boreholes and CPT probes can generally be divided into four strata: hydraulically placed sand fill; native Yerba Buena Shoals sand and clay; bay mud, consisting primarily of soft to stiff olive-gray silty clay; and older bay sedimentary deposits, consisting of brownish- and greenish-gray, very stiff sandy, silty, and (or) peaty clay and dense sand. The generalized subsurface stratigraphic conditions across the island are illustrated in three north-south and two east-west cross sections in figure 6, and several cross sections through the perimeter dike are shown in figure 7. Additional cross sections through the perimeter dike, as identified in figure 5, were presented by Geomatrix Consultants (1990b); these cross sections provide additional details regarding the various subsurface materials. A generalized circumferential cross section illustrating the stratigraphy of the subsurface materials penetrated in the boreholes and CPT probes along and adjacent to the perimeter dikes is shown in figure 8.

The sand fill and shoal sand range in combined thickness from approximately 30 to 50 ft, except in a small area on the north side of the island where a key was dredged below the bay bottom. In this area, the sand fill is approximately 70 ft thick (see cross sec. *D–D'*, fig. 7). The bay mud, which ranges in thickness from approximately 10 to 120 ft, is thinnest on the eastern perimeter and thickest on the northwest side of the island. The older bay sedimentary deposits below the bay mud extend to Franciscan bedrock. The thickness of these older bay sedimentary deposits is not definitely known because only a few boreholes on the island reached bedrock. One borehole, drilled in 1966 during a study for the proposed U.S. Naval School Command Barracks, indicates that bedrock is about 280 ft below the ground surface (borehole 69, fig. 5). Two boreholes drilled during the same year for an office building indicate bedrock at about 125 and 200 ft below the ground surface (boreholes 154 and 152, respectively, fig. 5). An additional borehole drilled in 1992 (de Alba and others, 1992) indicates bedrock at about 300-ft depth near the fire station (fig. 5) and strong-motion-recording instrument. On the basis of this information and the data of Goldman (1969), we believe that the depth to bedrock on Treasure Island ranges from approximately 100 to 400 ft below the ground surface and is shallowest on the south side of the island (nearest Yerba Buena Island, fig. 3) and deepest to the north.

Ground-water levels on Treasure Island are affected by tidal fluctuations. During floodtide, ground-water

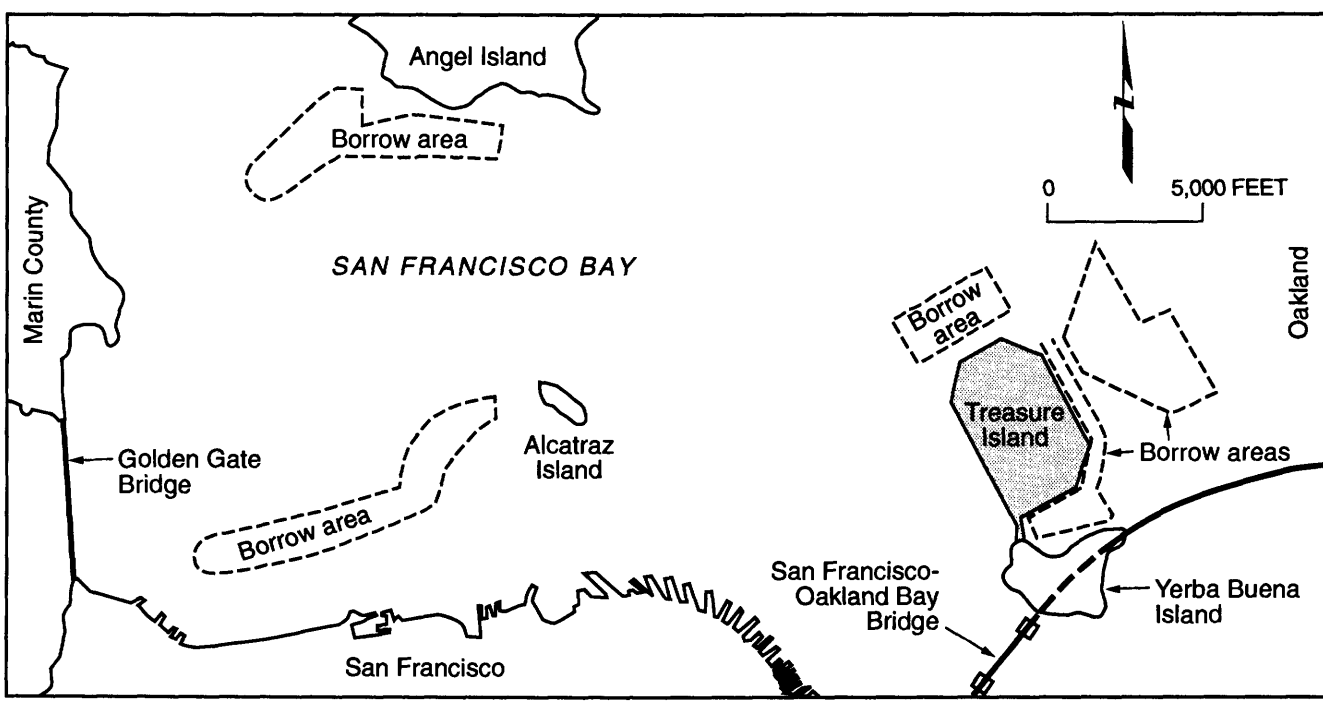


Figure 4.—San Francisco Bay, showing locations of dredge borrow areas used in construction of Treasure Island.

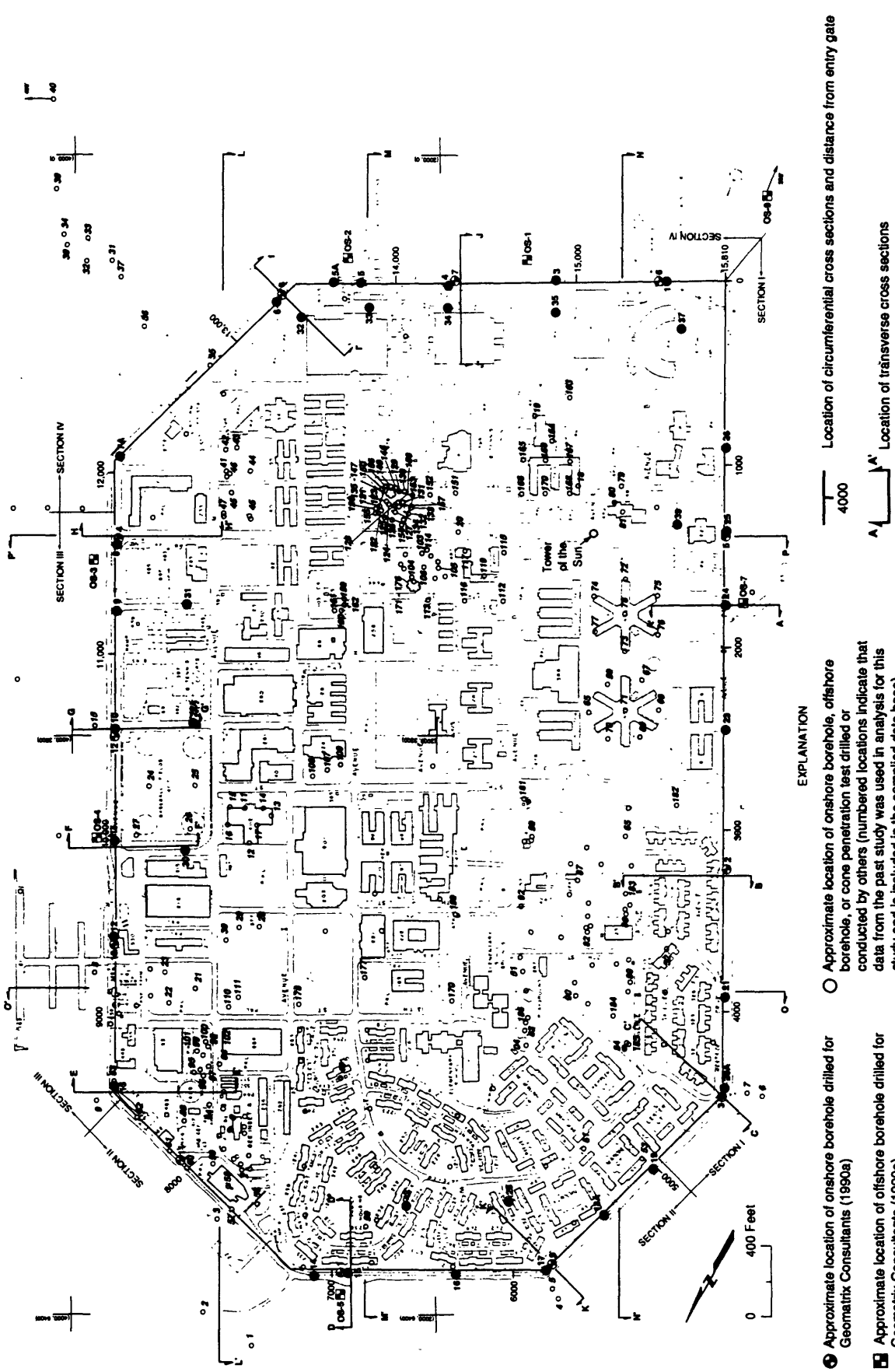


Figure 5.—Treasure Island, showing locations of subsurface explorations and cross sections in figures 6 through 8, and 10. Sections I through IV indicate areas for which $(N_1)_{60}$ values were compared with critical $(N_1)_{60}$ values for liquefaction.

levels rise, reaching an average elevation of 6 ft above MLLW; during ebbtide, ground-water levels fall, reaching an elevation of 0 ft above MLLW. Ground-water levels on the island are affected by the rate of seepage into and out of the sand-fill materials and may not reach the same height as the bay. During the 1989 Loma Prieta earthquake, the tide was between high and low; thus, we believe that the ground-water level and the elevation of the bay were approximately 3 ft above MLLW.

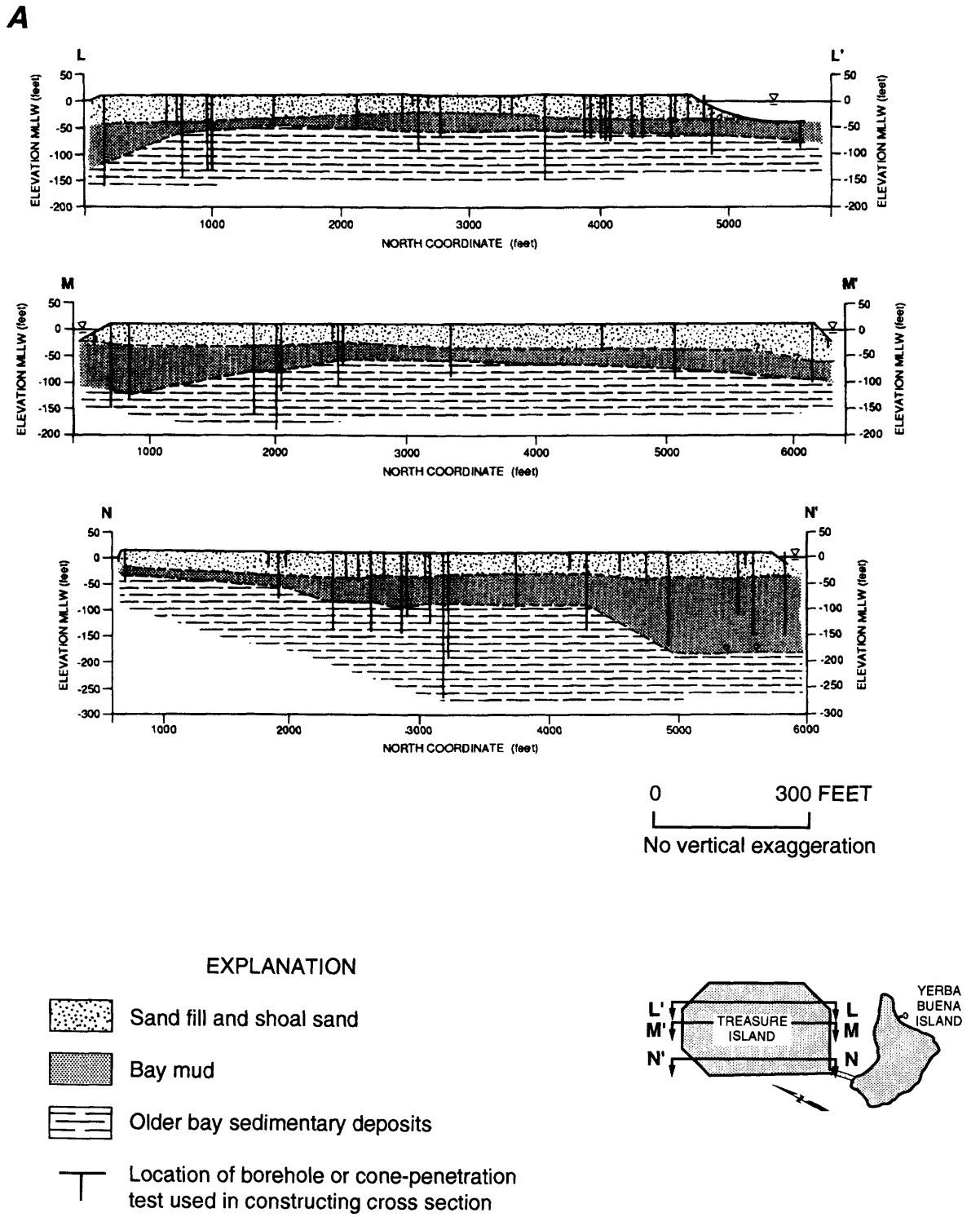


Figure 6.—Stratigraphic cross sections in longitudinal (north-south) (*A*) and transverse (east-west) (*B*) directions on Treasure Island (see fig. 5 for locations).

## SOIL CHARACTERISTICS

### SAND FILL AND SHOAL SAND

The fill material penetrated in boreholes matches well the material described by Lee (1969). The fill is a clean to silty sand with a few clayey-sand zones. Generally, the sand is poorly graded, but it contains well-graded zones. The underlying Yerba Buena Shoals materials consist of clean to clayey sand with clay layers. In boreholes, the sand fill is typically difficult to distinguish from the underlying shoal sand. The fill generally is somewhat looser and has a lower penetration resistance and a lower shell content. On average, however, the sand fill and shoal sand appear to be nearly identical in engineering characteristics, and their behavior during earthquakes may be expected to be similar.

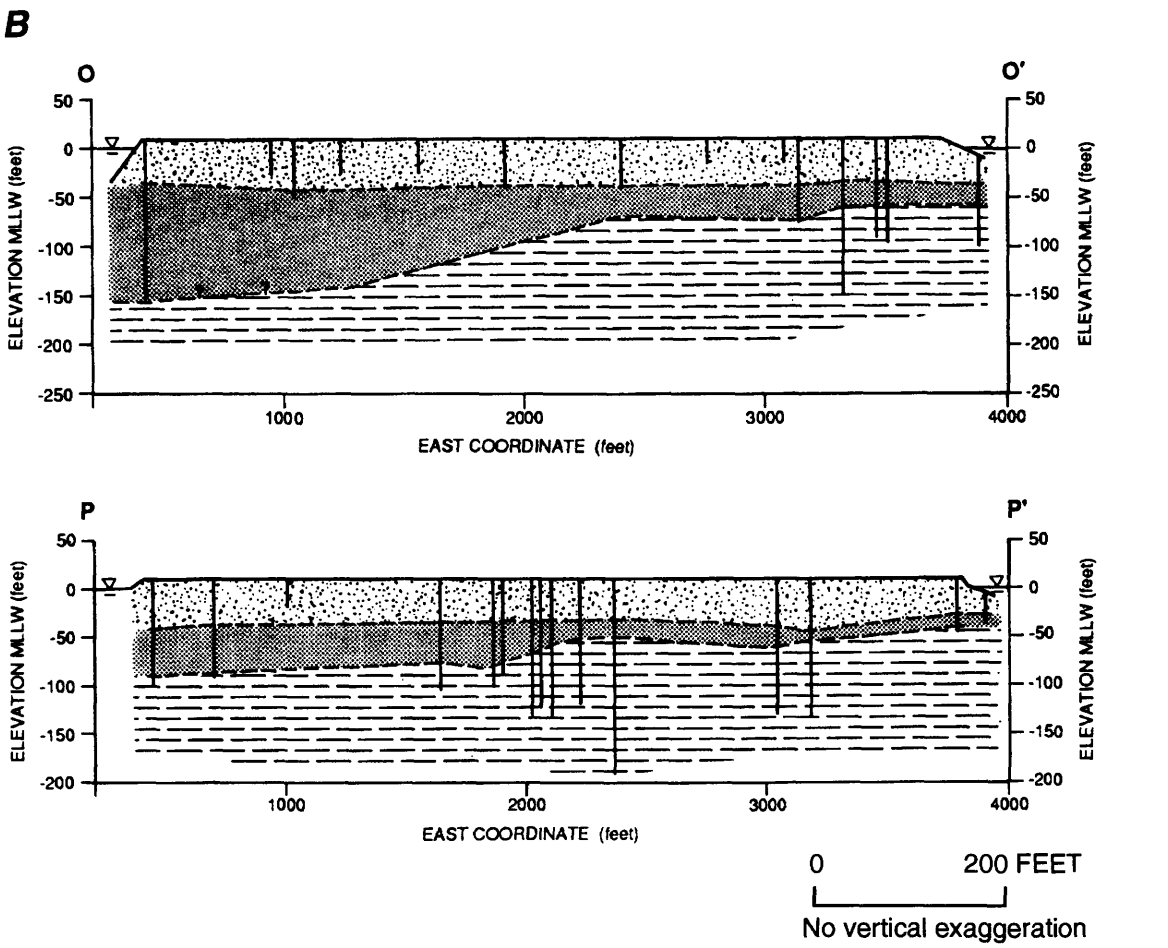


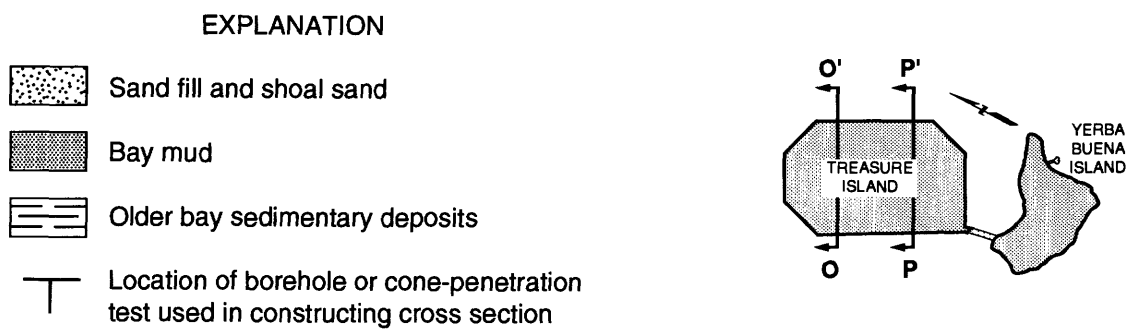


Figure 6.—Continued.

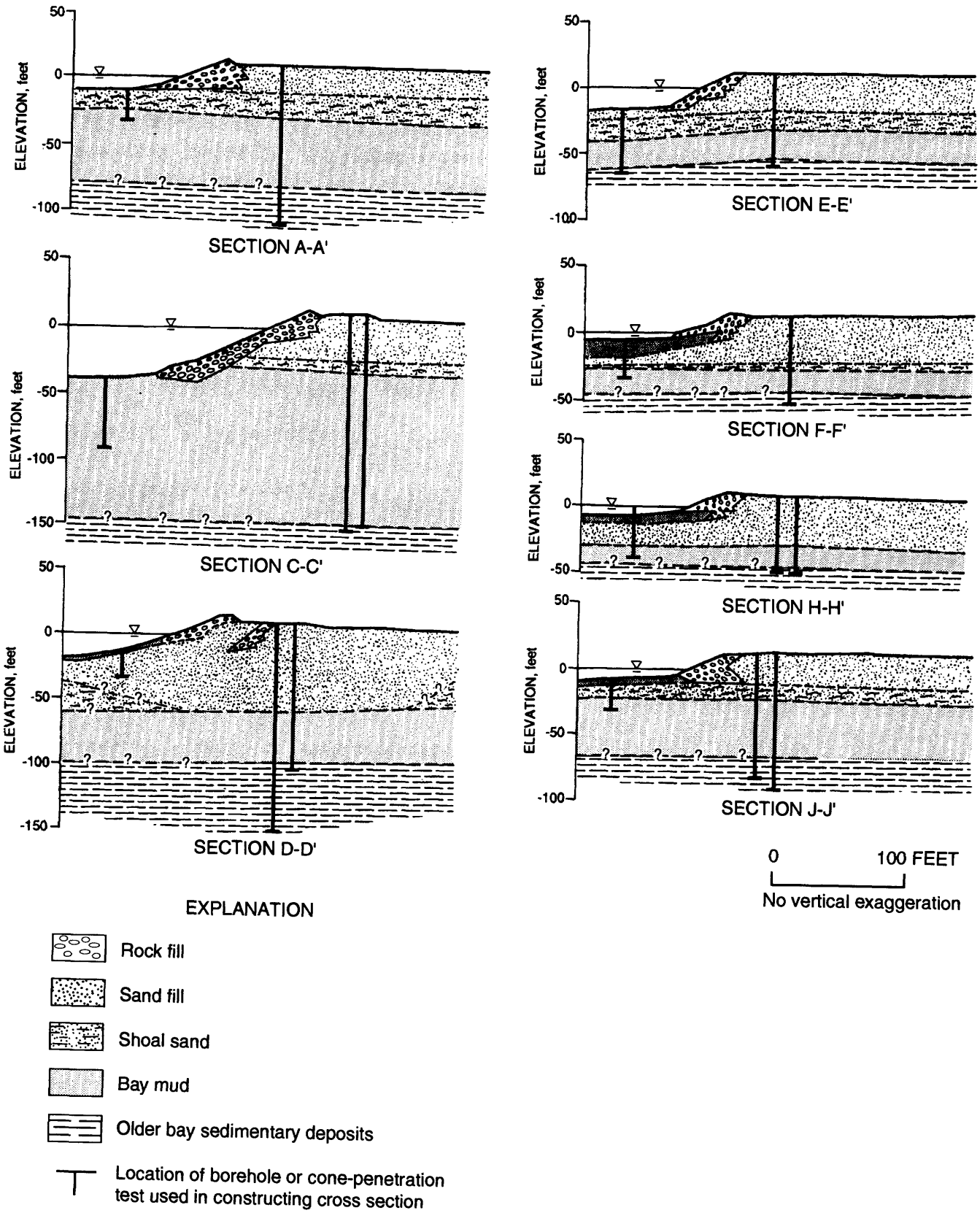


Figure 7.—Stratigraphic cross sections through perimeter dikes on Treasure Island (see fig. 5 for locations).

The grain-size distributions in the sand fill and shoal sand are plotted in figure 9, and cross sections of standard penetration resistance in the sand fill and shoal sand are shown in figure 10, corresponding to the stratigraphic cross sections in figures 6 and 8. A standard penetration test (SPT) is used to measure the relative density and lique-

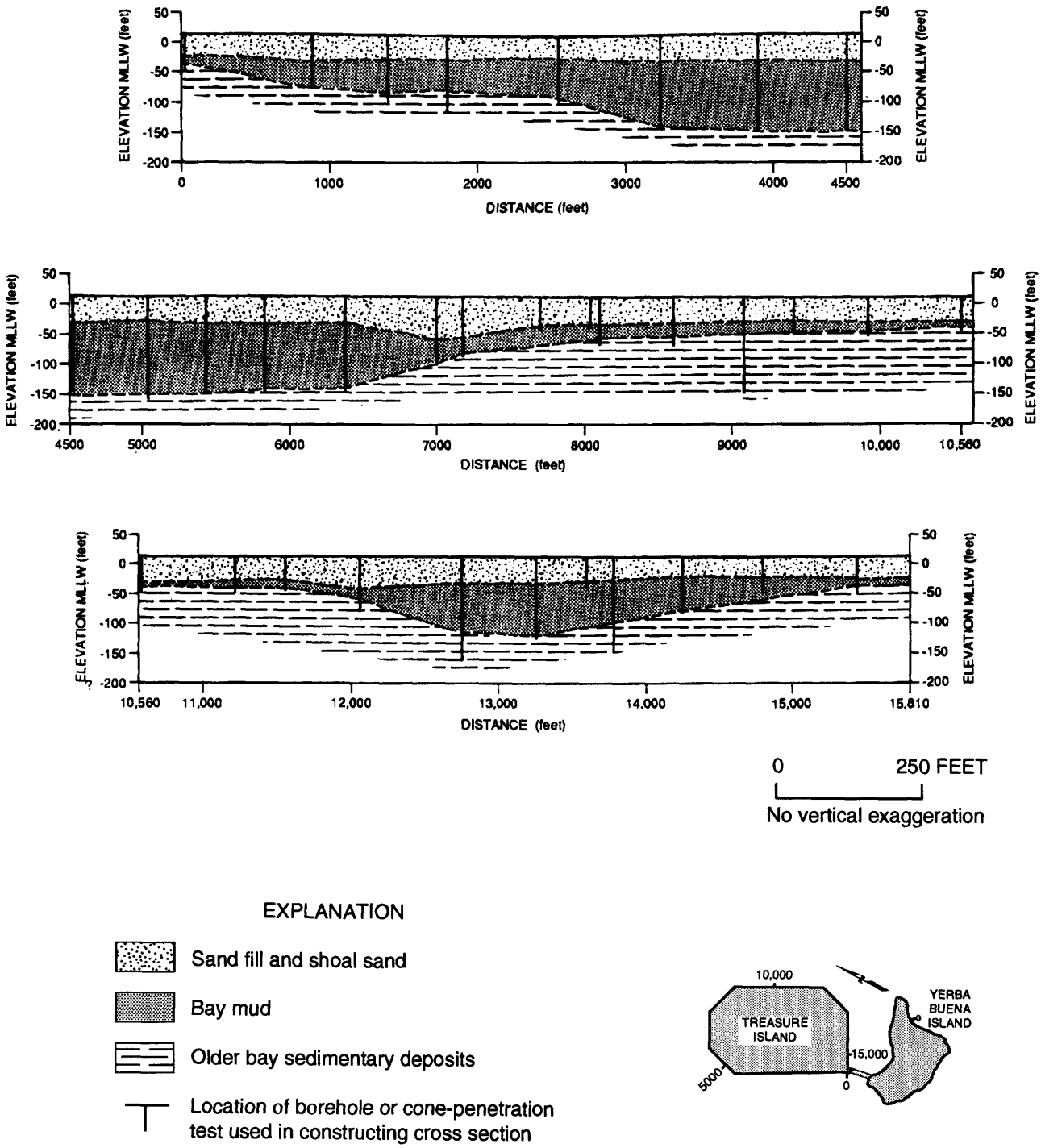


Figure 8.—Stratigraphic cross sections around perimeter of Treasure Island (see fig. 5 for locations), beginning at southwest corner of island at entry gate to U.S. Naval Station and extending clockwise along entire perimeter dike, for a total distance of 15,800 ft. Soil conditions portrayed in cross sections are based on data on materials penetrated in boreholes and cone-penetration tests contained in geotechnical data base, as well as on information on original bay-bottom elevations before island construction and on construction methods used.

faction susceptibility of granular materials; materials with high blowcounts are generally denser and more resistant to liquefaction. The SPT values were calculated by using the data from boreholes and CPT probes in the geotechnical data base. CPT data obtained in this study were converted to SPT values, using an SPT–CPT correlation developed during this study from the SPT data, soil classification, and CPT data from sites where SPT boreholes and CPT probes were immediately adjacent to one another. The site-specific SPT–CPT correlation is described below in the appendix.

All blowcounts were corrected to a normalized standard penetration resistance $(N_1)_{60}$ at an effective overburden stress of 1 ton/ft$^2$, as detailed by Seed and others (1985). The cross sections in figure 10 were constructed by using geostatistical-analysis techniques. The various contours define regions where $(N_1)_{60}$ values are less than 10, 10 to 15, and greater than 16 blows/ft. These regions are meant only to show spatial trends of $(N_1)_{60}$ value and not to be deterministic indicators of the conditions in specific places.

The $(N_1)_{60}$ values contoured in figure 10 indicate that the sand fill and shoal sand generally are relatively loose and susceptible to liquefaction under seismic loading. Liquefaction susceptibility is discussed in the next section. Near-surface materials are generally denser than the deeper materials. This layer of denser surficial material appears to vary in thickness across the island in no consistent pattern.

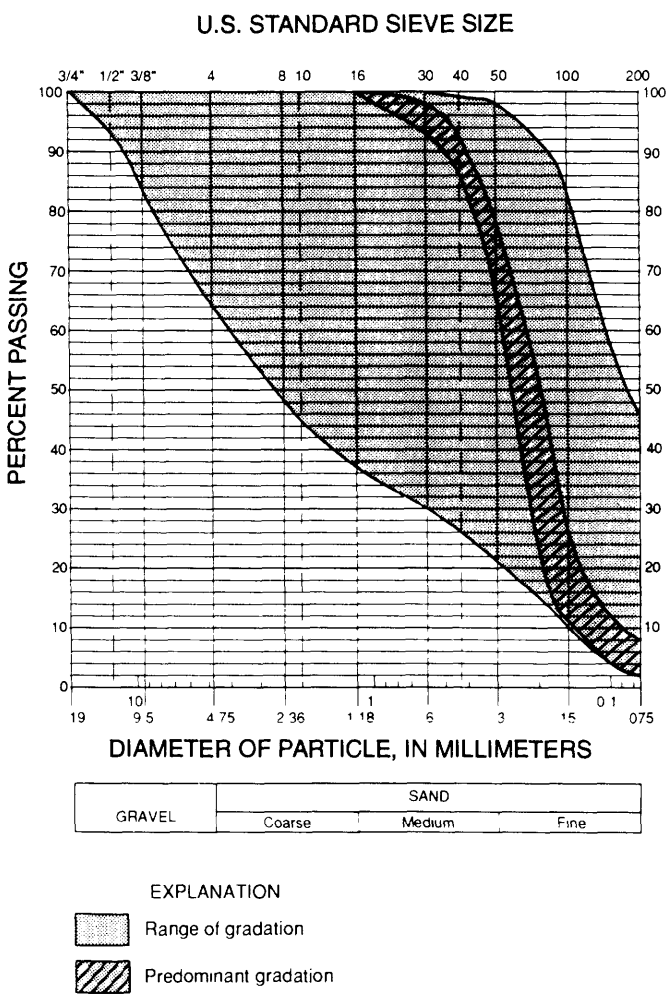


Figure 9.—Grain-size distribution in sand fill and shoal sand on Treasure Island.

## BAY MUD

The bay mud, which has been consolidated by the overlying sand fill and shoal sand, is soft to stiff in consistency. Off shore, where currents are weak, is also a layer of siltation material, as much as 10 ft thick, that has been deposited since the construction of Treasure Island on top of the sand fill and shoal sand. This material, which is essentially young bay mud, is very soft to soft in consistency. Available field and laboratory data indicate that consolidation of the bay mud by the overlying sand fill and shoal sand has increased the strength of the clay. The bay mud is assessed to be essentially normally consolidated, that is, fully consolidated under the overburden imposed by the sand fill and shoal sand. Undrained strengths for the bay mud, characterized by using a SHANSEP (stress history and normalized soil engineering property) approach (Ladd and Foott, 1974), are represented by strength-effective-stress ratios $(S_u/p')$ of 0.35 for vertical-plane-strain conditions and 0.30 for horizontal-plane-strain conditions, where $S_u$ is the undrained strength and $p'$ is the consolidation effective stress on the potential failure plane.

We also evaluated the potential for changes in the strength of the bay mud due to cyclic effects during earthquake shaking. Based on the remolded UU triaxial test results, the sensitivity of the bay mud ranges from 1.5 to 4, where sensitivity is defined as the ratio of the peak to the remolded shear strength. However, review of the stress-strain curves from the CU test results indicates that postpeak strength reductions are less than 20 percent for axial-strain levels lower than 20 percent. Possible strength reductions were also examined by considering potential pore-water-pressure accumulation during ground shaking, using the relations to soil compressibility described by Egan and Sangrey (1978). Estimates of the possible shaking-induced strength reduction in the bay mud using that approach range from 10 to 20 percent.

Strength reductions in the bay mud may also be associated with large deformations that may result from slope movements, with the limit of this reduction corresponding to the undrained residual strength. Testing of other clay soils indicates that comparisons of cone-tip and friction-

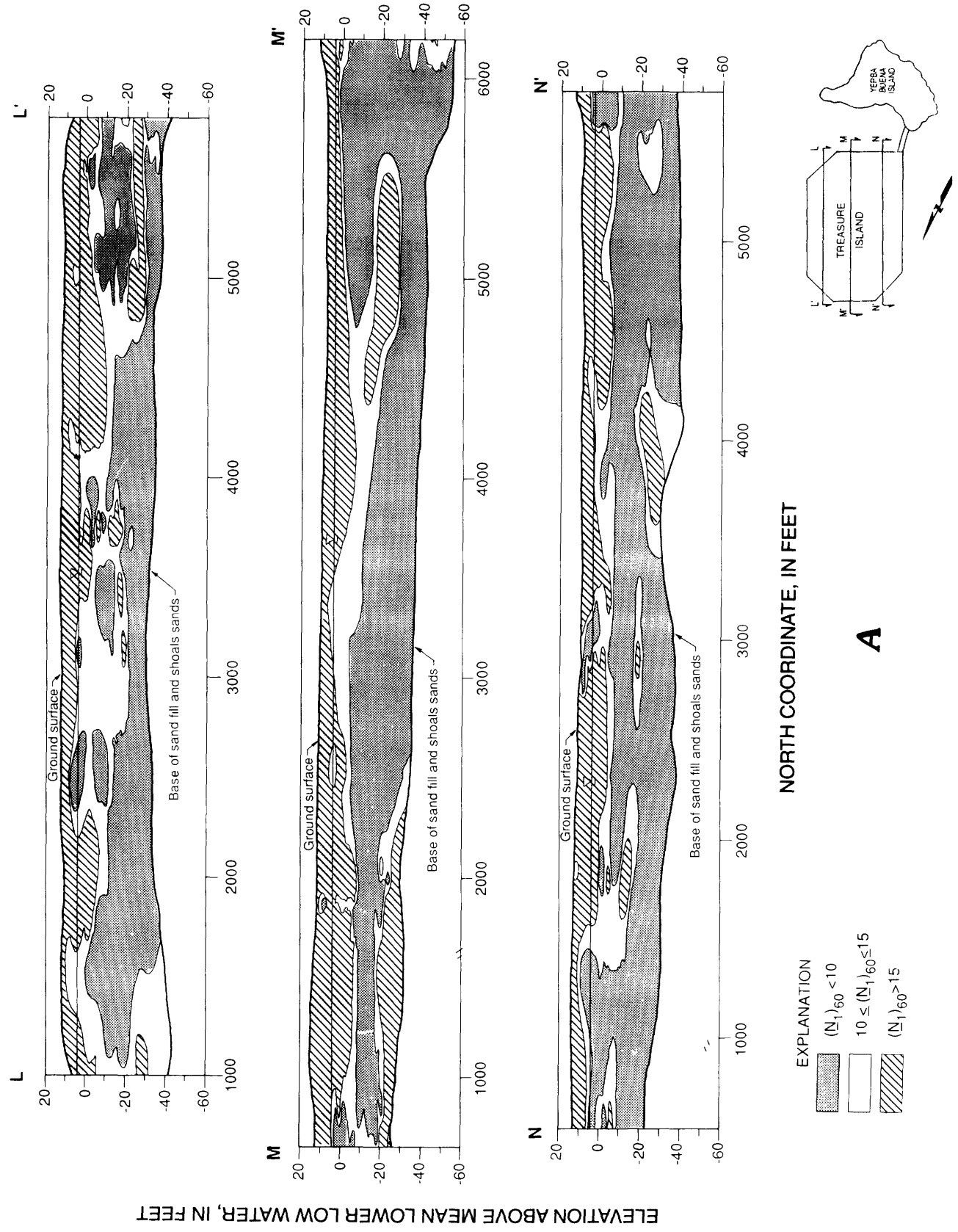


Figure 10.—Stratigraphic cross sections in longitudinal (north-south) (*A*), transverse (east-west) (*B*), and circumferential (*C*) directions on Treasure Island (see fig. 5 for locations), showing distribution of normalized standard penetration resistance, $(N_1)_{60}$, in sand fill and shoal sand. Cross sections extend horizontally to top of perimeter slope at island edge; contours of $(N_1)_{60}$ value (in blows per foot) only indicate trends and do not represent actual $(N_1)_{60}$ values at any point.

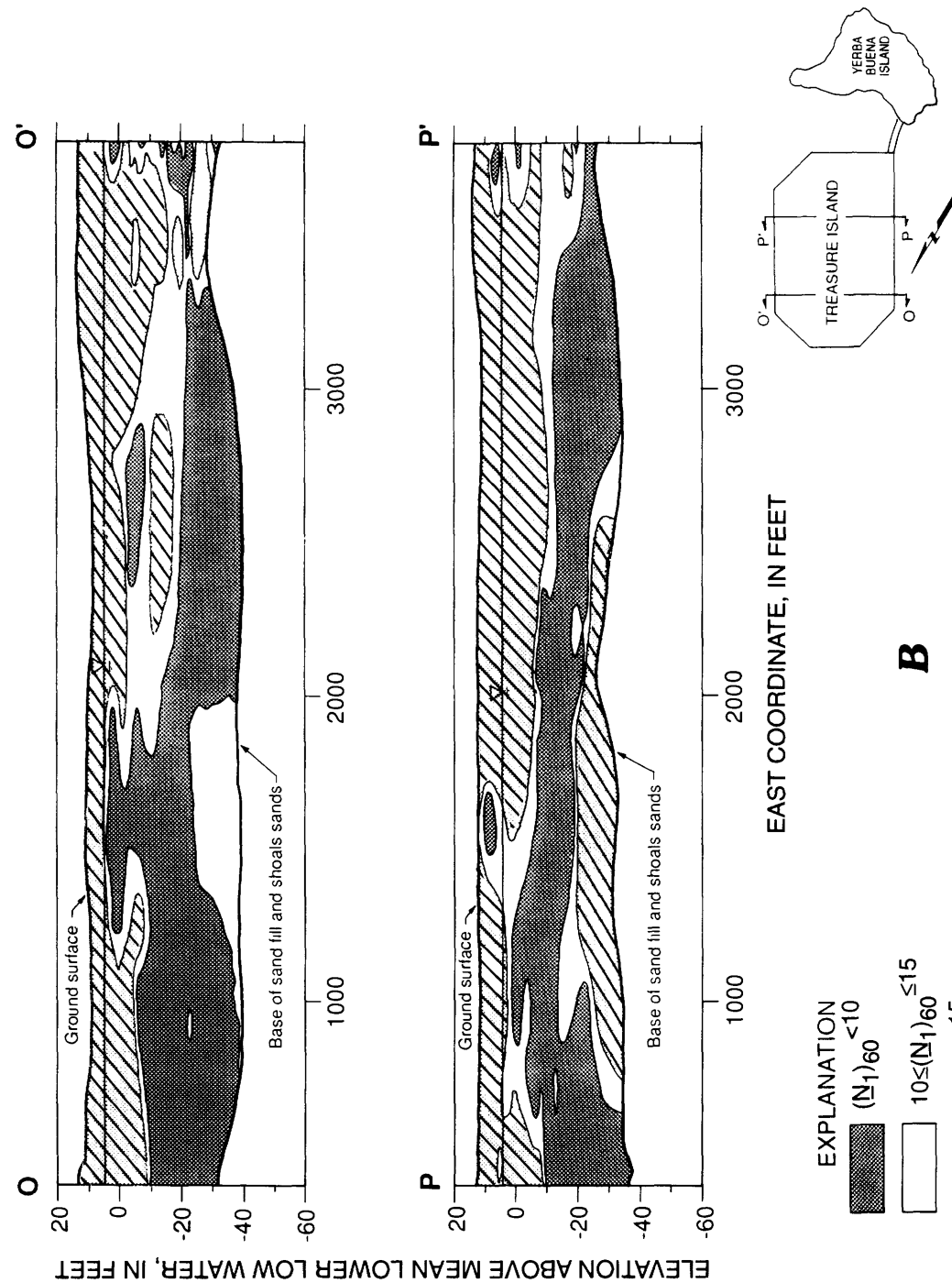


Figure 10.—Continued.

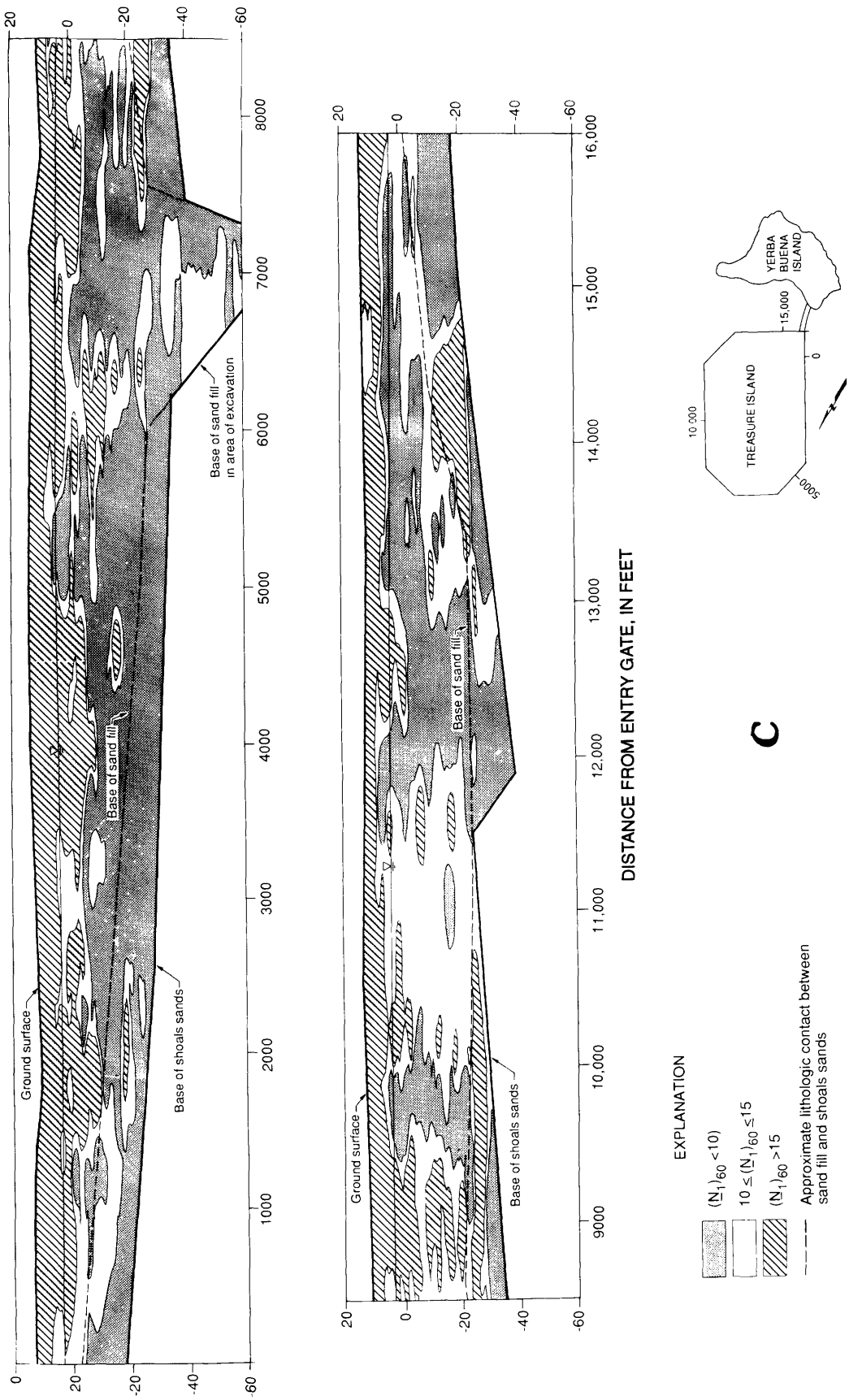


Figure 10.—Continued.

sleeve measurements may be used to estimate undrained residual strength. For the bay mud underlying Treasure Island, the CPT results indicate that the undrained residual strength is about 50 percent of the undrained peak strength of the soil. On the basis of testing of other soils, we estimate that the undrained residual strength of the bay mud would be developed at deformation levels of 1 to 2 ft or more.

### OLDER BAY SEDIMENTARY DEPOSITS

Below the bay mud, sandy, silty, and peaty clay and sand layers were penetrated. These materials, which are commonly referred to as older bay sedimentary deposits, are generally stiff to very stiff or dense. They have not been characterized in detail because, being deep and relatively strong, they are believed to have less influence on the earthquake performance of the island than the shallower materials. In particular, the older bay sedimentary deposits are believed to be relatively insusceptible to earthquake-induced lateral movements or compaction settlements beneath Treasure Island.

## OBSERVATIONS OF LIQUEFACTION AND GROUND DEFORMATION DURING THE EARTHQUAKE

### EARTHQUAKE GROUND SHAKING

Treasure Island is approximately 50 mi (80 km) north of the closest part of the Loma Prieta rupture zone (fig. 1). Ground motion was recorded at the fire station (fig. 5) on Treasure Island, and a recording on bedrock was obtained on Yerba Buena Island. The recorded east-west components of ground motion on Yerba Buena Island and the corresponding ground motion on Treasure Island are plotted in figure 11. As shown, the peak acceleration of 0.06 *g* on Yerba Buena Island was amplified to 0.16 *g* on Treasure Island.

Figure 11 indicates that the strong motion recorded on Treasure Island decreases greatly after approximately 13 s. This substantial decrease in shaking intensity is thought to correspond to the onset of liquefaction in the sand fill and shoal sand; because liquefied sand cannot transmit as much energy from bedrock to the ground surface, lower acceleration results.

### LIQUEFACTION AND DEFORMATIONS

#### SAND BOILS

In addition to indirect evidence of liquefaction from the ground-motion recordings discussed above, abundant evidence of liquefaction was observed on Treasure Island in the form of sand boils. In mapping conducted by the U.S. Geological Survey in November 1989, sand boils were documented at 18 locations on the island, as shown on plate 1. A large sand boil is shown in figure 12. At several other locations on the island, the U.S. Geological Survey (in November 1989) or Geomatrix Consultants (in January and February 1990) noted sinkholes that may have indicated the locations of earlier sand boils where the sand had been removed (see pl. 1).

#### GROUND CRACKS

Geologists of Geomatrix Consultants conducted detailed mapping of ground cracks around the perimeter of the island in January and February 1990 (Geomatrix Consultants, 1990a, b). Cracks and other features were mapped onto 1:240-scale aerial photographs from a topographic survey conducted by the U.S. Navy in November and December 1989. The most conspicuous features are shown on plate 1. Horizontal crack widths are indicated, and the sense and amounts of vertical displacements at cracks are also noted where significant vertical offsets were observed. In general, cracks were as much as 4 in. wide. Vertical displacements at cracks were as large as 2 in., with the bay side of the cracks generally displaced downward. (One notable exception to the sense of displacement was along the western dike at the south edge of the housing area shown in fig. 5, where the downward displacement of a conspicuous crack was landward. The perimeter dike is several feet above the housing area in this location, and the sense of displacement of the crack appeared indicative of some lateral spreading of the dike landward toward the housing area.) As shown in plate 1, almost all cracks parallel the island edge. Cracking was most prevalent along the east side of the island. The maximum distance of cracks from the island edge was approximately 550 ft, along Avenue M in the southeastern part of the island (fig. 5). In most other areas of the island, cracks were limited to a much lesser inland extent: Cracks at the northeast corner showed movements as far as about 200 ft from the dike, those on the west side were generally limited to inland distances of 150 ft or less, and those on the north side were observed as far as 100 ft from the dike, where the zone of noticeable movement was localized within the area of deep fill.

#### SETTLEMENT AND LATERAL SPREADING

The ground cracks mapped in the perimeter areas of the island indicate relatively small amounts of bayward lateral spreading (except that localized landward, lateral spreading apparently occurred in the housing area, as men-

tioned above). Summation of horizontal crack widths indicates that as much as about 12 in. of bayward lateral spreading may have occurred along the east side of the island. The extent of ground cracks indicate that lesser amounts, as well as a lesser extent inland, of lateral spreading occurred along the north, south, and west sides of the island relative to the east side.

Several bench marks on Treasure Island could provide measurements of horizontal and vertical movements associated with the 1989 Loma Prieta earthquake. Only two bench marks, TI N2 and TI N3, at the southeast corner of the island, had preearthquake locations that were sufficiently accurately determined to derive horizontal movements from comparison of preearthquake and postearthquake surveys. Bench mark TI N3, located near the perimeter dike near the interaction of Avenue N and Third Avenue (pl. 1), indicated approximately 10 in. of primarily eastward lateral movement, in good agreement with observations of ground cracks in this area. Bench mark TI N2, located adjacent to Pier 1 at the southeast corner of the island, is in an area of ground improvement (densification of the sand, using vibroflotation). This bench mark moved less than 3/4 in. horizontally, indicating negligible lateral spreading of this area.

Ground-surface settlement was quite obvious across Treasure Island, especially differential settlement adjacent to or inside of buildings, localized sinkholes, or vertical slumping associated with lateral spreading. Observations of ground-surface settlements adjacent to piled structures and (or) old pilings indicated that settlements were generally as much as approximately 6 in. Approximately 4 to 6 in. of settlement was evident adjacent to pile-supported Buildings 2 and 3 on the south side of the island, and a similar amount around the old pile foundation for the Tower of the Sun on Fourth Avenue (pl. 1). The preearthquake and postearthquake data from survey monuments indicated that total settlements generally ranged from 2 to 6 in. The actual settlements at survey monuments are mapped in figure 13.

One area of greater settlement was the area along the northern dike where the bay bottom had been excavated and thicker fills placed. Comparison of preearthquake and postearthquake topographic-survey aerial photographs indicated a maximum settlement of about 2 ft in this area. The causes of this large settlement are poorly established. Our estimate (see subsection below entitled "Ground Settlement") of the shaking-induced compaction settlement in this area is about 8 in., suggesting that about 1 ft of the elevation change may be associated with bayward lateral spreading. Extensive fissuring indicative of extensive lateral spreading was not evident in this area; however, most of the area was covered by lawns that may have obscured surface evidence of cracks.

## DISTRESS TO BUILDINGS AND UTILITIES

The effects of the 1989 Loma Prieta earthquake on the U.S. Naval Station facilities on Treasure Island varied across the island and appeared to correlate reasonably well with areas of more significant ground motion. Most of the buildings at the U.S. Naval Station reportedly sustained

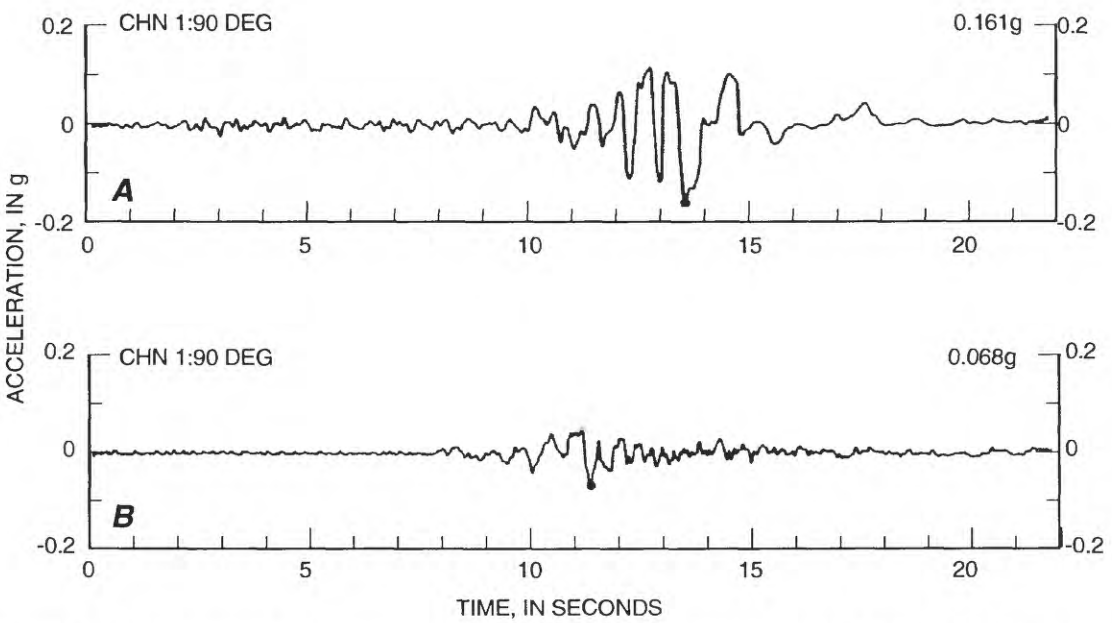


Figure 11.—Accelerograms of east-west ground motion recorded on Treasure Island (*A*) and Yerba Buena Island (*B*). After California Strong Motion Instrumentation Program (1989)

no or insignificant damage or distress. The locations of 34 buildings for which formal inspections were conducted (Applied Management Engineering, Inc., 1990) and repairs discussed are shown on plate 1. Earthquake damage to many of these buildings was, in fact, limited to minor cracks or differential settlement. Several buildings, however, fell into the category of greater damage (that is, Buildings 7, 107, and 461 and residential units 1211, 1218, 1233, 1235, and 1237, pl. 1). The buildings that were more severely damaged were generally located near the perimeter dike and in areas of mapped significant ground distress, primarily lateral spreading. In addition to lateral spreading, Building 7 is located in an area that underwent estimated settlements of 6 to 10 in. Residential unit 1211, which is located near the perimeter dike as well, may have undergone some minor lateral spreading (although no significant cracks were noted in its vicinity); however, this unit is located in an area of settlement estimated at about 6 in., and sand ejected from a boil adjacent to the unit may have resulted in differential settlement. Building 107 and residential unit 1218, both in the interior of the island (more than 1,000 ft from the perimeter dike), are located in areas with relatively large estimated settlements (8 in.). We note that an increased likelihood of differential settlement exists in areas of larger estimated settlement, owing to potential variation in fill conditions and (or) foundation loads. These factors may have contributed to the differential settlement sustained by the northwest wing of Building 107 relative to the rest of the building. A correlation is possible between ground effects and building performance at those buildings that sustained generally minor damage. These buildings are generally located in the areas of settlements estimated at less than 6 in.

Nearly all the buildings on Treasure Island are supported on shallow footing foundations; a few are supported on pile foundations. The pile-supported buildings performed well; however, these buildings are not located in areas of significant lateral spreading. The ground around pile-supported Buildings 1, 2, and 3 settled noticeably, but the pile foundations for these buildings, as well as the structure itself, performed reasonably well. The slab-on-grade interior floor systems, however, were damaged from settlement of the underlying fill. Large areas of the slabs settled differentially and required repair. An attached section of Building 2 that is supported on shallow footings settled differentially from pile-supported Building 2, causing substantial distress at the interface between the original and attached sections. Building 369, the only other structure on the island known to have a pile foundation, also performed reasonably well in the earthquake.

Underground utilities were also affected by lateral spreading and ground settlements associated with liquefaction. A total of 44 utility-line breaks were reported on maps provided by the Public Works section of the U.S. Naval Supply Center, distributed across the island at locations shown on plate 1. These utility-line breaks included 28 freshwater-line breaks, 10 sewage-line breaks, and 6 gas-line breaks. Many of the breaks occurred in the area adjacent to the perimeter dike, probably primarily owing to lateral spreading. However, it is unclear from the available data how much lateral spreading was required to cause breaks in different types of utility lines, although at some locations, spreading cracks about 1 in. wide are mapped near the breaks. Some breaks also appeared to occur as a result of differential vertical (slumping) movement on lateral-spreading cracks. In the interior of the island, breaks cannot be associated with lateral spreading but instead

Figure 12.—Sand boil on Treasure Island. Photograph courtesy of Michael J. Bennett, U.S. Geological Survey.

appear to be generally associated with ground settlement and (or) areas where liquefied fill materials are at shallow depths below the ground surface. Comparison of the break locations shown on plate 1 with the settlement contours estimated for the island shown in figure 13 (see subsection below entitled "Ground Settlement") indicates that breaks typically occurred in areas with ground settlements of at least 6 to 8 in.

## PERFORMANCE OF IMPROVED-GROUND AREAS

In several areas of Treasure Island, ground improvements of different types had been implemented before the earthquake. Ground-improvement methods included compaction piles, Terraprobe, and vibroflotation/stone columns. Generally, buildings founded on improved ground performed well during the earthquake. No major structural damage was detected in Buildings 450 (sand-compaction pile densification), 452, and 453 (nonstructural-timber pile densification), although a concrete spall was noted at the end of one wing of Building 453 (see pl. 1). The area of Buildings 487, 488, and 489 was densified by using vibroflotation; these buildings sustained no to little damage. At Pier 1 (fig. 5), the areas densified by Terraprobe exhibited no signs of ground movement, whereas sinkholes and sand boils were observed in immediately adjacent areas. As noted above, significant lateral movement did not occur at the bench mark located in the area of improved ground at Pier 1. (Note that preearthquake vertical control for this bench mark was not established, and so earthquake-induced settlements (or the absence thereof) at this location could not be determined.)

The medical/dental facility located in the south-central part of the island (fig. 5) was under construction at the time of the earthquake. The area of improved ground at this facility apparently performed well during the earthquake; no evidence of liquefaction, differential settlement, or other ground-failure-related distress was observed at the surface. Sand flows did occur within a 22-ft-deep elevator-shaft excavation.

# ANALYSIS OF GROUND PERFORMANCE DURING THE EARTHQUAKE

We analyzed the ground performance on Treasure Island during the 1989 Loma Prieta earthquake to help

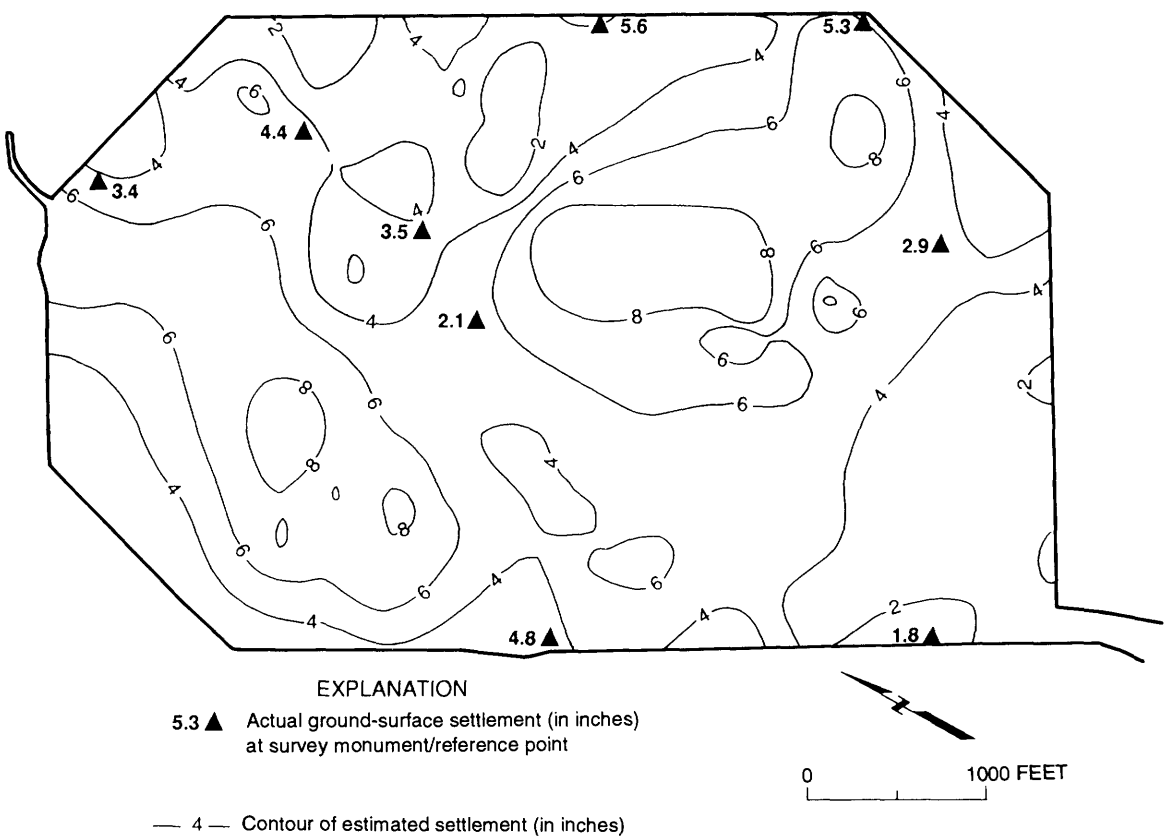


Figure 13.—Sketch map of Treasure Island, showing actual ground-surface settlements and contours of estimated settlement caused by compaction (see text for discussion).

understand the behavior of the island during that event, as well as to provide a quantitative basis for extrapolating to the behavior anticipated during potential future earthquakes on the San Andreas and Hayward faults closer to the island. Analyses conducted for the 1989 Loma Prieta earthquake included ground shaking (site response), liquefaction, slope stability and lateral spreading, and ground settlement.

## GROUND SHAKING

A significant observation regarding the ground motions resulting from the 1989 Loma Prieta earthquake was the amplification of shaking intensity at sites around the margin of San Francisco Bay underlain by deep, relatively soft bay mud. To examine the site-amplification effects observed on Treasure Island during the 1989 Loma Prieta earthquake, we conducted site-response analyses, using the computer program *SHAKE* (Schnabel and others, 1972). The accelerograms recorded on Yerba Buena Island during the earthquake were used as input motions for the *SHAKE* analyses. During the analyses conducted for this study, site-specific measurements of dynamic soil properties were unavailable; therefore, these properties were estimated on the basis of published correlations of shear-wave velocity or shear modulus with penetration-resistance data for sands (Sykora, 1987) and with undrained shear strengths for clayey soils (Egan and Ebeling, 1985), as well as values measured for similar soils at other bay-margin sites (Fumal, 1978). The estimated shear-wave-velocity profile used in the analyses is illustrated in figure 14. Measurements of shear-wave velocity made on Trea-

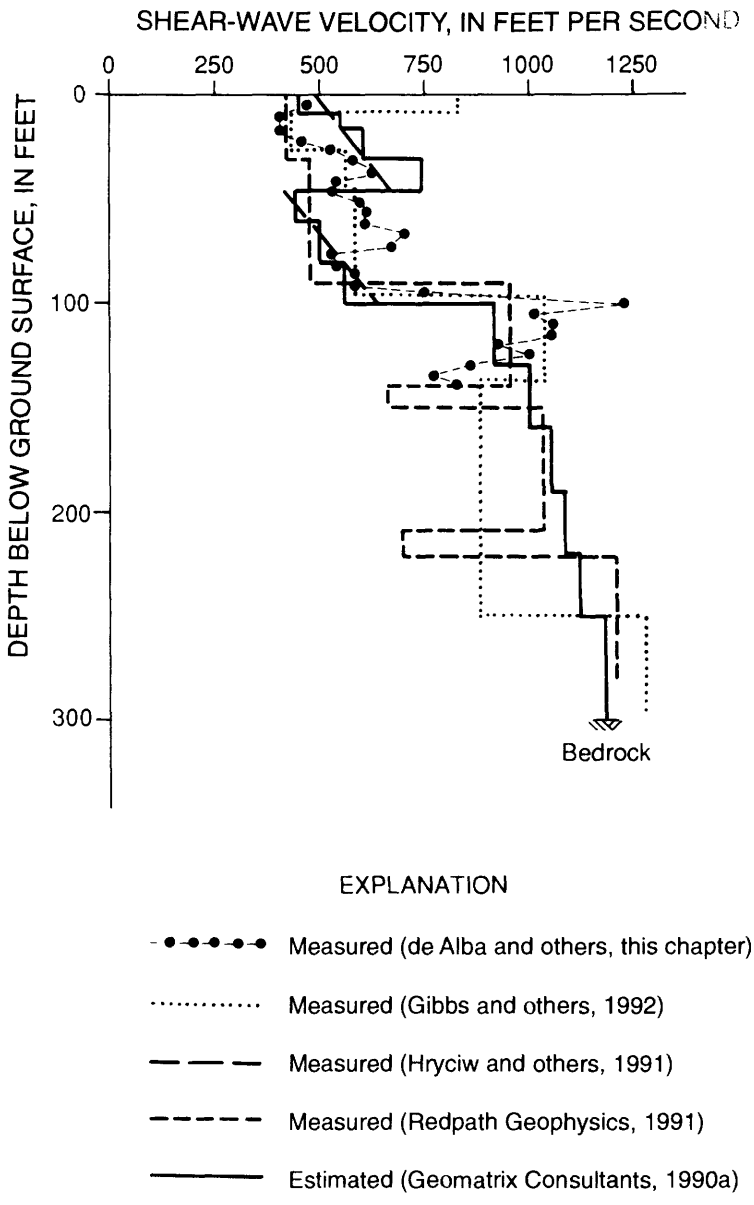


Figure 14.—Shear-wave velocity versus depth on Treasure Island.

sure Island after the analyses conducted for this study are also shown in figure 14 for comparison, illustrating that the estimated analysis profile is reasonable.

Ground surface motion computed in a typical analysis is illustrated in figure 15 for the east-west horizontal component, in comparison with the east-west component of ground motion recorded on Treasure Island during the 1989 Loma Prieta earthquake. The input motion is also plotted. The computed and recorded ground motions show generally similar amplitudes and strong-shaking duration; however, the *SHAKE* analysis does not capture the reduction in motion at 13 s that is thought to be due to liquefaction. Softening of the sand due to liquefaction cannot be modeled well with *SHAKE* analysis, and so postliquefaction motions are overestimated by the analysis. Results of several *SHAKE* analyses modeling the various subsurface conditions across the island are illustrated in figure 16. Computed peak accelerations were in the range of about 0.14–0.18 *g*, in good agreement with the peak acceleration of 0.16 *g* recorded on Treasure Island, indicating that the intensity of ground shaking probably did not vary greatly in different places on the island.

## LIQUEFACTION

As previously discussed, sand boils were observed in many places across the island, substantiating that subsurface materials had liquefied during the earthquake. The sand fill and shoal sand of Treasure Island located below the water table are considered susceptible to such liquefaction. To assess the occurrence of liquefaction in these materials during the 1989 Loma Prieta earthquake, SPT and CPT data obtained during the present study, as well as during previous studies, were used as indices of liquefaction susceptibility. Using SPT and CPT data to assess the liquefaction susceptibility of soils in an earthquake is presently considered to be a reasonable engineering approach (Seed and Idriss, 1982; Seed and others, 1985; U.S. National Research Council, 1985) because many of the factors affecting SPT and CPT data similarly affect the liquefaction susceptibility of sandy soils and because state-of-the-art liquefaction-evaluation procedures are based on the actual performance of soil deposits during worldwide historical earthquakes.

The approach used in this study to assess liquefaction potential was the empirical method of Seed and Idriss (1971, 1982; Seed and others, 1985). Peak acceleration, total and effective overburden pressures at the point of interest, and SPT blowcounts are needed for the assessment. As described below in the appendix, CPT data were converted to equivalent SPT blowcounts, using a site-specific correlation to provide supplementary resistance data. The standardized index used in the method is $(N_1)_{60}$, which represents the SPT blowcount to advance a 2-in. (51 mm)-outer-diameter split-spoon sampler 1 ft (0.3 m)

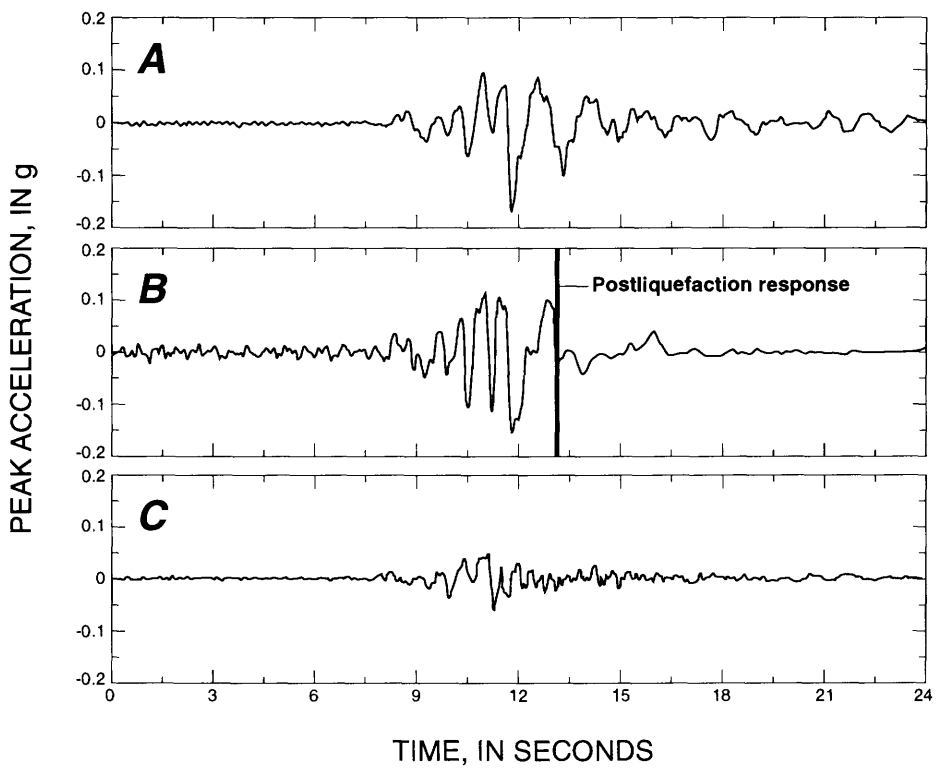


Figure 15.—Computed (*A*) and recorded (*B*) peak acceleration at ground surface on Treasure Island and recorded peak acceleration on bedrock on Yerba Buena Island (*C*).

at 60-percent hammer-energy efficiency, corrected to an overburden pressure of 1 ton/ft$^2$ (98 kPa). The method is based on the empirical correlation between cyclic-stress ratio (computed from peak acceleration or from site-response analyses, for example, *SHAKE* analyses) and $(N_1)_{60}$ value, differentiating the observed occurrence or nonoccurrence of liquefaction in sand deposits during earthquakes. The basic correlation presented by Seed and others (1985) is illustrated in figure 17, which was developed for an $M$=7.5 earthquake in sandy materials with different fines contents but may be adjusted to other-magnitude earthquakes by using the correction factors of Seed and others. The set of curves appropriate to an $M$=7 earthquake (that is, a Loma Prieta-type event) would be obtained by multiplying the ordinates of the curves in figure 17 by a correction factor of 1.06. The curve for clean sand (≤5 percent fines) in figure 17 was used, and SPT resistances for silty sand were converted to equivalent blowcounts in clean sand on the basis of the fines content of the soil samples and the curves in figure 17. Cone-penetration resistances, however, cannot be converted to equivalent blowcounts in clean sand because of uncertainty in the fines content associated with the CPT data (see appendix). Thus, the $N_1$ values inferred from CPT data may be slightly underestimated overall by no more than 1 to 2 blows/ft, a difference that would not significantly change the comparisons presented below.

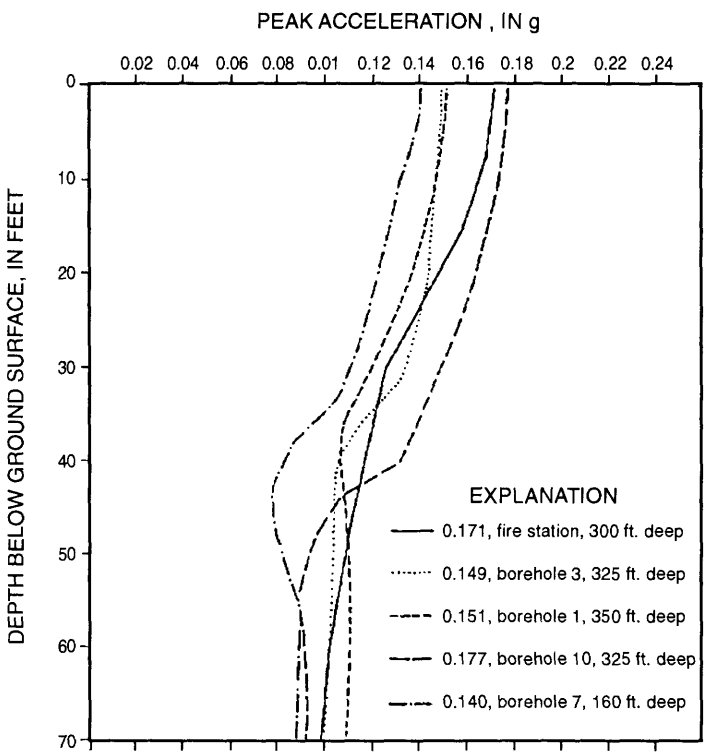


Figure 16.—Peak acceleration versus depth at sites on Treasure Island (see pl. 1 and fig. 5 for locations), calculated from analyses of soil profiles above bedrock using computer program *SHAKE* (Schnabel and others, 1972). Description of curves lists peak acceleration at ground surface at each site.

For a given peak acceleration ($a_{max}$) and the total and effective overburden pressures at the depth of interest ($\sigma_o$ and $\bar{\sigma}_o$, respectively), the average induced cyclic-stress ratio ($\tau_a/\bar{\sigma}_o$) can be computed, using the expression (Seed and Idriss, 1971)

$$\frac{\tau_a}{\bar{\sigma}_o} = 0.65 \frac{a_{max}}{g} \frac{\sigma_o}{\bar{\sigma}_o} r_d,$$

where $r_d$ is the stress-reduction factor, which decreases from 1 at the ground surface to 0.9 at a depth of about 35 ft. Thus, given a cyclic-stress ratio calculated for a peak acceleration and using the curve for clean sand plotted in figure 17, a critical $(N_1)_{60}$ value can be determined, such that those materials with an $(N_1)_{60}$ value greater than the critical value would not be likely to liquefy and those with an $(N_1)_{60}$ value less than the critical value would be likely to liquefy. By comparing the critical with the measured $(N_1)_{60}$ value of the sand material, its liquefaction likelihood can then be assessed.

For a peak acceleration of 0.16 $g$, the seismically induced cyclic-stress ratio was computed as a function of elevation, and the corresponding critical $(N_1)_{60}$ value was determined. These critical $(N_1)_{60}$ values were then compared with the $(N_1)_{60}$ values from boreholes and CPT soundings located close to the perimeter of the island. Comparisons were made for four different sections or reaches of the perimeter dike (Geomatrix Consultants, 1990b). The comparison for Section II (fig. 5), which is the reach located from 4,950 to 8,500 ft from the entry gate, proceeding clockwise around the island's perimeter, is shown in figure 18; the comparisons are similar for the other three reaches. As can be seen, a substantial number of the $(N_1)_{60}$ data fall below the critical value, indicating that much of the sand below the ground-water level probably liquefied during the 1989 Loma Prieta earthquake. However, because some of the data below the ground-water level also fall above the critical $(N_1)_{60}$ value, liquefaction probably did not occur in some zones within the sand fill and shoal sand.

The spatial distribution of expected occurrence and nonoccurrence of liquefaction can be illustrated by examining the contours of $(N_1)_{60}$ data for typical island cross sections, such as those in figure 10. As shown in figure 18, the critical $(N_1)_{60}$ value was estimated at 10 to 15 blows/ft. Figure 10 indicates that substantial proportions of the island's subsurface materials have an $(N_1)_{60}$ value less than 10 and so could reasonably be expected to have liquefied during the 1989 Loma Prieta earthquake. For the zones of material in figure 10 with an $(N_1)_{60}$ value of 10 to 15 blows/ft, the occurrence of liquefaction was only marginal, and materials with an $(N_1)_{60}$ value greater than

15 blows/ft are not expected to have liquefied. Such materials are located primarily near the ground surface, in many places above the ground-water level, and were not expected to liquefy anyway. Sand-boil evidence was especially prevalent in the northwest quadrant of the island. Examination of subsurface conditions in that area indicated that liquefied zones may have been within about 5 ft of the ground surface in some places. In fact, comparisons of reported sand-boil locations from across the island with contours of $(N_1)_{60}$ values generally indicates that sand boils formed where the liquefied fill was within about 10 ft of the ground surface.

## PERIMETER-DIKE STABILITY AND LATERAL SPREADING

As previously discussed, the perimeter dike and areas adjacent to it on Treasure Island moved laterally (bayward), with associated cracking and slumping. Postearthquake observations indicate that these areas moved laterally during the ground shaking and did not continue to move after the earthquake. These observations are consistent with the phenomenon of lateral spreading, which is a form of ground failure whereby earthquake ground shaking affects the stability of slopes (for example, the perimeter dikes on Treasure Island) containing potentially liquefiable soils by seismic inertial forces within the slope and by shaking-induced strength reductions in the liquefiable soil materials. Temporary instability due to seismic inertial forces are manifested by lateral (in this case, bayward) movements of the slope, and such movements can potentially involve large land areas. For the duration of ground shaking associated with the 1989 Loma Prieta earthquake, several such occurrences of temporary instability could have caused an accumulation of downslope (bayward) movement. The 1989 Loma Prieta earthquake was of unusually short duration for an $M$=7 event. Had its duration been longer, more lateral spreading would undoubtedly have occurred.

The primary objective of our analyses of perimeter-dike stability and lateral-spreading movement was to evaluate the residual strength exhibited by the sand fill and shoal sand in a state of earthquake-induced liquefaction, so that this information could then be used to predict the amount of lateral spreading during potential future

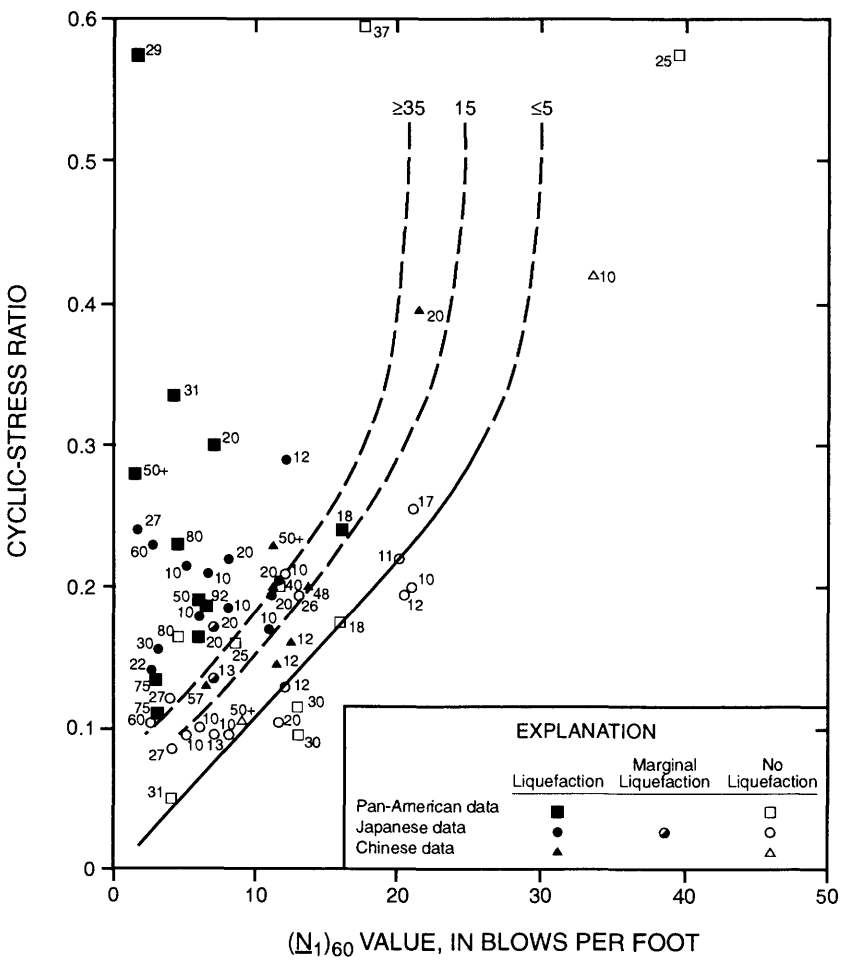


Figure 17.—Cyclic-stress ratio versus $(N_1)_{60}$ value for hypothetical $M$=7.5 earthquake (after Seed and others, 1985). Data points are shown only for sites with >5 percent fines; considerable data for <5 percent fines omitted for clarity.

earthquakes. To estimate the residual strength of the sand deposits, we conducted stability and deformation analyses for several cross sections through mapped lateral-spreading zones, given the Loma Prieta ground-shaking conditions and observed deformation patterns.

During ground shaking, excess pore-water-pressure buildup tends to reduce the strength of the sand. For a loose sand, the strength associated with a liquefied state may be drastically less than the static strength, although strength is not completely lost. On the basis of observations from several historical liquefaction-failure sites, Seed and Harder (1990) postulated that liquefied sand has a small residual postliquefaction undrained shear strength. The relation between $(N_1)_{60\text{-cs}}$ value and residual undrained shear strength based on several case histories is plotted in figure 19, where $(N_1)_{60\text{-cs}}$ is a "clean sand"-corrected equivalent blowcount that accounts for the residual strength of a sand on the basis of its density and fines content. The $(N_1)_{60}$ value for the liquefied sand on Treasure Island typically ranges from 5 to 15 blows/ft. From figure 19, the undrained residual strength of liquefied sand for such $(N_1)_{60}$ values is estimated to generally range from 50 to 700 lb/ft$^2$.

To determine a representative site-specific value of undrained residual shear strength for the sand materials on Treasure Island that liquefied during the 1989 Loma Prieta earthquake, we performed deformation analyses, using the method of Newmark (1965) as modified by Makdisi and Seed (1978) to calculate seismically induced ground displacements for a slope. After analyzing several cross sections, we found that a residual shear strength of 375 to 450 lb/ft$^2$ was necessary to make the calculated displacement compatible with the observed. However, because liquefaction may not have occurred completely, the strengths mobilized in nonliquefied or partially liquefied zones may have exceeded these values, whereas the residual strengths of fully liquefied sand were less than these values.

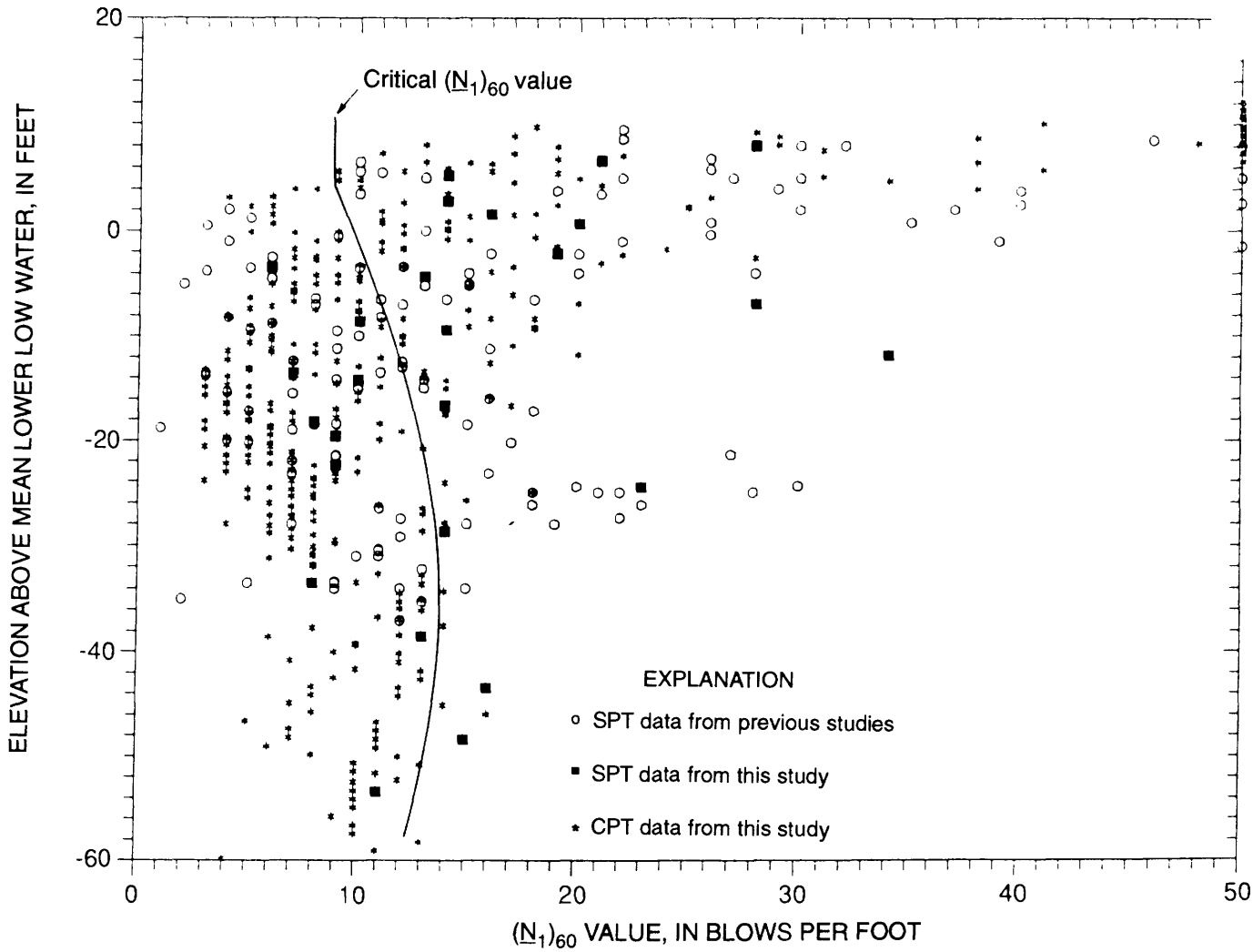


Figure 18.—$(N_1)_{60}$ value versus elevation, based on SPT and CPT data. Curve shows critical $(N_1)_{60}$ value at various elevations.

The range of residual shear strength calculated from our analyses give quite low postliquefaction static factors of safety for the slopes, in the range 1.03–1.23, consistent with the observation of no continued movement after the earthquake shaking ceased. These low factors of safety result in very low yield accelerations for the postliquefaction slopes, about 0.015 to 0.05 *g*, indicating that if postliquefaction ground-shaking intensity during the 1989 Loma Prieta earthquake had been greater or the duration longer, larger deformations of the perimeter dike would have occurred.

## GROUND SETTLEMENT

To develop a more complete picture of the settlement variation across Treasure Island than that provided by the limited survey data, we estimated ground-surface settlements associated with shaking-induced compaction by using the compiled $(N_1)_{60}$ data, the observed 1989 Loma Prieta earthquake ground motions, and a method for estimating the magnitude of earthquake-induced compaction settlement of sandy materials modified from that of Tokimatsu and Seed (1987), which we found to overestimate the shaking-induced compaction settlement for the 1989 Loma Prieta earthquake. Our modified method was developed to utilize the simplified framework of Tokimatsu and Seed as a basis and to incorporate the influence of grain size on postcyclic volumetric strain, as described by Lee and Albaisa (1974).

Examination of the empirical data of Tokimatsu and Seed (1987) to develop their volumetric-strain relations indicates that the soils from the various sites/studies had a similar median grain size ($D_{50}$). The laboratory-testing results of Lee and Albaisa (1974) indicate that the postliquefaction volumetric strains of sandy soils depend on grain size, such that a soil with a smaller $D_{50}$ value would undergo smaller strains than coarser soils. On the basis of the data of Lee and Albaisa, we calculated $D_{50}$-dependent adjustments to the volumetric strains computed by the method of Tokimatsu and Seed (1987) for a given layer/zone of soil. Because the sand deposits on Treasure Island are typically finer than the soils used by Tokimatsu and Seed, the net effect was a general reduction of settlement computed by their method.

The results of our analysis are illustrated in figure 13, which shows contours of estimated ground-surface compaction settlements associated with the 1989 Loma Prieta earthquake, as well as elevation changes at survey monuments or reference points determined from available ground-survey measurements. The settlements estimated from nearby SPT–CPT data agree reasonably well with the surveyed elevation changes. Figure 13 indicates that in some areas, compaction settlements may have been as large as 8 to 10 in. These areas typically correspond to places where the thickest zones of liquefied fill/soil were expected, on the basis of examination of cross sections throughout the island.

Again, we note that settlements near the island's perimeter were locally greater than the compaction settlements estimated herein, owing to slumping movements accompanying lateral spreading. At the north end of the island, where thicker fills are present (see cross sec. *D–D'*, fig. 7), the 2 ft of settlement that occurred in this area exceeds

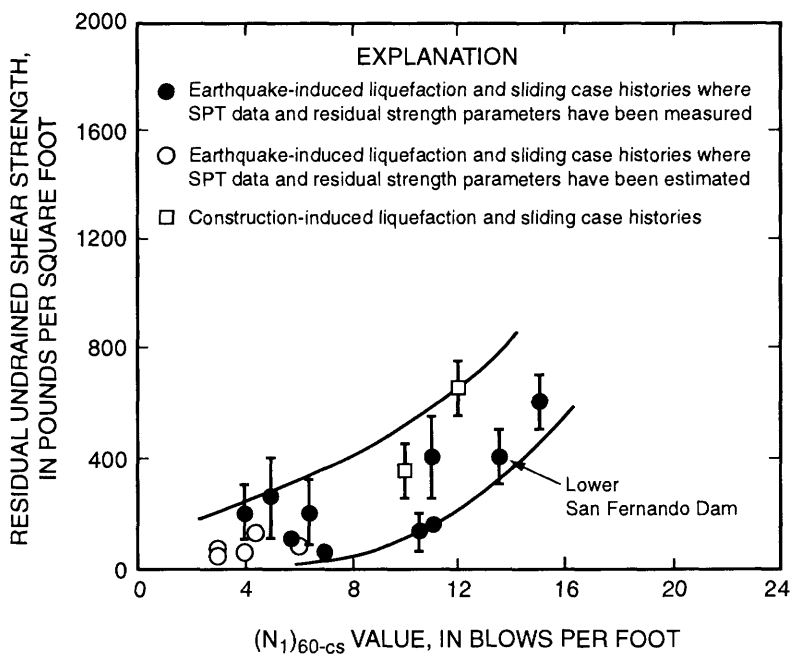


Figure 19.—Corrected standard penetration resistance for "clean sand" ($(N_1)_{60\text{-cs}}$ value) versus residual undrained shear strength from case studies (after Seed and Harder, 1990).

by more than 1 ft the amount of settlement estimated to be due to compaction; this greater settlement is due to lateral spreading or unknown local soil variations.

# POTENTIAL FOR GROUND FAILURE DURING FUTURE EARTHQUAKES

## POTENTIAL FUTURE EARTHQUAKES AND GROUND SHAKING

We evaluated the potential for ground failure on Treasure Island for an $M$=7 earthquake on the Hayward fault and an $M$=8 earthquake on the San Andreas fault, both assumed to occur on sections of these faults closest to Treasure Island (fig. 1). The postulated $M$=7 earthquake on the Hayward fault is similar in size to earthquakes that occurred on this fault in 1836 and 1868. The probability of such an earthquake has been assessed at 28 percent within the time period 1990–2020 (Working Group on California Earthquake Probabilities, 1990), and so it is a relatively likely event. The postulated $M$=8 earthquake on the San Andreas fault would be essentially the same size as the 1906 San Francisco earthquake. The probability of such an earthquake has been assessed as being low (approx 2 percent) within the time period 1990–2020 (Working Group on California Earthquake Probabilities, 1990), and so it is a relatively unlikely event.

The characteristics of these potential future earthquakes and the resulting ground motions on Treasure Island are compared with the characteristics of the 1989 Loma Prieta earthquake in table 1, which illustrates that the earthquake ground motions to which Treasure Island may be subjected in the future will be considerably more severe than those recorded on the island during the 1989 Loma Prieta earthquake. We note from table 1 that peak accelerations on Treasure Island are estimated to be equal on rock and on soil for nearby potential future earthquakes, whereas during the 1989 Loma Prieta earthquake, the peak acceleration recorded on soil was 2 1/2 times that recorded on rock. The estimates for potential future earthquakes reflect the expected strong nonlinear soil behavior during intense strong ground shaking, on the basis of both the *SHAKE* analyses conducted for Treasure Island during this study and the correlation developed by Idriss (1991) between peak accelerations on rock and soft soil, as shown in figure 20.

## LIQUEFACTION AND DEFORMATIONS

Using the method of Seed and others (1971, 1982, 1985) discussed earlier in connection with the 1989 Loma Prieta earthquake analysis, we estimated critical $(N_1)_{60}$ values for liquefaction for potential future earthquakes of $M$=7 on the Hayward fault and $M$=8 on the San Andreas fault. A typical comparison of the critical $(N_1)_{60}$ values for these earthquakes with that for the sand deposits on Treasure Island is shown in figure 21, which illustrates that essentially complete liquefaction of the sand would be expected during these earthquakes.

The most severe potential effect of liquefaction would be lateral spreading. Using a simplified version of the deformation-analysis method of Newmark (1965), along with values of residual strength inferred from the 1989 Loma Prieta earthquake analysis discussed earlier, we estimate that lateral displacements could be about 4 and 10 ft for potential future earthquakes on the Hayward and San Andreas faults, respectively. Because of the large uncertainties inherent in this method, these estimated displacements are not upper-bound values and could well be exceeded. The lateral-spreading movements could extend several hundred feet into the island and thus cause severe damage to facilities in the affected areas.

We estimated anticipated compaction settlements associated with potential future earthquakes on the Hayward and San Andreas faults in the same way as for the 1989 Loma Prieta earthquake. The resulting contours of compaction settlements of the ground surface are mapped in figure 22. These settlements are considerably larger than the 1989 Loma Prieta earthquake settlements mapped in figure 13. The contours in figure 22 indicate that areal subsidence of Treasure Island resulting from earthquakes on the Hayward or San Andreas fault would be approximately 1 ft, although some parts of the island may subside as much as 2 ft. In particular, this much shaking-induced compaction settlement may occur in the area of thicker sand fill near the perimeter dike on the north side of the island. These shaking-induced settlements are expected to occur within several hours to a day after the earthquake. We emphasize that the estimated settlements mapped in figure 22 are due to compaction as excess pore-water pressures in the liquefied sand dissipate. In areas of lateral spreading, additional, larger settlements (slumping) would accompany the lateral spreading. The differential settlements associated with slumping would also be expected to be greater than those associated with compaction. In general, compaction settlements would generally vary relatively smoothly from area to area in a pattern similar to that shown in figure 22; however, local, more abrupt differential settlements could also occur in the vicinity of sand boils.

## MEASURES TO MITIGATE GROUND FAILURE

Mitigation of the lateral-spreading hazard appears to be the highest priority action to reduce the severity of ground-failure effects on Treasure Island during potential future

Table 1.—*Characteristics of the 1989 Loma Prieta earthquake and potential future earthquakes affecting Treasure Island*

| Earthquake | Closest distance to Treasure Island, in miles (km) | Estimated mean peak rock acceleration (*g*) | Estimated mean peak soil acceleration (*g*) | Estimated mean duration of strong motion on rock (s) |
|---|---|---|---|---|
| Loma Prieta, Oct. 17, 1989. | 50 (80) | [1]0.06 | [2]0.16 | [1]8 |
| Maximum earthquake on the San Andreas fault (*M*=8). | 11 (18) | .4 | .4 | 45 |
| Maximum earthquake on the Hayward fault (*M*=7). | 7 (11) | .4 | .4 | 15 |

[1]Yerba Buena Island recording.
[2]Fire Station recording.

earthquakes. Creation of a buttressing, stabilized area of sand adjacent to the perimeter slope by the vibroreplacement method was found to be the most cost effective means of mitigating the hazard. By this method, the sand would be densified by vibroflotation at approximately 7 ft on center, and stone columns approximately 3 ft in diameter would be constructed at the vibroflotation locations. Analysis indicated that a stabilized buttressing zone approximately 50 ft wide extending back from the top of the perimeter slope would be enough to effectively retain any liquefied sand behind (landward of) this zone and thus reduce lateral-spreading displacements through the sand to less than approximately 1 ft. A plan view of the stone-column configuration is shown in figure 23, and a cross section of the stabilized zone is shown in figure 24.

Before proceeding with this mitigation scheme, one must assess the potential for movements in the underlying bay mud, which, though not susceptible to liquefaction, is a relatively soft material that could be further reduced in strength and deform during strong earthquake shaking. With the sand-stabilization measures in place, the area susceptible to lateral-spreading movements then shifts below the stabilized zone into the bay mud (fig. 24). Larger movements might occur on sliding surfaces that pass through the bay mud below the stabilized zone than on sliding surfaces passing through this zone. Within the scope of our studies, we could not assess in detail the potential for such movements through the bay mud around the perimeter of Treasure Island. Preliminary analyses using the method of Newmark (1965) indicate that movements of several feet might occur and that therefore more detailed consideration of this potential hazard would be desirable.

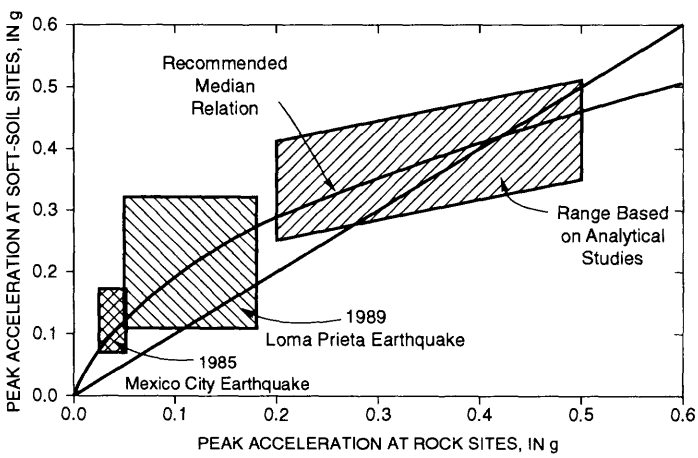


Figure 20.—Peak acceleration at rock sites versus soft-soil sites (after Idriss, 1991).

Extending the stone columns into the bay mud would be relatively ineffective in resisting deformations through the bay mud. If it were found that unacceptably large amounts of lateral spreading could be associated with deformations in the bay mud, then other or complementary ground-stabilization techniques would be needed. For example, creating 3-ft-diameter soil-cement columns extending into the bay mud by the deep-soil-mixing technique could add significant strength to the bay mud, but this technique is relatively expensive in comparison with vibroreplacement (Geomatrix Consultants, 1990b).

If the lateral-spreading hazard were effectively mitigated, then the main remaining ground-failure hazard would be compaction settlements. The differential movements accompanying these settlements would be damaging to many buildings and facilities, but overall, the island would be much less severely affected by these movements than by those caused by several feet or more of lateral spreading.

For certain facilities on the island judged to be relatively more critical or more susceptible to damage due to

settlement, inplace ground stabilization or structural modifications of the foundation systems could be considered. Ground-improvement techniques that may be appropriate include compaction, permeation, or jet grouting; vibrodrains, which are essentially small-diameter stone columns; and small-displacement compaction piles. Structural-foundation modifications may include installing deeper foundations (for example, small-diameter steel piles) and tying shallow foundation elements together for increased rigidity.

Because of the presence of a structure, costs of such retrofit stabilization would be considerably higher than open-space ground improvement or new construction. A detailed seismic-safety evaluation of existing structures would be needed to determine those facilities where improvements would be most beneficial.

Settlement of Treasure Island due to lateral spreading and compaction would also increase the potential for flooding or inundation of parts of the island by bay waters, particularly during periods of high tide and storm waves. The flooding hazard, however, would be largely mitigated by mitigating the lateral-spreading hazard. In addition, it might be desirable to fill low-lying areas of the island to above the high-tidal elevations (after accounting for earthquake-induced compaction settlements). This filling would mitigate shallow flooding due to seepage through the perimeter dike.

## CONCLUSIONS

The behavior of Treasure Island during the 1989 Loma Prieta earthquake again illustrated the liquefaction susceptibility of sand fills placed through water without compaction. Although significant ground failure and consequent damage occurred during the earthquake, these effects could have been much more severe had the earthquake been closer and (or) larger, as might affect the island and other parts of the San Francisco Bay region in the future.

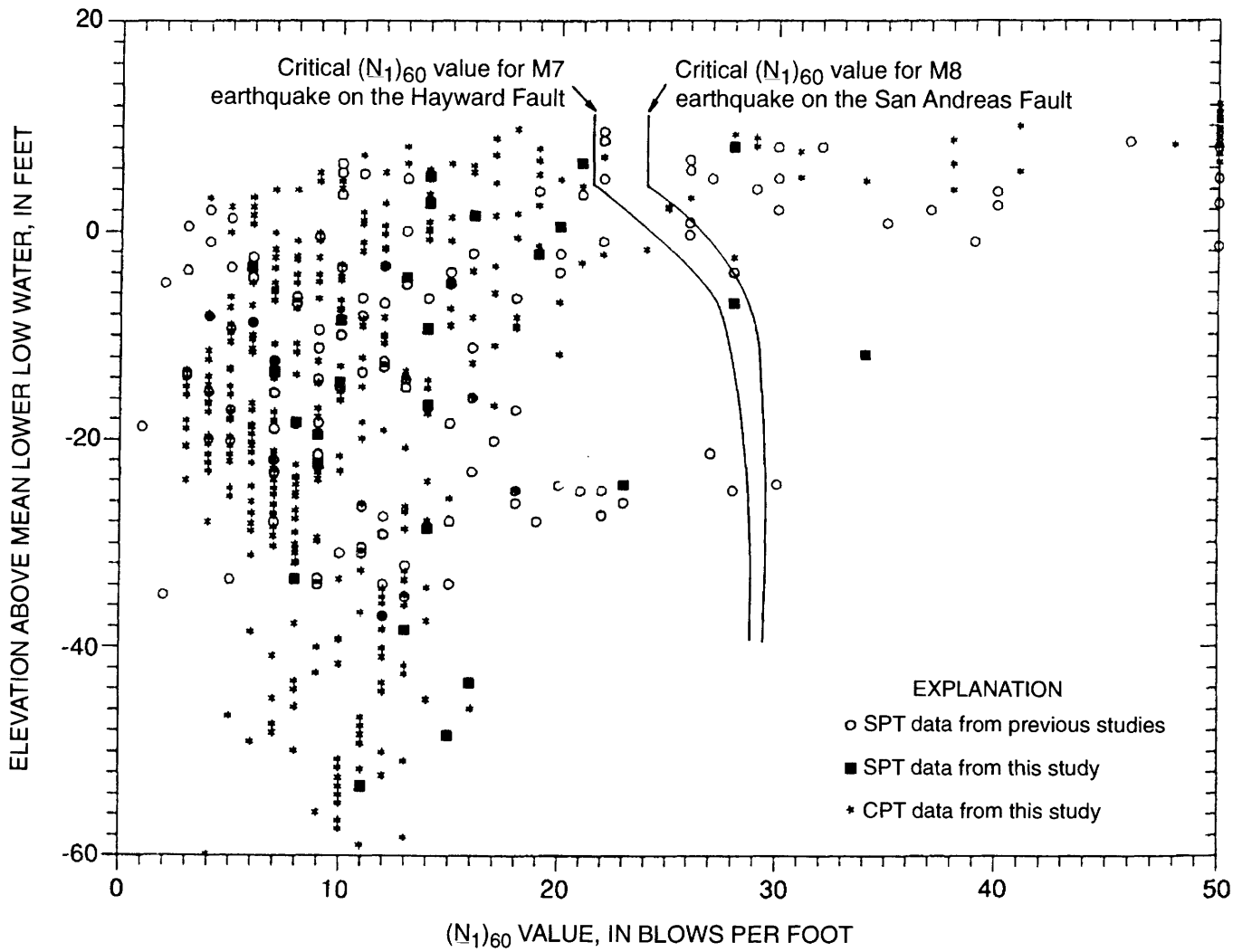


Figure 21.—$(N_1)_{60}$ value versus elevation, based on SPT and CPT data. Curves show critical $(N_1)_{60}$ values for hypothetical $M$=7 earthquake on the Hayward fault and $M$=8 earthquake on the San Andreas fault.

Most buildings on the island performed satisfactorily during the 1989 Loma Prieta earthquake. Thus, liquefaction does not necessarily imply severe damage to construction; the effects depend on the amount and types of ground movement resulting from liquefaction and the type of the design and the construction. Compaction settle-

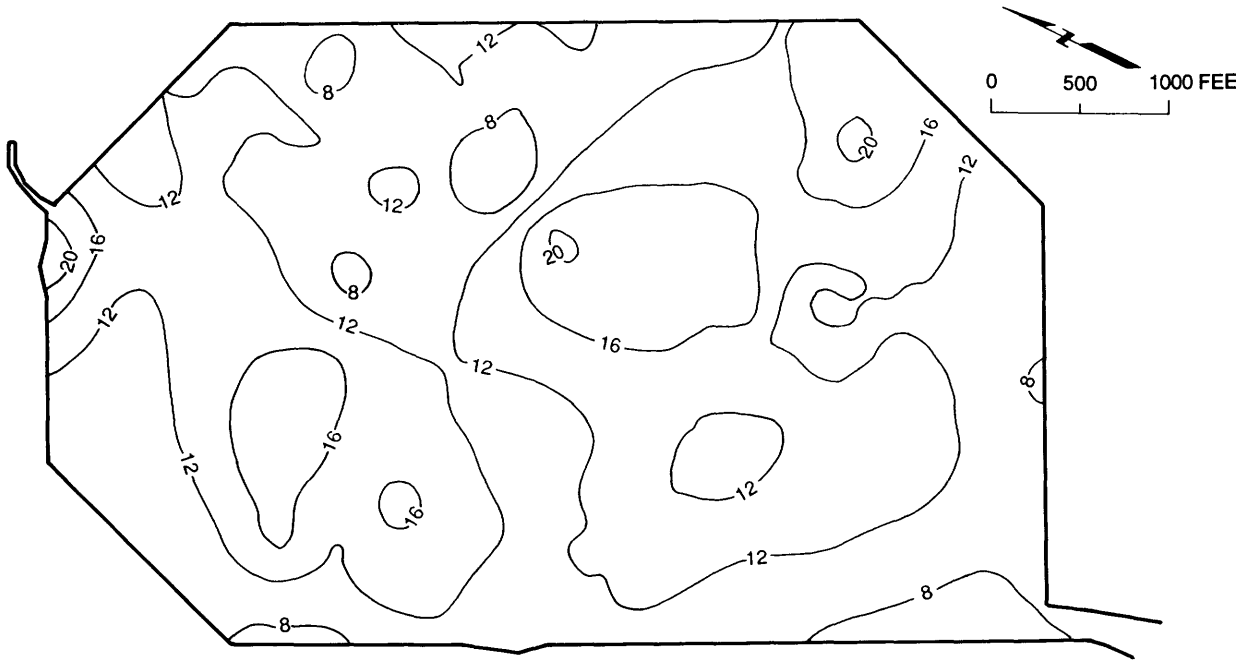


Figure 22.—Sketch map of Treasure Island, showing contours of estimated ground-surface settlement (in inches) caused by compaction for hypothetical $M$=7 earthquake on the Hayward fault and $M$=8 earthquake on the San Andreas fault.

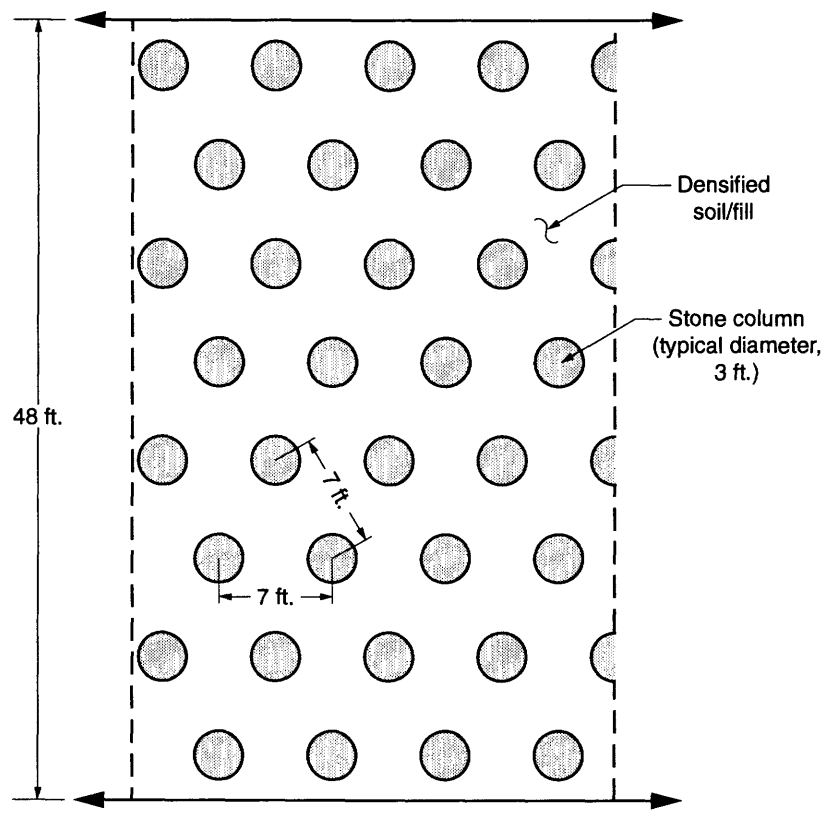


Figure 23.—Plan view of stone-column configuration for remedial scheme to mitigate liquefaction-induced lateral spreading.

ments of several inches caused relatively minor damage overall. Lateral-spreading movements of several inches were more damaging; potentially much larger lateral-spreading movements during larger, nearer earthquakes could be extremely damaging. The lateral spreading associated with liquefaction of sand could be effectively mitigated by using the vibroreplacement technique to create a stabilized buttressing zone near the island's perimeter. Before implementing this technique, however, the potential for deformations in the soft to stiff clay (bay mud) that underlie the liquefiable sand should be assessed.

The intensity of ground shaking recorded on Treasure Island during the 1989 Loma Prieta earthquake agrees reasonably well with that predicted from current ground-response-analysis methods. The occurrence of liquefaction on the island was consistent with the behavior predicted by using the method of Seed and others (1971, 1982, 1985). Applying a modified version of the method of Tokimatsu and Seed (1987) results in estimates of compaction settlement that agree reasonably well with observed settlements. Residual strengths of liquefied sand inferred from analysis of the lateral-spreading behavior on the island fall within the range reported by Seed and Harder (1990).

## REFERENCES CITED


Applied Management Engineering, Inc., 1990, Facility inspection for Naval Station Treasure Island, San Francisco, California (Treasure Island complex): Citrus Heights, Calif., 2 v.

California Strong Motion Instrumentation Program, 1989, Plots of the processed data for the interim set of 14 records from the Santa Cruz Mountains (Loma Prieta) earthquake of October 17, 1989: California Division of Mines and Geology, Office of Strong Motion Studies Report OSMS 89–08.

Egan, J.A., and Sangrey, D.A., 1978, Critical state model for cyclic load pore pressure: American Society of Civil Engineers Specialty Conference on Earthquake Engineering and Soil Dynamics, Pasadena, California, 1978, Proceedings, v. 1, p. 410–424.

Egan, J.A., and Ebeling, R.M., 1985, Variation of small-strain shear modulus with undrained shear strength of clay: International Conference on Soil Dynamics and Earthquake Engineering, 2d, Queen Elizabeth II, 1985, Proceedings, p. 2–27 to 2–36.

Engineering News-Record, 1937, Large dredging fleet assembled for filling Golden Gate Fair site: March 18, p. 412–414.

———1938, An island built to order: October 13, p. 459–461.

Fumal, T.E., 1978, Correlations between seismic wave velocities and physical properties of near-surface geologic materials in the southern San Francisco Bay region, California: U.S. Geological Survey Open-File Report 78–1067, 114 p.

Geomatrix Consultants, 1990a, Evaluation of interior area performance, Naval Station Treasure Island, San Francisco, California, v. 5 *of* report prepared for U.S. Navy, Naval Facilities Engineering Command, Western Division: San Bruno, Calif., 52 p.

———1990b, Perimeter dike stability evaluation, Naval Station Treasure Island, San Francisco, California, v. 3 *of* report prepared for U.S. Navy, Naval Facilities Engineering Command, Western Division: San Bruno, Calif., 55 p.

Gibbs, J.F., Fumal, T.E., Boore, D.M., and Joyner, W.B., 1992, Seismic velocities and geologic logs from borehole measurements at seven strong-motion stations that recorded the 1989 Loma Prieta earthquake: U.S. Geological Survey Open-File Report 92–287, 139 p.

Goldman, H.B., 1969, Geology of San Francisco Bay, *in* Goldman, H.B., ed., Geologic and engineering aspects of San Francisco Bay fill: California Division of Mines and Geology Special Report 97, p. 11–29.

Hagwood, J.J., 1980, Engineers at the Golden Gate, a history of the San Francisco District, U.S. Army Corps of Engineers, 1866–1980: U.S. Army Corps of Engineers, San Francisco, California, p. 158–166.


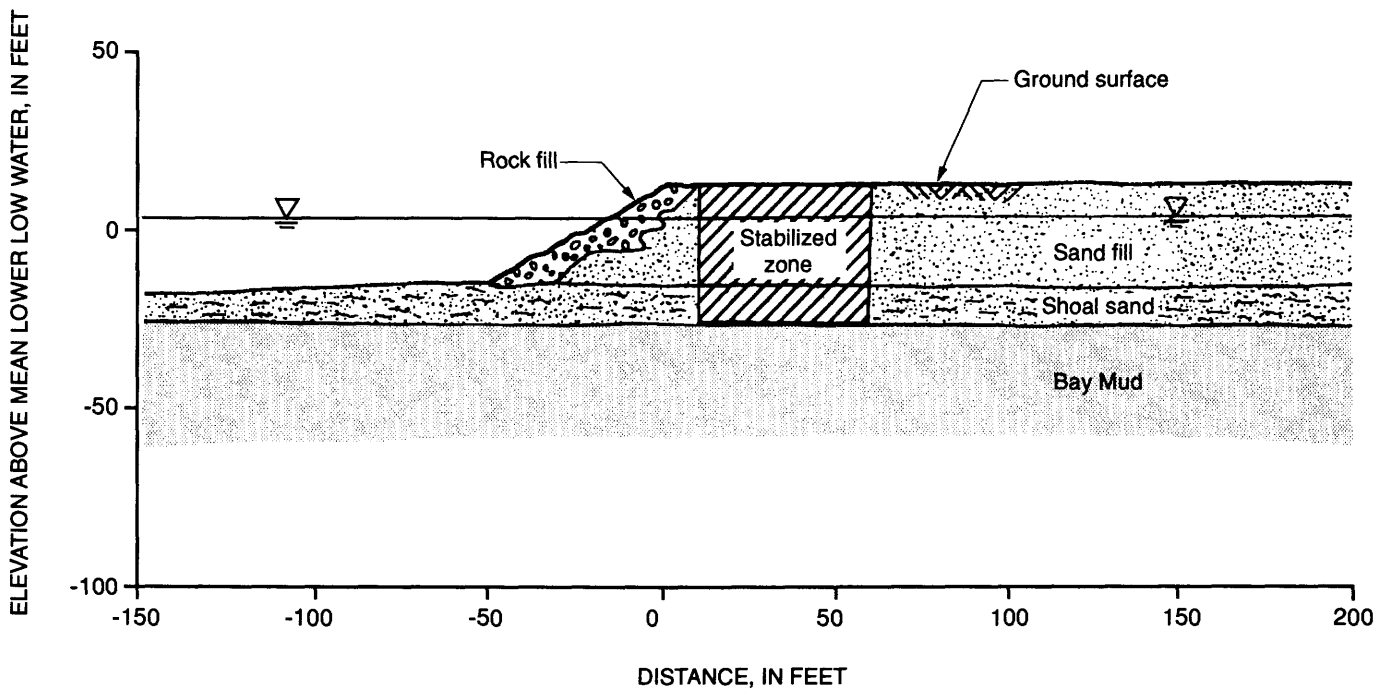


Figure 24.—Cross section of remedial scheme to mitigate liquefaction-induced lateral spreading.

Hryciw, R.D., Rollins, K.M., Homolka, Matthew, Shewbridge, S.E., and McHood, M.D., 1991, Soil amplification of Treasure Island during the Loma Prieta earthquake: International Conference on Recent Advances in Geotechnical Earthquake Engineering and Soil Dynamics, 2d, St. Louis, Mo., 1991, Proceedings, v. 2, p. 1679–1695.

Idriss, I.M., 1991, Earthquake ground motions at soft soil sites: International Conference on Recent Advances in Geotechnical Earthquake Engineering and Soil Dynamics, 2d, St. Louis, Mo., 1991, Proceedings, v. 3, p. 2265–2272.

Ladd, C.C., and Foott, Roger, 1974, New design procedure for stability of soft clays: American Society of Civil Engineers Proceedings, Geotechnical Engineering Division Journal, v. 100, no. GT7, p. 763–786.

Lee, C.H., 1969, Treasure Island fill, case history 2 *of* Lee, C.H., and Praszker, Michael, Bay mud developments and related structural foundations, *in* Goldman, H.B., ed., Geologic and engineering aspects of San Francisco Bay fill: California Division of Mines and Geology Special Report 97, p. 69–72.

Lee, K.L., and Albaisa, Aurelio, 1974, Earthquake induced settlements in saturated sands: American Society of Civil Engineers Proceedings, Geotechnical Engineering Division Journal, v. 100, no. GT4, p. 387–406.

Makdisi, F.I., and Seed, H.B., 1978, Simplified procedure for estimating dam and embankment earthquake-induced deformations: American Society of Civil Engineers Proceedings, Engineering Division Journal, v. 104, no. GT7, p. 849–867.

Newmark, N.M., 1965, Effects of earthquakes on dams and embankments: Geotechnique, v. 15, no. 2, p. 139–160.

Redpath Geophysics, 1991, Seismic velocity logging in the San Francisco Bay Area: report prepared for Electric Power Research Institute under agreement RP3014–06, 5 p.

Robertson, P.K., and Campanella, R.G., 1984, Guidelines for use and interpretation of the electric cone penetration test: Hogentogler and Co., Inc., and University of British Columbia, 175 p.

Schnabel, P.B., Lysmer, John, and Seed, H.B., 1972, SHAKE—a computer program for earthquake response analysis of horizontally layered sites: Berkeley, University of California, Earthquake Engineering Research Center Report EERC 72–12, 88 p.

Seed, H.B., and Idriss, I.M., 1971, Simplified procedures for evaluating soil liquefaction potential: American Society of Civil Engineers Proceedings, Soil Mechanics and Foundation Division Journal, v. 91, no. SM9, p. 1249–1273.

———1982, Ground motions and soil liquefaction during earthquakes: El Cerrito, Calif., Earthquake Engineering Research Institute, 134 p.

Seed, H.B., Tokimatsu, K., Harder, L.F., and Chung, R.M., 1985, Influence of SPT procedures in soil liquefaction resistance evaluations: Journal of Geotechnical Engineering, v. 111, no. 12, p. 1425–1445.

Seed, R.B., and Harder, L.F., 1990, SPT-based analysis of cyclic pore pressure generation and undrained residual strength, *in* Proceedings, H. Bolton Seed Memorial Symposium: Berkeley, Calif., BiTech, v. 2, p. 351–376.

Sykora, D.W., 1987, Examination of existing shear wave velocity and shear modulus correlations in soil: Vicksburg, Miss., U.S. Army, Waterways Experiment Station Miscellaneous Paper GL–87–22, 101 p.

Tokimatsu, Kohji, and Seed, H.B., 1987, Evaluation of settlements in sands due to earthquake shaking: Journal of Geotechnical Engineering, v. 113, no. 8, p. 861–878.

U.S. National Research Council, 1985, Liquefaction of soils during earthquakes: Washington, D.C., National Academy Press, 240 p.

Working Group on California Earthquake Probabilities, 1990, Probabilities of large earthquakes in the San Francisco Bay region: U.S. Geological Survey Circular 1053, 51 p.

# APPENDIX: TREASURE ISLAND SPT–CPT CORRELATION

The standard penetration test (SPT) is the most commonly used inplace soil test in North America. Although the relation between penetration resistance as measured by corrected standard blowcounts $(N_1)_{60}$ and liquefaction resistance is well established (Seed and others, 1985), a similar well-established correlation is unavailable for the cone-penetration test (CPT). Therefore, most engineers have relied on correlations between cone-penetration resistance, soil type, and the ratio of cone-penetration resistance to standard penetration resistance to determine the liquefaction susceptibility of a soil. Knowing the soil type (typically expressed as mean grain size), the penetration resistance is converted to a blowcount by using typical values of the ratio $Q_c/N$ (cone-penetration resistance to standard penetration resistance). The liquefaction susceptibility can then be determined by using the standard SPT correlations. Typical values of this ratio are plotted along with the soil-classification scheme of Robertson and Campanella (1984) in figure 25. Because the correlation shown in figure 25 was calculated by using data from numerous case studies, the soil types and $Q_c/N$ ratios represent average values. Indeed, Robertson and Campanella suggested that local observations should be used to establish relations more representative of local soil conditions.

In our study, the CPT data were converted to "standard" blowcounts by correlating the SPT resistance with the soil classification and cone-penetration resistance at sites immediately adjacent to one another. The soil was classified into a soil-behavior zone on the basis of the cone-penetration resistance and friction ratio, using the classification scheme of Robertson and Campanella (1984). Cone-penetration resistances were then averaged over a 2 $^1/_2$-ft depth interval and compared with the SPT resistance at an adjacent site at the same elevation. Most of the materials were classified as belonging to soil-behavior zones 5 through 9. Cone-penetration resistance is plotted against friction ratio and measured $Q_c/N$ ratio for the sand fill and shoal sand on Treasure Island in figure 26, with the soil-classification zones of Robertson and Campanella superimposed. The measured $Q_c/N$ ratios for each zone were averaged, giving typical values for Treasure Island materials (fig. 26). The Treasure Island $Q_c/N$ ratios are greater than the averages used by Robertson and Campanella, possibly owing to the looseness of the materials. As such, the blowcounts estimated from cone-penetration resistances on Treasure Island are lower than would have been calculated by using the standard correlations of Robertson and Campanella.

Liquefaction analyses also require an estimation of the fines content of the materials. Typically, the fines content

is estimated from the soil-behavior type identified by using the standard correlation of Robertson and Campanella (1984). As stated above, most of the materials were classified as belonging to soil-behavior zones 5 through 9, which range from clayey silt to clean sand. The fines content of these materials ranges from less than 5 percent (clean sand, highly susceptible to liquefaction) to nearly 100 percent (clayey silt, insusceptible to liquefaction). However, sieve analyses of the materials retrieved from adjacent SPT sites indicated that the actual material ranges from silty sand to clean sand. Cone-penetration resistance is plotted against friction ratio in figure 27, with the soil classification and fines content based on sieve analyses and the Unified Soil Classification System (USCS). Figure 27 indicates that the CPT-based soil-classification scheme of Robertson and Campanella cannot be used to estimate the fines content of the materials on Treasure Island.

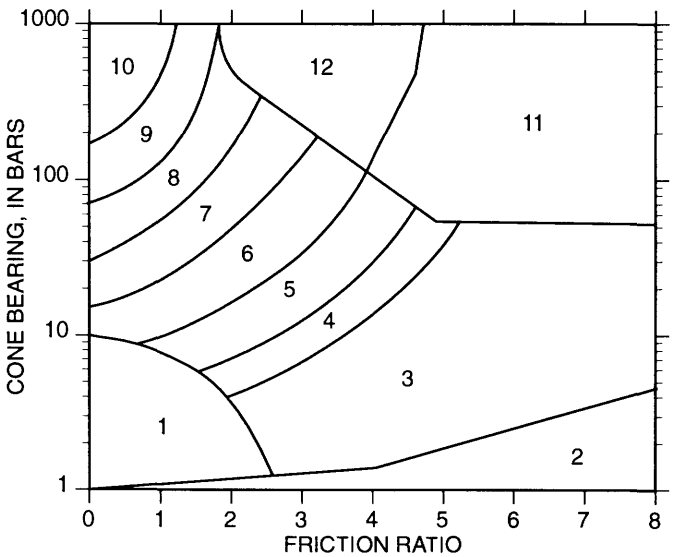


| Zone | Soil-behavior type | $Q_c/N$ |
|---|---|---|
| 1 | Sensitive fine-grained | 2 |
| 2 | Organic material | 1 |
| 3 | Clay | 1 |
| 4 | Silty clay to clay | 1.5 |
| 5 | Clayey silt to silty clay | 2 |
| 6 | Sandy silt to clayey silt | 2.5 |
| 7 | Silty sand to sandy silt | 3 |
| 8 | Sand to silty sand | 4 |
| 9 | Sand | 5 |
| 10 | Gravelly sand to sand | 6 |
| 11 | Very stiff, fine grained[1] | 1 |
| 12 | Sand to clayey sand[1] | 2 |

[1]Overconsolidated or cemented.

Figure 25.—Cone bearing versus friction ratio for standard electronic friction cone (after Robertson and Campanella, 1984).

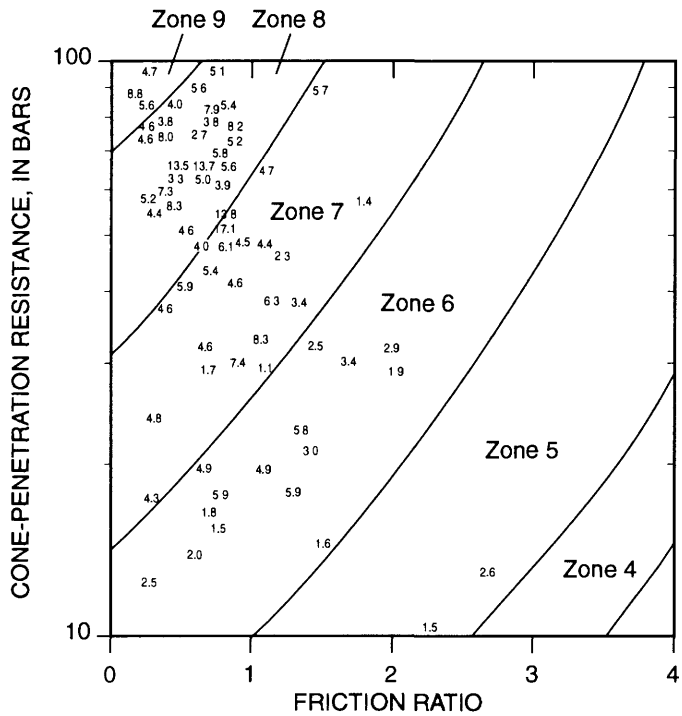


| Classification Zone | Average $Q_c/N$ Value |
|---|---|
| 4 | 1.5 |
| 5 | 2.1 |
| 6 | 3.4 |
| 7 | 4.4 |
| 8 | 5.2 |
| 9 | 5.5 |

Figure 26.—Cone-penetration resistance versus friction ratio at sites of adjacent cone-penetration and standard penetration tests, showing soil-classification zones of Robertson and Campanella (1984) and average $Q_c/N$ values used for Treasure Island.

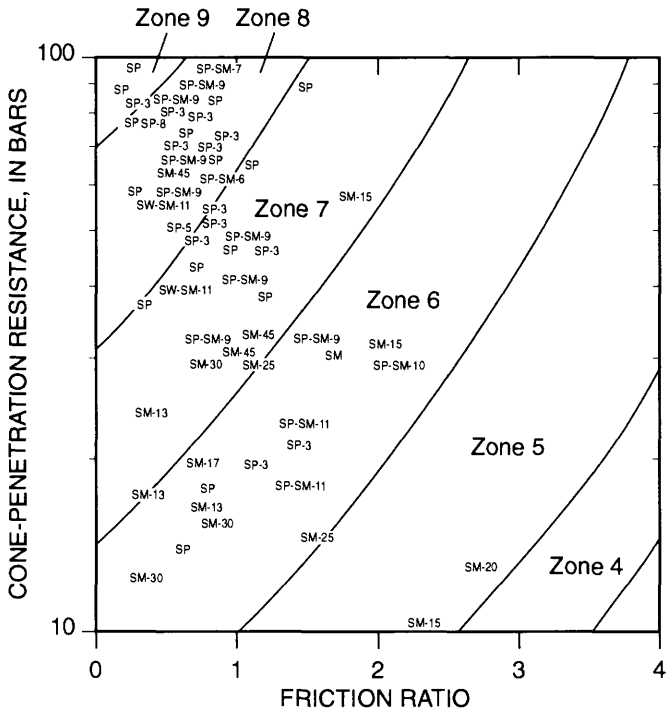


Figure 27.—Cone-penetration resistance versus friction ratio at sites of adjacent cone-penetration and standard penetration tests, showing soil-classification zones of Robertson and Campanella (1984), soil types in Unified Soil Classification System (alphabetic symbols), and fines content (in percent passing No. 200 sieve; numeric values).

STRONG GROUND MOTION AND GROUND FAILURE

# SAND BOILS AND SETTLEMENT ON TREASURE ISLAND AFTER THE EARTHQUAKE

By Michael J. Bennett,
U.S. Geological Survey

## CONTENTS



ABSTRACT

After the 1989 Loma Prieta earthquake, a reconnaissance survey was made on Treasure Island, a manmade island underlain by hydraulic fill, to document liquefaction effects and settlement. During the earthquake, parts of the fill liquefied and was redeposited as sand boils on the ground surface. On the basis of grain size and color, at least three groups of sand boils are distinguishable. Although dredging and transportation during filling, as well as venting of sand during liquefaction, induced changes in the grain-size distribution of the sand, the sand-boil deposits are correlatable with the natural deposits before they were dredged. Differential settlement is most clearly evident where piles are associated with buildings, and in a few other places. The maximum measured differential settlement is 120 mm.

## INTRODUCTION

On Treasure Island, a manmade island in San Francisco Bay, strong ground shaking during the 1989 Loma Prieta earthquake liquefied a part of the subsurface and caused liquefaction effects, such as sand boils and differential settlement, at the U.S. Naval Station (fig. 1). Between November 14 and 20, 1989, a reconnaissance survey was made to document the sand boils and differential settlement caused by the earthquake. A more complete description of the subsurface conditions and ground effects on Treasure Island is given by Power and others (this chapter).

Treasure Island was constructed on Yerba Buena Shoals, a shallow-water area just north of Yerba Buena Island (fig. 1). Before construction, the shallowest of the shoals was a sand spit that was just exposed at low tide. Hydraulic filling for the construction of Treasure Island began in 1936 and was completed in 1937. The hydraulic fill was dredged from the area immediately surrounding the shoals and from areas adjacent to the Presidio and Angel Island (fig. 1).

Lee (1969) characterized the types of sedimentary materials used as fill (in decreasing percentage of total volume) and its source area as (1) soft blue marine sand (49 percent), 50 to 60 percent held on No. 200 sieve, transported from east and north of Treasure Island by pipeline from dredges; (2) "yellow" alluvial sand (24 percent), 98 percent held on No. 150 sieve, transported from the east bay by pipeline dredges, containing clayey sand that was discharged as "clay balls"; (3) soft blue marine sand (22 percent), 70 to 80 percent held on No. 200 sieve, transported from a channel south of Treasure Island by pipeline from dredges; (4) "heavy sand" (4 percent), coarse and well graded, transported by hopper dredges from the Presidio and Alcatraz and Knox Shoals; and (5) miscellaneous (1 percent), black sandy mud, transported by clamshell dredge over the seawall. Lee also stated that the texture of the fill was determined soon after placement. The predominate texture was fine sand, in some places clayey, with some medium to coarse sand and gravelly sand. Lee noted that shells and clay balls (a result of hydraulic transportation) were a common component of the fill. The clay balls ranged from small gray clay balls from the central bay, only 2 percent greater than 0.075 mm, to large yellow clay balls from the east bay, 70 percent greater than 0.075 mm.

## SAND BOILS

Gravel and sand contents were determined by using sieves; silt and clay fractions were determined with a hy-

drometer. Grain-size characteristics of the sand boils are listed in table 1. The sand boils are composed of very fine gray sand and fine to medium, gray and brown sand. Shell fragments are abundant and large (19-cm diam) clay balls are present in some of the brown sand-boil deposits. The frequency of the median grain size ($D_{50}$) of all the sand boils is bimodal: Two distinct peaks occur on the grain-size-frequency graph (fig. 2). The grain-size distribution is plotted in figure 3. On the basis of grain size and color, the sand boils can be divided into three groups. Group 1 consists of gray, very fine sand, with an average $D_{50}$ value of 0.108 mm, an average coefficient of uniformity ($C_u$) of 3.8, and an average sand content (No. 200 sieve) of 69 percent; shells are common (similar to fill type 1). Group 2 consists of brown, fine to medium sand, with an average $D_{50}$ of 0.236 mm, an average $C_u$ value of 2.6, and an average sand content of 94 percent; shells and large clay balls are present (similar to fill type 2). Group 3 consists of gray, fine to medium sand; shells are common (similar to fill type 3).

Sand-boil samples can be correlated with their original sources by using color, grain size, and other features, such as shells and clay balls. The gray, very fine sand (sand-boil group 1) originated from fill type 1 (soft blue marine sand, 50 to 60 percent held on No. 200 sieve). The increase in sand content from the original 50–60 percent to the average of 69 percent in the sand-boil samples occurred during dredging and placement of fill, when engineers flushed the fines out of the construction zone. Of the original 22,464,000 $m^3$ of material dredged, only 16,015,000 $m^3$ was retained as fill; the rest (28 percent) was lost by erosion or flotation of fines (Lee, 1969). Similarly, in sand-boil group 2, the brown, fine to medium sand originated from fill type 2. In this group the change in sand content is less because the original deposit had a lower fines content. Sand-boil group 3 (gray, fine to me-

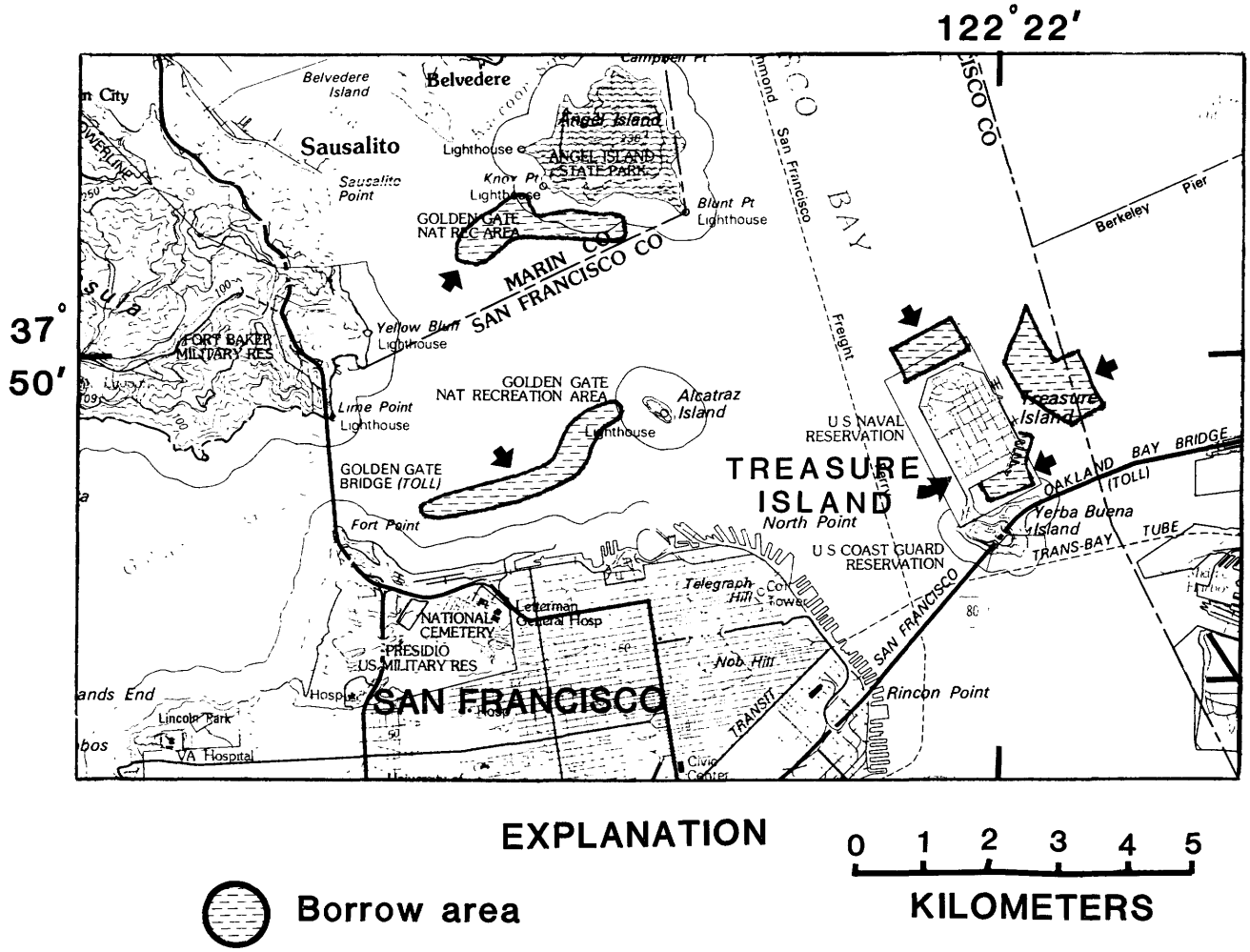


Figure 1.—San Francisco Bay, showing locations of Treasure Island and borrow areas used for fill in its construction.

Table 1. *Grain-size characteristics of sand boils on Treasure Island*

[C, clay (<0.005 mm); G, gravel (>4.75 mm); M, silt (>0.005 to <0.075 mm); S, sand (>0.075 to <4.75 mm). $D_{50}$, median grain size; $C_u$, coefficient of uniformity, defined as grain size at the 60th percentile divided by grain size at the 10th percentile ($D_{60}/D_{10}$)]

| Locality (Fig. 4) | G | S | M | C | M+C | $D_{50}$ | $C_u$ |
|---|---|---|---|---|---|---|---|
| 1 | 0 | 96 | - | - | 4 | 0.220 | 2.1 |
| 2 | 2 | 97 | - | - | 1 | 0.289 | 1.9 |
| 3 | 0 | 96 | - | - | 4 | 0.225 | 2.4 |
| 4 | 0 | 76 | 19 | 5 | - | 0.119 | 6.2 |
| 5 | 0 | 94 | - | - | 6 | 0.245 | 2.8 |
| 6 | 0 | 99 | - | - | 1 | 0.378 | 1.9 |
| 7 | 0 | 89 | - | - | 11 | 0.192 | 3.0 |
| 8 | 0 | 98 | - | - | 2 | 0.320 | 2.3 |
| 9 | 0 | 98 | - | - | 2 | 0.243 | 2.1 |
| 10 | 1 | 58 | 36 | 5 | - | 0.090 | 4.8 |
| 11 | 0 | 99 | - | - | - | 0.335 | 2.0 |
| 12 | 0 | 97 | - | - | 3 | 0.210 | 2.0 |
| 13 | 0 | 98 | - | - | | 0.230 | 2.0 |
| 14 | Large clay balls | | | | | | |
| 15 | 0 | 54 | 31 | 15 | - | 0.113 | 178.0 |
| 16 | 0 | 98 | - | - | | 0.211 | 1.6 |
| 17 | Shells | | | | | | |
| 18 | 0 | 93 | - | - | 7 | 0.187 | 2.3 |
| 19 | 0 | 91 | - | - | 9 | 0.200 | 2.8 |
| 20 | 0 | 92 | - | - | 8 | 0.204 | 2.6 |
| 21 | 0 | 91 | - | - | 9 | 0.194 | 2.6 |
| 22 | 6 | 86 | - | - | 8 | 0.270 | 2.8 |
| 23 | 0 | 54 | 40 | 6 | - | 0.085 | 7.1 |
| 24 | 0 | 80 | 17 | 3 | - | 0.119 | 2.8 |
| 25 | 0 | 72 | 25 | 3 | - | 0.112 | 4.6 |
| 26 | 0 | 88 | - | - | 12 | 0.282 | 7.0 |
| 27 | 0 | 77 | 21 | 2 | - | 0.110 | 2.7 |
| 28 | 0 | 75 | 21 | 4 | - | 0.105 | 3.3 |
| 29 | 0 | 37 | 61 | 2 | - | 0.062 | 2.2 |
| 30 | 1 | 88 | - | - | 11 | 0.168 | 2.9 |
| 31 | 0 | 90 | - | - | 10 | 0.153 | 2.2 |
| 32 | 0 | 85 | - | - | 15 | 0.123 | 2.2 |
| 33 | 0 | 87 | - | - | 13 | 0.148 | 2.5 |
| 34 | 0 | 91 | - | - | 9 | 0.197 | 2.6 |

dium sand) is postulated to have originated from fill type 3 (70–80 percent fines).

Identification of the subsurface units that liquefied from material deposited above ground in the form of sand boils is important in liquefaction studies. Knowing what units liquefied can be used to confirm estimates of liquefaction potential determined from penetration tests.

Although sand boils were common on Treasure Island, their areal distribution was not uniform (fig. 4). A zone, 100 m wide by 1,000 m long, of sand boils (brown, fine to medium sand) occurred on the east (fig. 5, locality 5) and southeast sides of the island. The source of this fill, which was located 300 m east of the island, consisted of "yellow" fine to medium sand. Some sand in this elongate

zone erupted through the pavement and left collapse features.

Sand boils were concentrated in three areas on the island. The highest concentration was on the baseball field in the central part of the island (fig. 4), where the sand deposits were large and consisted of gray, fine shelly sand. Three large sand boils (brown sand; vent diameter, 1.0 m) erupted on the west side of the island at the storm-pump station (fig. 4). Four sand boils erupted in the area of residential buildings 1315 and 1321 (gray sand, some of which was erupted into a residence; see fig. 4, locs. 32, 33). The sand boils in the northern part of the island did not occur in closely spaced groups; they consisted of the finest sand and the second-coarsest sand within 100 m of each other. The largest individual sand deposit, approximately 11 to 19 $m^3$ in volume (Tom Cuckler, oral commun., 1989), occurred in this group in the schoolyard (fig. 4). Of the 32 sand boils sampled, 20 occurred within 100 m of the perimeter dike that surrounds the island.

Except for the baseball field and schoolyard, most of the central part of the island was free from sand boils. The sand-spit area of the shoals (southwestern part of the island), especially an area that was originally under less than 3.7 m of water, had only one definite occurrence of a sand boil but displayed well-defined differential settlement.

## SETTLEMENT

The best-defined examples of settlement involve piles that were emplaced to support structures. Although it is uncertain that piles did not rise, it is known from survey data (Egan and Power, 1990) that the surface of the island subsided from 5 to 15 cm. Buildings 2 and 3 (fig. 4) are pile supported around the building perimeter; settlement occurred where there was no pile support, on the floors inside or the ground outside. Building 2 consistently showed 60 to 110 mm of differential settlement around its perimeter. Piles that had been cut off at an unknown depth below ground were thrust through the pavement as the ground around the piles settled; piles poking through the asphalt pavement in the parking lot near building 450 show about 90 mm of differential settlement (fig. 6). Without a stable(?) pile in the ground, settlement in these areas would be difficult to see without a precise survey. Measurements of differential settlement are listed in table 2, and the locations of settlement sites are shown in figure 4.

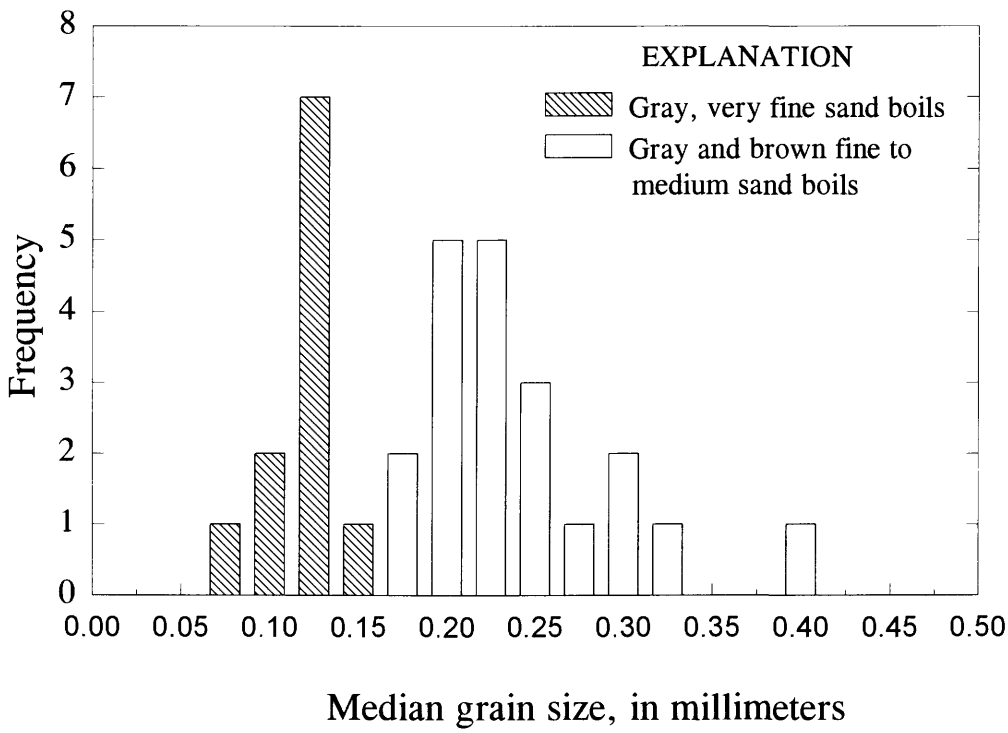


Figure 2.—Frequency of median grain sizes for all sand boils on Treasure Island. Three groups of sand boils are identifiable by color and size: (1) gray, very fine sand; (2) brown, fine to medium sand; and (3) gray, fine to medium sand.

## CONCLUSIONS

By using color, grain size, and other features, sand-boil deposits can be correlated with their original sources. Without stable references, however, such as piles or buildings supported by piles, settlement on Treasure Island would be difficult to measure without a precise survey.

## ACKNOWLEDGMENTS

I thank Capt. Thomas Vaught, Commander of Treasure Island Naval Station; Thomas Cuckler of the Civil Engineering Department, Treasure Island Naval Station; and Richard Faris of the U.S. Navy's Naval Engineering Command, Western Division, for their cooperation and assistance. I also thank David Keefer and Raymond Wilson for their reviews of the manuscript.

## REFERENCES CITED

Egan, J.A., and Power, M.S., 1990, Evaluation of interior area performance, Naval Station, Treasure Island, San Francisco, California: report to Geomatrix Consultants on project 1539.09, v. 5, 52 p.

Lee, C.H., 1969, Treasure Island fill, case history 2 *of* Lee, C.H., and Praszker, Michael, Bay mud developments and related structural foundations, *in* Goldman, H.B., ed., Geologic and engineering aspects of San Francisco Bay fill: California Division of Mines and Geology Special Report 97, p. 69–72.

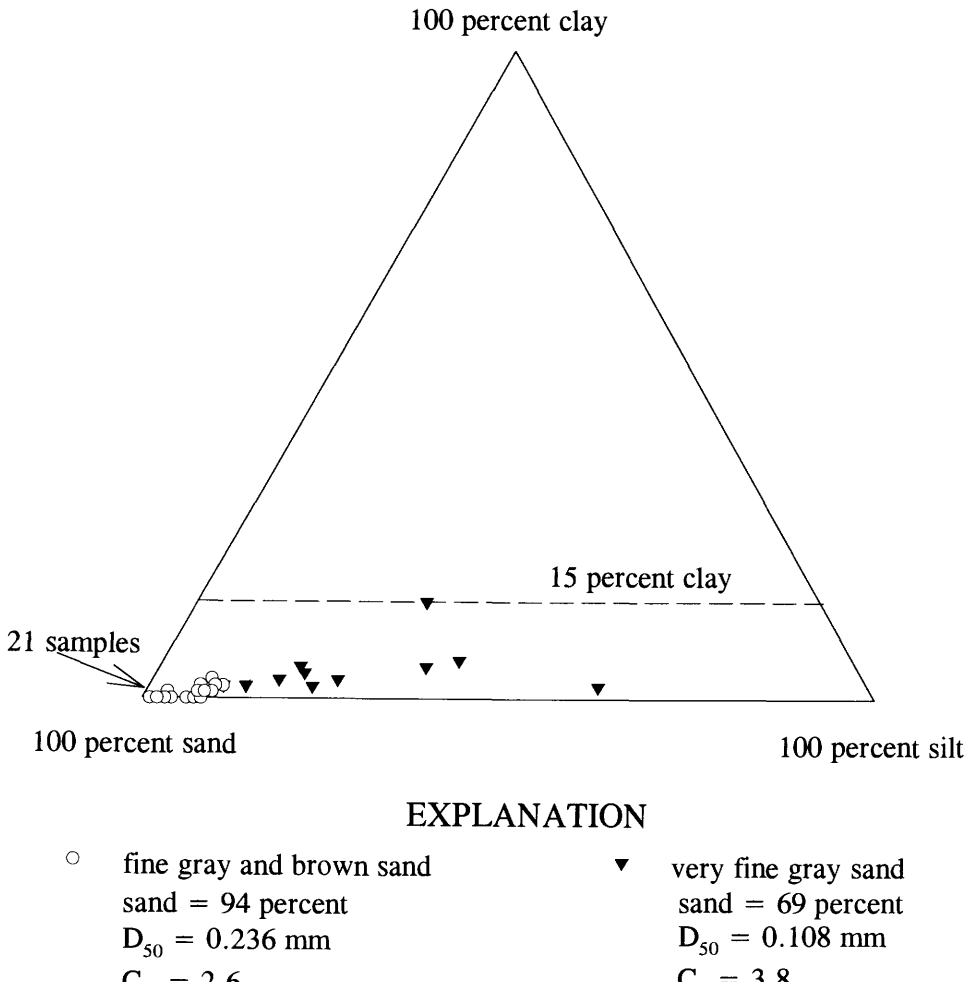


Figure 3.—Triangular diagram showing grain-size distribution in all sand boils on Treasure Island. Dashed line labeled "15 percent" represents 15 percent clay (0.005 mm); subsurface samples plotting above this line would not be expected to liquefy.

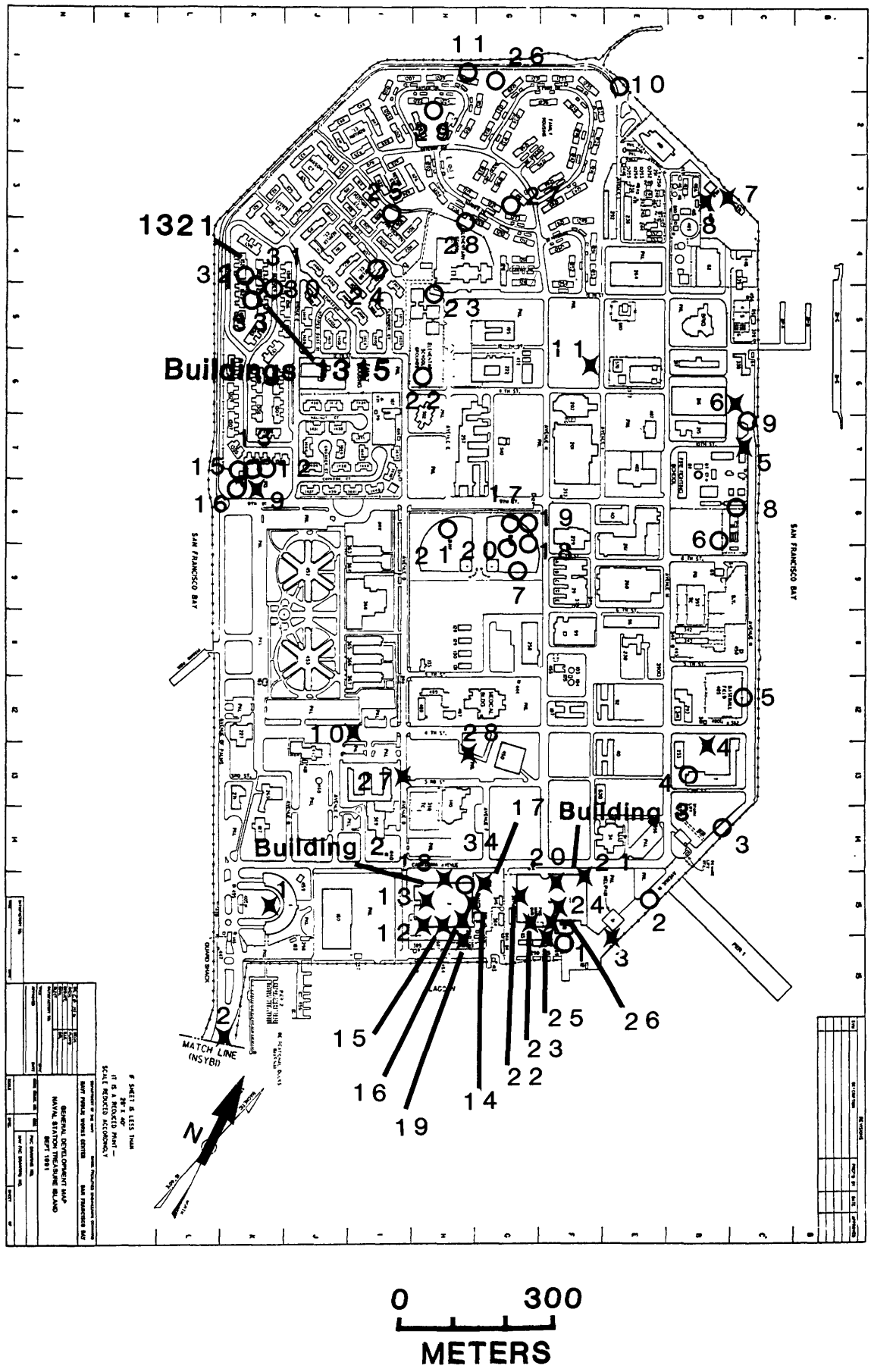
Buildings
Building 2
Building 3
SAN FRANCISCO BAY
MATCH LINE (NSYBI)
N
0 300
METERS

Figure 5.—Sand boil on east side of Treasure Island at locality 5 (fig. 4).

Figure 6.—Differential settlement (approx 90 mm) on Treasure Island where piles erupted through pavement in parking lot near Building 450 (loc. 28, fig. 4).

◀ Figure 4.—Treasure Island (see fig. 1 for location), showing localities (numbers) where sand boils were sampled (circles) and settlements measured (crossed dots).

Table 2. *Settlement measurements at sites on Treasure Island*

| Locality (fig. 4) | Settlement (mm) | Description |
|---|---|---|
| 1 | 5-20 | Along cracks at headquarters parking lot. |
| 2 | 0-20 | Along cracks on causeway. |
| 3 | 70 | Along crack on east side, east side down. |
| 4 | 70 | Piles thrust through parking lot, building 7. |
| 5 | 30 | Along crack, east side down. |
| 6 | 15-50 | Along crack, west side down. |
| 7 | 90 | At tank that extends 1.9 m below ground level. |
| 8 | 35 | Along crack, east side down. |
| 9 | 75 | At pump station, associated with sand boil. |
| 10 | ? | Octahedral pattern caused by settlement on piles (old main tower from fair ?). |
| 11 | 750 | Sinkhole, recently active. |
| 12 | 70 | Building 2, room 1131, separation of southern. wall and floor |
| 13 | 95 | Building 2, foundation and floor, stable between October 20, and November 20, 1989. |
| 14 | 110 | Building 2, eastern wall, floor and pile supported foundation for old sliding door. |
| 15 | 30 | At floor and wall, but as much as 580 mm, void space beneath floor. |
| 16 | 40 | Building 2, floor and wall. |
| 17 | <120 | Building 2, flashing on outside corner of building indicates maximum settlement is less than 120 mm. |
| 18 | 60 | Building 2, paint overlap on awning. |
| 19 | 80 | Building 2, pull down of pipe brace. |
| 20 | 35 | Building 3, fence damaged when floor settled. |
| 21 | 50 | Building 3, northeast corner. |
| 22 | 50 | Building 3, floor and foundation. |
| 23 | 65 | Building 3, around structural support. |
| 24 | 70 | Building 3, settlement due to heavy equipment (?). |
| 25 | 90 | Building 3, ground and building outside. |
| 26 | 65 | Building 3, floor. |
| 27 | 5-50 | Piles, Avenue D. |
| 28 | 90 | Piles, parking lot near Building 450. |

THE LOMA PRIETA, CALIFORNIA, EARTHQUAKE OF OCTOBER 17, 1989:
LIQUEFACTION

STRONG GROUND MOTION AND GROUND FAILURE

# LIQUEFACTION AT MOSS LANDING

By Lelio H. Mejia,
Woodward-Clyde Consultants

## CONTENTS



ABSTRACT

The 1989 Loma Prieta earthquake caused extensive liquefaction in the Monterey Bay area, Calif. Liquefaction was widespread in the coastal area of Moss Landing at the confluence of Elkhorn and Moro Cojo Sloughs and the Old Salinas River some 15 mi south of the epicenter. Liquefaction damage was particularly severe on the Moss Landing sand spit, a 500- to 1,000-ft-wide shoreline peninsula deposited by beach sedimentation and by the Old Salinas River. The Moss Landing Marine Laboratory (MLML) operated by the California State University was damaged beyond repair by liquefaction of the natural subsurface soils and ensuing lateral spreading and differential settlement of the site. In contrast, permanent lateral ground displacements at the site of the new Monterey Bay Aquarium Research Institute (MBARI) technology building and pier were small, and these facilities were essentially undamaged. This paper describes some of the liquefaction effects in the Moss Landing area and reports on an investigation of the liquefaction failure at the MLML site and of the absence of liquefaction damage at the MBARI facilities. Liquefaction occurred in loose to medium-dense sand underlying the MLML site at about 10- to 20-ft depth. In addition, liquefaction appears to have occurred in clayey silt underlying the east side of the site at similar depths. The good performance of the MBARI facilities is attributable to more favorable soil conditions and the type of construction at this site. Liquefaction damage in the Moss Landing area from a future larger and closer earthquake could be more severe than that observed during the 1989 Loma Prieta earthquake unless measures to mitigate the damage are implemented.

## INTRODUCTION

The 1989 Loma Prieta earthquake caused extensive liquefaction and ground failure throughout the San Francisco Bay and Monterey Bay regions. In the Monterey Bay region (fig. 1), liquefaction was widespread in alluvial deposits of the San Lorenzo, Pajaro, and Salinas Rivers, along the channels of Watsonville and Struve Sloughs, and in unconsolidated deposits along the coast from Santa Cruz to the mouth of the Salinas River. Notably, liquefaction generally occurred in areas that had previously been identified as having a high liquefaction susceptibility and that had liquefied during the great 1906 San Francisco earthquake (Youd and Hoose, 1978; Dupré and Tinsley, 1980; Seed and others, 1990).

Liquefaction was widespread in the coastal area of Moss Landing at the confluence of Elkhorn and Moro Cojo Sloughs and the Old Salinas River about 15 mi south of the epicenter, as shown in figure 1. Liquefaction was particularly severe on Moss Landing spit, a 500- to 1,000-ft-wide shoreline peninsula deposited by beach sedimentation and by the Salinas River. Water and sewer services on the spit could not be restored for more than 3 months, severely affecting the operation of several commercial fisheries, the Monterey Bay Aquarium Research Institute (MBARI) facilities, and the Moss Landing harbor.

The $6-million Moss Landing Marine Laboratory (MLML) operated by the California State University was damaged beyond repair by liquefaction of the natural subsurface soils and ensuing lateral spreading and differen-

tial settlement of the site. Even though the buildings were practically torn apart at the foundation, the structures did not collapse, and no casualties or severe injuries were reported among the approximately 50 people occupying the facility at the time.

North of the MLML, evidence of liquefaction, settlement, and lateral spreading was observed along the entire length of the spit. Damage from liquefaction to other buildings, however, was not as severe as to the MLML. At the site of the new MBARI technology building and pier, permanent lateral ground displacements were small, and these facilities were essentially undamaged.

The purpose of this paper is to describe some of the observed liquefaction effects in the Moss Landing area in relation to subsurface soil conditions, and to evaluate the liquefaction failure at the MLML site and the absence of damage at the MBARI facilities.

## SETTING

Moss Landing is situated on the east shoreline of Monterey Bay approximately midway between Santa Cruz and Monterey, about 7.5 mi southwest of Watsonville and about 15 mi south of the earthquake epicenter (fig. 1). The area is a focal point for regional surface drainage entering Monterey Bay through three main watercourses: Elkhorn Slough, the Pajaro River about 3 mi to the north, and the Salinas River about 4.5 mi to the south. Before the 1906 San Francisco earthquake, the Salinas River flowed into Monterey Bay through the Moss Landing harbor to an outlet about 1.5 mi north of Moss Landing (Griggs, 1990). As shown in figure 2, the harbor now occupies part of the old river channel.

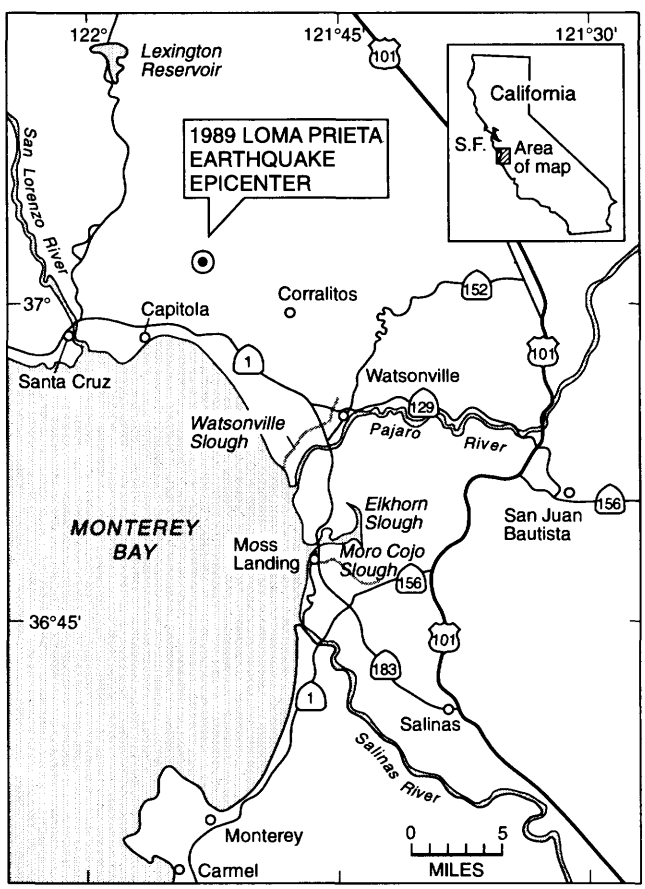


Figure 1.—Monterey Bay region, Calif., showing location of epicenter of 1989 Loma Prieta earthquake.

The Moss Landing area is underlain by a sequence of Holocene deposits consisting of relatively thick sand offshore and estuarine and fluvial deposits onshore, as much as about 180 ft deep (Dupré and Tinsley, 1980). Wood penetrated at 110-ft depth in a borehole near Units 6 and 7 at the Pacific Gas & Electric (PG&E) powerplant was found to be about 7,000 years old by radiocarbon dating (Dames & Moore, 1963).

The Moss Landing spit is underlain by littoral soils deposited in a shoreline environment within the zone of tidal fluctuation. These soils consist predominantly of sand with interbedded silt and clay, underlain by Pleistocene and Miocene deposits to about 7,000-ft depth, where oil-exploration logs indicate Mesozoic granite.

## EARTHQUAKE GROUND MOTIONS

No ground-motion-recording instruments were operating near Moss Landing at the time of the 1989 Loma Prieta earthquake; however, several instruments operated by the California Strong Motion Instrumentation Program (CSMIP) of the California Division of Mines and Geology recorded earthquake motions in the Monterey Bay region. The peak horizontal accelerations recorded at the strong-motion stations closest to Moss Landing are listed in table 1 (Shakal and others, 1989), along with the epicentral distance, approximate closest distance to the earthquake source, and site conditions for the recording stations.

Because Moss Landing is about 13 mi from the earthquake source (approx 15 mi from the epicenter) and the area is underlain by deep alluvium that is generally soft near the surface, the data listed in table 1 suggest a peak acceleration of about 0.2 to 0.3 *g* at Moss Landing. Numerical simulations using the techniques of Wald and others (1988) and the source and crustal-structure models of Sommerville and Yoshimura (1990) for the 1989 Loma Prieta earthquake suggest that the peak acceleration on a hypothetical rock outcrop at Moss Landing would have been about 0.15 *g* (Woodward-Clyde Consultants, 1990). These simulations, together with the relation between peak accelerations on rock and soft soils proposed by Idriss (1991), suggest a peak acceleration of about 0.25 *g* at Moss Landing.

A peak ground acceleration of 0.25 *g* is consistent with the felt intensity of ground motions reported by occupants of the MLML and other people on the spit at the time of the earthquake (Larry Jones, oral commun., 1989), and with the relatively slight damage to building contents at the MLML (Jon Raggett, oral commun., 1989). Buildings on the spit that were unaffected by soil liquefaction and lateral spreading sustained little to no structural damage. At the MLML, a few books fell off shelves in the library, and the damage to freestanding equipment, museum specimens, and pictures on walls was minimal. The shear walls between door openings were intact (without stress cracks) after the earthquake. A few freestanding bookshelves that had not been braced fell over on the second floor; however, new sheetrock partitions showed very small cracks at the door corners, and the roof diaphragms and chords were intact. Freestanding masonry walls around the loading dock area had only minor hairline cracks (J.D. Raggett and Associates, 1989).

On the basis of ground motions recorded in the Monterey Bay region, the results of the aforementioned numeric simulations, the level of shaking intensity reported by oc-

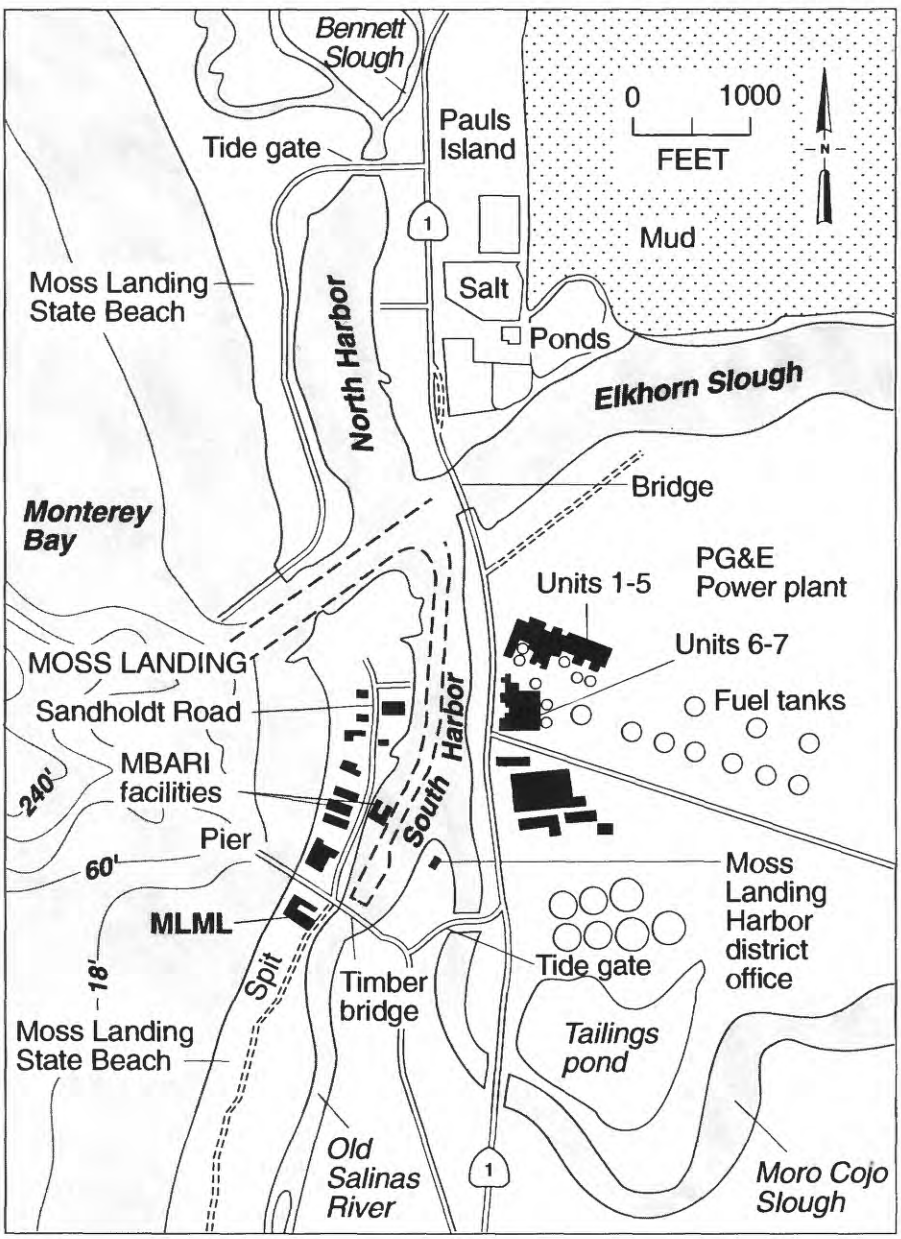


Figure 2.—Moss Landing area, showing locations of Moss Landing Marine Laboratory (MLML), Monterey Bay Aquarium Research Institute (MBARI), and Pacific Gas & Electric (PG&E) Co. powerplant. Depth contours in feet below mean lower low water.

Table 1.—*Peak horizontal accelerations recorded in the Moss Landing area*

| Recording station | Epicentral distance (mi) | Distance to source (mi) | Site conditions | Peak horizontal acceleration (g) |
|---|---|---|---|---|
| Watsonville | 11.3 | 5 | Alluvium | 0.39 |
| San Juan Bautista. | 20.6 | 12.5 | Stiff alluvium. | 0.15 |
| Salinas | 28.8 | 22.5 | Alluvium | 0.12 |
| Monterey | 30.6 | 29.9 | Rock | 0.07 |

cupants of the MLML, and the level of shaking inferred from damage to structures and their contents unaffected by liquefaction, I estimate that a peak acceleration of about 0.25 *g* is reasonable for evaluating the effects of soil behavior during the earthquake at Moss Landing.

## OVERVIEW OF LIQUEFACTION EFFECTS IN THE MOSS LANDING AREA

The earthquake caused widespread liquefaction throughout the Moss Landing area. Liquefaction resulted in extensive lateral spreading and settlement of the access road to Moss Landing State Beach west of the Moss Landing north harbor (fig. 2), leaving numerous motorists stranded. The road embankment at the tide gate across Bennett Slough slumped about 5 ft as a result of liquefaction and lateral spreading of the foundation soils. The California Highway 1 bridge across Elkhorn Slough was intermittently closed for repairs for a few days after the earthquake. Liquefaction of the subsurface natural soils resulted in settlement and lateral deformation of the approach fills of about 1/2 ft.

In contrast, the 2,000-MW PG&E powerplant at Moss Landing sustained relatively minor damage during the earthquake except at the 500-kV switchyard, where many pieces of electrical equipment, including several transformers, were damaged. An aerial photograph of the powerplant taken the day after the earthquake is shown in figure 3. No major damage was sustained in the boiler or generator buildings, or to the large smokestacks for Units 6 and 7 (fig. 3), and no evidence of liquefaction or significant soil movements was observed in the area of these main facilities. This area is relatively flat, at an elevation[1] of 27 ft, and is underlain by medium-dense to dense sand to about 20-ft depth, in turn underlain by dense to very dense gravelly sand with occasional thin layers of medium-stiff to stiff plastic clay and silt. The water table in the area is generally at an elevation of about 0 ft. The generators and boilers are founded on thick concrete mats at elevations of 0 and 21 ft, respectively, whereas the smokestacks are founded on piles, 20 to 25 ft long, bearing in the dense to very dense gravelly sand (Dames & Moore, 1963).

The large fuel tanks east of Units 6 and 7 were undamaged. These tanks are founded on grade at an elevation of 20 ft and are underlain by about 10 ft of medium-dense sand and silty sand, in turn underlain by about 25 ft of dense sand and stiff silty clay and 50 ft of stiff clay. The water table in the area is at an elevation of 0 to 5 ft (Dames & Moore, 1963).

Considerable liquefaction damage occurred in the area of the parking lot at the Moss Landing Harbor District offices (fig. 2); however, structural damage to the buildings was minor, amounting to small cracks in the floor slabs. The parking lot is located in an area underlain by fill in turn underlain by alluvial silt and sand (Dupré and Tinsley, 1980), and liquefaction appears to have occurred in the sand below the fill. Sand boils along a 1-in.-wide crack parallel to the west waterfront slope of the fill facing the Old Salinas River are shown in figure 4, and cracks in the pavement at the north end of the parking lot associated with lateral movements of the waterfront fill of about 1/2 ft and settlements of about 1 ft are shown in figure 5.

Liquefaction was widespread on Moss Landing spit. Evidence of lateral spreading and liquefaction in the form of sinuous cracks and a few grabenlike features could be followed for several hundred feet along Moss Landing State Beach south of the MLML. The south access road to the spit, beginning at the south tide gate on the Old Salinas River and joining Sandholdt Road at the single-lane timber bridge across the river, was damaged as a result of settlement and lateral deformations associated with liquefaction. For a few weeks, however, this road was the only land access to the spit because the timber bridge across the river was heavily damaged during the earthquake. Repairs to the west approach of the bridge a few days after

[1] All elevations refer to the National Geodetic Vertical Datum (NGVD).

the earthquake are shown in figure 6. Liquefaction resulted in more than 4 ft of settlement of the approach fill and about 1 ft of lateral deformation toward the river. The bridge piles near the approach were shifted laterally at the mudline by an average of 1/2 ft, making the bridge impassable except by light emergency vehicles.

Liquefaction damage along the spit was severe, extending to the north end of the spit and offshore. A good summary of liquefaction effects offshore was presented by Greene and others (1991). Below, I present more detailed description of the liquefaction effects along Sandholdt Road, and at the sites of the MLML and MBARI facilities, and of the relation between subsurface soil conditions and liquefaction at these sites.

## SANDHOLDT ROAD

Typical liquefaction effects observed along Sandholdt Road north of the MBARI facilities are shown in figure 7. The roadbed is underlain by sandy soil to a depth of as much as about 30 ft; the water table is at about 5- to 6-ft depth. Liquefaction of the sandy soil generally resulted in settlements of as much as several inches (fig. 7), lateral deformations toward the harbor, sand boils, and sinkholes.

About halfway between the timber bridge and the MBARI facilities (fig. 8), the road parallels the waterfront at an elevation of about 6 ft and is approximately 50 ft wide. The waterfront slope has an inclination of about 3:1 in the upper 20 ft and is covered with riprap. The bottom of the harbor is at an elevation of about -20 ft.

A subsurface profile along the road between the timber bridge and the MBARI facilities is shown in figure 9. In this area, the road is underlain by loose to medium-dense sand, in turn underlain by soft to medium-stiff clay, dense gravelly sand, and medium-dense to dense interbedded sand and silty sand. The upper sand layer contains about 3 to 10 percent fines. The clay has a water content of 37 to 47 percent, a dry density of about 80 lb/ft$^3$, a plasticity index (PI) of 20 to 36 percent, and a liquid limit (LL) of 46 to 66 percent. The standard penetration resistances ($N$ values) plotted in figure 9 were calculated by correcting blowcounts measured using a 2.43-in.-ID split-barrel sampler (Harding Lawson Associates, 1988).

Horizontal deflections measured after the earthquake with a slope inclinometer on the east edge of Sandholdt Road within 10 ft of borehole HB–2 (fig. 9) are plotted in figure 10. This inclinometer and two others farther to the north were installed in early 1989 by Harding Lawson Associates to monitor slope movements associated with riprap filling of the waterfront slopes (Kevin Tillis, oral commun., 1991). These inclinometer measurements indicate that the edge of the road moved about 11 in. toward the harbor and about 4 in. southward nearly parallel to the waterfront. Clearly, the deformations resulted from liquefaction of the saturated part of the upper sand layer, and no permanent deformations occurred below. These deformations correspond to an approximately uniform shear strain of about 10 percent over a depth interval of about 10 ft.

As shown in figure 8, lateral deformations of the road were accompanied by settlements of 2 to 3 in. and cracking of the road surface approximately 15 to 20 ft landward of the slope crest. No evidence of significant deformation of the road was observed farther west at this site. Assuming that the observed cracks represent the sur-

Figure 3.—Pacific Gas & Electric Co. powerplant at Moss Landing (see fig. 2 for location). Moss Landing spit and Moss Landing State Beach are visible in background.

face expression of the lateral extent of deformation at depth and that liquefaction occurred early in the shaking, a simplified deformation analysis using a Newmark-type approach (Newmark, 1965; Makdisi and Seed, 1978) suggests that the strength of the liquefied sand was about 100 lb/ft$^2$ during deformation.

Because the penetration resistance of the sand was determined by using nonstandard procedures, a measured $N_{60}$ value[2] in the sand at this site is unavailable. The data plotted in figure 9, however, suggest that the $N_{60}$ value in the sand is about 5 to 8 blows/ft; the corresponding $N_{60}$ value, normalized to an effective overburden of 1 kg/cm$^2$ (2,048 lb/ft$^2$), $(N_1)_{60}$, would be about 8 to 12 blows/ft. Because the sand contains less than about 10 percent fines, the equivalent clean sand $(N_1)_{60cs}$ value, as defined by Seed (1987), would also be about 8 to 12 blows/ft. Downhole shear-wave velocities measured in the slope-inclinometer casing after the earthquake were 480 ft/s from 0- to 15-ft depth, 610 ft/s from 15- to 40-ft depth, and 930 ft/s from 40- to 60-ft depth (Bruce Redpath, written commun., 1991).

The slope-inclinometer casing appears to have undergone small lateral deformations in the upper 2 ft of the soft clay directly below the liquefied sand, probably as a result of the lateral loading induced by deformation of the sand. The clay itself, however, does not appear to have been strained significantly during the earthquake because such strains would have caused deformation of the casing throughout the depth of the clay. At this site, an $N$ value of about 2 blows/ft, a water content of 43 percent, an LL value of 46 percent, and a PI value of 21 percent were measured in the clay (Harding Lawson Associates, 1988).

## MOSS LANDING MARINE LABORATORY

### DESCRIPTION OF THE FACILITY

As shown in figure 11, the MLML consisted of two main buildings and a west wing surrounding a courtyard. The northern building was a one- and two-story wood-frame structure with a raised wood floor, founded on shallow footings. The southern building and the west wing were one-story wood-frame-and-shear-wall structures with slab-on-grade floors. The east half of the southern building was founded on 16-in.-diameter cast-in-place concrete piers, as much as 18 ft deep. The west half and the west wing were founded on shallow strip footings.

The MLML facility included several concrete fishtanks and planters and a 35-ft-high, 15-ft-diameter concrete seawater-storage tank. The fishtanks and planters were founded on grade; the seawater-storage tank was supported on a 2-ft-thick concrete mat founded 2 ft below the ground surface. A 15-ft-high concrete seawall founded at an elevation of about 0 ft protected the facility from wave action in Monterey Bay.

The northern building was more than 30 years old at the time of the earthquake; the other facilities were built in 1983 and 1984. The facilities were demolished after the earthquake, and the site has since been reclaimed as a dune-sand area. A new facility has been constructed at a site across the river immediately north of the Moss Landing cemetery.

### EARTHQUAKE EFFECTS

The general pattern of damage to the MLML indicated east-west lateral spreading of the entire site from soil liquefaction. A postearthquake survey by Brian Kangas Foulk (1989) indicated that the buildings spread 3.5 to 4 ft at the

Figure 4.—Sand boils in Moss Landing Harbor District parking lot. Smokestacks for Units 6 and 7 of Pacific Gas & Electric powerplant are visible in background.

[2] Standard penetration resistance corresponding to a hammer energy of 60 percent of the theoretical maximum, as defined by Seed and others (1985).

ground surface in the east-west direction, and that displacements in the north-south direction were relatively small. Racking of the director's office at the southwest corner of the MLML is shown in figure 12; this corner moved about 2.5 ft toward Monterey Bay and settled about 1.2 ft. Similarly, the northwest corner of the MLML was displaced laterally about 2 ft toward the bay. A settlement of 1.2 ft was measured at the northwest corner of the seawall.

Racking of the southeast corner of the MLML is shown in figure 13; this corner of the facility moved laterally toward the river about 1.5 ft and settled about 1 foot. Similar displacements were observed at the northeast corner. Measured lateral displacements on the east side of Sandholdt Road were 2.5 to 4.5 ft toward the river (fig. 11). Thus, the total extension of the spit due to lateral spreading at the site appears to have ranged from about 4.5 ft on the north side of the MLML to 7 ft on the south side. This difference in displacement appears to be related mainly to slight differences in topography between the north and south sides of the site and to slight differences in soil conditions.

Figure 5.—Ground cracks at north end of Moss Landing Harbor District parking lot.

Figure 6.—West approach to single-lane timber bridge across the Old Salinas River (see fig. 2 for locations).

As shown in figure 11, lateral spreading resulted in extensive cracking throughout the site and formation of an approximately 15-ft-wide, 1-ft-deep graben south of the MLML. The southern building sustained severe cracking in the foundation and slab floor; cracks as much as 6 in. wide formed in the slab, and separations of as much as 10 in. occurred between building floors and walls. Cracking of the concrete floor in the southern building, just north of the graben, is shown in figure 14. The northern building also sustained severe cracking at the roof and foundation levels, and separations of more than 18 in. in some places.

Soil boils, which geysered as much as 3 ft high, flowed for 30 to 45 minutes after the earthquake at the volleyball court south of the MLML (Greene and others, 1991). As shown in figure 15, the soil-boil ejecta consisted of predominantly fine clayey silt, although medium sand also flowed to the surface at this site. Sand boils of

Figure 7.—Settlement across Sandholdt Road near north end of Moss Landing spit (see fig. 2 for locations).

Figure 8.—Sandholdt Road halfway between timber bridge and Monterey Bay Aquarium Research Institute facilities (see fig. 2 for locations). Photograph taken 3 days after earthquake. View northward.

medium sand erupted at the southeast corner of the southern building and on the north side of the MLML. In addition, considerable upwelling of muddy water occurred through cracks in the corporation-yard pavement shown in figure 16. The pavement heaved upward about 2 ft and resettled as muddy water erupted through the cracks,

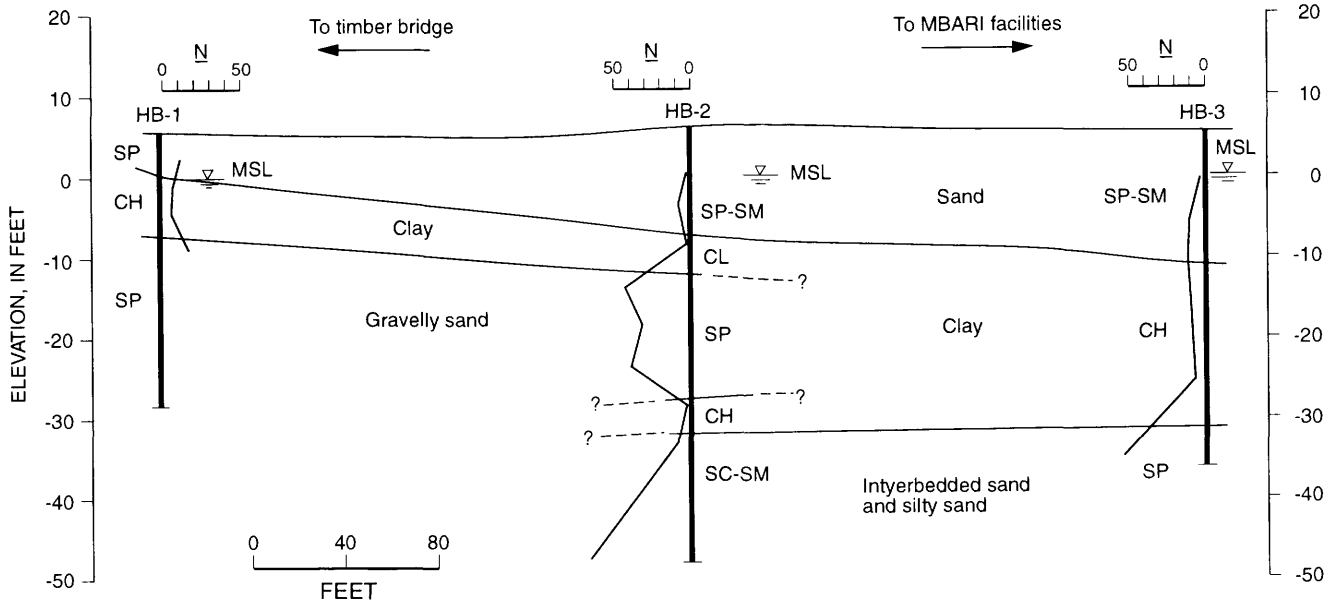


Figure 9.—Subsurface profile along Sandholdt Road between timber bridge and Monterey Bay Aquarium Research Institute facilities (see fig. 2 for locations). *N*, standard penetration resistance (in blows per foot) in boreholes HB–1 through HB–3 (see fig. 11 for locations). CH, fat clay; CL, lean clay; SC, clayey sand; SM, silty sand; SP, poorly graded sand. MSL, mean sea level. View westward.

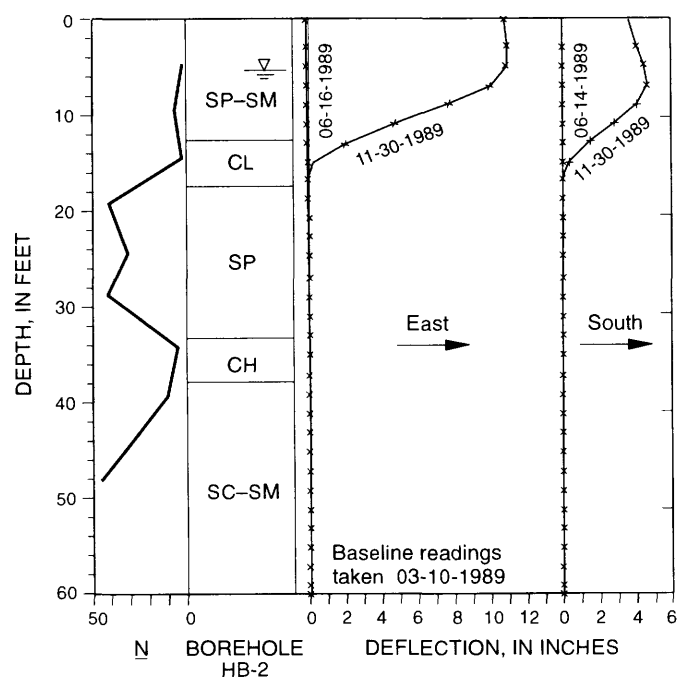


Figure 10.—Slope-inclinometer deflections on east edge of Sandholdt Road midway between timber bridge and Monterey Bay Aquarium Research Institute facilities (see fig. 2 for locations). CH, fat clay; CL, lean clay; SC, clayey sand; SM, silty sand; SP, poorly graded sand.

several times after the earthquake (Larry Jones, oral commun., 1989).

Water sloshed out of the seawater-storage tank shown in figure 16; the tank settled about 2 to 3 in. with respect to the pavement and tilted about 2°–3° W.

## FIELD EXPLORATION

An investigation was undertaken soon after the earthquake to evaluate the liquefaction failure at the MLML site (Woodward-Clyde Consultants, 1990). The investigation included a topographic survey to measure lateral and vertical deformation, drilling of boreholes, cone-penetration tests (CPT's), and excavation of a test pit at the site of the soil boils in the volleyball court. In addition, samples of the subsurface soils and of the soil-boil ejecta were tested in the laboratory to help establish the source of liquefaction at the site. The location of field explorations at the site, including boreholes drilled before the earthquake, are shown in figure 11. For clarity, the locations of boreholes and CPT's performed in the corporation-yard area by Martin and Douglas (1980) are omitted.

The boreholes drilled by Woodward-Clyde Consultants were advanced by using a rotary-wash drill rig with a

4 7/8-in. tricone bit. Standard penetration tests (SPT's) were performed at about 2.5-ft intervals in the upper 40 ft and at larger intervals below. A Central Mine Equipment (CME) 140-lb automatic triphammer and a 140-lb safety hammer, operated using a rope-and-pulley system with two rope turns around the cathead, were used to drive a 2-in.-OD SPT split spoon without liners.

The operator's throw of the safety hammer was carefully monitored during the SPT's, and it was noted that the operator consistently delivered a 31.5-in. fall to the

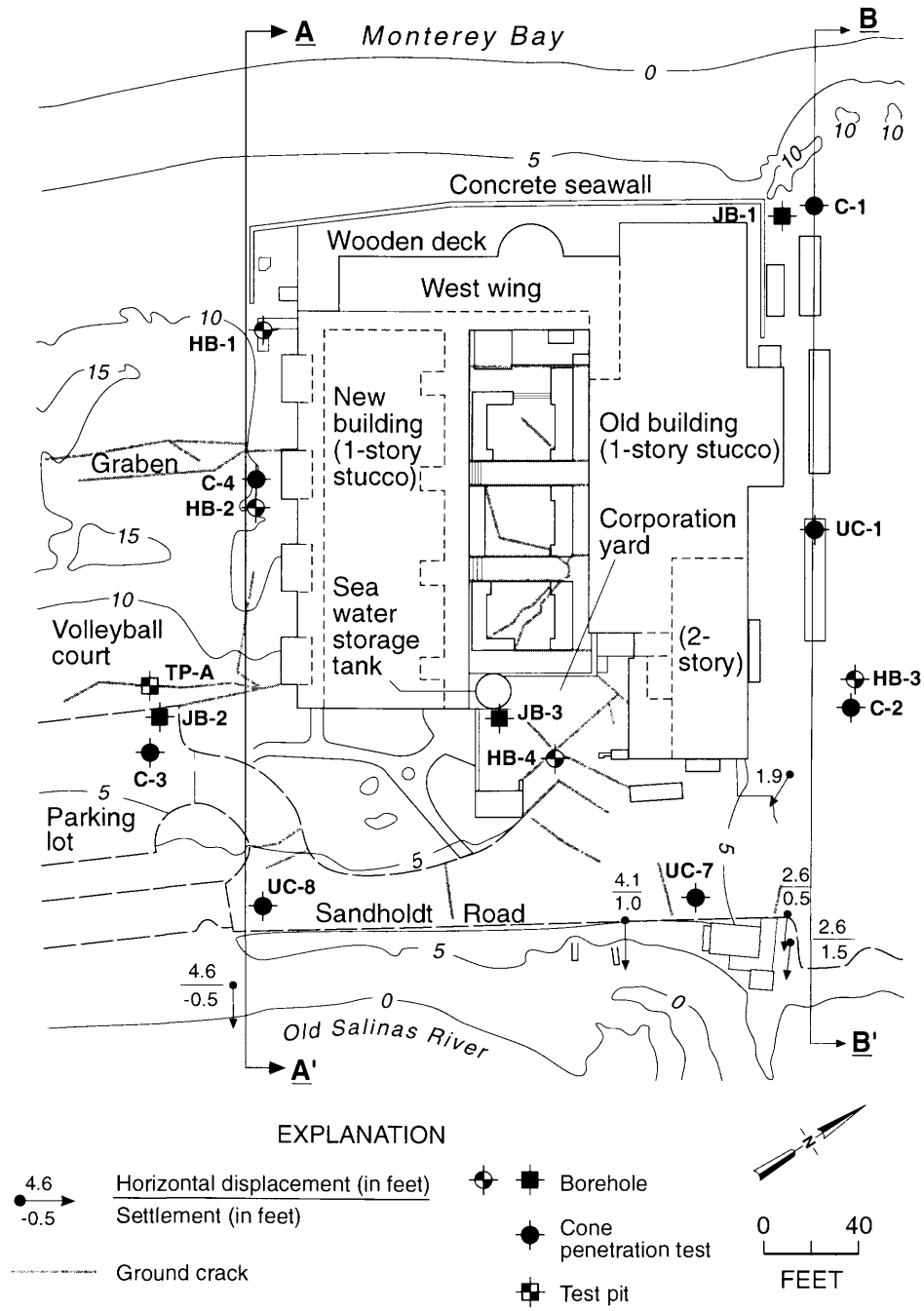


Figure 11.—Site plan of Moss Landing Marine Laboratory (fig. 2), showing locations of boreholes and cone-penetration-test soundings, contours of elevation (in feet), and lines of cross sections *A–A′* and *B–B′* in figure 17.

hammer. Previous calibration tests of the CME triphammer indicate that this hammer delivers about 15 percent more energy than the standard safety hammer with a 30-in. fall (Riggs and others, 1984). This information was used to correct the measured $N$ values to $N_{60}$ values, as proposed by Seed and others (1984). Details of the hammer energies used for SPT's at the site by other investigators are unavailable.

The CPT's were conducted by using a 20-ton Hogentogler piezoelectric cone with a 10-$cm^2$ tip, a 20-cm-long side friction sleeve, and a pore-pressure sensor behind the tip.

Figure 12.—Racking of director's office at southwest corner of Moss Landing Marine Laboratory (fig. 11).

Figure 13.—Racking of southern building at southeast corner of Moss Landing Marine Laboratory (fig. 11).

## SUBSURFACE SOIL CONDITIONS

As shown in figure 17, the MLML site is underlain by dune, beach, marshland, and alluvial deposits. The central part of the sand spit at the site is blanketed by 5 to 8 ft of loose to medium-dense, fine- to medium-grained, light-brown dune sand with a median grain size ($D_{50}$) of about 0.2 to 0.3 mm and a fines content of generally less than 4 percent passing a No. 200 sieve.

A 10- to 20-ft-thick deposit of medium-grained, light-brown beach sand underlies the dune sand on the west side of the spit. The beach sand is generally loose to medium dense except at the location of CPT C–1 (fig.11), where it appears to be dense. It contains abundant seashell and calcareous particles, and has a $D_{50}$ value of 0.35 to 0.5 mm and a fines content of about 3 to 5 percent.

On the east side of the spit, a 5- to 10-ft-thick marshland deposit of gray clayey silt and clay is interbedded between the dune and beach sand (fig. 17). An LL value of 32 percent, a PI value of 6 percent, a fines content of 72 percent, a minus-5-μm fraction of 14 percent, a water content of 37 percent, and a dry density of 83 lb/ft$^3$ were measured in a sample of the silt. A sample of the clay had a measured LL of 57, a PI of 27, a fines content of 98 percent, and a minus-5-μm fraction of 42 percent.

On the north side of the site (cross sec. *B–B′*, fig. 17), the beach sand is underlain by 5 ft of interbedded sand and clay that, in turn, is underlain by 5 to 15 ft of dense, medium-grained to coarse gravelly sand. On the south side of the site, the gravelly sand directly underlies the beach sand. The gravelly sand has a $D_{50}$ value of about 0.6 to 1.2 mm and a fines content of 5 to 8 percent.

Except at the location of CPT C–1 (fig. 11), the gravelly sand is underlain by a layer of loose to medium-dense silty sand to about 40-ft depth. This silty sand is fine grained, with a $D_{50}$ value of about 0.15 mm and a fines content of about 27 to 34 percent.

Below about 40-ft depth, a layer of soft to medium-stiff clay, 5 to 8 ft thick, was penetrated. This layer is underlain by interbedded gravelly sand and silty sand, with some silt and clay, and clayey sand. A deposit of medium-stiff, highly plastic clay was penetrated at 75- to 85-ft depth in CPT C–3 and borehole B–2 (fig. 11), respectively (cross sec. *A–A′*, fig. 17); this deposit extends to at least 120-ft depth.

Figure 14.—Cracks in concrete floor in southern building of Moss Landing Marine Laboratory (fig. 11).

## EVALUATION OF OBSERVED SOIL BEHAVIOR

Surficial evidence of earthquake effects indicates that the ground failure at the MLML site was due to liquefaction. A comparison between samples of the soil-boil ejecta at the site and samples of the subsurface soils in terms of color, general appearance, and particle-size gradation from laboratory tests clearly indicates that liquefaction occurred in the loose to medium-dense beach sand below the water table, including the beach sand below the clayey silt underlying the east side of the site.

The soil-boil ejecta at the volleyball court indicates that the clayey silt underlying the dune sand in this area also appears to have developed high excess pore pressures (fig. 15). Several liquefaction vents through the dune sand were carefully examined in an 8-ft-deep test pit at this site. The appearance of the clayey silt in these vents suggests that the silt flowed to the surface in a liquefied state. An LL value of 38 percent, a PI value of 17 percent, a fines content of 78 percent, and a minus-5-μm fraction of 24 percent were measured in a sample of the soil ejecta at the surface.

Liquefaction of the beach sand would be anticipated based on the SPT data from boreholes at the site and currently available empirical correlations between $(N_1)_{60}$ values and liquefaction susceptibility. In figure 18, cyclic-stress ratio induced by the earthquake is plotted against stress ratio required for liquefaction, calculated by using the procedure of Seed and others (1984) and $(N_1)_{60}$ data from the Woodward-Clyde Consultants boreholes. Figure

Figure 15.—Sand-boil ejecta in volleyball court of Moss Landing Marine Laboratory (fig. 11).

Figure 16.—Cracks in corporation-yard pavement of Moss Landing Marine Laboratory (fig. 11). Seawater-storage tank in background settled differentially 2 to 3 in.

18 shows that liquefaction would be expected in the beach sand between elevations of 0 and –10 ft and suggests that liquefaction occurred relatively early during the shaking. Figure 18 also suggests that the dense gravelly sand at elevations of –20 to –10 ft probably did not liquefy and that limited liquefaction may have occurred in the silty sand at elevations of –30 to –20 ft.

Liquefaction of the subsurface soils was accompanied by lateral spreading of the site in the east-west direction and formation of a graben near the middle of the spit, as shown in figure 11. Measured horizontal and vertical displacements from a postearthquake topographic survey of the site are shown in figure 17. The maximum lateral displacement toward the east on the south side of the laboratory was about 4.5 ft, and on the north side about 2.5 ft. The average lateral displacement of the ground between the graben and the east shore of the spit appears to have been about 1.5 to 2.5 ft, and between the graben and the west shore about 2.5 ft.

Assuming that liquefaction occurred relatively early in the earthquake shaking and that the average displacement toward the east of a soil block extending horizontally from the graben to the Salinas River and vertically to an elevation of –8 ft was 1.5 to 2.5 ft, a simplified analysis of deformations using a Newmark-type approach suggests that the strength of the beach sand ranged from about 70 to 100 lb/ft$^2$ during lateral spreading. SPT and CPT data indicate an average $(N_1)_{60cs}$ value corresponding to the assumed deformation mechanism of about 16 to 18 blows/ft. A similar analysis of lateral-spreading displacements toward the west suggests a strength of about 100±40 lb/

ft$^2$. The corresponding average $(N_1)_{60cs}$ value is about 12 to 16 blows/ft.

The above-calculated strengths during lateral spreading at the MLML site are significantly lower than the residual strengths that might be anticipated on the basis of correlations between $(N_1)_{60cs}$ value and residual strength (Seed and Harder, 1990). However, several of the case histories that exhibited higher strengths in materials with similar $(N_1)_{60cs}$ values involved strains and deformations significantly larger than those that developed at the MLML site.

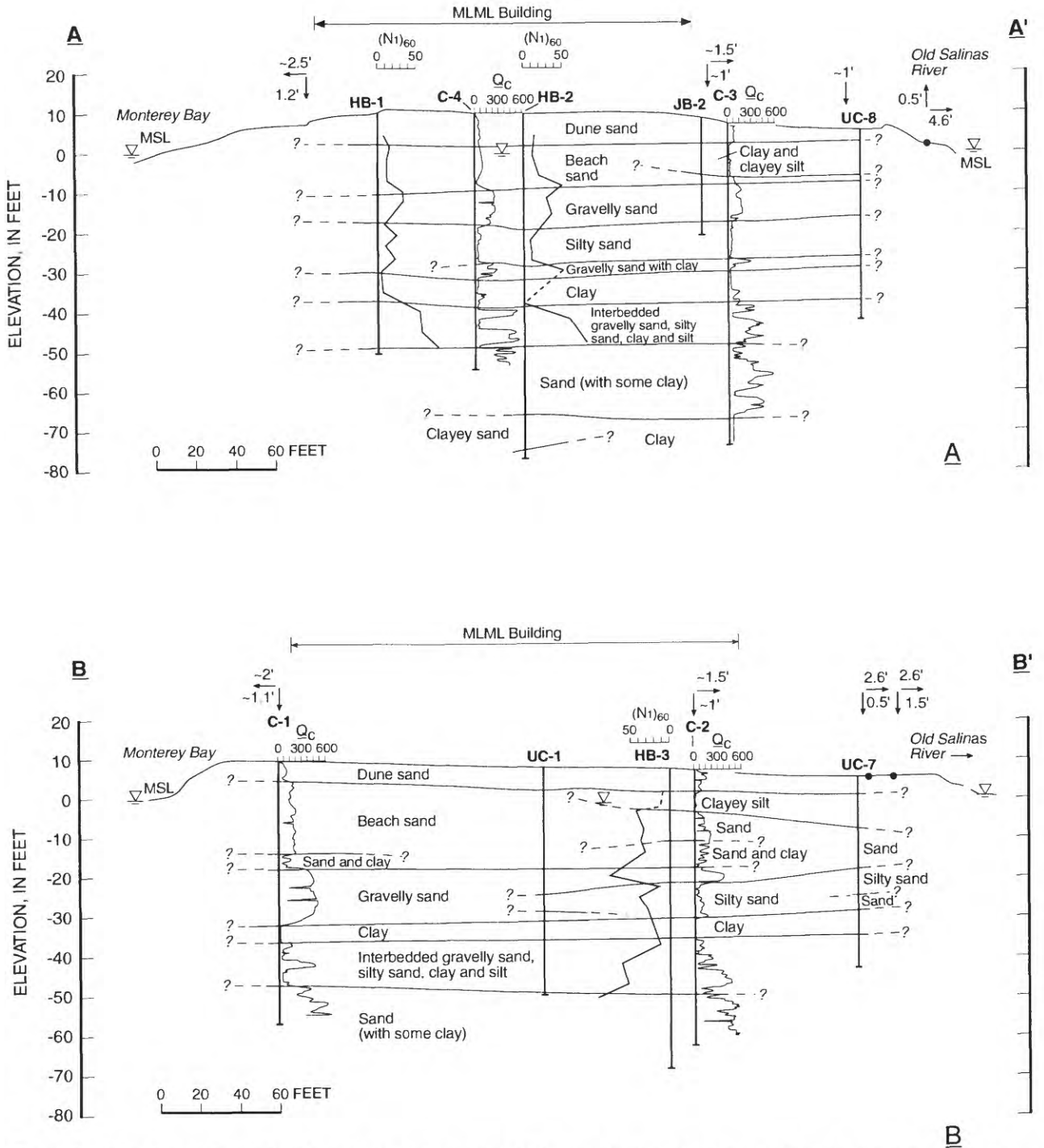


Figure 17.—Subsurface profiles at Moss Landing Marine Laboratory (MLML) (see fig. 11 for locations). *A*, Cross section *A–A′*. *B*, Cross-section *B–B′*. MSL, mean sea level; $(N_1)_{60}$, normalized standard penetration resistance (in blows per foot) in boreholes HB–1 through HB–3; $Q_c$, cone-penetration resistance (in tons per square foot) in tests C–1 through C–4.

Thus, the above-calculated strengths suggest that larger strains and deformations than those that developed at the MLML site may be required to mobilize the full residual strength of the materials under conditions where full stress reversal occurs, as suggested by Seed (1987).

## MONTEREY BAY AQUARIUM RESEARCH INSTITUTE

### DESCRIPTION OF THE FACILITIES

The MBARI facilities are located about 800 ft north of the MLML on the Moss Landing spit. A site plan of the facilities at the time of the earthquake is shown in figure 19. They consist of a reinforced-concrete pier on the Moss Landing harbor and a high one-story building across Sandholdt Road from the pier, known as the technology building. A one-story masonry storage building is built on the pier and fronts Sandholdt Road. The facilities, which were built in 1988 and 1989, were being completed at the time of the earthquake.

The pier deck ramps up from the road (elev, approx 6 ft) to an elevation of about 8 ft. It is supported on driven 20-in.-diameter circular prestressed-concrete piles. The channel mudline was dredged to an elevation of about -15 ft in the pier area. The waterfront slope from the edge of the road to the mudline is covered with riprap and has inclinations of 2H:1V just south of the pier and of 3H:1V under and north of the pier. The bottom of the harbor channel is dredged to an elevation of –18 ft.

The technology building is a concrete tiltup structure founded on spread footings embedded about 3 ft below the ground surface. The footings are structurally connected. The building has a concrete slab-on-grade floor that rests on a 12-in.-thick compacted-gravel subbase that extends 3 ft beyond the building footprint (Rutherford and Chekene, 1988).

### EARTHQUAKE EFFECTS

In contrast to the MLML, the MBARI facilities performed very well during the earthquake. The exterior and interior of the technology building 3 days after the earthquake are shown in figures 20*A* and 20*B*, respectively. The structure was undamaged by the shaking, and no evidence of damage to the foundation or concrete floor was observed. Permanent ground deformations at the site were small, and the building appears to have settled uniformly. A few cracks, less than about $^1/_2$ in. wide, were observed in the paved area in front and around the sides of the building. No evidence of sand boils was observed in the immediate area of the building, although sand boils erupted on Sandholdt Road in front, north, and south of the pier.

The MBARI pier was essentially undamaged by the earthquake. The south side of the pier and the underside

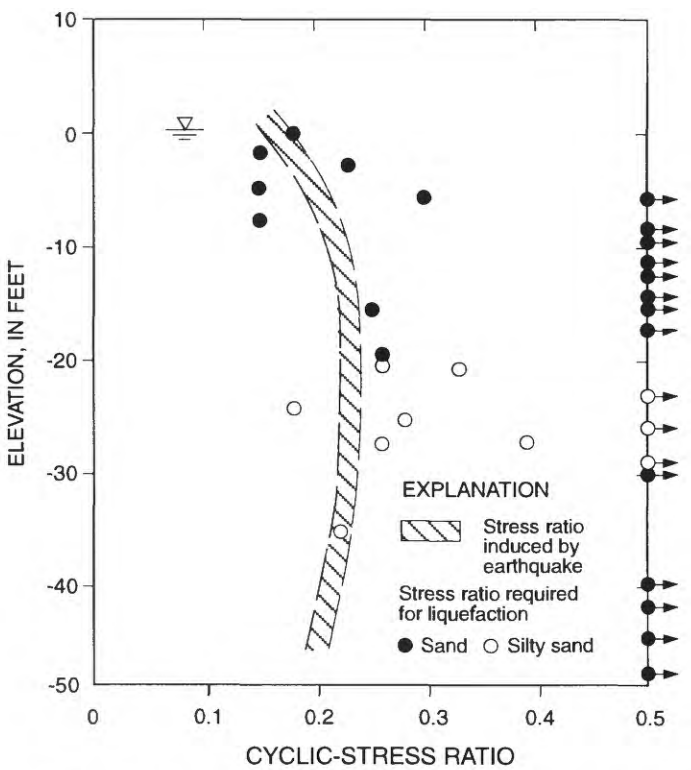


Figure 18.—Cyclic-stress ratio required for liquefaction versus depth, based on standard-penetration-test data from Moss Landing Marine Laboratory.

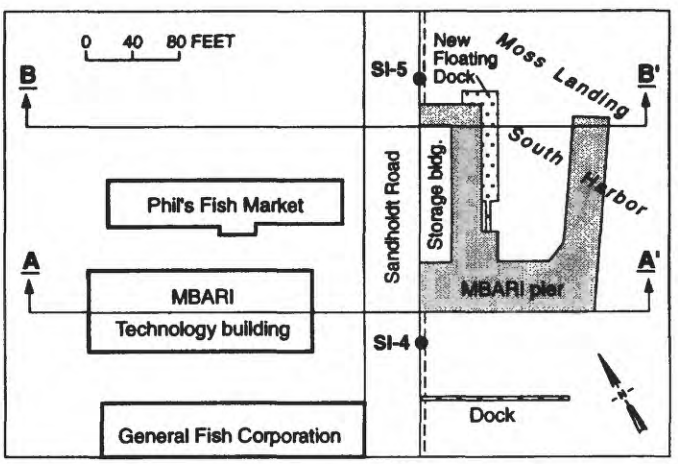


Figure 19.—Site plan of Monterey Bay Aquarium Research Institute facilities, showing locations of slope inclinometers SI–4 and SI–5 in which measurements were made after earthquake, and lines of cross sections *A–A′* and *B–B′* in figure 22.

of the concrete deck on the north side of the pier are shown in figures 21*A* and 21*B*, respectively. Evidence of small movements in the form of minor concrete spalling was observed at the joints between some of the piles and the deck. Lateral displacements of the edge of the road toward the harbor were about 10 in. and 3 in. just north and south of the pier, respectively; however, the pier appears to have been displaced laterally toward the harbor less than about 1 in.

## SUBSURFACE SOIL CONDITIONS

Subsurface conditions in the MBARI area were explored by Rutherford and Chekene (1988) as a part of the design studies for the facilities. As shown in figure 22, the area is underlain by poorly graded sand that is loose to medium dense under Sandholdt Road and medium dense to dense under the technology building. The sand, which contains generally less than 10 percent fines, is 10 to 15 ft

*A*


*B*

Figure 20.—Appearance of Monterey Bay Aquarium Research Institute technology building 3 days after earthquake. *A*, Building exterior. *B*, Building interior.

thick under Sandholdt Road and as much as 25 ft thick at the west side of the technology building.

The sand is underlain by dense gravelly sand with a few seams of clay, and lenses of sand and silty sand. The gravelly sand is underlain by 10 to 25 ft of interbedded silt, clay, and silty sand. These materials are generally soft or loose to medium dense. The underlying soils consist of interlayered dense sand and clayey sand and stiff clay. A very dense silty and clayey sand was penetrated at an elevation of about -75 ft.

## EVALUATION OF OBSERVED SOIL BEHAVIOR

On the basis of the observed absence of damage, widespread liquefaction, such as that observed at the MLML site, clearly did not occur at the site of the MBARI technology building. The small deformations observed around this building suggest that localized liquefaction may have occurred in the medium-dense to dense sand underlying the site. The marked difference in observed performance between the MLML and MBARI sites appears to be due

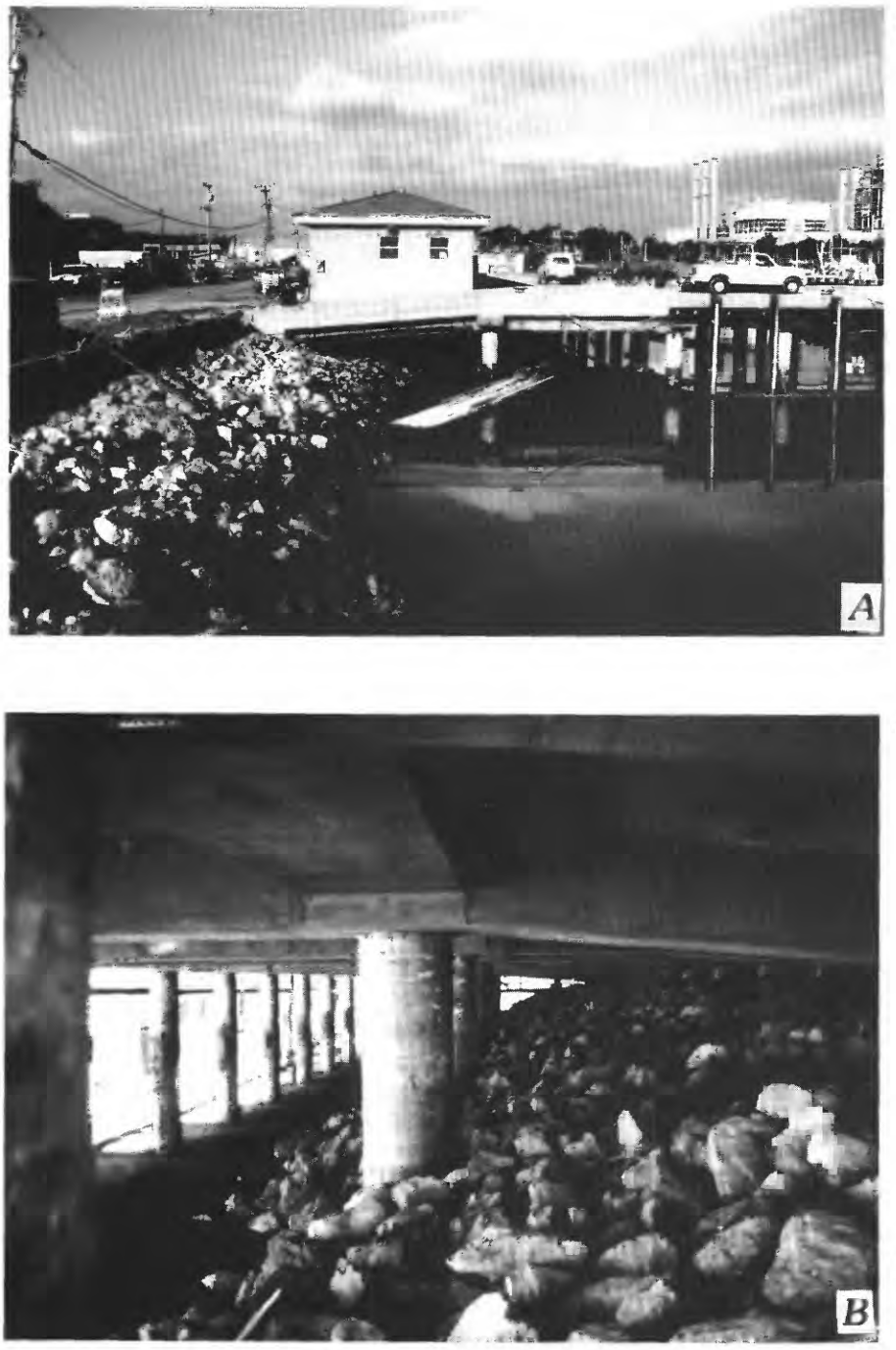


Figure 21.—Appearance of Monterey Bay Aquarium Research Institute pier 3 days after earthquake. *A*, South side of pier. *B*, Underside of concrete deck.

to the apparently higher density of the near-surface sand at the MBARI site.

The sand boils and deformations observed along Sandholdt Road indicate that liquefaction occurred in the near-surface loose to medium-dense sand underlying the road. On the basis of the observed difference in lateral displacements of the pier and the waterfront slopes to the north and south, the pier apparently buttressed the liquefied soils and prevented larger lateral deformations from occurring on Sandholdt Road in front of the pier and, possibly, at the building sites across the road.

The apparent distribution of liquefaction at the site of the MBARI facilities is consistent with SPT data from boreholes at the site and with the empirical correlations

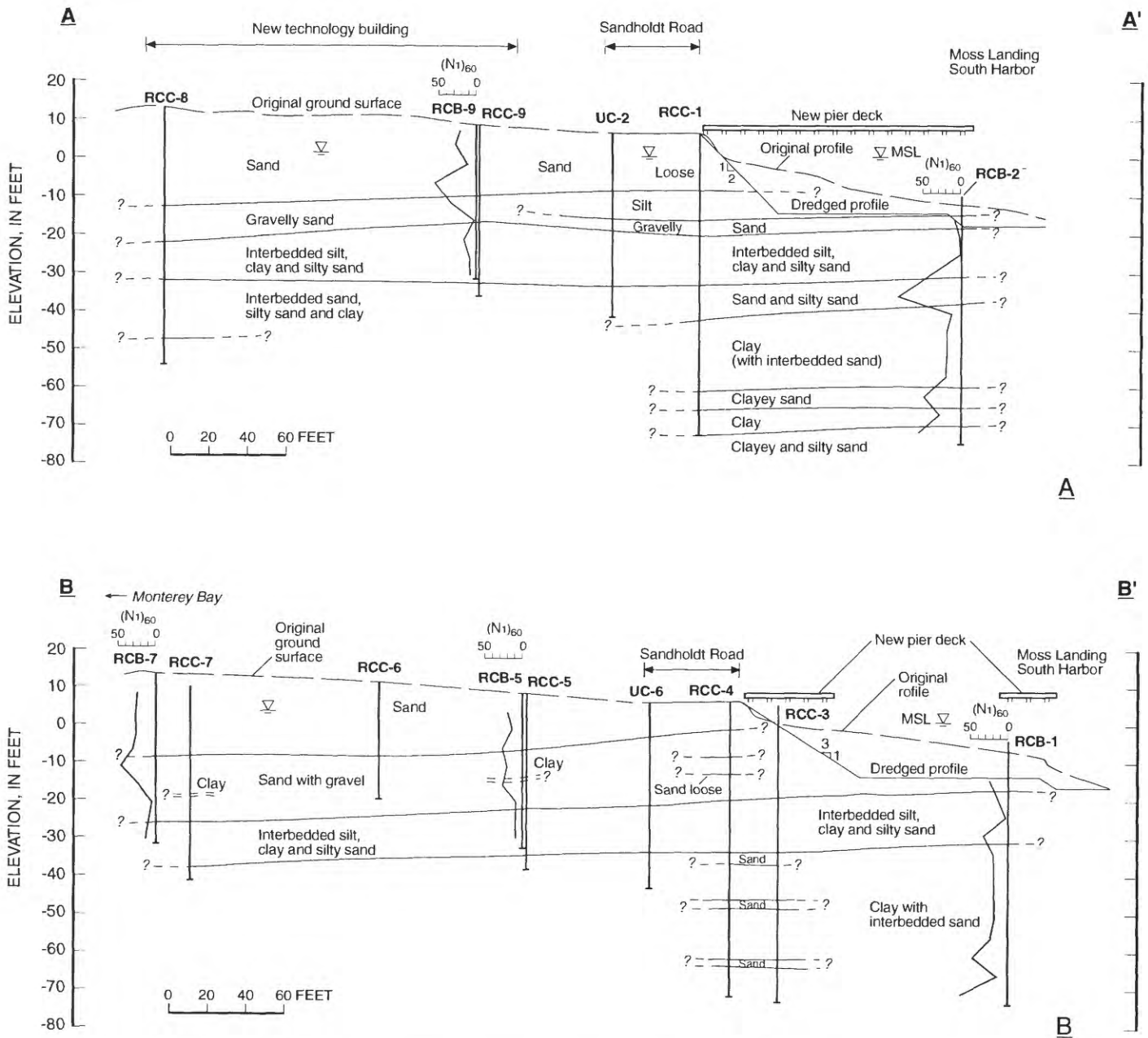


Figure 22.—Subsurface profiles at Monterey Bay Aquarium Research Institute facilities (see fig. 19 for locations). *A*, Cross section *A–A′*. *B*, Cross section *B–B′*. MSL, mean sea level; $(N_1)_{60}$, normalized standard penetration resistance (in blows per foot).

between $(N_1)_{60}$ value and liquefaction resistance proposed by Seed and others (1984). The cyclic-stress ratio induced by the earthquake is plotted against the stress ratio required for liquefaction calculated from the $(N_1)_{60}$ values at the site in figure 23. On the basis of the SPT data, limited liquefaction would be expected in the sand underlying the technology building at elevations of –20 to 0 ft, and more widespread liquefaction would be expected in the sand in the pier area at the same elevations, in good agreement with the observed surface evidence. Figure 23 also indicates that liquefaction probably occurred in the loose to medium-dense silty sand and silt at elevations of -30 to -20 ft.

The horizontal deflections measured after the earthquake with a slope inclinometer (SI–5, fig. 19) located on the east edge of Sandholdt Road, about 20 ft north of the MBARI pier, are plotted in figure 24A, along with the log of a CPT sounding by Rutherford and Chekene (1988) located within about 10 ft of the inclinometer. The deflections measured with another slope inclinometer (SI–4, fig. 19) located about 20 ft south of the pier, within about 5 ft of another Rutherford and Chekene CPT sounding, are plotted in figure 24*B*. The edge of the road north of the pier moved about 10 in. towards the harbor, and south of the pier about 3 in. Movements parallel to the road were small.

The movements north of the MBARI pier appear to have resulted primarily from liquefaction of a medium-dense lens of sand at 13- to 19-ft depth. The observed deformations correspond to an approximately uniform shear strain of about 8 percent over a depth interval of 6 ft. Interestingly, the slope-inclinometer deflections suggest that deformation also occurred in the clayey silt and silty sand at about 28- to 36-ft depth. South of the pier, liquefaction appears to have occurred in the loose to medium-dense sand immediately below the water table at 5- to 7-ft depth, and in the clayey silt and silty sand at about 15- to 22-ft and 28- to 40-ft depth. No deformations occurred in the soils below 40-ft depth.

The lateral displacements of the road edge north of the pier were accompanied by movements and significant cracking of the road surface to a distance of about 15 to 30 ft from the road edge. Assuming that liquefaction occurred midway to late in the earthquake shaking, a simplified Newmark-type analysis of the observed deformations suggests that the strength of the liquefied sand while it deformed was about 150±30 lb/ft$^2$. The adjacent CPT data indicate that the $(N_1)_{60cs}$ value of the liquefied sand is about 20 to 21 blows/ft. The above-calculated strengths suggest that the strength after liquefaction of sand with an $(N_1)_{60cs}$ value of as much as about 20 blows/ft can be quite low for strains as high as about 10 percent and that larger strains may be required to mobilize the full residual strength of the materials, in cases where full stress reversal occurs.

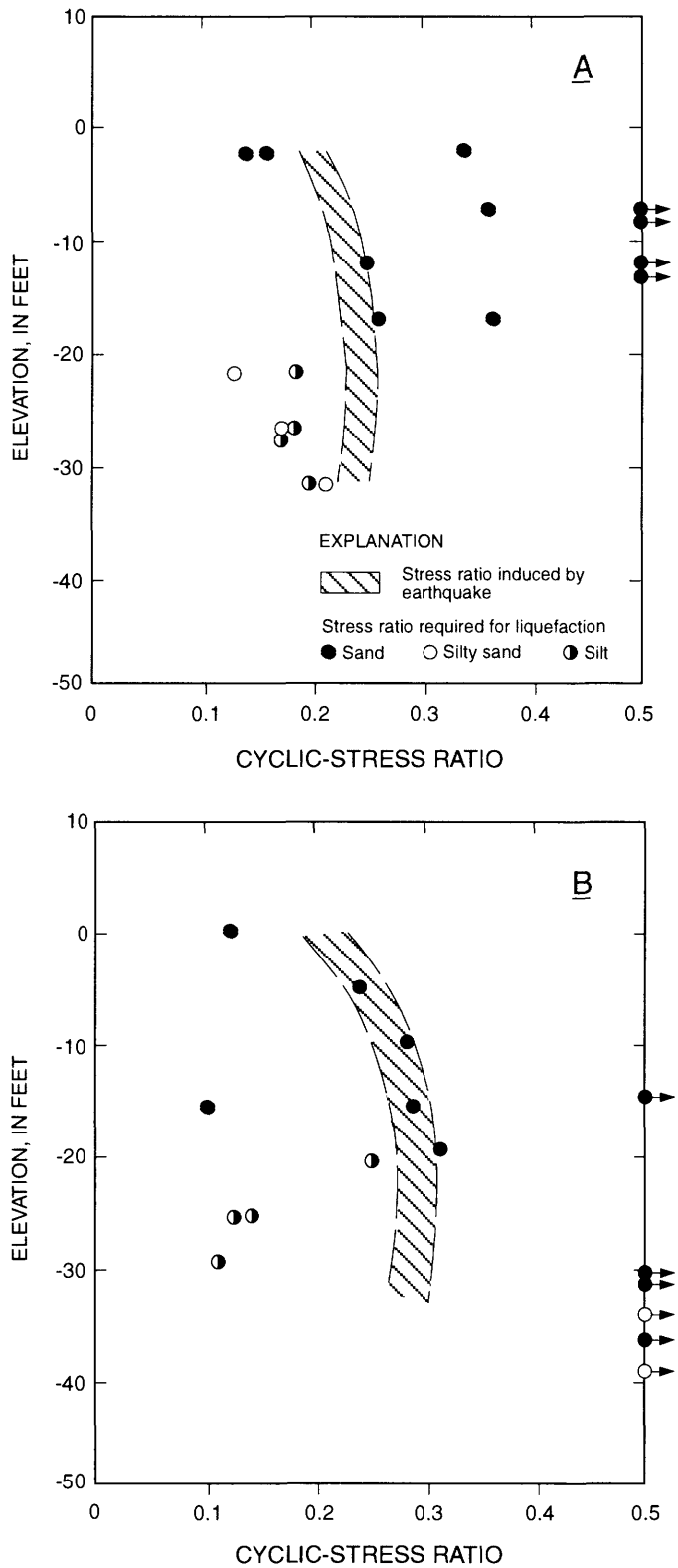


Figure 23.—Cyclic-stress ratio required for liquefaction versus depth, based on standard-penetration-test data. *A*, Monterey Bay Aquarium Research Institute technology building. *B*, Monterey Bay Aquarium Research Institute Pier.

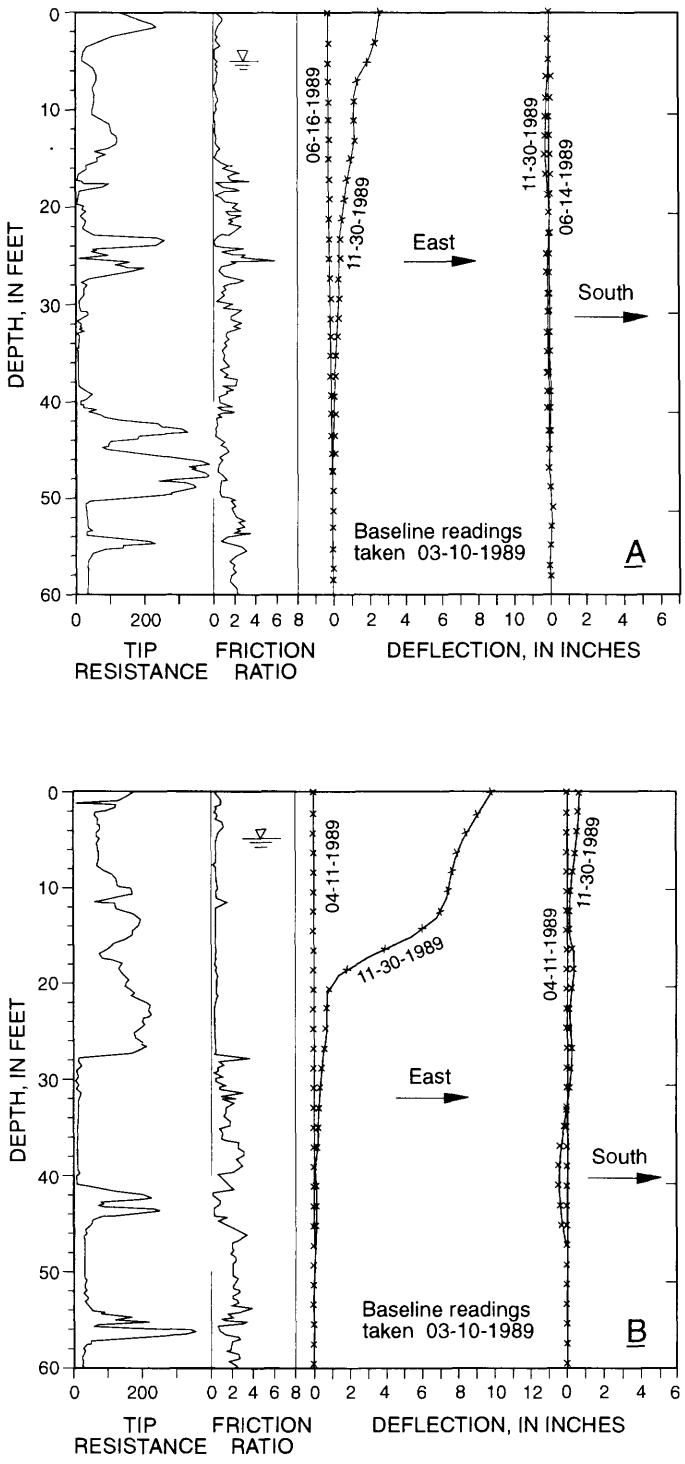


Figure 24.—Cone-penetration resistance (in tons per square foot), friction ratio (in percent), and deflection measured in slope inclinometers SI–4 (*A*) and SI–5 (*B*) (see fig. 19 for locations) versus depth at east edge of Sandholdt Road north (*B*) and south (*A*) of Monterey Bay Aquarium Research Institute pier.

Downhole shear-wave velocities were measured by Bruce Redpath in the slope-inclinometer casings after the earthquake. Shear-wave velocities of 480 ft/s from 0- to 20-ft depth, 585 ft/s from 20- to 50-ft depth, and 865 ft/s from 50- to 60-ft depth were measured in slope inclinometer SI–4 (fig. 19), and a shear-wave velocity of 570 ft/s at 10- and 30-ft depth in slope inclinometer SI–5 (fig. 19).

## SUMMARY AND CONCLUSIONS

The 1989 Loma Prieta earthquake caused extensive liquefaction and ground failure in the coastal area of Moss Landing. Liquefaction was widespread on the Moss Landing spit and resulted in extensive damage to structures, waterlines, and sewerlines, thus affecting for a few months operation of several commercial fisheries, the MBARI facilities, and the Moss Landing harbor.

Ground motions in the Moss Landing area, though strong, were not particularly severe. Recordings of ground motions in the area by CSMIP, together with the reported felt intensity of motions on the spit, the level of shaking inferred from damage to structures not affected by liquefaction, and the results of numeric simulations, indicate that the peak acceleration at Moss Landing was about 0.25 *g*.

Liquefaction does not appear to have been a major factor in the performance of the PG&E powerplant at Moss Landing, even though liquefaction caused significant damage to the north and west, including at Moss Landing State Beach and in the Moss Landing Harbor District parking lot. The soils in the area of the powerplant are generally medium dense to dense, and the water table is at least 20 ft deep.

On the Moss Landing spit, evidence of liquefaction and lateral spreading was observed from several hundred feet south of the MLML to the north end of the spit and offshore. Liquefaction of near-surface loose to medium-dense sand along Sandholdt Road resulted in sand boils, sinkholes, settlements, and lateral deformations toward the harbor. Lateral deformations of as much as about 1 ft, accompanied by cracking of the road surface, were observed along the waterfront.

The MLML was damaged beyond repair by liquefaction and lateral spreading in the east-west direction. Lateral extension of the building foundations ranged from about 3.5 to 4 ft; total lateral extension of the spit at the site was about 4.5 to 7 ft. In spite of these deformations, the structures did not collapse, and no casualties or severe injuries were reported among the laboratory occupants. Liquefaction occurred in loose to medium-dense sand un-

derlying the site at 10- and 20-ft depth. In addition, liquefaction appears to have occurred in a marshland deposit of clayey silt underlying the east side of the site at similar depths.

In contrast to the MLML, the MBARI facilities performed very well during the earthquake. Permanent ground deformations at the site of the technology building were small, and the structure appears to have settled uniformly. A few cracks less than about 1/2 in. wide were observed in the paved area in front and around the sides of this building. The observed deformations suggest that limited liquefaction may have occurred in the medium-dense to dense sand underlying the building to about 25-ft depth.

Sand boils and deformations observed along Sandholdt Road between the technology building and the pier indicate that liquefaction occurred in the near-surface loose to medium dense sand underlying the road. Even though lateral displacements of several inches toward the harbor were observed on the waterfront edge of the road immediately north and south of the pier, deformations of the pier were small. The pier and its pile foundation appear to have buttressed the liquefied soils and prevented larger deformations from occurring on Sandholdt Road in front of the pier and, possibly, across the road.

Thus, the main reasons for the marked difference in performance between the MLML and MBARI facilities appear to include the more favorable soils at the site of the MBARI technology building, which did not liquefy extensively; the type of construction used for the building, which was not susceptible to damage from small ground deformations; and the buttressing action of the pier on the liquefied soils along Sandholdt Road, which prevented larger deformations from occurring on the road in front of the pier.

Lateral deflections observed in three slope inclinometers along the east edge of Sandholdt Road indicate that strains of as high as 10 percent developed in the liquefied sand along the road. Analyses of the deformations observed along the road suggest that the strength of liquefied sand of similar densities can be quite low for small strains and that large strains may be required to mobilize the full residual strength of these materials, in cases where full stress reversal occurs.

Significantly, extensive liquefaction and ground failure occurred throughout the Moss Landing spit during the great 1906 San Francisco earthquake. Reports of the observed damage indicate that ground failure was significantly more extensive and ground deformations throughout the spit were larger than those observed during the 1989 Loma Prieta earthquake, probably owing to the higher intensity and longer duration of strong ground motion likely to have occurred in the area during the 1906 earthquake. Thus, I conclude that liquefaction damage in the Moss Landing area from a future larger and closer earthquake is likely to be more severe than that observed during the 1989 Loma Prieta earthquake unless measures to mitigate this damage are adopted.

## ACKNOWLEDGMENTS

The investigation of the failure at the MLML was funded by the California State University through a contract with Woodward-Clyde Consultants administered by Will Nighswonger and Herb Zuidema of the university. I appreciate the efforts of David Hughes and Joseph Sun, who supervised and assisted with the fieldwork. Special thanks are due to Kevin Tillis of Harding Lawson Associates who provided the slope-inclinometer data; to Bruce Redpath, who provided the shear-wave velocities measured in the slope-inclinometer casings, to Ross Boulanger and Les Harder, who provided data on the subsurface conditions at the MLML site; and to Larry Jones of MLML, who provided information on earthquake effects at the laboratory. This research was supported by the professional development program of Woodward-Clyde Consultants.

## REFERENCES CITED

Brian Kangas Foulk, 1990, Crack and foundation separation survey, marine biology research center: survey map prepared for California State University, scale 1:250.

Dames & Moore, 1963, Foundation investigation Moss Landing power plant, Units 6 and 7, Moss Landing: report prepared for Pacific Gas & Electric Co., 90 p.

Dupré, W.R., and Tinsley, J.C., 1980, Maps showing geology and liquefaction potential of northern Monterey and southern Santa Cruz Counties, California: U.S. Geological Survey Miscellaneous Field Studies Map MF–1199, scale 1:62,500, 2 sheets.

Greene, H.G., Gardner-Taggart, Joan, Ledbetter, M.T., Barminski, Robert, Chase, T.E., Hicks, K.R., and Baxter, Charles, 1991, Offshore and onshore liquefaction at Moss Landing spit, central California—result of the October 17, 1989, Loma Prieta earthquake: Geology, v. 19, no. 9, p. 945–949.

Griggs, G.B., 1990, An evaluation of coastal hazards at the Moss Landing Marine Laboratory site: report prepared for Chancellor's Office of California State University, 42 p.

Harding Lawson Associates, 1988, Geotechnical investigation, dredging and slope improvements, Moss Landing South Harbor, Moss Landing, California: report prepared for Moss Landing Harbor District, 35 p.

Idriss, I.M., 1991, Earthquake ground motions at soft soil sites: International Conference on Recent Advances in Geotechnical Earthquake Engineering and Soil Dynamics, 2d, St. Louis, Mo., 1991, Proceedings, v. 3, p. 2265–2273.

Makdisi, F.I., and Seed, H.B., 1978, Simplified procedure for estimat-

ing dam and embankment earthquake-induced deformations: American Society of Civil Engineers Proceedings, Geotechnical Engineering Division Journal, v. 104, no. GT7, p. 849–867.

Martin, G.R., and Douglas, B.J., 1980, Evaluation of the cone penetrometer for liquefaction hazard assessment: Menlo Park, Calif., report prepared for U.S. Geological Survey, 95 p.

Newmark, N.M., 1965, Effects of earthquakes of dams and embankments: Geotechnique, v. 15, no. 2, p. 139–159.

Raggett, J.D., & Associates, Inc., 1989, Post-earthquake (10/17/89) structural survey, Moss Landing Marine Laboratory, California State University, Moss Landing, California: report prepared for California State University, 21 p.

Riggs, C.O., Mathes, G.M., and Raissieur, C.L., 1984, A field study of an automatic SPT hammer system: Geotechnical Testing Journal, v. 7, no. 3, p. 158–163.

Rutherford and Chekene, 1988, Geotechnical investigation, Moss Landing Facility, Technology Building: report prepared for Monterey Bay Aquarium Research Institute, Moss Landing, 85 p.

Seed, H.B., 1987, Design problems in soil liquefaction: Journal of Geotechnical Engineering, v. 113, no. 8, p. 827–845.

Seed, R.B., Dickenson, S.E., Riemer, M.F., Bray, J.D., Sitar, Nicholas, Mitchell, J.K., Idriss, I.M., Kayen, R.E., Kropp, Alan, Harder, L.F., Jr., and Power, M.S., 1990, Preliminary report on the principal geotechnical aspects of the October 17, 1989 Loma Prieta earthquake: University of California, Earthquake Engineering Research Center Report UCB/EERC–90/05, 137 p.

Seed, R.B., and Harder, L.F., Jr., 1990, SPT-based analysis of cyclic pore pressure generation and undrained residual strength, in H. Bolton Seed Memorial Symposium Proceedings, Berkeley, Calif., BiTech, v. 2, p. 351–376.

Seed, H.B., Tokimatsu, Kohji, Harder, L.F., and Chung, R.M., 1985, Influence of SPT procedures in soil liquefaction resistance evaluations: Journal of Geotechnical Engineering, v. 111, no. 12, p. 1425–1445.

Shakal, A.F., Huang, M.J., Reichle, M.S., Ventura, C.E., Cao, T.Q., Sherburne, R.W., Savage, M.K., Darragh, R.B., and Petersen, C.P., 1989, CSMIP strong-motion records from the Santa Cruz Mountains (Loma Prieta), California earthquake of 17 October 1989: California Division of Mines and Geology, Office of Strong Motion Studies Report OSMS 89–06, 196 p.

Somerville, P.G., and Yoshimura, Joanne, 1989, Strong motion modeling of the October 17, 1989 Loma Prieta earthquake [abs.]: Eos (American Geophysical Union Transactions), v. 71, no. 8, p. 290.

Wald, D.J., Burdick, L.J., and Somerville, P.G., 1988, Simulation of acceleration time histories close to large earthquakes, *in* Von Thun, J.L., ed., Proceedings; Earthquake Engineering and Soil Dymanics II; recent advances in ground-motion evaluation: American Society of Civil Engineers Geotechnical Special Publication 20, p. 430–444.

Woodward-Clyde Consultants, 1990, Phase I—geotechnical study marine biology laboratory, California State University, Moss Landing: Los Alamitos, Calif., report prepared for California State University, 54 p.

Youd, T.L., and Hoose, S.N., 1978, Historic ground failures in northern California triggered by earthquakes: U.S. Geological Survey Professional Paper 993, 177 p.

STRONG GROUND MOTION AND GROUND FAILURE

# OBSERVATIONS OF MULTIPLE LIQUEFACTION EVENTS AT SODA LAKE, CALIFORNIA, DURING THE EARTHQUAKE AND ITS AFTERSHOCKS

By John D. Sims and Cristofer D. Garvin,
U.S. Geological Survey

## CONTENTS



ABSTRACT

Sandblows in modern lake sediment near Watsonville, Calif., were caused by the $M$=7.1 October 17, 1989, Loma Prieta earthquake, the $M$=5.5 April 18, 1990, aftershock, and the $M$=4.6 March 23, 1991, aftershock. In June 1990, we dug four trenches in the dry lakebed of Soda Lake to expose the subsurface structure of the sandblows induced by the 1989 and 1990 events; we made additional observations 3 days after the March 23, 1991, aftershock. This study describes the structural relations among three liquefaction events that occurred in the same place during these three earthquakes. We discuss in detail the structures that resulted from the 1989 main shock and the April 18, 1990, aftershock.

Ground fissures formed in the lake sediment during the 1989 main shock, and the host sediment was vertically offset 3 to 6.5 cm. The sandblow vents opportunistically followed the zones of weakness formed by these fissures. Liquefied sand was ejected onto the dry lakebed and formed sandblow deposits ranging from low-angle conical structures, 30 to 50 cm thick and about 2 to 5 m in diameter, to elongate deposits of similar thickness and width but as much as 35 m long. Sand dikes formed in the fissures that extend to the liquefied layer at depth as the rising liquefied sand dewatered and solidified. Sandblows associated with the April 18, 1990, aftershock commonly reoccupied preexisting fissures but also formed new vents outside of preexisting fissures. Sandblows from the March 23, 1991, aftershock erupted only through large preexisting vents. Vents reactivated by the April 18, 1990, sandblows contained sediment clasts of sandblow deposits formed in the 1989 main shock. Xenoclasts of host sediment, probably from the source zone, are also present in the sand dikes.

Textural and color differences define laminations within vents and surface cones. These laminations show that the sandblow cones and sand dikes were not formed in a single episode. The three generations of sandblows are represented by cone and dike deposits that are composed of several subunits, suggesting that the cone deposits were formed by pulses of water and sediment which were expelled from the vent. We interpret these pulses to result from cyclic phases of locally increased pore pressure in the liquefied bed at depth. Episodes of liquefaction and sandblow formation can yield two types of sandblows, compound and complex. Compound sandblows result from multiple episodes of sediment and water ejection from a single fissure, and complex sandblows result from the interaction of sandblows formed by ejecta from two or more fissures. Although the two older generations of structures were formed about 6 months apart, they have color and textural differences that mimic liquefaction structures formed in earthquakes separated by intervals of decades or centuries.

## INTRODUCTION

The 1989 Loma Prieta earthquake induced liquefaction in various types of sediment at numerous locations (U.S. Geological Survey staff, 1990). Importantly, some of the largest aftershocks caused repeated liquefaction at some

sites in precisely the same places in the San Francisco Bay region (Wills and Manson, 1990). One site, Soda Lake near Watsonville, Calif. (fig. 1), reveals a record of three liquefaction events. The sedimentary deposits of Soda Lake, which are particularly sensitive to liquefaction (Dupré and Tinsley, 1980), are near the epicenters of the October 17, 1989, $M$=7.1 Loma Prieta earthquake and the April 18, 1990, $M$=5.5 and March 23, 1991, $M$=4.6 aftershocks. The March 23, 1991, aftershock is the smallest earthquake known to have induced liquefaction in the sediment; however, nearness of the epicenter to the sensitive deposits at Soda Lake and preexisting fissures in the sediment were factors in the induction of this liquefaction event.

Both the 1989 Loma Prieta earthquake and its predecessor, the 1906 San Francisco earthquake, caused liquefaction in sediment in the Watsonville, Calif., area. The distributions of earthquake-induced liquefaction triggered by the 1906 and 1989 earthquakes in this area are remarkably similar (fig. 2). The relations among liquefaction structures formed in 1906, 1989, and, possibly, earlier earthquakes are likely to provide information on multiple liquefaction structures separated by intervals of decades to centuries. This paper describes the morphology and

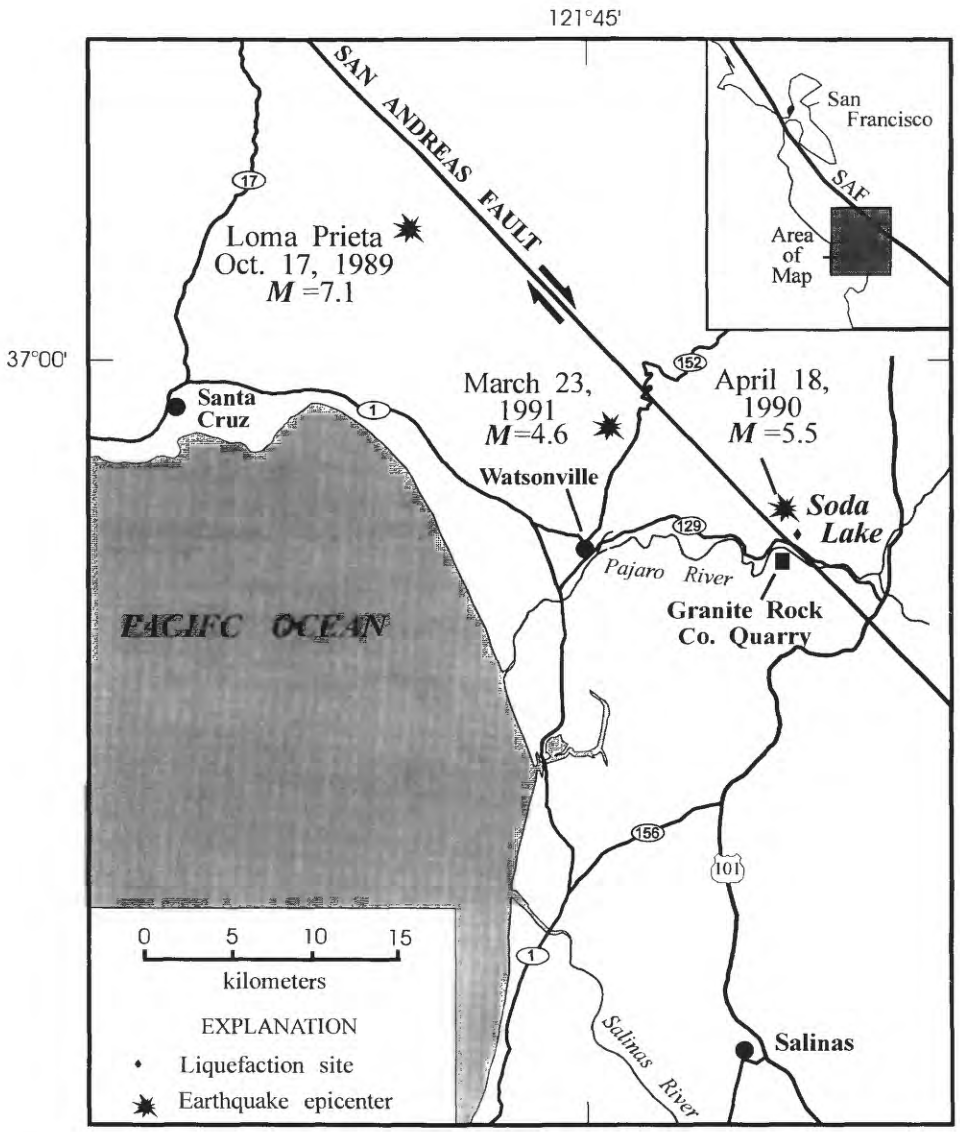


Figure 1.—Soda Lake, Calif., showing locations of epicenters of October 17, 1989, Loma Prieta earthquake and April 18, 1990, and March 23, 1991, aftershocks that caused liquefaction in lakebed. In October 1989, liquefaction also occurred in Santa Cruz and Watsonville, along the Salinas and Pajaro Rivers, and along other, smaller coastal streams. Paired arrows show direction of movement on the San Andreas fault (SAF).

sedimentary relations of liquefaction structures at a site where multiple liquefaction events were associated with the Loma Prieta main shock and the stronger aftershocks. Most importantly, the locations and times of the earthquakes that caused the liquefaction are known. Thus, the sequence of liquefaction events at Soda Lake can easily be reconstructed, and its potential for aiding studies of paleoliquefaction events is significant.

Liquefaction occurs when a metastable, loosely packed grain framework is suddenly broken down; the grains become temporarily suspended in the pore fluid and settle through the fluid, displacing it upward, until a grain-supported structure is reestablished (Lowe, 1975; Lowe and LoPiccolo, 1975). Most of the data pertaining to the cause, process, and effect of liquefaction come from engineering studies (Lee and Seed, 1967). These studies primarily focus on the response of soils and critical engineered structures, such as dams and foundations, to the effects of earthquake-induced liquefaction (Housner, 1958; Youd and Hoose, 1978; Seed and others, 1981; Seed and Idris, 1983; Bennett and others, 1984; Youd and Wieczorek, 1984; Holzer and others, 1989).

The occurrence of liquefaction-induced deformation in earthquakes depends on the shaking intensity and the presence of liquefiable sediment. Preservation of the deformational structures largely depends on environment. The potential range of earthquake-induced deformational structures in soft sediment is large (Sims, 1978a, b); however, the most common liquefaction structures in subaerial environments are sandblows. Liquefaction structures that

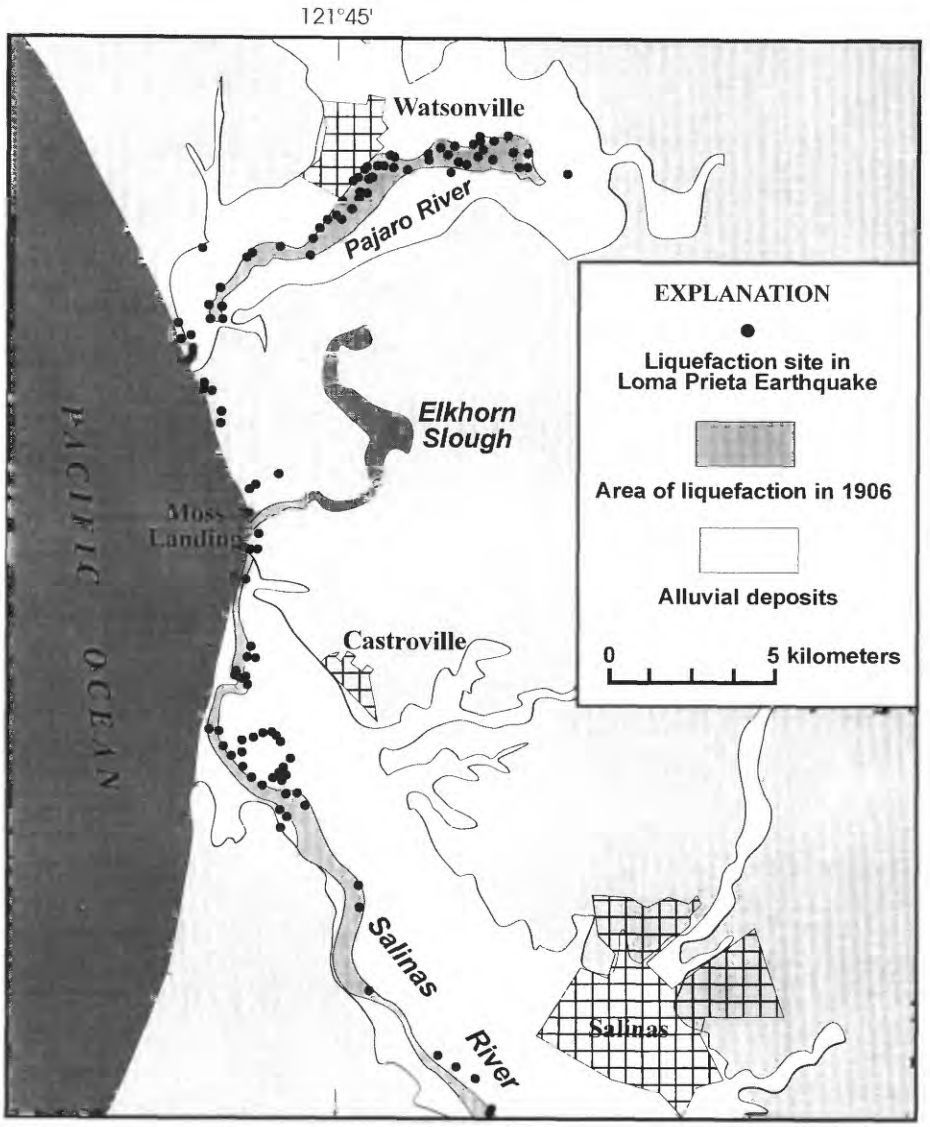


Figure 2.—Area of Salinas and Pajaro Rivers, showing regional distribution of earthquake-induced liquefaction in 1906 San Francisco and 1989 Loma Prieta earthquakes.

form subaqueously in lacustrine deposits contain a larger variety of earthquake-induced structures than do those in other depositional environments (Sims, 1973, 1975, 1978b; Rymer and Sims, 1976).

## SANDBLOWS OF SODA LAKE

Soda Lake is a now-inactive settling basin of the nearby Granite Rock Co. quarry (fig. 1). The basin was constructed over a preexisting natural lake in an abandoned meander loop of the Pajaro River near Watsonville, Calif. Deposits in the basin are derived from the washing of crushed rock to remove sand, silt, and clay particles at the quarry. Rock washings were pumped as a slurry from the quarry to Soda Lake, where the sediment settled out and accumulated to a total thickness of about 10 to 12 m. The sediment that liquefied was deposited in the basin between about 1968 and the mid-1980's (Wills and Manson, 1990). The surface of Soda Lake slopes slightly southeast toward a 2- to 3-m-deep marshy depression on the southeast side of the basin. Loose sand and silt cover the sparsely vegetated surface of the dry lakebed.

Three liquefaction events were induced in the sediment of Soda Lake: the October 17, 1989, Loma Prieta earthquake, the April 18, 1990, aftershock, and the March 23, 1991, aftershock. Strong aftershocks at about 5:30 a.m. P.d.t. on October 18, 1989, probably renewed or continued liquefaction at Soda Lake induced by the main shock at 5:04 p.m. the evening before; however, we have no observations to confirm this interpretation. Liquefaction structures, if any, from these aftershocks were indistinguishable from those that resulted from the main shock and so are not included as a discrete suite in this paper. Shortly after the 1989 Loma Prieta main shock, scientists from the U.S. Geological Survey and the California Division of Mines and Geology visited Soda Lake (Wills and Manson, 1990), where they noted numerous sandblows and fissures on the surface of the basin (J.C. Tinsley, oral commun., 1990).

One of us (J.D.S.) visited the site on April 19, 1990, after the April 18 aftershock, when I observed the later stages of formation of the second generation of sandblows. At that time, water was flowing from many of the sandblow vents. Although some of the larger vents still carried suspended sediment, none was actively adding to the cones built during this phase of formation. Water flowing from some of the larger vents still carried suspended clay- and silt-size sediment, but none of the cones was being actively built during that phase of the eruptions. Water that lacked suspended sediment flowed from some of the vents and actively cut rills into the newly built cones. Sandblows that resulted from the 1989 Loma Prieta main shock were easily distinguishable from the newly formed second-generation sandblows. The first-generation cones were slightly eroded by raindrops, deflation, and desiccation in response to the sparse winter rains that fell between October 1989 and April 1990.

In May 1990, we mapped the distribution of fissures in the lakebed and the first two generations of sandblows (fig. 3). Fissures nearest the lake margin have associated sandblows. We recorded the diameter of each vent and, for elliptical vents, the average of the dimensions of the major and minor axes. Most of these sandblows are aligned along fissures in the lake sediment and are identifiable as discrete features, even though the cones of closely spaced sandblows overlap. Some vents, however, are elongate and stretch as much as 13 m along the fissures. At Soda Lake, the diameter and volume of a sediment cone is generally proportional to the size of its vent. The map of sandblow distribution shows that about 70 percent of second-generation cones overlap those of the first generation (fig. 3). In some places, only second-generation cones are visible on the surface because they completely mantle first-generation cones.

In June 1990, we excavated four trenches across selected fissures and their associated sandblows to examine the subsurface relations of the two existing generations of sandblows and the lake sediment. Trench 1 reached a liquefiable water-saturated sand unit at about 3 m below the surface of the lake (fig. 3). When the excavation penetrated the water-saturated layer, however, the liquefiable sediment flowed, and the trench walls collapsed. Thus, our study was limited to only about the upper 1.5 m of the lake sediment.

After the March 23, 1991, aftershock, one of us (C.D.G.) again visited Soda Lake. At that time, only a few of the larger preexisting sandblows near the center of the lake showed signs of recent liquefaction, and no new vents had formed. On March 26, water laden with fine sediment was flowing from the reactivated vents and had breached and incised the surfaces of the cones (fig. 4). The fresh surfaces of reactivated cones showed no signs of erosion from recent rainfall and were easily distinguishable from the slightly eroded and partly vegetated older cones (fig. 5). Microvents, 3 to 5 mm in diameter with associated cones 1 to 3 mm high, flanked the sides of the main vents and also issued water and fine sediment (fig. 6). Water was ponded on the lake surface, and the lake sediment was saturated from several days of heavy rainfall, which prevented even shallow excavation. Several older vents were partly filled with clear water and showed no signs of recent cone deposition (fig. 7). These vents apparently filled with rainwater or perched ground water and, like most of the preexisting vents, were not reactivated during the March 23 aftershock. The fact that this aftershock reactivated only preexisting vents at Soda Lake suggests that had there not been preexisting vents, the earthquake would not have produced sandblow deposits. Thus, liquefaction at depth could occur without the presence of surface or vent deposits to record such an event.

## INTERNAL STRUCTURE OF SANDBLOW DEPOSITS

The sandblows exposed in the trenches typically consist of a surface cone and vent and a subsurface feeder dike (fig. 8). The cone is composed of sand, silt, and clay expelled onto the ground surface from the vent. Some vents are filled with dewatered liquefied material to within a few centimeters of the high point on the cone; other vents remained open to depths of as much as 1 m. The near-vertical, planar feeder dike is filled with sand, silt, and a minor amount of clay that was derived from the liquefied layer at depth.

The excavations in Soda Lake reveal subsurface details of the sandblow structures and the thin-bedded, finely laminated deposits through which fissures opened and liquefied sediment vented to the surface of the lakebed (fig. 9). We observed the three-dimensional aspect of the sandblows and their feeder dikes in seven sequential vertical cross sections taken at 10-cm intervals along the strike of the fissure in trench 2 (fig. 3). These serial sections of the sandblow structures reveal the relations among the fissures, feeder dikes, cones, and vertical separation across the fissure. The amount of offset on fissures, relations among graded subunits in the surface cones, and textural zonation and lamination in the feeder dikes all suggest that the sandblows formed episodically.

### FISSURES

Numerous fissures cut the bed of Soda Lake and facilitated the eruption of sandblows. These fissures generally

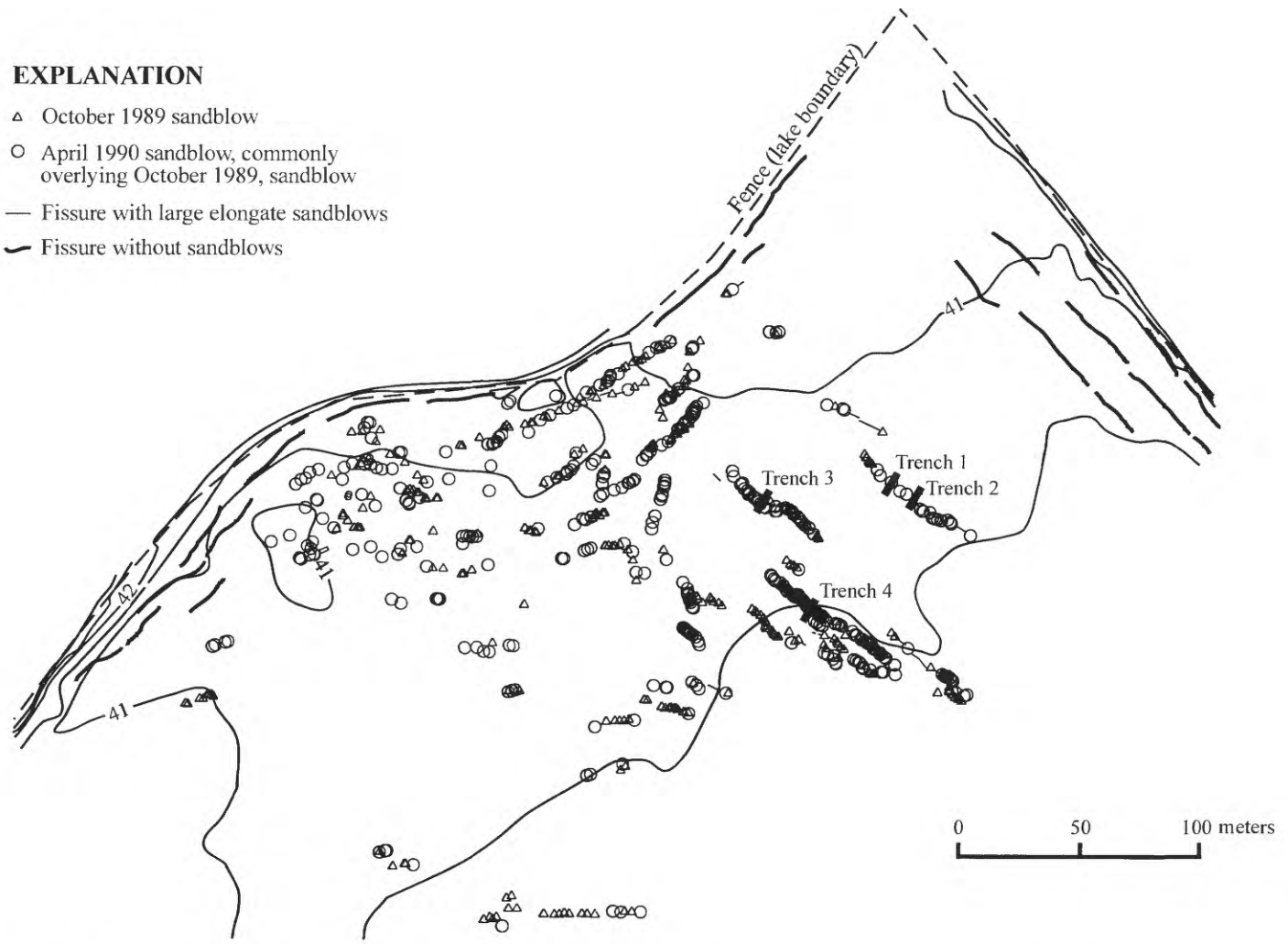


Figure 3.—Topographic map of Soda Lake, Calif., showing distribution of fissures and sandblows formed in October 17, 1989, Loma Prieta earthquake and April 18, 1990, aftershock, and locations of four trenches. Contour interval, 0.5 m.

consist of two intersecting sets of echelon straight segments, subparallel to parallel to the lake margin, that range in length from less than 1 to about 35 m. One set of fissures is subparallel to the northwest lake boundary formed by a hillslope; the other set is parallel to the northeast lake boundary formed by a manmade dike (fig. 3). Fissures that lack sandblows lie principally along the margin of the lake and have an aggregate vertical displacement of 50 to 70 cm. Fissures along which sandblows erupted have vertical separations that range from 3 to 6.5 cm. The sense of movement on all of the fissures with vertical displacement was down toward the center of the lake.

Figure 4.—Sandblow reactivated by March 23, 1991, $M$=4.6 aftershock. Surface is smooth in comparison with eroded and vegetated cones shown in figures 5 and 7. Diameter of vent between arrows is approximately 30 cm. Photograph taken March 26, 1991.

Figure 5.—Photograph of eroded and vegetated cone first formed in October 17, 1989, Loma Prieta earthquake and reactivated in April 18, 1990, aftershock but not in March 23, 1991, aftershock. Photograph taken March 26, 1991.

As of April 18, 1990, open fissures were most common along the margin of the lake where sandblows were absent. Open fissures were also present in places where sediment-free water continued to flow from sandblow vents. At the time of our excavations in June 1990, however, most of the fissures were partly to completely filled by eolian sand.

## DIKES

Sand dikes are subsurface deposits of dewatered liquefied sediment that fill fissures. The dikes are composed of well-sorted, fine to medium sand (fig. 10). Some of the sand-dike deposits contain laminations subparallel to parallel to the fissure wall (fig. 11). In cross section, the walls of sand dikes are undulatory, and most of the con-

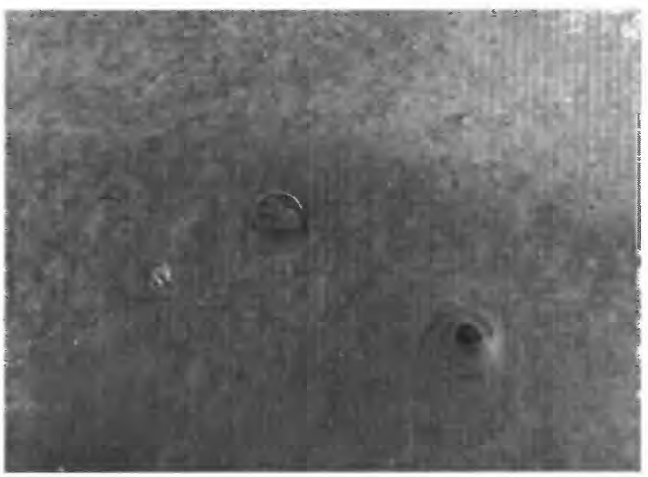

Figure 6.—Microvent on flank of cone reactivated in March 23, 1991, aftershock. Diameter of microvent is approximately 1 cm. Photograph taken March 26, 1991.

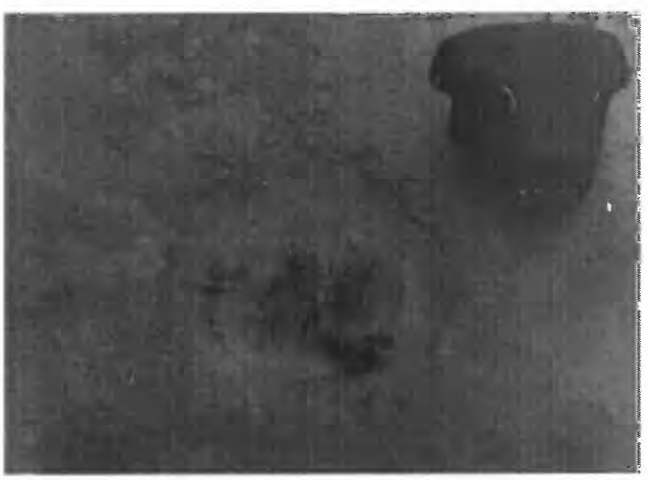

Figure 7.—Weathered cone filled with rainwater or perched ground water. Photograph taken March 26, 1991.

cave sections are filled by dark sand lenses. The dark sand in the sidewall lenses is traceable to the dark-sand subunit at the bottom of the surface cone (fig. 9*C*). Thin, fine-grained laminations separate the sand lenses along the sidewall from the coarser, lighter colored dike interior.

When viewed normal to the strike of the fissure, contemporaneous dikes can terminate at different stratigraphic levels that do not necessarily reach the free surface (fig. 12). Three of the dikes shown in figure 12*D* have a complex crosscutting relation in which dike I is cut by dikes II and III. In turn, dike II is truncated by dike III where dike II emerges from the dike I sediment. Dike deposits discontinuously occupy some fissures. In trench II, we observed dike deposits between vertical cross sections 0 and about 35 cm and an open fissure from about 35 to 60 cm; the open fissure coincides with the vent of the sandblow.

Dikes are the structures most likely to be preserved in the geologic record, and cones the least likely. Vents present in the geologic record are likely to be difficult to distinguish from dikes after erosion and modification of the surface cone.

## CONES

Two major depositional units from the two earlier liquefaction events are easily distinguishable in the stratigraphy of the cone deposits of the sandblows. Each major unit, in turn, contains a varying number of subunits commonly separated by darker laminations. Although the number of subunits varies between vertical sections through the sandblow, most of the subunits are identifiable and correlatable in all cross sections. The major stratigraphic units of the cone deposits represent the first two genera-

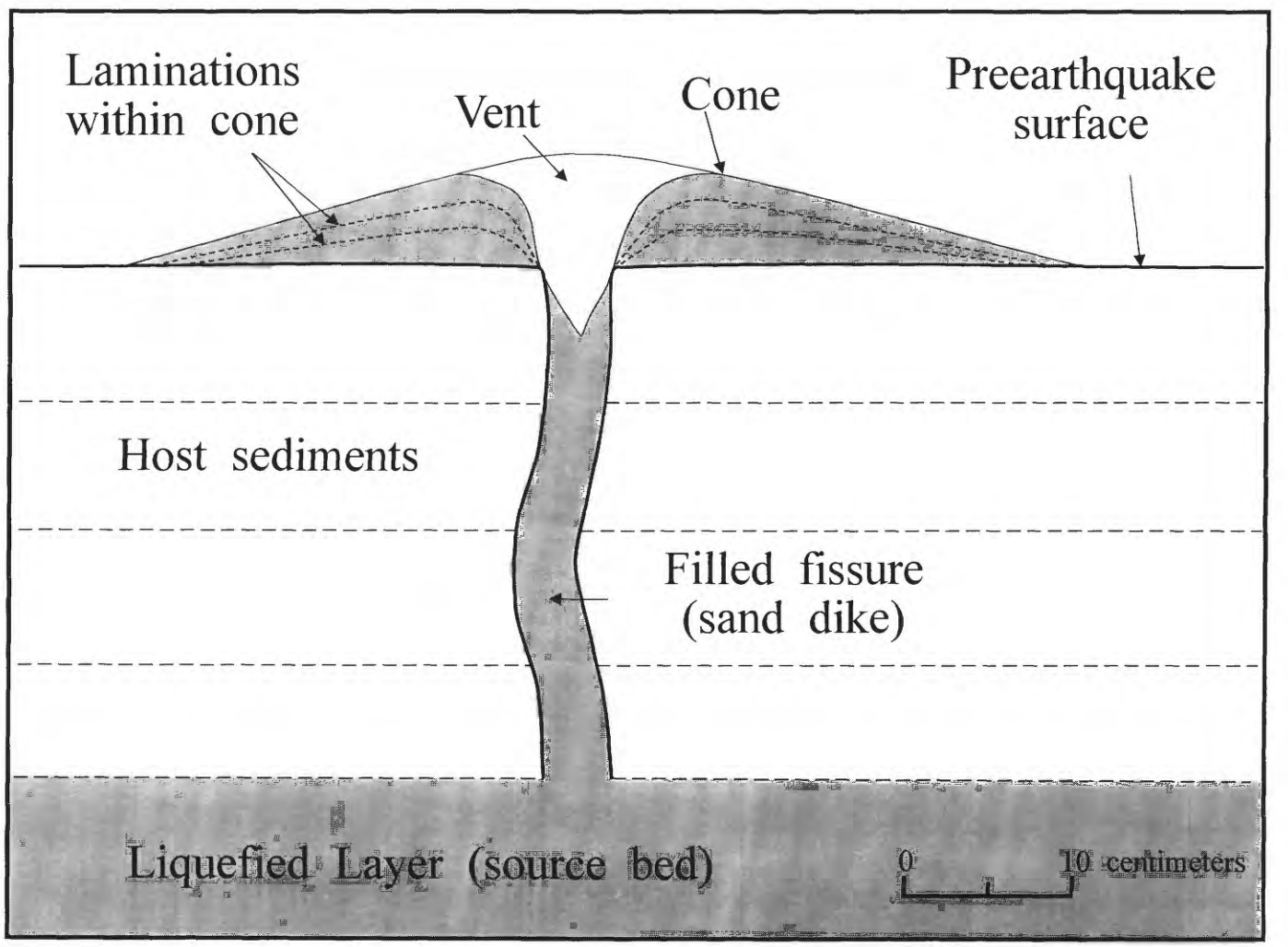


Figure 8.—Schematic cross section of a sandblow, showing typical stratigraphic and structural relations and terminology used in this paper.

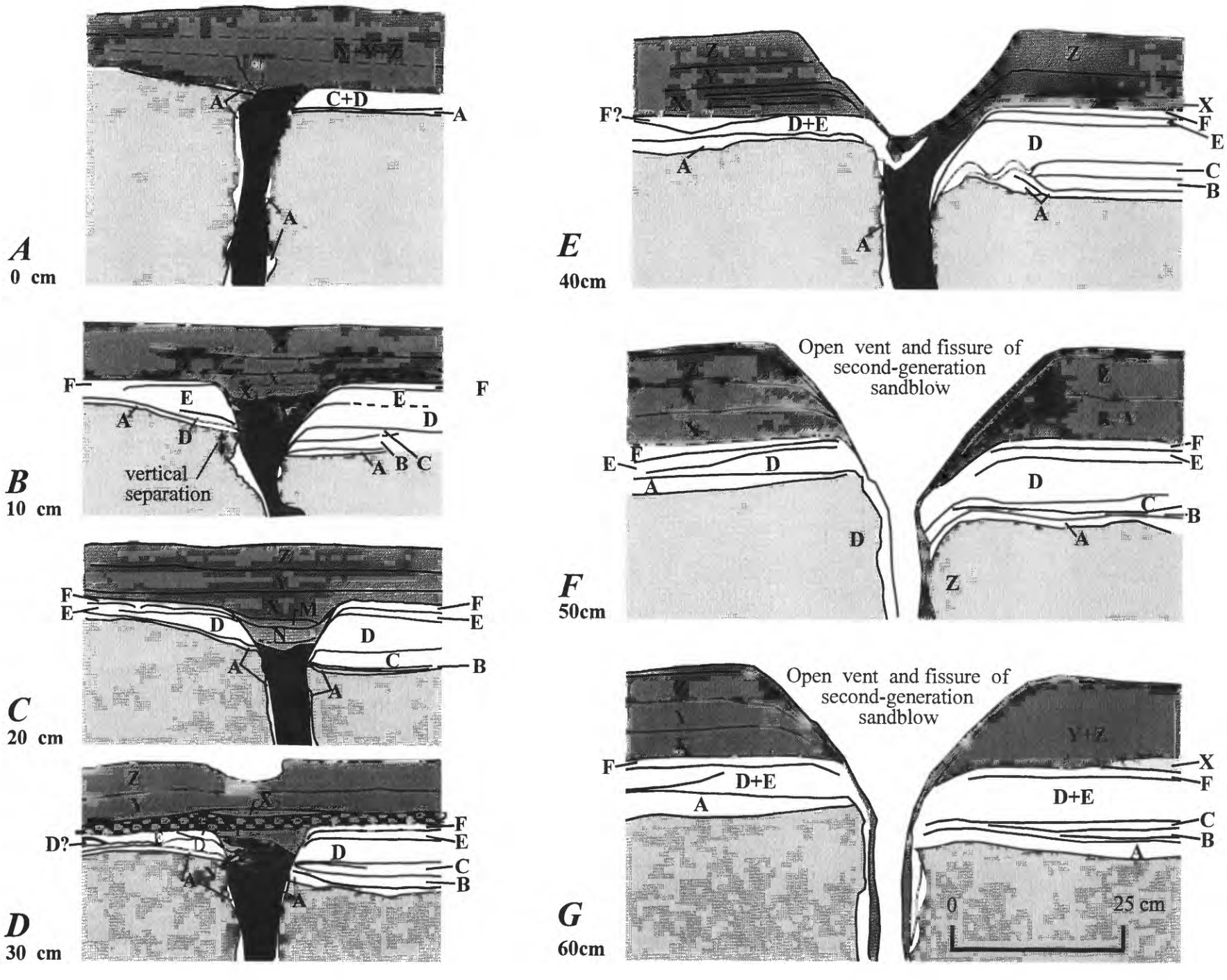
A
0 cm
C+D
A
A
B
10 cm
F
E
E
D
A
D
A B C
vertical
separation
C
20 cm
F
E
D
C
B
D
30 cm
D?
D
C
B
E
40cm
F?
D+E
A
D
C
B
F
50cm
Open vent and fissure of
second-generation
sandblow
E
D
A
D
D
C
B
G
60cm
Open vent and fissure of
second-generation
sandblow
F
D+E
A
D+E
C
B
0
25 cm

tions of sandblows: Unit I formed in response to the 1989 Loma Prieta earthquake, and unit II accompanied the April 18, 1990, aftershock. Unit I is commonly darker than the overlying unit II. Subunits within the two major units correspond to different eruptive phases during a liquefaction event.

### UNIT I

Unit I, consisting of subunits A through F (fig. 9), is composed of laminated fine sand and silt that overlies a basal subunit of coarse sand. The upper surface of unit I consists of an irregular silt lamina, about 3 to 5 mm thick, with desiccation cracks and raindrop impressions (fig. 9*B*).

At least six subunits, A through F, are present on the downthrown side of the fissure (fig. 9). Subunit A, the basal subunit of the cone, is composed of wavy-laminated, laterally discontinuous coarse sand that rests directly on the lake bed surface. Subunit B consists of parallel-laminated, fining-upward, medium to fine sand that is laterally more extensive than subunit A. The upper boundary of subunit B is a zone of discontinuous dark mineral laminations composed of silt-size grains. Subunit C consists of wavy-laminated, fining-upward, fine to medium sand. The upper contact of subunit C is marked by a diffuse, thick, dark lamina (fig. 9*B*). Subunit C is overlain by subunits D through F, a sequence of three layers of fining-upward, fine to medium sand with faint dark, discontinuous laminae (figs. 9*B*, 9*C*)

Cone deposits on the upthrown side of the fissure are less complex and less extensive (fig. 9). The basal subunit is a thin, coarse sand identical to subunit A on the downthrown side. In cross sections at intervals 40, 50, and 60 cm, subunit A is overlain by dark deposits similar to, but thinner than, subunits B and C. This subunit is overlain by a sequence of three subunits identical to subunits D through F on the downthrown side of the fissure.

The above-mentioned relations are common to serial sections at intervals 0, 10, 20, and 30 cm. The open vent of the second-generation sandblow was exposed in the section at interval 40 cm. The principal change in this section is that subunit N, the wavy-laminated silt and sand at the top of the feeder dike, is no longer present (fig. 9).

### UNIT II

Unit II consists of subunits X through Z (fig. 9), formed as the result of liquefaction during the April 18, 1990, aftershock. Unit II is composed of medium sand and silt and thus lacks a coarse basal subunit. This younger unit is lighter in color and about 1.5 times thicker than unit I. Unit II has no vertical offset, is generally massive, and contains several faint dark laminae throughout and multiple dark laminations in the upper 1 to 1.5 cm. Unit II is not offset vertically.

## MODEL FOR SANDBLOW FORMATION

Sandblow formation proceeds from liquefaction of a sand layer(s) at depth. The process of liquefaction yields a sand-and-water layer with little or no shear strength; liquefied sediment is then forced to migrate through weak zones in the overlying confining deposits. Weak zones at Soda Lake most commonly are created by fissures formed through brittle deformation and foundering of the sedi-

◄ Figure 9.—Schematic drawing based on photographs of serial sections through sediment in trench 2 in Soda Lake (see fig. 3 for location), showing host sediment, feeder dikes, and cone deposits that formed after October 17, 1989, Loma Prieta earthquake and April 18, 1990, aftershock. Feeder sand dikes cut well-bedded, laminated host sediment that is vertically offset as much as 3 cm across fissure. Downdropped side of fissure is to right toward center of lake. Finely laminated surface cone deposit is composed of two groups of subunits: A through F are deposits from October 17, 1989, Loma Prieta earthquake, and X through Z are from April 18, 1990, aftershock. October 17, 1989, deposits are subdivided into two depositional stages represented by subunits A through C and D through F. Serial sections at intervals 40, 50, and 60 cm progressively expose open vent and fissure that resulted from the April 18, 1990, episode of sandblow deposition. This vent probably remained open after October 17, 1989, earthquake and was reactivated during April 18, 1990, aftershock. Subunits N and M in serial sections at intervals 10, 20, and 30 cm are deposits of windborne and waterborne sediment that filled vent depression after first phase of sandblow formation.

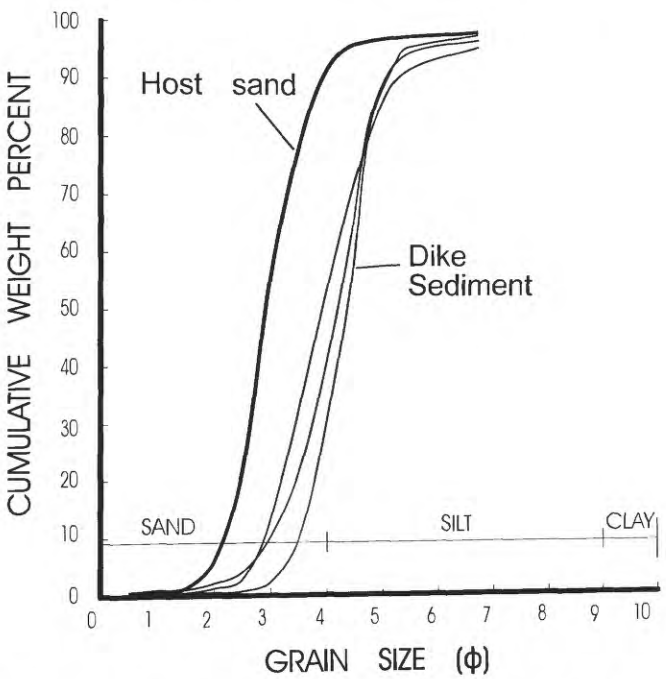


Figure 10.—Grain size versus cumulative weight percent of sand-dike material and sandy host sediment.

Figure 11.—Vertical section through sand dike and sandblow, showing internal lamination subparallel to dike walls in sand dike. Dike walls are undulatory, and most concave sections are filled with lenses of darker silt- and clay-rich sediment (arrows). Note details of stratigraphy of host sediment. Dotted line, contact between finely laminated host sediment and erupted sand of sandblow surface shield; dashed line, upper contact of basal subunit of coarse sand that was first material erupted from fissure.

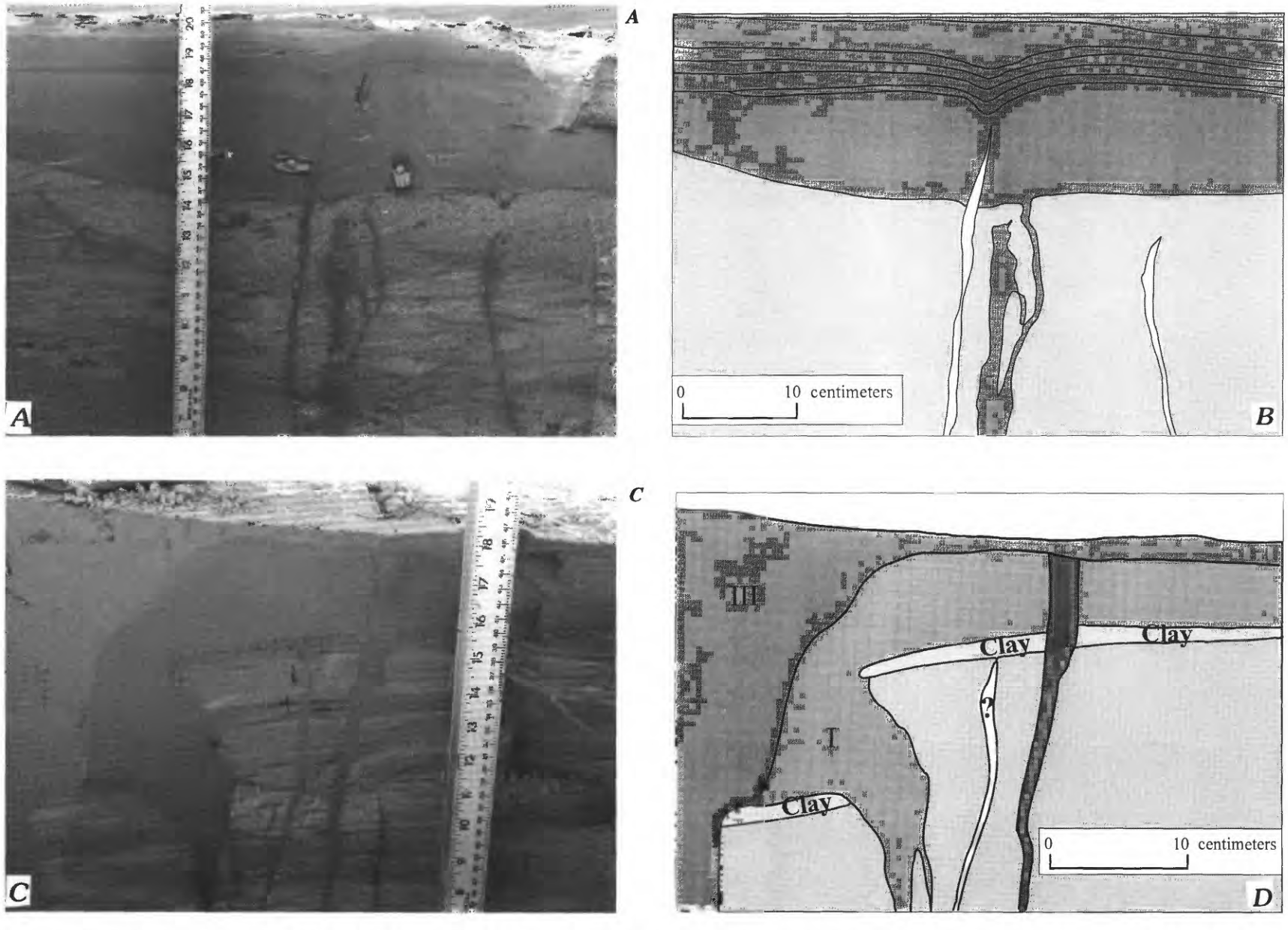


Figure 12.—Sediment exposed in trenches 3 (*A*) and 4 (*C*) (see fig. 3 for locations), with sketches illustrating stratigraphic relations (*B* and *D*, respectively). Photograph in figure 12*A* shows small sand dikes, terminating at different stratigraphic levels, that formed on either October 17, 1989, or April 18, 1990. Photograph in figure 12*C* shows three crosscutting liquefaction structures, I through III, and a small sand dike that terminates at a clay layer.

ment that overlies the liquefied zone during lateral spreading. These weak zones then develop into cracks that become the fissures through which water and sediment are expelled. The expelled sediment forms the distinctive elongate or cone-shaped deposits on the ground surface.

The two generations of sandblow cone deposits at Soda Lake show several fining-upward subunits with fine-grained dark laminae at the top. The presence of these fining-upward subunits indicates that the cone was constructed by the expulsion of several pulses of sediment and water during an episode of liquefaction. This episodic deposition of cone subunits is probably associated with cyclic redistribution of local excess pore pressure in the liquefied bed. This phenomenon, which has been observed in other sandblows, appears to be a common feature during liquefaction (Holzer and others, 1989; Scott, 1974).

Deposition of the lowest subunits of unit I was strongly controlled by vertical separation along the fissure (fig. 9). Cone building on the lower side of the fissure was favored until the vertical offset on the lakebed surface was eliminated. Deposition of multiple subunits built the cone during a second stage of formation. These two stages of cone building are also apparent in the dike of this sandblow. The final stage of formation of the sandblow was during the waning stages of flow, when waterflow had decreased to the point that sedimentation occurred in part of the vent. Deposition in standing water resulted in an irregularly laminated sequence in the vent depression. These late-stage deposits overlie, in part, the feeder-dike deposits (fig. 9*B*–9*D*).

Sand-dike deposits are intermediate to late-stage deposits. Initially, the water and sediment flow through open fissures created by lateral spreading of the deposits that overlie the liquefied unit. The fissure walls show little evidence of differential erosion by the escaping water and sediment, suggesting that the overall velocity of escaping sediment and water is low. Although water continues to escape for as long as several days, sediment is carried only early in the process, owing to redeposition of sediment in the liquefied layer after release of the hydrostatic pressure and the initial escape of water and sediment. Any erosion of the dike wall probably ceases after the initial release of hydrostatic pressure or when the fissure has widened enough to accommodate the flow of water and sediment at a particular time. Thus, erosion of the sidewall probably is strongly controlled by the number of fissures and their width, the water and sediment flux, and the cohesive strength of the sidewall. After the fissure opens, concave pockets in the sidewall are the first to receive deposition. The color and textural differences between the lenses and the interior of the dike suggest that the lenses formed early in the formation of the sandblow. Therefore, erosion of the dike wall occurs only during the early phase of sandblow formation.

Interior laminations in the dike, which parallel the flow direction, were probably formed as the flow of water and sediment began to wane. These laminations are probably analogous to the differing suites of depositional structures formed at varying fluid velocities and sediment grain sizes in stream deposits (Allen, 1984). Sediment is deposited along the conduit wall as a response to decreasing water and sediment flux. Once the sediment fills a segment of a fissure vent, the solid dike structure continues to grow along strike of the fissure. Thus, as a segment of fissure becomes clogged, it is buried by sediment issuing from the adjacent section of fissure (figs. 10*A*, 10*B*).

We interpret three crosscutting dike structures in trench 4 (fig. 10*C*, 10*D*) to have formed in at least four ways. (1) All three visible dikes are discrete and represent three separate earthquakes. Dike 1 formed first and was followed in succession by dikes 2 and 3. (2) Dike 1, from the main shock, is crosscut by dikes 2 and 3 that resulted from an aftershock. Dike 2 clogged, while dike 3 remained active and eroded the surface sediment from dike 2. (3), Dikes 1 and 2 resulted from the main shock and immediate large aftershocks. Dike 1 formed first and was pinched off by a downdropped block of host sediment, thus forcing the formation of dike 2. Dike 3 formed in an aftershock and cut through both previously formed dikes. (4) All three dikes formed during the same earthquake. Dikes 1 and 3 were active simultaneously until a block of host sediment dropped and pinched off the conduit that fed dike 1. Dike 3 remained active and cut into dike 1. Lateral pressure release, caused by the dropped sediment block, allowed dike 2 to open. Dike 2's relatively small size caused it to clog before dike 3 stopped flowing; thus, dike 3 truncated dike 2.

## CONCLUSIONS

Individual sandblow formations are not formed in a single simple eruption but through several pulses of eruption of liquefied sand. These eruptions are episodic, and if liquefaction is renewed during large aftershocks, the resulting sandblow features may mimic liquefaction structures caused by seismic events separated by intervals of decades or centuries. The multiple phases of cone deposition observed in Soda Lake are associated with the pulsed expulsion of water and sediment from the vents. These pulses probably result from local cyclic buildup and redistribution of pore pressure in the liquefied bed. The sand dike and surface cone also form in several phases associated with pulsed expulsion of water and sediment. The dike material filling the fissure is deposited progressively along strike as the water and sediment flux decreases. Stratigraphic relations within the dike are more complex than those within the cone because the water and

its suspended sediment are constrained to flow within a conduit. A strong pulse that increases discharge can erode the walls of the conduit and thus erase evidence of previous pulses. Pulsating discharges during eruption were observed in sandblows in the Imperial Valley after the 1987 Superstition Mountain, Calif., earthquake (Holzer and others, 1989).

From our work at Soda Lake, we distinguish two main groups of sandblows, compound and complex. Compound sandblows result from multiple episodes of water and sediment expulsion from a single fissure, and complex sandblows result from the interaction of sandblows formed in two or more fissures. Compound sandblows result from successive events of liquefaction and consequent intrusion and extrusion of the liquefied sand. Different episodes of dike and cone deposition are distinguishable by such features as textural gradation of conduit fill, crosscutting conduit-fill sequences, and compound extrusion features. Compound sandblows can be further subdivided into (1) compound sandblows truncated by an unconformity or erosional surface, and (2) compound sandblows that do not reach a free surface; that is, the upper or lateral end of sandblow or hydrofracture terminates in a tapered point.

Complex sandblows can also be further subdivided into (1) crosscutting conduits terminated at a single level, (2) conduits terminated at different stratigraphic levels by unconformities, (3) two or more conduits truncated at a single level with no crosscutting, and (4) compound sandblows with complex structures. The eruptive structures may or may not be present with each sandblow type.

## ACKNOWLEDGMENTS

The final phases of this research were supported by the U.S. Nuclear Regulatory Commission. We thank John Rocha for granting us access to his property. John Hamilton and Dan Meier surveyed the sandblows of Soda Lake and prepared the map in figure 3. Allyn Foss expertly prepared the illustrations for this paper and assisted in the fieldwork. We thank S.F. Obermeier and J.C. Tinsley for their reviews of the manuscript.

## REFERENCES CITED

Allen, J.R.L., 1984, Sedimentary structures; their character and physical basis: Amsterdam, Elsevier, 2 v.

Bennett, M.J., McLaughlin, P.V., Sarmiento, J.S., and Youd, T.L., 1984, Geotechnical investigation of liquefaction sites, Imperial Valley, California: U.S. Geological Survey Open-File Report 84–252, 103 p.

Dupré, W.R., and Tinsley, J.C., III, 1980, Map showing geology and liquefaction potential of northern Monterey and southern Santa Cruz Counties, California: U.S. Geological Survey Miscellaneous Field Studies Map MF–1199, scale 1:62,500, 2 sheets.

Holzer, T.L., Youd, T.L., and Hanks, T.C., 1989, Dynamics of liquefaction during the 1987 Superstition Hills, California, earthquake: Science, v. 244, no. 4900, p. 56–59.

Housner, G.W., 1958, The mechanism of sandblows: Seismological Society of America Bulletin, v. 48, no. 2, p. 155–161.

Lee, K.L., and Seed, H.B., 1967, Cyclic stress conditions causing liquefaction of sand: American Society of Civil Engineers Proceedings, Soil Mechanics and Foundations Division Journal, v. 93, no. SM1, p. 47–70.

Lowe, D.R., 1975, Water escape structures in coarse-grained sediments: Sedimentology, v. 22, no. 2, p. 157–204.

Lowe, D.R., and LoPiccolo, R.D., 1974, The characteristics and origins of dish and pillar structures: Journal of Sedimentary Petrology, v. 44, no. 2, p. 484–501.

Rymer, M.J., and Sims, J.D., 1976, Preliminary survey of modern glaciolacustrine sediments for earthquake-induced deformational structures, south-central Alaska: U.S. Geological Survey Open-File Report 76–373, 20 p.

Scott, R.F., 1974, Observations of sandblows: California Institute of Technology, Pasadena, California Institute of Technology, Division of Engineering and Applied Science, 23 p.

Seed, H.B., Arango, I., Chan, C.K., Gomez-Masso, Alberto, and Ascoli, R.G., 1981, Earthquake-induced liquefaction Near Lake Amatitlan, Guatemala: American Society of Civil Engineers Proceedings, Geotechnical Engineering Division Journal, v. 107, no. GT4, p. 501–518.

Seed, H.B., Idriss, I.M., and Arango, Ignacio, 1983, Evaluation of liquefaction potential using field performance data: Journal of Geotechnical Engineering, v. 109, no. 3, p. 458–482.

Sims, J.D., 1973, Earthquake-induced structures in sediments of Van Norman Lake, San Fernando, California: Science, v. 182, no. 4108, p. 161–163.

———1975, Determining earthquake recurrence intervals from deformational structures in young lacustrine sediments: Tectonophysics, v. 29, no. 1–4, p. 141–153.

———1978a, Annotated bibliography of penecontemporaneously formed deformational structures in sediments: U.S. Geological Survey Open-File Report 78–510, 79 p.

———1978b, Environments of formation of earthquake-induced deformational structures in sediments: International Congress on Sedimentology, 10th, Jerusalem, 1978, Abstracts, v. 10, no. 2, p. 612–613.

U.S. Geological Survey staff, 1990, The Loma Prieta, California, earthquake; an anticipated event: Science, v. 247, no. 4940, p. 286–293.

Wills, C.J., and Manson, M.W., 1990, Liquefaction at Soda Lake; effects of the Chittenden earthquake swarm of April 18, 1990: California Geology, v. 43, no. 10, p. 225–232.

Youd, T.L., and Hoose, S.N., 1978, Historic ground failures in northern California triggered by earthquakes: U.S. Geological Survey Professional Paper 993, 177 p.

Youd, T.L., and Weiczorek, G.F., 1984, Liquefaction during the 1981 and previous earthquakes near Westmorland, California: U.S. Geological Survey Open-File Report 84–680, 36 p.

THE LOMA PRIETA, CALIFORNIA, EARTHQUAKE OF OCTOBER 17, 1989:
LIQUEFACTION

STRONG GROUND MOTION AND GROUND FAILURE

# POSTEARTHQUAKE INVESTIGATIONS AT LIQUEFACTION SITES IN SANTA CRUZ AND ON TREASURE ISLAND

By Roman D. Hryciw, University of Michigan;
Scott E. Shewbridge, Scott Shewbridge Associates;
Alan Kropp, Alan Kropp and Associates;
and Matthew Homolka, CH2M Hill

## CONTENTS



ABSTRACT

After the 1989 Loma Prieta earthquake, we conducted cone-penetration tests (CPT's), flat-plate-dilatometer tests (DMT's), and seismic cone-penetration tests (SCPT's) at saturated-sand sites in Santa Cruz and on Treasure Island. Tests were performed both at sites with surface evidence of liquefaction and at sites without such evidence. Tests on Treasure Island confirmed existing CPT, DMT, and shear-wave-velocity liquefaction criteria in the cyclic-stress-ratio range from 0.1 to 0.2. In Santa Cruz, where cyclic-stress ratios were estimated to range from 0.3 to 0.6, surface evidence of liquefaction was absent when the ratio of the thickness of a liquefiable layer to its center depth ($t/z$) was less than 0.4. DMT material-index values, however, suggest that fines content may also have played a role in limiting liquefaction at some sites. Nevertheless, considering $t/z$ ratios, liquefaction evidence appears to confirm the most recent DMT-based criteria, whereas current shear-wave-velocity criteria may require further evaluation.

## INTRODUCTION

The 1989 Loma Prieta earthquake resulted in significant liquefaction of cohesionless soil as far as 120 km from the epicenter, which was located in the Santa Cruz Mountains approximately 15 km northeast of Santa Cruz, Calif. (fig. 1). Although the earthquake caused widespread liquefaction in Santa Cruz, it also caused significant, if not major, damage nearly 100 km to the north in San Francisco, most notably in the Marina District and on Treasure Island (fig. 1). Liquefaction also occurred along the coastal areas of Oakland and the Alameda, as well as along the Pacific Coast from the Marin Peninsula to Monterey Bay.

Because of the earthquake's relatively large size and its far-reaching effects, it has provided an excellent opportunity to evaluate existing in-situ-test-based liquefaction criteria over a wide range of ground motions. This paper summarizes the results of postearthquake cone-penetration tests (CPT's), flat-plate-dilatometer tests (DMT's), and seismic cone-penetration tests (SCPT's) in Santa Cruz and on Treasure Island that were performed during June 1991 by the University of Michigan.

## SANTA CRUZ

### GROUND MOTIONS

Ground motions in Santa Cruz were measured at the University of California, Santa Cruz, Lick Observatory in a one-story building founded on limestone rock (sta. 135, fig. 1). The station, located 16 km due west of the epicenter, registered peak accelerations of 0.44 and 0.47 $g$ in the horizontal directions and 0.40 $g$ in the vertical direction. Because the recording station is on rock, ground motions on the alluvial deposits of the San Lorenzo River in which liquefaction occurred could have been greater or smaller,

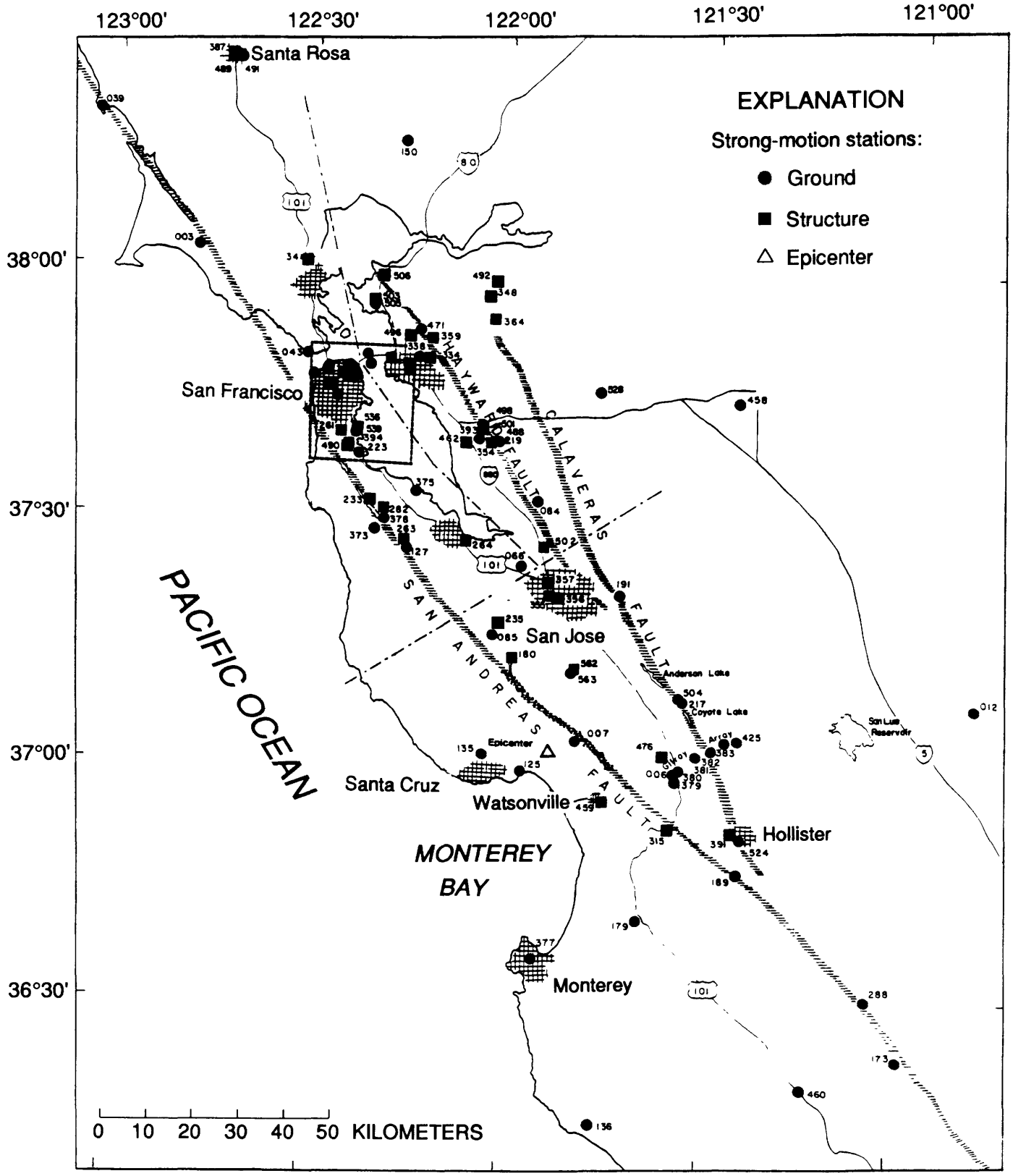


Figure 1.—San Francisco Bay region, showing locations of epicenter of 1989 Loma Prieta earthquake and strong-motion-recording stations maintained by California Division of Mines and Geology's California Strong Motion Instrumentation Program. From Shakal and others (1989).

owing to site effects. The station in nearby Capitola (sta. 125, fig. 1) is at an epicentral distance of 9 km and is located on alluvium. Peak accelerations measured at Capitola were 0.47 and 0.54 *g* in the horizontal directions and 0.60 *g* in the vertical direction. The Santa Cruz liquefaction sites were at distances of 11 to 12 km southwest of the epicenter. Thus, it is reasonable to assume that the peak accelerations on solid ground near liquefaction sites in Santa Cruz ranged from 0.47 to 0.54 *g*; we used 0.50 *g* in our analysis.

### LIQUEFACTION FEATURES AT TEST SITES

Kropp and Thomas (1991) performed detailed mapping of ground-failure features in downtown Santa Cruz on October 18, 19, and 20, 1989. By October 21 and 22, heavy rains had obscured much of the ground failure evidence. The locations of ground-failure features, mostly along San Lorenzo Creek are shown in figure 2. Note that the investigation and mapping were conducted after at least one tidal fluctuation in the San Lorenzo River. Therefore, more sand boils and lateral spreads probably formed in the immediate river channel than are shown in figure 2.

Liquefaction from the earthquake occurred primarily within an area of undifferentiated Holocene alluvial deposits previously mapped by Dupré (1975) and Brabb (1986) (fig. 3). The city of Santa Cruz had previously classified these deposits as having a high liquefaction susceptibility (fig. 4). Kropp and Thomas (1991) compared the observed damage features after the earthquake with Dupré's mapping and found that the area in which liquefaction had actually occurred in 1989 was included within Dupré's area of predicted high liquefaction susceptibility.

Nonetheless, liquefaction features were absent in a significant part of zone A in figure 4. Therefore, in our investigation, we conducted tests both at sites where liquefaction was observed and at sites where no evidence of liquefaction was observed (fig. 5). Liquefaction was confirmed at sites SC03 and SC14 by sand boils. At site SC02, lateral spreading had been reported. At the other three test sites (SC04, SC05, SC13), no clear evidence of liquefaction was observed. DMT's and SCPT's were performed at each site approximately 2 m apart.

## TREASURE ISLAND

### SOIL STRATIGRAPHY

Treasure Island is a 1.6 $km^2$-area manmade island immediately northwest of Yerba Buena Island in San Francisco Bay (fig. 6). Treasure Island was constructed in 1936–37 by hydraulic and clamshell dredging; details of its construction were reported by Lee (1969), who indicated that a perimeter rock dike was built in two to four stages on a bed of coarse sand placed over young bay mud. This dike acted as a retaining system for the sand that was pumped or placed inside. The structure is thus essentially an upstream-constructed hydraulic fill.

The soils at Treasure Island can be grouped into four categories: fill, native shoal sand, young bay mud, and old bay mud. Both the fill and the native shoal sand consist predominantly of sand containing varying amounts of gravel, silt, and clay. Our study confirms an earlier effort by Shewbridge and others (1990), who reported that the fill is somewhat looser and locally has a lower cone-tip resistance ($q_c$) than the native shoal sand. Typical $q_c$ values for the fill range from 10 to 50 kg/$cm^2$, and for the native shoal sand typically from 40 to 100 kg/$cm^2$. The young bay mud is a relatively soft, medium-plastic, silty clay (Shewbridge and others, 1990) with $q_c$ values increasing with depth and ranging from 8 to 14 kg/$cm^2$; its cone-friction ratio is about 1 percent. At the southeast end of the island, nearest to Yerba Buena Island, the deposits include a mixture of young bay mud interbedded with sand. Much stiffer sandy or silty clay of Pleistocene age underlies the young bay mud.

The depth and thickness of the soils vary significantly throughout the island. Shewbridge and others (1990) reported that the fill and native shoal sand range in thickness from less than 10 m at the south end to more than 15 m in the north. The young bay mud begins at about 10-m depth in the south and extends to only about 15-m depth. At the southeast corner of the island, however, the soils, which include both young bay mud and interlayered sand, extend to 35-m depth. The young bay mud extends from 14–17-m depth in the north to 21-m depth at the northeast corner and 49-m depth at the west corner of the island. The thicknesses of the fill and native shoal sand at each test site on Treasure Island are listed in table 1.

### GROUND MOTION

The strong-motion-recording seismographs on Treasure Island (sta. 117, fig. 6) and Yerba Buena Island (sta. 163, fig. 6) are both located on the floors of small one-story buildings, at epicentral distances of 98 and 95 km, respectively. Peak accelerations in the east-west direction were 0.16 *g* on Treasure Island and 0.06 *g* on Yerba Buena Island. In the north-south direction, peak accelerations were smaller: 0.11 *g* on Treasure Island and 0.03 *g* on Yerba Buena Island.

Idriss (1990) and Hryciw and others (1991) showed that the computer model *SHAKE90* (Schnabel and others, 1972) predicts the amplification of ground motions on Treasure Island reasonably well when the Yerba Buena

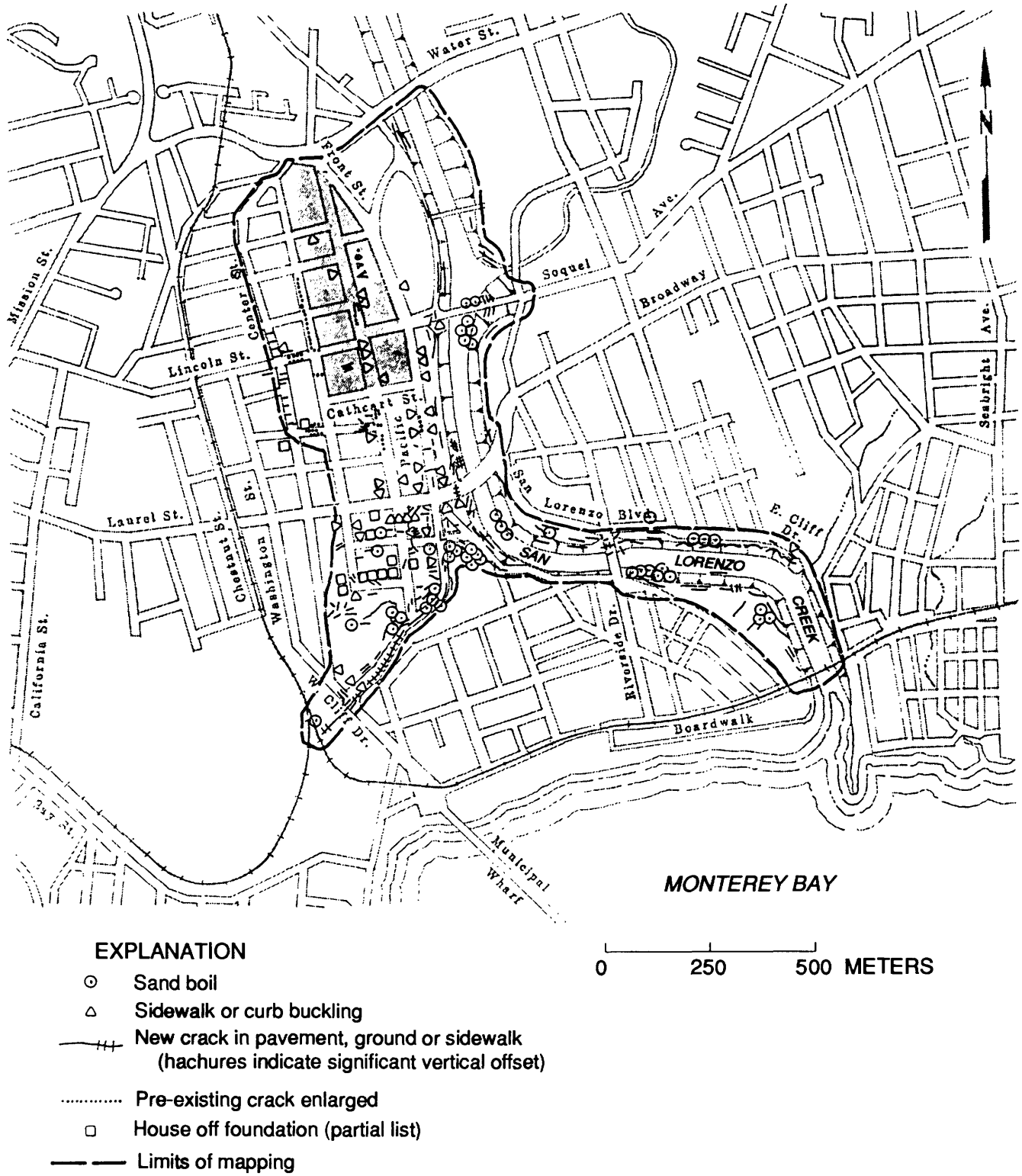


Figure 2.—Downtown Santa Cruz, showing locations where surface evidence of liquefaction was observed after earthquake. From Kropp and Thomas (1991).

Island time history is used as the base rock input motion. The program *SHAKE90* assumes an equivalent linear soil response; dynamic soil properties are iteratively adjusted until they are compatible with the computed cyclic strain. We used the data of Seed and others (1986) for the variations in normalized shear modulus and damping with shear strain for the fill, and the information of Lodde (1982) for the young bay mud and old bay mud.

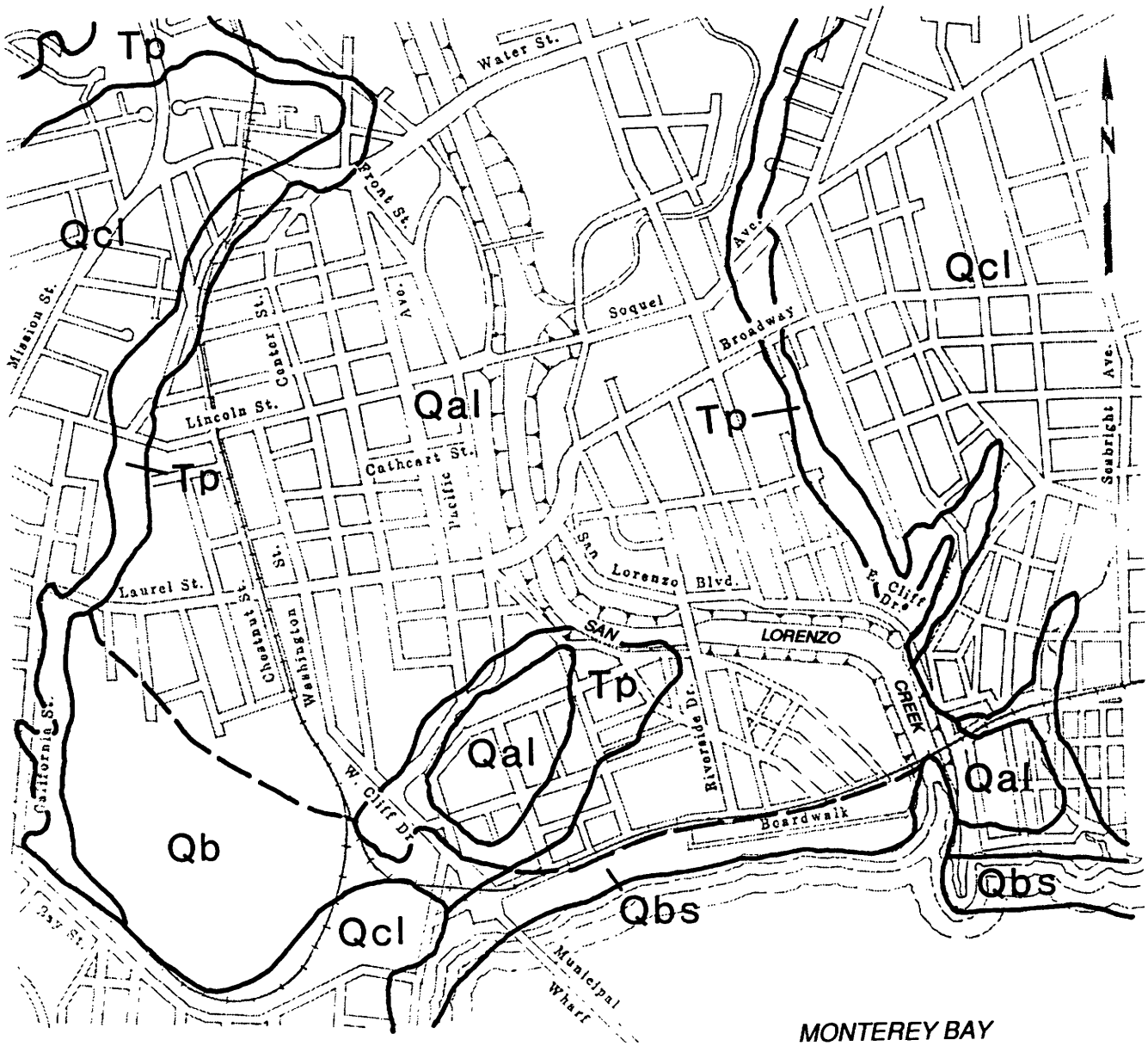


Figure 3.—Geologic map of downtown Santa Cruz. After Dupré (1975) and Brabb (1986).

On the basis of the soil stratigraphy and shear-wave velocities that we measured at various sites on Treasure Island, we used the program *SHAKE90* to compute the peak accelerations at all test sites. Complete details of the *SHAKE90* analyses, including input parameters, were provided by Rollins and others (1994). The computed peak accelerations are summarized in table 1. The differences in stratigraphy around the island clearly resulted in different computed ground motions. The peak accelerations in the east-west direction ranged from 0.13*g* at site UM03 to 0.20 *g* at site UM09 (fig. 7).

## LIQUEFACTION FEATURES AT TEST SITES

Shewbridge and others (1990) performed an extensive postearthquake assessment of damage to the retaining system on Treasure Island. Seed and others (1990) discussed

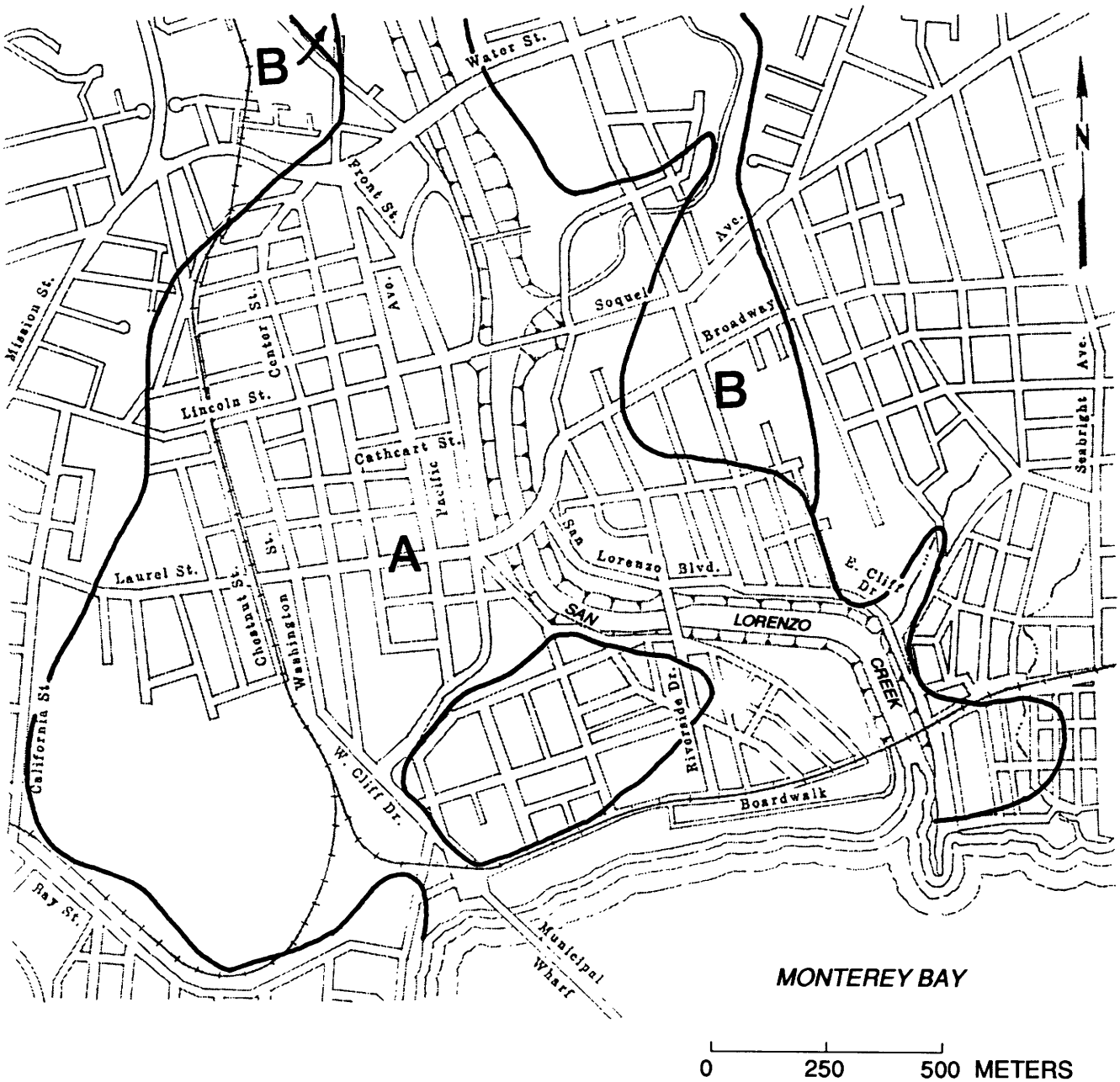


Figure 4.—Downtown Santa Cruz, showing zones of high (A) and moderately high (B) liquefaction susceptibility. From City of Santa Cruz (1976).

damage in the interior of the island. Damage features to the levee system included lateral spreads, slope failures, pavement cracking and collapse, and soil settlement. Evidence of soil liquefaction was pervasive on the interior of the island, and numerous large sand boils were observed. Settlements of as much as 30 cm occurred, accompanied by numerous pipe breaks and water ponding at the surface.

The best performance of the retaining systems was on the west and north sides of the island. No damage was evident at site UM03 (fig. 7), although some liquefaction did occur in adjacent inland areas and a large slump of the retaining system occurred northeast of site UM03. As much as 9 cm of vertical settlement was observed adjacent to a building approximately 60 m inland from site UM09. At site UM05, some 9 cm of horizontal dis-

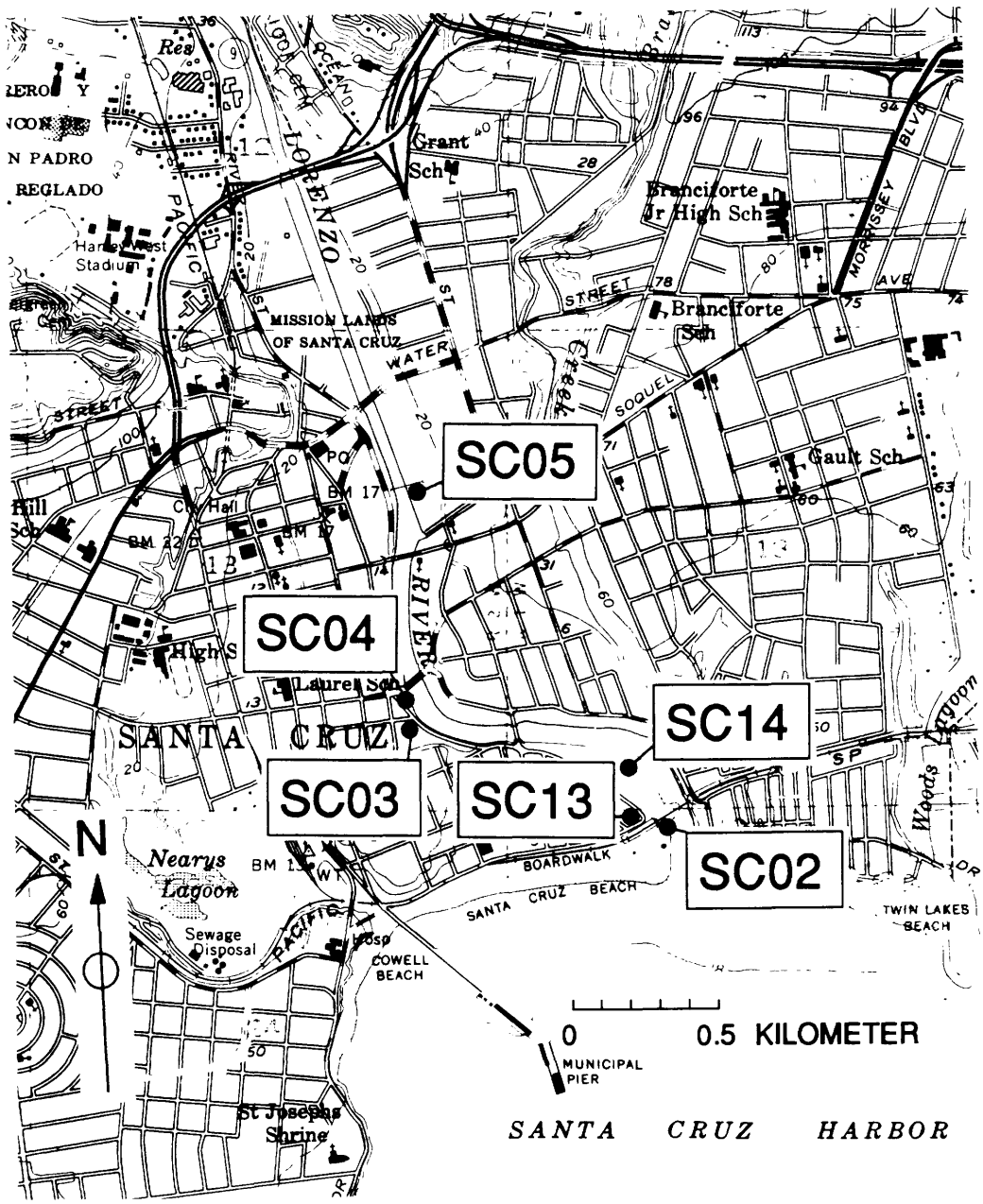


Figure 5.—Santa Cruz, showing locations of test sites.

placement of the soil was observed. In addition, 5 cm of vertical settlement was observed 30 m away. At site UM06, sand boils and 12 to 15 cm of horizontal movement of the levee were observed. Liquefaction was observed at site UM11; however, soils in an area immediately south of site UM11 has been improved by vibroflotation and were undamaged. We were unable to perform any tests in this area.

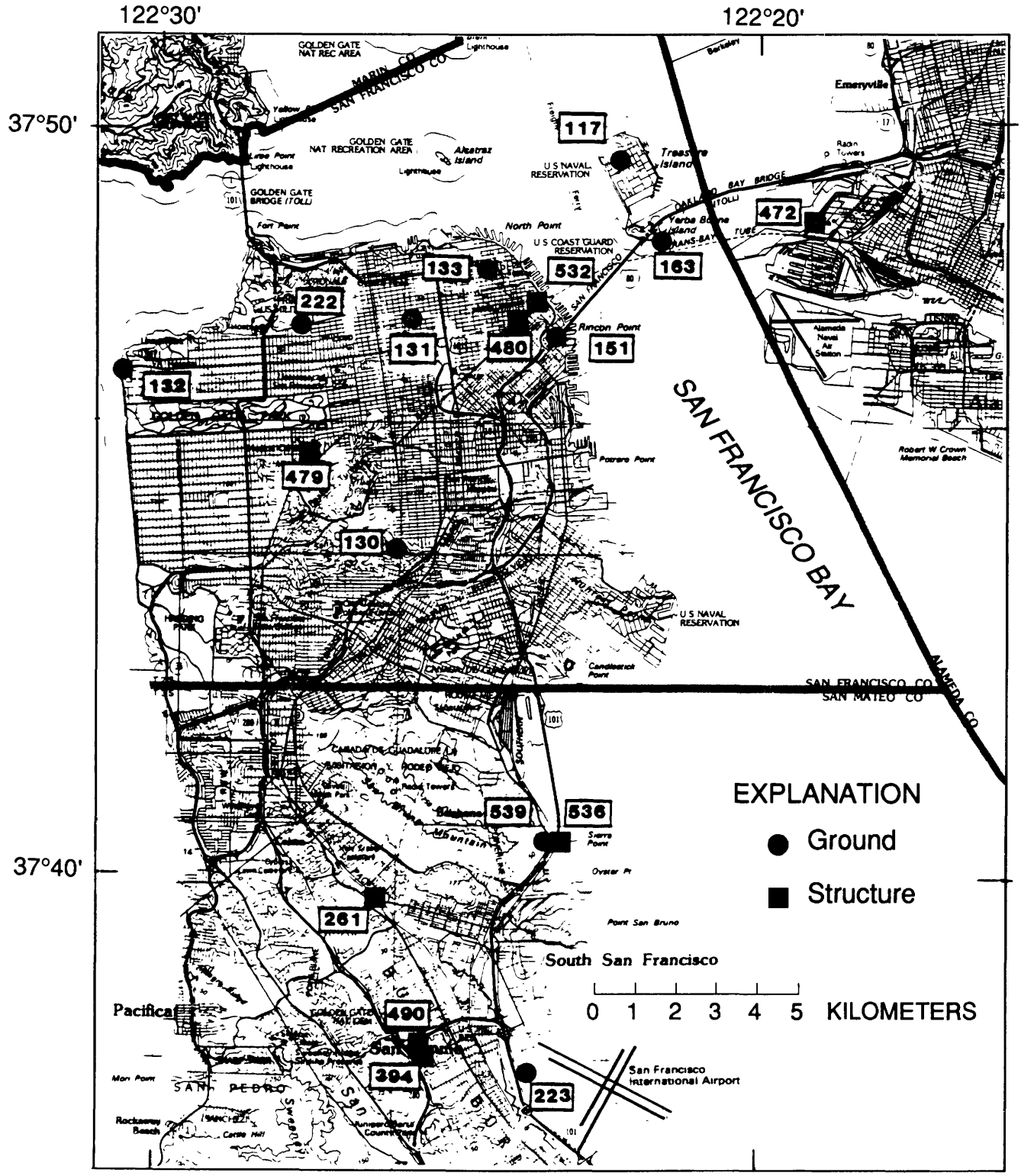


Figure 6.—San Francisco area, showing locations of strong-motion-recording stations maintained by California Division of Mines and Geology's California Strong Motion Instrumentation Program. From Shakal and others (1989).

Table 1.—*Thicknesses of fill and native shoal sand and computed peak accelerations on Treasure Island*

| Test site | Thickness (m) | Computed Peak Acceleration | |
|---|---|---|---|
| | | East-West Component (*g*) | North-South Component (*g*) |
| UM03 | 15.5 | 0.13 | 0.06 |
| UM05 | 11.9 | .19 | .07 |
| UM06 | 14.6 | .17 | .08 |
| UM09 | 9.3 | .20 | .09 |
| UM11 | 14.1 | .16 | .07 |
| Recorded | 11.7 | .16 | .11 |

## ONSITE TESTING FOR ASSESSMENT OF LIQUEFACTION SUSCEPTIBILITY

Although the liquefaction susceptibility of a site is most commonly evaluated by standard penetration test (SPT) (for example, Seed and Idriss, 1971; Seed and de Alba, 1986), the test's inherent shortcomings, which include discontinuous profiling, operator sensitivity, and nonstandardization, has motivated the development of other onsite tests for assessing liquefaction susceptibility, including CPT's, DMT's, and SCPT's.

The electronic CPT, which provides a nearly continuous profile of soil stratigraphy, is more repeatable than the SPT and is relatively operator independent. Although a sample is not retrieved in the CPT, the combination of tip resistance and friction ratio may provide an estimate of the grain size. Early efforts to establish CPT-based liquefaction criteria were based on correlations with existing SPT-based criteria; more recent efforts have sought relations independent of the SPT (Ishihara, 1985; Robertson and Campanella, 1985; Seed and de Alba, 1986; and Tseng, 1990).

For an assessment of liquefaction susceptibility, the cyclic-stress ratio required to cause liquefaction is compared with the modified cone-tip resistance, $q_{c1}$, where $q_{c1}$ is the tip resistance corrected to an effective overburden pressure of 1.0 kg/cm$^2$. "Cyclic-stress ratio" is defined as the ratio of cyclic shearing stress, $\tau$, to effective overburden pressure, $\sigma_v'$. Procedures for determining $\tau$ from earthquake accelerations are identical to those followed for the SPT, as reported by Seed and Idriss (1971). A peak acceleration of 0.50 *g* was used for Santa Cruz, and the larger of the peak accelerations listed in table 1 was used for each test site on Treasure Island.

The DMT is a more recently developed tool for geotechnical investigations (Marchetti, 1980). Through a series of empirical and semiempirical relation, the DMT provides soil strengths, compressibilities, in-situ stresses, and material identification. The DMT horizontal-stress index, $K_D$, has been related to liquefaction susceptibility (Marchetti, 1982; Robertson and Campanella, 1986; Reyna and Chameau, 1991). In the CPT, the $q_c$ value depends somewhat on the soil conditions to several cone diameters below and above the advancing tip. In contrast, DMT's are conducted at discrete test depths, and so the $K_D$ value is not so sensitive to conditions above and below the test depth. As such, the DMT is less prone to "vertical smear"

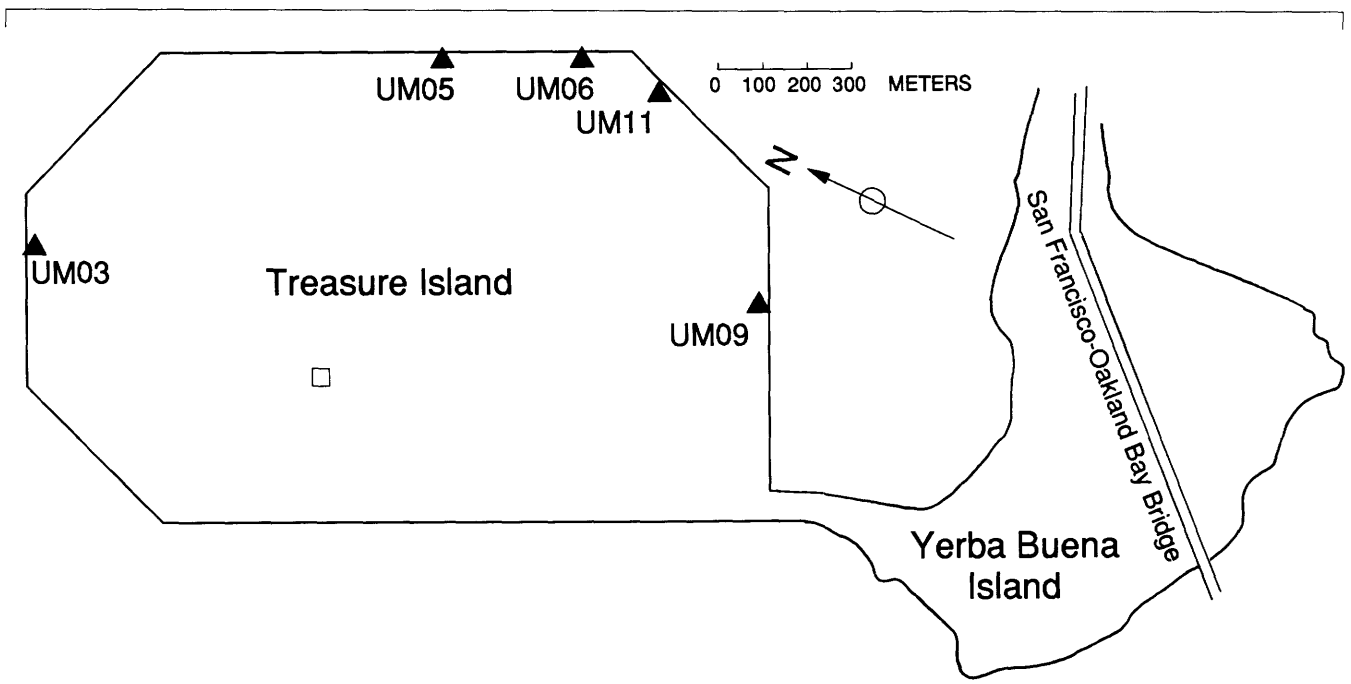


Figure 7.—Sketch map of Yerba Buena Island and Treasure Island, showing locations of test sites.

of the data and thus may afford better resolution of anomalous strata, such as loose and liquefiable sand seams. The DMT material index, $I_D$, may well be a better indicator of soil type than CPT-based relations.

Because liquefaction susceptibility is known to be a function of the same parameters that control seismic-wave-propagation velocity, including confining stress, density, stress history, aging, and cementation, attempts have also been made to correlate the cyclic-stress ratio for liquefaction with the normalized shear-wave velocity, $V_{s1}$ (Andrus and others, 1991; Finn, 1991; Robertson and others 1992). Finn (1991) and Robertson and others (1992) defined the normalized shear-wave velocity as $V_{s1}=V_s(P_a/\sigma_v')^{0.25}$, where $P_a$ is a reference pressure of 100 kPa. One drawback of the shear-wave velocity is that soil type is not easily determined. However, with the advent of the SCPT (Robertson and Campanella, 1986), both $q_{c1}$ and $V_{s1}$ may be determined simultaneously. Earlier, Bierschwale and Stokoe (1984) attempted to relate shear-wave velocities to liquefaction susceptibility on the basis of the Imperial Valley earthquakes of 1979 and 1981; however, because these earthquakes were of $M$=6.5 and 5.6, respectively, the results could not be applied to Loma Prieta studies.

## TEST RESULTS

After the 1989 Loma Prieta earthquake, CPT's, DMT's and SCPT's were conducted at six sites in Santa Cruz (fig. 5) and at five sites on Treasure Island (fig. 7). The complete reduced test results at each site, along with the local liquefaction evidence, estimate peak acceleration, ground-water table, and computed cyclic-stress ratios, were reported by Hryciw (1991).

At each test site, potentially liquefiable layers were identified; the data for these layers in Santa Cruz and on Treasure Island are summarized in tables 2 and 3, respectively. We note some variations in layer identification by the three tests. The data listed in tables 2 and 3 are also plotted in figures 8 through 10 for Santa Cruz and in figures 11 through 13 for Treasure Island, for comparison with existing liquefaction criteria by DMT, CPT, and shear-wave-velocity measurements.

The soil stratigraphies in Santa Cruz and on Treasure Island differ significantly. Whereas the fill on Treasure Island is relatively clean, uniform, and continuous, natural alluvial deposition in Santa Cruz has created highly stratified, inhomogeneous soil conditions, commonly with sandy-silt and silty-sand and even clayey-silt layers and lenses. Thus, whereas on Treasure Island soil liquefaction was clearly evident at the ground surface, in Santa Cruz sand-boil formation could have been hindered by fines, stratification, or nonliquefiable surface layers.

For ground failure to occur, the liquefiable layer must be either close to the surface or sufficiently thick to be significant. If $t$ is the layer thickness and $z$ is the depth to the center of the layer, then $t/z$ may serve as an index of the probability that subsurface liquefaction would cause ground damage. The $t/z$ ratio has an upper limit of 2.0, which occurs when the top of the liquefiable layer coincides with the ground surface and the water table is also at the surface.

In figures 8 through 13, the $t/z$ ratio is given for each data point. The $t/z$<0.1 criterion provides an intuitively logical first test by which to eliminate probably inconsequential layers from consideration.

For Treasure Island, the $t/z$ ratio is not so meaningful a parameter because the layers listed in table 3 generally represent small to moderate variations in $q_c$, $K_d$, or $V_{s1}$ rather than significant layering. In most places on Treasure Island, several successive layers are likely to be liquefiable, and so the $t/z$ ratio as an indicator of sand-boil formation loses its meaning.

The estimated cyclic-stress ratio is plotted against the normalized cone-tip resistance, $q_{c1}$, for the test sites in Santa Cruz in figure 8. On the basis of liquefaction criteria, liquefaction or, at least, cyclic mobilization should have occurred at all six test sites; however, no surface evidence of liquefaction was observed at site SC04, SC05, or SC13 (fig. 5). The liquefiable layers at these three test sites are generally characterized by $t/z$<0.40. Conversely, at the three sites where sand boils formed, the maximum $t/z$ ratios were 0.40, 0.75, and 0.77.

Ishihara (1985) studied the effects of nonliquefiable surface layers. He suggested that the ground damage at sites with nonliquefiable surface layers is also related to the peak accelerations. Ishihara compared the thickness of the liquefiable layer with that of the surface layer, as shown in figure 14, rather than using a $t/z$ ratio. Nevertheless, the $t/z$ ratio is easily convertible to Ishihara's approach, as shown in figure 14. The test data for Santa Cruz are also plotted in figure 14. We note that the observed $t/z$=0.4 threshold for ground damage corresponds to a suggested peak acceleration slightly smaller than that believed to have occurred in Santa Cruz. Therefore, an upward shift of the lower part of Ishihara's 0.4- to 0.5-$g$ line may be warranted.

The $K_D$-based data for the test sites in Santa Cruz are plotted in figure 9. Considering the low $t/z$=0.13 of the outlying point for site SC13 and the fact that the higher-$K_D$ layer at site SC02 is not a critical layer, both the criteria of Marchetti (1982) and Reyna and Chameau (1991) appear to have performed well in the cyclic-stress range 0.35–0.60. Although the criterion of Robertson and Campanella (1985) appears to be somewhat conservative, we again emphasize that the absence of ground damage does not exclude the possibility of subsurface liquefaction.

An alternative explanation for the data plotted in figure 9 is grain size. The average DMT material-index ($I_D$ )

Table 2.—*Summary of cone-penetration tests (CPT's), flat-plate-dilameter tests (DMT's), and shear wave velocities at test sites in Santa Cruz*

[CSR, cyclic-stress ratio; GWT, ground-water table. Values in parentheses indicate layers with a thickness less than 10 percent of their center depth]

| Test site (fig. 5) | GWT (m) | Ground failure | CPT | | | DMT | | | Shear-wave-velocity | | |
|---|---|---|---|---|---|---|---|---|---|---|---|
| | | | Depth (m) | $q_{c1}$ (kg/cm$^2$) | CSR | Depth (m) | $K_D$ | CSR | Depth (m) | $V_{s1}$ (m/s) | CSR |
| SC01 | 1 | yes | 2.0-3.0 | 75 | 0.53 | 2.4-2.7 | 5.46 | 0.54 | 1.0-2.7 | 140 | 0.50 |
| | | | 3.8-4.6 | 40 | .59 | 4.1-4.7 | 3.80 | .59 | 4.3-4.9 | 104 | .59 |
| SC03 | 2.1 | yes | 2.0-2.4 | 88 | .38 | 2.9-3.5 | 2.76 | .38 | 3.5-4.0 | 118 | .41 |
| | | | (5.3.5.7) | 80 | .46 | (5.3-5.8) | 3.38 | .46 | (6.4-6.7) | 97 | .48 |
| | | | (6.3-6.5) | 68 | .48 | (6.5-7.2) | 1.94 | .49 | --- | --- | --- |
| SC04 | 1.8 | no | 2.0-2.9 | 101 | .33 | --- | --- | --- | 2.1-2.9 | 120 | .33 |
| | | | 3.0-4.2 | 125 | .40 | --- | --- | --- | --- | --- | --- |
| SC05 | 2.8 | no | 3.0-4.2 | 82 | .38 | 3.0-4.1 | 6.80 | .37 | 3.0-4.6 | 146 | .40 |
| | | | 4.2-4.7 | 51 | .41 | 4.2-4.8 | 9.17 | .41 | --- | --- | --- |
| | | | 5.2-6.0 | 180 | .44 | --- | --- | --- | --- | --- | --- |
| SC13 | 1.8 | no | 2.0-2.7 | 54 | .36 | 1.8-3.1 | 4.20 | .37 | 1.8-2.8 | 130 | .36 |
| | | | 3.3-5.0 | 174 | .46 | (3.1-3.4) | 8.40 | .42 | 2.8-3.4 | 167 | .41 |
| | | | 5.6-7.0 | 155 | .50 | 3.5-4.0 | 2.70 | .45 | (4.6-4.9) | 123 | .47 |
| | | | --- | --- | --- | 7.0-7.8 | 7.00 | .55 | --- | --- | --- |
| SC14 | 1.2 | yes | 1.2-2.7 | 50 | .42 | 1.2-2.7 | 3.10 | .42 | 1.5-3.0 | 153 | .44 |
| | | | --- | --- | --- | (4.1-4.5) | 1.92 | .54 | (3.7-4.0) | 129 | .52 |
| | | | --- | --- | --- | --- | --- | --- | (6.2-6.5) | 104 | .57 |

Table 3.—*Summary of cone-penetration tests (CPT's), flat-plate-dilatometer tests (DMT's), and shear-wave velocities at test sites on Treasure Island*

[CSR, cyclic-stress ratio; GWT, ground-water table. Values in parentheses indicate layers with a thickness less than 10 percent of their center depth]

| Test site (fig. 7) | GWT (m) | Ground failure | CPT | | | DMT | | | Shear-wave-velocity | | |
|---|---|---|---|---|---|---|---|---|---|---|---|
| | | | Depth (m) | $q_{c1}$ (kg/cm$^2$) | CSR | Depth (m) | $K_D$ | CSR | Depth (m) | $V_{s1}$ (m/s) | CSR |
| UM03 | 1.5 | no | 4.4-6.5 | 110 | 0.14 | 2.7-5.2 | 4.2 | 0.13 | 6.3-8.0 | 190 | 0.15 |
| | | | 6.5-8.2 | 62 | .15 | 9.0-11.0 | 3.4 | .15 | 8.7-11.7 | 169 | .15 |
| | | | 8.2-10.0 | 72 | .15 | 12.0-14.7 | 3.9 | .14 | 14.9-16.9 | 168 | .12 |
| | | | --- | --- | --- | 15.0-17.7 | 4.3 | .11 | --- | --- | --- |
| UM05 | 24 | yes | 3.5-4.7 | 77 | .15 | 3.9-4.5 | 3.4 | .15 | 2.2-3.1 | 95 | .13 |
| | | | 4.8-6.0 | 70 | .17 | 4.8-6.0 | 3.1 | .17 | 3.1-4.6 | 145 | .15 |
| | | | 6.0-8.0 | 60 | .18 | 6.3-7.4 | 3.5 | .18 | (5.2-5.5) | 170 | .17 |
| | | | --- | --- | --- | (7.9-8.4) | 3.7 | .19 | 5.5-8.3 | 183 | .18 |
| UM06 | 1.4 | yes | 2.0-4.0 | 36 | .16 | 5.7-7.2 | 3.5 | .19 | 2.9-3.7 | 95 | .14 |
| | | | 5.0-9.0 | 67 | .19 | --- | --- | --- | 3.7-8.0 | 200 | .18 |
| | | | --- | --- | --- | --- | ---- | --- | 8.0-10.4 | 160 | --- |
| UM09 | 2.7 | yes | 1.5-3.0 | 40 | .13 | 2.2-3.9 | 3.1 | .14 | 2.4-3.4 | 130 | .18 |
| | | | 4.0-5.7 | 43 | .17 | --- | --- | --- | 3.4-4.3 | 168 | .19 |
| | | | --- | --- | --- | --- | --- | --- | 4.3-4.9 | 245 | .20 |
| | | | --- | --- | --- | --- | --- | --- | 4.9-7.0 | 159 | .21 |
| UM11 | 1.4 | yes | 4.0-6.2 | 84 | .21 | (4.3-4.6) | 3.7 | .20 | 1.5-2.5 | 267 | .15 |
| | | | 7.0-7.7 | 73 | .22 | (6.8-7.2) | 4.1 | .22 | 2.5-3.0 | 167 | .17 |
| | | | --- | --- | --- | --- | --- | --- | 3.0-4.9 | 175 | .20 |
| | | | --- | --- | --- | --- | --- | --- | 4.9-7.0 | 191 | .21 |

values for the test sites without evidence of liquefaction (open symbols, fig. 9) are lower than for the test sites with evidence of liquefaction (solid symbols). For the test sites without evidence of liquefaction, representative $I_D$ values range from 2.0 to 4.3 and average 3.0; for the test sites with evidence of liquefaction, $I_D$ values range from 2.8 to 6.8 and average 4.3. Silty sand typically has an $I_D$ values of 1.8 to 3.4, whereas clean sand typically has an $I_D$ value greater than 3.3.

On the basis of existing shear-wave-velocity criteria, figure 10 predicts that liquefaction should have occurred at all the test sites in Santa Cruz. Nevertheless, we note that the data points corresponding to the test sites with surface evidence of liquefaction invariably plot closer, albeit at some distance, from the criteria of Finn (1991) and Robertson and others (1992).

For Treasure Island, the CPT-based criteria of Ishihara (1985) and Seed and de Alba (1986) correctly predict the field behavior, as shown in figure 11. The criterion of Robertson and Campanella (1985) is slightly overconservative in predicting liquefaction at site UM03 (fig. 7). The data for the test sites on Treasure Island also

show (fig. 12) that the DMT-based criterion of Marchetti (1982) seriously overpredicts the field performance at cyclic-stress ratios in the range 0.10–0.25. Both the criteria of Robertson and Campanella (1986) and Reyna and Chameau (1991) perform well in this range. According to figure 13, the shear-wave-velocity-based criteria of Finn (1991) and Robertson and others (1992) predict liquefaction on Treasure Island well.

The combined data for the test sites in Santa Cruz and on Treasure Island are plotted in figures 15 through 17; however, in these figures only the layers estimated to be most critical are represented. Again, we note that the fill on Treasure Island, represented by data points with cyclic-stress ratios less than 0.25, behaved as expected, with a reasonable agreement between the conclusions from the CPT, DMT, and shear-wave-velocity results. The notable exception was the $K_D$-based criterion of Marchetti (1982). For the test sites in Santa Cruz (cyclic-stress ratios >0.3), when low $t/z$ ratios are accounted for, the CPT-based criteria (fig. 15) appear to be reasonable. The DMT-based criterion of Reyna and Chameau (1991) (fig. 15) appears to improve on Robertson and Campanella's (1986) more conservative recommendations. The shear-wave-velocity results for the test sites in Santa Cruz remain somewhat inconsistent with field observations.

## SUMMARY AND CONCLUSIONS

We performed CPT, DMT, and SCPT tests in the aftermath of the 1989 Loma Prieta earthquake at sites in Santa Cruz and on Treasure Island. Our results, when correlated with the field performance on Treasure Island, verify the most recent CPT-, DMT-, and shear-wave-velocity-based liquefaction criteria in the cyclic-stress-ratio range 0.1–0.2.

For Santa Cruz, correlation of our results with field performance is more difficult, owing to soil stratification. On the basis of CPT results, it appears that when the ratio of layer thickness to center depth ($t/z$) was less than approximately 0.4, ground damage and the formation of surface liquefaction features did not occur, despite possible subsurface liquefaction. We also note that the material index averages 4.3 (suggesting clean sand) at test sites with surface evidence of liquefaction but only 3.0 (suggesting silty sand) at test sites with no surface evidence of liquefaction.

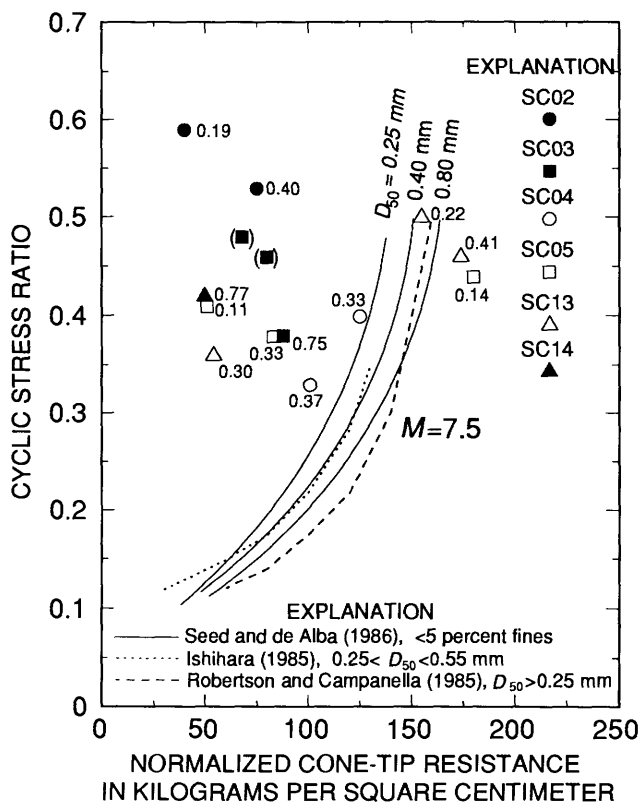


Figure 8.—Cone-penetration-test results at sites in Santa Cruz (see fig. 5 for locations). Solid data points denote sites with surface evidence of liquefaction. Values near data points indicate ratio of thickness of liquefiable layer to its center depth ($t/z$); data points in parentheses denote sites where $t/z$<0.1.

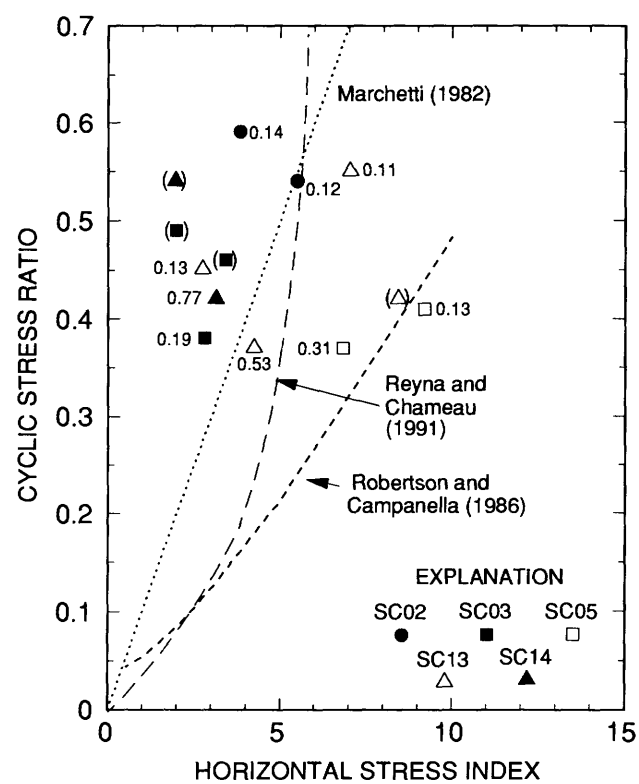


Figure 9.—Flat-plate-dilatometer-test results at sites in Santa Cruz (see fig. 5 for locations). Solid data points denote sites with surface evidence of liquefaction. Values near data points indicate ratio of thickness of liquefiable layer to its center depth ($t/z$); data points in parentheses denote sites where $t/z$<0.1.

The DMT-based criterion of Reyna and Chameau (1991) clearly improves on Marchetti's (1982) unconservative recommendations in the low-cyclic-stress-ratio range. Reyna and Chameau's criterion may also be an improvement over Robertson and Campanella's (1986) more conservative recommendations in the high-cyclic-stress-ratio range.

Although, CPT-, DMT-, and SCPT-based criteria for assessment of liquefaction susceptibility are not yet widely used, the resolution of liquefiable strata by these tests is much better than by the SPT. Future assessments of liquefaction susceptibility must rely more heavily on these techniques.

## ACKNOWLEDGMENTS

This research was supported by U.S. Geologic Survey research grant DOI–G–14–08–0001–G1985 and National Science Foundation grants NSF–9011121 and NSF–CES–8807134 to the University of Michigan. We thank John A. Debecker of the Western Division, U.S. Naval Facilities Engineering Command and his staff for their support and assistance with our testing on Treasure Island. We appreciate the assistance of Geomatrix Consultants, Inc., of San Francisco. The test sites in Santa Cruz were selected with the assistance of Alan Kropp and Associates. Brian Evers and other city of Santa Cruz officials encouraged our study. Kevin Schmidt assisted with test-vehicle operation both in Santa Cruz and on Treasure Island.

## REFERENCES CITED

Andrus, R.D., Stokoe, K.H., II, and Roesset, J.M., 1991, Liquefaction of gravelly soil at Pence Ranch during the 1983 Borah Peak, Idaho earthquake: International Conference on Soil Dynamics and Earthquake Engineering, 5th, Karlsruhe, Germany, 1991, Proceedings, p. 251–262.

Bierschwale, J.G., and Stokoe, K.H., II 1984, Analytical evaluation of liquefaction potential of sands subjected to the 1981 Westmorland Earthquake: Austin, University of Texas, Civil Engineering Department Report GR–84–15.

Brabb, E.E., 1986, Preliminary geologic map of Santa Cruz County, California: U.S. Geological Survey Open-File Report 86–577, scale 1:62,500.

City of Santa Cruz, 1976, City of Santa Cruz general plans, seismic safety and safety elements: Santa Cruz, Calif., Planning Depart-

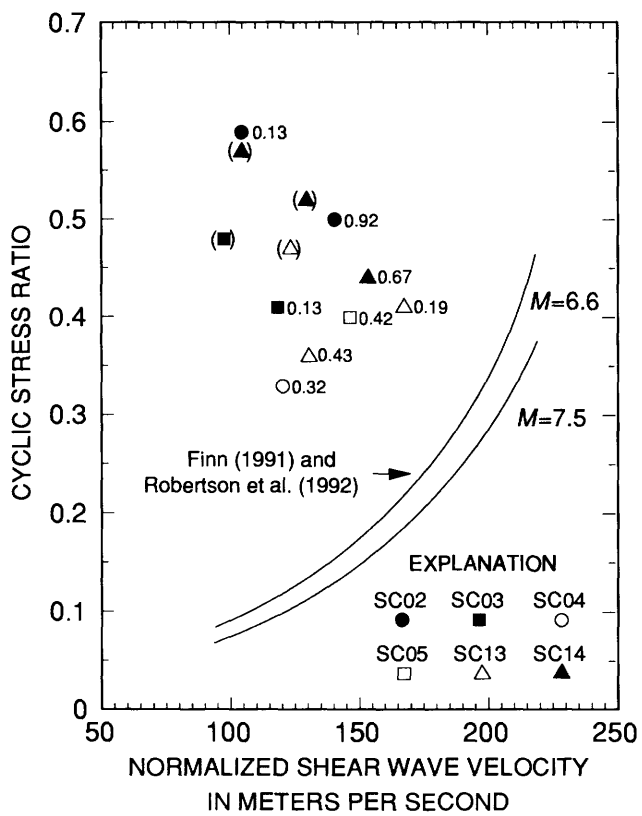


Figure 10.—Shear-wave-velocity results at sites in Santa Cruz (see fig. 5 for locations). Solid data points denote sites with surface evidence of liquefaction. Values near data points indicate ratio of thickness of liquefiable layer to its center depth ($t/z$); data points in parentheses denote sites where $t/z<0.1$.

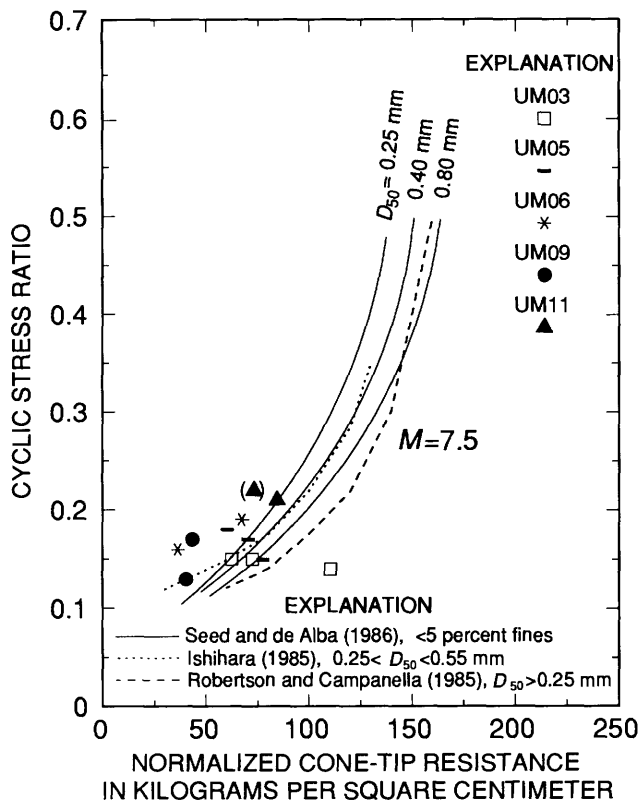


Figure 11.—Cone-penetration-test results at sites on Treasure Island (see fig. 7 for locations). Solid data points denote sites with surface evidence of liquefaction. Data point in parentheses denotes site where $t/z<0.1$.

ment.

Dupré, W.R., 1975, Maps showing geology and liquefaction potential of Quaternary deposits in Santa Cruz County, California: U.S. Geological Survey Miscellaneous Field Studies Map MF–648, scale 1:62,500.

Finn, W.D.L., 1991, Assessment of liquefaction potential and post-liquefaction behavior of earth structures: International Conference on Recent Advances in Geotechnical Earthquake Engineering and Soil Dynamics, 2d, St. Louis, Mo., 1991, Proceedings, p. 1833–1850.

Hryciw, R.D., 1991, Report on post Loma Prieta Earthquake CPT, DMT and shear wave velocity investigations of liquefaction sites in Santa Cruz and on Treasure Island: report to U.S. Geological Survey on grant 14–08–0001–G1865, 68 p.

Hryciw, R.D., Rollins, K.M., Homolka, Matthew, Shewbridge, S.E., and Mchood, M.D., 1991, Soil amplification at Treasure Island during the Loma Prieta earthquake: International Conference on Earthquake Engineering and Soil Dynamics, 2d, St. Louis, Mo., 1991, Proceedings, p. 1679–1685.

Idriss, I.M., 1990, Response of soft soil sites during earthquakes, in Proceedings, H. Bolton Seed Memorial Symposium: Berkeley, Calif., BiTech, v. 2, p. 273–289.

Ishihara, Kenji, 1985, Stability of natural deposits during earthquakes: International Conference on Soil Mechanics and Foundation Engineering, 11th, San Francisco, 1985, Proceedings, v. 1, p. 321–376.

Kropp, Alan, and Thomas, Michael, 1991, Ground failure in downtown Santa Cruz [Calif.]: International Conference on Earthquake Engineering and Soil Dynamics, 2d, St. Louis, Mo., 1991, Proceedings, v. 3, p. 226–229.

Lee, C.H., 1969, Treasure Island fill, case history 2 *of* Lee, C.H., and Praszker, Michael, Bay mud development and related structural foundations, *in* Goldman, H.B., ed., Geological and engineering aspects of San Francisco Bay fills: California Division of Mines and Geology Special Report 97, p. 69–72.

Lodde, P.F., 1982, Dynamic response of San Francisco Bay Mud: University of Texas, Austin, M.S. thesis.

Marchetti, Silvano, 1980, In-situ tests by flat dilatometer: American Society of Civil Engineers Proceedings, Geotechnical Engineering Division Journal, v. 106, no GT3, p. 299–321.

———Detection of liquefiable sand layers by means of quasi-static penetration tests: European Symposium on Penetration Testing, 2d, Amsterdam, 1982, Proceedings, p. 458–482.

Mitchell, J.K., and Tseng, D.-J., 1990, Assessment of liquefaction potential by cone penetration resistance, *in* Proceedings, H. Bolton Seed Memorial Symposium: Berkeley, Calif., BiTech, v. 2, p. 335–350.

Reyna, Fernando, and Chameau, J.L., 1991, Dilatometer based liquefaction potential of sites in the Imperial Valley [Calif.]: International Conference on Earthquake Engineering and Soil Dynamics, 2d, St. Louis, Mo., 1991, Proceedings, p. 385–392.

Robertson, P.K., and Campanella, R.G., 1985, Estimating liquefaction potential of sand using the flat dilatometer: American Society for Testing and Materials Geotechnical Testing Journal, v. 9, no. 1, p. 38–40.

———Liquefaction potential of sands using the CPT: Journal of Geotechnical Engineering, v. 111, no. 3, p. 384–403.

Robertson, P.K., Woeller, D.J., and Finn, W.D.L., 1992, Seismic cone penetration testing for evaluating liquefaction potential under cyclic loading: Canadian Geotechnical Journal, v. 29, no. 4, p. 686–695.

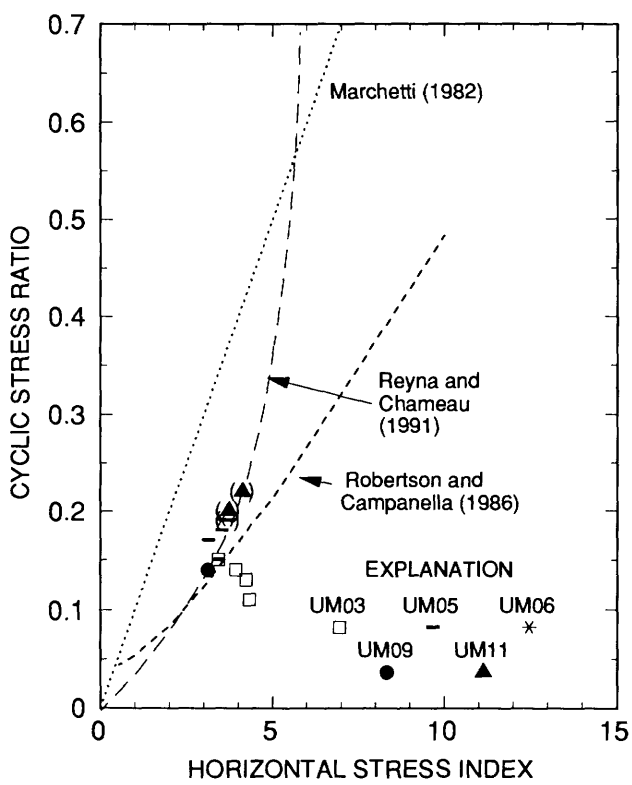


Figure 12.—Flat-plate-dilatometer-test results at sites on Treasure Island (see fig. 7 for locations). Solid data points denote sites with surface evidence of liquefaction. Data points in parentheses denote sites where $t/z<0.1$.

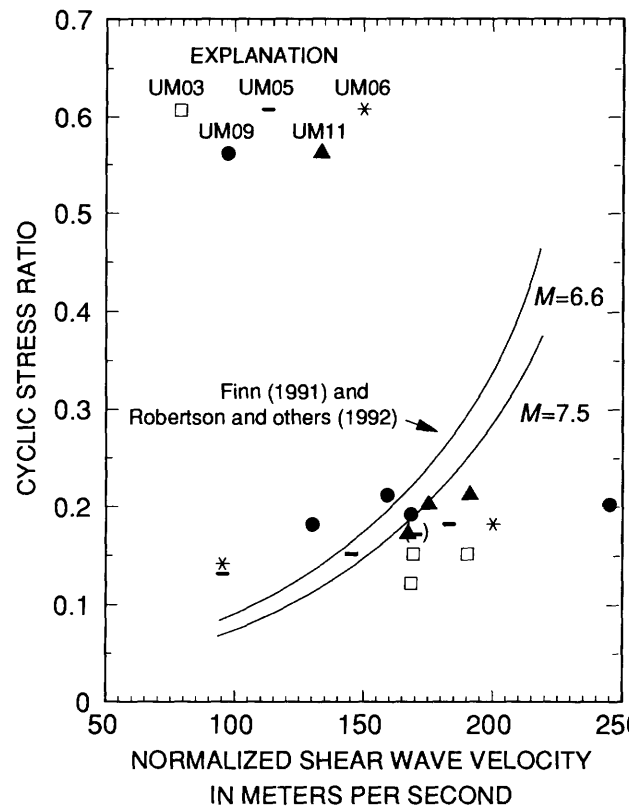


Figure 13.—Shear-wave-velocity results at sites on Treasure Island (see fig. 7 for locations). Solid data points denote sites with surface evidence of liquefaction. Data point in parentheses denotes site where $t/z<0.1$.

Rollins, K.M., McHood, M.D., Hryciw, R.D., Homolka, Matthew, and Shewbridge, S.E., 1994, Ground response on Treasure Island, *in* Borcherdt, R.D., ed., The Loma Prieta, California, earthquake of October 17, 1989—strong ground motion: U.S. Geological Survey Professional Paper 1551–A, p. A109–A121.

Schnabel, P.B., Lysmer, John, and Seed, H.B., 1972, SHAKE; computer program for earthquake response analysis of horizontally layered sites: Berkeley, University of California, Earthquake Engineering Research Center Report EERC 72–12, 88 p.

Seed, H.B., and de Alba, Pedro, 1986, Use of SPT and CPT tests for evaluating the liquefaction resistance of sands, in Clemence, S.P., ed., Proceedings of In Situ #86, a specialty conference; use of in situ tests in geotechnical engineering: American Society of Civil Engineers Geotechnical Special Publication 6, p. 281–302.

Seed, H.B. and Idriss, I.M., 1971, Simplified procedure for evaluating soil liquefaction potential: American Society of Civil Engineers Proceedings, Soil Mechanics and Foundations Division Journal, v. 97, no. SM9, p. 1249–1273.

Seed, H.B., Wong, R.T., Idriss, I.M., and Tokimatsu, Kohji, 1986, Moduli and damping factors for dynamic analyses of cohensionless soils: Journal of Geotechnical Engineering, v. 112, no. 11, p. 1016–1032.

Seed, R.B., Dickenson, S.E., Riemer, M.F., Bray, J.D., Sitar, Nicholas, Mitchell, J.K., Idriss, I.M., Kayen, R.E., Kropp, Alan, Harder, L.F., Jr., and Power, M.S., 1990, Preliminary report on the principal geotechnical aspects of the October 17, 1989 Loma Prieta earthquake: Berkeley, University of California, Earthquake Engineering Research Center Report, UCB/EERC–90/05, 137 p.

Shakal, A.F., Huang, M.J., Reichle, M.S., Ventura, C.E., Cao, T.Q., Sherburne, R.W., Savage, M.K., Darragh, R.B., and Peterson, C.P., 1989, CSMIP strong-motion records from the Santa Cruz Mountains (Loma Prieta), California earthquake of 17 October, 1989: California Division of Mines and Geology, Office of Strong Motion Studies Report OSMS 89–06, 196 p.

Shewbridge, S.,E., Power, M.S., and Basore, C., 1990, Perimeter dike stability evaluation, Naval Station Treasure Island: San Bruno, Calif., U.S. Navy, Naval Facilities Engineering Command, Western Division, 23 p.

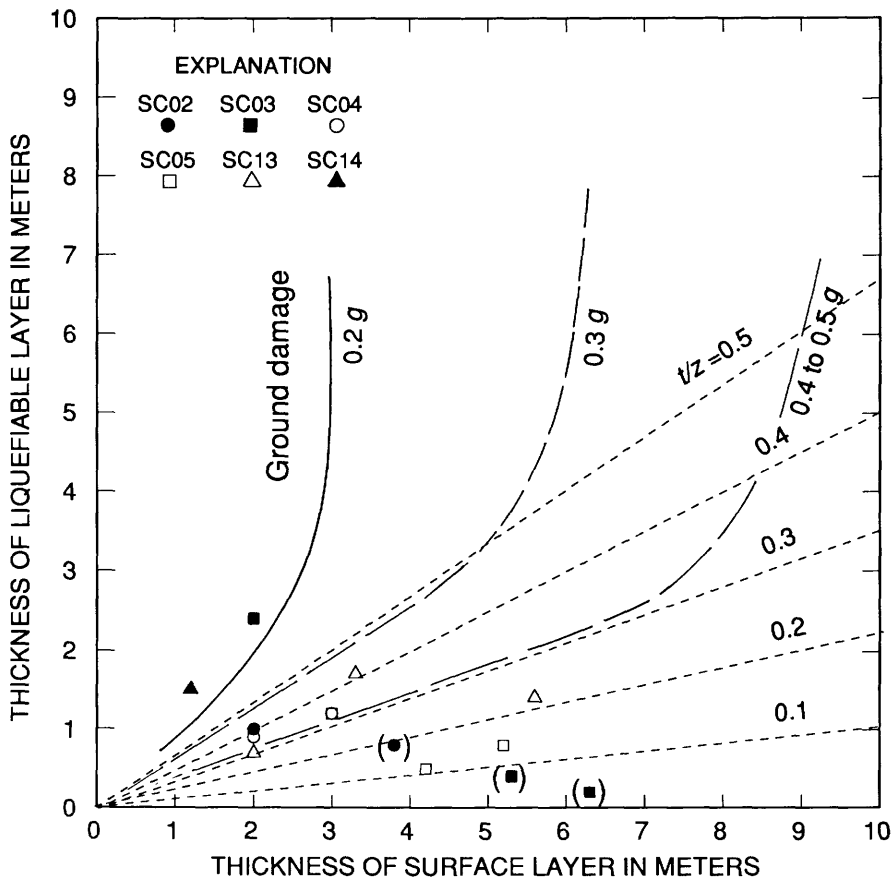


Figure 14.—Comparison of criterion of Ishihara (1985) for ground damage with observed *t*/*z* ratios at sites in Santa Cruz (fig. 5). Solid data points denote sites where ground damage occurred; data points in parentheses denote sites where ground damage was probably not attributable to secondary liquefiable layers. Three sloping curves illustrate approximate peak accelerations suggested by Ishihara.

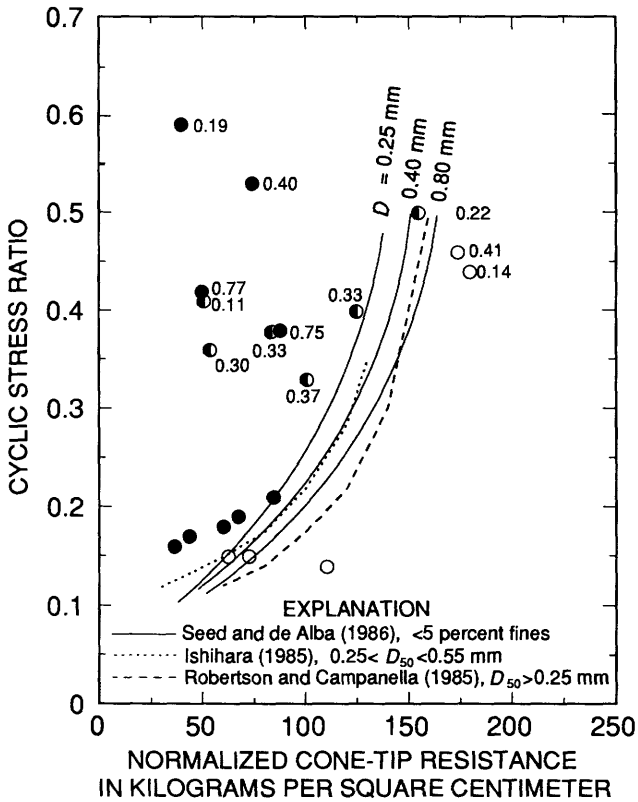


Figure 15.—Combined cone-penetration-test results (for critical layers only) at sites in Santa Cruz (fig. 5) and on Treasure Island (fig. 7). Values near data points indicate ratio of thickness of liquefiable layer to its center depth ($t/z$). Dots, sites with surface evidence of liquefaction; circles, sites with no surface evidence of liquefaction where $t/z>0.4$; half-solid circles, sites with no surface evidence of liquefaction where $t/z<0.4$. Data for sites in Santa Cruz where $t/z<0.1$ are omitted.

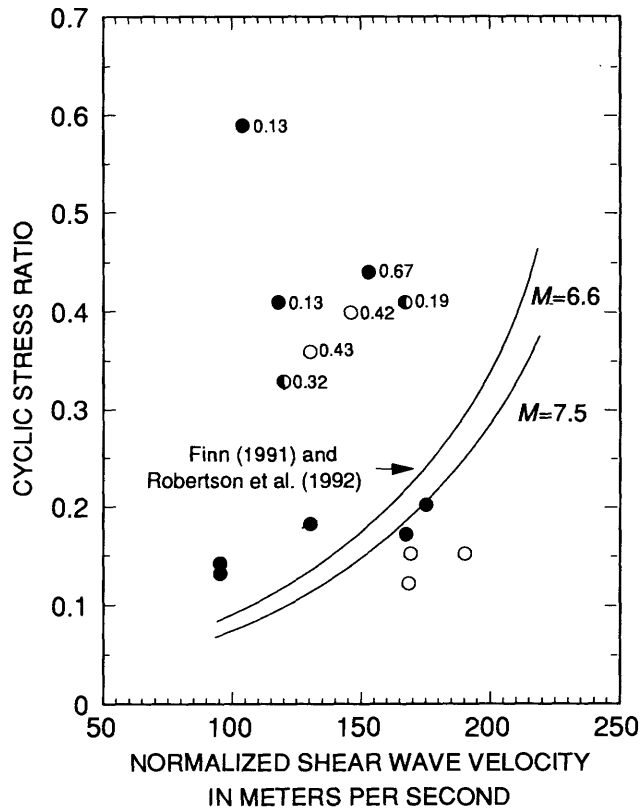


Figure 17.—Combined shear-wave-velocity results (for critical layers only) at sites in Santa Cruz (fig. 5) and on Treasure Island (fig. 7). Values near data points indicate ratio of thickness of liquefiable layer to its center depth ($t/z$). Dots, sites with surface evidence of liquefaction; circles, sites with no surface evidence of liquefaction where $t/z>0.4$; half-solid circles, sites with no surface evidence of liquefaction where $t/z<0.4$. Data for sites in Santa Cruz where $t/z<0.1$ are omitted.

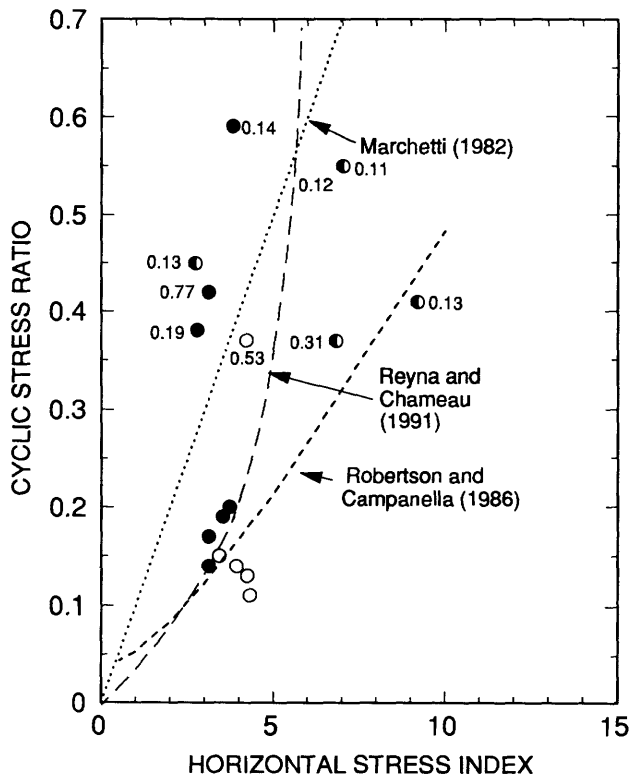


Figure 16.—Combined flat-plate-dilatometer-test results (for critical layers only) at sites in Santa Cruz (fig. 5) and on Treasure Island (fig. 7). Values near data points indicate ratio of thickness of liquefiable layer to its center depth ($t/z$). Dots, sites with surface evidence of liquefaction; circles, sites with no surface evidence of liquefaction where $t/z>0.4$; half-solid circles, sites with no surface evidence of liquefaction where $t/z<0.4$. Data for sites in Santa Cruz where $t/z<0.1$ are omitted.

THE LOMA PRIETA, CALIFORNIA, EARTHQUAKE OF OCTOBER 17, 1989:
LIQUEFACTION

STRONG GROUND MOTION AND GROUND FAILURE

# DIRECT MEASUREMENT OF LIQUEFACTION POTENTIAL IN SOILS OF MONTEREY COUNTY, CALIFORNIA

By Wayne A. Charlie, Donald O. Doehring, Jeffrey P. Brislawn, and Hassen Hassen,
Colorado State University

## CONTENTS



ABSTRACT

The Piezovane, invented at Colorado State University, is a vane-shear device equipped with a pressure transducer to measure changes in pore-water pressure so as to identify contractive and dilative soils. Contractive soils may undergo extensive lateral spreading and flow. Laboratory tests show that the Piezovane generates positive pore-water pressures in contractive soils and negative pressures in dilative soils. The advantage of the Piezovane is that it directly measures the soil property associated with flow liquefaction.

This study, which constitutes the first field test of the Piezovane, was conducted at three study sites where extensive liquefaction occurred during the 1989 Loma Prieta earthquake; these sites have also been studied by U.S. Geological Survey scientists. The Piezovane correctly identified zones of contractive soils in areas where extensive lateral spreading occurred during the earthquake, and zones of dilative soils in areas where no lateral spreading occurred.

## INTRODUCTION

This paper reports on our efforts to field-test the Piezovane, an instrument invented at the Colorado State University for the direct measurement of soil-liquefaction potential. The study was conducted in Monterey County, Calif., where liquefaction occurred during the 1989 Loma Prieta earthquake. The sites chosen for this study were also studied by scientists of the U.S. Geological Survey (see Tinsley and others, this chapter).

The term "liquefaction" has various meanings in the literature. According to Seed and Lee (1966), liquefaction occurs when pore pressures, increased by cyclic loading, reduce a soil's effective stress to zero. Castro and Poulos (1977) defined liquefaction according to a decrease in soil shear resistance at large strains. According to this approach, liquefaction is "a phenomenon wherein a mass of soil loses a large percentage of its shear resistance, when subjected to undrained monotonic, cyclic, or shock loading, and flows in a manner resembling a liquid until the shear stresses acting on the mass are as low as the reduced shear resistance." Castro and Poulos' definition, which is appropriate for the analytical approach used in this paper to analyze the Piezovane data, is denoted as "flow-liquefaction potential," and Seed and Lee's definition as "level-ground-liquefaction potential." Flow failure can occur only in contractive soils (Casagrande, 1936; Castro and others, 1992), whereas liquefaction-induced

sand boils, ground settlement, and limited lateral spreads can occur in both contractive and dilative soils.

The need to improve and develop onsite methods for evaluating the liquefaction potential of sand layers was expressed, for example, by Peck (1979) and Poulos (1988). Methods using the standard penetration test (SPT) and cone-penetration test (CPT) for the prediction of level-ground liquefaction are restricted to empirical correlations. Dilative/contractive tendencies and steady-state shear strength are currently determined by laboratory tests complemented with field-index tests (Marcuson and others, 1980; Housner, 1985; Castro and others, 1992).

Addition of pore-pressure measurement to onsite techniques is thought to assist in the direct measurement of flow-liquefaction potential because pore pressure is critical to liquefaction. A few field studies have attempted to use the piezocone, a cone for measuring pore pressure, to evaluate liquefaction potential (Schmertmann, 1978; Forest and others, 1981; Campanella and others, 1983; East and others, 1988). Interpretations from such studies are conjectural, owing to complex failure modes, volumetric strains caused by cavity expansion, and uncertainty in the effect of pore-pressure-measurement location. A detailed study by Norton (1983) concluded that the piezocone could not distinguish between liquefiable and nonliquefiable soils on the basis of pore-pressure response.

Absence of a reliable onsite device for direct, quantitative evaluation of flow-liquefaction potential prompted us to invent the Piezovane, a vane-shear device for measuring pore pressure (Charlie and Butler, 1990). This new onsite device has several advantages over others, including its ability to induce large, unidirectional shear strains that closely simulate those associated with liquefaction.

The purpose of this study was to use the Piezovane technique to identify contractive and dilative soils at sites where liquefaction is known to have occurred during the earthquake. We believed that this systematic investigation would validate the Piezovane approach and provide useful information about the study sites.

## THE PIEZOVANE

The concept of the Piezovane was based on a patent application by Charlie and Butler (1990) and tested in the laboratory by Scott (1989) and Butler (1992). Its design, which is based on the field vane-shear device used to determine the undrained shear strength of clay layers, consists of four blades attached to a shaft; when rotated, the vane induces large shear deformation in the enclosed and surrounding soil. The Piezovane is equipped with a pressure transducer that measures pore-pressure changes during vane shear. The rectangular vane, in accordance with American Society for Testing and Materials (ASTM) (1987) standard method D2573, is 63.5 mm in diameter by 127 mm high and has a blade 3.2 mm thick. The vane shaft is 19 mm in outside diameter, in contrast to the ASTM's recommended 12.7 mm, to accommodate an electronic pore-pressure transducer. At least 18 percent of the soil volume enclosed within the vane's diameter, in contrast to the ASTM's recommended 15 percent, is displaced at the time of vane insertion. The Piezovane is rotated at approximately 30°/s, in contrast to the ASTM's recommended 0.1°/s; this rapid rate of rotation requires electronic data acquisition with a sampling rate exceeding 1 sample per second.

Details of the Piezovane are shown in figures 1 and 2. Soil pore-water pressure is monitored through four 1.5-mm-diameter ports that provide continuous fluid paths from the vane-blade edges to a pressure transducer mounted at the top of the device. Figure 3 shows the Piezovane's torque rod being rotated by hand during field testing. This torque rod and, thus, the vane were rotated 100° during field testing. Field methods for the Piezovane shear test are summarized below in the section entitled "Supplementary Information," and details were given by Brislawn (1992).

The Piezovane is designed to identify zones of contractive and dilative soils by determining changes in pore pressure during shearing. According to Castro and Poulos (1977) and Poulos and others (1985), soils exhibiting dilative tendencies are nonliquefiable with respect to flow failure, whereas soils exhibiting contractive tendencies may undergo flow liquefaction under certain conditions. A soil's steady-state deformation varies with void ratio and effective stress; this variation is represented by the steady-state curve in figure 4, where each point on the curve represents a condition of continuous deformation (Poulos, 1981). Thus, the steady-state curve marks the boundary between contractive and dilative tendencies. A contractive soil's void ratio lies above the steady-state curve (point B, fig. 4). In such a soil, the pore pressure increases and the shear strength decreases during undrained shearing. The undrained steady-state strength, which is reached during continuous deformation at a point on the steady-state curve, is the minimum shear strength of a contractive soil. Flow-liquefaction failure occurs when shear stresses on an undrained contractive soil exceed the soil's steady-state shear strength. In contrast, a dilative soil's void ratio lies below the steady-state curve, and the soil cannot liquefy because of an increase in effective stress (decrease in pore pressure) during undrained loading (point A, fig. 4). The undrained strength is greater than the drained strength for dilative soils.

Scott (1989) and Butler (1992) tested the Piezovane in a large calibration chamber designed to simulate field conditions. As recorded by the Piezovane, positive pore-pressure changes occurred in contractive-soil samples

compacted to void ratios above the steady-state curve (fig. 5), whereas negative pore-pressure changes occurred in dilative-soil samples with void ratios below the steady-state curve (fig. 6). Vertical spikes in both pore pressure and resisting torque occurred during very short pauses in rotation as a result of moving the vane by hand. During these short pauses in rotation, both the pore pressure and resisting torque decreased for contractive sand (fig. 5), whereas the pore pressure increased and the resisting torque decreased for dilative sand (fig. 6). Scott (1989) and Butler (1992) concluded from their calibration-chamber tests that the Piezovane can identify zones of contractive and dilative soils.

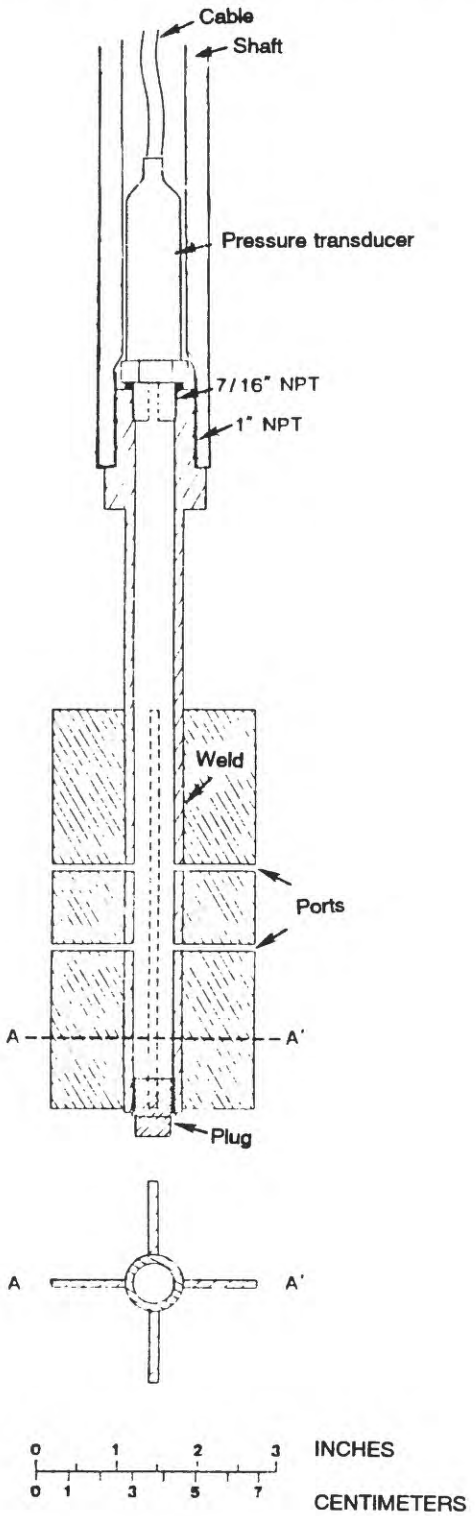


Figure 1.—Details of Piezovane construction. NPT, national taper pipethread.

## STUDY SITES

The epicenter of the 1989 Loma Prieta earthquake was located near Loma Prieta peak in the Santa Cruz Mountains, approximately 16 km northeast of Santa Cruz and 80 km southeast of San Francisco, Calif. (fig. 7). The $M$=7.1 earthquake was responsible for 63 deaths and more than $8 billion in property damage (Seed and others, 1990). During 8 to 10 s of strong shaking, it caused structural failure of many commercial and residential buildings and disrupted transport, communication, and utility lines. Most of the damage resulted from soft-sediment intensification of ground shaking, liquefaction-induced lateral spreading, and landslides (Seed and others, 1990, 1991).

Soil liquefaction and liquefaction-induced lateral spreading resulted in considerable damage to structures, facilities, and lifelines in the Monterey Bay area (fig. 7). Damage was most prevalent in coastal and alluvial deposits and in uncompacted artificial fills. In and near Santa Cruz, Watsonville, and Castroville (fig. 7), liquefaction and lateral spreading were responsible for pavement buckling, building settlement, and levee damage (Plafker and Galloway, 1989). Other liquefaction-related damage included thousands of meters of levee cracking from lateral spreading, highway- and railroad-bridge failures, and the destruction of the Moss Landing Marine Laboratory.

We conducted Piezovane tests at three sites where extensive lateral spreading, ground cracking, and sand boils had occurred during the earthquake. These sites, situated in Monterey County, Calif., were selected in concert with scientists of the U.S. Geological Survey who have also studied these sites (see Tinsley and others, this chapter). The locations of the three study sites are shown in figure 7.

## REGIONAL GEOLOGY

The geologic setting of the coastal region of Monterey Bay is a depositional basin bounded by mountains of the Coast Ranges to the north, east, and south and by the

Pacific Ocean to the west (fig. 7). The Pajaro and Salinas Rivers supply sediment to the basin. Tectonics and eustatic sea-level changes have controlled patterns of deposition and erosion in the past. The northern part of Monterey Bay is a region of Quaternary uplift, and sand dunes have formed along the stable central and south coast (Dupré, 1975).

The entrenched valleys of the Salinas and Pajaro Rivers formed during the Pleistocene glacial sea-level lowstand and were later filled with younger sedimentary materials during a rise in sea level; 70 to 100 m of river deposits are preserved in the Salinas and Pajaro River valleys. The lowermost 20 m of gravel, deposited in a braided-stream environment, forms a ground-water aquifer in the region (Muir, 1983). Overlying sand, silt, and clay are thought to represent a change to a fine-grained meandering-stream and estuarine environment during a period of relatively stable sea level from 7,000 yr B.P. to the present (Greene,

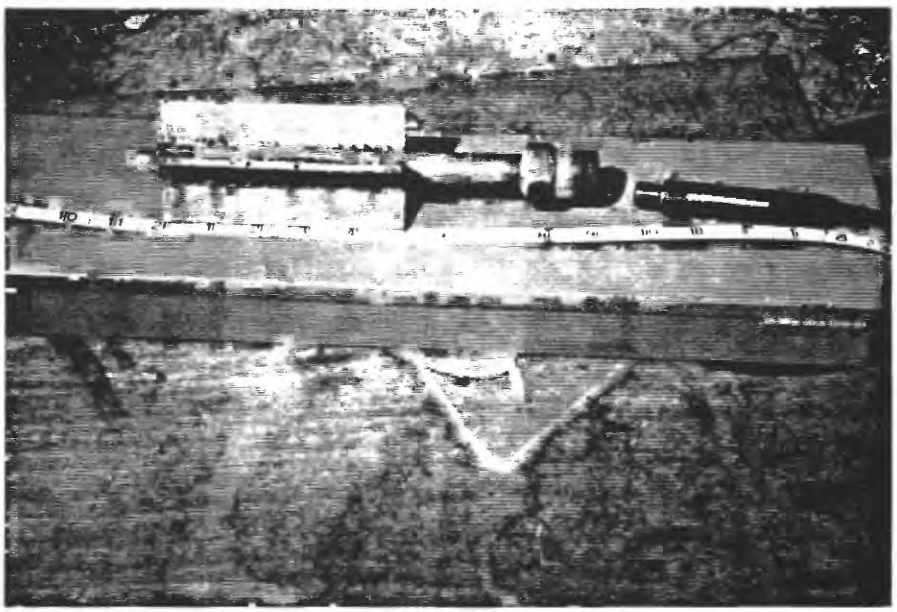

Figure 2.—Piezovane and pore-pressure transducer.

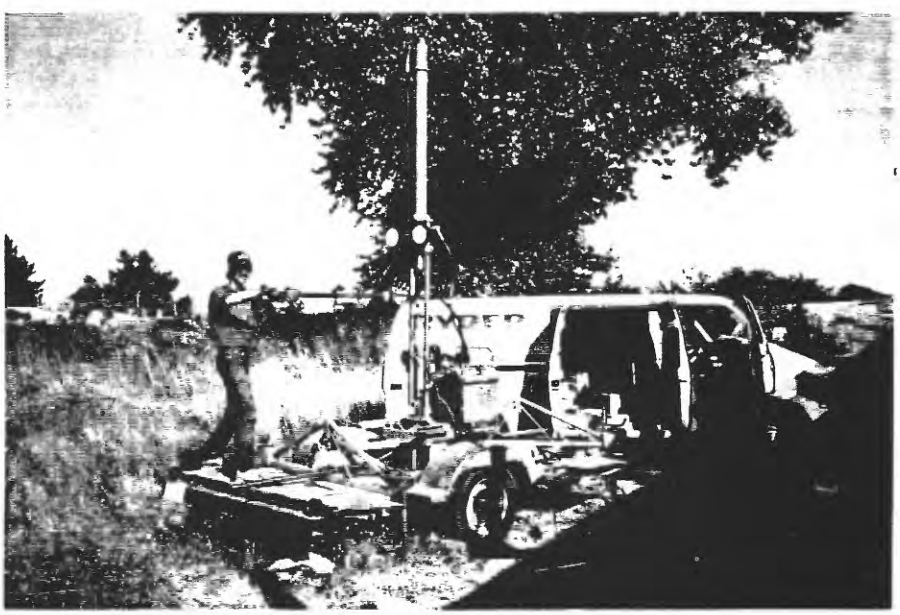

Figure 3.—Field testing with the Piezovane.

1970). Sources of sediment are primarily Tertiary sandstone and shale in the nearby Coast Ranges. The recently deposited (post-Pleistocene) saturated sand and silt are most susceptible to liquefaction (Dupré and Tinsley, 1980).

## SEA MIST-LEONARDINI FARMS

The Sea Mist-Leonardini Farms study site is located in the Salinas River valley approximately 34 km southeast

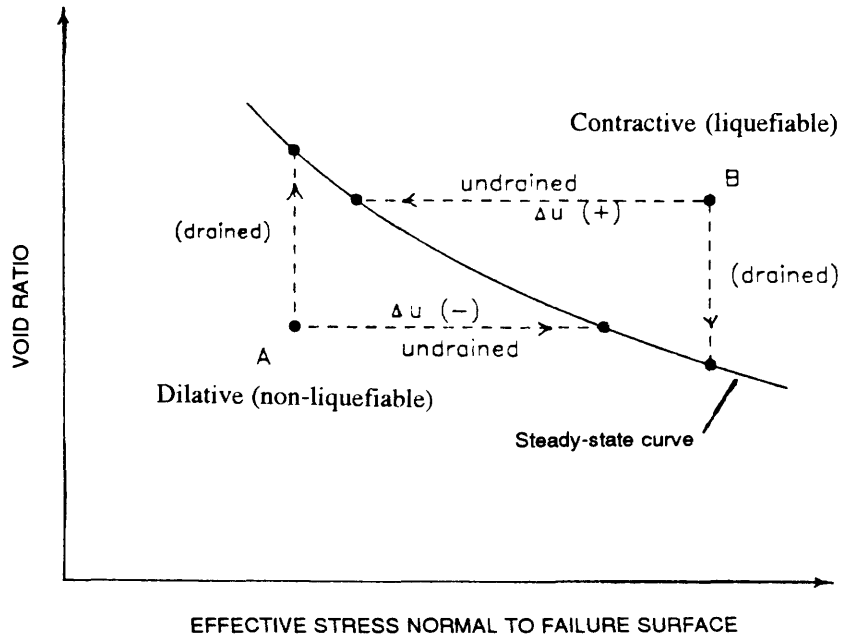


Figure 4.—Void ratio versus effective normal stress, showing steady-state curve (Poulos and others, 1985).

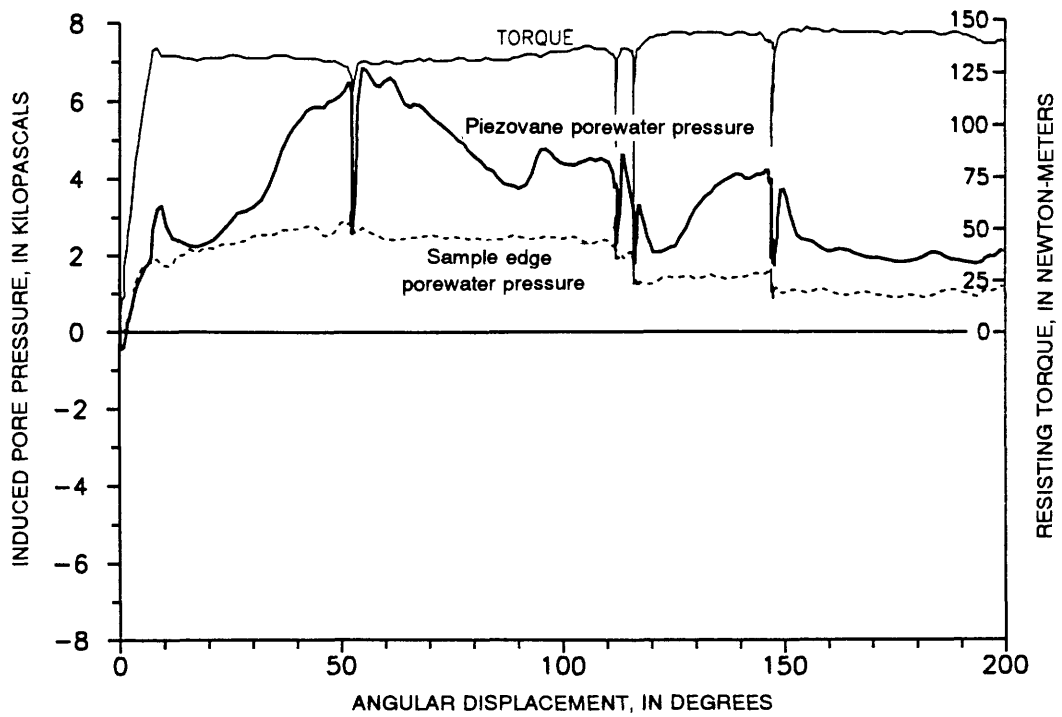


Figure 5.—Induced pore pressure and resisting torque versus angular displacement, showing typical behavior in contractive soil. Test VP3B: rotation rate, 30°/s; effective static stress, 552 kPa; void ratio, 0.782.

of the Loma Prieta earthquake epicenter (fig. 7). Site details and the locations of test sites are shown in figure 8; the Piezovane equipment at test sites CSU 29 and 38 is shown in figures 9 and 10, respectively. Liquefaction during the earthquake caused sections of the farmland to crack and spread toward the Salinas River (fig. 11), and formed numerous sand boils (fig. 12). Ground cracking and extensive lateral spreading also occurred in the area during the 1906 San Francisco earthquake (fig. 13; Youd and Hoose, 1978). The elevation at this study site ranges from 1 to 3 m above sea level. The ground-water table at the study site ranged from 1 to 3 m in depth at the time of our testing in August 1990. Sedimentary deposits at the study site are predominately loose sand and silty sand, with a few beds of silt and clay.

We conducted four Piezovane tests (CSU 30, 31, 38, 39, fig. 8) at the study site in soils in which extensive lateral spreading had occurred during the 1989 Loma Prieta earthquake, and two Piezovane tests, CSU 29 and 37, in soils in which no lateral spreading had occurred.

## MILLER FARM

The Miller Farm study site is located on the south bank of the Pajaro River across from the town of Watsonville, 17.5 km from the Loma Prieta earthquake epicenter (fig. 7). Site details and the locations of test sites are shown in figure 14; the Piezovane equipment at test site CSU 8 is shown in figure 15. Liquefaction during the earthquake caused extensive lateral spreading, ground settlement, and large sand boils, and a levee that separates the farm from the river was severely cracked. Ground cracking and extensive lateral spreading also occurred in the area during the 1906 San Francisco earthquake (fig. 13). The elevation at this study site ranges from 8 to 9 m above sea level. The ground-water table at the study site ranged from 3 to 4.6 m in depth at the time of our testing in August 1990. Sedimentary deposits at the study site range from silt and silty fine sand to coarse sand, with local clay-rich zones.

We conducted three Piezovane tests (CSU 3, 8, 9, fig. 14) at the study site in soils in which extensive lateral spreading had occurred during the earthquake, and two Piezovane tests, CSU 1 and 10, in soils in which no lateral spreading had occurred.

## SOUTHERN PACIFIC RAILROAD BRIDGE

The Southern Pacific Railroad Bridge study site is located where the railroad crosses the Pajaro River, between the levee and the river channel, near the community of Pajaro (fig. 7). Site details and the locations of test sites

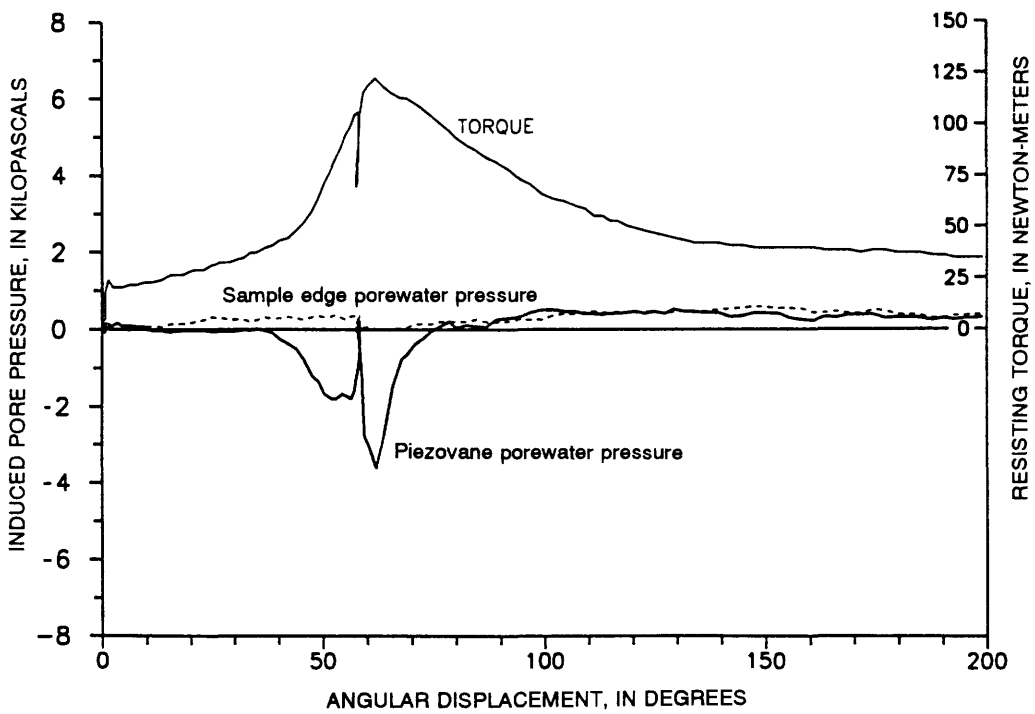


Figure 6.—Induced pore pressure and resisting torque versus angular displacement, showing typical behavior in dilative soil. Test PV7A: rotation rate, 30°/s; effective static stress, 206 kPa; void ratio, 0.674.

are shown in figure 16; the location of the borehole at test site CSU 48 is shown in figure 17. Extensive lateral spreading during the earthquake caused ground cracking and disrupted bridge pile supports that later required repairs. Ground cracking and extensive lateral spreading also occurred in the area during the 1906 San Francisco earthquake (fig. 13). The elevation at this study site is about 5.5 m above sea level. The ground-water table at the study site was 5.2 m deep at the time of our testing in August 1990.

We conducted one Piezovane test (CSU 48, fig. 16) at the study site 10 m west of the damaged piles in soils in

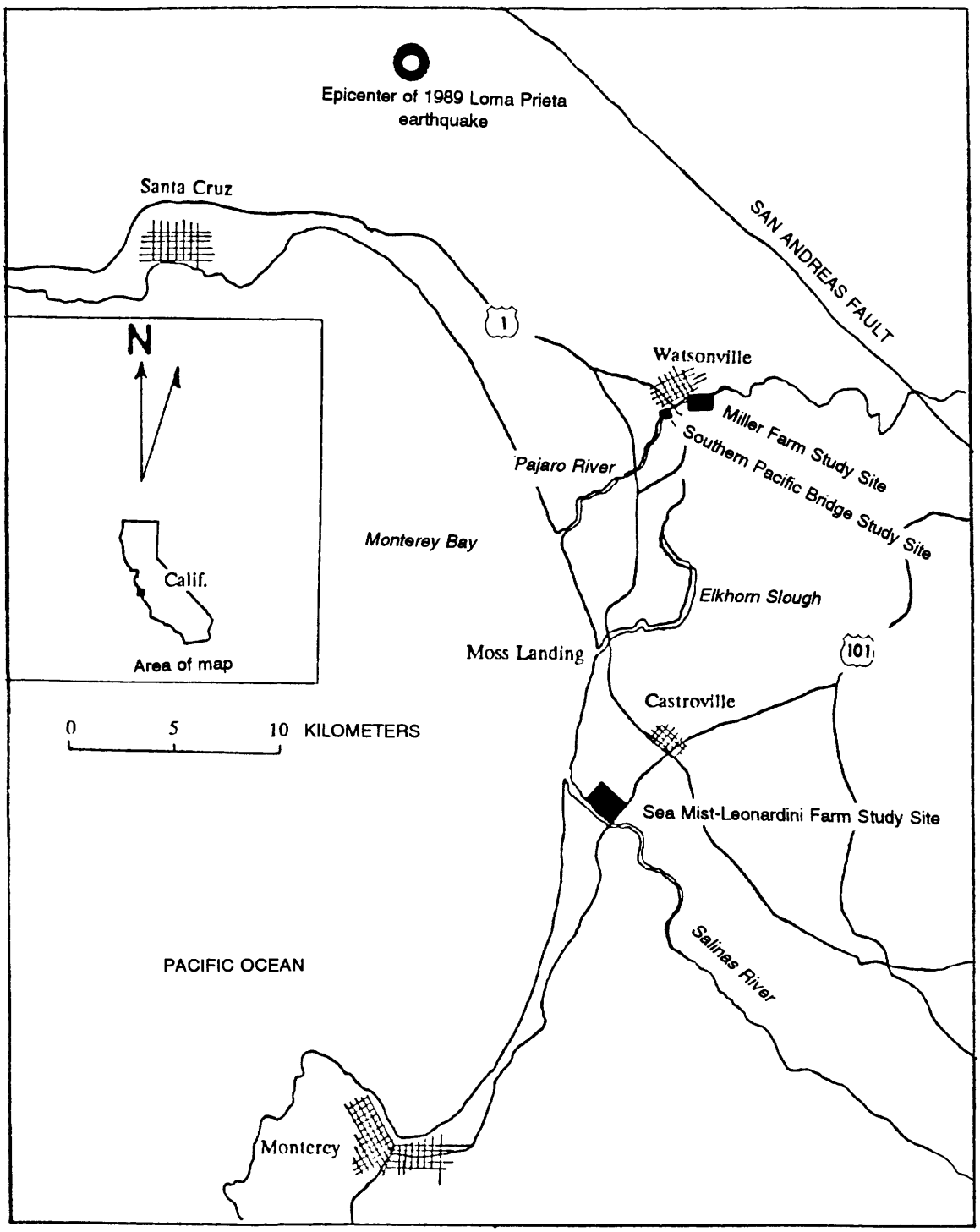


Figure 7.—Monterey Bay area, Calif., showing locations of test sites.

which extensive lateral spreading had occurred during the 1989 Loma Prieta earthquake.

## RESULTS

We located zones of contractive and dilative soils at the study sites from the pore-pressure response induced during Piezovane rotation. We then compared the zones of contractive soils with the areas in which extensive lateral spreading had occurred during the earthquake. Level-ground-liquefaction potential was determined from site geology, sand-boil samples, shear-wave velocities, and the U.S. Geological Survey geotechnical information of Tinsley and others (this chapter).

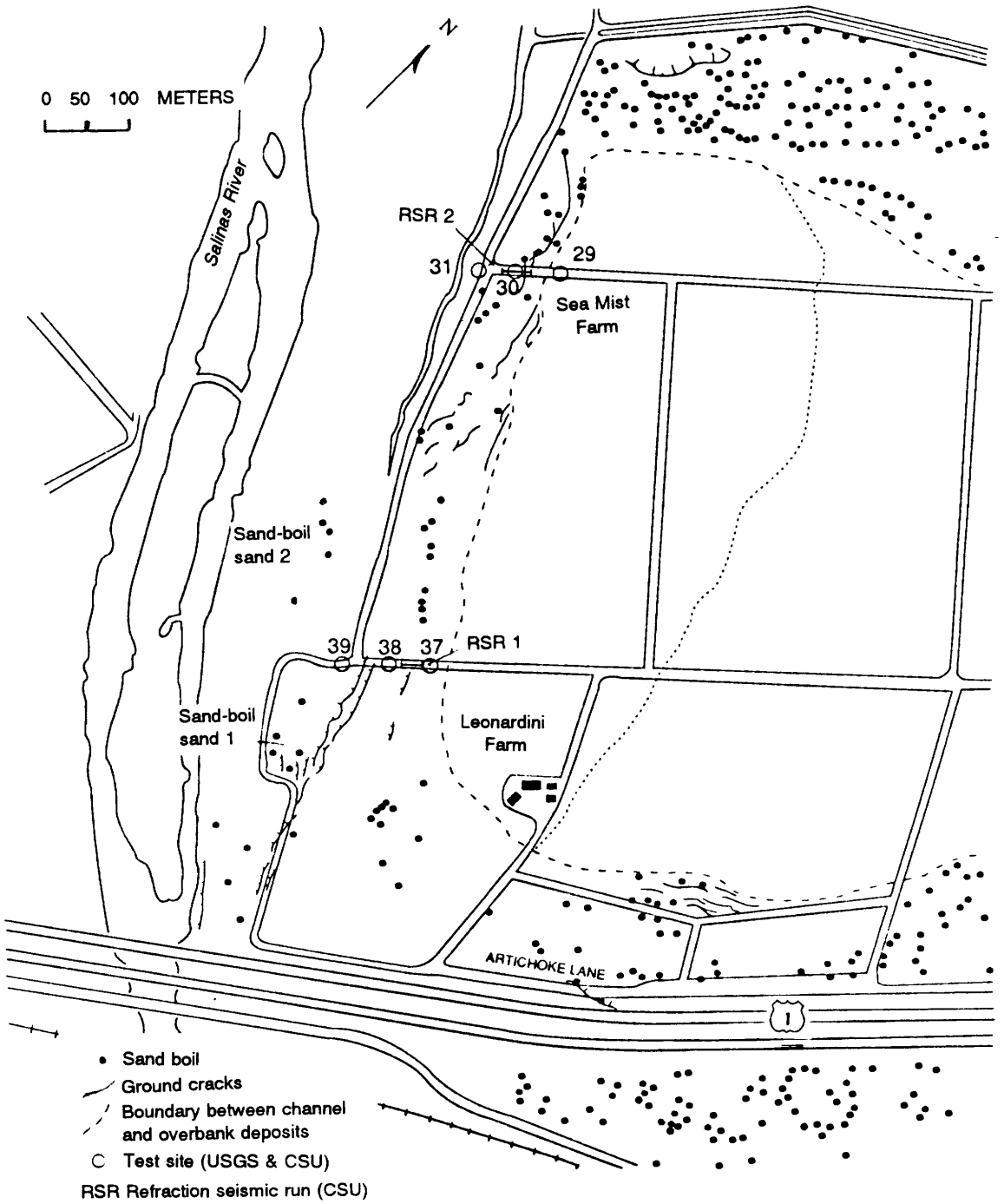


Figure 8.—Sea Mist-Leonardini Farms study site (fig. 7), showing locations of liquefaction features and tests by Colorado State University (CSU) and U.S. Geological Survey (USGS).

## PIEZOVANE DATA

Identifying contractive and dilative soils with the Piezovane is a straightforward procedure. On the basis of previous laboratory work by Scott (1989) and Butler (1992), this study interpreted field pore-pressure increases during vane shearing to indicate contractive soils with a potential for liquefaction-induced lateral spreading and flow as defined by Castro and Poulos (1977) and Poulos (1981), and field pore-pressure decreases to indicate dilative soils resistant to lateral spreading. Peak changes in pore pressure during vane rotation versus depth are plotted below in the section entitled "Supplementary Information," and typical Piezovane pore-pressure changes are plotted in figure 18.

The Piezovane recorded positive pore-pressure changes at specific depths at 8 of the 12 test sites. Significant lateral spreading occurred at all eight of these sites during the earthquake. At the four sites where no lateral spreading occurred, three tests (CSU 1, 10, 29) were conducted in clays and are omitted from this analysis. One test (CSU 37, fig. 8), performed in stable sand, yielded all negative pore-pressure changes, except for two points where no pore-pressure change was detected.


Figure 9.—Piezovane in operation at test site CSU 38 (fig. 8) on the Leonardini Farm (fig. 7).


Figure 10.—Piezovane in operation at test site CSU 29 (fig. 8) on the Sea Mist Farm (fig. 7).

The zones of contractive soils are at 2-, 2.4-, and 7.5-m depth on the Sea Mist Farm, at 2- and 2.4-m depth on the Leonardini Farm, at 5.2-, 5.8-, 6.7-, and 7.6-m depth on the Miller Farm, and at 5.8-, 6.7-, and 7.5-m depth at the Southern Pacific Railroad Bridge.

## GEOLOGIC DATA

Both the 1906 San Francisco and 1989 Loma Prieta earthquakes induced ground failures and sand boils at the three study sites, indicating the presence of liquefiable soils. At the Sea Mist-Leonardini Farms study site (figs. 8, 13), extensive lateral spreads, ground cracks, and sand boils were confined to sedimentary deposits within a paleochannel meander bend. Sand boils, ground cracking, and lateral spreading at the Miller Farm (figs. 13, 14) decreased away from the Pajaro River where fine-grained sedimentary deposits are present. Sand layers that appear susceptible to liquefaction are interpreted as fluvial or estuarine in origin. Overbank deposits consist of silt and clay that did not liquefy. The channel sand layers shown

Figure 11.—Ground cracks southwest of the sea Mist Farm (fig. 7). Pen is 15 cm long.

Figure 12.—Sand boils on the Leonardini Farm (fig. 7). Pen is 15 cm long.

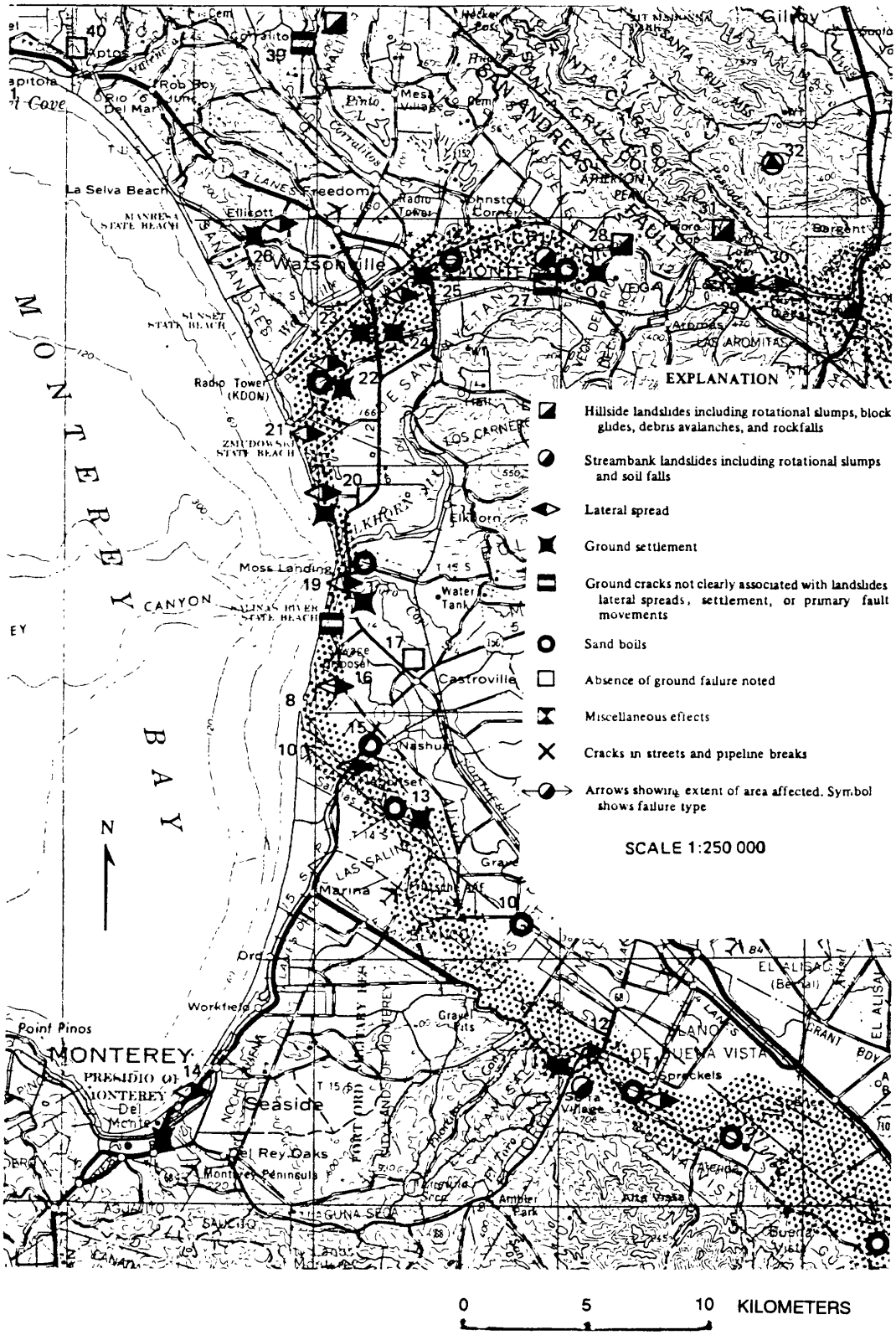


Figure 13.—Monterey Bay area, Calif., showing locations of ground failures induced by 1906 San Francisco earthquake. From Youd and Hoose (1978).

in U.S. Geological Survey soil logs (see Tinsley and others, this chapter) within 10 m of the ground surface are thought to be liquefiable on the basis of their proximity to the water table and ground surface, their age, their size distribution, and their low relative densities based on low blowcounts and cone-tip resistances. Liquefiable sand layers with the above-mentioned characteristics are at 1.5- to 8.5-m depth on the Sea Mist-Leonardini Farms, at 4.5- to 9.2-m depth on the Miller Farm, and at 5.2- to 9.2-m depth at the Southern Pacific Railroad Bridge.

## SAND-BOIL DATA

We collected samples of sand-boil material at both the Sea Mist-Leonardini Farms and Miller Farm study sites. Sand-boil material from the Sea Mist-Leonardini Farms study site was erupted from small-diameter (0.3–1 m) isolated vents (figs. 8, 12). Sand-boil material from the Miller Farm study site was deposited on the surface in massive amounts from long ground fissures (locs. 5, 6, fig. 14). At several boreholes, sand samples near the water table were collected with a sand-bucket auger before inserting the Piezovane; the samples were analyzed for grain-size distribution, mineral contents, and color.

We compared the physical properties of the sand-boil material with those of subsurface samples in an attempt to determine the depth of the sand-boil source bed for each study site. The grain-size distributions of these samples are plotted in figure 19, and their physical properties are listed in table 1. The most likely source for the sand-boil material at both study sites appears to be the uppermost sand layer. These sand layers are capped by silt and clay at both study sites. Void ratios of these zones, estimated

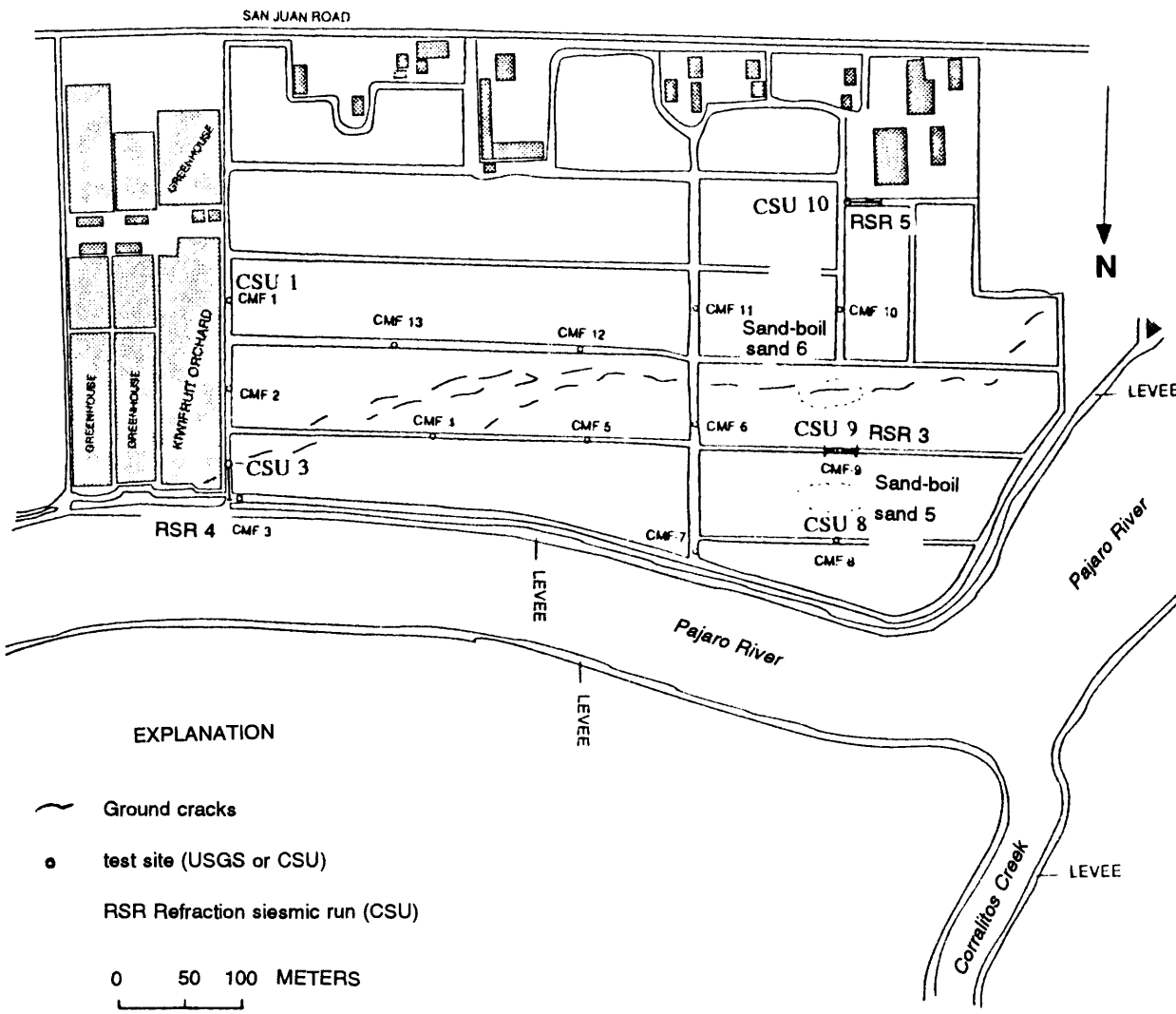


Figure 14.—Miller Farm study site (fig. 7), showing locations of liquefaction features and tests by Colorado State University (CSU) and U.S. Geological Survey (USGS).

Figure 15.—Test site CSU 8 (fig. 14) on the Miller Farm (fig. 7).

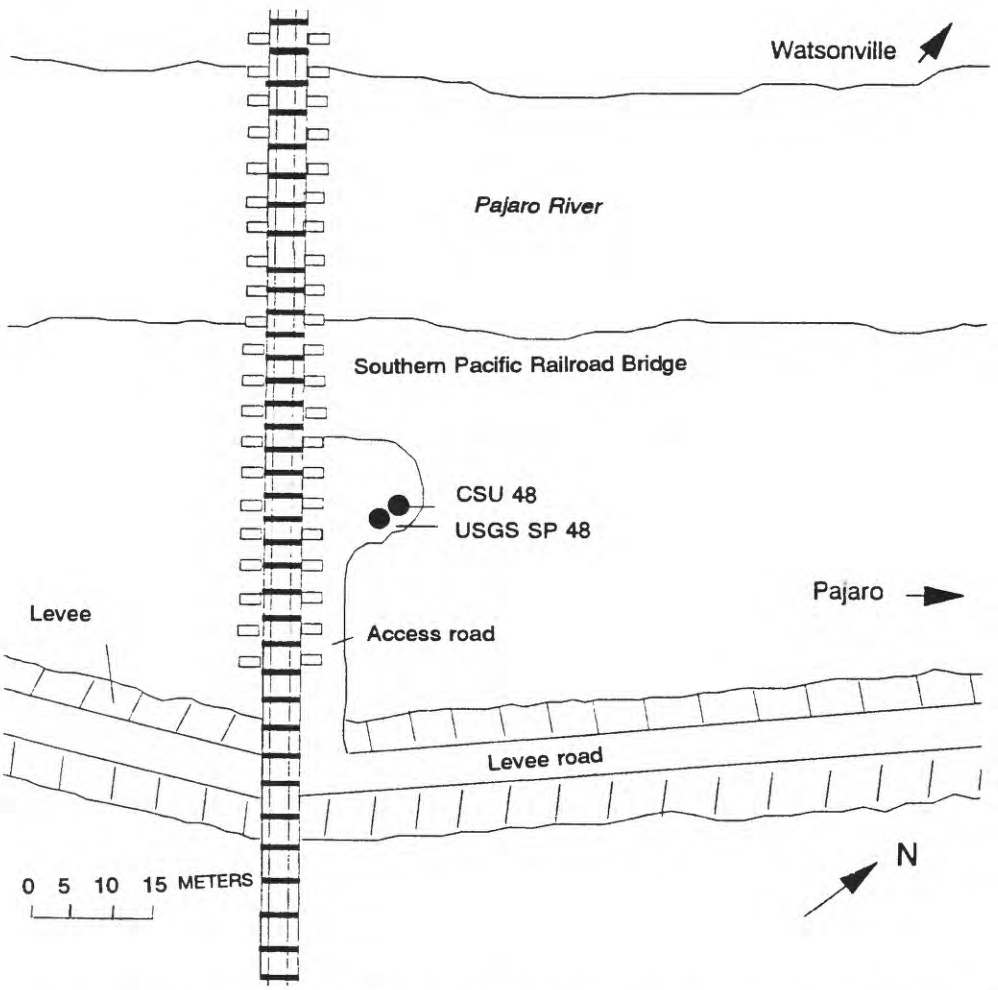


Figure 16.—Southern Pacific Railroad Bridge study site (fig. 7), showing locations of tests by Colorado State University (CSU) and U.S. Geological Survey (USGS).

from field SPT blowcounts and laboratory tests, and the steady-state curves of Poulos and others (1985) for similar sand layers suggest contractive soils. Approximate depths of the sand-boil source beds are 2.2 m at the Sea Mist-Leonardini Farms study site, 5.2 m at the Miller Farm study site, and 5.5 m at the Southern Pacific Railroad Bridge study site.

### SHEAR-WAVE-VELOCITY DATA

We conducted seismic-refraction shear-wave tests at the Sea Mist-Leonardini Farms and Miller Farm study sites. The test results, listed in table 2, indicated a low-shear-wave-velocity layer at each study site. Shear-wave velocities fall within the typical range for recent loose sand deposits (table 3). We were unable to correlate shear-wave velocity with potential for pore-pressure buildup under cyclic loading, as discussed by Dobry and others (1981), because reverse-velocity profiles inhibited calculation of the depth to the low-velocity layers.

### STANDARD-PENETRATION-TEST DATA

The U.S. Geological Survey performed SPT's at 9 of the 12 Piezovane test sites. SPT's were performed at various intervals to a maximum depth of 7 m. Each geotechnical log presents grain-size analyses and detailed soil descriptions of SPT samples from various depths; examples of the U.S. Geological Survey logs used in this study (see Tinsley and others, this chapter) are shown in figure 18. We performed quantitative level-ground-liquefaction analyses on the SPT blowcounts; the analysis followed the procedure of Seed and others (1984). A factor of safety against liquefaction was calculated from the site SPT blowcounts, using estimates of soil conditions and earthquake ground motion. We used estimated peak accelerations of 0.14 *g* for the Sea Mist-Leonardini Farms study site and 0.39 *g* for the Miller Farm and Southern Pacific Railroad Bridge study sites. The data, assumptions, and methods used for factor-of-safety calculations are summarized below in the section entitled "Supplementary Information," and details were given by Brislawn (1992). Zones with SPT factors of safety against liquefaction of less than 1 are shown in figure 18.

### CONE-PENETRATION-TEST DATA

The results of CPT's are also presented in the U.S. Geological Survey geotechnical logs (see Tinsley and others, this chapter). Soil type, relative density, and equivalent SPT blowcount can be estimated from charts of friction ratio versus tip resistance. We performed level-ground-liquefaction analysis on cone-tip resistances at depths that matched those of the Piezovane tests. We converted the CPT data to an equivalent SPT blowcount (*N* value) and used the same procedure for liquefaction analysis of the SPT data. The results are summarized below in the section entitled "Supplementary Information," and details were given by Brislawn (1992). Zones with a CPT factor of safety against liquefaction of less than 1 are shown in figure 18.

## DISCUSSION

Most positive pore pressures were recorded by the Piezovane in the uppermost layer of sand bodies, beneath

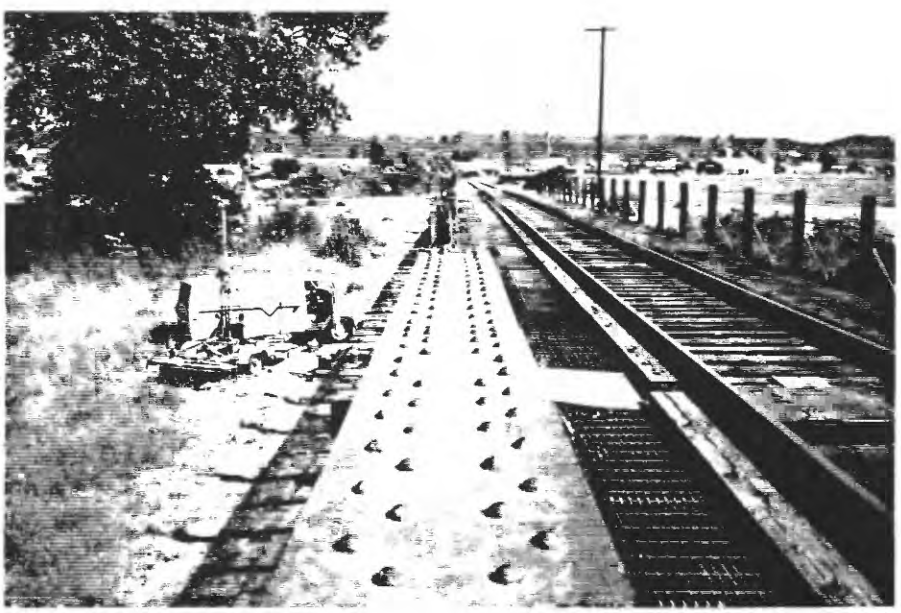

Figure 17.—Test site CSU 48 (fig. 16) at Southern Pacific Railroad Bridge study site (fig. 7).

silt-clay layers. Grain-size analysis, color, and mineral contents suggest that the sand-boil material at the Sea Mist-Leonardini Farms and Miller Farm study sites were derived from these zones. Estimated onsite void ratios of these zones and the steady-state curves of Poulos and others (1985) for similar sand layers suggest contractive soils. Although Piezovane tests and subsequent analyses indicate that these zones are contractive, additional study is needed to confirm this conclusion.

Piezovane pore-pressure increases are consistent with the areas of extensive lateral spreading, as illustrated by the soil profile for the Leonardini Farm (fig. 20). The Piezovane data indicate a zone of contractive soil in the uppermost sand layers in USGS boreholes 38 and 39 but not in USGS borehole 37 (fig. 8). USGS boreholes 38 and 39 were drilled in areas where extensive lateral spreading occurred during the earthquake, and USGS borehole 37 in an area where lateral spreading did not occur.

On the soil profile for the Leonardini Farm (fig. 20), the Piezovane data indicate a zone of contractive soil wherever the SPT and CPT factors of safety are less than 1, except in USGS borehole 39 (fig. 8) at 6-m depth. SPT's and CPT's at the Miller Farm and Southern Pacific Railroad Bridge study sites indicate a higher potential for level-ground liquefaction than the Piezovane data indicate for flow liquefaction. SPT and CPT data, predictions of level-ground liquefaction during the 1989 Loma Prieta earthquake, and the Piezovane identification of zones of contractive soils are compared in figure 18.

## CONCLUSIONS

This study applied and evaluated the Piezovane, a new field device that identifies soils susceptible to liquefaction-induced lateral spreading and flow failure. Field measurements of shear-induced pore-pressure changes indicate that the Piezovane identifies contractive and dilative cohesionless soils.

Horizons of contractive or dilative soils at the Sea Mist-Leonardini Farms, Miller Farms, and Southern Pacific Railroad Bridge study sites are shown as zones of positive or negative peak induced pore-pressure change during shearing. Contractive soils have a potential for significant lateral spreading. The zones of contractive soils are at 2-, 2.4-, and 7.5-m depth on the Sea Mist Farm, at

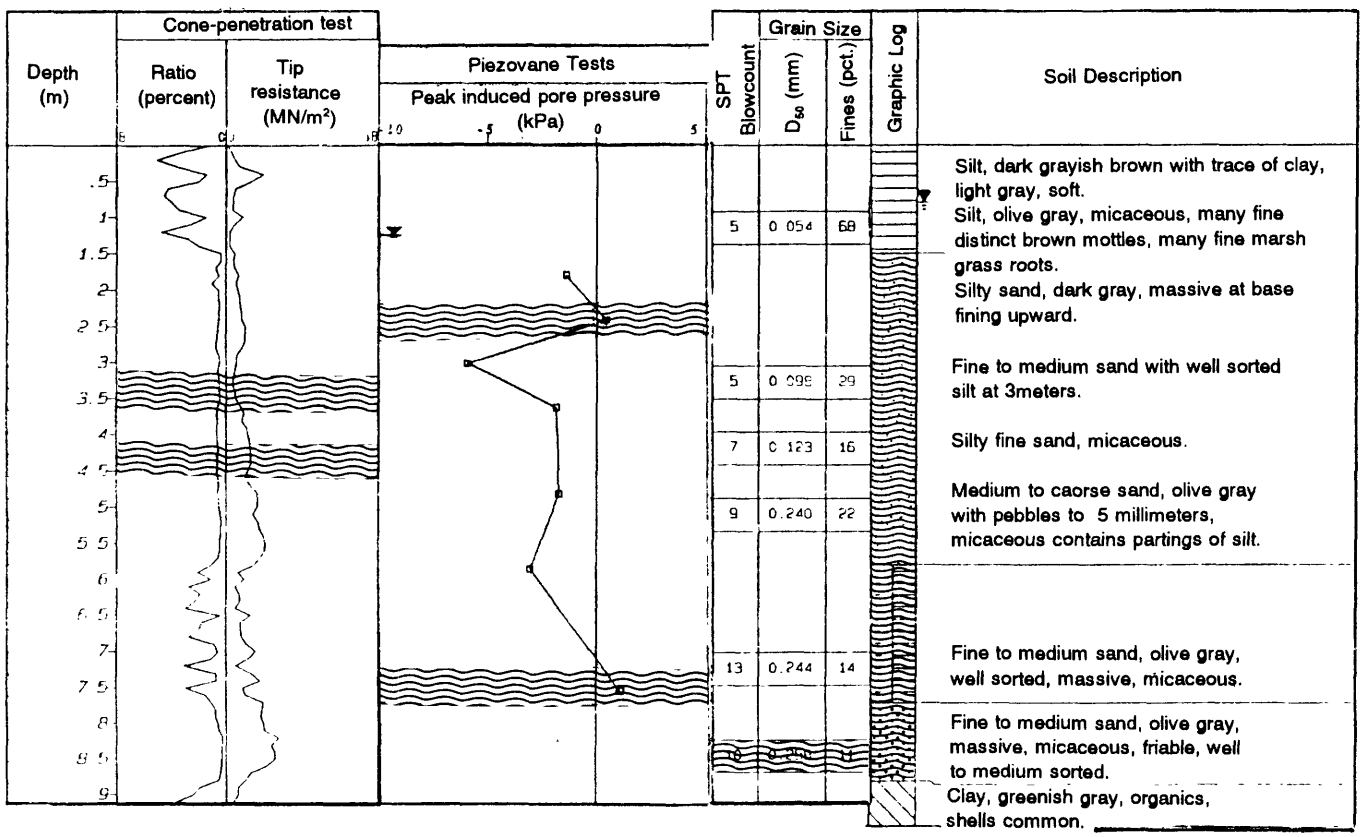


Figure 18.—Pore-pressure logs of U.S. Geological Survey cone-penetration tests (CPT's) (left), Colorado State University Piezovane tests (middle), and U.S. Geological Survey standard penetration tests (SPT's) (right) (*A*) on the Sea Mist Farm (site CSU 31, fig. 8), (*B*) on the Miller Farm (site CSU 3, fig. 14), and (*C*) on the Southern Pacific Railroad Bridge (site CSU 48, fig. 16). Shading denotes zones with liquefaction potential based on factors of safety; inverted solid triangle, depth to water table. CPT and SPT data from Tinsley and others (this chapter); soil descriptions from U.S. Geological Survey.

2- and 2.4-m depth on the Leonardini Farm, at 5.2-, 5.8-, 6.7-, and 7.6-m depth on the Miller Farm, and at 5.8-, 6.7-, and 7.5-m at the Southern Pacific Railroad Bridge. Comparison of the evidence for liquefaction potential indicated by other tests and geology supports the Piezovane test results. The Piezovane recorded positive pore pressures in soil horizons that appear to be the source of sand boils from the 1989 Loma Prieta earthquake. Zones of contractive soils identified by the Piezovane are consistently identified in areas where extensive lateral spreading occurred during the earthquake. Positive pore pressures were measured in sand layers with the highest level-ground-liquefaction potential as indicated by SPT's and CPT's. Evidence presented in this study indicates that the Piezovane accurately identifies zones of contractive soils with a potential for excessive lateral spreading and flow failure.

## ACKNOWLEDGMENTS

This research was supported by U.S. National Science Foundation grant 9011319 as part of the National Earthquake Hazards Reduction Program. Thomas L. Holzer, John C. Tinsley, and Michael J. Bennett of the U.S. Geological Survey provided invaluable technical information and advice, as well as site access, site maps, and geotechnical data. Clint Miller, Silvio Bernardi, and employees of the Sea Mist, Leonardini, and Miller Farms in Monterey County, Calif., provided access to the study sites and much helpful information. C. Peter Wroth of the Department of Engineering Science, Oxford University, encouraged us to experimentally test our concept of the Piezovane. John W. France of GEI Consultants, Inc., provided special expertise during laboratory testing of the Piezovane. "Piezovane" is a trademark of the Colorado State University; the Piezovane was invented by Wayne A. Charlie and William L. Butler (U.S. patent No. 5109702).

## REFERENCES CITED

American Society for Testing and Materials, 1987, Standard test method for field vane shear test in cohesive soil, designation D2573 of Annual book of ASTM standards: Philadelphia, p. 424–427.

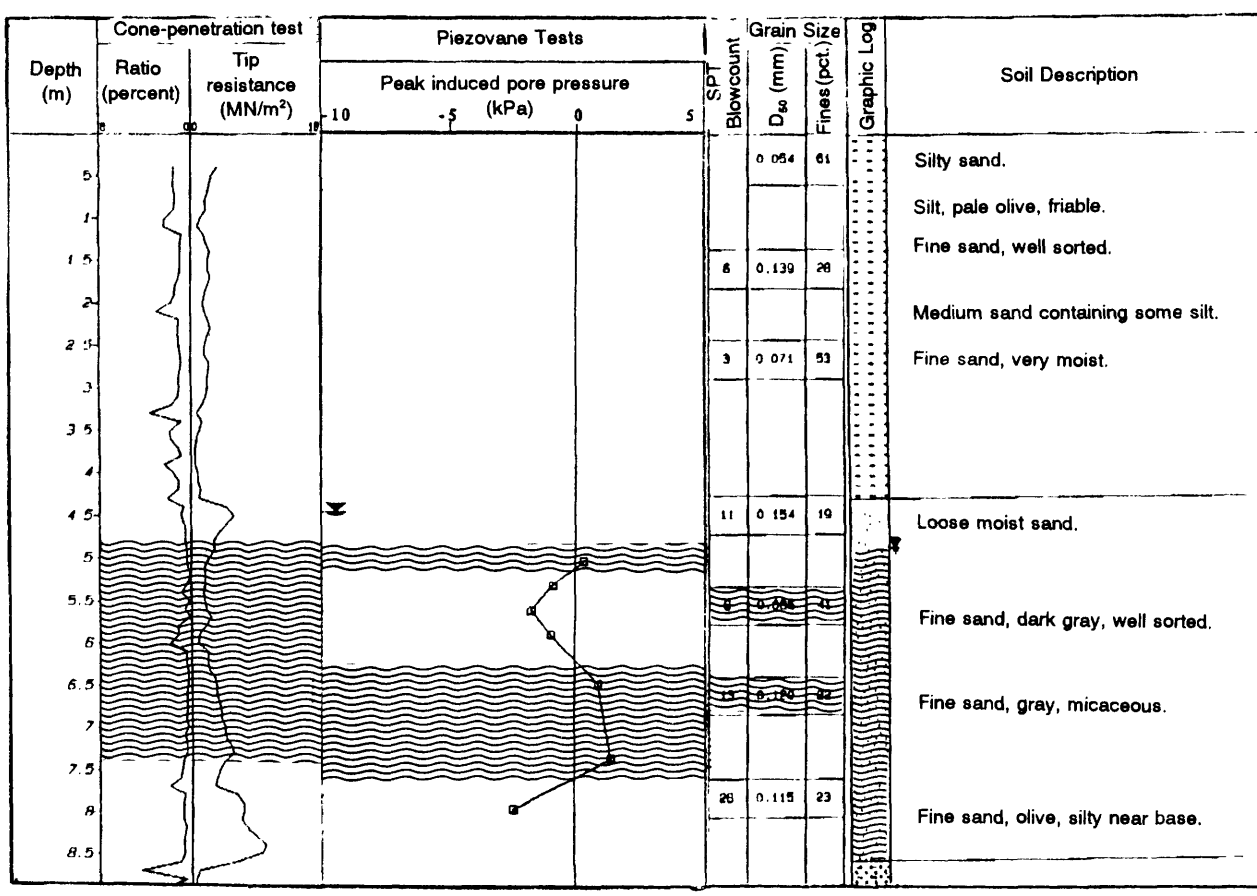


Figure 18.—Continued.

Brislawn, J.P., 1992, Site liquefaction investigation with the CSU Piezovane: Fort Collins, Colorado State University, M.S. thesis, 143 p.

Butler, L.W., 1992, Development of the CSU Piezovane for estimating liquefaction potential of saturated sands: Fort Collins, Colorado State University, M.S. thesis, 138 p.

Campanella, R.G., Robertson, P.K., and Gillespie, D.G., 1983, Cone penetration testing in deltaic soils: Canadian Geotechnical Testing Journal, v. 20, no. 2, p. 23–35.

Casagrande, Arthur, 1936, Characteristics of cohesionless soils affecting the stability of slopes and earth fills: Boston Society of Civil Engineers Journal, v. 23, no. 1, p. 13–32.

Castro, Gonzalo, and Poulos, S.J., 1977, Factors affecting liquefaction and cyclic mobility: American Society of Civil Engineers Proceedings, Geotechnical Engineering Division Journal, v. 103, no. GT6, p. 501–516.

Castro, Gonzalo, Seed, R.B., and Keller, T.O., 1992, Steady-state strength analysis of Lower San Fernando Dam slide: Journal of Geotechnical Engineering, v. 118, no. 3, p. 406–427.

Charlie, W.A., and Butler, L.W., 1990, A method for determining liquefaction potential of cohesionless soils; Air Force invention no. 18,634, declaration for patent application: Washington, D.C., U.S. Patent and Trademark Office, 29 p.

Dobry, Ricardo, Stokoe, K.H., II, Ladd, R.S., and Youd, T.L., 1981, Liquefaction susceptibility from *S*-wave velocity, *in* In situ testing to evaluate liquefaction susceptibility: American Society of Civil Engineers National Convention, St. Louis, Mo., 1981, Proceedings, p. 55–64.

Dupré, W.R., 1975, Quaternary history of the Watsonville lowlands north-central Monterey Bay Region, California: Stanford, Calif., Stanford University, Ph.D. thesis, 145 p.

Dupré, W.R., and Tinsley, J.C., 1980, Maps showing geology and liquefaction potential of northern Monterey and southern Santa Cruz Counties, California: U.S. Geological Survey Miscellaneous Field Studies Map MF–1199, scale 1:62,500, 2 sheets.

East, D.R., Hughes, J.M.O., Cincilla, W.A., and Benoit, Jean, 1988, The use of electric Piezocone for mine tailings deposits, *in* International Symposium on Penetration Testing, 1st, Orlando, Fla., 1988, Proceedings: Rotterdam, A.A. Balkema, v. 2, p. 745–750.

Forrest, J.B., Ferritto, J.M., and Wu, George, 1981, Site analysis for seismic soil liquefaction potential: International Conference on Recent Advances in Geotechnical Earthquake Engineering and Soil Dynamics, St. Louis, Mo., 1981, Proceedings, v. 1, p. 155–160.

Greene, H.G., 1970, Geology of southern Monterey Bay and its relationship to the ground water basin and salt water intrusion: U.S. Geological Survey Open-File Report, 50 p.

Housner, G.W., ed., 1985, Liquefaction of soils during earthquakes: U.S. National Research Council, Committee on Earthquake Engineering, Commission on Engineering and Technical Systems Report CET–EE–001, 240 p.

Martin, G.R., 1991, Site investigation using the CPT and CPT/SPT correlations: San Francisco, Calif., San Francisco State University Seismic Short Course, 100 p.

Marcuson, W.F., Franklin, A.G., and Hadala, P.F., 1980, Liquefaction potential of dams and foundations: Vicksburg, Miss., U.S. Army Corps of Engineers, Waterways Experiment Station Research Report S–76–2, 28 p.

Muir, K.S., 1973, Preliminary report on geology and ground water of

*C*

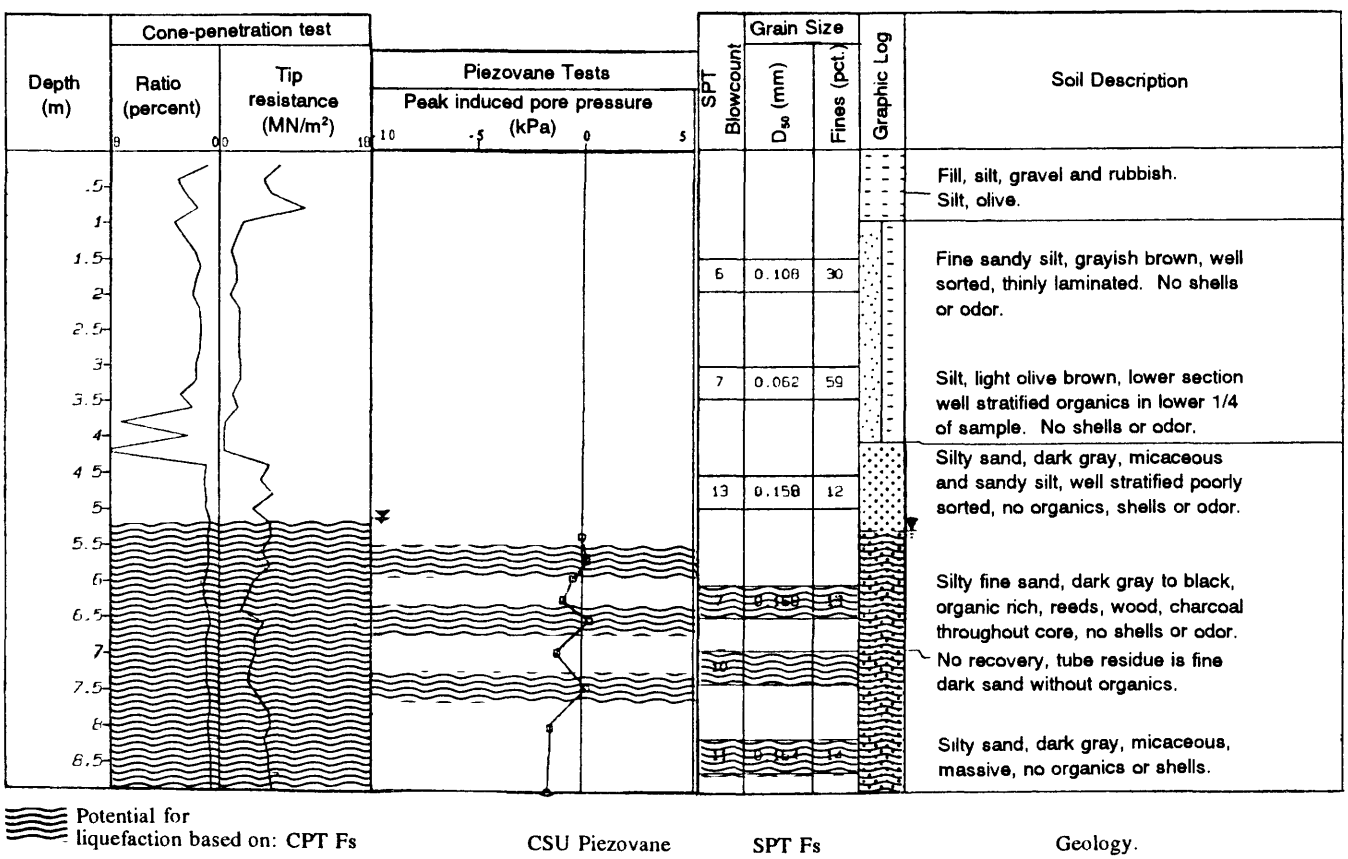


Figure 18.—Continued.

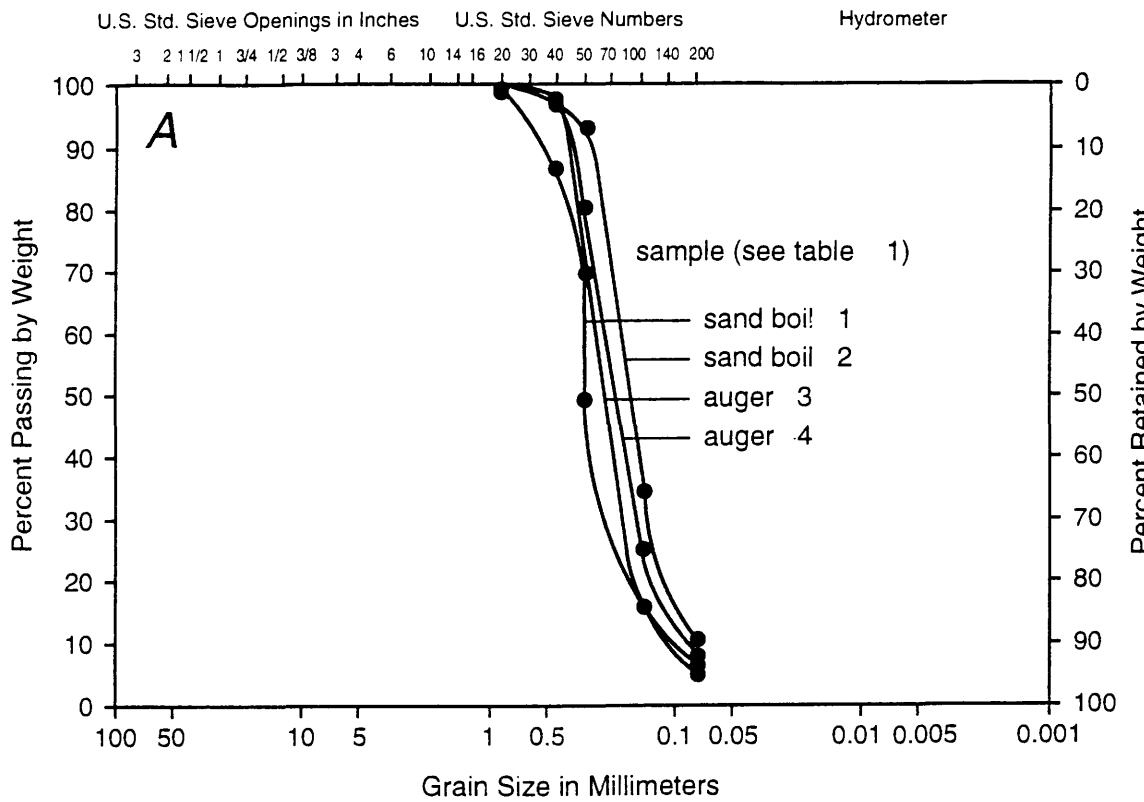


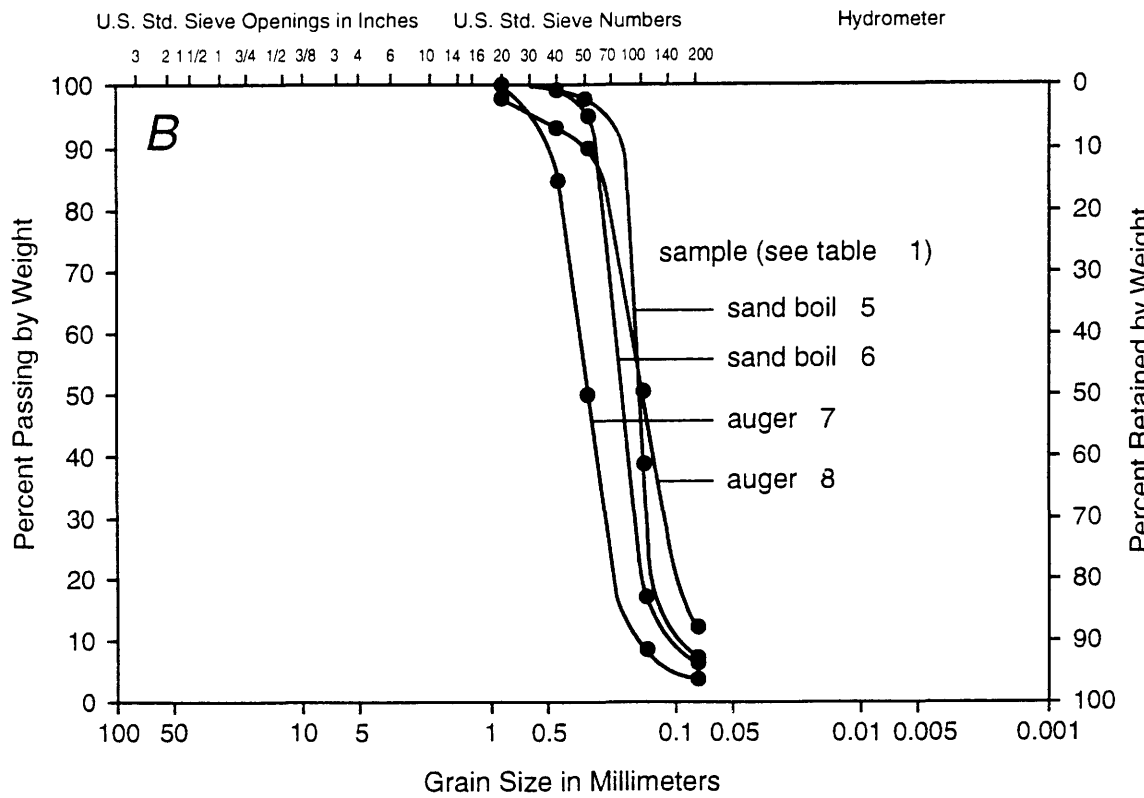


| | GRAVEL | | SAND | | | SILT or CLAY |
|---|---|---|---|---|---|---|
| | Course | Fine | Coarse | Medium | Fine | |

Table 1.—*Physical properties of sand-boil and auger samples*

| sample # | D50(mm) | %fines | Cu | USCS | color(Munsell) | shape |
|---|---|---|---|---|---|---|
| #1 Leonardini sand boil, 60-150m S BH39 | 0.29 | 5 | 2.7 | SP-SM | 5Y5/2 light olive grey | SA-SR |
| #2 Sea Mist sand boil, 800m NW BH39 | 0.17 | 10 | 2.5 | SP-SM | 5Y5/2 light olive grey | SA-SR |
| #3 Leonardini auger, 1.3m depth, BH38 | 0.20 | 8 | 2.7 | SP-SM | 10YR6/2 pale yellow brown | SA-SR |
| #4 Leonardini auger, 1.3m depth, BH39 | 0.22 | 4 | 2.3 | SP | 10YR6/2 pale yellow brown | SA-SR |
| #5 Miller sand boil, 30m N BH9 | 0.15 | 7 | 1.6 | SP-SM | 5Y5/2 light olive grey | SR |
| #6 Miller sand boil, 40m S BH9 | 0.20 | 5 | 1.8 | SP-SM | 5Y5/2 light olive grey | SR |
| #7 Miller auger, 4m depth, BH9 | 0.30 | 3 | 2.0 | SP | 10Y6/2 grayish olive | SR |
| #8 Miller auger, 4.3m depth, BH3 | 0.15 | 11 | 2.4 | SP-SM | 10Y6/2 grayish olive | SR |

Notes: USCS is ASTM D-2487 soil classification
BH = borehole
SA = subangular grain shape
SR = subrounded grain shape

Table 2.—*Minimum shear-wave velocities calculated from seismic lines*

| Seismic line | Site | Minimum shear wave velocity | Liquefaction |
|---|---|---|---|
| #1 | Leonardini | 154 m/s | yes |
| #2 | Sea Mist | 198-231 m/s | yes |
| #3 | Miller | 111 m/s | yes |
| #4 | Miller | 100-111 m/s | yes |
| #5 | Miller (clay) | 75-90 m/s | no |

◀ Figure 19.—Grain-size distributions of sand-boil and auger samples from (*A*) Sea Mist-Leonardini Farms and (*B*) Miller Farm study sites (see fig. 7 for locations).

Table 3.—*Typical ranges of shear-wave velocities in saturated sand*

[From Dobry and others (1981)]

| Material | Vs |
|---|---|
| Very recent non-compacted sands | 90-215 m/s |
| Other Holocene sands (<10,000 years) | 150-305 m/s |
| Pleistocene sands (>10,000 years) | 180-425 m/s |

Pajaro Valley area, Santa Cruz and Monterey Counties, California: U.S. Geological Survey Open-File Report, 80 p.

Norton, W.E., 1983, In-situ determination of liquefaction potential using the PQS probe: Vicksburg, Miss., U.S. Army Corps of Engineers, Waterways Experiment Station Technical Report GL-83-1, 101 p.

Peck, R.B., 1979, Liquefaction potential; science versus practice: American Society of Civil Engineers Proceedings, Geotechnical Engineering Division Journal, v. 105, no. GT3, p. 393-398.

Plafker, George, and Galloway, J.P., eds., 1989, Lessons learned from the Loma Prieta, California, earthquake of October 17, 1989: U.S. Geological Survey Circular 1045, 48 p.

Poulos, S.J., 1981, The steady state of deformation: American Society of Civil Engineers Proceedings, Geotechnical Engineering Division Journal, v. 107, no. GT5, p. 533-562.

———1988, Strength for static and dynamic stability analysis, *in* Hydraulic fill structures: American Society of Civil Engineers, Geotechnical Division, Specialty Conference, Fort Collins, Colo., 1988, Proceedings, p. 452-474.

Poulos, S.J., Castro, Gonzalo, and France, J.W., 1985, Liquefaction evaluation procedure: Journal of Geotechnical Engineering, v. 111, no. 6, p. 772-792.

Schmertmann, J.H., 1978, Study of feasibility of using Wissa-type piezometer probe to identify liquefaction potential of fine sands: Vicksburg, Miss., U.S. Army Corps of Engineers, Waterways Experiment Station Technical Report S-78-2, 73 p.

Scott, C.E., 1989, Estimating liquefaction potential of sands using the piezovane: Fort Collins, Colorado State University, M.S. thesis, 111 p.

Seed, H.B., and Idriss, I.M., 1971, Simplified procedure for evaluating soil liquefaction potential: American Society of Civil Engineers Proceedings, Soil Mechanics and Foundations Division Journal, v. 97, no. SM9, p. 1249-1273.

Seed, H.B., Idriss, I.M., and Arango, Ignacio, 1983, Evaluation of liquefaction potential using field performance data: Journal of Geotechnical Engineering, v. 109, no. 3, p. 458-482.

Seed, H.B., and Lee, K.L., 1966, Liquefaction of saturated sands during cyclic loading: American Society of Civil Engineers Proceedings, Soil Mechanics and Foundations Division Journal, v. 97, no. SM8, p. 1099-1119.

Seed, H.B., Tokimatsu, Kohji, Harder, L.F., and Chung, R.M., 1984, The influence of SPT procedures on soil liquefaction resistance evaluations: Berkeley, University of California, Earthquake Engineering Research Center, Report UCB/EERC-84/15, 20 p.

Seed, R.B., Dickenson, S.E., and Idriss, I.M., 1991, Principal geotechnical aspects of the 1989 Loma Prieta earthquake: Soils and Foundations, v. 31, no. 1, p. 1-26.

Seed, R.B., Dickenson, S.E., Riemer, M.F., Bray, J.D., Sitar, Nicholas, Mitchell, J.K., Idriss, I.M., Kayen, R.E., Kropp, Alan, Harder, L.F., Jr., and Power, M.S., 1990, Preliminary report on the principal geotechnical aspects of the October 17, 1989 Loma Prieta earthquake: Berkeley, University of California, Earthquake Engineering Research Center Report UCB/EERC-90/05, 137 p.

Shakal, A.F., Huang, M.J., Reichle, M.S., Ventura, C.E., Cao, T.Q., Sherburne, R.W., Savage, M.K., Daragh, R.B., and Peterson, C.P., 1989, CSMIP strong-motion records from the Santa Cruz Mountains (Loma Prieta), California earthquake of 17 October 1989: California Division of Mines and Geology, Office of Strong Motion Studies Report OSMS 89-06, 196 p.

Terzaghi, Karl, and Peck, R.B., 1967, Soil mechanics in engineering practice (2d ed.): New York, John Wiley and Sons, 729 p.

U.S. Department of the Navy, 1983, Soil dynamics, deep stabilization, and special geotechnical construction: Facilities Engineering Command Design Manual 7.3, 115 p.

Youd, T.L., and Hoose, S.N., 1978, Historic ground failures in northern California triggered by earthquakes: U.S. Geological Survey Professional Paper 993, 177 p.

# SUPPLEMENTARY INFORMATION

## FIELD METHODS FOR THE PIEZOVANE SHEAR TEST

### SCOPE

This method covers the field Piezovane test to determine whether uncemented saturated, cohesionless soils are contractive or dilative. The Piezovane is a field vane equipped with a pore-pressure transducer to record the pore-pressure changes induced during rotation of the vane. W.A. Charlie and L.W. Butler invented this patented device (Charlie and Butler, 1990).

### SUMMARY OF METHOD

The Piezovane test consists of placing a four-bladed vane in uncemented, undisturbed, saturated, cohesionless soils and rapidly rotating it from the surface to determine the pore-pressure response of the surrounding soil sheared by the vane. In addition, the torsional force required to cause a cylindrical surface to be sheared can be converted to a unit shear resistance of the cylindrical surface. The torque can be applied by hand or, preferably, with a geared drive. The rate of rotation should be 30°/s.

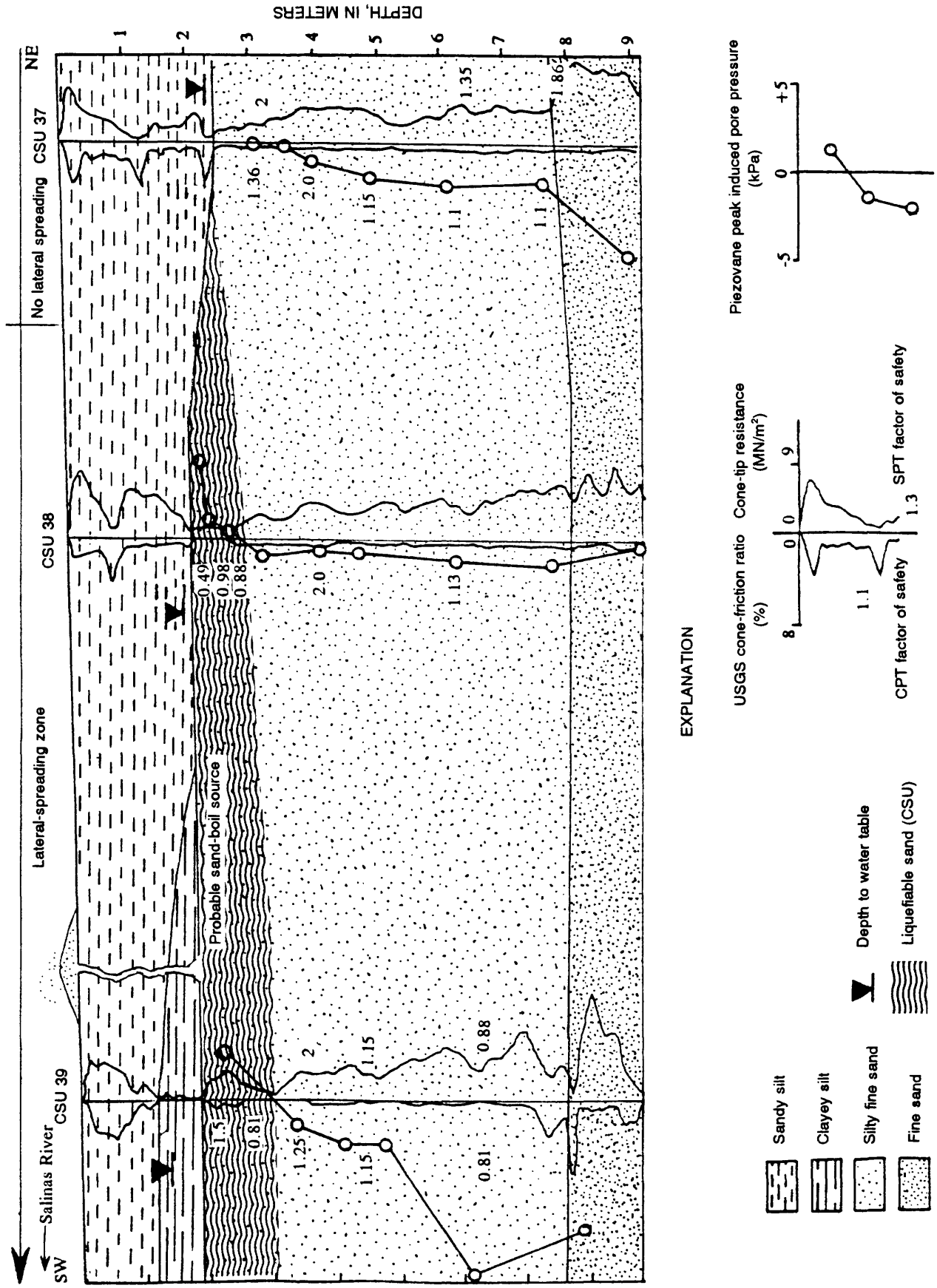


Figure 20.—Soil profile along line of Piezovane test sites CSU 37 through 39 (fig. 8) on the Leonardini Farm (fig. 7). CPT, cone-penetration test; CSU, Colorado State University; SPT, standard penetration test; USGS, U.S. Geological Survey.

### PROCEDURE FOR SATURATING THE PIEZOVANE

1. Full saturation of the vane's ports, internal areas, and the pressure transducer is critical.
2. Saturation of the vane requires immersing it in deaired hot water, using a hypodermic needle to flush hot deaired water through the vane's ports, sealing the ports with silicone grease, vibrating the vane to dislodge any remaining air bubbles, attaching the pressure transducer, and enclosing the vane in a latex-rubber membrane filled with deaired water.

### PROCEDURE FOR INSERTING THE PIEZOVANE

1. Auger a borehole to below the water table.
2. Connect the Piezovane to steel torque rods and insert the Piezovane into the borehole.

### PROCEDURE FOR CONDUCTING A PIEZOVANE TEST

1. Advance the Piezovane to the test depth. Do not rotate the torque rods or vane during advancement. Insert the vane into the soil by pushing at a uniform rate.
2. Following Piezovane advancement, allow any advancement-induced pore pressure to dissipate.
3. Apply torque to the steel torque rods to rotate the vane at a constant rate of 30°/s. Hold the Piezovane at a constant elevation during rotation.
4. Rotate the vane at least 100° (180°–360° preferred).
5. Record the pore pressure, torque, and rotation rate for at least 30 s before the onset of rotation, during rotation, and for 30 s after stopping. Measure and record the pore pressure, torque, and rotation rate at intervals not exceeding 1 s.
6. After the test, rotate the vane 10 revolutions to determine remolded behavior of the soil.
7. Advance the Piezovane to the next depth.

## SPT–CPT FACTOR OF SAFETY AGAINST LIQUEFACTION

### GROUND-MOTION ESTIMATION

Peak accelerations at each site during the 1989 Loma Prieta earthquake were estimated from seismogram data recorded at nearby sites with similar soil conditions. Peak accelerations at the Miller Farm and Southern Pacific Railroad Bridge study sites were determined from a seismograph positioned in the basement of a four-story commercial building in Watsonville (fig. 7). This structure, which is located on fill over alluvium, recorded a peak acceleration of 0.39 *g* (Shakal and others, 1989). The ground motion measured closest to the Sea Mist-Leonardini Farms study site was a peak acceleration of 0.12 *g* at a station located 14.6 km away in the town of Salinas. Modified Mercalli intensities (fig. 21; Plafker and Galloway, 1989) and soil/rock attenuation relations reported by the U.S. Department of the Navy (1983, p. 22–34) were used to independently estimate peak accelerations at the three study sites. Modified Mercalli intensities of VIII and IX for the Miller Farm and Southern Pacific Railroad Bridge study sites correspond to a peak acceleration of 0.21 to 0.39 *g*, which agrees with the 0.39 *g* recorded in Watsonville. The modified Mercalli intensity at the Sea Mist-Leonardini Farms study site is almost VII, which corresponds to a peak acceleration of 0.07 to 0.13 *g*. We used distance and soil/rock attenuation relations to estimate a peak acceleration of 0.16 *g* for the Sea Mist-Leonardini Farms study site. We used peak accelerations of 0.39 *g* for the Miller Farm and Southern Pacific Railroad Bridge study sites and 0.14 *g* for the Sea Mist-Leonardini Farms study site for this study, on the basis of the information described above.

### LEVEL-GROUND-LIQUEFACTION ANALYSIS

#### STANDARD PENETRATION TEST

The cyclic-stress ratio, $R_i$, during the 1989 Loma Prieta earthquake at different depths in the field was calculated by the following equation, proposed and outlined by Seed and Idriss (1971) and outlined by the U.S. Department of the Navy (1983):

$$R_i = \frac{\tau}{\sigma'} = 0.65 a_{\max} \frac{\sigma}{\sigma'} r_d,$$

where $\tau$ is the average cyclic shear stress generated by design ground motion; $\sigma'$ is the initial static effective overburden stress on the sand layer under consideration; $\sigma$ is the total overburden stress on the sand layer under consideration; $a_{\max}$ is the peak acceleration (in *g*); and $r_d$ is a stress-reduction factor, decreasing from 1 at the ground surface to 0.9 at about 10-m depth. Estimated soil densities used to determine the total overburden stress are listed in table 4.

The SPT blowcounts (*N* values) at particular depths were used to determine the cyclic-stress ratio required to cause level-ground liquefaction during an earthquake of a particular magnitude ($R_f$). Field blowcounts were initially adjusted to a standard hammer-energy efficiency of 60 percent, as recommended by Seed and others (1984):

$$N_{60} = N\left(\frac{\mathrm{ERm}}{60}\right),$$

where $N_{60}$ is the blowcount adjusted to 60 percent of free-fall energy, *N* is the field blowcount, and ERm is the rod energy ratio for the investigative method used (in

percent). A rod-energy ratio of 68 percent was used in the SPT investigation (M.J. Bennett, oral commun., 1990), yielding a multiplication factor of 1.13*N*. $N_{60}$ values were adjusted to an overburden pressure of 100 kPa by determining the appropriate $C_n$ value of Seed and others (1983):

$$(N_1)_{60} = C_n N_{60}.$$

The $(N_1)_{60}$ value was used to determine the cyclic-stress ratio, $R_f$, required to cause liquefaction during an $M$=7.5 earthquake (Seed and others, 1983).

This $R_f$ value was corrected for an $M$=7.1 earthquake (Loma Prieta) by dividing the appropriate correction factor proposed by Seed and others (1984), listed in table 5. The 1989 Loma Prieta earthquake induced an estimated 12 loading cycles with an amplitude of 65 percent of the peak amplitude. The correction factor used was 1.08. The corrected $R_f$ value was used to determine the factor of safety against level-ground liquefaction for each layer by the relation

$$\mathrm{FS} = \frac{R_f}{R_i}$$

where $R_i$ is the cyclic-stress ratio for the $i$th layer.

The data required for SPT liquefaction analysis of the study sites are listed in table 6, along with the calculated factors of safety. SPT liquefaction analysis was omitted for certain boreholes and depths, owing to absence of SPT blowcounts.

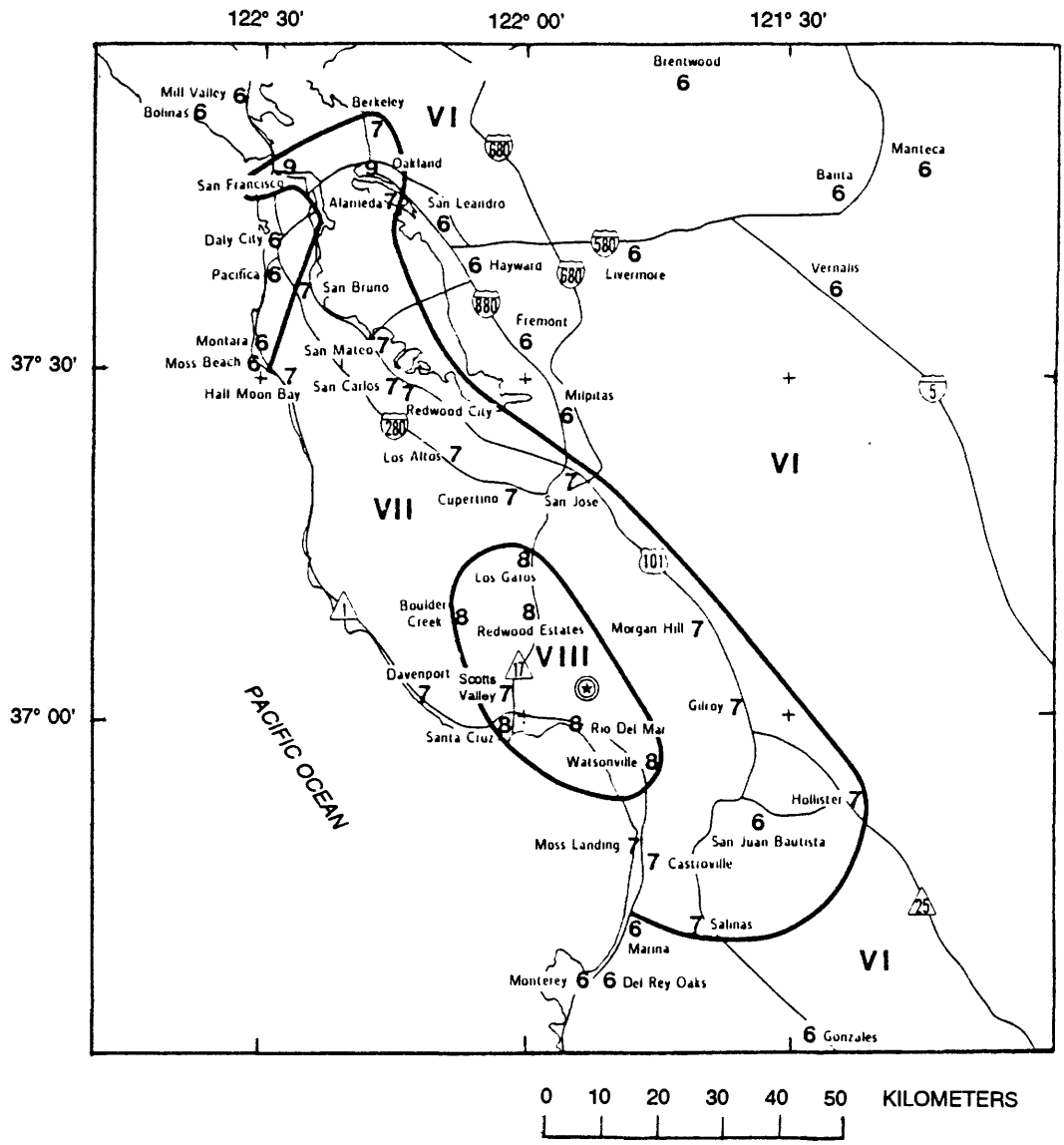


Figure 21.—San Francisco-Monterey Bay region, showing distribution of modified Mercalli intensities (Roman and Arabic numerals) from 1989 Loma Prieta earthquake. After Plafker and Galloway (1989).

Table 4.—*Estimated unit weights used in field stress calculations*

[After Terzaghi and Peck (1968)]

| Soil description | Moisture | Unit weight ($kN/m^3$) | Density ($kg/m^3$) |
|---|---|---|---|
| Micaceous silty sand ($G_s$=2.7) | Dry | 13.4 | 1,263 |
| | Saturated | 18.0 | 1,841 |
| | Moist (50 percent saturated) | 14.5 | 1,400 |
| Uniform subangular sand ($G_s$=2.67) | Dry | 16.5 | 1,681 |
| | Saturated | 19.3 | 1,978 |

Table 5.—*Relation between earthquake magnitude, number of equivalent uniform load cycles, and magnitude- or duration-correction factor*

| Magnitude, $M$ | Number of representative cycles at $0.65\tau_{cyclic,max}$ | Magnitude or duration correction factor; $C_M$ |
|---|---|---|
| 8.5 | 26 | 0.89 |
| 7.5 | 15 | 1.0 |
| 6.75 | 10 | 1.13 |
| 6 | 5-6 | 1.32 |
| 5.25 | 2-3 | 1.5 |

## CONE-PENETRATION TEST

Cone-tip resistances and friction ratios at various depths were converted to equivalent SPT blowcounts for level-ground-liquefaction analysis of questionable intervals in which blowcounts had not been measured. As with the SPT analysis, soil conditions and ground motions at the sites must be determined to use the CPT for liquefaction analysis. We used the same unit weights and estimated peak accelerations discussed previously. Cone-tip resistance, $q_c$, at a particular depth is adjusted for overburden pressure by multiplying by a correction factor (Martin, 1991):

$$q_{c1} = q_c C_p,$$

where $q_{c1}$ is the normalized cone-tip resistance to 100 kPa, $q_c$ is the field tip resistance, and $C_p$ is the overburden-correction factor. The normalized cone-tip resistance, $q_{c1}$, and friction ratio were used with Martin's (1991) chart to estimate the SPT blowcount, $N_1'$. $R_f$ values were read from Seed and others' (1983) SPT chart and corrected for an $M$=7.1 earthquake. Factors of safety calculated from this analysis, along with the data required for CPT liquefaction analysis, are listed in table 7, and the estimated CPT and SPT factors of safety against liquefaction are compared in figure 22.

Table 6.—*Standard-penetration-test data for level-ground-liquefaction analysis*

[$a_{max}$=0.14 *g* for Sea Mist-Leonardini Farms study site; $a_{max}$=0.39 *g* for Miller Farm and Southern Pacific Railroad Bridge study sites. Unit weight of soil estimated from table 4. σ, total static overburden stress; σ′, initial static overburden effective stress; $r_d$, stress-reduction factor for depth; $D_{50}$, particle diameter of 50-percent passing, by weight; *N*, field blowcount; $C_n$, overburden-correction factor; $N_1$, field blowcount adjusted to overburden pressure of 100 kPa, $(N_1)_{60}$, blowcount adjusted to 60 percent of free-fall energy and to overburden pressure of 100 kPa, with correction factor of 1.13; $R_i$, cyclic-stress ratio; $R_f$, cyclic-stress ratio required to cause liquefaction; τ, average cyclic shear stress; FS, factor of safety]

| CSU test site (figs. 8,14,16) | Depth (m) | σ (kPa) | σ′ (kPa) | $r_d$ | $D_{50}$ (mm) | Fines content (pct) | *N* | $C_n$ | $N_1$ | $(N_1)_{60}$ | $R_i(\tau/\sigma')$ | $R_f(\tau/\sigma)$ 7.5 | $R_f$ 7.1 | FS 7.1 |
|---|---|---|---|---|---|---|---|---|---|---|---|---|---|---|
| 3 | 5.4 | 76.8 | 70.9 | 0.96 | 0.086 | 41 | 6 | 1.15 | 6.9 | 7.8 | 0.26 | 0.19 | 0.20 | 0.77 |
| 3 | 6.7 | 98.9 | 81.0 | .95 | .120 | 22 | 13 | 1.13 | 14.7 | 16.6 | .29 | .255 | .27 | .93 |
| 3 | 7.9 | 120.9 | 91.0 | .94 | .115 | 23 | 26 | 1.04 | 27.0 | 30.5 | .32 | .60 | .70 | 2.50 |
| 8 | 4.5 | 62.5 | 61.0 | .97 | .082 | 45 | 11 | 1.24 | 13.6 | 15.4 | .25 | .33 | .36 | 1.44 |
| 8 | 5.7 | 85.3 | 71.8 | .96 | .143 | 17 | 9 | 1.14 | 10.3 | 11.6 | .29 | .18 | .19 | .66 |
| 8 | 7.3 | 114.7 | 86.3 | .95 | .263 | 14 | 9 | 1.06 | 9.5 | 10.8 | .32 | .16 | .17 | .53 |
| 31 | 1.2 | 19.0 | 14.8 | .99 | .054 | 68 | 5 | 1.93 | 9.6 | 10.8 | .11 | .25 | .27 | 2.50 |
| 31 | 3.3 | 57.5 | 32.5 | .98 | .098 | 29 | 5 | 1.65 | 8.2 | 9.3 | .16 | .17 | .18 | 1.12 |
| 31 | 4.2 | 74.1 | 40.0 | .97 | .123 | 16 | 7 | 1.42 | 9.9 | 11.2 | .16 | .17 | .18 | 1.12 |
| 31 | 5.1 | 90.6 | 47.5 | .96 | .240 | 22 | 9 | 1.37 | 12.3 | 13.9 | .17 | .206 | .22 | 1.30 |
| 31 | 7.3 | 129.1 | 65.2 | .95 | .240 | 14 | 13 | 1.21 | 15.7 | 17.7 | .17 | .24 | .26 | 1.50 |
| 31 | 8.5 | 151.2 | 75.3 | .93 | .260 | 11 | 10 | 1.12 | 12.1 | 13.7 | .17 | .17 | .18 | 1.08 |
| 37 | 3.3 | 49.7 | 41.0 | .98 | .105 | 13 | 9 | 1.50 | 13.5 | 15.2 | .11 | .21 | .22 | 2 |
| 37 | 6.4 | 104.8 | 66.2 | .95 | .195 | 8 | 11 | 1.19 | 13.1 | 14.8 | .14 | .178 | .19 | 1.35 |
| 37 | 7.9 | 132.3 | 78.8 | .94 | .197 | 6 | 17 | 1.12 | 19.0 | 21.5 | .14 | .24 | .26 | 1.86 |
| 39 | 3.2 | 49.7 | 36.6 | .98 | .185 | 11 | 10 | 1.55 | 15.5 | 17.5 | .12 | .23 | .25 | 2.00 |
| 39 | 4.2 | 69.0 | 45.4 | .97 | .210 | 10 | 7 | 1.38 | 9.7 | 10.9 | .13 | .14 | .15 | 1.15 |
| 39 | 6.4 | 107.5 | 63.0 | .95 | .305 | 5 | 8 | 1.18 | 9.4 | 10.8 | .15 | .122 | .13 | .88 |
| 48 | 6.4 | 91.2 | 80.8 | .95 | .168 | 13 | 7 | 1.10 | 7.7 | 8.7 | .27 | .12 | .13 | .48 |
| 48 | 7.3 | 116.3 | 96.9 | .95 | --- | --- | 10 | 1.05 | 10.5 | 11.9 | .29 | .17 | .18 | .62 |
| 48 | 8.5 | 129.8 | 98.4 | .93 | .164 | 14 | 11 | .98 | 10.8 | 12.2 | .31 | .18 | .19 | .63 |

Notes: $a_{max}$ = 0.14*g* for Sea Mist-Leonardini sites
$a_{max}$ = 0.39*g* for Miller-SP sites
$(N_1)_{60}$ SPT correction factor = 1.13
FS = factor of safety
unit weight of soil estimated from Table 4

Table 7.—*Cone-penetration-test data for level-ground-liquefaction analysis*

[$a_{max}$=0.14 *g* for Sea Mist-Leonardini Farms study site; $a_{max}$=0.39 *g* for Miller Farm and Southern Pacific Railroad Bridge study sites. Unit weight of soil estimated from table 4. s, total static overburden stress; σ′, initial static overburden effective stress; $C_p$, overburden correction factor for cone; $q_{c1}$, tip resistance corrected to overburden pressure of 100 kPa; SPT, standard peentration test; $(N_1)_{60}$, blowcount adjusted to 60 percent of free-fall energy and to overburden pressure of 100 kPa; $R_i$, cyclic-stress ratio; τ, average cyclic shear stress; $R_f$, cyclic-stress ratio required to cause liquefaction; FS, factor of safety]

| CSU test site (figs. 8,14,16) | Depth (m) | σ (kPa) | σ′ (kPa) | Cone (kPa) | $C_p$ | $q_{c1}$ | Friction ratio | Equivalent SPT blowcount | Actual SPT $(N_1)_{60}$ | $R_i$ (τ/σ′) | $R_f$(τ/σ′) | $R_f$ | FS |
|---|---|---|---|---|---|---|---|---|---|---|---|---|---|
| 3 | 5.4 | 76.8 | 70.9 | 23.0 | 1.28 | 29.4 | 0.3 | 5 | 7.8 | 0.26 | 0.15 | 0.16 | |
| 3 | 5.7 | 82.4 | 73.4 | 21.9 | 1.14 | 24.9 | .9 | 6 | --- | .27 | .15 | .16 | 0.61 |
| 3 | 6.7 | 98.9 | 81.0 | 41.7 | 1.17 | 48.8 | .5 | 9 | 16.6 | .29 | .15 | .16 | .59 |
| 3 | 7.9 | 120.9 | 91.1 | 76.2 | 1.05 | 80.0 | .8 | 19 | 30.5 | .32 | .30 | .32 | .55 |
| 8 | 5.4 | 79.0 | 68.6 | 64.7 | 1.28 | 82.8 | 1.0 | 20 | --- | .28 | .29 | .31 | |
| 8 | 5.7 | 85.3 | 71.9 | 81.4 | 1.25 | 101.7 | 1.0 | 28 | 11.6 | .29 | .35 | .38 | 1.00 |
| 8 | 7.3 | 114.7 | 86.4 | 44.9 | 1.10 | 49.4 | .4 | 9 | 10.8 | .32 | .15 | .2 | |
| 9 | 5.1 | 82.2 | 70.2 | 62.6 | 1.30 | 81.4 | .7 | 18 | --- | .28 | .25 | .27 | 1.10 |
| 9 | 6.0 | 99.8 | 79.0 | 38.6 | 1.19 | 46.0 | .5 | 8 | --- | .30 | .15 | .16 | |
| 9 | 7.6 | 129.3 | 93.5 | 57.4 | 1.02 | 58.5 | .5 | 10 | --- | .33 | .15 | .16 | 1.30 |
| 30 | 2.1 | 28.4 | 22.5 | 10.4 | 2.70 | 28.1 | .8 | 7 | --- | .11 | .10 | .11 | .47 |
| 30 | 2.7 | 44.2 | 32.3 | 10.4 | 2.13 | 22.1 | .7 | 5 | --- | .12 | .11 | .12 | .96 |
| 30 | 3.0 | 49.7 | 34.6 | 15.7 | 2.00 | 31.4 | .6 | 7 | --- | .13 | .13 | .14 | .53 |
| 30 | 3.3 | 55.3 | 37.4 | 15.7 | 1.85 | 29.0 | 1.0 | 7 | --- | .13 | .12 | .13 | .48 |
| 30 | 4.5 | 76.2 | 46.9 | 47.0 | 1.66 | 78.0 | .8 | 18 | --- | .14 | .26 | .28 | .98 |
| 30 | 6.0 | 104.8 | 60.0 | 80.4 | 1.40 | 112.5 | .6 | 21 | --- | .15 | .32 | .35 | |
| 30 | 8.2 | 98.6 | 76.9 | 40.4 | 1.20 | 48.5 | .8 | 10 | --- | .16 | .15 | .16 | 1.00 |
| 31 | 2.4 | 41.0 | 24.9 | 22.9 | 2.38 | 54.5 | .5 | 10 | --- | .15 | .17 | .18 | |
| 31 | 3.3 | 57.5 | 32.5 | 10.4 | 2.13 | 22.1 | .5 | 5 | 8.2 | .16 | .12 | .13 | 1.10 |
| 31 | 4.2 | 74.1 | 40.1 | 27.1 | 1.80 | 48.8 | .5 | 9 | 9.9 | .16 | .15 | .16 | |
| 31 | 5.1 | 90.6 | 47.6 | 41.8 | 1.65 | 68.9 | .3 | 11 | 12.3 | .17 | .18 | .19 | 1.00 |
| 31 | 7.6 | 134.6 | 66.9 | 41.8 | 1.33 | 55.6 | 1.2 | 15 | --- | .18 | .21 | .23 | |
| 37 | 3.3 | 49.7 | 41.1 | 31.3 | 1.75 | 54.8 | .5 | 9 | 13.5 | .11 | .14 | .15 | 2.00 |
| 37 | 3.9 | 60.7 | 46.1 | 47.0 | 1.65 | 77.5 | .6 | 16 | --- | .12 | .22 | .24 | |
| 37 | 4.8 | 77.2 | 53.7 | 41.7 | 1.50 | 62.5 | .4 | 10 | --- | .13 | .14 | .15 | 2.30 |
| 37 | 5.4 | 88.2 | 58.7 | 23.0 | 1.45 | 33.3 | .5 | 6 | --- | .13 | .09 | .10 | |
| 37 | 6.4 | 104.8 | 66.3 | 49.0 | 1.33 | 65.2 | .5 | 11 | 13.1 | .14 | .15 | .16 | 1.00 |
| 37 | 7.6 | 126.8 | 76.3 | 41.7 | 1.20 | 50.0 | .6 | 10 | --- | .14 | .14 | .15 | |
| 38 | 2.1 | 31.6 | 26.6 | 15.7 | 2.50 | 39.2 | .1 | 5 | --- | .11 | .05 | .05 | 1.20 |
| 38 | 2.1 | 32.7 | 27.1 | 12.5 | 2.50 | 31.2 | .1 | 5 | --- | .11 | .10 | .11 | .81 |
| 38 | 2.4 | 37.1 | 29.1 | 13.6 | 2.20 | 29.7 | .1 | 4 | --- | .11 | .09 | .10 | .98 |
| 38 | 3.9 | 55.5 | 33.1 | 52.2 | 2.10 | 109.6 | .5 | 20 | --- | .15 | .29 | .31 | 1.1 |
| 38 | 6.0 | 55.3 | 59.3 | 43.8 | 1.40 | 61.3 | .5 | 11 | --- | .15 | .16 | .17 | |
| 39 | 2.1 | 30.4 | 27.8 | 31.3 | 2.50 | 78.3 | .4 | 13 | --- | .1 | .14 | .15 | 1.27 |

Table 7.—*Continued.*

| CSU test site (figs. 8,14,16) | Depth (m) | σ (kPa) | σ′ (kPa) | Cone (kPa) | $C_p$ | $q_{c1}$ | Friction ratio | Equivalent SPT blowcount | Actual SPT $(N_1)_{60}$ | $R_t$ ($\tau/\sigma'$) | $R_f(\tau/\sigma')$ | $R_f$ | FS |
|---|---|---|---|---|---|---|---|---|---|---|---|---|---|
| 39 | 2.7 | 42.0 | | 10.4 | 1.95 | 20.4 | .1 | 3 | --- | .11 | .08 | .09 | |
| 39 | 3.2 | 49.7 | | 33.4 | 1.88 | 62.8 | .2 | 9 | 17.5 | .12 | .14 | .15 | 1.36 |
| | | | | 3_3.4 | | | .3 | | | | | | |
| 39 | | | | 5_2.2 | 1.67 | | .3 | | | | | | 2.00 |
| 39 | | | | | | | | | | | | | |
| 48 | | | | | | | | | | | | | 1.15 |
| | | | | | | | | | | | | | .74 |
| | | | | | | | | | | | | | 1.10 |
| | | | | | | | | | | | | | 1.07 |
| | | | | | | | | | | | | | .49 |
| | | | | | | | | | | | | | .98 |
| | | | | | | | | | | | | | .88 |
| | | | | | | | | | | | | | 2.00 |
| | | | | | | | | | | | | | 1.13 |
| | | | | | | | | | | | | | 1.50 |
| | | | | | | | | | | | | | .81 |
| | | | | | | | | | | | | | 1.25 |
| | | | | | | | | | | | | | 1_.1 |
| | | | | | | | | | | | | | 5 |
| | | | | | | | | | | | | | .81 |
| 39 | 2.7 | 42.1 | 33.1 | 10.4 | 1.95 | 20.4 | .1 | 3 | --- | .11 | .08 | .09 | .81 |
| 39 | 3.2 | 49.8 | 36.6 | 33.4 | 1.88 | 62.8 | .2 | 9 | 17.5 | .12 | .14 | .15 | |
| Table 7 | 4.2 | 69.0 | 45.4 | 33.4 | 1.67 | 55.8 | .3 | 9 | 10.9 | .13 | .14 | .15 | 1.25 |
| (cont.) | 6.4 | 107.5 | 63.1 | 52.2 | 1.37 | 71.5 | .3 | 10 | 10.8 | .15 | .11 | .12 | |
| 39 | 5.7 | 80.2 | 75.7 | 62.6 | 1.22 | 76.4 | 1.0 | 19 | --- | .26 | .24 | .26 | 1.15 |
| 39 | 6.4 | 48.1 | 80.8 | 26.1 | 1.17 | 30.5 | 1.0 | 8 | 8.7 | .27 | .14 | .15 | .81 |
| | 7.0 | 116.6 | 85.8 | 41.8 | 1.12 | 46.8 | 1.0 | 10 | 10.6 | .29 | .15 | .16 | |
| 48 | 7.3 | 116.3 | 96.9 | 39.7 | 1.1 | 43.7 | 1.0 | 11 | 10.5 | .29 | .16 | .17 | 1.00 |
| 48 | 8.5 | 129.8 | 98.4 | 57.4 | .99 | 56.8 | .8 | 11 | 12.2 | .31 | .16 | .17 | .56 |
| 48 | | | | | | | | | | | | | .55 |
| 48 | | | | | | | | | | | | | .59 |
| 48 | | | | | | | | | | | | | .54 |

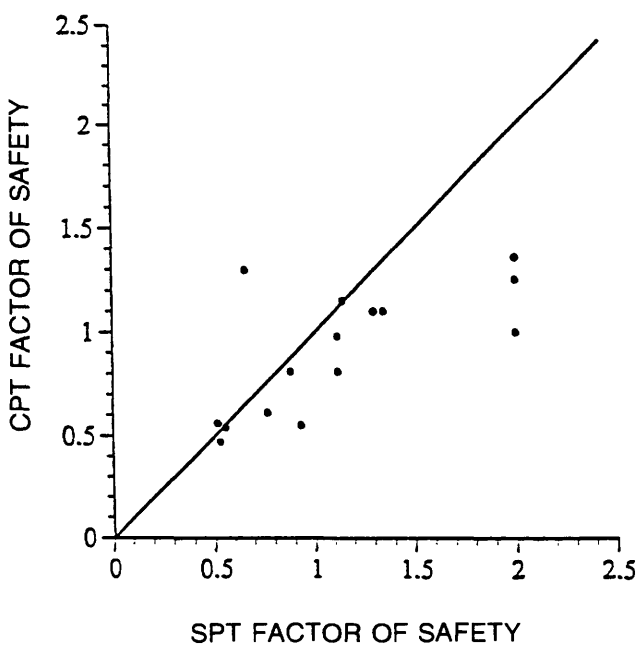


Figure 22.—Cone-penetration-test (CPT) versus standard-penetration-test (SPT) factors of safety against liquefaction, calculated from data of this study.

# APPENDIX

## PIEZOVANE TESTS

## COLORADO STATE UNIVERSITY GEOTECHNICAL LOG

HOLE NUMBER CSU Miller 1[1] PROJECT LIQUEFACTION POTENTIAL USING CSU PIEZOVANE

LOCATION WATSONVILLE, CALIFORNIA COORDINATES

DATE TESTED 8/17/90 GROUND WATER 10.0 ft.

PERSONNEL D: J. BRISLAWN, L: H. HASSEN ELEVATION

CSU PIEZOVANE TESTS

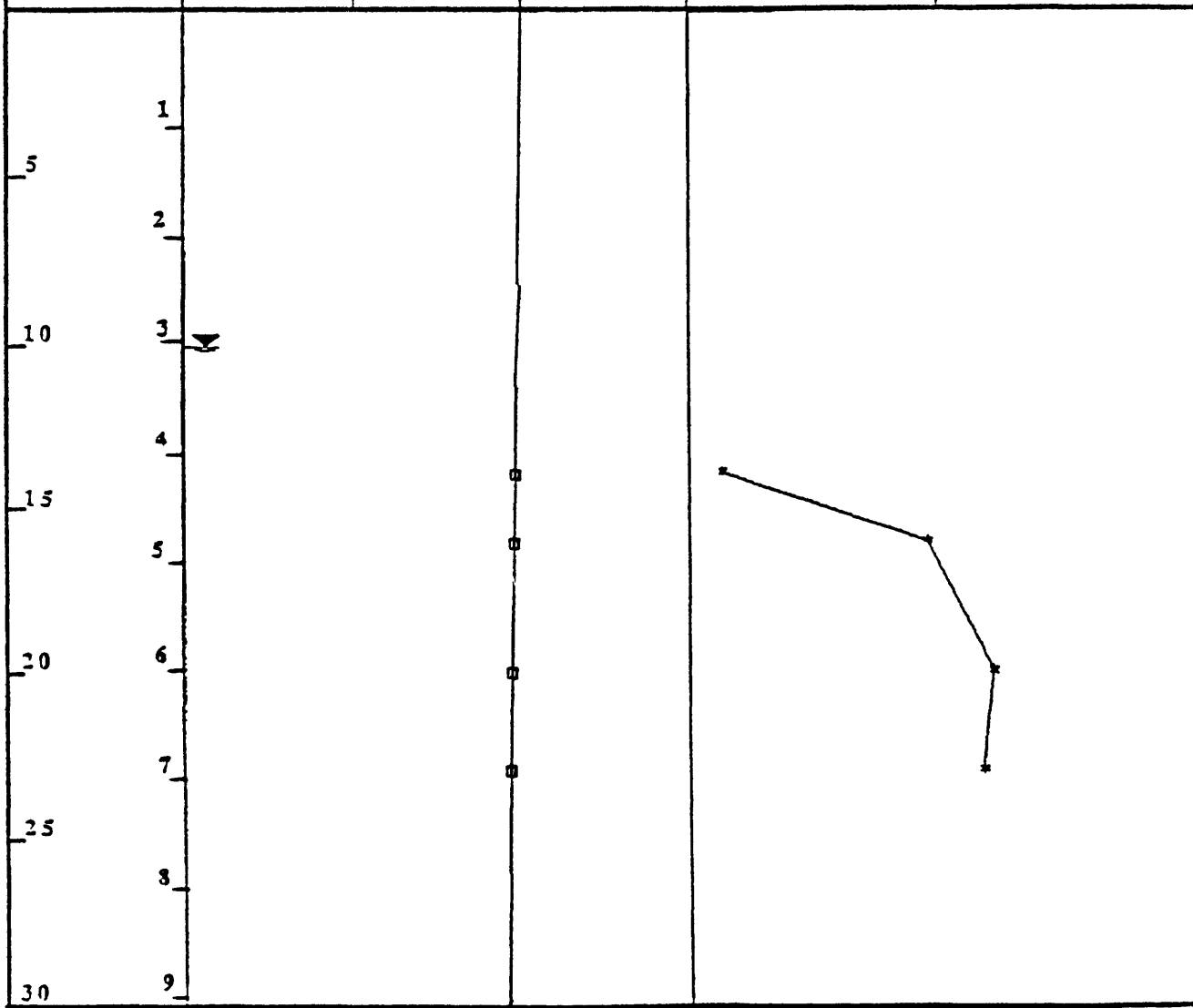


REMARKS:

1. Clint Miller Strawberry Farms.

* Not corrected for rod friction.

## COLORADO STATE UNIVERSITY GEOTECHNICAL LOG

HOLE NUMBER CSU Miller 3 [1]
PROJECT LIQUEFACTION POTENTIAL USING CSU PIEZOVANE
LOCATION WATSONVILLE, CALIFORNIA
COORDINATES
DATE TESTED 8/18/90
GROUND WATER 15.0 ft.
PERSONNEL D: J. BRISLAWN, L: H. HASSEN
ELEVATION

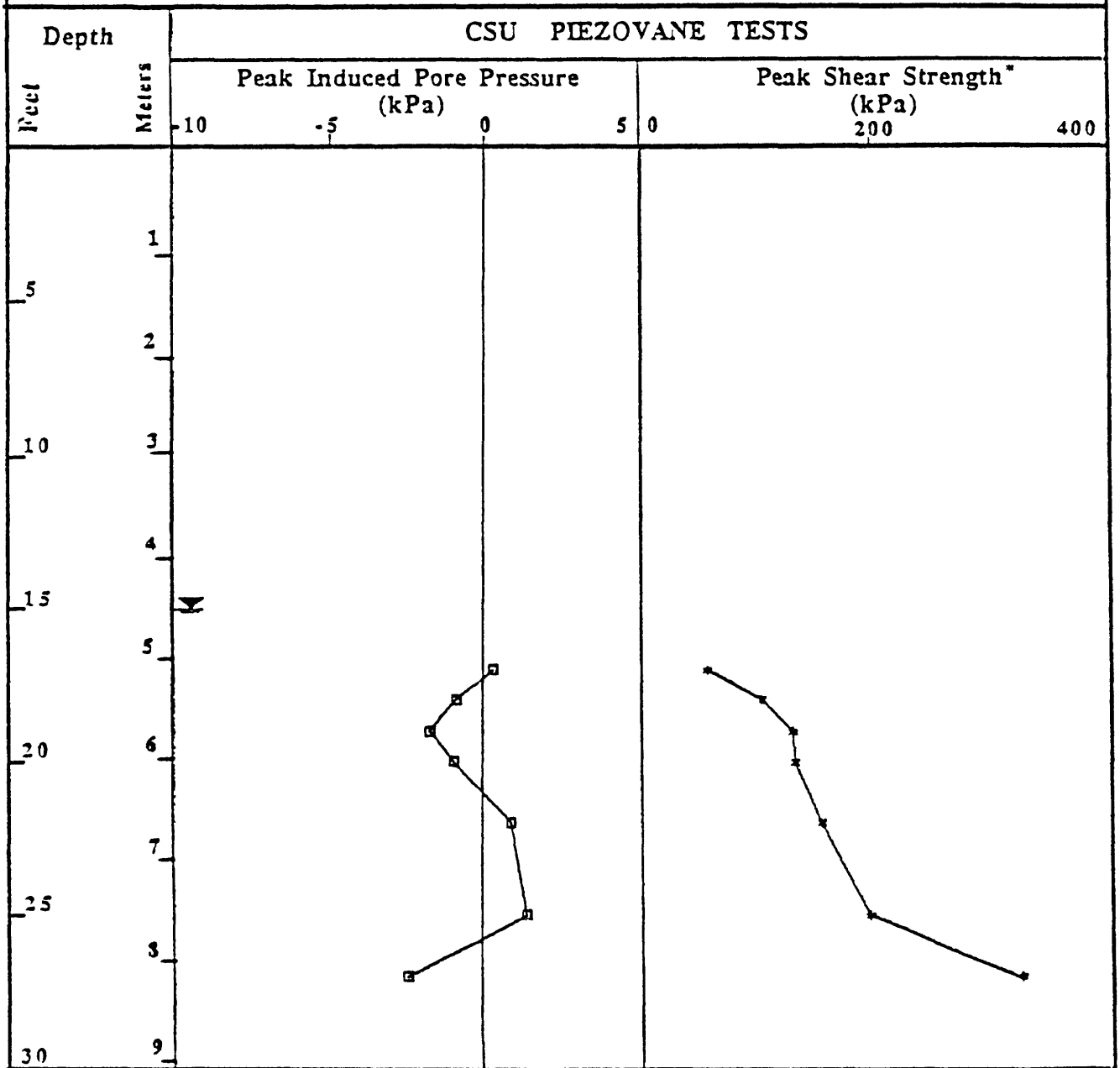


REMARKS:
1. Clint Miller Strawberry Farms.

* Not corrected for rod friction.

# COLORADO STATE UNIVERSITY GEOTECHNICAL LOG

HOLE NUMBER CSU Miller 8 [1]
LOCATION WATSONVILLE, CALIFORNIA
DATE TESTED 8/15/90
PERSONNEL D: J. BRISLAWN, L: H. HASSEN

PROJECT LIQUEFACTION POTENTIAL USING CSU PIEZOVANE
COORDINATES
GROUND WATER 15.5 ft.
ELEVATION

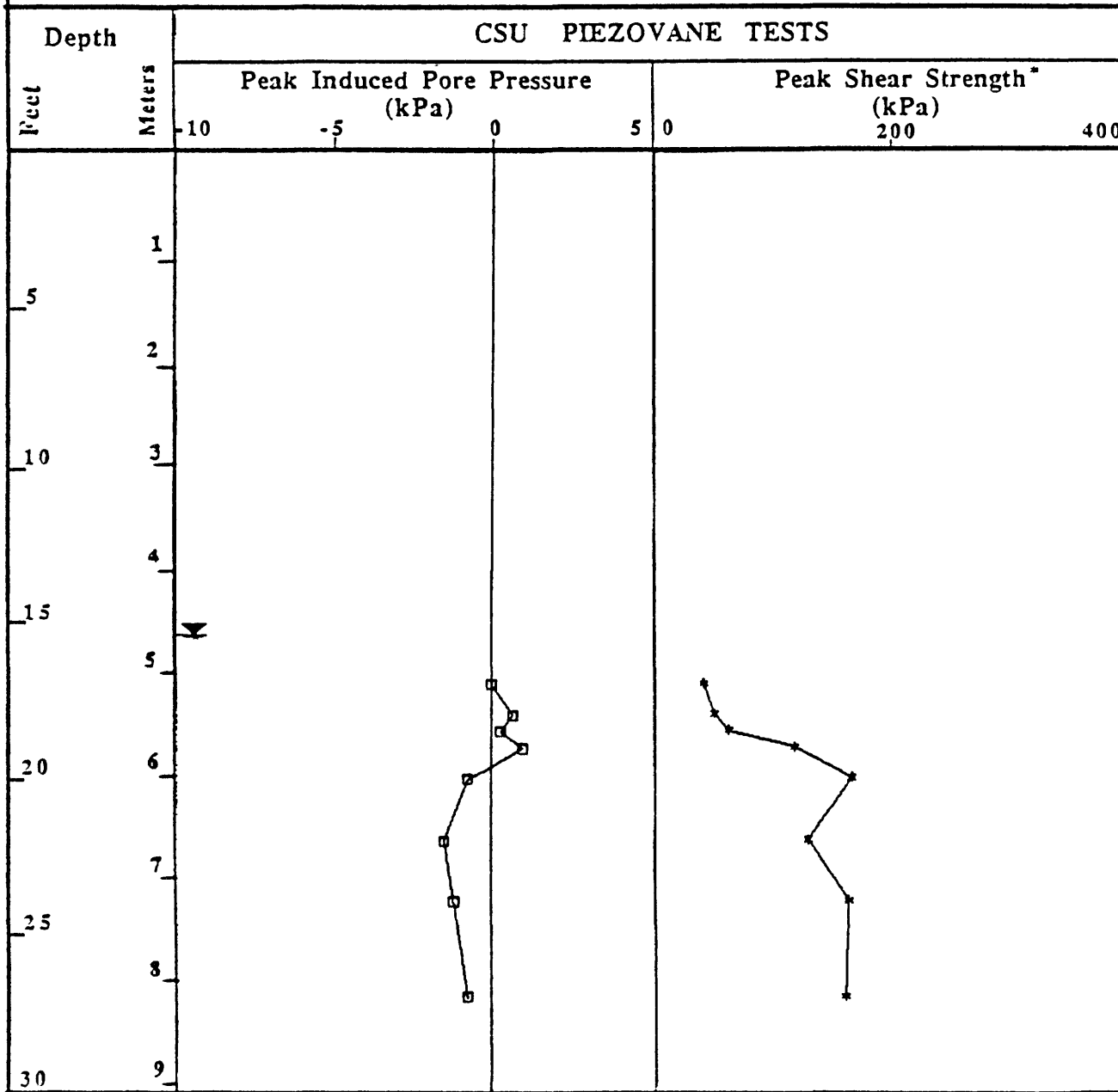


REMARKS:

1. Clint Miller Strawberry Farms

* Not corrected for rod friction.

## COLORADO STATE UNIVERSITY GEOTECHNICAL LOG

HOLE NUMBER CSU Miller 9 [1]
PROJECT LIQUEFACTION POTENTIAL USING CSU PIEZOVANE
LOCATION WATSONVILLE, CALIFORNIA
COORDINATES
DATE TESTED 8/14/90
GROUND WATER 13.6 ft.
PERSONNEL D: J. BRISLAWN, L: H. HASSEN
ELEVATION

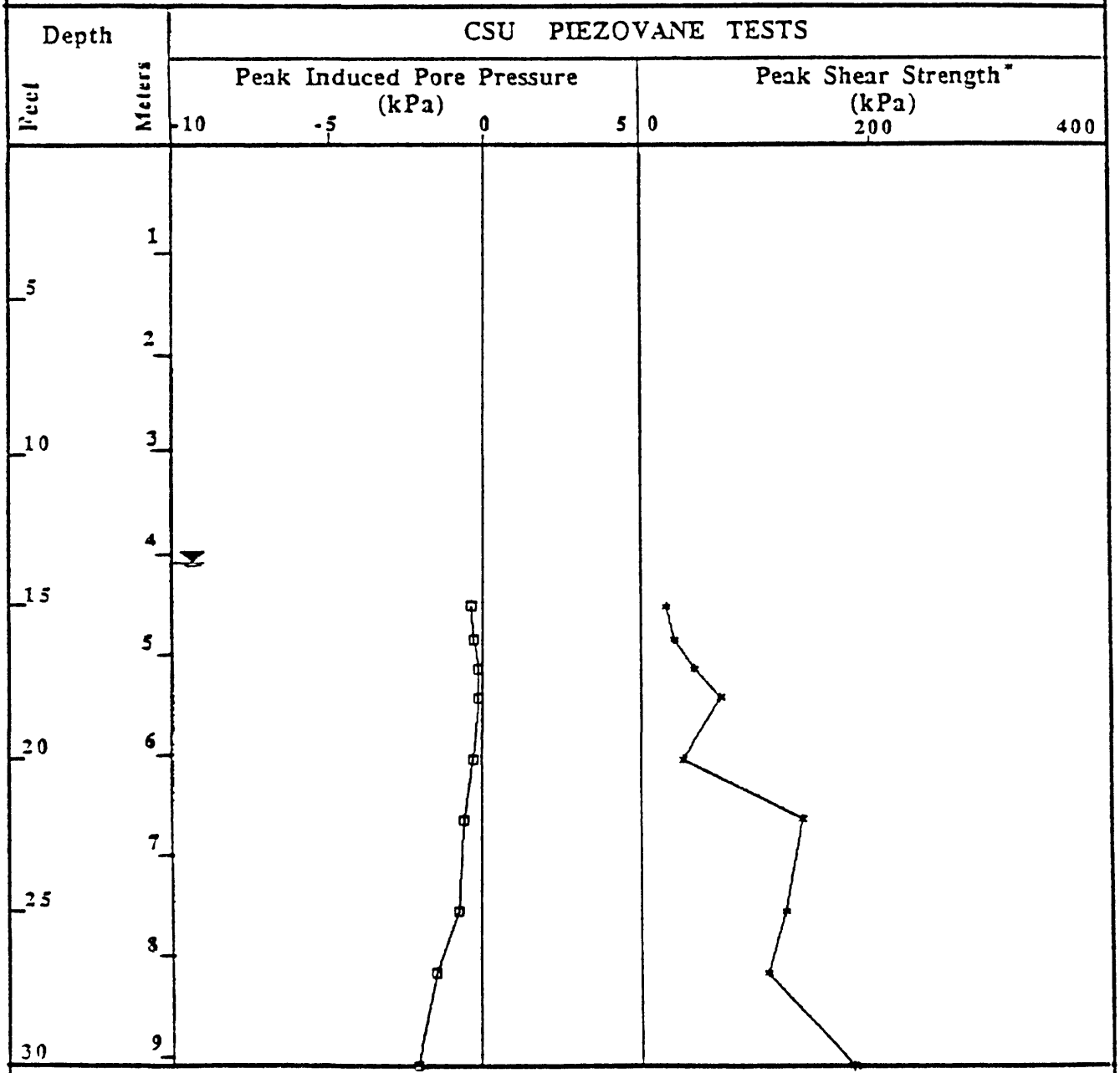


REMARKS:

1. Clint Miller Strawberry Farms

* Not corrected for rod friction.

## COLORADO STATE UNIVERSITY GEOTECHNICAL LOG

HOLE NUMBER CSU Miller 10 [1]
LOCATION WATSONVILLE, CALIFORNIA
DATE TESTED 8/16/90
PERSONNEL D: J. BRISLAWN, L: H. HASSEN

PROJECT LIQUEFACTION POTENTIAL USING CSU PIEZOVANE
COORDINATES
GROUND WATER 12.0 ft.
ELEVATION

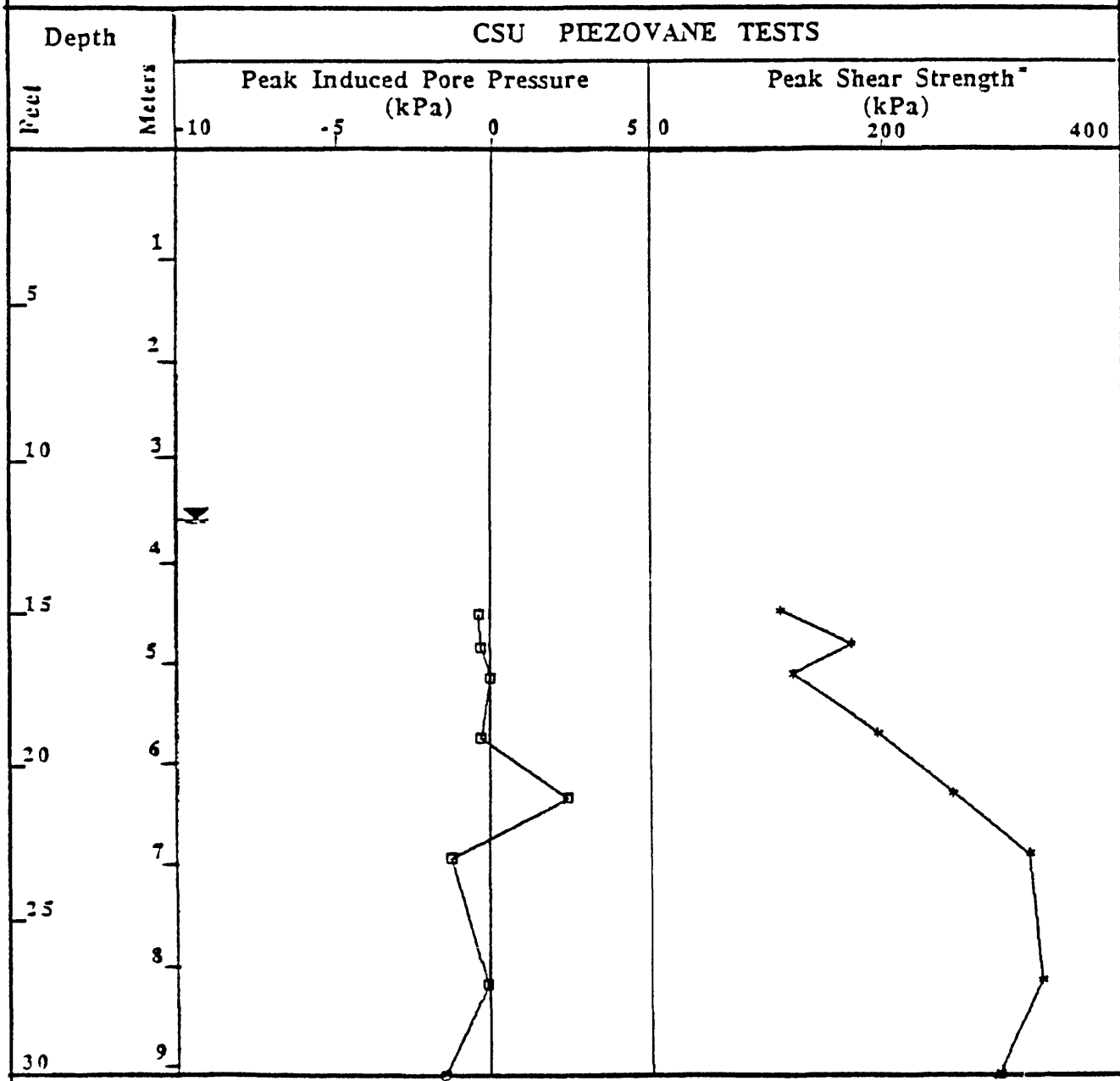


REMARKS:

1. Clint Miller Strawberry Farms

* Not corrected for rod friction.

## COLORADO STATE UNIVERSITY GEOTECHNICAL LOG

HOLE NUMBER CSU Sea Mist 29
PROJECT LIQUEFACTION POTENTIAL USING CSU PIEZOVANE
LOCATION NEAR CASTROVILLE,[1] CALIFORNIA
COORDINATES
DATE TESTED 8/13/90
GROUND WATER 9.0 ft.
PERSONNEL D: J. BRISLAWN, L: H. HASSEN
ELEVATION

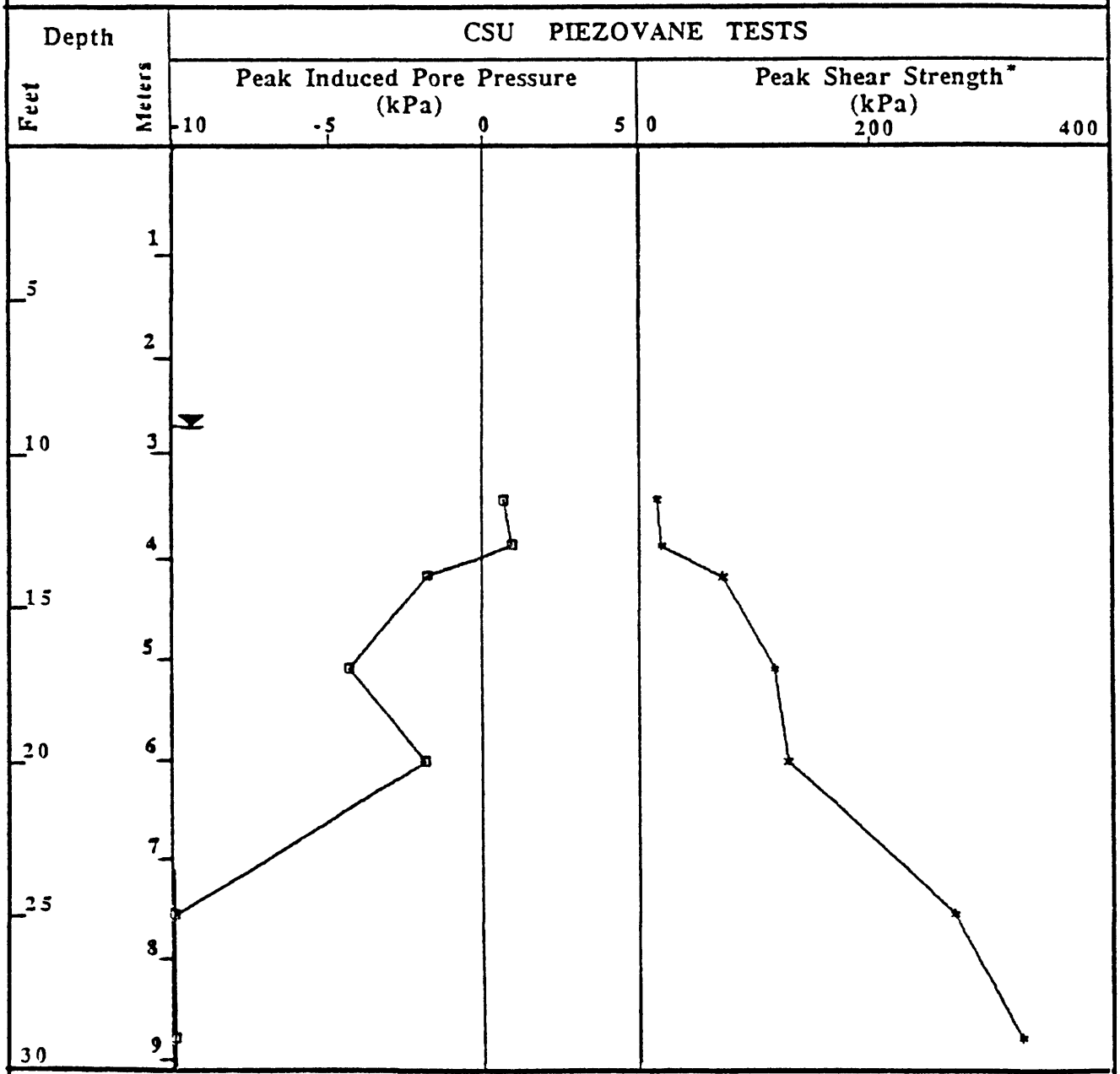


REMARKS:
1. Sea Mist Farms

* Not corrected for rod friction.

## COLORADO STATE UNIVERSITY GEOTECHNICAL LOG

HOLE NUMBER CSU Sea Mist 30
PROJECT LIQUEFACTION POTENTIAL USING CSU PIEZOVANE
LOCATION NEAR CASTROVILLE,[1] CALIFORNIA
COORDINATES
DATE TESTED 8/12/90
GROUND WATER 6.33 ft.
PERSONNEL D: J. BRISLAWN, L: H. HASSEN
ELEVATION

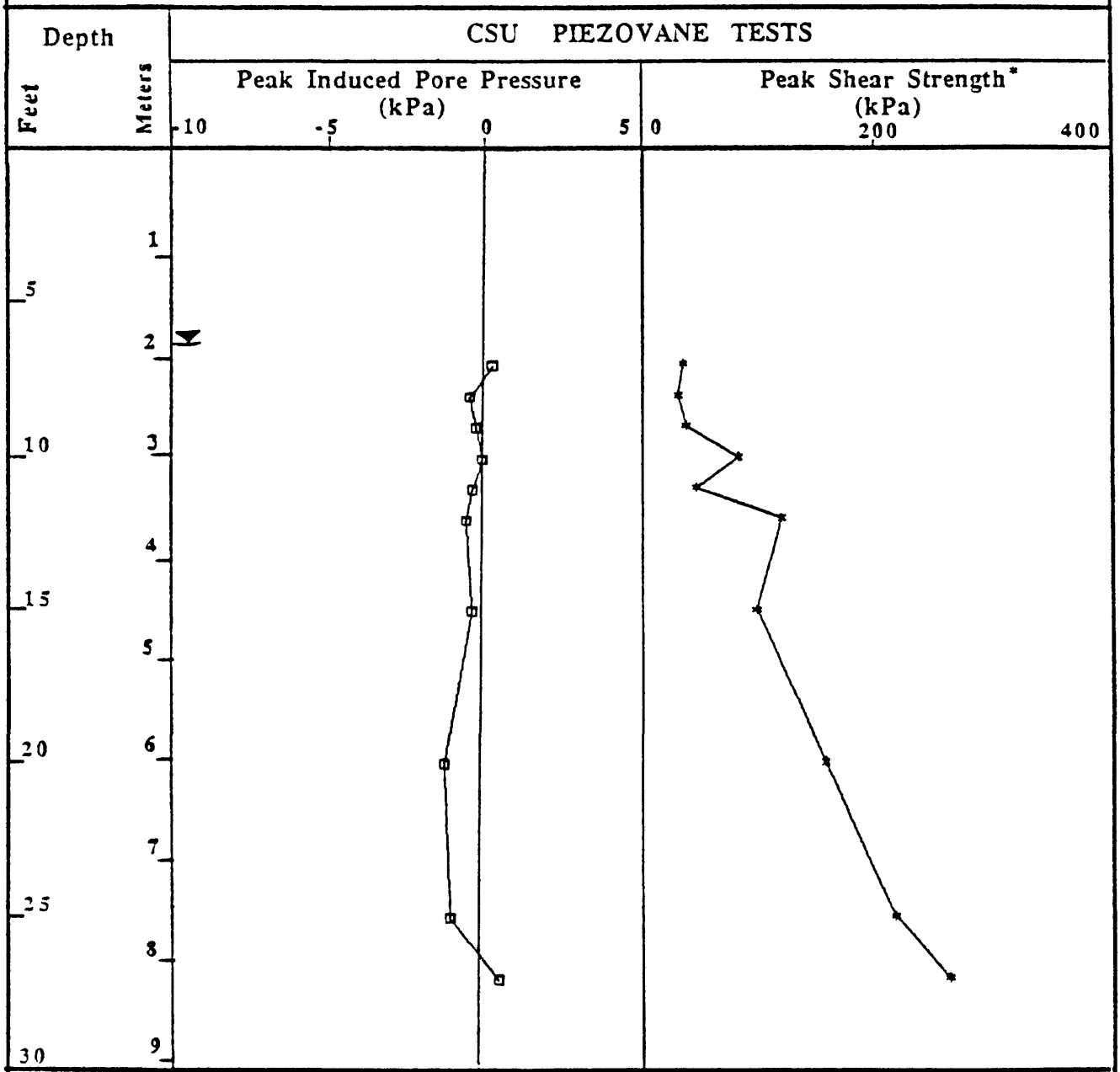


REMARKS:
1. Sea Mist Farms

* Not corrected for rod friction.

## COLORADO STATE UNIVERSITY GEOTECHNICAL LOG

HOLE NUMBER CSU Sea Mist 31
PROJECT LIQUEFACTION POTENTIAL USING CSU PIEZOVANE
LOCATION NEAR CASTROVILLE,[1] CALIFORNIA
COORDINATES
DATE TESTED 8/9/90
GROUND WATER 4.0 ft.
PERSONNEL D: J. BRISLAWN, L: H. HASSEN
ELEVATION

CSU PIEZOVANE TESTS

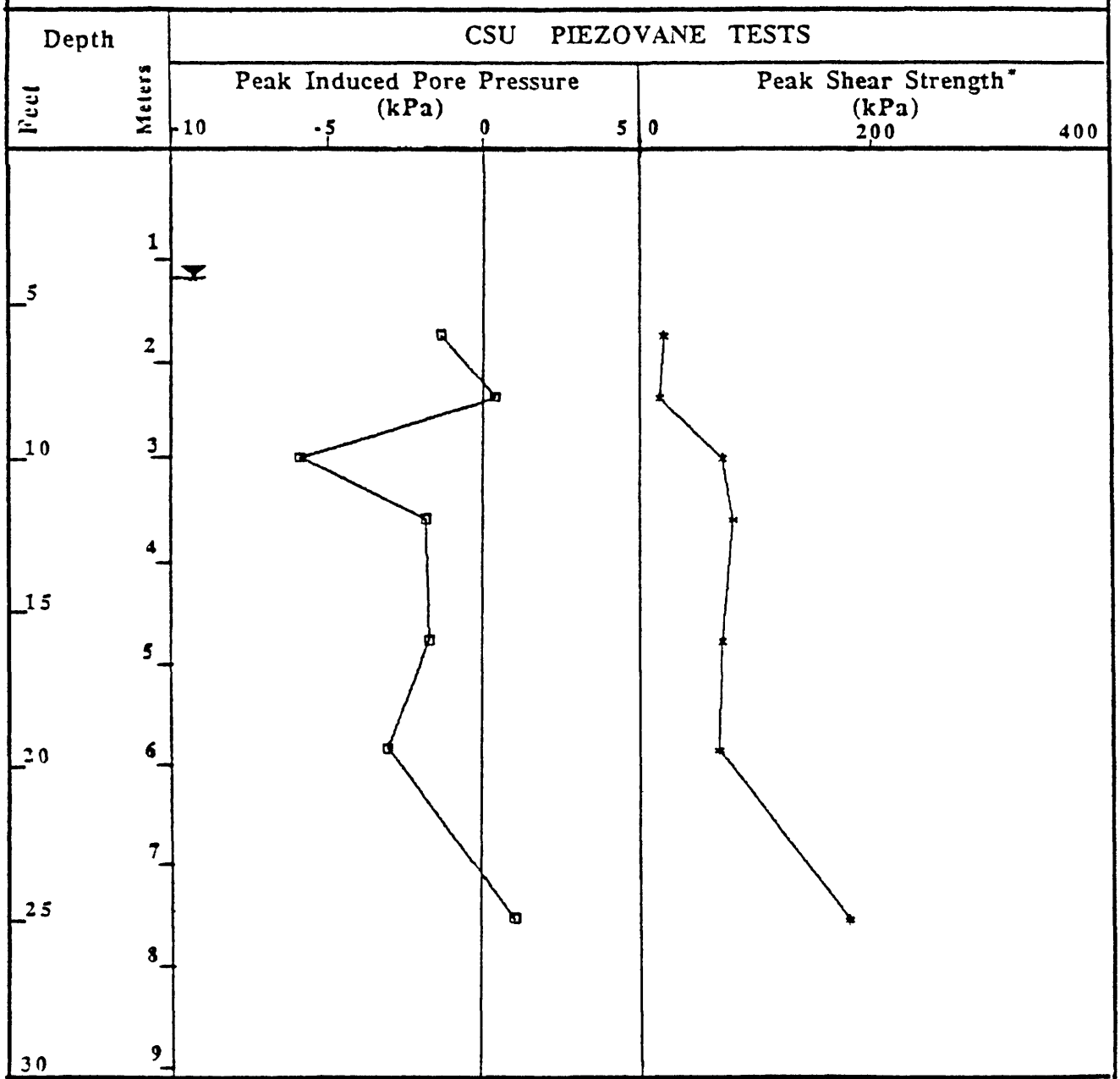


REMARKS:
1. Sea Mist Farms

* Not corrected for rod friction.

## COLORADO STATE UNIVERSITY GEOTECHNICAL LOG

HOLE NUMBER CSU Leonardini 37
PROJECT LIQUEFACTION POTENTIAL USING CSU PIEZOVANE
LOCATION NEAR CASTROVILLE,[1] CALIFORNIA
COORDINATES
DATE TESTED 8/8/90
GROUND WATER 7.5 ft.
PERSONNEL D: J. BRISLAWN, L: H. HASSEN
ELEVATION

CSU PIEZOVANE TESTS

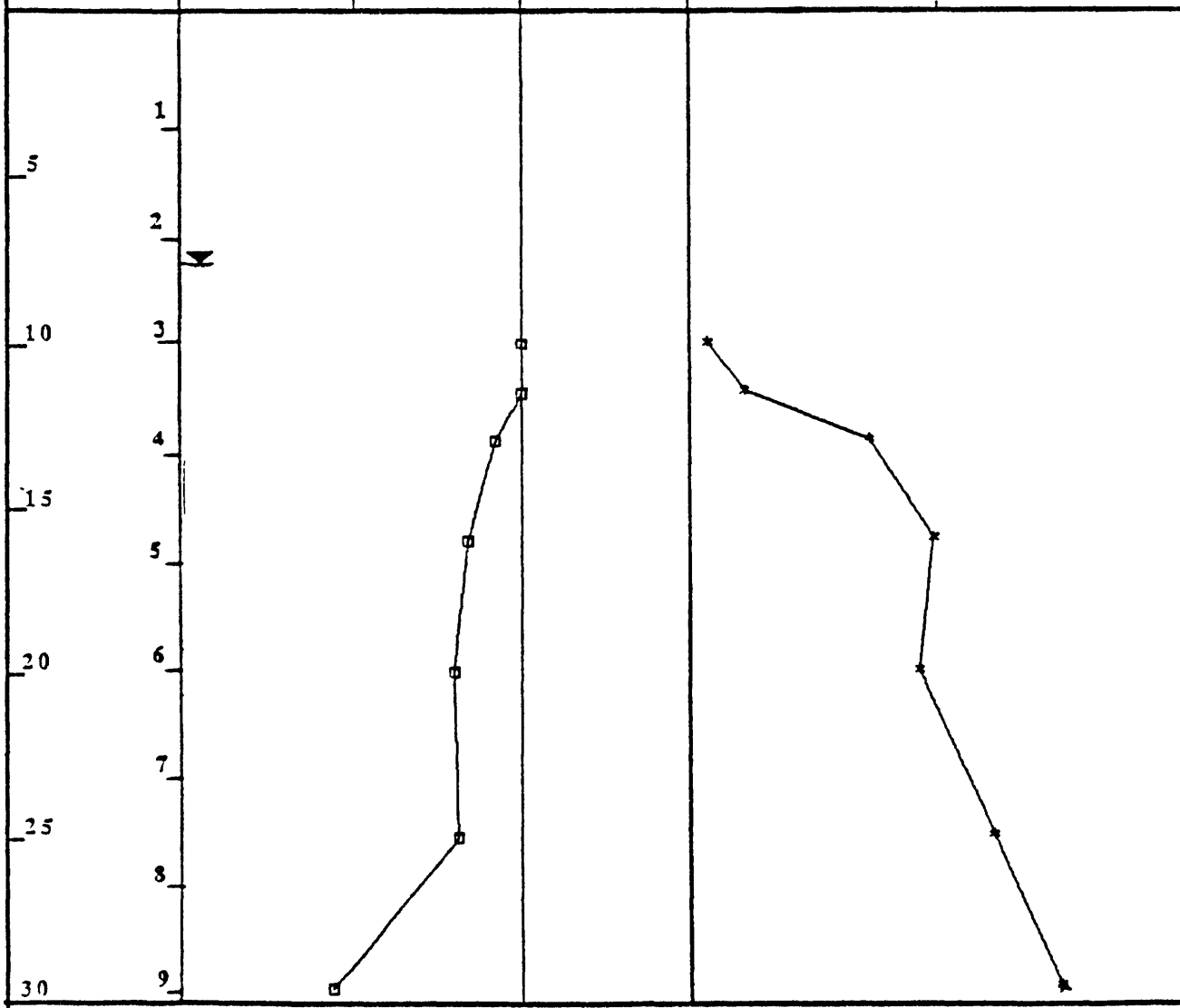


REMARKS:
1. Leonardini Farms

* Not corrected for rod friction.

## COLORADO STATE UNIVERSITY GEOTECHNICAL LOG

HOLE NUMBER CSU Leonardini 38
PROJECT LIQUEFACTION POTENTIAL USING CSU PIEZOVANE
LOCATION NEAR CASTROVILLE,[1] CALIFORNIA
COORDINATES
DATE TESTED 8/7/90
GROUND WATER 5.67 ft.
PERSONNEL D: J. BRISLAWN, L: H. HASSEN
ELEVATION

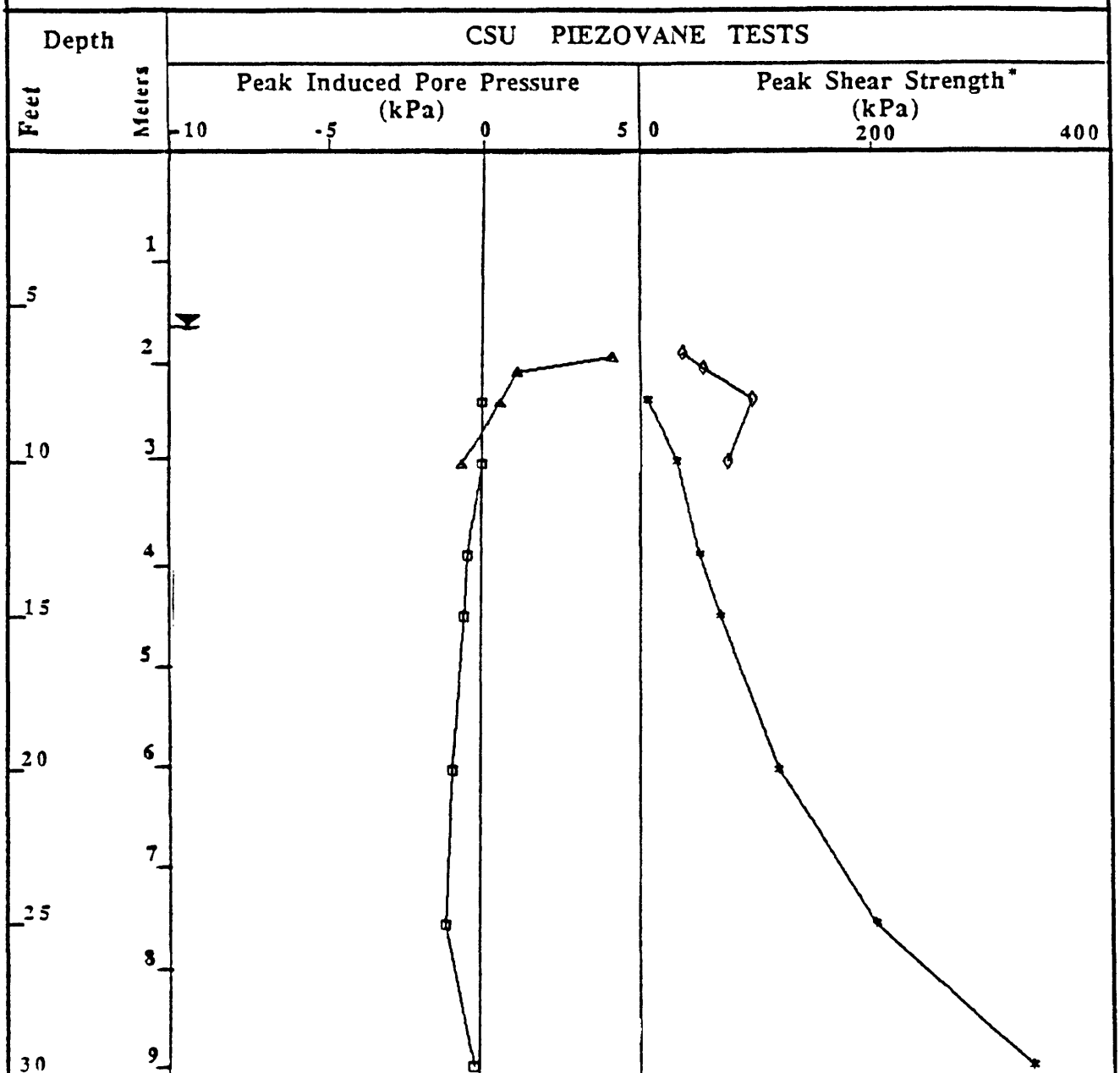


REMARKS:
1. Leonardini Farms

* Not corrected for rod friction.

## COLORADO STATE UNIVERSITY GEOTECHNICAL LOG

HOLE NUMBER CSU Leonardini 39

PROJECT LIQUEFACTION POTENTIAL USING CSU PIEZOVANE

LOCATION NEAR CASTROVILLE,[1] CALIFORNIA

COORDINATES

DATE TESTED 8/6/90

GROUND WATER 4.25 ft.

PERSONNEL D: J. BRISLAWN, L: H. HASSEN

ELEVATION

CSU PIEZOVANE TESTS

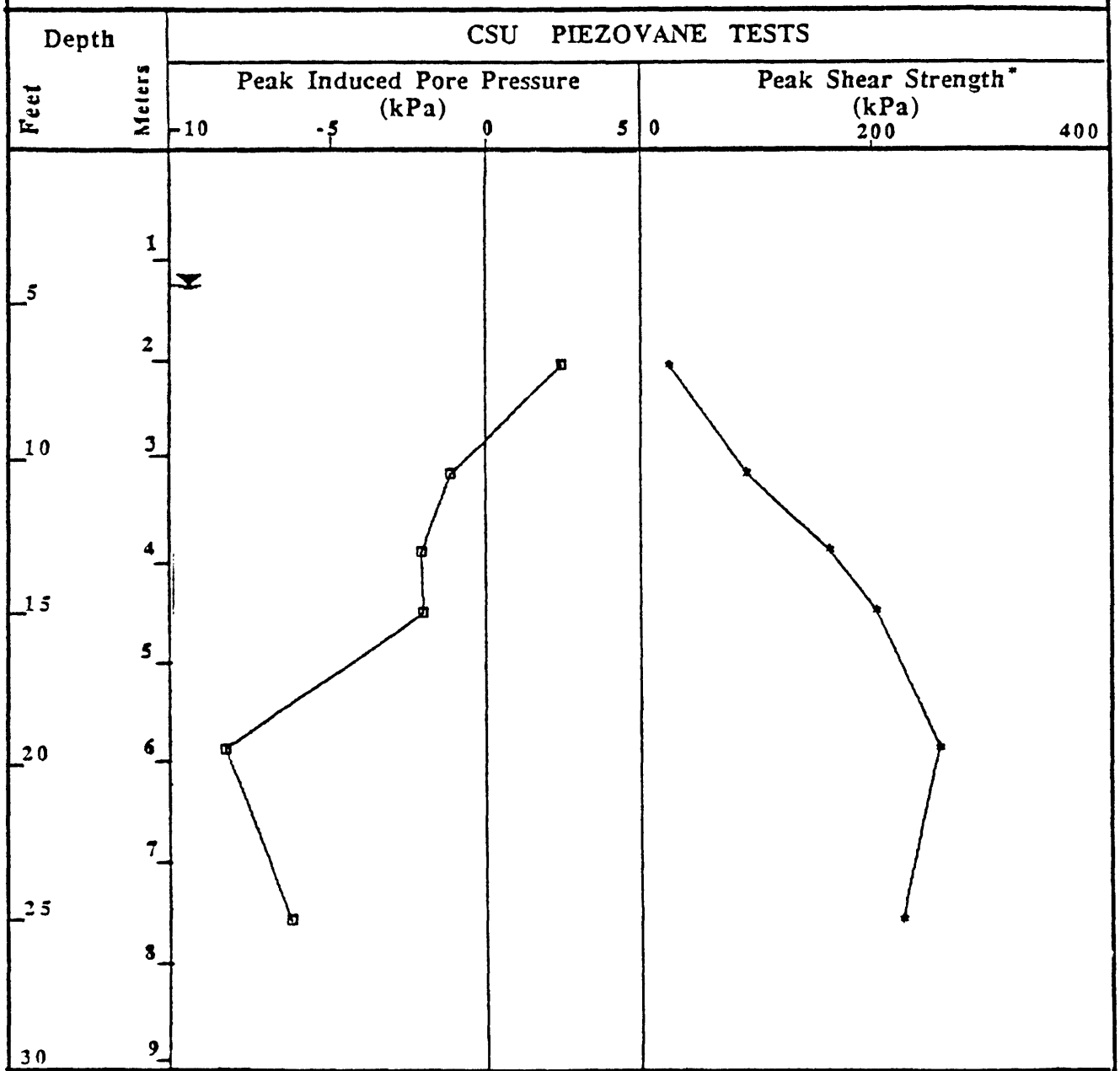


REMARKS:

1. Leonardini Farms

* Not corrected for rod friction.

## COLORADO STATE UNIVERSITY GEOTECHNICAL LOG

HOLE NUMBER CSU SP Bridge 48 [1]
PROJECT LIQUEFACTION POTENTIAL USING CSU PIEZOVANE
LOCATION WATSONVILLE, CALIFORNIA
COORDINATES
DATE TESTED 8/19/90
GROUND WATER 17.0 ft.
PERSONNEL D: J. BRISLAWN, L: H. HASSEN
ELEVATION

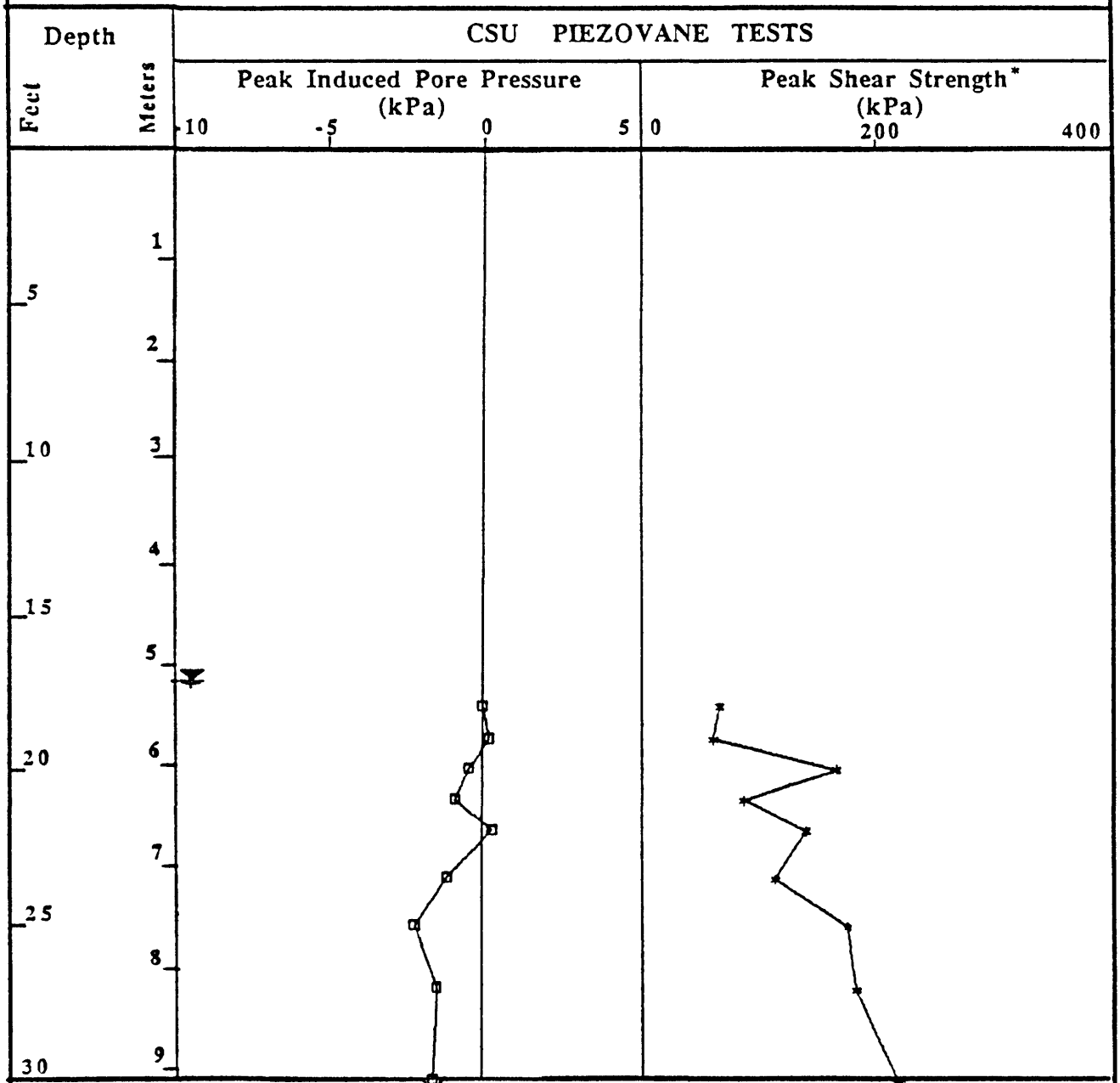


REMARKS: 1. Southern Pacific Railroad Bridge. Borehole is in the Pajaro river Channel next to Bridge.

* Not corrected for rod friction.

THE LOMA PRIETA, CALIFORNIA, EARTHQUAKE OF OCTOBER 17, 1989:
LIQUEFACTION

STRONG GROUND MOTION AND GROUND FAILURE

# COMPARISON OF COMPUTED AND MEASURED LIQUEFACTION-INDUCED SETTLEMENTS IN THE MARINA DISTRICT, SAN FRANCISCO

By Kyle M. Rollins and Michael D. McHood,
Brigham Young University

## CONTENTS



ABSTRACT

Dynamic ground-response analysis for the Marina District of San Francisco results in computed peak accelerations of 0.15±0.05 *g* during the 1989 Loma Prieta earthquake. The liquefaction-induced settlement computed for this level of earthquake shaking compares favorably with the measured settlement in the Marina District. Normalized spectral shapes determined from ground-response analysis are nearly identical to those recorded at other soft-soil sites during the earthquake. Normalized spectral shapes computed for the Marina District are also similar to those recorded on soft soil during other earthquakes and agree favorably with soft-soil (Applied Technology Council soil type 3) design-spectrum shapes. Additional ground-response analyses indicate that future near-field earthquakes would generate higher levels of earthquake shaking and cause more extensive liquefaction in the Marina District.

## INTRODUCTION

The 1989 Loma Prieta earthquake was the most costly earthquake in U.S. history (Seed and others, 1990). Much of the damage can be ascribed to geotechnical conditions that were recognized before the event. Geotechnical factors known to amplify earthquake shaking are deep soil profiles, loose granular soils, and thick clay layers. Liquefaction of loose sandy soils and their subsequent settlement is another geotechnical concern for engineers. This paper focuses on the Marina District and the geotechnical conditions that contributed to the damage there. Post-earthquake investigations indicate that liquefaction, in combination with amplified earthquake shaking, was responsible for the extensive damage in the Marina District (Mitchell and others, 1990; Seed and others, 1990; U.S. Geological Survey, 1990).

## SITE CHARACTERIZATION

The Marina District is located on the north end of the San Francisco peninsula. During the earthquake, the area was significantly damaged, although it was more than 60 mi from the epicenter. The geologic conditions, both natural and manmade, in the Marina District are described below.

## BEDROCK

The main geologic unit underlying the Marina District is the Franciscan Formation, consisting of serpentine, sandstone, and shale; the bedrock underlying the Marina District is mainly serpentine. The bedrock surface in the Marina District has not been mapped precisely; however, several drill holes in the area have reached bedrock. These drill holes hit bedrock at elevations ranging from 75 to 256 ft below mean sea level (Bonilla, 1990).

### NATURAL DEPOSITS

Three main sedimentary units overlie the bedrock in the Marina District: old bay mud, hardpan, and young bay mud. The old bay mud was deposited during the Pleistocene, approximately 125,000 to 75,000 years ago. This unit is a stiff clay with an undrained shear strength generally of 2,000 to 3,500 lb/ft$^2$ and a shear-wave velocity commonly ranging from 1,000 to 2,000 ft/s, increasing with depth. The hardpan, a dense cemented sand, is believed to be the top of an erosional surface that formed during the low sea level of the last glaciation; this unit probably marks the boundary between the Holocene and Pleistocene (Bonilla, 1990, p. A–13). The young bay mud was deposited during the Holocene, approximately 28,000 to 10,000 years ago. This unit is a soft to medium-consistency clay with an undrained shear strength generally of 100 to 1,000 lb/ft$^2$ and a shear-wave velocity ranging from 200 to 600 ft/s, increasing with depth.

### FILLS

Most of the upper soil profile in the Marina District consists of hydraulic fill built up mainly in 1912 and placed directly on young bay mud (Bonilla, 1990). Hydraulic fill is placed as a slurry in which solids settle out of suspension with no compactive effort. Standard-penetration-test (SPT) blowcounts measured in the hydraulic fill range from 3 to 11 blows/ft (Kayen and others, 1990). Owing to the loose saturated condition of these fills, the Marina District is highly susceptible to liquefaction.

### SOIL PROFILE

The U.S. Geological Survey (USGS) conducted a geotechnical investigation at Winfield Scott School in the Marina District, located at the corner of Beach and Divisadero Streets. This site was chosen because of the heavy earthquake damage in the immediate area (Kayen and others, 1990). On the basis of the data obtained from this investigation, a soil profile was constructed to study the amplification of earthquake motions in the Marina District. This profile (fig. 1) consists of sand fill extending to a depth of 11.5 ft, followed by 12.5 ft of dune or beach sand, and 13.0 ft of young bay mud. The young bay mud is underlain by 40 ft of dense sand (hardpan) and 184 ft of old bay mud. Serpentine of the Franciscan Formation is at a depth of 261 ft.

Shear-wave velocities were measured to a depth of 92 ft as part of the USGS investigation (Kayen and others, 1990). Shear-wave velocities at depths greater than 92 ft were estimated from studies of shear-wave velocities of old bay mud (Warrick, 1974; Joyner and others, 1976). The shear-wave-velocity profile used in subsequent analyses is shown in figure 1. Although this profile shows only 13 ft of young bay mud, about 25 ft of the near-surface material has a shear-wave velocity of less than 500 ft/s. In addition, the 12.5-ft-thick dune or beach sand has a shear-wave velocity of only 575 ft/s. On the basis of a strict interpretation of the seismic-code provisions outlined by the Structural Engineers Association of California (SEAOC) (1990), this location would be classified as a soil-type 2 (S2) site; however, a more liberal interpretation, considering the low shear-wave velocity of the loose surface fill, might result in an S3 classification. Previous ground-response studies on Treasure Island suggest that loose saturated sand at the ground surface may be as effective as young bay mud in amplifying ground motions (Rollins and others, 1994).

## GROUND-RESPONSE ANALYSIS

Earthquake damage in the Marina District resulted from both ground shaking and liquefaction, phenomena both influenced by local ground-response. Deep soil profiles, loose granular fills, and thick clay layers are all factors known to amplify earthquake shaking. All of these conditions are present in the Marina District. The soil profile at Winfield Scott School, which is 261 ft deep, shows loose fills and significant clay layers (fig. 1).

Because no records of ground motion are available for the Marina District, numerical analyses are required to quantify the influence of soil conditions on ground response. We performed a one-dimensional ground-response analysis for the Marina District by using *SHAKE90*, a personal-computer version of the computer program *SHAKE* (Schnabel and others, 1972), with the soil profile shown in figure 1. Time histories recorded during the earthquake at sites located on bedrock were used as input motions for the analysis; the time histories used were recorded at Diamond Heights, Rincon Hill, Pacific Heights, Telegraph Hill, Presidio, Cliff House, and Yerba Buena Island. These sites are all located on the San Francisco peninsula except for Yerba Buena Island, which is in San Francisco Bay. They are also all at similar epicentral distances, from 62 to 71 mi.

An examination of the response spectra from time histories recorded in San Francisco reveals a considerable variation in spectral amplitude with frequency (fig. 2), although all the sites are at similar epicentral distances, as well as a considerable variation in peak acceleration (table 1). This range of different motions, all recorded on bedrock, makes the task of choosing a representative bedrock motion for the Marina District more difficult. Each of these records was used in the analysis to examine the full range of possible bedrock motions for the Marina District.

Using the program *SHAKE90*, the soil profile was excited by each recorded bedrock motion after deconvolution, and the ground-surface-response spectrum was computed. The shear-modulus-degradation curves for young bay mud were based on the data of Lodde (1982), and the curves for sand and old bay mud were based on the data of Seed and Idriss (1970) and Sun and others (1988), respectively. The computed response spectra were statistically analyzed to determine the mean and mean±1σ spectra plotted in figure 3. Significant amplification of spectral acceleration is evident for periods of 0.2 to 1.5 s. Peak spectral ratios occur at periods of 1.0 to 2.0 s. The mean±1σ peak acceleration is 0.15±0.05 *g*. Although a peak in the response spectrum occurs at 0.45 s, the spectral amplitude remains relatively high to a period of 1.5 s.

## COMPARISON WITH OTHER LOMA PRIETA SOFT-SOIL SPECTRA

Although no seismometers were located on soft soil in the Marina District during the earthquake, time histories were recorded at 11 soft-soil sites in the San Francisco Bay region. Five of these sites are at epicentral distances between 54 and 65 mi, similar to the Marina District. These five soft-soil sites, which generally classify as S3 sites (Structural Engineers Association of California, 1990), include San Francisco International Airport, Oakland outer harbor wharf, Treasure Island, Alameda Naval Air Station, and Emeryville Christie Avenue. The mean and mean±1σ response spectra for these five sites are plotted in figure 4.

The recorded spectra shapes agree reasonably well with those computed for the Marina District; the main difference is the spectral amplitude. This variation results from the different input motions at the various sites and in the Marina District. By normalizing the response spectra with respect to peak acceleration, we can remove this effect and more readily compare the spectral shapes.

The normalized Loma Prieta earthquake response spectra recorded at the five soft-soil sites and computed for the Marina District are plotted in figures 5*A* and 5*B*, respectively. Both the measured and computed normalized spectra have peak amplitudes of nearly 5 in the period range 0.25–0.75 s, whereas peak amplitudes of 2 to 3 are common for periods as long as 1.5 s. The small differences in

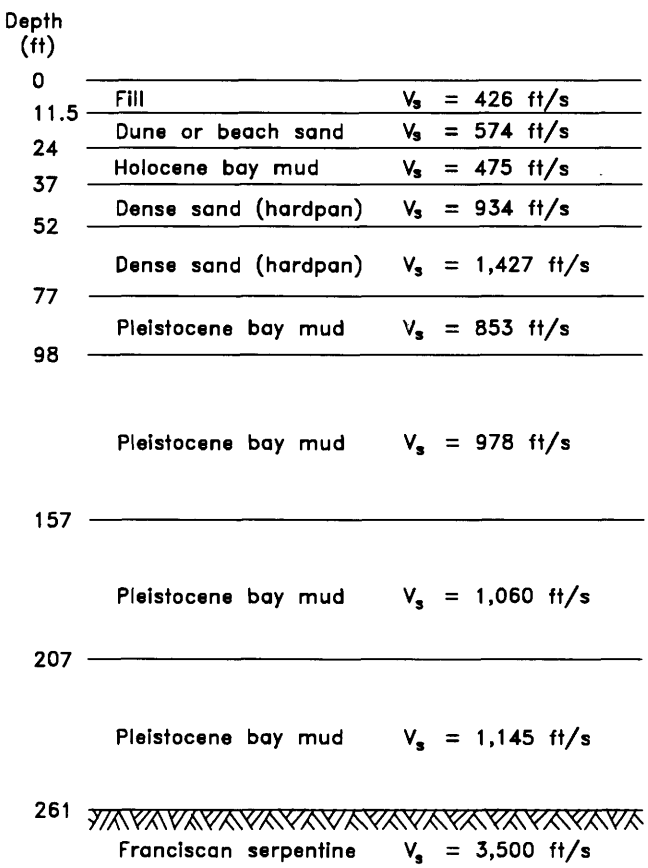


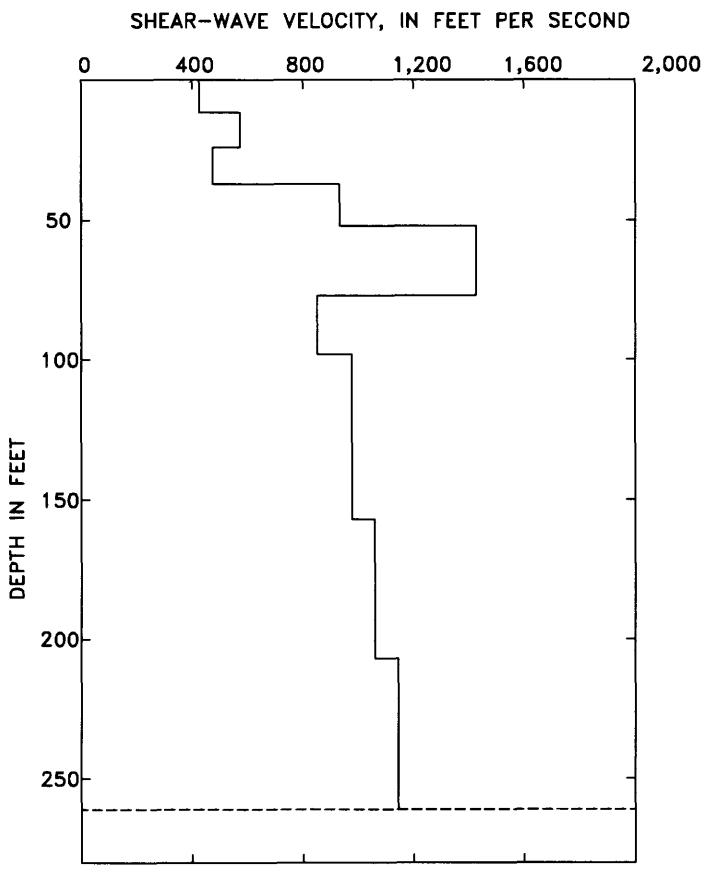


Figure 1.—Soil profile and variation in shear-wave velocity ($V_s$) with depth at Winfield Scott School in the Marina District of San Francisco.

these normalized spectra are attributable to local variations in the Marina District profile with respect to the soft-soil sites. We performed statistical analyses on each of these sets of normalized spectra; the mean and mean±1σ spectral shapes are compared in figure 6*A* and 6*B*, respectively. The normalized spectra for the Marina District agree closely with those for the five soft-soil sites.

## COMPARISON WITH OTHER NORMALIZED SPECTRA

Seed and others (1976) analyzed normalized response spectra to determine response-spectral shapes for different soil conditions. In their study of sites underlain by soft to medium clay and sand, they analyzed 15 time histories recorded in various places throughout the world. Their mean and mean±1σ response-spectral shapes normalized by peak acceleration are plotted in figure 7, and their mean and mean±1σ normalized spectra are compared with those for the Marina District in figure 8. The mean spectral shapes agree well, and the mean±1σ spectral shapes agree reasonably well except at periods of 0.75 to 1.0 s. Within this period range, the Marina District spectral shape has a trough corresponding to the peak in the spectral shape of Seed and others (1976). The trough in the mean±1σ normalized spectral shape may be a site-specific response characteristic of the Marina District. This anomaly is also seen in the mean spectral shapes, although it is not so pronounced.

Table 1.—*Peak east-west and north-south accelerations at recorded seven San Francisco bedrock sites in San Francisco*

[All values in *g*]

| Site | East-west | North-south |
|---|---|---|
| Cliff House---------- | 0.11 | 0.07 |
| Diamond Heights---------- | .11 | .10 |
| Pacific Heights---------- | .06 | .05 |
| Presidio---------- | .20 | .10 |
| Rincon Hill---------- | .09 | .08 |
| Telegraph Hill---------- | .09 | .05 |
| Yerba Buena Island-------- | .07 | .03 |

## COMPARISON WITH APPLIED TECHNOLOGY COUNCIL SPECTRUM

Since the early 1970's, the Applied Technology Council (ATC) (1978) has influenced standards for earthquake building codes. Included in these provisions are normalized response-spectral shapes for different soil types (fig. 9); these shapes are similar to those adopted by the SEAOC (Structural Engineers Association of California, 1990). The ATC normalized response spectra for an S3 site (soft to

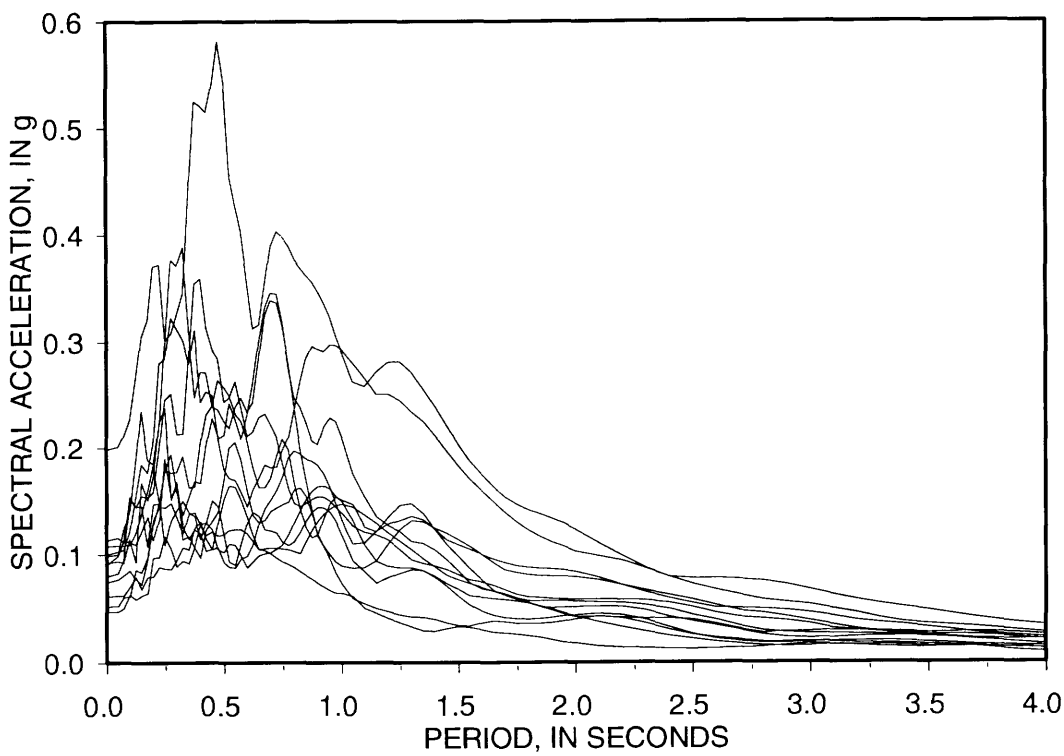


Figure 2.—Loma Prieta earthquake response spectra measured at seven bedrock sites in San Francisco.

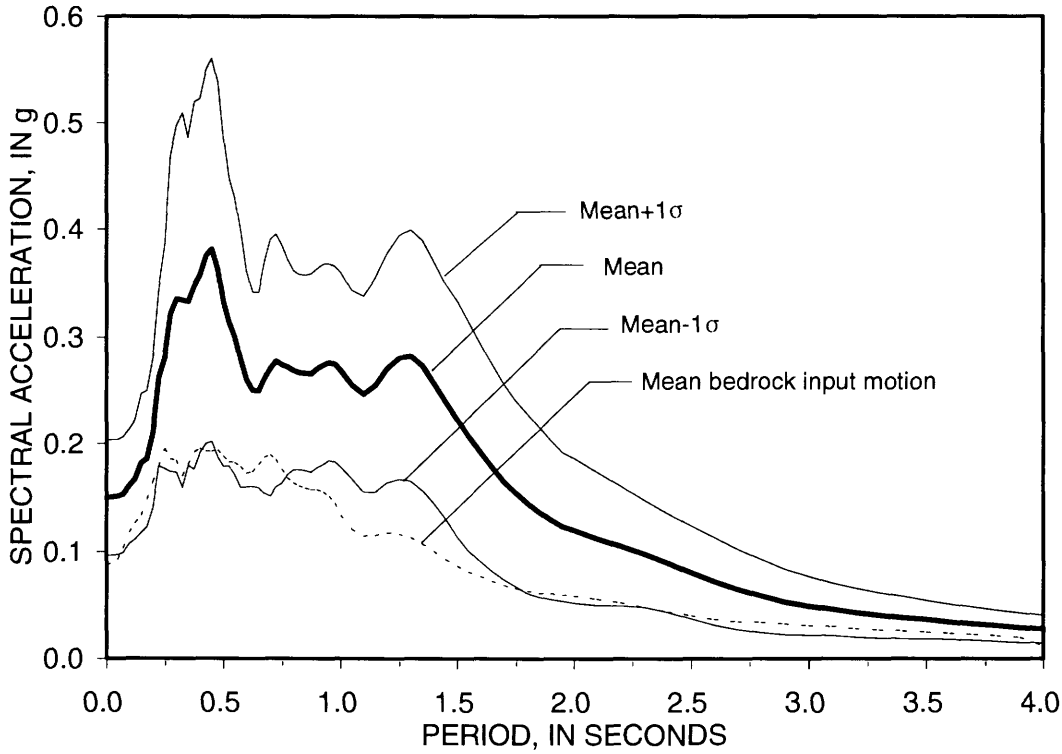


Figure 3.—Earthquake response spectra computed for the Marina District using records from bedrock sites in San Francisco. 5-percent damping.

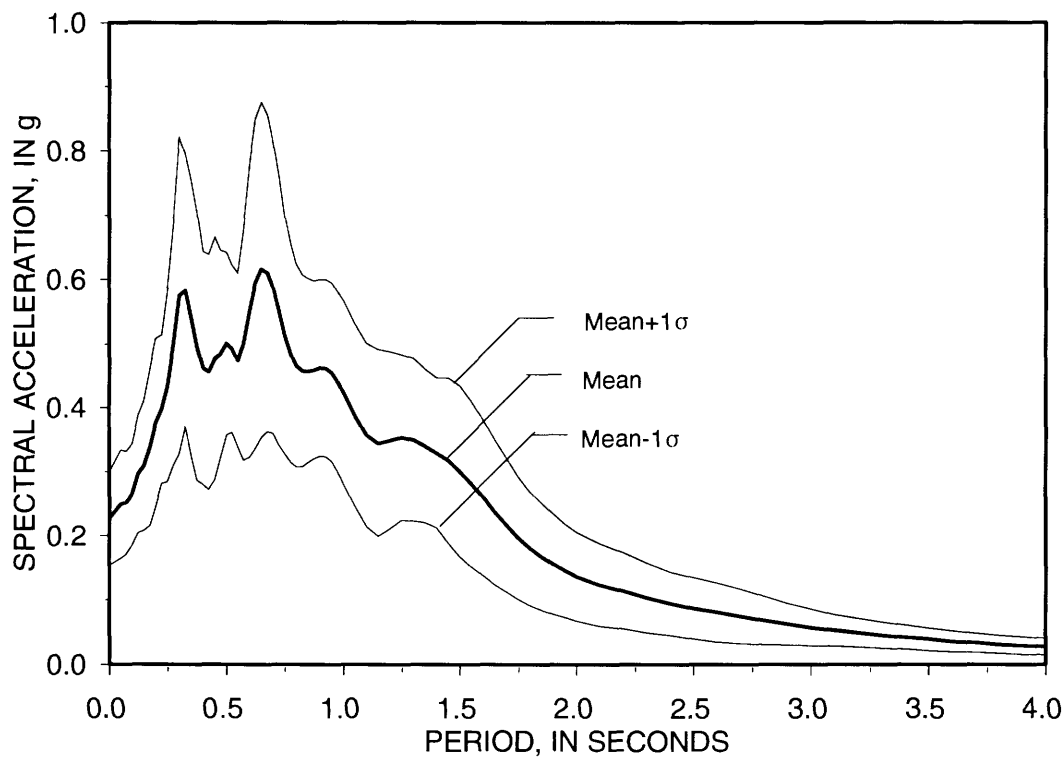


Figure 4.—Mean and mean±1σ Loma Prieta earthquake response spectra for five soft-soil (Applied Technology Council soil type 3) sites in the San Francisco Bay region. 5-percent damping.

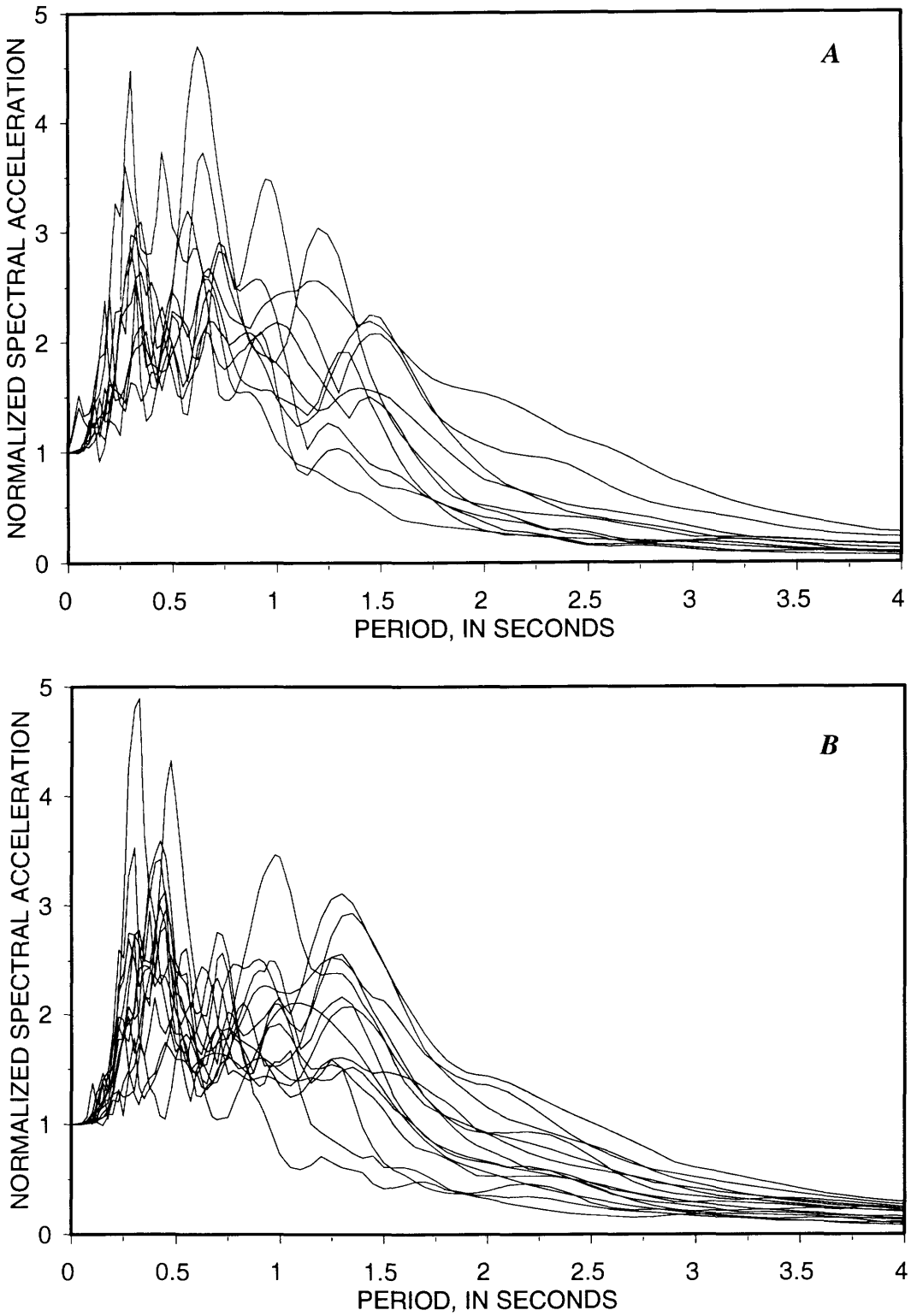


Figure 5.—Normalized Loma Prieta earthquake response spectra for five soft-soil (Applied Technology Council soil type 3) sites in the San Francisco Bay region (*A*) and computed for the Marina District (*B*).

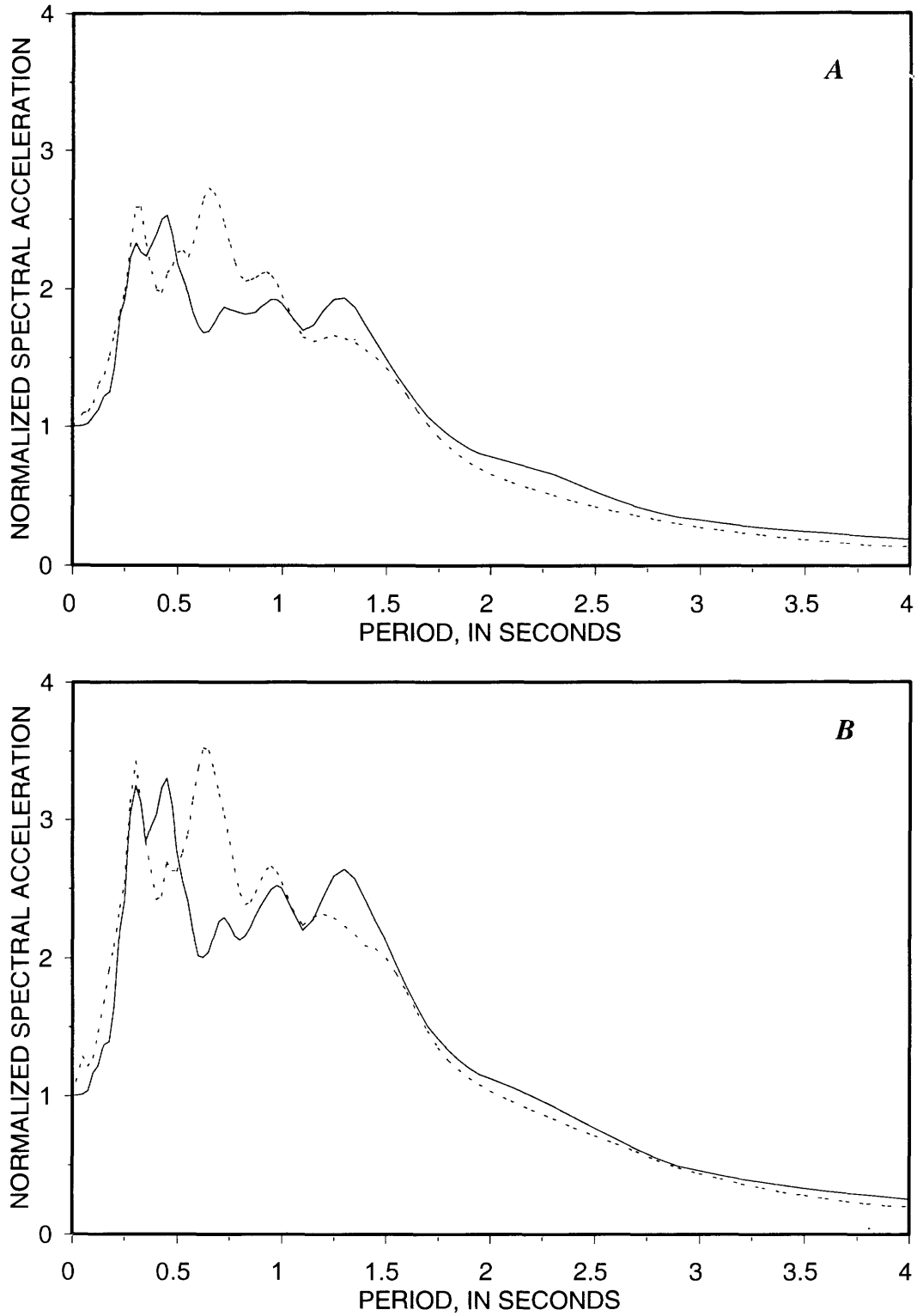


Figure 6.—Comparison of mean (*A*) and mean±1σ (*B*) normalized Loma Prieta earthquake response spectra for five soft-soil (Applied Technology Council soil type 3) sites in the San Francisco Bay region (dotted curve) and for the Marina District as computed from ground-response analysis (solid curve). 5-percent damping.

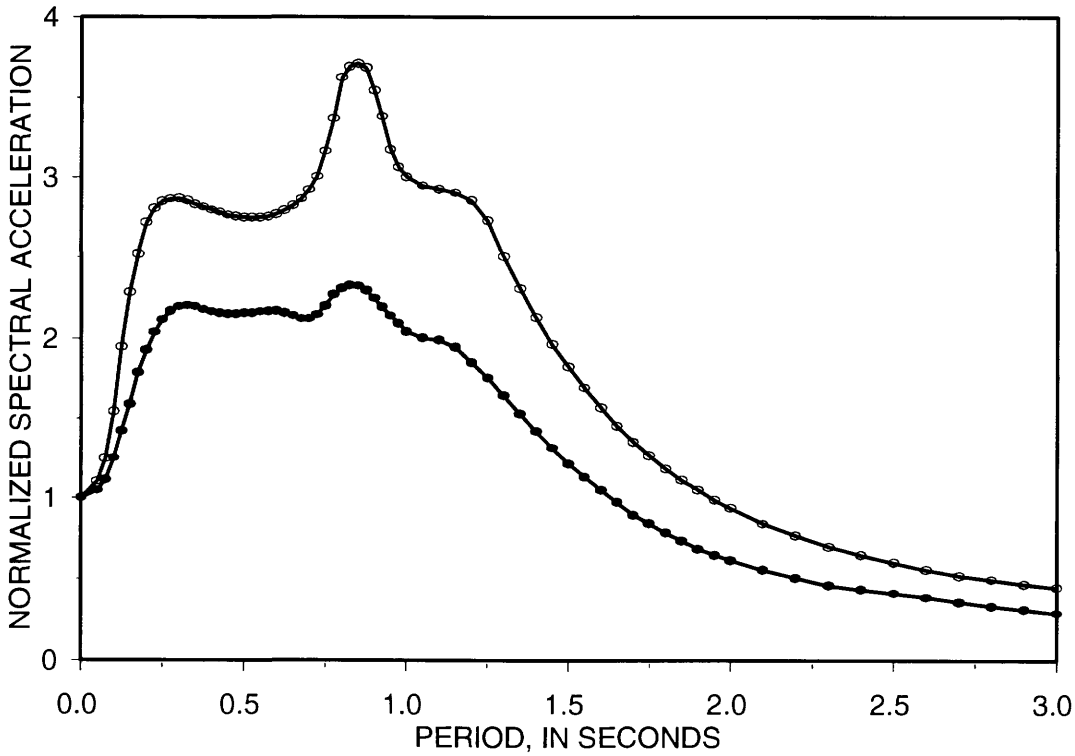


Figure 7.—Mean (dots) and mean±1σ (approx 84th percentile) (circles) normalized response spectra for sites underlain by soft to medium-stiff clay and sand, based on 15 records (from Seed and others, 1976). 5-percent damping.

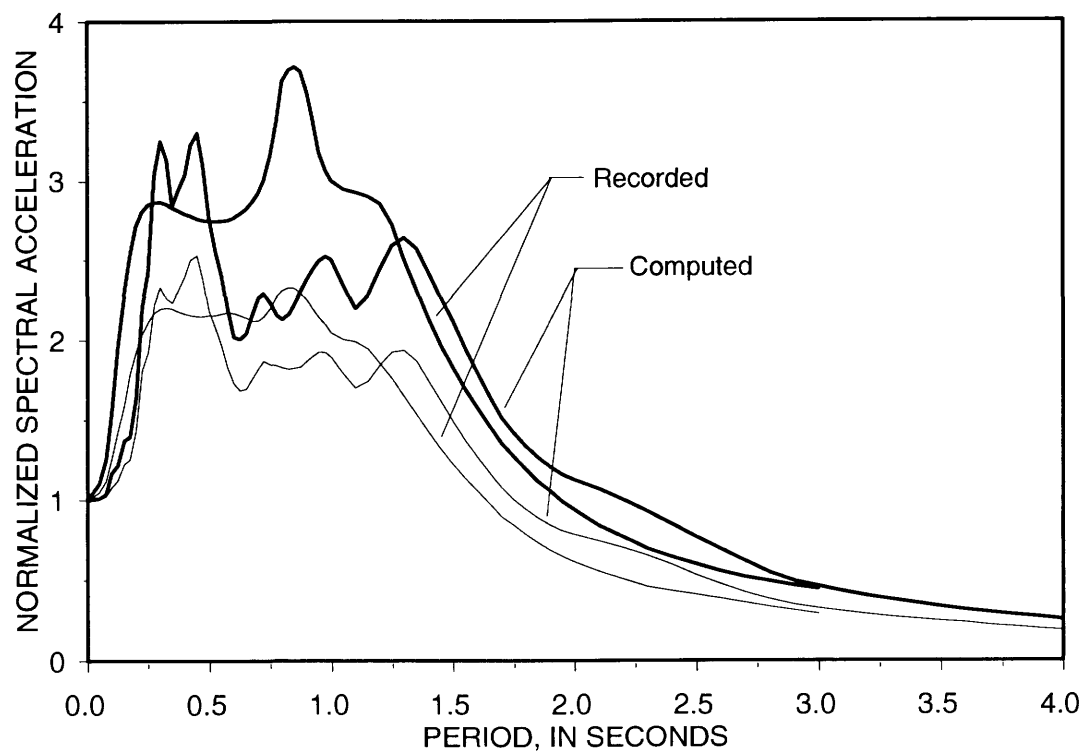


Figure 8.—Comparison of mean and mean±1σ (heavy) normalized response spectra from recorded data of Seed and others (1976) and for the Marina District as computed from ground-response analysis. 5-percent damping.

medium clay and sand) are compared with the computed normalized response spectra from the Marina District in figure 10. The ATC normalized spectrum generally bounds the mean normalized spectrum for the Marina District. Using the ATC S3 spectrum to design buildings within the Marina District should provide reasonable protection against earthquake shaking.

Many buildings in the Marina District, however, that were built before the implementation of the ATC provisions were heavily damaged in the earthquake. Amplification of earthquake shaking by clay layers and loose sandy fill played a major role in the destruction in the Marina District. The reasonably good agreement between the response spectra computed for the Marina District and those measured at other soft-soil sites at similar epicentral distances suggests that soil amplification can be predicted with sufficient accuracy for engineering purposes.

### FUTURE NEAR-FIELD EARTHQUAKES

The ground-response analyses discussed above were calculated by using Loma Prieta bedrock records from the San Francisco peninsula to re-create the level of shaking that occurred during the 1989 Loma Prieta earthquake. We also used Loma Prieta earthquake near-field records together with the Marina District soil profile to predict levels of ground shaking that would occur in a near-field earthquake of similar magnitude with an epicenter closer to the Marina District. The near-field time histories used in these analyses were recorded at Corralitos, Capitola, Gilroy No. 1, and Santa Cruz at epicentral distances of 3, 9, 14, and 15 mi, respectively. Although the Corralitos and Capitola stations were actually located on stiff soil sites, their spectral shapes were similar to typical bedrock spectra as defined by Seed and others (1976).

The mean and mean±1$\sigma$ spectral shapes computed for the Marina District using near-field motions are plotted along with the mean spectra for near-field input motions in figure 11. The calculated mean±1$\sigma$ peak acceleration is 0.46±0.04 *g*. Figure 11 predicts that spectral acceleration will attenuate for periods shorter than 0.35 s and amplify for periods longer than 0.35 s. Comparison of the computed near- and far-field response spectra shows that a significant increase in spectral acceleration may be expected in the Marina District during a future near-field earthquake (fig. 12).

## LIQUEFACTION-SETTLEMENT COMPUTATIONS

As indicated earlier, most of the Marina District is located on uncompacted fills. These fills are in a loose saturated condition and are highly susceptible to liquefaction.

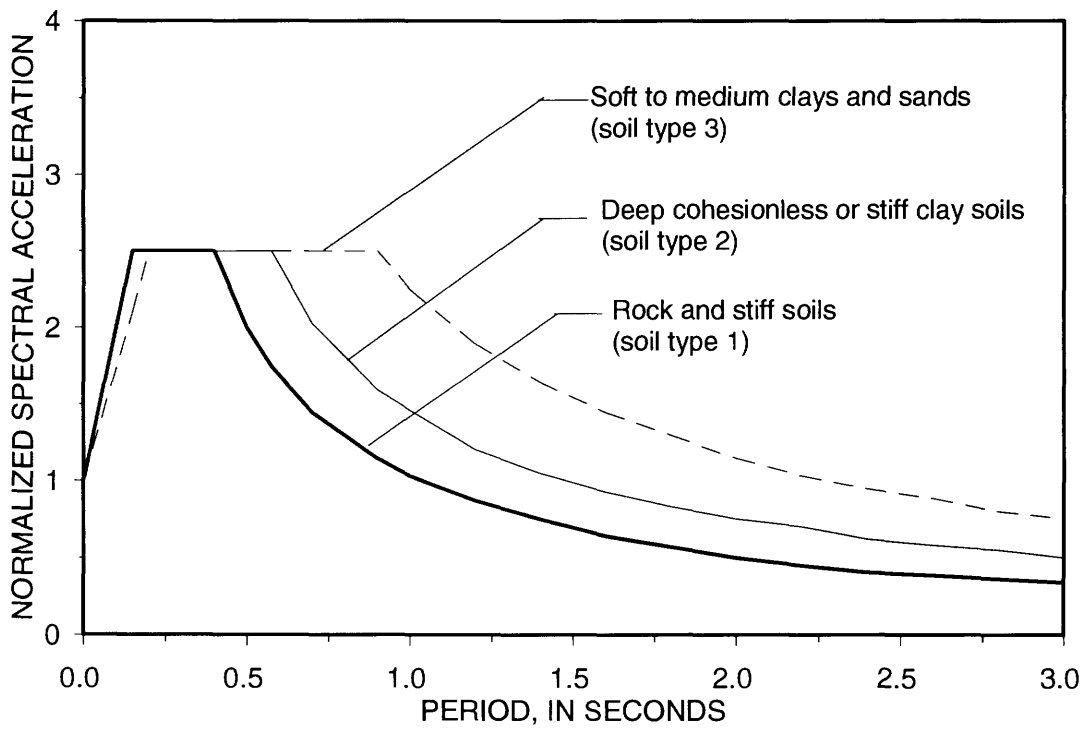


Figure 9.—Normalized design spectra for soil types 1 through 3 (S1–S3). From Applied Technology Council (1978) and Structural Engineers Association of California (1990).

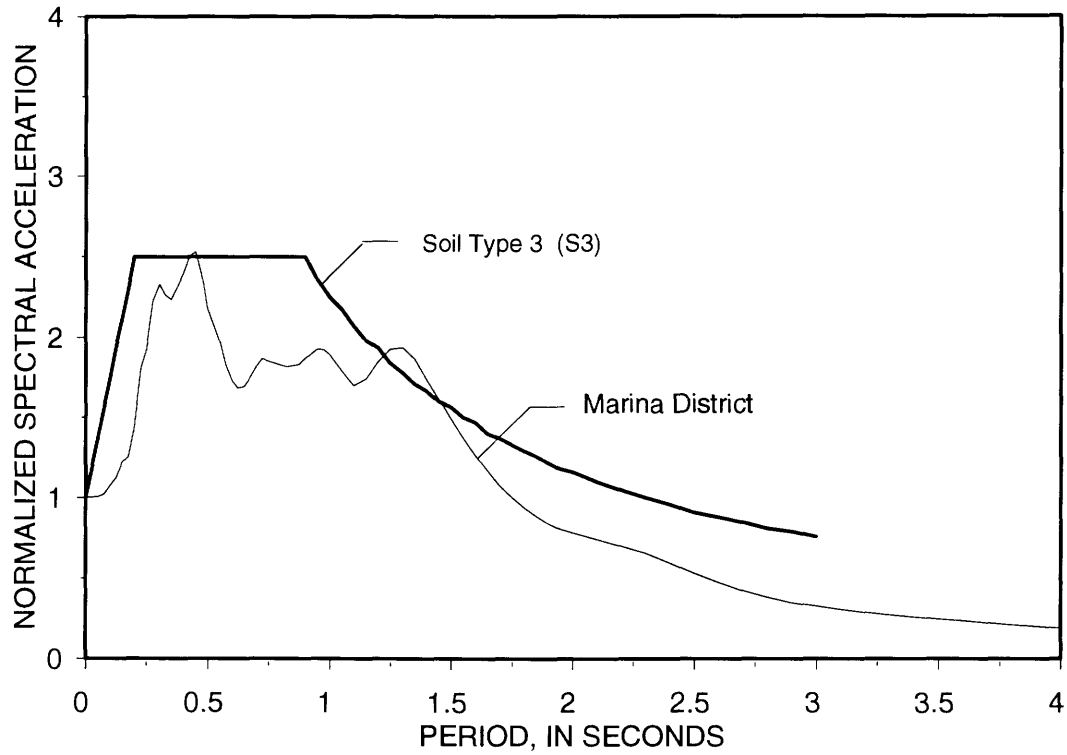


Figure 10.—Comparison of normalized response spectra for Applied Technology Council (1978) soil type 3 (S3) and for the Marina District as computed from ground-response analysis. 5-percent damping.

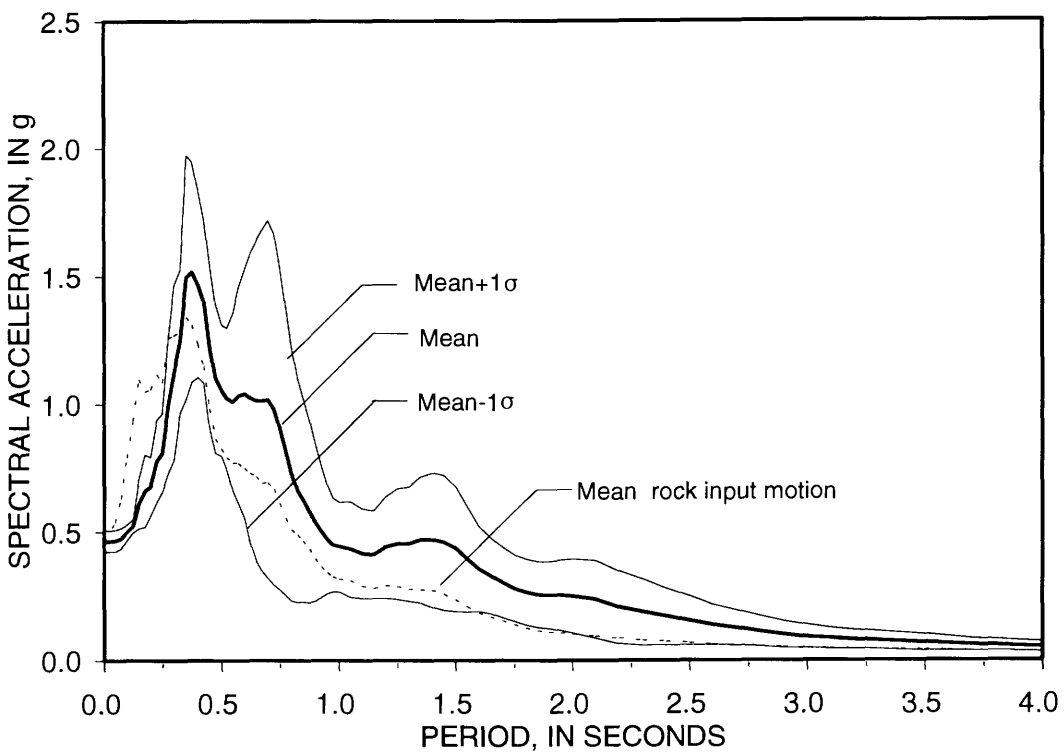


Figure 11.—Mean and mean±1σ Loma Prieta earthquake response spectra computed for the Marina District using near-field bedrock records. 5-percent damping.

Postearthquake investigations verified that liquefaction was widespread throughout the Marina District (Seed and others, 1990; U.S. Geological Survey, 1990)

Owing to the efforts of Bennett (1990), good information is available regarding liquefaction-induced settlement in the Marina District. These data allow calculation of settlement contours from measurements between 1974 and November 1989 (fig. 13). Most of this settlement resulted from liquefaction during the earthquake, although a small fraction may be due to other sources. The settlement ranges

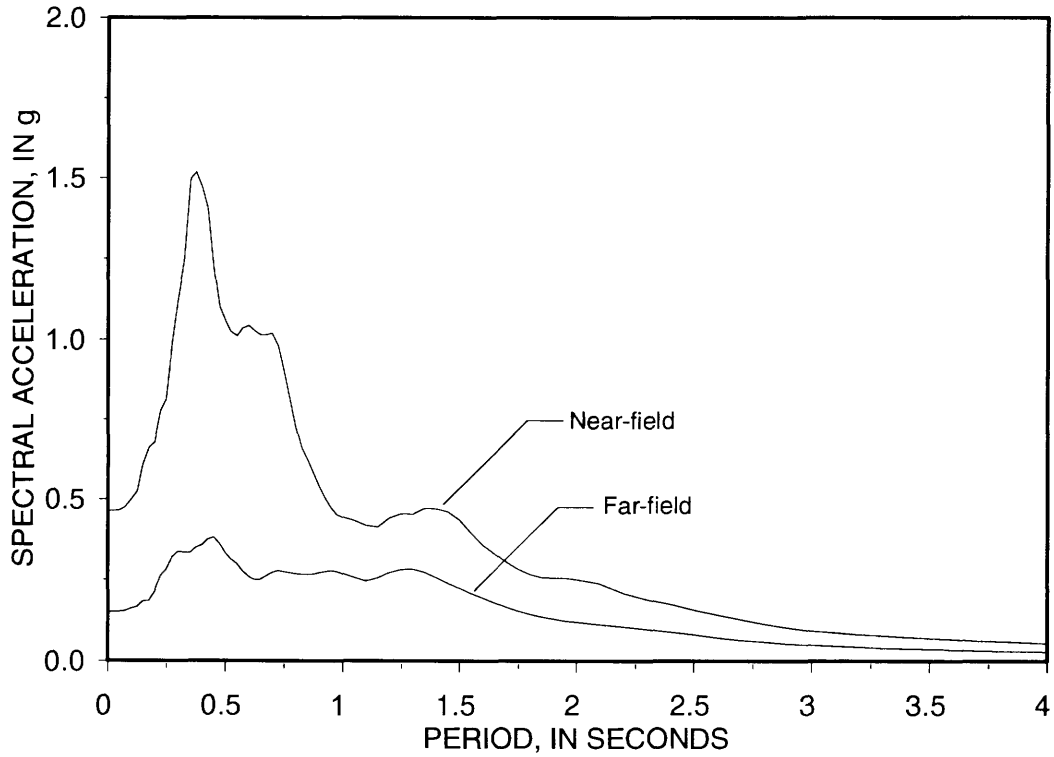


Figure 12.—Comparison of near- and far-field mean Loma Prieta earthquake response spectra computed for the Marina District.

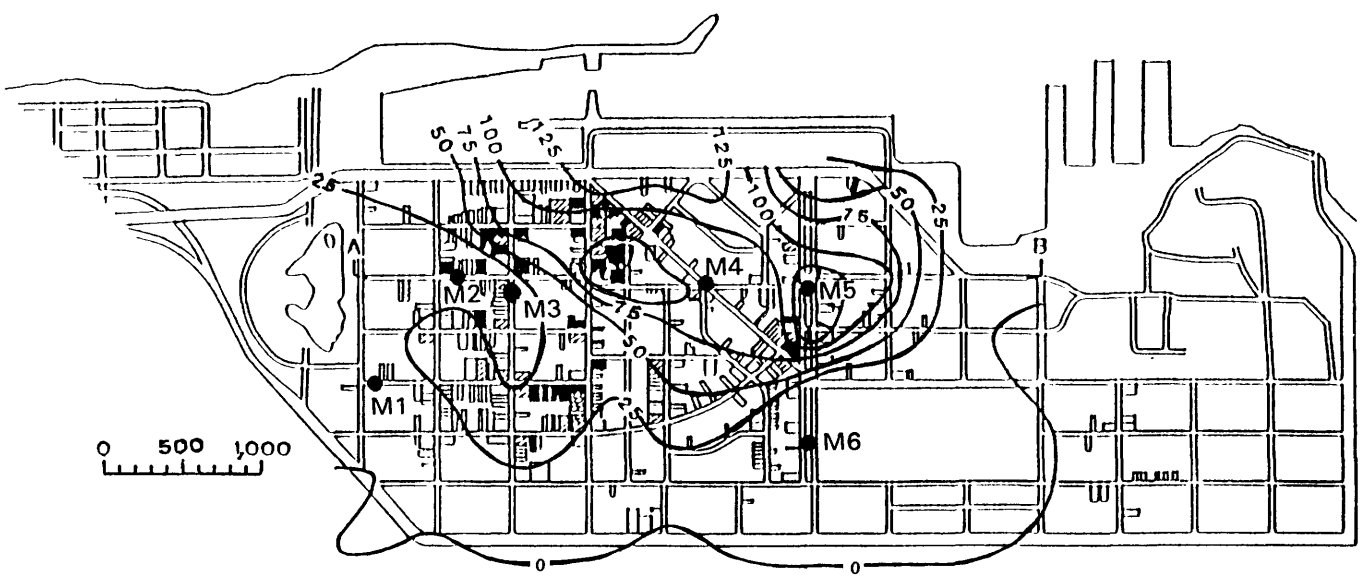


Figure 13.—Marina District of San Francisco, showing contours of settlement (in millimeters) and locations of boreholes drilled by the U.S. Geological Survey (Bennett, 1990).

from less than 25 mm at the margins of the hydraulic fill to more than 125 mm in certain places within the fill. After the earthquake, the U.S. Geological Survey drilled six test borings to depths of approximately 40 ft at locations shown in figure 13, and SPT's were conducted at each site. The soil profiles and SPT results for each borehole are shown in figure 14.

The liquefaction-settlement data collected in the Marina District provide an excellent opportunity to test methods for computing liquefaction-induced settlement against measurements. As part of this study, we computed the settlement at each site by using the simplified procedure of Tokimatsu and Seed (1987), which relates liquefaction-induced volumetric strain to the induced cyclic-stress ratio (CSR) and $(N_1)_{60}$ value in a layer by using the curves plotted in figure 15. The induced CSR is defined as the average horizontal induced shear stress ($\tau_{avg}$) divided by the initial vertical effective stress ($\sigma'_0$). The curves in figure 15 indicate that liquefaction of a loose sand results in substantially more strain than does liquefaction of a denser sand. Multiplication of the volumetric strain by the thickness of the layer gives the settlement in each layer;

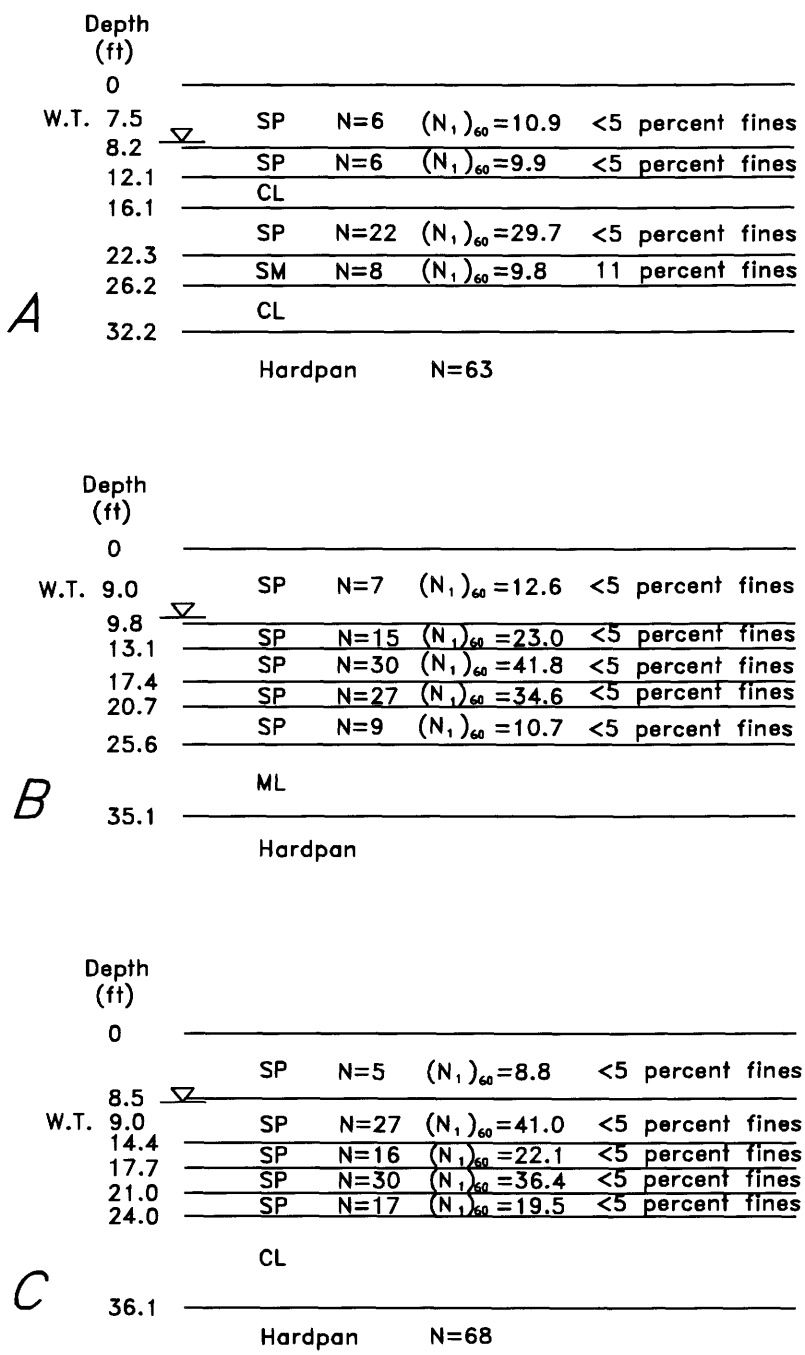


Figure 14.—Soil profiles in U.S. Geological Survey boreholes M1 (*A*), M2 (*B*), M3 (*C*), M4 (*D*), M5 (*E*), and M6 (*F*) in the Marina District (see fig. 13 for locations). From Bennett (1990).

the total settlement of the profile is the summation of the settlements of the individual layers.

## SETTLEMENT-COMPUTATION PROCEDURE

We computed the settlement separately for each of the six soil profiles with postearthquake geotechnical data (figs. 14). The plot in figure 15 is for an $M$=7.5 earthquake and relatively clean sand, and so application of this procedure requires a few adjustments. First, we converted the measured SPT blowcounts to $(N_1)_{60}$ values for each soil layer. Next, we shifted the volumetric-strain curves to correct for earthquake magnitude and fines content. The factor used to correct for earthquake magnitude was 1.13, corresponding to an $M$=6.75 event (Tokimatsu and Seed, 1987). We chose this magnitude after computing the number of equivalent uniform-stress cycles during the

*B*

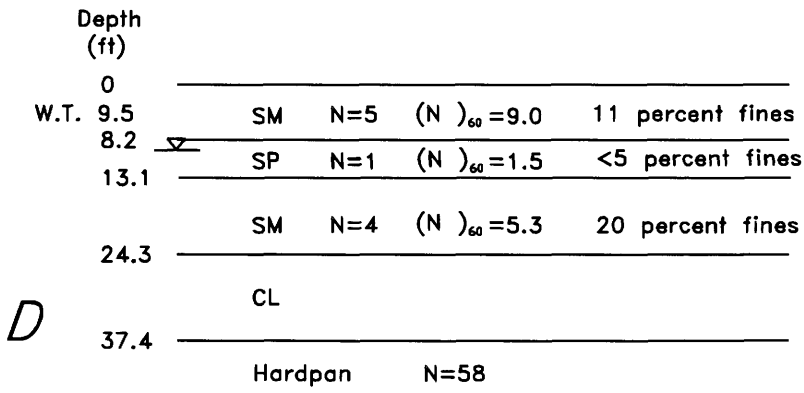


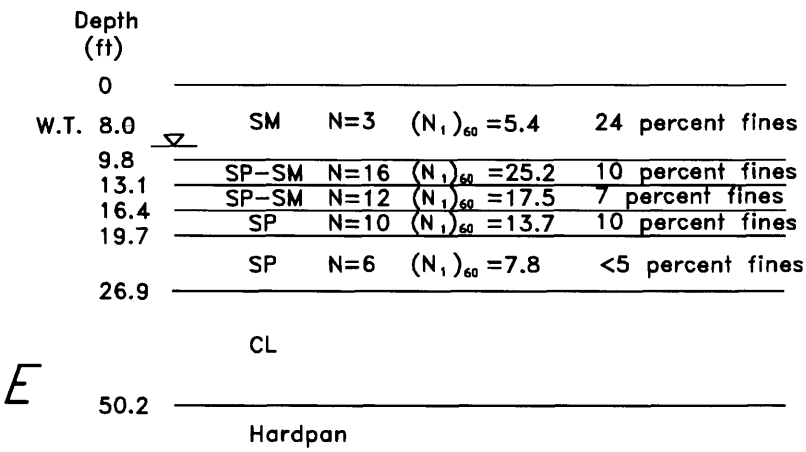


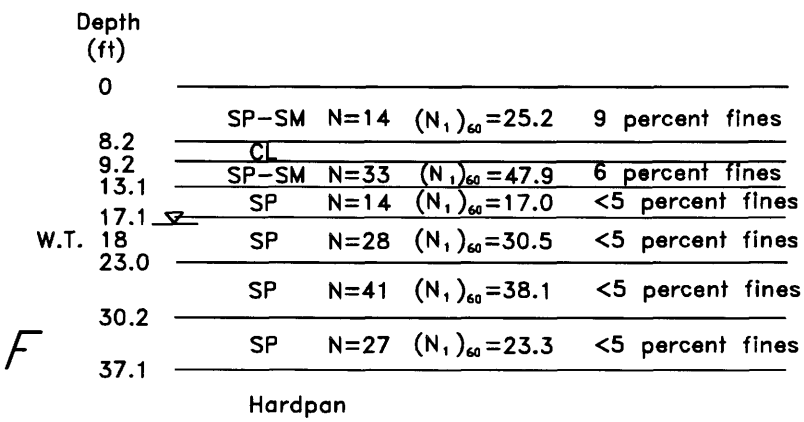


Figure 14.—Continued.

earthquake at several soft-soil sites in the San Francisco Bay region, using the procedure of Seed and others (1975). Various magnitudes for the 1989 Loma Prieta earthquake include a surface-wave magnitude ($M_S$) of 7.1, a body-wave magnitude ($m_b$) of 6.5, a moment magnitude ($M_w$) of 6.9, and a local magnitude ($M_L$) of 6.7 (California Institute of Technology, Pasadena) and 7.0 (University of California, Berkeley) (McNutt and Toppozada, 1990). These various magnitudes also justify the use of the $M$=6.75 correction factor.

Although Tokimatsu and Seed (1987) did not specify a procedure for correcting for fines content in the settlement computation, we were able to correct for fines content by adjusting the volumetric-strain curves in a manner consistent with the correction of Seed and others (1984) for liquefaction triggering. The near-coincidence of the strain boundary of Tokimatsu and Seed (1987) with the liquefaction boundary makes this approach appear more reasonable than adjusting the blowcount.

We calculated the induced CSR from the *SHAKE* analyses, using the various far-field bedrock records, as described previously. The mean CSR and mean CSR±1σ versus depth are plotted in figure 16. We used the induced CSR and $(N_1)_{60}$ value with the corrected strain

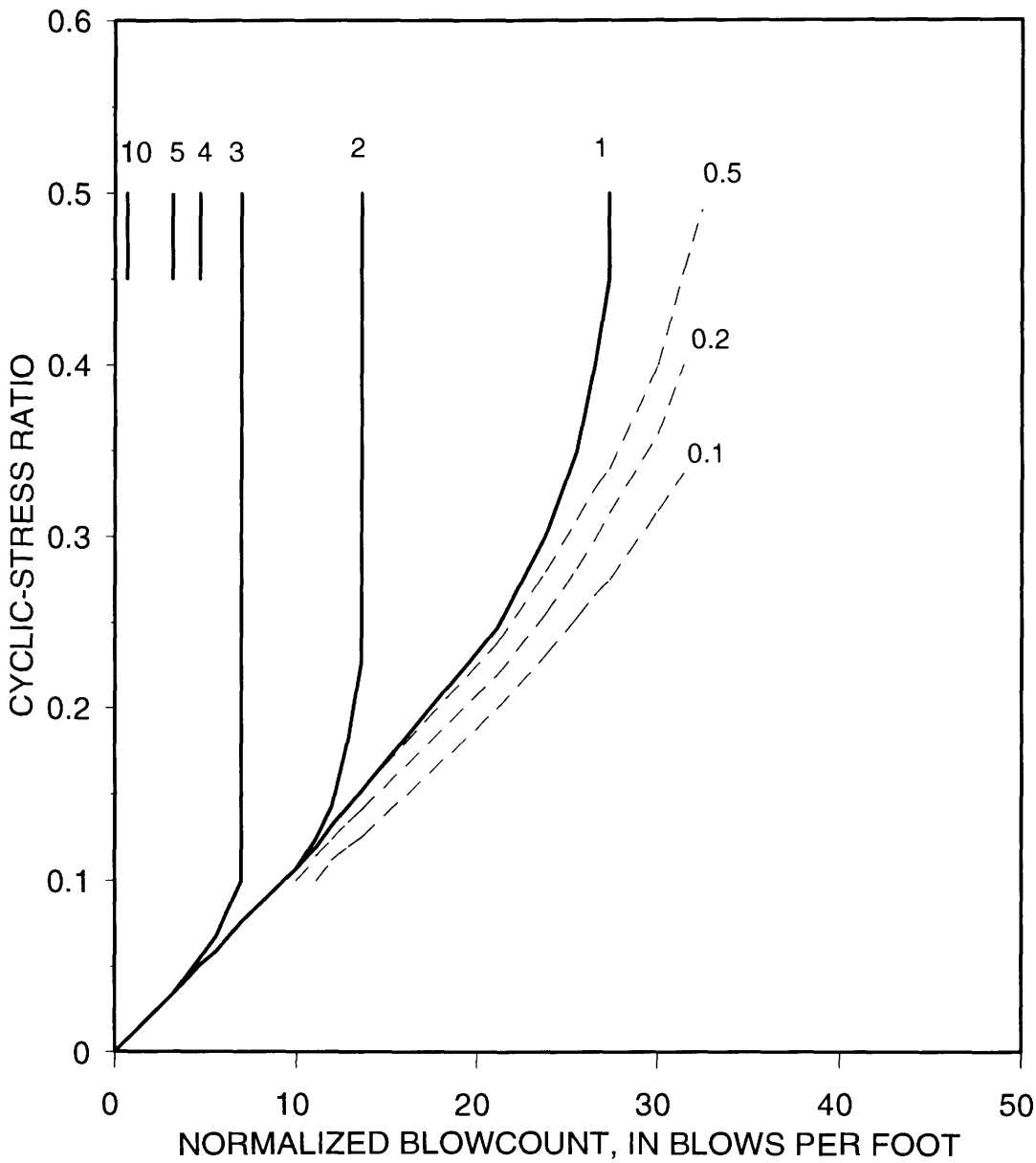


Figure 15.—Cyclic-stress ratio versus normalized blowcount, $(N_1)_{60}$, showing proposed curves of liquefaction-induced volumetric strain (in percent) for saturated clean sand for an $M$=7.5 earthquake. After Tokimatsu and Seed (1987).

curves to determine the volumetric strain for each soil layer. Owing to the diversity of bedrock motions used as input to the *SHAKE* analysis, a significant variation in CSR is evident throughout the Marina District soil profile. To account for this variation, we repeated the settlement computations for the mean CSR±1σ; the results of these computations and the measured settlements are shown in figure 17.

## COMPARISON OF COMPUTED AND MEASURED SETTLEMENTS

Considering the inherent variation of sand density, the use of correction factors, and the uncertainty in induced stresses from response analysis, the measured and computed settlements agree reasonably well for most of the soil profiles, although the predictions overestimate the settlement at borehole M4 and underestimate the settlement at borehole M5 (fig. 13). At borehole M4, one of the thicker layers had a CSR placing it just above the 2-percent-strain curve, leading to an overestimation of the settlement. At borehole M5, a similar layer with a slightly higher blowcount had a CSR just below the 2-percent-strain curve leading to an underestimation of the settlement. In these two soil profiles, better agreement with the measured settlement is obtained at the standard-deviation bounds. The two bounding points on either side of the 2-percent-strain curve tend to confirm the accuracy of the boundary-strain curve proposed by Tokimatsu and Seed (1987).

In certain parts of the strain curves (fig. 15), a small change in CSR can result in a significant difference in volumetric strain. This zone, which is the sensitive transition between no settlement and significant settlement, results from the fact that liquefaction and its ensuing settlement are an on/off phenomenon: The soil is stable up to a threshold point, beyond which a significant loss of shear strength and settlement occur.

The variation in settlement calculated for the different soil profiles is significant. The range of settlement calculated for boreholes M4 and M5 is 10 times larger than that for boreholes M3 and M6 (fig. 13). The sites with low blowcounts (boreholes M4, M5) vary widely in calculated settlement, whereas the sites with higher blowcounts (boreholes M3, M6) vary much less. This trend is inherent in the computation procedure for settlement in saturated sand. For low $(N_1)_{60}$ values (1–7 blows/ft), the volumetric strain can range from 0 to 10 percent; for moderate $(N_1)_{60}$ values (8–14 blows/ft), the volumetric strain is less than 3 percent; and for high $(N_1)_{60}$ values (greater than 15 blows/ft) the volumetric strain can be no greater than 2 percent.

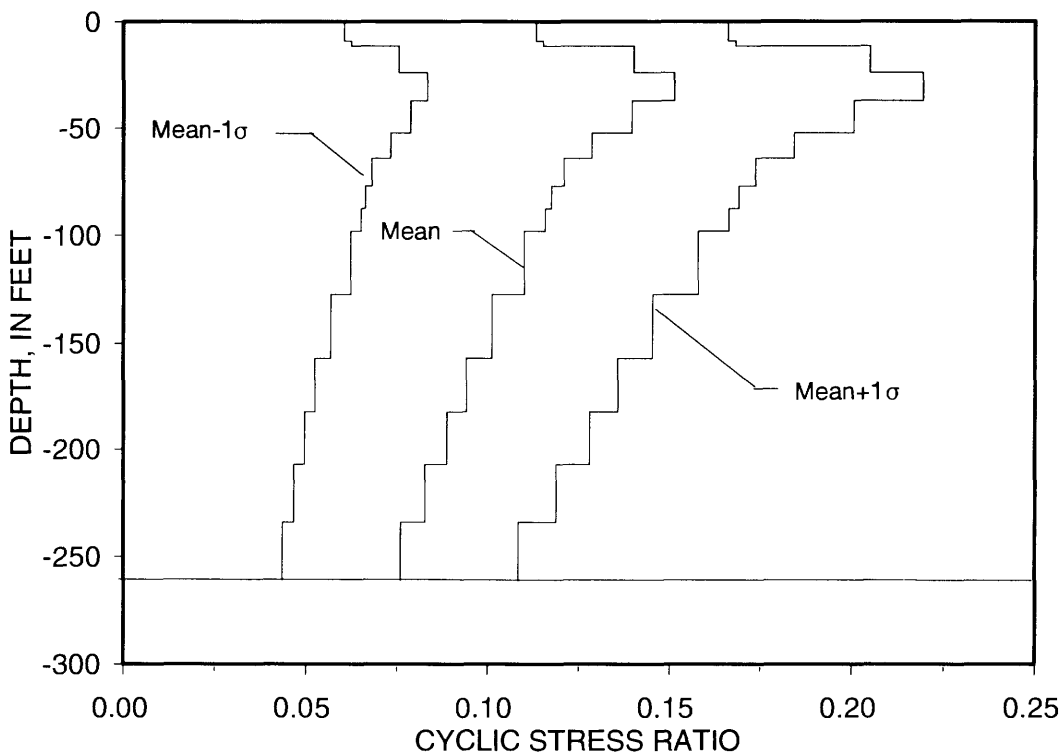


Figure 16.—Mean and mean±1σ curves of cyclic-stress ratio versus depth as calculated from ground-response analysis.

Overall, the measured settlements are generally within about 1σ of the mean settlements calculated by the procedure of Tokimatsu and Seed (1987). Estimates were less accurate for sites where large settlements (>80 mm) had occurred. The ratio of the measured settlement to the calculated settlement ranges from 0.4 to 1.6. We can gain some perspective on the success of this procedure by noting the accuracy and reliability of equations for predicting settlement of structures built on sand under static conditions. Tan and Duncan (1991) proposed that the most accurate static-settlement prediction be multiplied by 1.7 to ensure that 85 percent of the measured settlements would be less than the computed settlements. Considering these results, the agreement here between measured and computed settlements for earthquake shaking is encouraging.

## CONCLUSIONS

1. Computed peak accelerations in the Marina District are approximately 0.15±0.05 *g* whereas computed normalized spectral shapes are nearly identical to those recorded at other soft-soil sites in the 1989 Loma Prieta earthquake.
2. Although the Marina District classifies as an ATC S2 site, computed normalized spectral shapes agreed well with those recorded at distant soft-soil (ATC S3) sites in several other earthquakes and are generally enveloped by the ATC S3 design spectrum.
3. Computed peak acceleration in the Marina District for an $M_S$=7.1 earthquake on the closest segment of the San Andreas fault was 0.46±0.05 *g*. A future near-field earthquake would generate higher levels of earthquake shaking and cause more extensive liquefaction in the Marina District.
4. The procedure of Tokimatsu and Seed (1987) shows promise in providing reasonable predictions of earthquake-induced settlements, using relatively simple computation procedures; however, measured settlements may differ from the mean computed value by a factor of as much as 2. Additional study is needed to confirm the procedure and to determine the effect of fines content on the correlations.

## ACKNOWLEDGMENT

This research was supported by National Science Foundation grant NSF–BCS–9011294.

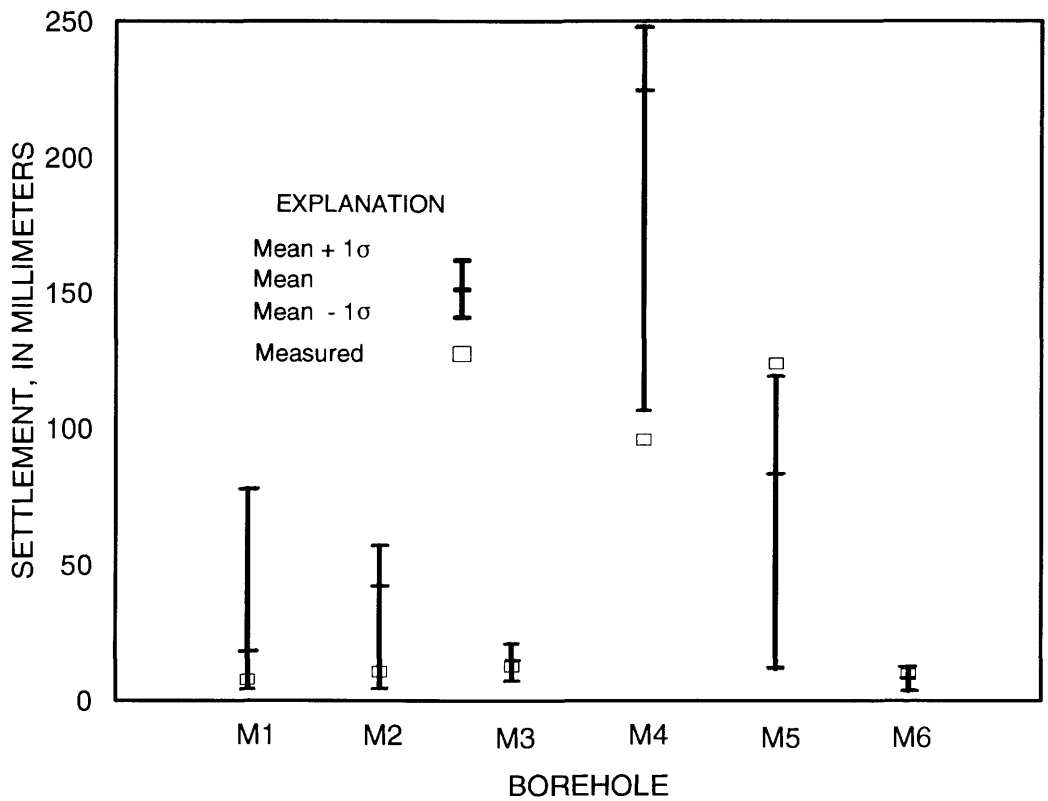


Figure 17.—Comparison of measured and calculated settlement at U.S. Geological Survey boreholes (see fig. 13 for locations) in the Marina District.

## REFERENCES CITED


Applied Technology Council, 1978, Tentative provisions for the development of seismic regulations for buildings: Publication ATC–3–06, 505 p.

Bennett, M.J., 1990, Ground deformation and liquefaction of soil in the Marina District, chap. D *of* U.S. Geological Survey, Effects of the Loma Prieta earthquake on the Marina District, San Francisco, California: Open-File Report 90–253, p. D–1 to D–36.

Bonilla, M.G., 1990, Natural and artificial deposits in the Marina District, chap. A *of* U.S. Geological Survey, Effects of the Loma Prieta earthquake on the Marina District, San Francisco, California: Open-File Report 90–253, p. A–1 to A–24.

Joyner, W.B., Warrick, R.E., and Oliver, A.A., 1976, Analysis of seismograms from a downhole array in sediments near San Francisco Bay: Seismological Society of America Bulletin, v. 66, no. 3, p. 937–958.

Kayen, R.E., Liu, H.-P., Fumal, T.E., Westerlund, R.E., Warrick, R.E., Gibbs, J.F., and Lee, H.J., 1990, Engineering and seismic properties of the soil column at Winfield Scott School, San Francisco, chap. G *of* U.S. Geological Survey, Effects of the Loma Prieta earthquake on the Marina District, San Francisco, California: Open-File Report 90–253, p. G–1 to G–18.

Lodde, P.F., 1982, Dynamic response of the San Francisco Bay Mud: Austin, University of Texas, M.S. thesis, 283 p.

McNutt, S.R., and Toppozada, T.R., 1990, Seismological aspects of the 17 October 1989 earthquake, in McNutt, S.R., and Sydnor, R.H., eds., The Loma Prieta (Santa Cruz Mountains), California, earthquake of 17 October 1989: California Division of Mines and Geology Special Publication 104, p. 11–27.

Mitchell, J.K., Masood, Tahir, Kayen, R.E., and Seed, R.B., 1990, Soil conditions and earthquake hazard mitigation in the Marina District of San Francisco: Berkeley, University of California, Earthquake Engineering Research Center Report UBC/EERC–90/08, 59 p.

Rollins, K.M., McHood, M.D., Hryciw, R.D., Homolka, Matthew, and Shewbridge, S.E., 1994, Ground response on Treasure Island, *in* Borcherdt, R.D., ed., The Loma Prieta, California, earthquake of October 17, 1989—strong ground motion: U.S. Geological Survey Professional Paper 1551–A, p. A109–A121.

Schnabel, P.B., Lysmer, John, and Seed, H.B., 1972, SHAKE; a computer program for earthquake response analysis of horizontally layered sites: Berkeley, University of California, Earthquake Engineering Research Center Report EERC 72–12, 88 p.

Seed, H.B., and Idriss, I.M., 1970, Soil moduli and damping factors for dynamic response analyses: Berkeley, University of California, Earthquake Engineering Research Center Report EERC 70–10, 15 p.

Seed, H.B., Idriss, I.M., Makdisi, F.I., and Banerjee, N.G., 1975, Representation of irregular stress time histories by equivalent uniform stress series in liquefaction analysis: Berkeley, University of California, Earthquake Engineering Research Center Report EERC 75–29, 13 p.

Seed, H.B., Tokimatsu, Kohji., Harder, L.F., and Chung, R.M., 1984, The influence of STP procedures in soil liquefaction resistance evaluations: Berkeley, University of California, Earthquake Engineering Research Center Report UBC/EERC–84/15, 50 p.

Seed, H.B., Ugas, Celso, and Lysmer, John, 1976, Site-dependent spectra for earthquake-resistant design: Seismological Society of America Bulletin, v. 66, no. 1, p. 221–243.

Seed, R.B., Dickenson, S.E., Riemer, M.F., Bray, J.D., Sitar, Nicholas, Mitchell, J.K., Idriss, I.M., Kayen, R.E., Kropp, Alan, Harder, L.F., Jr., and Power, M.S., 1990, Preliminary report on the principal geotechnical aspects of the October 17, 1989 Loma Prieta earthquake: Berkeley, University of California, Earthquake Engineering Research Center Report UBC/EERC–90/05, 137 p.

Structural Engineers Association of California, 1990, Recommended lateral force requirements and commentary: San Francisco, 60 p.

Sun, J.I., Golesorkhi, R., and Seed, H.B., 1988, Dynamic moduli and damping ratios for cohesive soils: Berkeley, University of California, Earthquake Engineering Research Center Report UCB/EERC–88/15, 42 p.

Tan, C.K., and Duncan, J.M., 1991, Settlement of footings on sands—accuracy and reliability, in Geotechnical Engineering Congress, Boulder, Colo., 1991, Proceedings: American Society of Civil Engineers Special Publication 27, v. 1, p. 446–455.

Tokimatsu, Kohji, and Seed, H.B., 1987, Evaluation of settlements in sands due to earthquake shaking: Journal of Geotechnical Engineering, v. 113, no. 8, p. 861–878.

U.S. Geological Survey, 1990, Effects of the Loma Prieta earthquake on the Marina District of San Francisco, California: Open-File Report 90–253.

Warrick, R.E., 1974, Seismic investigation of a San Francisco bay mud site: Seismological Society of America Bulletin, v. 64, no. 2, p. 375–385.

STRONG GROUND MOTION AND GROUND FAILURE

# IMPROVED-GROUND PERFORMANCE DURING THE EARTHQUAKE

By James K. Mitchell,
Virginia Polytechnic Institute and State University;
and
Frederick J. Wentz, Jr.,
Woodward-Clyde Consultants

## CONTENTS



ABSTRACT

Various ground-improvement methods have been used increasingly in recent years to reduce the potential for liquefaction and lateral spreading of loose cohesionless to slightly cohesive soils. Several deep-densification methods have been applied, including vibrocompaction, vibroreplacement, dynamic deep compaction, penetration grouting, and compaction grouting. The 1989 Loma Prieta earthquake provided one of the first opportunities to evaluate the behavior of improved ground that has actually been subjected to significant seismic shaking.

Using available data, we have evaluated 12 sites where the ground had been improved before the earthquake, including five sites on Treasure Island, two sites in Santa Cruz, and one site each in Richmond, Emeryville, Bay Farm Island, Union City, and South San Francisco. The ground-improvement methods that had been used included vibrating probe (Terraprobe), vibroreplacement with stone columns, sand-compaction piles, nonstructural-displacement piles, dynamic deep compaction, compaction grouting, and chemical-penetration grouting.

For each study site, we collected the available information and analyzed it with respect to type of structure or facility, initial soil conditions, level of ground improvement required, ground-improvement methods considered and selected, construction procedures and problems, level of ground improvement achieved, intensity of earthquake shaking, and performance of the improved ground. At all but one of the study sites, the soil was manmade fill. Seven of these sites contained a hydraulic sand fill. The required depths of ground improvement were as much as about 30 ft at most sites, with a treatment depth of 40 ft specified for one site. The peak ground accelerations recorded at the study sites ranged from 0.11 *g* at Marina Bay in Richmond and at the Kaiser-Permanente Medical Center in South San Francisco to 0.45 *g* at the two sites in Santa Cruz.

Without exception, little or no distress or damage due to ground shaking occurred either to the improved ground or to the facilities and structures built on it. At many study sites, unimproved ground adjacent to the improved ground cracked and (or) settled, primarily owing to liquefaction. At every study site where the ground shaking was severe enough that liquefaction of the unimproved ground would be predicted to occur, it did occur. Together, these results support our conclusions that (1) the procedures used for prediction of liquefaction are reliable and (2) ground improvement is an effective method for mitigation of liquefaction risk.

In assessing these results and their implications for the future, we note that the 1989 Loma Prieta earthquake was of only moderate intensity and unusually short duration. On average, at each study site, except for those nearest the epicenter, peak ground accelerations of only about 25 to 75 percent of the design-earthquake accelerations were recorded. How these sites will perform in an earthquake of greater local intensity and duration is unknown; however, almost certainly, soil liquefaction and related effects on the improved ground will be reduced in comparison with those on unimproved ground.

## INTRODUCTION

Since the late 1960's, various methods of soil stabilization or ground improvement have been used at several sites in the San Francisco Bay region specifically to mitigate the risk of damage to existing structures and other facilities due to liquefaction, lateral spreading, and other forms of ground distress caused by moderate to large earthquakes.

Evaluations conducted after the 1989 Loma Prieta earthquake showed that essentially no distress or damage occurred at any site where the ground had been improved. This observation provides evidence of the overall value of engineered fills and different ground-improvement methods, as well as an opportunity for a detailed study of the performance of improved-ground sites that were subjected to various levels of ground shaking during the earthquake.

Accordingly, we chose 12 sites (table 1) for study where the soil types and ground-improvement methods are well known: five sites on Treasure Island, two sites in Santa Cruz, and one site each in Richmond, Emeryville, Bay Farm Island, Union City, and South San Francisco (fig. 1). At each study site, we collected and analyzed as much information as was available concerning (1) the type of structures or facilities; (2) initial soil conditions; (3) level of ground improvement required; (4) ground-improvement methods considered and selected; (5) analytical studies performed, if any; (6) construction methods and problems; (7) field control and evaluation; and (8) performance during the earthquake. Where possible, we compared the behavior of areas of improved ground with that of adjacent areas of unimproved ground.

The peak accelerations and bracketed durations[1] of shaking for accelerations greater than 0.1 *g* at each study site during the earthquake are listed in table 2. These values were estimated on the basis of data from the U.S. Geological Survey (USGS) and the California Division of Mines and Geology (CDMG). At all but one study site, the actual intensity of ground shaking was substantially less than the design value. Furthermore, the total duration of ground shaking was less than 15 s, about half that expected for an $M$=7 earthquake. The bracketed durations for accelerations greater than 0.1 *g* were considerably shorter at all the study sites except those in Santa Cruz. Nevertheless, the ground motion was strong enough at most study sites to cause liquefaction of unimproved ground. At some study sites, especially on Treasure Island, little specific information is available concerning construction procedures, field testing, and evaluation of the final results of ground improvement. The ground at many of the study sites was improved during the late 1960's, and many project files are no longer available.

[1] The bracketed duration is the elapsed time between the first and last waves with accelerations greater than some specified value.

## GROUND-IMPROVEMENT METHODS

We describe briefly below the different ground-improvement methods that were used at the study sites. More complete descriptions and details of these methods were given by Mitchell (1981), Welsh (1986), and Hausmann (1990).

### VIBROSTABILIZATION

Vibrostabilization methods for deep compaction of cohesionless soils are characterized by the insertion of a cylindrical probe into the ground, followed by compaction by vibration during withdrawal. In some of these methods, a granular backfill is added so that a sand or gravel column is left behind within a volume of sand compacted by vibration. Sinking of the probe to the desired depth is generally accomplished by vibration, commonly supplemented by water jets at the tip.

### VIBRATING PROBE

The Terraprobe method, developed in the United States, uses a Foster Vibro-driver pile hammer on top of a 2.5-ft-diameter open tubular probe (pipe pile) that is 10 to 16.5 ft longer than the desired penetration depth. Other types of vibrating probes have recently been developed, including the Vibro-Wing and the Tri-Star or Y-Probe (Wightman, 1991).

### VIBROCOMPACTION (VIBROFLOTATION)

The vibrocompaction method (fig. 2) achieves good results in clean granular soils containing less than about 15

Table 1.—*Ground-improvement study sites in the San Francisco Bay region*

[Do., ditto]

| No. (Fig. 1) | Study site | Location | Soil conditions | Method | Year |
|---|---|---|---|---|---|
| 1 | Medical/Dental Building------ | Treasure Island------ | Hydraulic sand fill---------- | Stone columns | 1989 |
| 2 | Office Building 450---------- | --do---------- | --do---------- | Sand-compaction piles | 1967 |
| 3 | Facilities 487, 488, and 489- | --do---------- | --do ---------- | Vibrocompaction | 1972 |
| 4 | Approach to berthing pier---- | --do---------- | --do---------- | Stone columns | 1984 |
| 5 | Building 453---------- | --do---------- | --do---------- | Nonstructural timber piles | 1969 |
| 6 | East shore of Marina Bay---- | Richmond---------- | --do---------- | Stone columns | 1986 |
| 7 | East Bay Park Condominiums | Emeryville---------- | Silty, sandy, and gravelly fill | Vibrocompaction | 1981 |
| 8 | Harbor Bay Isle Development | Alameda---------- | Hydraulic sand fill---------- | Deep dynamic compaction | 1985 |
| 9 | Hanover Properties---------- | Union City---------- | Silty sand fill---------- | --do---------- | 1988 |
| 10 | Permanente Medical Center addition | So. San Francisco-- | Hydraulic sand fill---------- | Compaction grouting | 1978 |
| 11 | Riverside Avenue Bridge----- | Santa Cruz---------- | Sand and gravel---------- | Chemical grouting | 1986 |
| 12 | Santa Cruz County Detention Facility | --do---------- | Silty, sand fill---------- | Deep dynamic compaction | 1978 |

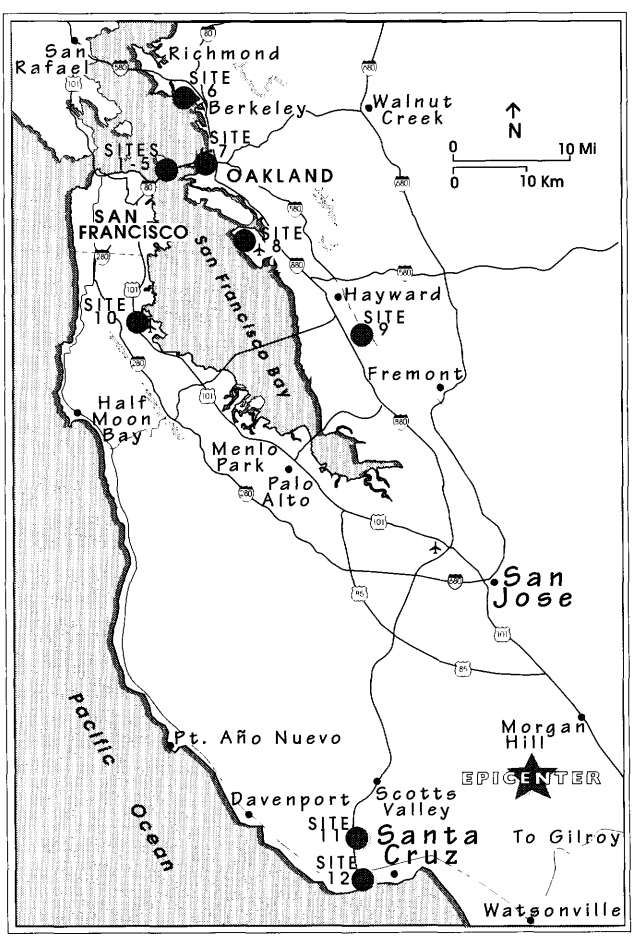


◀ Figure 1.—San Francisco Bay region, showing locations of ground-improvement study sites (dots): 1, Medical/Dental Building, Treasure Island; 2, Office Building 450, Treasure Island; 3, Facilities 487, 488, and 489, Treasure Island; 4, approach to berthing pier, Treasure Island; 5, Building 453, Treasure Island; 6, east shore of Marina Bay, Richmond; 7, East Bay Park Condominiums, Emeryville; 8, perimeter sand dikes, Harbor Bay Isle Development, Alameda; 9, Hanover Properties, Union City; 10, Kaiser-Permanente Medical Center addition, South San Francisco; 11, Riverside Avenue Bridge, Santa Cruz; 12, Santa Cruz County Detention Facility, Santa Cruz.

to 20 percent fines. The action of the vibrator, commonly accompanied by water jetting, reduces the intergranular forces between the soil particles, allowing the particles to move into a more compact configuration. After the optimum configuration has been reached, the vibrator is raised a short distance, and the procedure repeated. The increase in density is accompanied by a reduction in volume, which is compensated by backfilling the annulus around the vibrator with sand as the vibrator is withdrawn. In stratified soils where layers of soft cohesive material are present, the resulting column of compacted sand functions as compression and shear reinforcement.

## VIBROREPLACEMENT (STONE COLUMNS)

Vibroreplacement is used in soils with a higher fines content (>15–20 percent) than can be densified by

Table 2.—*Peak and design-earthquake accelerations at ground-improvement study sites in the San Francisco Bay region*

[Do., ditto]

| No. (Fig. 1) | Study site | Location | Distance from epicenter (mi) | Peak acceleration(g) Actual | Peak acceleration(g) Design | Bracketed duration (A ≥ 0.10 g) (s) |
|---|---|---|---|---|---|---|
| 1 | Medical/Dental Building----- | Treasure Island------ | 60 | 0.16 | 0.35 | 2.5 |
| 2 | Office Building 450---------- | --do---------- | 60 | .16 | .43* | 2.5 |
| 3 | Facilities 487, 488, and 489- | --do---------- | 60 | .16 | .43* | 2.5 |
| 4 | Approach to berthing pier--- | --do---------- | 60 | .16 | .35 | 2.5 |
| 5 | Building 453---------- | --do---------- | 60 | .16 | .45* | 2.5 |
| 6 | East shore of Marina Bay---- | Richmond---------- | 68 | .11 | .35 | 1.0 |
| 7 | East Bay Park Condominiums | Emeryville---------- | 60 | .26 | .35 | 2.0 |
| 8 | Harbor Bay Isle Development | Bay Farm Island--- | 49 | .25 | .35 | 4.0 |
| 9 | Hanover Properties---------- | Union City---------- | 39 | .16 | N/A | 3.0 |
| 10 | Permanente Medical Center addition | So. San Francisco | 51 | .11 | N/A | 2.0 |
| 11 | Riverside Avenue Bridge---- | Santa Cruz---------- | 10 | .45 | N/A | 15.0 |
| 12 | Santa Cruz County Detention Facility | --do---------- | 10 | .45 | .45 | 15.0 |

* Completed during the late 1960's; design earthquake used was the 1940 El Centro, Calif., earthquake (scaled to a peak acceleration of 0.43-0.45 g).

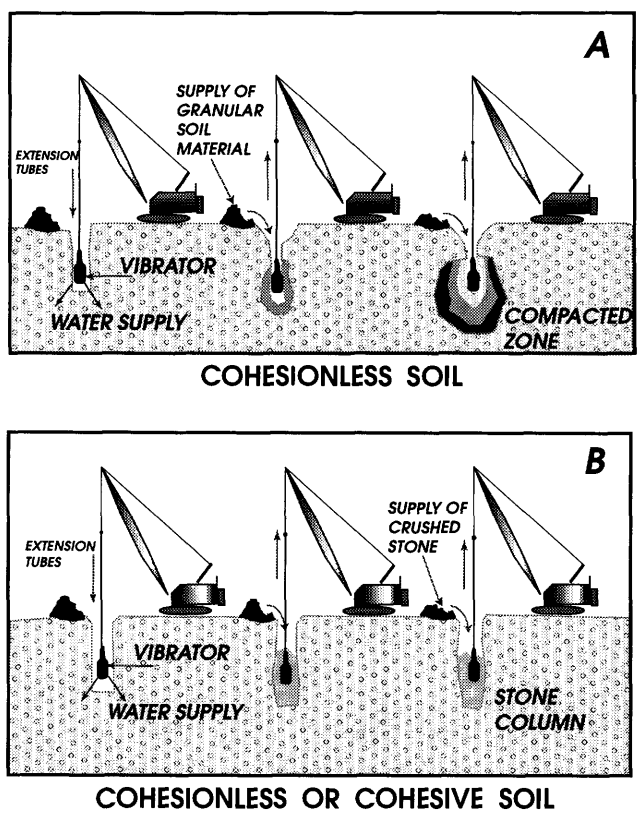


Figure 2.—Equipment and steps used in vibroflotation (*A*) and vibroreplacement (*B*).

vibroflotation, or even in clay soils where the strata do not respond satisfactorily to vibrations.

Most stone columns are installed by using the vibroreplacement method in a manner similar to vibrocompaction, as shown in figure 2. A probe penetrates to the desired depth by vibration and jetting. Gravel backfill is dumped into the hole in increments of 1.5 to 2.5 ft and compacted by the vibrating probe, simultaneously displacing the material radially into the soil.

The diameter of the resulting column, which can be estimated from the rock consumption, generally ranges from 2 to 3.5 ft. In the dry process, which is being increasingly used, a bottom-feed system is used in which the gravel or crushed-rock backfill is discharged at the bottom of the hole through a pipe attached to the side of the vibroflot.

Although clay and silt do not densify significantly by vibration, the stone columns confine the soil, thus increasing the bearing capacity and reducing settlement. In addition, in fine-grained liquefiable soils, besides stiffening the matrix, the stone column also acts as a vertical drain. Therefore, not only does vibroreplacement increase the relative density of the layers susceptible to liquefaction, but it also allows rapid dissipation of excess pore-water pressures induced by earthquake loading. In addition, the increased stiffness and shear resistance provided by the columns themselves create additional reinforcement of the soil mass.

## DYNAMIC DEEP COMPACTION

Dynamic deep compaction involves repeated dropping of 10- to 40-ton weights onto the ground surface from heights of as much as 120 ft in a grid pattern (fig. 3). Shockwaves generated by the impact densify the soil by rearranging the particles into a more compact arrangement. This method can substantially improve the engineering properties of a wide range of soils, including loose sand, mining spoils, collapsible soils, and construction rubble.

Layers or large obstructions that could inhibit the penetration of vibrators will not affect the dynamic-deep-compaction method, which is typically limited to a maximum improvement depth of about 40 ft. The major limitations of this method are the possible effects on nearby facilities from the vibrations, flying debris, and noise. Dynamic deep compaction is best employed in large open areas.

## COMPACTION PILES

Compaction piles densify the soil by displacement and provide compression and shear reinforcement in soft soils. Two types of compaction piles were used at the study sites: sand-compaction piles and nonstructural-displacement piles.

Figure 3.—Dynamic deep compaction in operation.

*Sand-compaction piles.*—A casing pipe is driven to the desired depth, using a mandrel, and then filled with sand. The pipe is withdrawn part way while compressed air is blown down inside the casing to hold the sand in place, and then the pipe is redriven down to compact the sand pile and enlarge its diameter. The process is repeated until the pipe reaches the ground surface.

*Nonstructural-displacement piles.*—Nonstructural-displacement piles are driven with a follower to a depth equal to the length of the pile. The soil surrounding the piles is compacted by displacement. The piles serve no structural function but remain in place permanently. This method is rarely used today.

### GROUTING

Grouting involves the injection of materials into voids in the soil, generally through boreholes and under pressure. A major advantage of grouting is that it can be used in small, difficult-to-access areas. Two grouting methods were used at the study sites: compaction grouting and chemical grouting.

*Compaction grouting.*—At sites where vibrostabilization methods and dynamic deep compaction may be impractical, particularly those with deep layers of loose liquefiable soils, compaction grouting can be used to displace and densify the soil. Typically, a stiff (1–2-in. slump) soil-cement-water mixture is injected into the soil, forming grout bulbs that displace and densify the surrounding ground without penetrating the soil pores. With slightly more fluid grout, thick fissures rather than bulbs may form; this process is sometimes referred to as "squeeze grouting" (Hausmann, 1990).

*Chemical grouting.*—Chemical grouting is used mainly to stabilize foundation soils under existing structures. With this method, pressure-injecting low-viscosity chemical grouts into granular-soil pores forms a strong, sandstone-like material. When grout gel fills voids in loose sandy soils, liquefaction is no longer possible, the cohesion added by the chemical grout provides increased bearing capacity, in addition to reducing liquefaction potential. The long-term stability of chemical grouts should be considered when selecting the type of grout to be used.

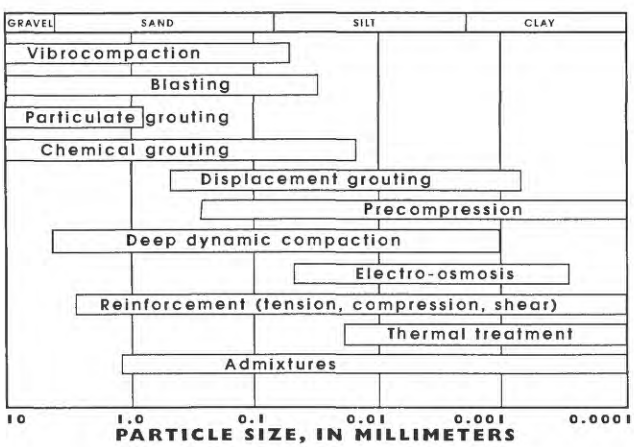


Figure 4.—Applicable grain-size ranges for various ground-improvement methods.

The choice of ground-improvement method generally depends on the prevailing soil profile, environmental conditions, and cost. The presence of near-surface ground water or soft, fine-grained soils, and the proximity to existing structures and utilities, place constraints on which methods can be used. The ground-improvement methods that are useful relative to different soil particle-size ranges are diagrammed in figure 4.

## CASE HISTORIES

### TREASURE ISLAND

Treasure Island is a manmade island in San Francisco Bay consisting of as much as 50 ft of hydraulically placed sand fill over natural bay deposits. A perimeter dike surrounds the island. A plan of the island with the relative locations of the five areas of improved ground is shown in figure 5. The effects of strong ground shaking during the earthquake were evident by the presence of liquefaction sand boils across most of the island. The peak acceleration recorded on Treasure Island was 0.16 *g*, in contrast to a peak acceleration of only 0.06 *g* on bedrock at Yerba Buena Island just to the south. The much stronger ground shaking on Treasure Island resulted from the amplification of relatively modest bedrock motions by the deep soil layer beneath the island.

Liquefaction of subsurface soils was evidenced by the presence of sand boils in many places. Settlements, both areal and localized, were also observed in many places. In the area of the perimeter dike, ground cracking caused by bayward lateral spreading was readily apparent. In addition, several buckled pavements, broken utility lines, and distressed buildings were observed across the island; however, little or no distress or damage occurred to structures or facilities built on improved ground.

#### MEDICAL/DENTAL BUILDING

##### SITE DESCRIPTION

The Medical/Dental Building (fig. 5; Harding Lawson Associates, 1986b, 1990) was under construction at the time of the earthquake, with about 40 percent of the building's footings cast and two 22-ft-deep elevator shafts

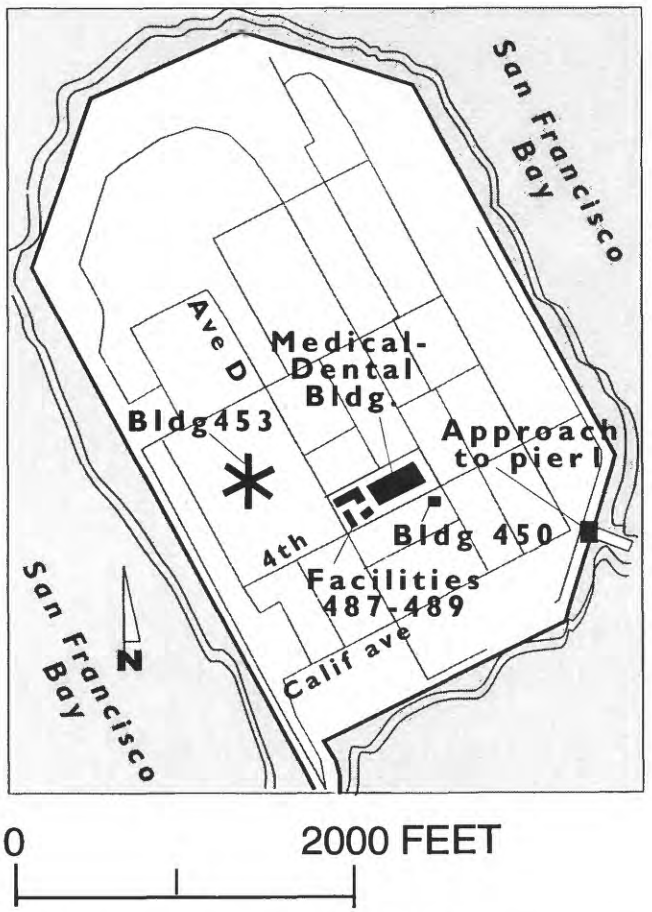


Figure 5.—Treasure Island, showing locations of ground-improvement study sites (1–5, fig. 1).

excavated. The building consists of a two-story steel-frame structure, with a total floor area of approximately 55,000 $ft^2$. The first floor is slab-on-grade, with a finish floor approximately 1 1/2 ft above the initial grade. The dead-plus-live column loads are as much as 115 tons; typically, the columns are spaced 30 ft apart.

## INITIAL CONDITIONS

The study site is nearly level, and the ground surface is approximately 13 ft above mean lower low water (MLLW). Near the west boundary of the study site is a maintained landscaped berm with small trees, shrubs, and grass. A subsurface cross section along the east-west centerline of the study site, illustrating the soil conditions in the boreholes, is shown in figure 6. The penetration-resistance profile is an average from several borings. The upper 31 to 43 ft of soil is composed of loose to medium-dense, hydraulically placed sand fill. The sand is generally fine to medium grained and contains an average of 12 percent of material finer than a No. 200 sieve. Above 20-ft depth, the fines content averages 8 percent, and below 20-ft depth 16 percent. A few thin layers of soft, compressible silt (dredged bay mud) were penetrated throughout the fill. The sand fill is underlain by a layer of soft to medium-stiff clayey silt (bay mud), approximately 30 ft thick, interspersed with thin sand lenses. The bay mud is underlain by alternating layers of dense to very dense sand and stiff to hard clay to the depth penetrated. The ground-water

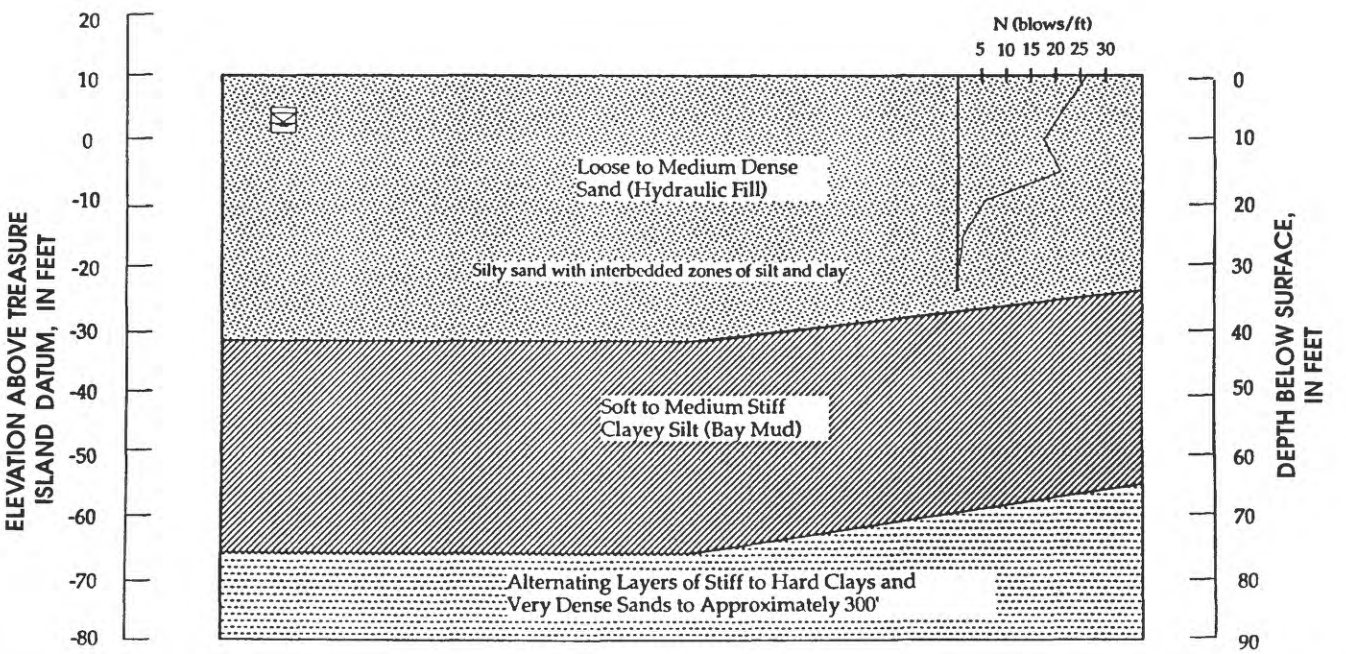


Figure 6.—Soil profile at Medical/Dental Building, Treasure Island (fig. 5). Standard-penetration-test blowcounts (*N* values) are averages from several boreholes.

level at the study sites was approximately 7 ft below the ground surface (approx 6 ft above MLLW) at the time of drilling.

## LIQUEFACTION POTENTIAL

The building designers evaluated the liquefaction potential of the hydraulically placed sand fill at three levels of ground shaking, using the empirical method of Seed and others (1983). The results, based on the assumptions of a water table at a depth of 7 ft and that accelerations can continue to be amplified after the soil liquefies, are summarized in table 3.

Table 3.—*Results of liquefaction-potential analysis for the hydraulic sand fill at the Medical/Dental Building on Treasure Island*

[See figure 1 for location of study site]

| Magnitude | Peak acceleration (g) | Depth of liquefiable zone (ft) |
|---|---|---|
| 6-1/4 | 0.15 | 17-43 |
| 6-3/4 | .25 | 17-43 |
| 7-1/2 | .35 | 7-43 |

## FOUNDATION ALTERNATIVES

The building could be founded on either spread footings or piles. However, if spread footings were used, then the sand fill would have to be densified to reduce its liquefaction potential. Alternatively, 12-in.-square prestressed/precast-concrete piles with a 125-ton load capacity, would be required, driven approximately 130 ft below the ground surface to reach their full bearing capacity. Thus, a pile-supported foundation would not be as economical as densifying the sand fill and founding the building on spread footings. In addition, movement of the subsiding ground surface relative to the stationary, pile-supported building during liquefaction would require that the utility connections be specially designed, thus increasing costs.

## GROUND-IMPROVEMENT GOALS AND METHODS

To prevent liquefaction, the upper layer of sand fill was to be improved to a minimum relative density of 75 percent beneath the building and to a distance of 20 ft beyond the building's perimeter. The densification achieved was measured by cone-penetration test (CPT) and standard penetration test (SPT).

Because deep-sand-densification methods are normally ineffective in the upper few feet of the soil layer, owing to the absence of confining pressure at the surface, specifications required that near-surface sand not densified to the required density as determined by CPT and SPT be excavated, backfilled, and compacted to a minimum relative compaction of 95 percent using surface compactors.

Several deep-densification methods believed to be appropriate for the soil conditions at the study site, including vibroreplacement, Terraprobe densification, dynamic compaction, conventional compaction piles, and sand-compaction piles, were investigated. The final recommendation was that either vibroreplacement or Terraprobe densification be used. Vibroreplacement, using gravel backfill, was ultimately chosen because this method would produce the greatest densification in the shortest time. Dynamic deep compaction was also considered, but the risk of disturbing neighboring structures was judged to be too great.

## CONSTRUCTION PROCEDURES AND PROBLEMS

A series of tests was done, using probe spacings of 8, 9, and 10 ft, to determine the largest spacing that would still satisfy the densification requirements. SPT's and CPT's were performed before and after ground improvement to evaluate the results of the densification. The SPT and CPT results showed that:

1. The uppermost 10 ft of the sand layer was already dense before treatment and was not densified further by vibroreplacement. The lowermost part (10–22 ft deep) of the sand layer was loose to medium dense before densification, and its density was increased. The closer the probe spacing, the higher was the cone-tip resistance after densification. The specified cone-tip resistances were achieved in the entire layer except the lowermost few feet for a probe spacing of 8 ft.
2. Silty-sand fill interbedded with zones of silt and clay underlay the upper part of the fill layer to about 40-ft depth. Adequate densification of this part of the fill layer was not achieved. CPT's indicated that the cone-tip resistance of the silty sand was practically unchanged by densification; however, SPT blowcounts increased from 2 to 5 blows/ft before densification to 3 to 19 blows/ft after densification. The postdensification blowcounts were still lower than specified.

Although the trial densification with the chosen spacings did not densify the soil enough to meet specifications, the contractor was allowed to proceed, using a 10-ft probe spacing penetrating to approximately 22-ft depth below the existing ground surface.

The measured cone-tip resistance indicated the presence of sand-fill layers at 10- to 22-ft depth where the specified resistance was not achieved. Using a volume-calculation method, however, the computed average final relative density of the sand at this depth was estimated at

77 to 80 percent. Ultimately, it was decided that the densification of the uppermost 22 ft of fill did meet specifications. No attempt was made to densify the soil at 22- to 40-ft depth, as required by the specifications. Therefore, we believe that layers of sandy fill are present at this depth that still have a potential for liquefaction in a large earthquake which could cause additional settlement of the structure. The additional total settlement caused by liquefaction was estimated at 1 to 3 in., and the differential settlement between adjacent columns at 1/2 in. After evaluating the risks and benefits of not densifying the lowermost part of the sand layer, it was decided to perform no further densification.

### PERFORMANCE DURING THE EARTHQUAKE

On the basis of data from a CDMG strong-motion-recording instrument located on Treasure Island, the study site was subjected to a peak acceleration of approximately 0.16 *g* within a bracketed duration of about 2.5 s during the earthquake. At that time, approximately 40 percent of the building's footings had already been cast. There was no visible cracking in the footings. It was observed, however, that the bottom 8 ft of the two 22-ft-deep elevator shafts that had been drilled before the earthquake was filled with sand. The engineers were also informed that sand flowed to the ground surface through one of the elevator shafts during the earthquake. From these observations, it was concluded that liquefaction had occurred in the lower, unimproved sand fill at 22- to 40-ft depth. In the area outside of the building footprint, which was not densified, sand boils and ground cracking were observed. The differential settlement of the footings measured in November 1989 was reported to be a maximum of 0.073 ft over a distance of 180 ft. The total settlement of the study site could not be determined because the bench mark had settled during the earthquake. No liquefaction appeared to have occurred in the uppermost 22 ft of sand fill that had been densified by stone columns.

## OFFICE BUILDING 450

### SITE DESCRIPTION

Office Building 450 (fig. 5; Woodward-Clyde-Sherard and Associates, 1966) was constructed in 1967. The study site actually consists of two buildings, each three stories high and of steel-frame construction, with concrete walls and floors. The larger building is 160 by 160 ft in plan and has a central court measuring 30 by 60 ft; the smaller building is 54 by 124 ft in plan and is located approximately 100 ft northwest of the first building. Typical dead-plus-live column loads are 125 to 150 tons. The finish floor elevation is approximately 2 1/2 ft above the initial grade.

### INITIAL CONDITIONS

The study site is nearly level, and the ground surface is approximately 11 ft above MLLW. A subsurface section along the north-south centerline of the study site is shown in figure 7. The uppermost 30 ft of soil is composed of loose to medium dense, hydraulically placed sand fill overlying 8 ft of medium-dense sand. The sand is generally fine to medium grained and contains less than 10 percent of material finer than a No. 200 sieve. Some coarse sand was penetrated in the uppermost 10 ft of the fill, and a few thin layers of soft, compressible silt (dredged bay mud) were penetrated throughout the fill. The sand fill is underlain by a layer of soft to medium-stiff gray silty clay (bay mud), approximately 20 ft thick. The bay mud is underlain by alternating layers of very dense sand and stiff to very stiff clay to the depth penetrated. The groundwater level at the study site was approximately 6 ft below the ground surface (approx 5 ft above MLLW) at the time of drilling.

The liquefaction potential of the saturated sand fill was analyzed by using the methods of Seed and Lee (1966), Lee and Seed (1967), and Seed and Idriss (1967). The results of this analysis showed that the fill would liquefy under the expected peak ground accelerations of 0.30 to 0.40 *g* during a large earthquake.

### FOUNDATION ALTERNATIVES

The building could be founded either on spread footings bearing on densified fill or on driven piles extending through the fill and underlying compressible clay into the bearing soils penetrated below 113-ft depth. The use of piles was ruled out for three reasons: (1) the extreme length of the piles and their associated high cost; (2) the fact that the piles under one corner of the building would be end bearing on bedrock, whereas the rest would be friction piles; and (3) the insufficient lateral stability of the piles, should the sand fill liquefy. It was decided, therefore, to found the buildings on spread footings bearing on densified fill.

### GROUND-IMPROVEMENT GOALS AND METHODS

The sand fill was to be improved to minimum relative densities of 75 percent to a depth of 30 ft beneath the building footings, and of 65 percent to a depth of 30 ft beneath the floor areas and to a distance of 10 ft beyond the building perimeter. Both vibroflotation and sand-compaction piles were considered as densification methods, and an extensive field-testing program was performed to determine which of these two methods would be more effective for the fill. This program and its results were

described by Basore and Boitano (1968) and summarized by Mitchell and Wentz (1991).

For a given spacing, vibrocompaction produced a much denser fill than the compaction piles, although both methods were judged to be effective. Vibrocompaction was estimated to cost about $1.10 less per cubic yard of densified fill than sand-compaction piles. Nonetheless, the owner, giving consideration to the time schedule for construction, the available funds, and existing contractual arrangements, decided to densify the building area with sand-compaction piles spaced 4 ft apart on centers beneath the footings and 5 ft apart on centers beneath the floor slabs.

## FINAL RESULTS OF GROUND IMPROVEMENT

The increase in density of the fill was measured by SPT and by calculating the relative density of samples of the densified fill recovered from 15 boreholes located throughout the building area. The results of control testing indicated that the density of the fill varied somewhat. The average minimum relative density measured at 13 of the 15 boreholes exceeded specifications, and it was concluded that although the average overall densification was adequate, isolated zones of silt and clay remained in the fill which were not densified to specifications.

## PERFORMANCE DURING THE EARTHQUAKE

On the basis of data from a CDMG strong-motion-recording instrument located on Treasure Island, the study site was subjected to a peak acceleration of approximately 0.16 *g* within a bracketed duration of about 2.5 s during the earthquake. A formal building inspection performed soon after the earthquake indicated no evidence of damage. Some lateral spreading, sand boils, and localized settlement were observed outside of the improved ground areas adjacent to the buildings, suggesting that had densi-

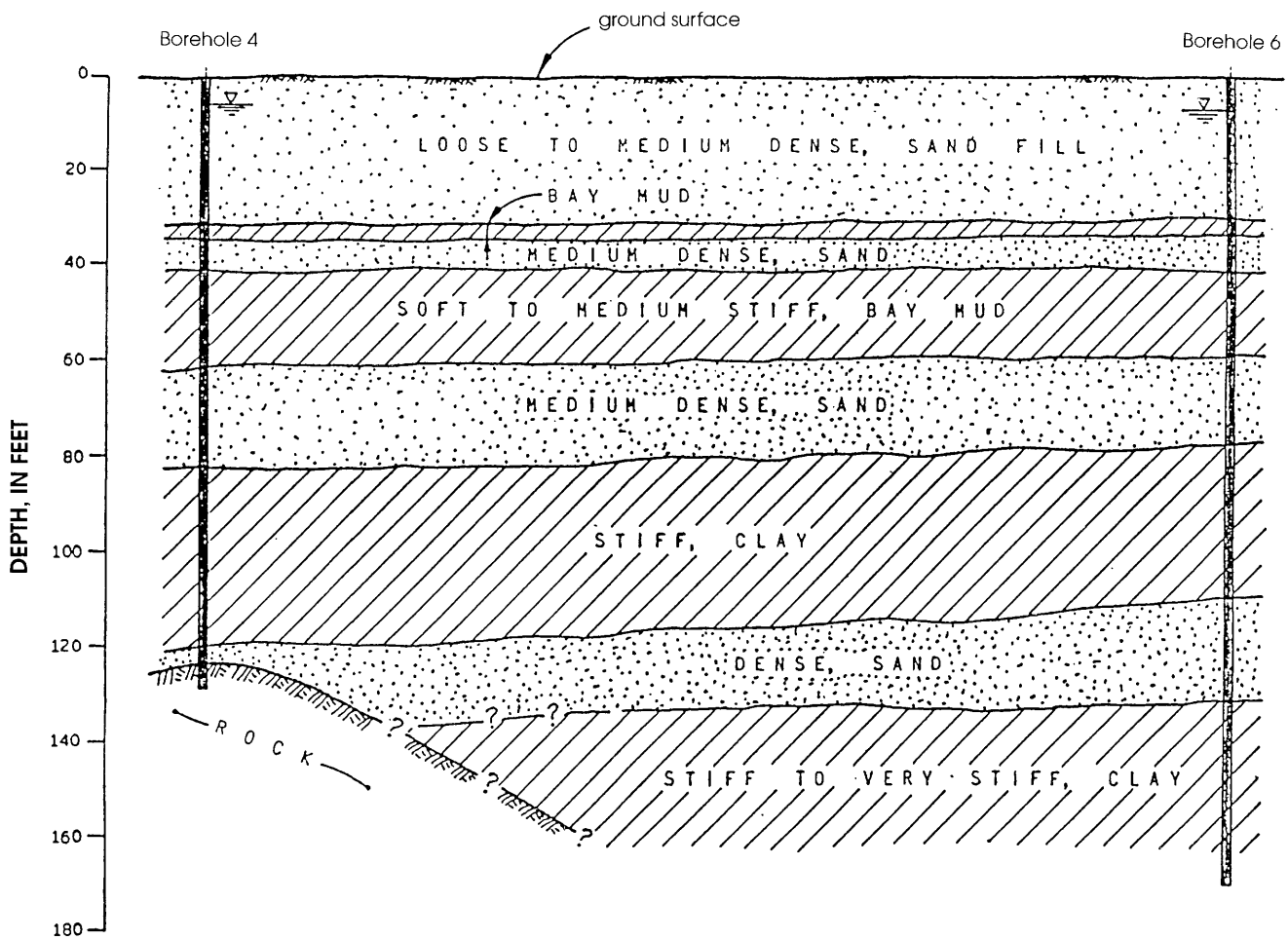


Figure 7.—Soil profile at Office Building 450, Treasure Island (fig. 5). From Woodward-Clyde-Sherard and Associates (1966).

fication not been performed, the soil beneath the building foundations would have liquefied.

## FACILITIES 487, 488, AND 489

### SITE DESCRIPTION

Facilities 487, 488, and 489 (fig. 5; Woodward-Lundgren and Associates, 1972), which were constructed in 1973, consist of three-story buildings with exterior and interior concrete-block walls, precast-concrete floor slabs, and concrete slab-on-grade first floors. Typical dead-plus-live loads for the longitudinal walls are approximately 1.5 tons/ft, for the exterior crosswalls (bearing walls) approximately 2.5 tons/ft, and for the interior crosswalls (bearing walls) approximately 3.5 tons/ft. There are no columns on independent footings.

### INITIAL CONDITIONS

The study site is nearly level, and the ground surface is approximately 10 ft above MLLW. A subsurface section along the east-west centerline of the study site is shown in figure 8. The uppermost 24 to 33 ft of soil is composed of very loose to medium-dense, hydraulically placed sand fill. The sand is generally fine grained and contains less than 12 percent of material finer than a No. 200 sieve. A few thin layers of soft, compressible silt and clay were penetrated in the fill below about 15-ft depth. The sand fill is underlain by a layer of soft silty clay (bay mud) approximately 4 ft thick. The bay mud is underlain by alternating layers of dense to very dense sand and stiff clay to the depth penetrated. The groundwater level at the study site was approximately 5 1/2 ft below the ground surface (4 1/2 ft above MLLW) at the time of drilling.

The liquefaction potential of the sand fill at the study site was evaluated by using the simplified procedure of Seed and Idriss (1971). According to the analysis, the existing saturated sand fill would be only marginally safe against liquefaction during earthquakes of "reasonably large magnitude" (peak accelerations of approx 0.30–0.40 *g*).

### FOUNDATION ALTERNATIVES

The buildings could be founded either on spread footings bearing on sand fill that had been densified to prevent liquefaction or on driven piles extending through the fill and soft bay mud into the bearing soils penetrated below 90-ft depth. The use of pile foundations was considered impractical for three major reasons: (1) long piles would be too expensive; (2) large downdrag forces would be exerted on the piles by settlement of the bay-mud layer; and (3) lateral resistance of the piles might be lost during

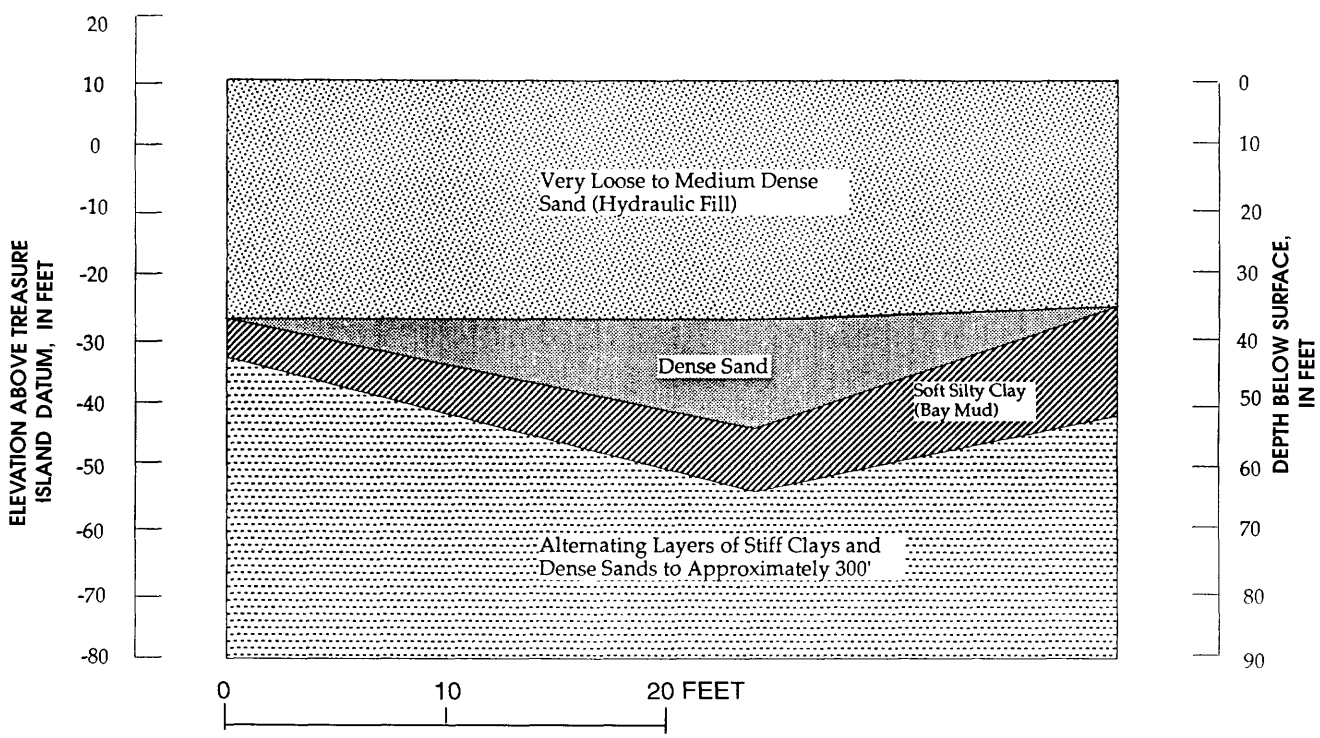


Figure 8.—Soil profile at Facilities 487, 488, and 489, Treasure Island (fig. 5).

an earthquake, owing to liquefaction of the sand. It was decided, therefore, to found the buildings on spread footings bearing on densified sand fill.

### GROUND-IMPROVEMENT GOALS AND METHODS

The hydraulic sand fill was to be improved to a minimum relative density of 75 percent to a depth of 30 ft beneath the buildings and to a distance of 10 ft beyond each building's perimeter. Three methods for densifying the sand fill were investigated: vibrocompaction, Terraprobe, and nonstructural-displacement piles. When the geotechnical engineer recommended either vibrocompaction or Terraprobe, the owner selected vibrocompaction.

A field-testing program was implemented before production densification to establish the optimum spacing for the compaction points. Before and after densifying a test area, SPT's were performed to evaluate the effectiveness of the different spacings used. The minimum spacing between compaction points was 6 1/2 ft, forming a grid of equilateral triangles.

The vibrator was to be inserted at each compaction point to a depth of 30 ft below the ground surface and maintained at that depth for a period of 1 minute, then withdrawn at a rate of not more than 1 ft per minute. Crushed rock no larger than 1 1/2 in. in largest particle dimension was continuously placed around the vibrator and follower pipe during the densification-and-withdrawal process.

### FINAL RESULTS OF GROUND IMPROVEMENT

The densification of the fill was measured by SPT; however, no records of the field-control testing are currently available. Geotechnical engineers at the U.S. Navy's Western Facilities Engineering Command indicated that the average minimum relative densities achieved at the site were no less than the specified minimum relative density of 75 percent.

### PERFORMANCE DURING THE EARTHQUAKE

On the basis of data from a CDMG strong-motion-recording instrument located on Treasure Island, the study site was subjected to a peak acceleration of approximately 0.16 *g* within a bracketed duration of approximately 2.5 s during the earthquake. A formal building inspection performed shortly after the earthquake revealed some minor cracking in the concrete floor of building 487 caused by differential settlement of the foundation; however, no repairs were required. The amount of settlement was not measured. Buildings 488 and 489 had no reported damage.

## APPROACH TO BERTHING PIER SITE

### DESCRIPTION

The general-purpose/berthing pier ("Approach to Pier 1," fig. 5), which was constructed in 1985, consists of a pile-supported reinforced-concrete structure and an approach area to the entrance of the pier. This approach area is the part of the site of interest herein.

### INITIAL CONDITIONS

The surface of the pier approach is nearly level and fronts San Francisco Bay for approximately 100 ft. A cross section along the centerline of the pier, illustrating the soil layers penetrated in boreholes, is shown in figure 9. The soil underlying the pier approach consists of a 43-ft-thick layer of loose to medium-dense, hydraulically placed sand fill. The sand is generally fine to medium and contains less than 10 percent of material finer than a No. 200 sieve. A few thin lenses of soft, compressible silt (bay mud) were penetrated in the upper 20 ft of the fill. The sand fill is underlain by a layer of soft, compressible silty clay (bay mud) approximately 80 ft thick. The bay mud is underlain by alternating layers of very stiff sandy clay and dense sand extending to the depth penetrated.

The geotechnical engineer estimated that the peak acceleration at the study site during the design earthquake would be at least 0.35 *g*. A major concern was possible seismic instability of the waterfront slope of the approach area beneath and adjacent to the pier. The liquefaction potential of the sand fill in the approach area was evaluated by the empirical method of Seed and others (1983), and it was concluded that the sand fill was susceptible to liquefaction. It was decided, therefore, to densify the sand fill underlying the approach area.

### GROUND-IMPROVEMENT GOALS AND METHODS

The sand fill was to be improved to a minimum relative density of 75 percent beneath the approach area to a depth of 40 ft. Because the top few feet of sand normally is not adequately densified by deep vibrators, owing to the absence of confining pressure at the surface, the uppermost layer of sand was compacted by conventional methods to a minimum relative compaction of 95 percent according to American Society for Testing and Materials (ASTM) method D1557–78.

Three methods were considered for densifying the sand fill at depth: compaction piles, vibroreplacement, and vibrating probe (Terraprobe). The final recommendation of the geotechnical engineer, based on a combination of cost, time, and effectiveness considerations was the Terraprobe.

A 30-in.-diameter open-ended steel pipe was used for the probe; several rectangular "windows" were cut into the side of the pipe to permit sand inflow from around the sides. Before densification, a blanket of coarse sand and gravel was placed over the site to compensate for the loss of elevation caused by densification of the underlying sand.

A series of densification tests was performed to establish the spacing criteria for the compaction probes and to determine static cone penetration resistance correlations to SPT $N$ values. A multiplier of 4.0 was used to convert the SPT $N$ values to equivalent $q_c$ values. The sand fill in the test sections was to be densified to the SPT $N$ values or CPT $q_c$ values listed in table 4.

In connection with these criteria, the SPT's were done at depth intervals of 2.5 ft. The average of three consecutive SPT $N$ values measured at the specified depth intervals above, at, and below any depth was to be no less than the value listed in table 4. The boreholes were located at points equidistant from three probe locations. The CPT's were performed at depth intervals not exceeding 1 ft. The CPT $q_c$ values were to be no less than the values listed in table 4, except where the friction ratio was greater than 2.0 percent. The CPT $q_c$ values were measured at points equidistant from three probe locations.

## FINAL RESULTS OF GROUND IMPROVEMENT

The CPT data indicated that the lower 5 to 7 ft of the fill consisted mainly of silty sand and sandy silt which did not meet the minimum densification requirements. It was judged that this material was potentially liquefiable but that reprobing the layer would probably not result in significant ground improvement. Overall, it was concluded that densification of the sand fill above this layer had been achieved to within the minimum relative density specified.

## PERFORMANCE DURING THE EARTHQUAKE

On the basis of data from a CDMG strong-motion-recording instrument located on Treasure Island, the study site was subjected to a peak acceleration of approximately 0.16 $g$ within a bracketed duration of about 2.5 s during the earthquake. A formal inspection of the pier approach performed shortly after the earthquake revealed no signs of ground movement in the improved areas; however, several sinkholes and sand boils were observed in the adjacent, unimproved areas.

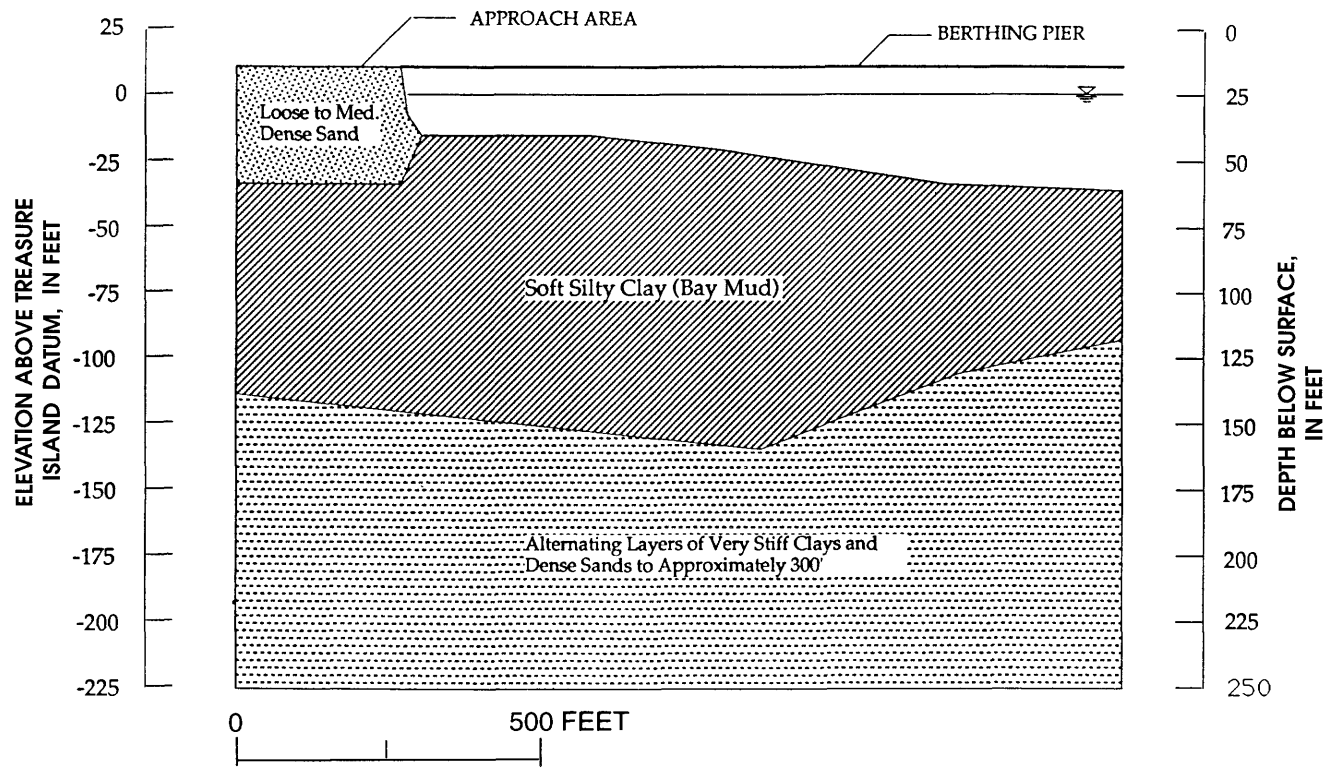


Figure 9.—Soil profile at approach to berthing pier, Treasure Island (fig. 5).

Table 4.—*Ground-improvement specifications for the approach to the berthing pier on Treasure Island*

[See figure 1 for location of study site. CPT, cone-penetration test; SPT, standard penetration test]

| Depth below ground surface (ft) | SPT N values | CPT $q_c$ = 4N (tons/ft$^2$) |
|---|---|---|
| 5 | 11 | 44 |
| 10 | 15 | 60 |
| 15 | 19 | 76 |
| 20 | 22 | 90 |
| 25 | 25 | 100 |
| 30 | 27 | 106 |
| 35 | 28 | 114 |
| 40 | 30 | 120 |

## BUILDING 453

### SITE DESCRIPTION

Building 453 (fig. 5), constructed in 1969, consists of six four-story reinforced-concrete wings radiating from a central core. The finish floor is approximately 2 1/2 ft above the existing grade. Estimated dead-plus-live loads for the wings are approximately 3.1 tons per linear foot for the exterior walls and 3.7 tons per linear foot for the interior walls. The core loads are carried by a series of circumferential and radial walls. The building loads average 735 and 560 lb/ft$^2$ over the gross core and wing areas, respectively.

### INITIAL CONDITIONS

The study site is nearly level, with a surface elevation of approximately 10 ft above MLLW. A north-south cross section of the study site is shown in figure 10. The uppermost 45 ft of soil is composed of loose to medium-dense, hydraulically placed sand fill. The sand is generally fine to medium grained and contains less than 12 percent of material finer than a No. 200 sieve. A few thin lenses of soft, compressible silt (dredged bay mud) were penetrated in the lower 20 ft of fill. The sand fill is underlain by a layer of soft to medium-stiff clayey silt (bay mud), approximately 20 ft thick. The bay mud is underlain by alternating layers of stiff clay and dense sand to the depth penetrated. The ground-water level at the study site was approximately 6 ft below the ground surface (4 ft above MLLW) at the time of drilling.

At the time of construction, the 1964 Niigata, Japan, earthquake was the only good previous case study for liquefaction analysis. The initial liquefaction analysis method of Seed and Idriss (1967) was used to evaluate the liquefaction potential of the sand fill at the study site. From this analysis, it was concluded that the upper 30 ft of sand fill could liquefy in a large earthquake (peak accelerations, >0.35 g).

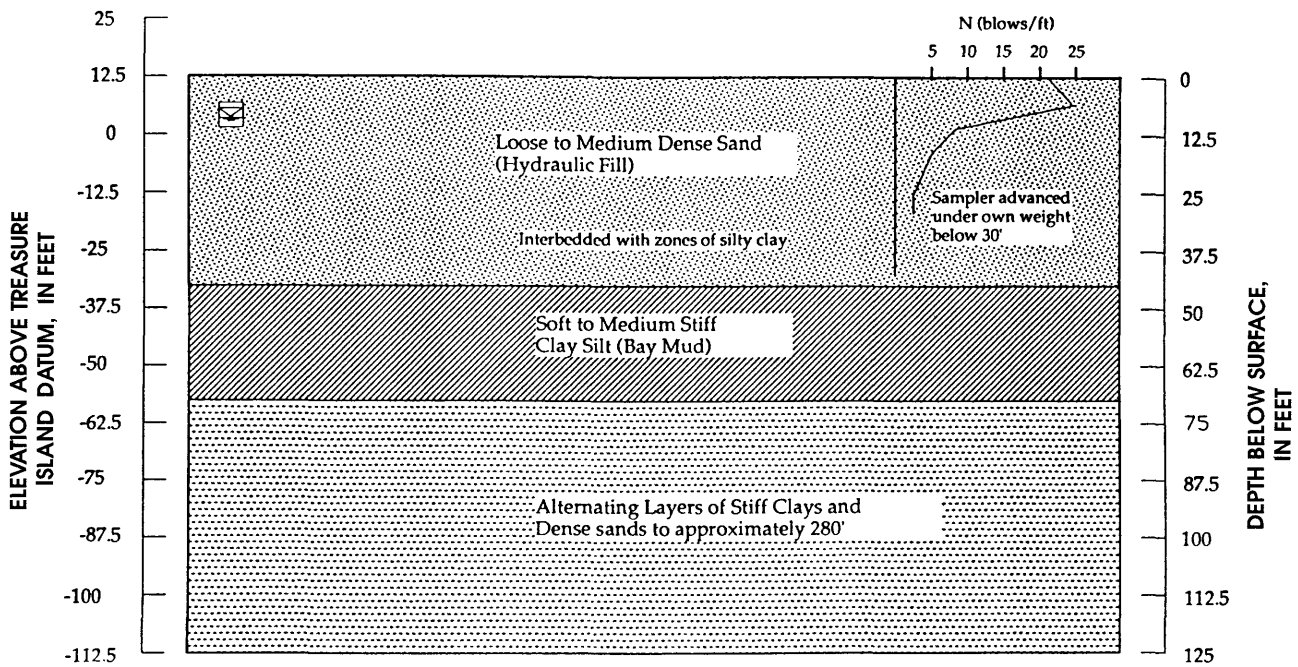


Figure 10.—Soil profile at Building 453, Treasure Island (fig. 5).

### FOUNDATION ALTERNATIVES

The building could be founded on either spread footings or piles. Because of the liquefaction potential of the sand fill, it was decided that if spread footings were used, the sand fill should be densified. The use of piles for structural support would not be as economical as spread footings bearing on densified fill because of the modest strength of the supporting soils and the large downdrag forces that would be exerted on the piles by settlement of the soft clay and fill.

### GROUND-IMPROVEMENT GOALS AND METHODS

The sand fill was to be improved to a minimum relative density of 70 percent to a depth of 30 ft under the building and to a distance of 10 ft beyond the building's perimeter. Because deep sand densification methods are ineffective in the uppermost few feet of the soil layer, owing to the absence of confining pressure at the surface, the uppermost four ft of fill was to be excavated, backfilled, and recompacted to a minimum relative compaction of 95 percent, according to ASTM method D1557.

Three methods were considered for densifying the sand fill: vibrocompaction, sand-compaction piles, and nonstructural-displacement piles. The sand-compaction piles were to be 14 in. in diameter and spaced approximately 3 1/2 ft apart on centers. The nonstructural-displacement piles were to be class C timber piles with an 8-in. minimum tip diameter and a 12-in. minimum diameter 3 ft from the butt; they were to be approximately 20 ft long and driven to a depth of approximately 25 ft into the fill. The tops of the piles would be driven below grade so that they would be below the permanent ground-water level and therefore immune to deterioration. The fill above the pile butts would then be excavated and recompacted to refill the voids created by the pile follower.

The costs (in 1969 dollars) of vibrocompaction, sand-compaction piles, and nonstructural-displacement piles were estimated at $3.00, $1.50, and $2.60 per square foot of ground surface, respectively. The owner chose nonstructural-displacement piles to densify the site.

### CONSTRUCTION PROCEDURES

Field tests were performed to determine the required spacing of the displacement piles. A relation between pile spacing and average pile diameter was formulated by assuming that the class C pile would have an average diameter of 10 in. in the "loose zone" (at 16–25-ft depth) and thus require a 4.3-ft center-to-center spacing in a triangular pattern. Because the nonstructural-displacement piles were driven approximately 6 1/2 ft below grade, the soil above the piles was excavated and recompacted to remove the voids created by the pile follower.

### FINAL RESULTS OF GROUND IMPROVEMENT

The densification of the fill was measured by SPT. The final average relative density of the sand fill is unknown. However, we conclude that the densification program was successful, on the basis of our discussions with U.S. Navy's Western Facilities Engineering Command engineers.

### PERFORMANCE DURING THE EARTHQUAKE

On the basis of data from a CDMG strong-motion-recording instrument located on Treasure Island, the study site was subjected to a peak acceleration of approximately 0.16 *g* within a bracketed duration of about 2.5 s during the earthquake. The building was inspected for damage shortly after the earthquake, but no major structural damage was observed inside the building, although there was a concrete spall at the end of one wing. In addition, some cracking was observed in the floor system, and some repairs were required for the slab-on-grade, owing to minor ground settlements (less than 3/8 in.). No foundation repairs were required, and no sinkholes, sand boils, or other evidence of liquefaction was observed near the building.

## EAST SHORE OF MARINA BAY, RICHMOND

### SITE DESCRIPTION

The study site (fig. 11; Harding Lawson Associates, 1986a) consists of an extension to Marina Bay Esplanade by approximately 1,000 ft along the east shore of Marina Bay constructed in 1987. This expansion includes walkways, landscape areas, and light standards. The walkways are supported at grade, with a finish-surface elevation of about 7.5 ft, relative to the National Geodetic Vertical Datum (NGVD). The adjacent shoreline is sloped 3:1 (horizontal to vertical) and protected with rock riprap. A large residential development is located just east of the esplanade.

### INITIAL CONDITIONS

At time of construction, the study site was nearly level, with a surface elevation of about 14 ft and an asphalt concrete pavement. Adjacent to Marina Bay, the ground surface sloped on an average of 2:1 toward the water. An

east-west cross section is shown in figure 12. The uppermost 13 ft of soil is composed of medium-dense to dense sandy and gravelly artificial fill interspersed with clay inclusions and construction debris. The artificial fill is underlain by a layer of loose, hydraulically placed silty sand and sandy silt, approximately 11 ft thick. The sand is generally fine grained and contains as much as to 55 percent of material finer than a No. 200 sieve. This fill is underlain by medium-stiff to stiff clay to the depth penetrated. The ground-water level at the study site was approximately 10 ft below the ground surface (5 ft NGVD) at the time of drilling.

The liquefaction potential of the hydraulically placed silt and sand fill was evaluated by using an analytical-empirical procedure based on the liquefaction behavior of saturated clean and silty sand during historical earthquakes (Seed and others, 1984). An $M$=6.5 design earthquake resulting in a peak acceleration of 0.30 $g$ at the study site was used in all the liquefaction analyses. The primary data used in the analyses consisted of SPT $N$ values obtained from field investigations and corrected for fines content (Seed, 1987). The resulting $(N_1)_{60}$ values ranged from 11 to 22 blows/ft and averaged 15 blows/ft. On the basis of these analyses, it was concluded that a continuous deposit of liquefiable soils was present between elevations of 5 and -11 ft along the entire length of the study site. This deposit was overlain by a dense surface layer of liquefaction-resistant material, approximately 9 ft thick.

In the event of liquefaction of the underlying deposit, the surface layer would prevent complete loss of bearing capacity. However, because the liquefiable deposit is ad-

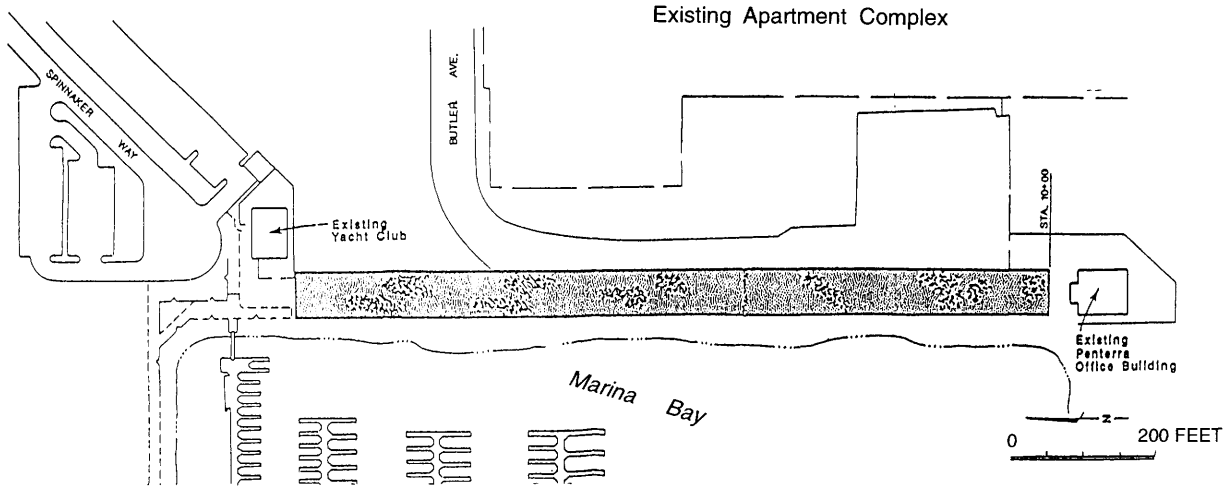


Figure 11.—East shore of Marina Bay, Richmond (study site 6, fig. 1). From Harding Lawson Associates (1987).

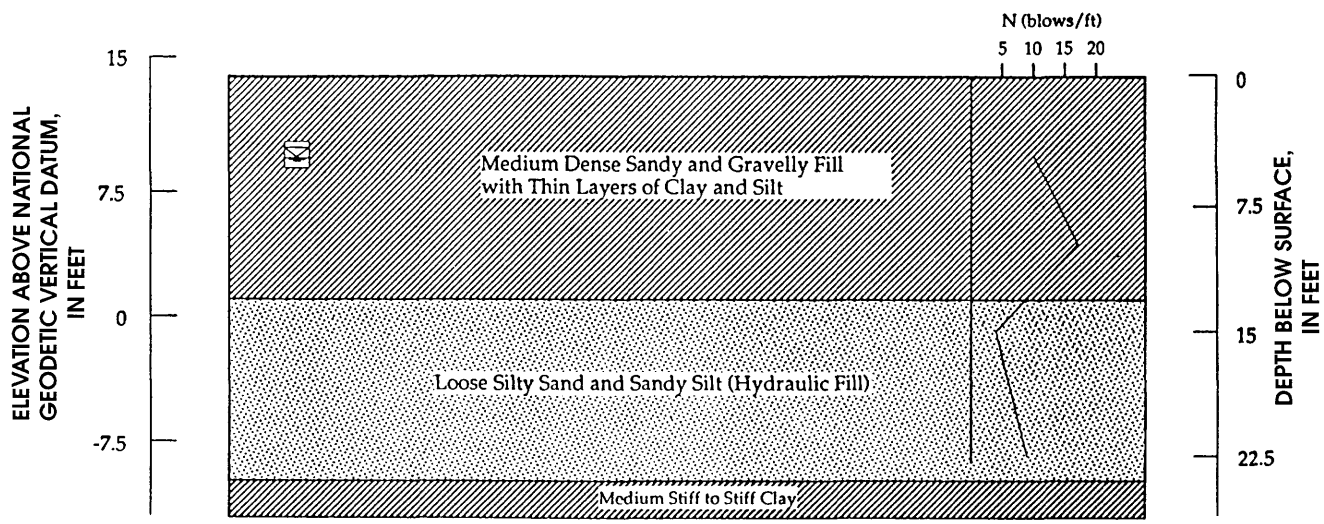


Figure 12.—Soil profile at Marina Bay Esplanade, Richmond (study site 6, fig. 1).

jacent to Marina Bay and lateral spreading during an earthquake was predictable, a significant risk to inland development existed. Both the city of Richmond and the developer agreed that it would be uneconomical to eliminate the liquefaction potential of the entire deposit under the study site. Therefore, it was decided to construct a "buttress" through the liquefiable deposit along the shoreline boundary to resist lateral spreading.

## GROUND-IMPROVEMENT GOALS AND METHODS

The specified level of ground improvement required that the liquefiable soils in the buttress area be densified enough to prevent liquefaction, on the basis of the CPT correlations proposed by Seed and others (1983) and Robertson and Campanella (1985), and by using SPT data (Seed and others, 1984).

Several densification methods were considered for developing a buttress that would be stable and buildable, given the economic and time constraints of the project. Because of the high fines content of the liquefiable deposit, it was believed that such ground-improvement methods as dynamic deep compaction or vibrocompaction would not densify the soil adequately to form an effective buttress. Therefore, it was decided to construct the buttress by using the vibroreplacement stone-column method (Rinne and others, 1988).

The buttress consists of 42-in.-diameter stone columns placed 6 ft apart on center in a square grid, extending about 1 ft below the bottom of the liquefiable zone at an elevation of -12 ft, as shown in figure 13. The buttress is trapezoidal in cross section, with crest and base widths of about 16 and 58 ft, respectively. The inland face of the buttress slopes at about 1:1, and the outboard (bayside) face at about 2:1. The crest elevation is 6 ft.

The stone-column buttress is intended to limit lateral spreading in two ways. First, the columns, which consist of dense, liquefaction-resistant crushed rock, reinforce the slope along the shoreline. Second, installation of the columns increases the liquefaction resistance of the sand and silt around the columns by densification and provides both increased lateral confinement and a drainage path to dissipate earthquake-induced pore pressures.

## CONSTRUCTION PROCEDURES

The stone columns were constructed by using two 1 1/2-ft-diameter, 12-ft-long downhole vibrators suspended from cranes. The vibrators were advanced into the ground dry, primarily by their vibratory energy. The hole created by the vibrator was backfilled with 3/8-in. by 1-in. crushed rock placed in about 3-ft-thick lifts, using a bottom-feed system. The amount of crushed rock required for each lift was determined by assuming an inplace relative density and computing the weight of rock required to achieve a 42-in.-diameter column at this density.

For the first several days of construction, the cranes were working from a pad excavated to an elevation of 8 ft and frequently became stuck in the soft subgrade soils. Therefore, the cranes were moved to the paved area just east of the buttress alignment. Minor slope failures and settlement occurred in the asphalt-paved area north of the Penterra office building (fig. 12), owing to construction-induced vibrations. In addition, tension cracks appeared in several areas behind the vertical slope parallel to the centerline of the buttress. Because of a concern that construction-induced vibrations might damage the Yacht Club at the north end of the buttress, the northernmost row of columns was eliminated. In addition, the vibrators were unable to penetrate the ground surface at five locations

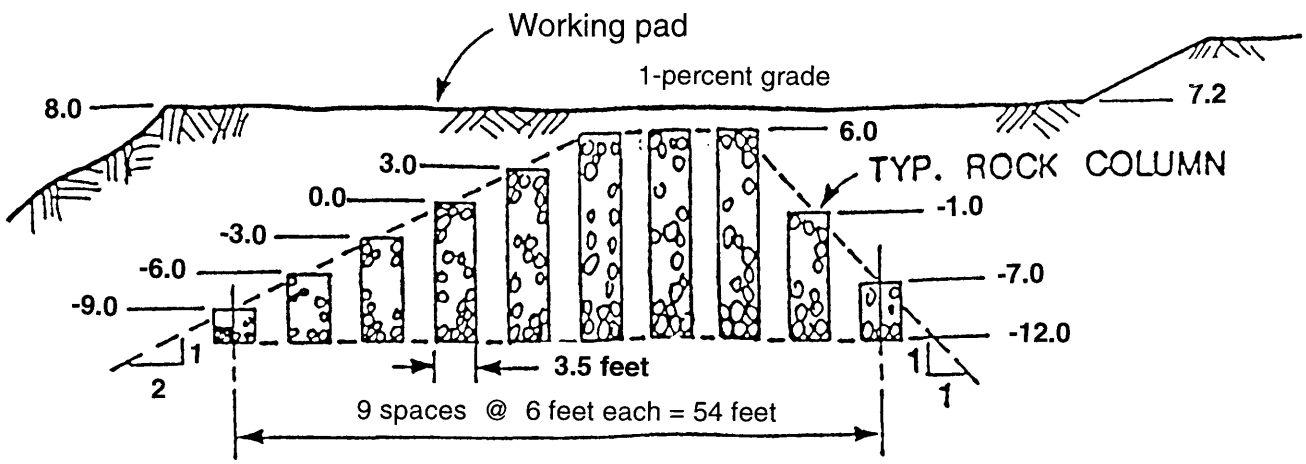


Figure 13.—Typical cross section of buttress on Marina Bay Esplanade, Richmond (study site 6, fig. 1). Numbers are elevations in feet above National Geodetic Vertical Datum. From Harding Lawson Associates (1987).

along the westernmost row of columns because of concrete debris in the fill. Therefore, the entire row of columns was shifted 6 ft eastward at these locations.

During the installation of each stone column, the as-built column-tip elevation and column length were recorded, and the amount of rock placed in each column was monitored. In addition, the maximum drive-motor resistance of the downhole vibrator was recorded for each column to give a qualitative indication of the increase in relative density of the rock.

## FINAL RESULTS OF GROUND IMPROVEMENT

To determine the effect of placing stone columns in the liquefiable deposit, 10 boreholes were drilled and 12 CPT probes were advanced in various locations between the stone columns. CPT $q_c$ values were converted to $q_{c1}$ values, using the correction factors of Robertson and Campanella (1985). The correlations between liquefaction resistance and $q_{c1}$ values proposed by Seed and others (1983) and Robertson and Campanella (1985), as well as SPT data (Seed and others, 1984), were used to evaluate the postconstruction liquefaction potential of the sand and silt in the buttress zone.

Average preconstruction and postconstruction $q_{c1}$ values are plotted in figure 14. The liquefaction potential of the deposits before densification was moderate to high, using the correlation of Seed and others (1983), and high, using the correlation of Robertson and Campanella (1985). The average $q_{c1}$ value increased by approximately 45 kg/cm$^2$ after column installation. It was concluded, on the basis of CPT correlations, that the postconstruction liquefaction potential of the hydraulic fill between the stone columns was low for the design earthquake. Increases in cone-tip resistance were greatest in zones with lower silt contents.

Average preconstruction and postconstruction $(N_1)_{60}$ values are plotted in figure 15, which shows the correlation between liquefaction resistance and $(N_1)_{60}$ values for the maximum credible earthquake ($M$=7.5). As shown, the average $(N_1)_{60}$ value increased by 7 blows/ft. Despite this increase, some liquefaction potential exists for the soil between the stone columns during a maximum credible earthquake. The estimated shear-strain potential of the liquefiable deposits, however, decreased from more than 20 percent to approximately 10 percent as a result of ground improvement. Overall, the combination of stone-

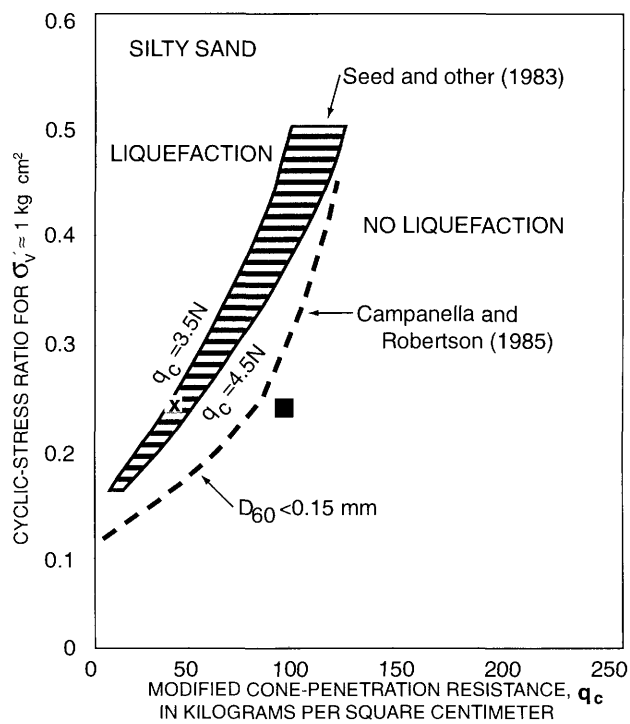


Figure 14.—Comparison of preconstruction (x) and postconstruction (square) cone-penetration-test data for an $M$=6.5 earthquake at Marina Bay Esplanade, Richmond (study site 6, fig. 1). From Rinne and others (1988).

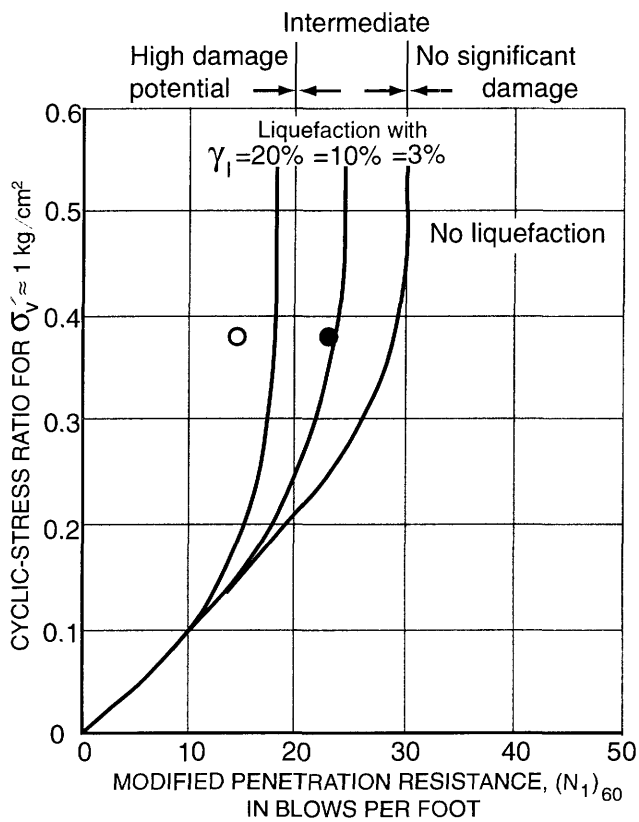


Figure 15.—Comparison of preconstruction (circle) and postconstruction (dot) standard-penetration-test data for an $M$=7.5 earthquake at Marina Bay Esplanade, Richmond (study site 6, fig. 1). From Rinne and others (1988).

column reinforcement and the increase in liquefaction resistance of the soil between the columns was judged to be sufficient to prevent lateral spreading into the bay in the event of liquefaction of the unimproved ground on the inland side of the buttress.

### PERFORMANCE DURING THE EARTHQUAKE

On the basis of data from a USGS strong-motion-recording instrument located in Richmond, the study site was subjected to a peak acceleration of approximately 0.11 *g* within a bracketed duration of about 1 s during the earthquake. No evidence of liquefaction or lateral spreading within or behind the buttress area was detected; however, some small sand boils were observed in undeveloped areas within about 1 mi of the study site.

## EAST BAY PARK CONDOMINIUMS, EMERYVILLE

### SITE DESCRIPTION

East Bay Park Condominiums in Emeryville, Calif. (Woodward-Clyde Consultants, 1981), which consists of a 30-story "tripod shaped" tower and a 4-story parking garage, was constructed in 1983. The tower is a reinforced-concrete, ductile-frame structure; its three wings measure approximately 70 by 140 ft in plan dimensions. Combined dead-plus-live loads on the interior and exterior columns in the tower are approximately 1,500 and 1,150 tons, respectively. The parking garage consists of a reinforced-concrete shear-wall structure, measuring approximately 125 by 514 ft in plan dimension. Combined dead-plus-live column loads in the parking garage are approximately 400 and 250 tons, respectively.

On the basis of bearing-capacity and settlement considerations, deep pile foundations were specified for support of the heavy column loads of both the tower and the parking garage. Other foundation types, including a mat foundation for the tower and footing foundations for the parking garage, were also considered; however, settlement analyses indicated that such foundations would be subject to marginal or excessive settlements. Thus, it was decided to support the tower on 14-in.-square prestressed-concrete piles, and the garage on 12-in.-square prestressed-concrete piles.

### INITIAL CONDITIONS

At the time of the geotechnical investigation, the study site was nearly level and cleared of all existing structures. The uppermost 10 to 20 ft of soil consists of medium dense, hydraulically placed sand interspersed with a few lenses and thin layers of soft silty and sandy clay and containing minor amounts of concrete, brick, and roofing paper. The sand fill is generally fine grained and contains less than 5 percent of material finer than a No. 200 sieve. The fill is underlain by a layer of soft to medium-stiff clayey silt (bay mud), approximately 5 to 12 ft thick. The bay mud is underlain by alternating layers of very stiff clay and dense sand and gravel to the depth penetrated. The ground-water level at the study site was approximately 5 ft below the ground surface at the time of drilling.

### REASON FOR GROUND IMPROVEMENT

This study site is unusual in that both deep foundations and ground improvement were used. The liquefaction potential of the sand fill was evaluated on the basis of SPT blowcount data from boreholes using the simplified analytical procedure of Seed (1979). The results indicated that because the sand fill is typically medium dense, liquefaction and a corresponding complete loss of soil strength were unlikely. However, the sand below the ground-water level could be subjected to some cyclic mobility (Seed, 1979) during moderate to strong earthquake ground shaking at the study site, and such movements could adversely affect the pile foundations. In addition, some areal settlements were expected to occur because of densification of the sand fill during moderate to strong earthquake ground shaking. On the basis of the data of Lee and Albaisa (1974), using SPT data for the study site, it was estimated that settlements of as much as 1 to 1.5 in. could occur. Although these settlements would not affect the pile foundation, they could damage underground utilities, pavements, and other surface improvements. From these considerations, the geotechnical engineer recommended that the sand fill be densified to minimize the potential for cyclic mobility and seismic compaction settlements and to optimize the overall seismic performance of the study site.

### GROUND IMPROVEMENT

The sand fill was densified by using vibrocompaction. Final construction reports are unavailable; however, the following information was provided by engineers who worked on the project (L.R. Houps and Tom Graf, written communs., 1991). More than 1,000 vibrocompaction probe points were spaced in a triangular pattern on 8-ft centers that extended a minimum of 20 ft beyond the footprint of the tower. Pea gravel was used as backfill in the vibrocompaction holes. The relative density of the hydraulic sand fill was increased to more than 100 percent, as inferred from SPT *N* values determined after densifica-

tion. The sand was so dense after treatment that it was necessary to predrill through it so as to drive the foundation piles for the highrise structure.

## PERFORMANCE DURING THE EARTHQUAKE

The study site was subjected to a peak acceleration of about 0.26 *g* within a bracketed duration of about 2 s. No ground settlement or damage to the 30-story tower was observed.

# PERIMETER SAND DIKES, HARBOR BAY ISLE DEVELOPMENT, ALAMEDA

## SITE DESCRIPTION

Perimeter dikes (fig. 16; Hallenbeck and Associates, 1985, 1986), were constructed beginning in 1965 around the bayside of a reclaimed landsite to retain hydraulic fill pumped into the area behind the dikes. The dikes were constructed by excavating a trench with a clamshell or dragline in the bottom of the bay adjacent to and generally outboard of the dike alignment. The excavated material was then placed as fill adjacent to the excavation until a dike extending above the high-water mark was formed. In some places, the excavated materials consisted of silty clay (bay mud), and in other places of sand. The filled area behind the dikes encompasses approximately 900 acres.

## INITIAL CONDITIONS

At the time of the geotechnical investigation, the average ground-surface elevation along the dikes was about 8 ft above bay level, or 108 ft referenced to the Harbor Bay Isle datum. Typically, the outboard (bayside) face of the dikes was covered with rip-rap, and three distinct slope

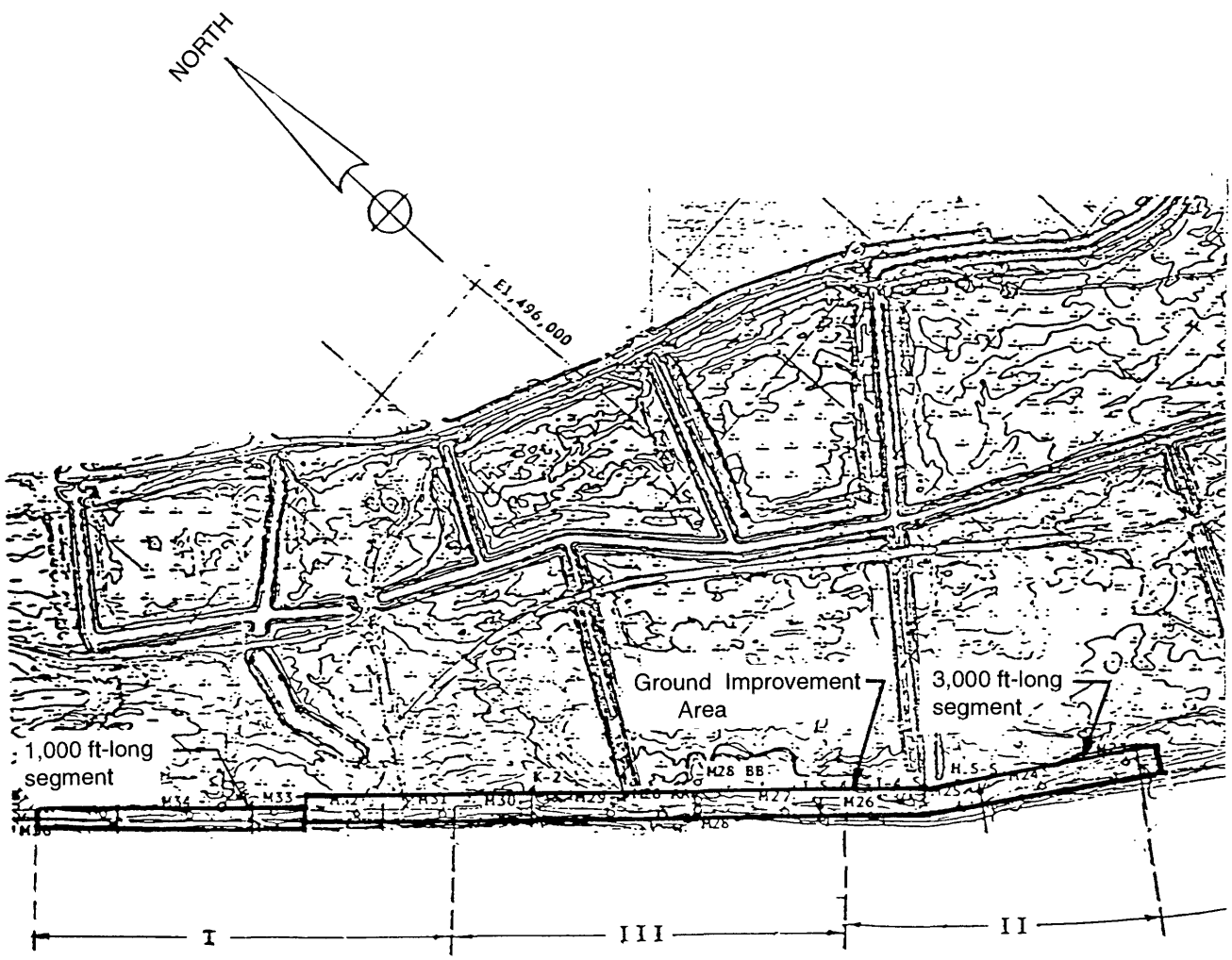


Figure 16.—Perimeter sand dikes at Harbor Bay Isle Development, Alameda (study site 8, fig. 1), showing locations of sections I through III in figure 17. From Hallenbeck and Associates (1985).

inclinations were visible in any one profile. The top parts of the dikes were sloped downward at about 1.5:1 (horizontal to vertical) or steeper for a height of about 10 ft. Below 10 ft, the slope became flatter and was inclined at about 3:1 for an additional height of about 10 ft. Below the toe of the second slope was a long, gradual slope inclined at about 10:1 or flatter for about 200 ft.

On the basis of the results of extensive geotechnical studies, the 4,000 ft of dikes can be divided into three different sections, as shown in figure 16; an idealized subsurface profile of each section is shown in figure 17. Section I consists of a 5- to 7-ft-thick upper layer of medium-dense to dense sand, with SPT blowcounts ranging from 15 to 35 blows/ft. This sand layer is underlain by a layer of loose to medium-dense silty sand, approximately 12 ft thick, with SPT blowcounts ranging from 3 to 10 blows/ft. Both the surface medium-dense to dense sand and the underlying loose sand consist of hydraulically placed fill. Medium-dense to dense silty and clayey sand, with SPT blowcounts of more than 25 blows/ft, was penetrated at 17-ft depth.

Section II similarly consists of 5 to 12 ft of medium-dense sand crust over a layer of loose sand fill; the medium-dense sand has SPT blowcounts ranging from 10 to 20 blows/ft. The loose sand layer is approximately 6 to 13 ft thick and is interspersed with thin clay lenses; this sand layer has SPT blowcounts ranging from 3 to 8 blows/ft. The loose sand is underlain by a layer of soft bay mud, approximately 3 ft thick. The bay mud, in turn, is underlain by a layer of natural loose to medium-dense sand extending to a maximum depth of 26 ft below the ground surface; this sand layer has SPT blowcounts ranging from 8 to 15 blows/ft. Below 26-ft depth, the sand is denser, with SPT blowcounts of more than of 30 blows/ft.

Section III consists of a surface fill layer of 10 to 16 ft of dense sand, with SPT blowcounts ranging from 30 to 40 blows/ft. The dense sand is underlain by a layer of loose to medium dense sand, 6 to 12 ft thick, with SPT blowcounts ranging from 5 to 10 blows/ft. The lower 5 ft of the loose sand layer consists of natural sand. Below 22-ft depth, the natural sand is denser, with SPT blowcounts of more than 30 blows/ft. The hydraulic sand fill is everywhere generally fine grained and contains an average of less than 11 percent of material finer than a No. 200 sieve. The natural sand also is generally fine grained, with an average fines content of about 22 percent. The ground-water level at the study site was at approximately the same elevation as mean sea level at the time of drilling.

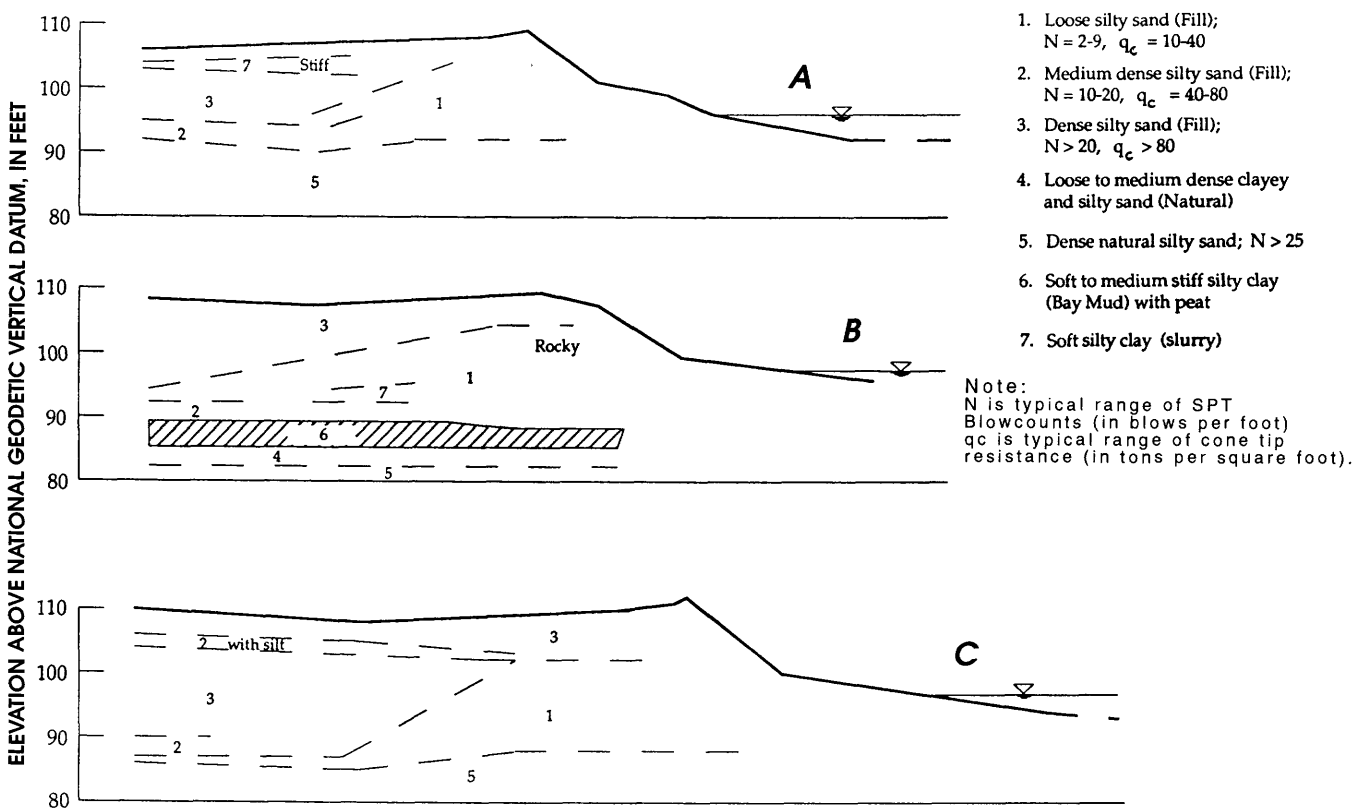


Figure 17.—Subsurface profiles of sections I (*A*), II (*B*), and III (*C*) (see fig. 16 for locations) of perimeter sand dikes at Harbor Bay Isle Development, Alameda (study site 8, fig. 1).

The liquefaction potential of the loose hydraulic sand fill was evaluated by using an analytical-empirical procedure based on SPT $N$ values corrected for fines content (Seed, 1987). An $M$=8.25 earthquake occurring on the San Andreas fault was used as the design earthquake. The results of this analysis showed that the liquefaction potential of the loose and medium-dense sand fill in the dikes was high, and it was concluded that the dikes could undergo excessive yielding or slope failure during a major earthquake. Such yielding or failure would reduce confinement of the interior soils and might allow lateral spreading in the interior of the Harbor Bay Isle development. On the basis of these conclusions, it was recommended that the loose sand fill in the dikes be densified to minimize its liquefaction potential.

### GROUND-IMPROVEMENT GOALS AND METHODS

The sand-fill dike was to be densified between depths of 5 and 26 ft below the ground surface. After ground improvement, the average cone-tip resistance in the sand layers was to be at least 100 kg/cm$^2$. In addition, no more than 10 percent of the recorded cone-tip resistances in any one layer were to be less than 90 kg/cm$^2$. A "layer" was defined as any continuous zone of sand or silty sand within the treatment area lying between any two elevations 3 ft apart.

Dynamic deep compaction, which was the most cost effective method for densifying the sand fill, was chosen for the study site. This method had been used to densify the southeast section of the dike in 1983 with excellent results. Other ground-improvement methods considered were chemical grouting and recompaction of the dikes, using standard grading equipment.

### CONSTRUCTION PROCEDURES

Densification of a 90-ft-wide strip of the 3,000-ft-long segment of dike (fig. 16) was carried out from June to October 1985. Specifications called for a total of five passes of the pounder throughout the entire ground-improvement area. The number and location of pounder drops varied with each pass. A 7- by 7-ft, 20-ton pounder was dropped from a height of 100 ft. The energy applied throughout the 3,000-ft-long segment was about 180 foot-tons per square foot of improved ground.

The required drop pattern for the 1,000-ft-long segment was nearly the same as for the 3,000-ft-long segment. The treatment area was narrowed to 75 ft, and because the soil conditions differed somewhat in the 1,000-ft-long segment from those in the 3,000-ft-long segment, the total number of drops was reduced. For this segment, a 5- by 5-ft, 20-ton pounder was dropped from a height of 95 ft. The total energy applied to the 1,000-ft-long segment was approximately 155 foot-tons per square foot of treated area. The work was done during December 1985 and January 1986.

### FINAL RESULTS OF GROUND IMPROVEMENT

CPT's were performed before, during, and after dynamic deep compaction. In addition, four boreholes were drilled at various locations in the 3,000-ft-long segment of dike when the ground improvement was about half completed, and SPT's were performed to provide a correlation between cone-tip resistance and SPT blowcount at the site. Changes in pore-water pressure in the sand fill after compaction were measured by using both open-standpipe and closed-porous-stone (hydraulic) piezometers. These measurements enabled monitoring the rate of pore-pressure dissipation in the fill after the compaction.

It was concluded that specifications were met or exceeded in the improved areas of the dike. CPT tip resistances in the densified sand averaged at least 100 kg/cm$^2$, except in the south third of the 3,000-ft-long segment. CPT's performed in this section indicated lenses of soil within the profile with tip resistances less than 80 kg/cm$^2$. It was concluded, on the basis of previous CPT data and sampling, that these lenses consist of clay or silt insusceptible to liquefaction. Therefore, no further ground improvement was required.

### PERFORMANCE DURING THE EARTHQUAKE

On the basis of data from a CDMG strong-motion-recording instrument located in downtown Oakland and a strong-motion-recording instrument at the Alameda Naval Air Station, the study site was subjected to a peak acceleration of approximately 0.25 $g$ within a bracketed duration of about 4 s during the earthquake. Evidence of extensive liquefaction (large sand boils, sinkholes) was observed in areas of Bay Farm Island behind the dikes, on the adjacent Oakland International Airport runways, and at the Alameda Naval Air Station. No liquefaction or permanent movement of the perimeter dikes was detected.

## HANOVER PROPERTIES, UNION CITY

### SITE DESCRIPTION

The Hanover properties consist of five relatively lightly loaded tiltup-panel buildings (R.A. Lopez, written commun., 1990) that were constructed in 1988. The buildings cover an area of approximately 200,000 ft$^2$.

### INITIAL CONDITIONS

The study site was nearly level and unimproved at the time of the geotechnical investigation. The uppermost 8 to 12 ft of soil is composed of 2 to 3 ft of hard clayey-silt fill underlain by alternating layers of loose sand and firm silt, approximately 2 ft thick. The sand is generally fine to medium grained. The sand and silt are underlain by a layer of soft to medium-stiff silty clay (bay mud) interspersed with organic materials, approximately 15 ft thick. The bay mud is underlain by stiff to very stiff clay to the depth penetrated. The ground-water level at the study site was approximately 7 ft below the ground surface at the time of drilling.

The liquefaction potential of the loose-sand layers was evaluated by using both SPT and CPT data. It was concluded that the liquefaction potential of the sand layers was moderate to high for a moderate to large earthquake occurring on either the Hayward or San Andreas fault. Therefore, it was decided that the buildings should be founded on spread footings bearing on previously densified soil.

### GROUND-IMPROVEMENT GOALS AND METHODS

The geotechnical engineer specified that the loose-sand layers be densified between a depth of 8 and 12 ft to a minimum relative density of 75 percent beneath the buildings and to a distance of 10 ft beyond each building perimeter.

Several ground-improvement methods believed to be appropriate for soil conditions at the study site, including vibrocompaction, Terraprobe densification, dynamic deep compaction, and excavation and recompaction of the sand, were investigated. It was ultimately decided that the loose sand could be densified by using dynamic deep compaction. This method was chosen because it was estimated to provide the most effective densification for the least cost. The only concern arising from the use of dynamic deep compaction was that improvement would be necessary within 60 ft of an existing warehouse structure and within approximately 25 to 50 ft of existing pavement, curbs, and utility lines. Therefore, it was necessary to provide vibration monitoring in the vicinity of the existing structures and utilities.

### CONSTRUCTION PROCEDURES

Before densification, two test areas of approximately 2,500 $ft^2$ each were treated to establish a drop pattern and the number of drops at each point. The relative success of densification was determined from three factors: (1) CPT's performed both before and after dynamic deep compaction; (2) elevation drop over the test area, indicating the soil-volume reduction; and (3) the amount of energy imparted to the ground. It was found that a 10-ton pounder dropped from a height of 25 ft 10 times at primary drop points and 6 times at secondary drop points satisfactorily densified the loose-sand layers in the test area. The drop pattern used is unknown. The production densification was done by using the procedure developed in the test program.

### FINAL RESULTS OF GROUND IMPROVEMENT

The increase in density of the sand layer was evaluated by comparing SPT and CPT data before densification with CPT data after densification, and by calculating the total soil-volume reduction. These results indicated that the liquefiable-sand layer underlying the study site had been densified to the required minimum. The elevation drop across the site after ground improvement averaged 1 1/2 to 2 ft.

### PERFORMANCE DURING THE EARTHQUAKE

On the basis of data from a USGS strong-motion-recording instrument located in Fremont, the study site was subjected to a peak acceleration of approximately 0.16 *g* within a bracketed duration of about 3 s during the earthquake. No evidence of liquefaction or ground settlement was observed during a postearthquake inspection of the study site.

## KAISER-PERMANENTE MEDICAL CENTER ADDITION, SOUTH SAN FRANCISCO

### DESCRIPTION

The Kaiser-Permanente Medical Center addition, completed in 1979, consists of a one-story structure immediately adjacent to an existing hospital. After the partial collapse of the Veterans' Administration Hospital during the 1971 San Fernando, Calif. earthquake, the State of California required more stringent conditions for seismic design in hospitals with the 1973 Hospital Act. Although the new code was not retroactive, the provisions were applied to hospital structures modified more than 10 percent and thus covered the planned expansion of the Kaiser-Permanente Medical Center.

### INITIAL CONDITIONS

The uppermost 8 ft of soil at the study site is unconsolidated fill consisting of sand, gravel, clay, and con-

struction debris. The fill is underlain by a layer of loose to medium-dense, hydraulically placed, predominantly sand fill extending from 8 to 35 ft below the ground surface. The sand is generally fine to medium grained, with a few samples containing as much as 50 percent fines. The liquefaction potential of the loose to medium-dense, hydraulically placed sand fill was considered to be moderate during a large earthquake; the liquefaction potential of the uppermost 8 ft of fill was considered to be low.

## FOUNDATION ALTERNATIVES

The building could be founded on either spread footings or piles. Because the study site is underlain by an approximately 27-ft-thick layer of potentially liquefiable sand fill, it was decided that if spread footings were to be used, the sand fill should be densified to reduce its liquefaction potential. The use of piles was eliminated because it was thought that the noise of pile driving would be too disruptive to continuing hospital operations.

## GROUND-IMPROVEMENT GOALS AND METHODS

The potentially liquefiable deposit was to be densified to a minimum relative density of 70 percent beneath the building and to a distance of 10 ft beyond the building perimeter. Three methods of densifying the potentially liquefiable layer were considered: nonstructural-displacement piles, compaction grouting, and excavation and recompaction of the liquefiable soils. From a technical standpoint, the preferred method was to use nonstructural-displacement piles; however, because the hospital was to remain in operation during densification, pile-driving operations would be unacceptable.

Excavation and recompaction of the liquefiable soils would have been too expensive and time consuming and so were not seriously considered. It was concluded that compaction grouting of the potentially liquefiable sand layer was the optimum method from both an economic and environmental standpoint, given the project constraints of budget and continuing operation of the hospital.

## CONSTRUCTION PROCEDURES

At the time of construction (1979), little was known quantitatively about the effects of compaction grouting in soils that were not initially loose. Therefore, a test section was constructed at the study site to evaluate the effectiveness of compaction grouting in medium-dense sand. Concrete grout with a 2-in. slump was injected into the sand layer located between depths of 8 and 35 ft. A variable injection-point spacing was used to determine the optimum grid pattern and spacing. Injection pressures and grout-take volumes were also monitored.

Each injection point was grouted from the top of the sand layer downward uniformly in stages to the bottom of the layer. Casing was first installed at each injection point to a depth of 8 ft. Grout was injected in all locations until a slight ground heave (approx $^1/_8$ in.) was observed or until the grout refused to flow at injection pressures as high as 600 lb/in$^2$. The grout was then allowed to harden, and the hole was advanced by drilling through the hardened grout to the next stage to be grouted; the stage lengths ranged from 3 to 4 ft. This procedure was repeated to the bottom of the sand layer. In effect, a grout "cap" was formed over the test section that helped prevent ground heave; thus, the grout at each level was progressively more effective in compacting the soil. The total surveyed ground heave after grouting averaged about $^1/_2$ in., corresponding to about 10 percent of the grout take.

To evaluate the effectiveness of the compaction grouting in densifying the fill layer, CPT's and SPT's were performed before and after grouting. The CPT $q_c$ values were converted to equivalent SPT N values, because most available liquefaction-potential relations were based on SPT blowcounts at the time. A comparison of the equivalent SPT blowcounts before and after grouting in the test section, using an 8-ft on center injection-point spacing in a triangular grid pattern, is shown in figure 18. This pattern was considered to be the optimum configuration to achieve the required minimum relative density.

Specifications called for the injection points to be spaced at a maximum of 8 ft on center and for a peripheral row of points to be located at least 5 ft beyond the planned building's perimeter. Alternative peripheral points were to be injected first. Grouting was to continue at each point until either a drop in injection pressure indicated shearing of the soil, the injection pressure remained at 400 lb/in$^2$ with a grout take of less than 0.75 ft$^3$ per minute, or a surface heave of $^1/_8$ in. occurred.

Before compaction grouting commenced, the contractor requested, and was granted, a modification of the injection procedures that consisted of injecting the grout from the top downward continuously at each injection point without allowing the grout to harden between stages. He also proposed leaving all but the uppermost section of grout pipe in the ground to further reinforce the soil. Using this method, the contractor had considerable difficulty in keeping the injection pipe open while driving between stages, resulting in injected grout volumes that were insufficient to provide the required compaction.

The contractor then requested another procedure consisting of changing the direction in which grouting was to proceed through the sand layer. The casing was first installed to the bottom of the liquefiable layer at 35-ft depth and gradually withdrawn in 3-ft stage intervals while grout

was continuously injected. The results of extensive field density testing performed in the area grouted by using this procedure showed that below about 17-ft depth the degree of compaction was adequate, whereas above 17-ft depth it was below the minimum required. Although it was unclear why less compaction was achieved at the shallow depths, it may have been due either to placement of the lower density fill over the liquefiable sand in this area, or to the grouting procedure.

Several alternative grouting schemes were proposed by the contractor. Ultimately, it was decided to grout the liquefiable layer in two phases: from 14- to 7-ft depth and from 35- to 7-ft depth, using 3-ft stage lengths. The final spacing between injection points was 4 ft on center.

## FINAL RESULTS OF GROUND IMPROVEMENT

Extensive CPT and SPT testing was performed during production grouting to evaluate the increase in densification. Surface heave was monitored throughout the grouting process. Surveyed heave contours (conical in shape) were observed across the study site after the completion of production grouting; maximum heave across the study site averaged less than $^1/_2$ in. The CPT and SPT results are summarized in figure 19. It was concluded that the hydraulic-fill-sand layer was adequately densified to prevent most liquefaction from occurring. The actual cost of densification was higher than originally estimated but still less than a third that of the alternative methods considered.

## PERFORMANCE DURING THE EARTHQUAKE

On the basis of data from a CDMG strong-motion-recording instrument located on Sierra Point in South San Francisco, the study site was subjected to a peak acceleration of approximately 0.11 *g* within a bracketed duration of about 2 s during the earthquake. There were no reports

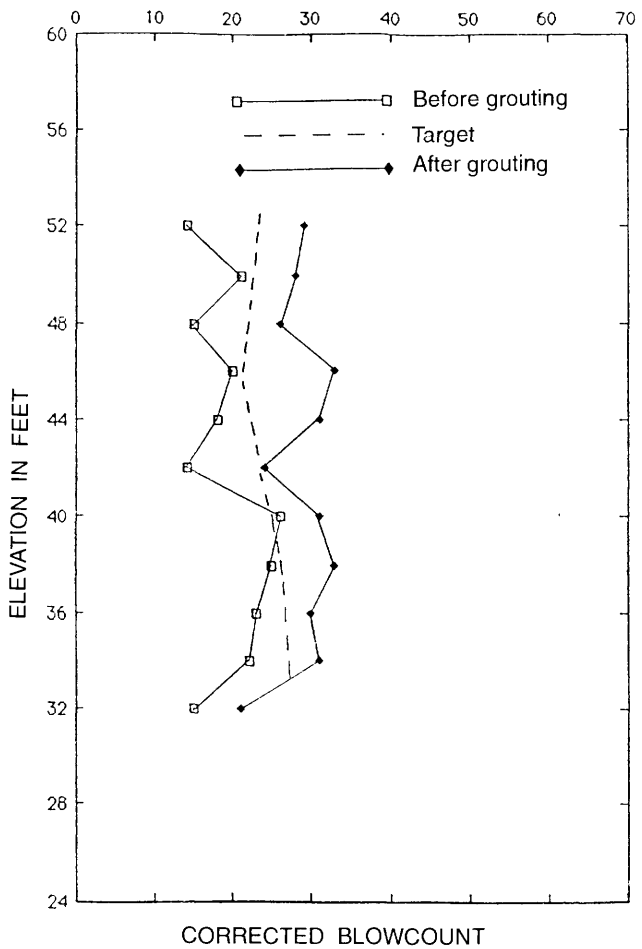


Figure 18.—Mean corrected blowcounts in test section before and after compaction grouting at Kaiser-Permanente Medical Center addition, South San Francisco (study site 10, fig. 1). From Donovan (1978).

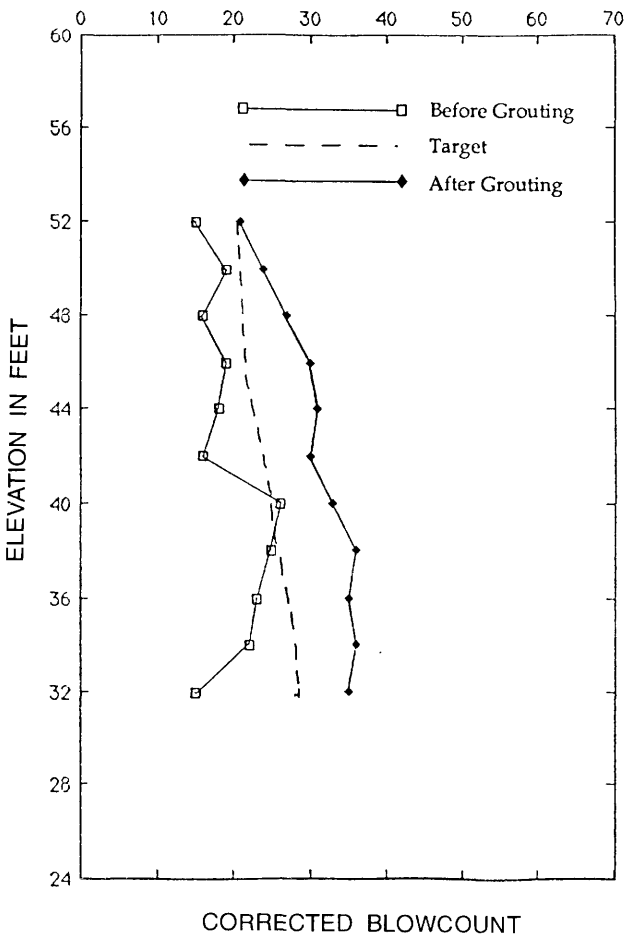


Figure 19.—Mean corrected blowcounts at end of compaction grouting at Kaiser-Permanente Medical Center addition, South San Francisco (study site 10, fig. 1). From Donovan (1978).

of damage to the facility or surrounding paved areas caused by the earthquake.

## RIVERSIDE AVENUE BRIDGE, SANTA CRUZ

### SITE DESCRIPTION

The Riverside Avenue Bridge consists of a reinforced concrete (Geo/Resource Consultants, 1986), two-lane traffic bridge spanning the San Lorenzo River. The bridge is supported by reinforced-concrete nose piers on each side; in addition, a concrete-slab apron lines the river channel beneath the bridge and nose piers. The soil area under the south nose pier, below the concrete-slab apron (fig. 20), is discussed here. Although the ground improvement was not undertaken for seismic strengthening, the behavior of the improved ground during strong shaking is nonetheless important.

### INITIAL CONDITIONS

The upper 5 ft of soil (beneath the concrete-slab apron) at the study site is composed of saturated, loose to medium-dense sandy gravel, with particles as much as 1 in. in diameter. The gravel is underlain by a layer of dense gravelly sand, approximately 11 ft thick. The sand is generally fine to medium grained and contains less than 5 percent of material finer than a No. 200 sieve; the gravel particles are 1 to 2 in. in diameter. The sand, in turn, is underlain by alternating layers of soft to medium-stiff silty clay and sandy silt to the depth penetrated. The water level of the river is approximately 9 ft above the bottom of the concrete-slab apron at high tide.

The granular bearing soils underneath the south nose pier were being eroded by the river, thereby undermining the pier. The resulting settlement of the pier was damaging the bridge decking above. Over time, the erosion and resulting settlement appeared to be increasing, and so it

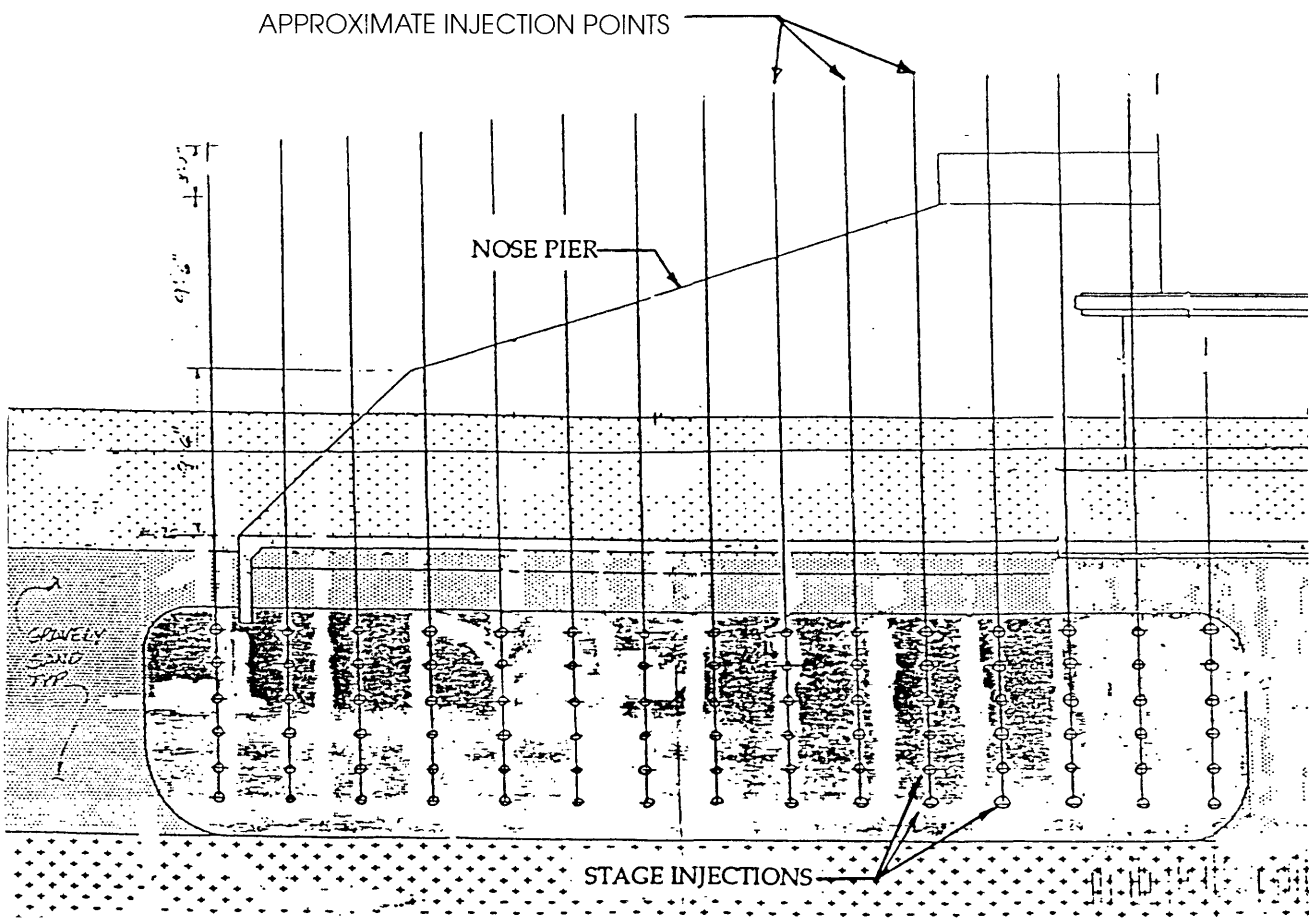


Figure 20.—Cross section of Riverside Avenue Bridge, Santa Cruz (study site 11, fig. 1), showing typical grouting pattern. From Georesource Consultants (1986).

was decided that some method of improving the granular soils to prevent further erosion must be implemented.

## GROUND-IMPROVEMENT GOALS AND METHODS

The ground improvement method had to prevent additional settlement of the pier and had to be performed with the existing nose pier, slab apron, and bridge deck in place. Santa Cruz city officials required one lane of traffic to remain open at all times during construction. Work was to proceed only between the hours of 8 a.m. and 6 p.m. and was required to be completed within 15 days of the start of construction.

Because of the soil problem and space constraints at the study site, grouting was the only ground-improvement method seriously considered. It was decided to use chemical grouting to "cement" the sand grains into a single, erosion-resistant mass.

## CONSTRUCTION PROCEDURES

The chemical grout was composed of N-grade sodium silicate and MC 500 microfine cement. Less than 0.1 volume percent of phosphoric acid was used to control setting time. The grouting was accomplished by placing sleeve port grout pipes (SPGP's) into the granular bearing soils and injecting grout in a zone around and underneath the nose pier, as shown in figures 20 and 21.

Casing pipe was set through the river sediment and holes were drilled through the 8-in.-thick concrete slab for SPGP access. A total of 12 vertical holes were drilled through the nose pier for grout injection directly beneath the footing. The steel SPGP's were vibrated or jetted into the granular soil. The grout was pumped into the SPGP's through an internal packer in multiple stages at each injection point. When grouting operations were completed, the lower part of each SPGP was backfilled with cement grout, and the rest removed, along with the casing pipe. All holes in the nose pier were also grouted.

To evaluate the effectiveness of chemical grouting, 76 additional SPGP's were incorporated into the original grouting plan and field-grouted specifically for testing purposes. From these SPGP's, grouted sand samples were made and strength-tested. In addition, the nose pier and bridge deck were surveyed before and after the grouting to check for movement due to ground heave.

Approximately 40,000 gal of chemical grout were injected into 77 locations around and beneath the nose pier. A total of about 550 injection points was used in the zone to be stabilized. On the basis of the unconfined compressive strengths of field samples and the volume of grout injected, it was concluded that the sand underneath the nose pier was suitably strengthened and that settlement of the pier would no longer occur.

## PERFORMANCE DURING THE EARTHQUAKE

On the basis of data from a CDMG strong-motion-recording instrument located on the University of California, Santa Cruz, campus, the study site was subjected to a peak acceleration of approximately 0.45 *g* within a brack-

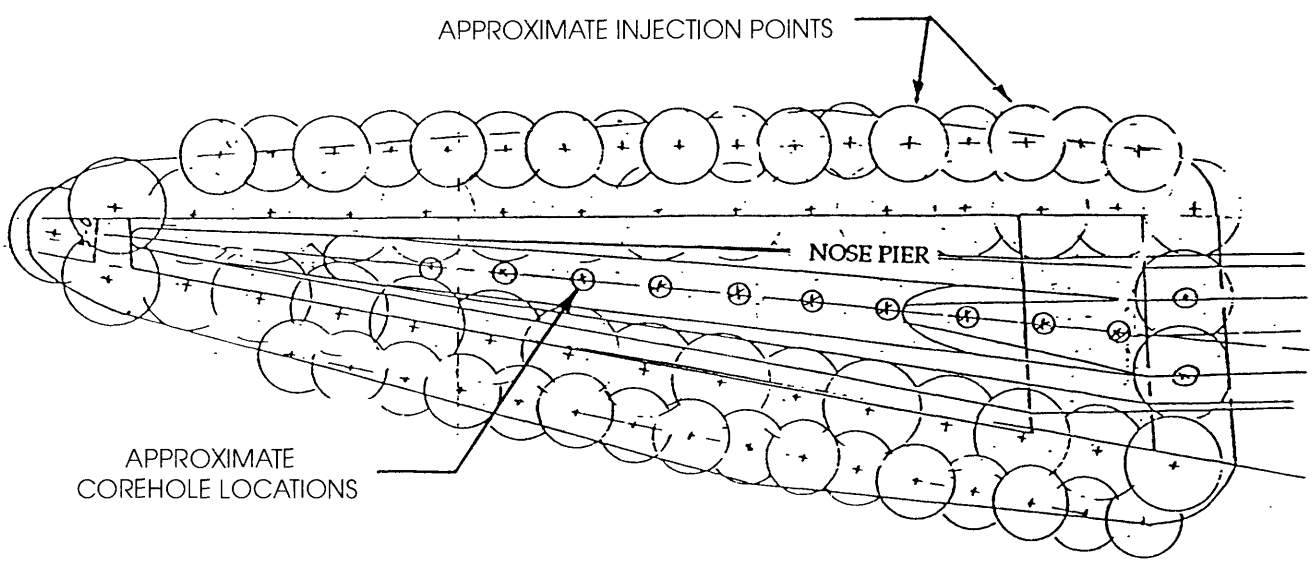


Figure 21.—Plan view of Riverside Avenue Bridge, Santa Cruz (study site 11, fig. 1), showing typical grouting pattern. From Georesource Consultants (1986).

eted duration of 15 s during the earthquake. According to the Santa Cruz city engineer, no settlement of the bridge pier or other detrimental ground movements were observed.

## SANTA CRUZ COUNTY DETENTION FACILITY, SANTA CRUZ

### SITE DESCRIPTION

The Santa Cruz County Detention Facility, constructed in 1979, consists of a one- and two-story building, a recreation yard, and two buffer zones. The structure is of a modular, split-level design, with maximum plan dimensions of 200 by 220 ft.

### INITIAL CONDITIONS

The study site was nearly level and paved for use as a parking lot at the time of the geotechnical investigation. The upper 4 to 12 ft of soil is composed of firm to very stiff clay and silt and medium to very dense sand and gravel. These materials consist of engineered fill placed during a redevelopment project in 1964. The fill is underlain by a layer of soft to stiff sandy silt and loose to medium-dense silty sand ranging in thickness from 20 to 70 ft. The silt and sand are underlain by siltstone bedrock to the depth penetrated. The ground-water level was 12 to 17 ft below the ground surface at the time of drilling.

A seismic investigation of the study site concluded that an earthquake occurring on either the San Gregorio or San Andreas fault ($M$=6.0–8.0), would result in peak accelerations at the site of 0.15 to 0.45 $g$. A liquefaction analysis of the silt and sand layer below the water table, using the simplified procedure of Seed and others (1983), indicated that widespread liquefaction was likely to occur in this layer at peak accelerations of 0.15 to 0.20 $g$. Liquefaction of the uppermost 4 to 12 ft of fill was considered unlikely because of its position above the ground-water table.

### FOUNDATION ALTERNATIVES

The primary consideration for foundation design was the high compressibility and liquefaction potential of the soft, clayey and sandy silt underlying the study site. It was concluded that total settlements of approximately 1 to 2 in. and differential settlements of about 1 in. could occur because of consolidation of the silt layer by the foundation loads of the proposed building. In addition, settlements of as much as 5 to 10 in. were expected to occur should the silt liquefy during an earthquake. Because of these potential settlements, the geotechnical engineer recommended that the building, including its ground-floor slab, be supported on driven piles end-bearing in the siltstone bedrock. The county of Santa Cruz decided, however, that the proposed pile foundation was too expensive and asked for an alternative foundation design. Therefore, the building was to be supported on spread footings, and the silt layer was to be densified so as to minimize consolidation and liquefaction potential.

### GROUND-IMPROVEMENT GOALS AND METHODS

The silty-sand fill was to be densified to a minimum relative density of 70 percent between depths of 5 and 35 ft beneath the building and to a distance of 10 ft beyond the building's perimeter. Because the study site was level and open, with no existing structures nearby, dynamic deep compaction was well suited as a densification method because of its simplicity and relatively low cost.

### CONSTRUCTION PROCEDURES

Before dynamic deep compaction commenced, a 20-ft-square test area was densified by this method to evaluate its effectiveness in the soils between 5- and 35-ft depth. Three test boreholes were drilled in the test area, and SPT's were performed at various depths. In addition, a piezometer was installed in the center of the square.

The contractor determined that a pounder about 6 ft square and weighing 20 tons would be dropped from a height of 60 ft to densify the site. The drop points were along the perimeter of the test area, as shown in figure 22. A total of 20 drops were made at each corner of the square, and 8 drops at the midpoint of each side of the square.

A comparison of the subsurface profile in the test area before and after improvement, indicating that a substantial amount of densification was achieved in the layers above about 25- to 30-ft depth, is shown in figure 23. A significant increase in SPT blowcounts was achieved in the silty-sand layer above about 30-ft depth (fig. 24). Overall, it was concluded that the liquefiable layer in the test area had been adequately densified.

Dynamic deep compaction of the study site proceeded by using the same drop pattern and number of drops as was used in the test area. No problems were reported during the densification.

### FINAL RESULTS OF GROUND IMPROVEMENT

A total of 12 boreholes were drilled across the study site, and SPT's were performed to evaluate the resulting densification. Induced ground settlements were also measured across the study site. On the basis of the SPT

results, it was concluded that the potentially liquefiable soils extending from 5- to 35-ft depth were densified to an average minimum relative density of 75 percent. Total induced ground-surface settlements across the study site ranged from 12 to 31 in.

### PERFORMANCE DURING THE EARTHQUAKE

On the basis of data from a CDMG strong-motion-recording instrument located on the University of California, Santa Cruz, campus, the study site was subjected to a peak acceleration of approximately 0.45 *g* within a bracketed duration of 15 s during the earthquake. There were no reports of any damage to the building or surrounding facilities due to liquefaction or associated ground failure phenomena.

## DISCUSSION AND CONCLUSIONS

All of the study sites with improved ground performed well during the earthquake. Without exception, little or no distress or damage due to ground shaking occurred to either the improved ground or the facilities and structures built on it. At many of the study sites, unimproved ground adjacent to the improved ground was badly cracked and (or) settled, primarily owing to liquefaction, resulting in some damage to the facilities and structures built on the unimproved ground. At every study site where peak accelerations were great enough that liquefaction of the unimproved ground would have been predicted to occur, it did occur. Together, these results support the conclusions that (1) the procedures used for prediction of liquefaction were reliable and (2) ground improvement is effective for mitigation of liquefaction risk.

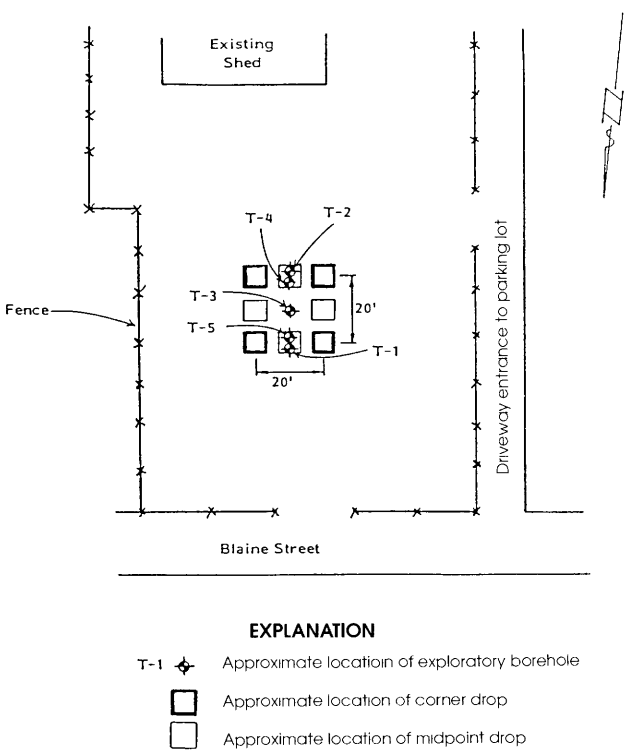


Figure 22.—Sketch map of Santa Cruz County Detention Facility, Santa Cruz (study site 12, fig. 1), showing drop pattern for dynamic deep compaction. Not to scale. From Peter Kaldveer and Associates (1977).

Nonetheless, in assessing these results and their implications for the future, we note that the 1989 Loma Prieta earthquake was of only moderate intensity and short duration. On average, each of the study sites sustained peak accelerations of only about 25 to 75 percent of the design earthquake values (table 2), and the durations of ground shaking were short relative to the common values for an $M$=7 event. How these improved-ground sites would perform during an earthquake of larger magnitude and longer duration is unknown; however, almost certainly, soil liquefaction and related effects at the sites would be reduced in comparison with the unimproved ground. The question is, by what amount?

Detailed ground-response analyses have not been made for the study sites. Thus, our analyses and interpretations of behavior are based on estimated peak accelerations and durations of ground shaking that were obtained from the nearest available ground-motion records. Additional ground-response studies would be useful to establish more exactly the actual ground motions that occurred and the influence, if any, of ground improvement on the surface motions.

One of the most important aspects of any ground-improvement project is accurate measurement of the improvement achieved. At almost every study site, there were questions as to the overall increase in relative density obtained. As CPT's and shear-wave-velocity methods for liquefaction-potential assessment become more established and better validated, testing programs for measurement of the overall ground improvement at a given site will become less expensive and simpler to perform. We expect that more complete quantitative documentation of postimprovement properties will be retained for all future ground-improvement projects so that more quantitative studies of behavior during future earthquakes will be possible.

Finally, we emphasize that ground improvement, in spite of its great benefits as demonstrated by the 1989 Loma Prieta earthquake, is not a panacea for mitigation of all earthquake risk at a site. Its functions are mainly mitigation of liquefaction potential and the prevention of lateral spreading. Analyses indicate that ground improvement has little effect on the ground-surface response. Thus, surface shaking remains a function of the input rock motions and the characteristics of the soil profile. Because soft-soil

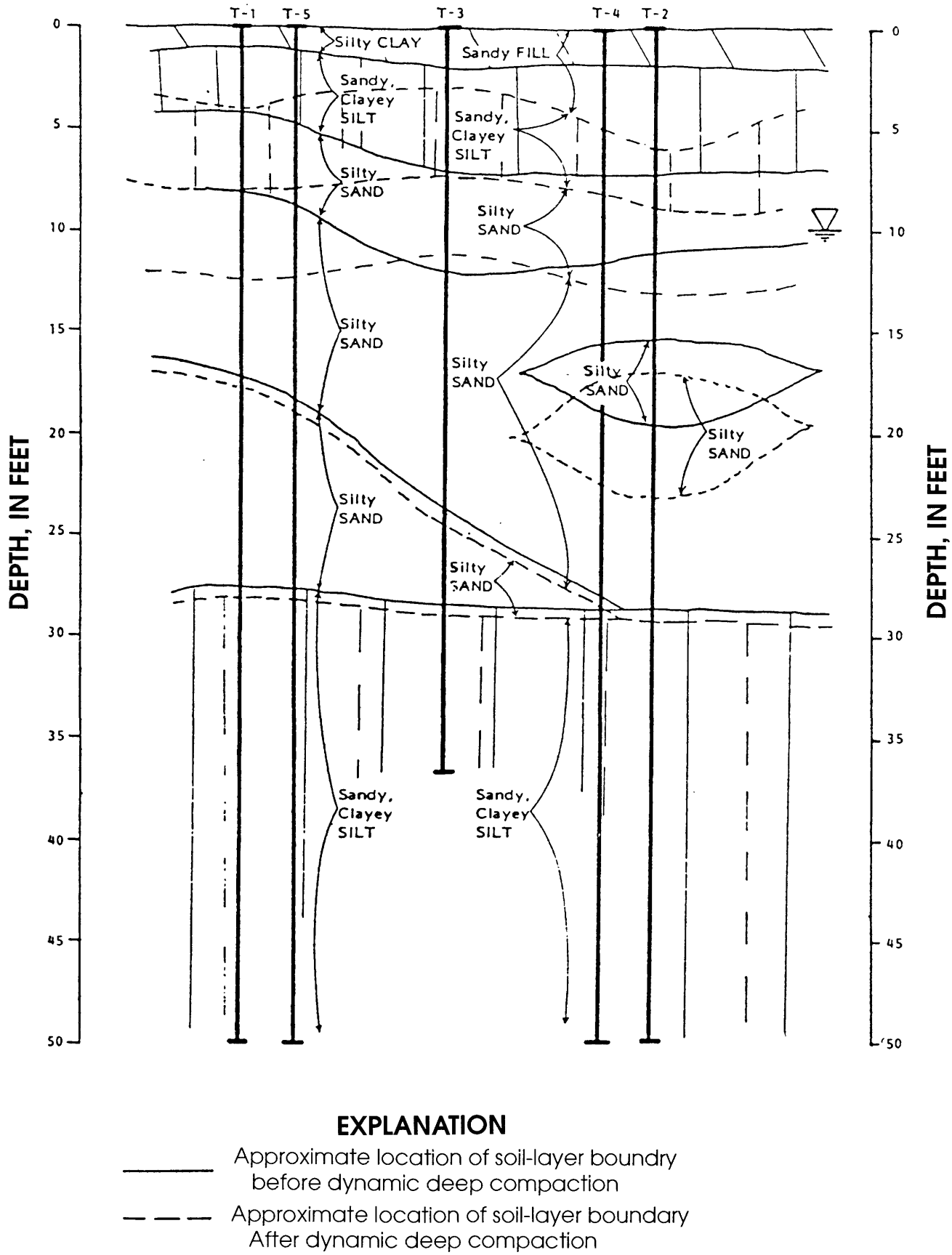


Figure 23.—Comparison of subsurface profile before and after dynamic deep compaction at Santa Cruz County Detention Facility, Santa Cruz (study site 12, fig. 1). T–1 through T–5, exploratory boreholes (see fig. 22 for locations). From Peter Kaldveer and Associates (1977).

sites generally amplify rock motions and ground improvement is most commonly used at soft-soil sites, structures that are at risk from shaking before ground improvement will remain so afterward unless structural strengthening is carried out.

## ACKNOWLEDGMENTS

Many individuals and organizations kindly provided data and information about the study sites described in this paper. In particular, we thank Steve Dickenson of Oregon State University, Corvallis; Lelio Mejia and Larry Houps of Woodward-Clyde Consultants, Oakland, Calif.; Richard Short of Peter Kaldveer and Associates, Oakland; Craig Shields of Treadwell & Rollo, Inc., San Francisco; H.R. Al-Alusi of the Pressure Grout Co., Hayward, Calif.; Henry Taylor of Harding Lawson Associates, San Francisco; John Debecker and Vitauts Ozols of the U.S. Navy's Western Facilities Engineering Command, San Bruno, Calif.; Larry Karp of Orinda, Calif.; Mahmut Otus and John Egan of Geomatrix Consultants, San Francisco; and Robert Lopez and Francis Gularte of Hayward-Baker, Inc., Ventura, Calif.

## REFERENCES CITED

Basore, C.E., and Boitano, J.D., 1969, Densification of sand fill with compaction piles and vibroflotation—a case history: American Society of Civil Engineers Proceedings, Soil Mechanics and Foundations Division Journal, v. 95, no. SM6, p. 1303–1323.

Donovan, N.C., 1978, Site improvement in a sensitive environment: San Francisco, Dames and Moore.

GeoMatrix Consultants, 1990, Draft report—evaluation of interior area performance Naval Air Station Treasure Island: San Francisco, project 1539.

Geo/Resource Consultants, 1986, Field and laboratory data report—Riverside Avenue Bridge: Santa Cruz, Calif., project 447–055–00–1, September 24, 1986.

Hallenbeck and Associates, 1985, Seismic performance evaluation and mitigation requirements for the perimeter sand dike; Harbor Bay Business Park, Harbor Bay Isle: jobs 4188–2 and 4189–2.

———1986, Final report of geotechnical engineering monitoring and testing program, dynamic consolidation work: Harbor Bay Parkway, phase III, job 4296–3–8510.

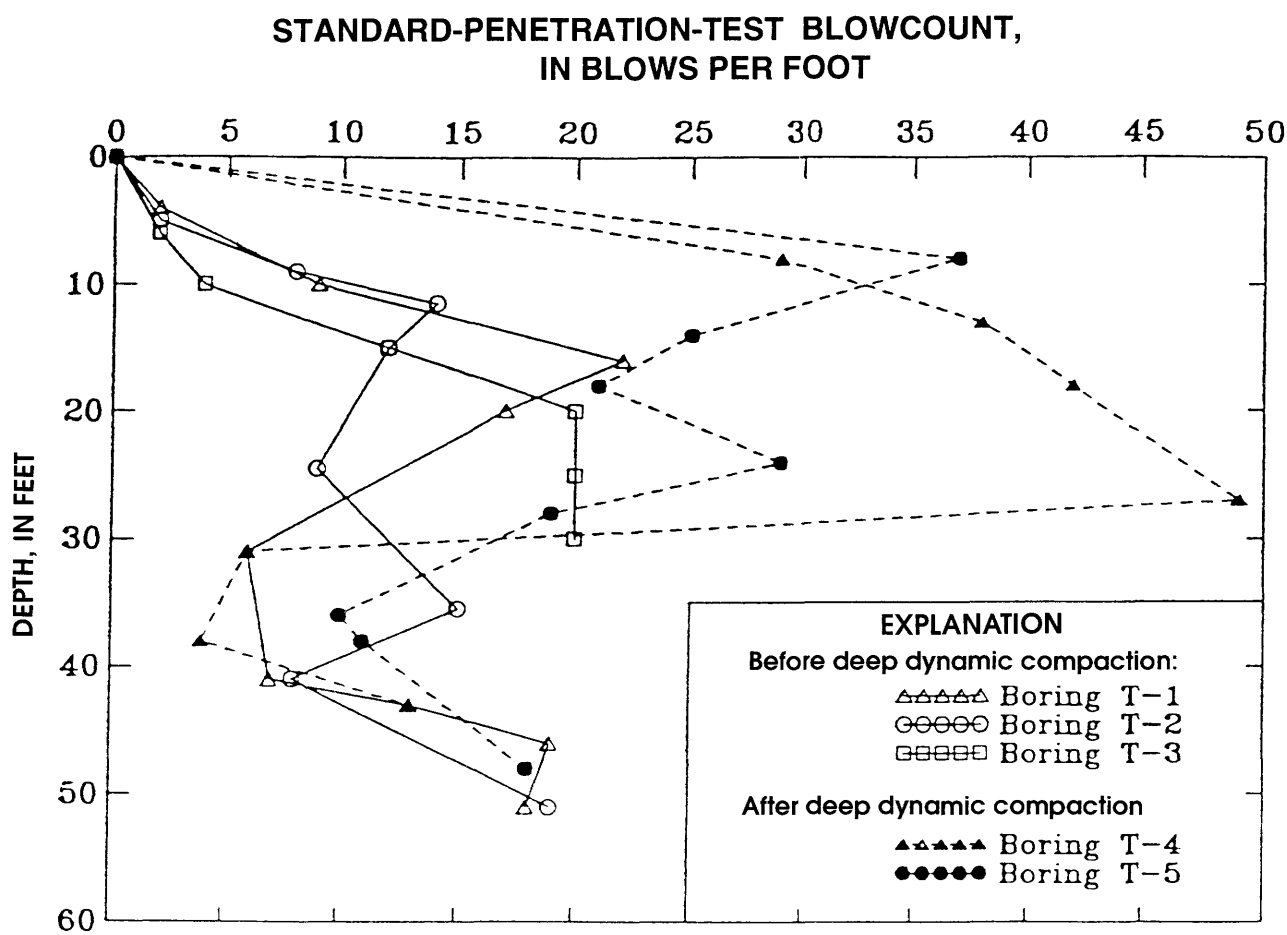


Figure 24.—Comparison of standard-penetration-test blowcount before and after dynamic deep compaction at Santa Cruz County Detention Facility, Santa Cruz (study site 12, fig. 1). See figure 22 for locations of boreholes T–1 through T–5. From Peter Kaldveer and Associates (1977).

Harding Lawson Associates, 1983, Geotechnical investigation—proposed general purpose/berthing pier, Treasure Island: San Francisco, project 2177,057.04.

———1986a, Geotechnical investigation—proposed Esplanade Extension East Shore, Marina Bay: Richmond, Calif., project 8003,069.04.

———1986b, Soil investigation—medical/dental clinic, Treasure Island: San Francisco, project 17916,002.04.

———1987, Final report—geotechnical engineering services during construction stone column installation, Eastern Shore, Marina Bay: Richmond, Calif., project 8003,071.04.

———1990, Geotechnical investigation subsequent to October 17, 1989 earthquake—medical/dental clinic: Treasure Island, Calif., project 17916,006.04, January 18, 1990.

Hausmann, M.R., 1990, Engineering principles of ground modification: New York, McGraw-Hill, 632 p.

Lee, K.L., and Albaisa, Aurelio, 1974, Earthquake induced settlements in saturated soils: American Society of Civil Engineers Proceedings, Geotechnical Engineering Division Journal, v. 100, no. GT4, p. 387–406.

Lee, K.L., and Seed, H.B., 1967, Cyclic stress conditions causing liquefaction of sand: American Society of Civil Engineers Proceedings, Soil Mechanics and Foundations Division Journal., v. 93, no. SM1, p. 44–70.

Mitchell, J.K., 1981, Soil improvement; state-of-the-art: International Conference on Soil Mechanics and Foundation Engineering, 10th, Stockholm, 1981, Proceedings, v. 4, p. 509–565.

Mitchell, J.K., and Wentz, F.J., 1991, Performance of improved ground during the Loma Prieta earthquake: Berkeley, University of California, Earthquake Engineering Research Center Report UCB/EERC–91/12, 93 p..

Peter Kaldveer and Associates, 1977, Geotechnical investigation—Santa Cruz County detention facility: Santa Cruz, Calif., project K480–2A, April 26, 1977.

Rinne, E.E., Shields, C.S., and Nardi, C.R., 1988, Mitigation of liquefaction potential: International Conference on Earthquake Engineering, Tokyo, 1988, Proceedings.

Robertson, P.K., and Campanella, R.G., 1985, Liquefaction potential of sands using the CPT: Journal of Geotechnical Engineering, v. 111, no. 3, p. 384–403.

Seed, H.B., 1979, Soil liquefaction and cyclic mobility evaluation for level ground during earthquakes: American Society of Civil Engineers Proceedings, Geotechnical Engineering Division Journal, v. 105, no. GT2, p. 201–255.

———1987, Design problems in soil liquefaction: Journal of. Geotechnical. Engineering, v. 113, no. 8, p. 827–845.

Seed, H.B., and Idriss, I.M., 1967, Analysis of soil liquefaction; Niigata earthquake: Americal Society of Civil Engineers Proceedings, Soil Mechanics and Foundations Division Journal, v. 93, no. SM3, p. 83–108.

———1971, Simplified procedure for evaluating soil liquefaction potential: American Society of Civil Engineers Proceedings, Soil Mechanics and Foundations Division Journal, v. 97, no. SM9, p. 1249–1274.

Seed, H.B., Idriss, I.M., and Arango, Ignacio, 1983, Evaluation of liquefaction potential using field performance data: Journal of Geotechnical Engineering, v. 109, no. 3, p. 458–482.

Seed, H.B., and Lee, K.L., 1966, Liquefaction of saturated sands during cyclic loading: American Society of Civil Engineers Proceedings, Soil Mechanics and Foundations Division Journal, v. 92, no. SM6, p. 105–134.

Seed, H.B., Tokimatsu, Kohji, Harder, L.F., and Chung, R.M., 1984, The influence of SPT procedures in soil liquefaction resistance evaluations: Berkeley, University of California, Earthquake Engineering Research Center Report UCB/EERC–84/15, 20 p.

Welsh, J.P., 1986, Construction considerations for ground modification projects: International Conference on Deep Foundations, Beijing, 1986, Proceedings.

Wightman, Adrian, 1991, Ground improvement by vibrocompaction: Geotechnical News, v. 9, no. 2, p. 39–41.

Woodward-Clyde Consultants, 1981, Geotechnical engineering study final design report—East Bay Park Condominium: Emeryville, Calif., projects 14884B through 14884D.

Woodward-Clyde-Sherard and Associates, 1966, Soil investigation for the proposed Office Building No. 450: Treasure Island, Calif., project S–10439.

Woodward-Lundgren and Associates, 1972, Foundation design recommendations for the proposed barracks buildings: Treasure Island, Calif., project S–12610.

THE LOMA PRIETA, CALIFORNIA, EARTHQUAKE OF OCTOBER 17, 1989:
LIQUEFACTION

STRONG GROUND MOTION AND GROUND FAILURE

# EVALUATION OF LIQUEFACTION-HAZARD MAPPING IN THE MONTEREY BAY REGION, CENTRAL CALIFORNIA

By William R. Dupré, University of Houston; and
John C. Tinsley III, U.S. Geological Survey

## CONTENTS



ABSTRACT

The 1989 Loma Prieta earthquake provided an opportunity to evaluate the accuracy of geologic and liquefaction-susceptibility maps of Quaternary deposits in the central Monterey Bay region. The relative liquefaction susceptibility was determined by combining detailed geologic mapping of Quaternary deposits with information on the geotechnical properties of these deposits, depth to the water table, and the response of these and similar units in previous earthquakes. The geologic maps were compiled from regional Quaternary maps, augmented by additional field mapping in selected areas.

Liquefaction-induced ground failure manifest as vented sand (sand boils), differential settling, and lateral spreading was widespread in the Monterey Bay region during the 1989 Loma Prieta earthquake ($M_S$=7.1). The areal extent of this liquefaction was less than that caused by the 1906 San Francisco earthquake ($M_S$=8+), as would be expected given its smaller magnitude. Nonetheless, within the area affected by the 1989 Loma Prieta earthquake, almost all of the 1906 failures were reactivated, clearly demonstrating that the phenomenon of recurrent liquefaction is an important consideration and cannot be ignored on the basis of a previous history of liquefaction.

Liquefaction occurred mainly in areas underlain by water-saturated, late Holocene alluvial and estuarine deposits along the San Lorenzo, Pajaro, and Salinas Rivers, as well as along estuaries and spits in the Moss Landing area. All of the major occurrences of liquefaction were in areas previously mapped as having a high to very high liquefaction susceptibility; however, large areas mapped as having a high to very high liquefaction susceptibility did not fail, even though similar units in adjacent areas did liquefy. The absence of failure in these large areas largely appears to reflect the absence of sand-rich facies within those geologic units (for example, younger fluvial deposits and basin deposits), which had not been recognized on the basis of surficial-materials and geomorphic mapping. Future maps of liquefaction susceptibility should delineate these sand-poor units wherever possible. In addition, lowered water tables due to the recent drought may in some areas have prevented liquefaction from occurring in some younger fluvial deposits.

The strong correlation between areas of observed liquefaction and areas mapped as having a high to very high liquefaction susceptibility demonstrates the potential utility of regional geologic mapping in helping regional planners minimize the losses caused by liquefaction in future earthquakes.

## INTRODUCTION

In 1973, the U.S. Geological Survey began a cooperative program with Santa Cruz County to provide a series of maps to aid regional planners evaluate potential geologic hazards in the county (fig. 1). These maps included active and potentially active faults (Hall and others, 1974), landslide deposits (Cooper, Clark & Associates, 1975), and Quaternary deposits and their liquefaction susceptibility (Dupré, 1975a). The maps were incorporated within Santa Cruz County's Seismic Safety Element. The mapping of Quaternary deposits and their liquefaction susceptibility was extended into central Monterey Bay region by Dupré and Tinsley (1980), funded in part by Monterey County, and into southern Monterey Bay region by Dupré (1990). The 1989 Loma Prieta earthquake ($M_S$=7.1) pro-

vided an opportunity to test these maps. This paper describes the methods by which the maps were prepared and documents the extent to which they predicted the distribution of earthquake-induced liquefaction and ground failure in that event.

## METHODOLOGY

Liquefaction is the transformation of a granular material from a solid to a liquid state, owing to an increase in pore-fluid pressure. This transformation, which typically is caused by seismic cyclic loading (Youd, 1973), is largely restricted to water-saturated, relatively unconsolidated (loose), well-sorted sand and silt in regions of high seismicity. Predicting the susceptibility of sedimentary deposits to earthquake-induced liquefaction requires knowledge of their age and mode of deposition, their physical properties and degree of water saturation, and the distribution of sand and silt within the deposits. Detailed mapping of Quaternary deposits, in combination with information on depth to the water table, geotechnical properties of the geologic units, and evidence of previous liquefaction, provide the data necessary for such mapping (Youd, 1973; Youd and others, 1973; Youd and Perkins, 1978). The methodology of Youd and Perkins (1978) was

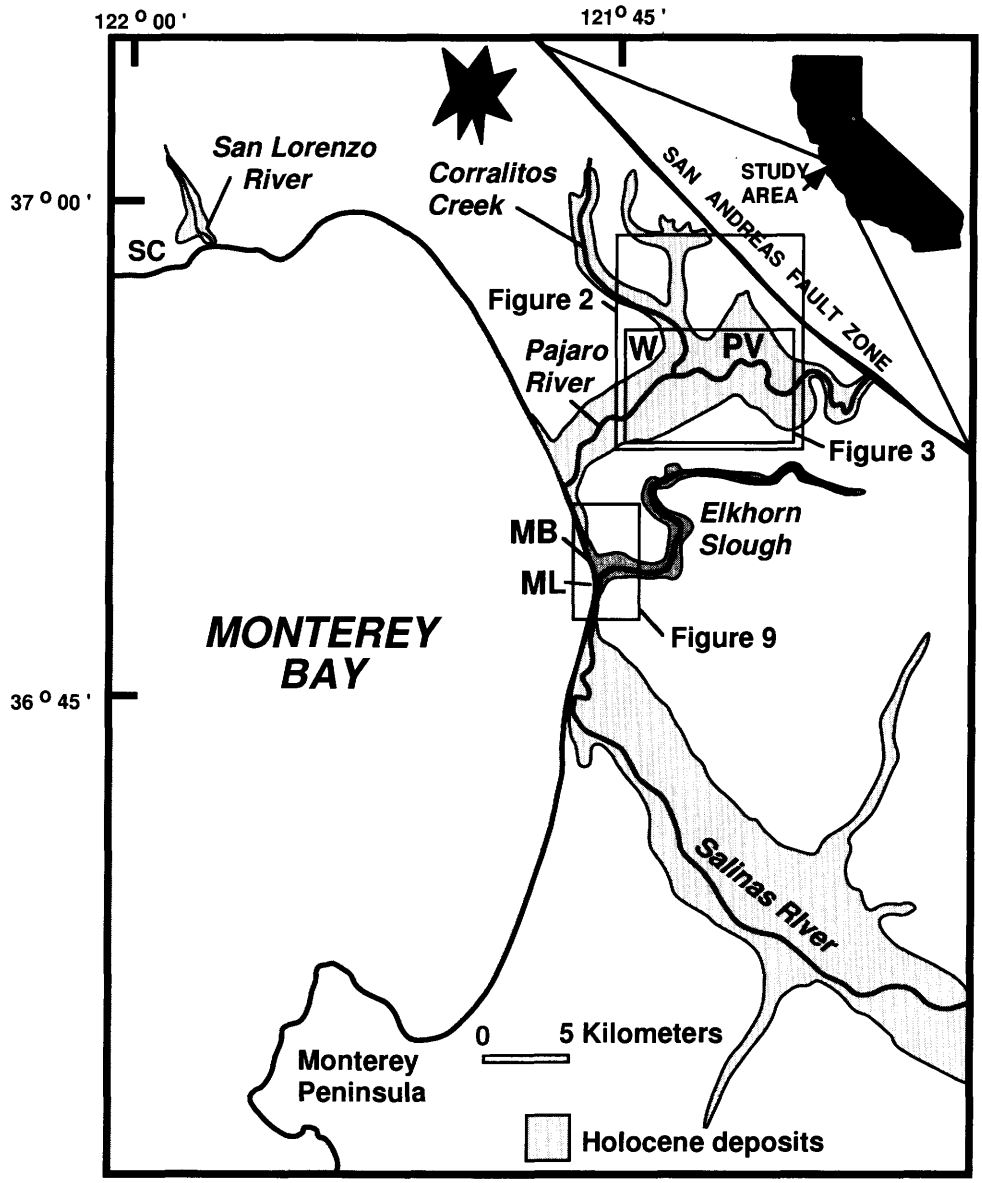


Figure 1.—Monterey Bay region, central California, showing locations of areas of figures 2, 3, and 5. Star, epicenter of 1989 Loma Prieta earthquake; MB, Moss Beach; ML, Moss Landing; PV, Pajaro Valley; SC, Santa Cruz; W, Watsonville.

Table 1.—*Probable liquefaction susceptibilities of cohesionless, granular, nongravelly layers used to compile liquefaction-susceptibility map*

[Modified from Tinsley and others (1985). Do., ditto]

| Age | Depth to water table (ft) | | | |
|---|---|---|---|---|
| | 0–10 | 10–30 | 30–50 | 50+ |
| Holocene: | | | | |
| Latest | High to very high | Moderate | Low | Very low. |
| Pre-latest | High | do | do | do. |
| Late Pleistocene | Low | Low | Very low | do. |
| Pre-late Pleistocene | Very low | Very low | do | do. |

the basis for making our maps (Dupré, 1975a; Dupré and Tinsley, 1980; Dupré, 1990); we describe how we used their method in the following sections of this paper. Other studies of liquefaction, using the methodology of Youd and Perkins (1978), sometimes with slight modifications, include those by Roth and Kavazanjian (1984), Tinsley and others (1985), and Youd and Perkins (1987b).

## PREPARATION OF A GEOLOGIC MAP

The first step requires the preparation of a geologic map of Quaternary deposits; such mapping allows the delineation of geologic units on the basis of their relative age and lithology. The most significant age distinctions for defining liquefaction susceptibility are between late Holocene, early Holocene, late Pleistocene, and pre-late Pleistocene deposits (table 1). In the Monterey Bay region, these four groups of deposits can generally be recognized on the basis of pedogenic-soil development (Dupré, 1975b; Tinsley, 1975). For example, late Holocene deposits are characterized by an undeveloped or very minimally developed soil profile, whereas early Holocene deposits have a minimally developed soil profile; late Pleistocene deposits typically have a medially developed soil profile, whereas pre-late Pleistocene deposits generally have a maximally developed soil profile. (See Janda and Croft, 1967, Tinsley, 1975, and Birkeland, 1984, for a description of the soil characteristics used in making these types of age distinctions.) Such first-order age distinctions can commonly be made by using soil maps from the U.S. Soil Conservation Service. In the Monterey Bay region, for example, the maps of Carpenter and Cosby (1925) and Storie (1944) were found to be especially useful. Because much of this definitive mapping was done early in the 20th century, most earth scientists are unaware of the value of the information in these old soils maps (Hatheway, 1991).

Additional information was obtained from aerial photographs taken in the 1920's and 1930's by the U.S. Soil Conservation Service. These photographs allow a more accurate identification and delineation of Holocene depositional environments because they predate much of the urbanization and intensive agricultural development in the region. The resulting geologic map of Quaternary deposits in the region delineates 23 Pleistocene and 12 Holocene units (fig. 2*A*). The recognition and delineation of genetically related Quaternary depositional environments and associated deposits provided by such mapping are essential in determining the age and distribution of potentially liquefiable sand and silt, and provide the basis for the subsequent preparation of liquefaction-susceptibility maps.

## PREPARATION OF A LIQUEFACTION-SUSCEPTIBILITY MAP

Information on the physical properties of the sedimentary deposits was limited to a few engineering reports. Correlation of the geologic units tested in these reports with similar deposits in nearby areas greatly expanded the data base on which our study rests. Similarly, information on the depth to the free-water surface (unconfined water table) was largely limited to a few engineering boreholes and water-well logs. The occurrence of unconfined near-surface water is locally complicated by perched water tables, the presence and seasonal persistence of which is hard to predict because shallow ground water is seldom monitored.

The engineering properties of the deposits (mainly standard-penetration-test data), coupled with information on the depth to the water table, were used to estimate the liquefaction susceptibility of the deposits in the event of an earthquake of $M$=8.3 on the San Andreas fault, using the criteria of Youd (1973); Youd and others (1975), Youd

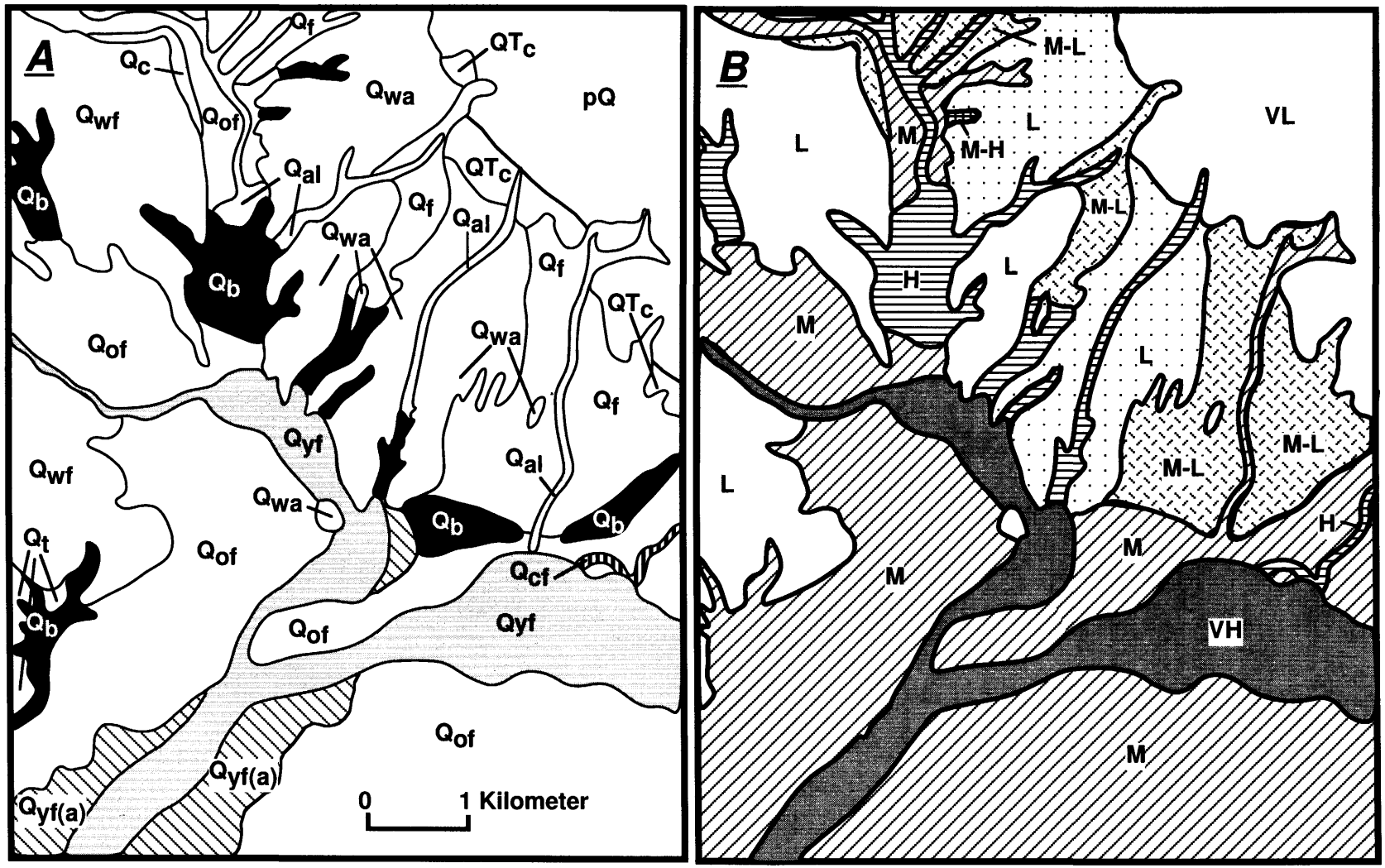


Figure 2.—Watsonville, Calif., area (see fig. 1 for location. *A*, Geologic map of mainly Quaternary deposits (modified from Dupré and Tinsley, 1980), from which liquefaction-susceptibility map in figure 2*B* was constructed. Units: pQ, pre-Quaternary rocks; Qal, Quaternary alluvial deposits, undivided (Holocene); Qb, Quaternary basin deposits (Holocene); Qc, Quaternary colluvium (Holocene); Qcf, Quaternary channel-fill deposits (Holocene); Qf, Quaternary alluvial-fan deposits (Holocene); Qof, Quaternary older flood-plain deposits (Holocene); Qt, Quaternary terrace deposits, undivided (Pleistocene); QTc, continental deposits, undivided (Pliocene and Pleistocene); Qwa, alluvial-fan facies of Quaternary terrace deposits of Watsonville (Pleistocene); Qyf, Quaternary younger flood-plain deposits (Holocene); Qyf(a), Quaternary younger flood-plain deposits (Holocene) as a veneer overlying Quaternary older flood-plain deposits. *B*, Liquefaction-susceptibility map (modified from Dupré and Tinsley, 1980). Zones: H, high; L, low; M, moderate; VH, very high; VL, very low.

and Perkins (1978), and Tinsley and others (1985). These estimates, in combination with historical evidence of the liquefaction-induced ground failure caused by the great San Francisco earthquake of 1906 (Lawson, 1908; Youd and Hoose, 1978), demonstrate a clear correlation between the mapped geologic units and their relative liquefaction susceptibility (table 1). These relations, together with the geologic maps of Quaternary deposits, are the foundations for the liquefaction-susceptibility maps (fig. 2*B*).

The zones listed in table 2 are based on the relative liquefaction susceptibility in a possible future earthquake similar in magnitude to the 1906 San Francisco earthquake ($M$=8.3). Given the magnitude of that event and the nearby proximity of the San Andreas fault, this zonation may be considered to represent the maximum likelihood for liquefaction under present-day water-table conditions. We tried to take into account the susceptibility for liquefaction-induced ground failure as well. (See Youd and Perkins, 1987a, or Bartlett and Youd, 1992; 1995 for alternative empirical approaches to estimate the magnitude of potential ground failure). Youd and Perkins (1987a) describe the "liquefaction-severity index," LSI; this approach has been revised by Bartlett and Youd, (1992, 1995). Deposits that had an estimated high liquefaction susceptibility but that showed little or no historical evidence of ground failure, such as the Quaternary older flood-plain deposits (unit Qof, fig. 2*A*), were zoned lower than those that sustained widespread failure in the 1906 earthquake, for example, the Quaternary younger flood-plain deposits (unit Qyf). There is more to this issue, however, than a simple dependency of liquefaction susceptibility on age, especially when deposits do not differ widely in age. That a sedimentary deposit becomes increasingly resistant to liquefaction as its geologic age substantially increases is clearly shown by regional studies (for example, Tinsley and others, 1985); this trend is used to assign a zonation to a deposit chiefly on the basis of age. For example, distinguishing Holocene from Pleistocene deposits works well enough in basins where erosional and depositional cycles reflect glacioeustatically controlled changes in sea level and the respective deposits differ in age by tens of thousands of years. The decrease in liquefaction susceptibility over time, however, is less evident when the deposits differ in age by hundreds to possibly a few thousands of years, as is the case for the Quaternary younger and older flood-plain deposits (units Qyf and Qof, respectively, fig. 2*A*). In these cases attributes other than relative age may control the liquefaction susceptibility. An especially relevant study of the effects of numerous earthquakes worldwide by Youd (1984) showed that deposits which have liquefied in the past are more likely to liquefy subsequently than those which show no historical evidence of liquefaction.

It is important to indicate the degree of confidence with which the liquefaction susceptibility is determined. A query ("?") indicates that the identification of the geologic unit is doubtful. A combination of two liquefaction-susceptibility categories, such as moderate-low (M-L), indicates that the area or geologic unit varies in its susceptibility; a single unit may underlie the entire area, for example, but such factors as sand thickness or continuity may vary, and so the susceptibility may be low in one part and moderate in another. For such units, we typically lack the data to distinguish which zonation to apply to subdivisions in the area, and so we must combine categories. A geologic unit that has a lower liquefaction susceptibility due to an artificially depressed water table is indicated by a subscript "w" (for example, $L_w$). Deposits in this area may have a higher susceptibility in the event of a rise in the water table. (For example, an increase in the elevation of the water table may reflect a decreased rate of ground-water pumping or an increased rate of irrigation.) Water levels, whether perched or not, may be significantly lower during periods of drought or higher after periods of heavy precipitation. Perched water tables may create a condition of an unexpectedly shallow depth to ground water in some areas. In any event, the depth to ground water is commonly the most difficult parameter to estimate with precision, because it may vary in time and space and is rarely monitored (Tinsley and others, 1985)

The maps by Dupré (1975a) and Dupré and Tinsley (1980), which were intended for regional land-use planning, are unsuitable for determining the actual hazard at any specific site. The local absence of sandy or silty layers in high-susceptibility zones would inhibit liquefaction, as would locally deep water tables. Similarly, we have not tried to estimate the relative amount of ground displacement that may accompany ground failure due to liquefaction. The proximity of a free face or scarp might increase the probable severity of a failure within a zone of moderate or high liquefaction susceptibility. Finally, some units (for example, artificial fill) may be too small in area to be delineated on the scale of the published map (1:62,500). Thus, the safety of a particular site with respect to a liquefaction hazard should be determined only after field investigations by qualified engineering geologists and soils engineers. Nonetheless, a comparison of the liquefaction-induced ground failures formed during the 1989 Loma Prieta earthquake with published liquefaction-susceptibility maps clearly demonstrates their utility, as discussed in the next section.

## LIQUEFACTION DURING THE EARTHQUAKE

Liquefaction and associated ground failure in the Monterey Bay region during the 1989 Loma Prieta earthquake were widespread (fig. 3; see Tinsley and others,

Table 2.—*Description of zones of liquefaction susceptibility*

[Modified after Dupré and Tinsley (1980) and Dupré (1990)]

| Liquefaction susceptibility | Description |
|---|---|
| **Very High** | Very likely to liquefy in the event of even a moderate earthquake. Deposits characterized by high susceptibility (on the basis of engineering tests and high water table) and for which evidence exists of extensive liquefaction-induced ground failure in the 1906 San Francisco earthquake. Chiefly restricted to younger flood-plain deposits but also includes some basin deposits and estuarine, beach, and dune sands in the vicinity of the coast. |
| **High** | Likely to liquefy in the event of a nearby major earthquake. Includes deposits for which engineering tests, shallow water tables, and nearby free faces indicate a potential for liquefaction and resulting ground failure but for which no historical evidence of liquefaction has been reported. Includes some basin deposits and younger flood-plain deposits, as well as most undifferentiated alluvial deposits and abandoned channel-fill deposits. |
| **Moderate** | May liquefy in the event of a nearby major earthquake. Includes deposits for which a moderate susceptibility was calculated but that lack historical evidence of liquefaction, as well as deposits with high susceptibilities but where water table is from 10 to 30 ft below the ground surface. Includes beach and older flood-plain deposits, most basin and colluvial deposits, most undifferentiated alluvial deposits, and some Holocene eolian deposits. |
| **Low** | Unlikely to liquefy, even in the event of a nearby major earthquake. Includes younger Pleistocene deposits (older dunes and landslide deposits) as well as Holocene deposits where the water table is more than 30 ft deep (for example, most alluvial-fan deposits and some older flood-plain deposits in areas where ground-water pumping has lowered the water table). |
| **Very Low** | Very unlikely to liquefy, even in the event of a nearby major earthquake. Includes all pre-late Quaternary deposits. |
| **Varying** | Restricted to areas of artificial fill. Susceptibility may range from low to very high depending on type of fill and method of emplacement. Much liquefaction-induced ground failure associated with the 1906 San Francisco earthquake occurred in hydraulically emplaced fill over bay and estuarine mud. |

this chapter). Mappable effects of liquefaction were manifest as ejected sand (sand boils) issuing from isolated vents or from extensional fissures; differential settling of buildings, levees, or other overburden into a liquefied substrata; loss of bearing capacity; and lateral spreading. Liquefaction-induced ground failure caused extensive damage to flood-control levees, pipelines, buildings, utilities, irrigation facilities (including water wells), bridges, and precisely graded agricultural tracts. Liquefaction occurred almost exclusively within areas underlain by water-saturated, late Holocene alluvial and estuarine deposits. It was especially conspicuous along the lower (tidewater) reaches of the San Lorenzo, Pajaro, and Salinas Rivers, where ground water is perpetually shallow, as well as along estuaries, abandoned channels, and adjacent fluvial tributaries in the Moss Landing area (ML, fig. 1). All of the major occurrences of liquefaction were in areas previously mapped by Dupré and Tinsley (1980) as having a high to very high liquefaction susceptibility.

Lateral spreading occurred along approximately 60 percent of the lower 15 km of the Pajaro River and was common along the lower 15 km of the lower Salinas River and the lower 2 km of the San Lorenzo River at Santa Cruz, Calif. Failures also occurred along the margins of estuaries and the tidal inlet in the vicinity of Moss Landing (ML, fig. 1). In all places but one, the lateral spread-

ing was restricted to late Holocene fluvial, basin, estuarine, or channel fill deposits (mostly mapped as units Qb, Qcf, and Qyf in fig. 2*A* by Dupré, 1975; Dupré and Tinsley, 1980). The one exception was a small lateral-spread failure in artificial road-fill along Carleton Road, approximately 4 km northeast of Watsonville (site 401 of Tinsley and others, this chapter).

The lateral-spread failures (figs. 4*A*–4*D*) typically occurred within 150 m of channel margins characterized by a free face or gently sloping point bar 3 to 5 m high. Some failures, however, occurred along the margins of abandoned channels filled with organic-rich sediment, where the free face was less than 1 m high but where the compressible material filling the channel readily accommodated the laterally displaced mass. Lateral displacements ranged from a few millimeters to as much as 2 m, measured cumulatively across a failure from its head to its toe; vertical displacements were similar but generally less than 0.3 m. Failure commonly occurred on both sides of the modern channel, and zones of failure were mappable for distances of as much as 2 km along the channel margins.

Differential settlement, fracturing, and sand boils were especially common over abandoned channels within the late Holocene flood plain (fig. 4*E*). For example, as part of a larger lateral failure in the town of Pajaro, just south of Watsonville (W, fig. 1), extensive fracturing and as much as 0.5 m of subsidence occurred over a filled channel approximately 15 m wide. The zone of deformation associated with this paleochannel extended approximately 2 km parallel to the river, as evidenced by sand boils, fractured ground, condemned buildings, and the damaged abutments of the Main Street and Southern Pacific bridges that cross the Pajaro River at Watsonville (see Tinsley and others, this chapter).

Most failures along the coast occurred in areas underlain by estuarine and tidal-channel deposits subsequently buried by channel migration, washover deposits, and landward-migrating dune deposits, as was particularly evident between the mouth of the Pajaro River and Moss Landing (fig. 5).

On the basis of observations during past earthquakes (Youd and Hoose, 1977, 1978), lateral spreading has been regarded as the principal mechanism causing significant property losses on gently sloping alluvial terrain. Events associated with the 1989 Loma Prieta earthquake, however, suggest that loss of bearing capacity and resulting differential settlement and sand extrusion were at least as important as lateral spreading in causing major damage to manmade structures, including flood-control levees.

## COMPARISON WITH PUBLISHED LIQUEFACTION-SUSCEPTIBILITY MAPS

Of the more than 70 liquefaction sites identified in the map area by Tinsley and others (this chapter), only 4

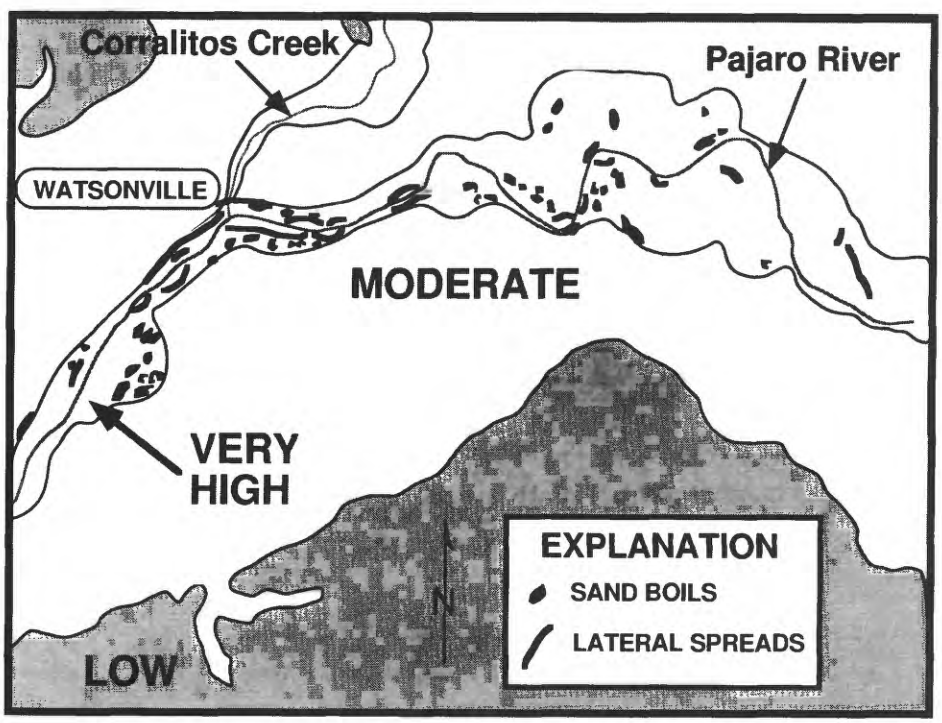


Figure 3.—Watsonville, Calif., area (see fig. 1 for location), showing distribution of liquefaction effects from 1989 Loma Prieta earthquake in relation to zones of predicted susceptibility as determined by Dupré and Tinsley (1980).

were not zoned by Dupré and Tinsley (1980) as having a high or very high liquefaction susceptibility. Minor sand boils occurred at two of these localities zoned as moderate (sites 100, 101) in basin deposits, along the lower part of the Pajaro Valley.

These sites appear to be associated with small paleochannels within the flood basin. Minor lateral spreading occurred at site 59 of Tinsley and others (this chapter), which was zoned as moderate, and differential subsidence without vented sand occurred at site 60, which was zoned as low. Both of these sites are in artificial roadfill too small to be mapped at the published scale of 1:62,500, and so the zonation was based on the underlying geologic units. In summary, the strong correlation of areas where liquefaction occurred during the 1989 Loma Prieta earthquake and areas mapped as having a high to very high liquefaction susceptible demonstrates the utility of the methodology of Youd and Perkins (1978).

The question remains why large areas zoned as having a high or very high liquefaction susceptibility did not fail, even when adjacent areas within the same zone did. A more careful examination of the geology of these sites reveals some important differences not noted during the original mapping.

Most of the 1989 liquefaction occurred within areas mapped as **abandoned channel fill** and **younger fluvial deposits** (units Qcf and Qyf of Dupré and Tinsley, 1980). Liquefaction within the younger fluvial deposits appeared to be largely restricted to the sandy point-bar facies of this unit. The areas of younger fluvial deposits that showed no evidence of liquefaction probably consist of locally undifferentiated areas of flood-basin deposits. These deposits are water saturated and mostly of late Holocene age, but they tend to lack beds of liquefiable sands and silts of any significant thickness; it is only where such beds are locally present (for example, near small tributaries) that minor liquefaction occurred (for example at site 101 of Tinsley and others, this chapter). Wherever possible, flood-basin deposits were mapped as **basin deposits** (unit Qb of Dupré and Tinsley, 1980). Basin deposits as mapped included a variety of clay rich depositional environments that differ in sand content and, thus, in liquefaction susceptibility. Although most of the flood-basin deposits within this map unit did not fail, large areas of


Figure 4.—Liquefaction features from 1989 Loma Prieta earthquake in Monterey Bay region. *A*, Lateral spread in channel and point-bar deposits beneath flood-control levee near mouth of the Pajaro River (fig. 1; site 103 of Tinsley and others, this chapter). Extension was from left to right, toward free face formed by river channel. *B*, Lateral spread along margin of lower course of the Pajaro River (fig. 1; site 99 of Tinsley and others, this chapter). Partial view emphasizes nearly 2 m of differential settlement of narrow strip of land adjacent to channel. Extension was right to left by nearly 1 m. *C*, Lateral spread in estuarine and overlying artificial fill deposits at the entrance to Moss Beach (MB, fig. 1; site 116 of Tinsley and others, this chapter). Extension was from right to left, toward tidal inlet north of Elkhorn Slough. *D*, Lateral spread in estuarine deposits and overlying dunes at Moss Beach (MB, fig. 1; site 116 of Tinsley and others, this chapter). Extension was from right to left, including differential settlement of about 0.4 m. *E*, Sand boils along paleochannel within younger fluvial deposits in the Pajaro Valley (PV, fig. 1; site 91 of Tinsley and others, this chapter).

estuarine, tidal-flat, and abandoned-tidal-channel deposits (also mapped as unit Qb) did fail, especially within a few hundred meters of the coast. Future mapping needs to distinguish between these different types of "basin" deposits.

In addition, **dune deposits** (unit Qd of Dupré and Tinsley, 1980), exhibited ground failure only where underlain by young estuarine or tidal-channel deposits; failure actually occurred within the underlying deposits (figs. 4*C*, 4*D*). The discontinuous patterns of failure in the Moss Landing area (ML, fig. 1; Tuttle and others, 1990; Greene and others, 1991), and at the mouth of the Pajaro River (sites 109 and 108 of Tinsley and others, this chapter) coincide largely with areas that were originally tidal inlets or estuaries which had been filled within the last 150 years (fig. 5). The geologic units as mapped at the surface, such as dunes and washover deposits, do not reflect these differences in subsurface stratigraphy. These differences become readily apparent, however, when historical maps of the shoreline are superimposed on the modern map (fig. 5).

One of the most puzzling questions remaining is why conclusive evidence of liquefaction was absent in younger fluvial deposits along all but the lowermost reaches of

*B*


Figure 4.—Continued.

*C*

Figure 4.—Continued.

Corralitos Creek (fig. 1), a major tributary to the Pajaro River, even though these deposits are similar in age to those that failed extensively along the Pajaro, and were much closer to the epicenter. Corralitos Creek is smaller and shorter, has a steeper gradient, and consists of slightly coarser and more poorly sorted sediment than the Pajaro River. We speculate that the Corralitos sediments may not fall within the optimum size distribution for liquefaction (median particle diameter, $D_{50}$, ranges from 0.08 to 0.7 mm; see Housner, 1985). Grain-size distributions currently being analyzed may help explain the observed anomaly. The water table may have been sufficiently deep along Corralitos Creek at the time of the earthquake that potentially liquefiable sediment was dry. However, information about the location of any perched or shallow ground water for the critical time in question is unavailable.

## EVIDENCE OF RECURRENT LIQUEFACTION

Within the area affected by the 1989 Loma Prieta earthquake, most of the failures that occurred during the 1906

*D*

Figure 4.—Continued.

*E*

Figure 4.—Continued.

San Francisco earthquake (as compiled by Youd and Hoose, 1978) were reactivated, clearly demonstrating the phenomenon of recurrent liquefaction (see Youd, 1984). The horizontal component of displacement and the differential vertical component of settlement observed in areas subject to lateral-spreading ground failure in 1989 were, however, generally significantly smaller than those in 1906. The 1989 earthquake ($M_S$=7.1) was significantly smaller, releasing energy amounting to only about $^1/_{60}$ of the energy released by the 1906 earthquake ($M_S$=8+). As the 1989 rupture nucleated near its center and propagated bilaterally, even the duration of shaking was unusually small for an $M$=7.1 event, and it paled in comparison with the 1906 earthquake. Predictably, the total areal extent of

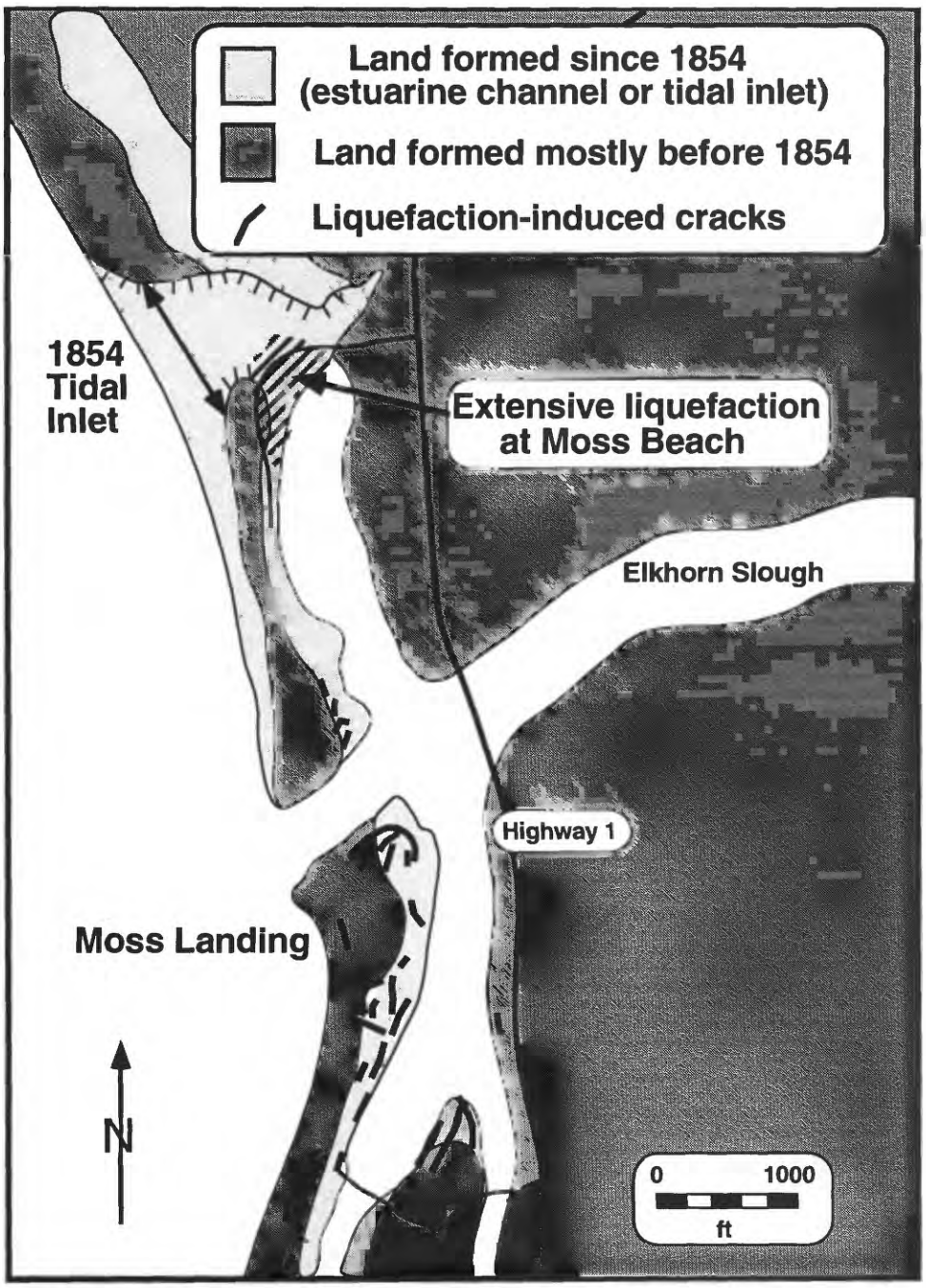


Figure 5.—Moss Landing area, Calif. (see fig. 1 for location), showing distribution of liquefaction-induced deformation (modified from Greene and others, 1991). Areas of young deposits (post-1854 estuarine-channel or tidal-inlet fill), are mapped on basis of comparisons with historical shoreline changes (modified from Hans Nielsen, unpub. data, 1991).

liquefaction was notably smaller in 1989 than in 1906. In addition, the 1906 earthquake followed an especially wet winter, and earthquake-triggered flow failures on hillsides were common. In contrast, the 1989 earthquake followed several years of drought, possibly accounting for the absence of liquefaction flow failures on hillsides.

Multiple liquefaction events occurred in artificial-fill deposits at Soda Lake (site 74 of Tinsley and others, this chapter; Sims and others, this chapter) as a result of two sets of aftershocks after the 1989 Loma Prieta earthquake. The first aftershock ($M$=5.4) occurred on April 18, 1990, 6 months after the main shock (Wills and Manson, 1990; Roger and others, 1991; Sims and others, this chapter), and the second ($M$=4.6?) occurred on March 23, 1991, almost 17 months after the main shock.

## SUMMARY

Detailed geologic mapping of Quaternary sedimentary deposits in the Monterey Bay region, in combination with application of the work by Youd and Perkins (1978), resulted in a regional map of relative liquefaction susceptibility (Dupré and Tinsley, 1980).

All of the major occurrences of significant liquefaction-induced ground failure during the 1989 Loma Prieta earthquake were in deposits mapped by Dupré and Tinsley (1980) as having a high to very high liquefaction susceptibility. These deposits were mainly late Holocene fluvial deposits, abandoned channel-fill deposits, and estuarine deposits.

Areas that did not appear to liquefy, yet were zoned as having a high to very high liquefaction susceptibility, mainly consisted of young, water-saturated deposits where a sandy facies was apparently absent in the subsurface. One exception may be the younger fluvial deposits along Corralitos Creek (fig. 1), where the absence of liquefaction might have been related to a low water table.

Future mapping should attempt to differentiate sand-poor and sand-rich facies within basin and fluvial deposits so as to more accurately delineate zones of liquefaction susceptibility. In addition, relatively young estuarine deposits should be differentiated from other types of basin deposits, because estuarine deposits are particularly prone to failure.

The strong correlation of areas of liquefaction in 1989 and areas mapped as having a high to very high liquefaction susceptibility clearly demonstrates the utility of regional geologic mapping for minimizing losses due to liquefaction in future earthquakes.

## ACKNOWLEDGMENTS

The original mapping by Dupré (1975a) and Dupré and Tinsley (1980) was initiated as part of the National Program for Earthquake Hazard Reduction of the U.S. Geological Survey. Earl E. Brabb of the U.S. Geological Survey, who established this project, provided base maps, aerial photographs, and other materials, as well as funding for most of the fieldwork, and helped edit the maps and facilitated their publication. Monterey County provided additional support of our fieldwork. Our 1989–92 postearthquake studies were primarily supported by the U.S. Geological Survey. Supplemental support was provided by the University of Houston's Coastal Center.

We are grateful to the numerous geologists and engineers who shared their expertise with us, as well as giving us access to historical maps and aerial photographs, engineering reports, and well logs. Lastly, we thank the many landowners and lessees who graciously gave us access to their property, without which this study could not have been completed.

## REFERENCES CITED

Bartlett, S.F., and Youd, T.L., 1992, Empirical prediction of lateral spread displacement: Buffalo, N.Y., National Center for Earthquake Engineering Technical Report 92–0019, p. 351–363.

———1995, Empirical prediction of liquefaction-induced lateral spread: Journal of Geotechnical Engineering, v. 121, no. 4, p. 316–329.

Birkeland, P.W., Soils and geomorphology: New York, Oxford University Press, 372 p.

Carpenter, E.J., and Cosby, S.W., 1925, Soil survey of the Salinas area, California: U.S. Department of Agriculture, Bureau of Chemistry and Soils, ser. 1925, no. 11, 80 p.

Cooper, Clark & Associates, 1975, Preliminary map of landslide deposits in Santa Cruz County, California, *in* Seismic Safety Element, Santa Cruz County, California: Palo Alto, Calif., 132 p.

Dupré, W.R., 1975a, Maps showing geology and liquefaction potential of Quaternary deposits in Santa Cruz County, California: U.S. Geological Survey Miscellaneous Field Studies Map MF–648, scale 1:62,500.

———1975b, Quaternary history of the Watsonville Lowlands, north-central Monterey Bay region, California: Stanford, Calif., Stanford University, Ph.D. thesis, 145 p.

———1990, Maps showing geology and liquefaction susceptibility of Quaternary deposits in the Monterey, Seaside, Spreckles, and Carmel Valley quadrangles, Monterey County, California: U.S. Geological Survey Miscellaneous Field Studies Map MF–2096, scale 1:24,000, 2 sheets.

Dupré, W.R., and Tinsley, J.C. III, 1980, Maps showing geology and liquefaction potential of northern Monterey and southern Santa Cruz Counties, California: U.S. Geological Survey Miscellaneous Field Studies Map MF–1199, scale 1:62,500, 2 sheets.

Greene, H.G., Gardner-Taggart, J.M., Ledbetter, M.T., Barminski, Robert, Chase, T.E., Hicks, K.R., and Baxter, Charles, 1991, Offshore and onshore liquefaction at Moss Landing spit, central California—result of the October 17, 1989, Loma Prieta earthquake: Geology, v. 19, no. 9, p. 945–949.

Hall, N.T., Sarna-Wojcicki, A.M., and Dupré, W.R., 1974, Faults and their potential hazards in Santa Cruz County, California; U.S. Geological Survey Miscellaneous Field Studies Map MF–626, scale 1:62,500, 3 sheets.

Hatheway, A.W., 1991, The value of historic American soil survey reports and maps: Association of Engineering Geologists News, v. 34, no. 3, p. 21–23.

Housner, G.W., chairman, 1985, Liquefaction of soils during earthquakes: Washington, D.C., National Academy Press, 240 p.

Janda, R.J., and Croft, M.G., 1967, The stratigraphic significance of a sequence of non-calcic brown soils formed on the Quaternary alluvium of the northeastern San Joaquin Valley, California, *in* Quaternary soils: International Association Quaternary Research (INQUA) Congress, 7th, Reno, Nev., 1967, Proceedings, v. 9, p. 158–190.

Lawson, A.C., chairman, 1908, The California earthquake of April 18, 1906; report of the State Earthquake Investigation Commission: Carnegie Institute of Washington Publication 87, 2 v.

Rogers, J.D., Wills, C.J., and Manson, M.W., 1991, Two sequences of fine grained soil liquefaction at Soda Lake, Pajaro River Valley, Santa Cruz County, California: International Conference on Recent Advances in Geotechnical Earthquake Engineering and Soil Dynamics, 2nd, St. Louis, Mo., 1991, Proceedings 3, p.2295-2308.

Roth, R.A., and Kavanjian, Edward, Jr., 1984, Liquefaction susceptibility mapping for San Francisco, California: Association of Engineering Geologists Bulletin, v. 21, no. 4, p. 459–478.

Storie, R.E., 1944, Soil survey: the Santa Cruz area, California: U.S. Department of Agriculture, Soil Conservation Service Soils Report, ser. 1935, no. 25, 90 p.

Tinsley, J.C., III, 1975, Quaternary geology of northern Salinas Valley, Monterey County, California: Stanford, Calif., Stanford University, Ph.D. thesis, 195 p.

Tinsley, J.C., III, Youd, T.L., Perkins, D.M., and Chen, A.T.F., 1985, Evaluating liquefaction potential, in Ziony, J.I., ed., Evaluating earthquake hazards in the Los Angeles region—an earth-science perspective: U.S. Geological Survey Professional Paper 1360, p. 263–316.

Tuttle, M.P., Cowie, P.A., Tinsley, J.C., III, Bennett, M.J., and Berrill, J.B., 1990, Liquefaction and foundation failure of Chevron oil and gasoline tanks at Moss Landing, California: Geophysical Research Letters, v. 17, no. 10, p. 1797–1800.

Wills, C.J., and Manson, M.W., 1990, Liquefaction at Soda Lake; effects of the Chittenden earthquake swarm of April 18, 1990, Santa Cruz County, California: California Geology, v. 43, no. 10, p. 225–232.

Youd, T.L., 1973, Liquefaction, flow, and associated ground failure: U.S. Geological Survey Circular 688, 12 p.

———1984, Recurrence of liquefaction at the same site: World Conference on Earthquake Engineering, 8th, 1984, Proceedings: Englewood Cliffs, N.J., Prentice Hall, p. 231–238.

Youd, T.L., and Hoose, S.N., 1977, Liquefaction susceptibility and geologic setting: World Conference on Earthquake Engineering, 6th, New Delhi, 1977, Proceedings, v. 3, p. 2189–2194.

———1978, Historic ground failures in northern California triggered by earthquakes: U.S. Geological Survey Professional Paper 993, 177 p.

Youd, T.L., Nichols, D.R., Helley, E.J., and Lajoie, K.R., 1975, Liquefaction potential, in Borcherdt, R.D., ed., Studies for seismic zonation of the San Francisco Bay region: U.S. Geological Survey Professional Paper 941–A, p. A68–A74.

Youd, T.L., and Perkins, D.M., 1978, Mapping liquefaction-induced ground failure potential: American Society of Civil Engineers Proceeding, Geotechnical Engineering Division Journal, v. 104, no. GT4, p. 433–446.

———1987a, Mapping of liquefaction severity index: Journal of Geotechnical Engineering, v. 113, no. 11, p. 1374–1392.

Youd, T.L., and Perkins, J.B., 1987b, Map showing liquefaction susceptibility of San Mateo County, California: U.S. Geological Survey Miscellaneous Investigations Series Map I–1257–G, scale 1:62,500.

THE LOMA PRIETA, CALIFORNIA, EARTHQUAKE OF OCTOBER 17, 1989:
LIQUEFACTION

STRONG GROUND MOTION AND GROUND FAILURE

# APPENDIX: MAPS AND DESCRIPTIONS OF LIQUEFACTION AND ASSOCIATED EFFECTS

By John C. Tinsley III [1], John A. Egan [2], Robert E. Kayen [1], Michael J. Bennett [1]
Alan Kropp [3], and Thomas L. Holzer [1]

## CONTENTS



## INTRODUCTION

This paper is an appendix that consists of a map explanation, two map sheets (Plate 1 and Plate 2, scale 1:100,000) and a compilation of observations at 170 sites that were examined by field personnel after the 1989 Loma Prieta earthquake for evidence of liquefaction, including sand boils, lateral spreading, settlement, and ground cracking. Included in this compilation are observations at sites (1) where liquefaction was reported in earlier earthquakes, primarily the 1906 San Francisco earthquake, but not in the 1989 Loma Prieta earthquake, and (2) where no liquefaction or ground failure was reported either in 1989 or in previous earthquakes. The second group of sites includes fills and earthworks constructed since 1906. The numbered sites are presented in three columns: the first column contains the number assigned arbitrarily to identify the site (generally numbered from north to south), the second column contains one or more graphic symbols indicating either the principal ground failure effects or absence of liquefaction observed at the location, and the third column contains a description of observations at the site. The location of the observations is indicated on the map by either a dot or a stippled area. Symbols are plotted for all of the effects that were observed at the site. Because surficial geologic maps and derivative liquefaction susceptibility maps were published before the 1989 Loma Prieta earthquake for the central Monterey Bay region (Dupré and Tinsley, 1980), table entries for that area include the surficial geologic unit at the site of liquefaction occurrence. Sites identified as U.S. Geological Survey special studies sites in the Monterey Bay area are also presented with supporting geotechnical data in Bennett and Tinsley (1995).

The compilers and their general geographic area of emphasis are John A. Egan and Michael J. Bennett, who compiled sites on Treasure Island and the west side of San Francisco Bay on plate 1; Robert E. Kayen, who compiled sites on the east side of San Francisco Bay on plate 1; Alan Kropp, who compiled sites in the Santa Cruz area on plate 2; and John C. Tinsley, who compiled the sites in the rest of the Monterey Bay region south of La Selva Beach on plate 2.

The sources of the observations in each entry, if not provided directly by the compilers or if supplemented by others, is given at the end of the entry. These additional sources include both published documents and written and oral communications to the compilers.

Author affiliation
[1] U.S. Geological Survey
[2] Geomatrix Consultants
[3] Alan Kropp and Associates

## SITES AND OBSERVATIONS

[Sites, types of ground failure, observations and descriptions of liquefaction-induced ground-failures. See plates 2 and 3, this volume, for locations of sites]

| Site | Failure Type | Observation |
|---|---|---|
| 1A | ◀▶ O | Bolinas Lagoon, Marin County. Sand boils and lateral spreading were observed on the adjacent beach. (Approximate location from Astaneh and others, 1989). |
| 1B | □ | Bolinas Lagoon, Sea Drift community, Marin County. No evidence of liquefaction was observed in a housing development on the spit across the mouth of lagoon (David M. Peterson, October 23, 1989). |
| 2 | ◀▶ | Rodeo Cove, Marin County. Lateral spreading, with cracks trending N. 30°-40° W., occurred in beach sand at the cove. Cumulative horizontal extension across cracks on the lagoon side of the beach ranged from 30 to 130 mm; differential vertical offset across cracks ranged from 50 to 100 mm. The ground-water level was 2 m below the ground surface at the time of observation (David M. Peterson, October 23, 1989). |
| 3 | O ◀▶ ⧓ × + | Treasure Island, San Francisco. The island consists of approximately 16 million $m^3$ of hydraulic fill emplaced over an area of 1.6 $km^2$. The fill, which was hydraulically dredged from local sources in 1936 and 1937, ranges in thickness from approximately 4.5 to 12.5 m. The island's perimeter consists of rock dikes. Sand boils, lateral spreading, and settlements occurred over most of the island, confirming that liquefaction was areally extensive. A detailed map of ground failure and distress to facilities is shown by Power and others (See plate 3).<br><br>Sand erupted through pavement, natural soils, and into homes and other buildings. The volume of sand in individual sand boils ranged from about 0.03 to 12 $m^3$.<br><br>Ground cracks caused by bayward lateral spreading were common along the island's perimeter, but were most prevalent along the east side of the island. The maximum distance of cracks from the edge of the island was approximately 170 m, but cracks were less than 60 m inland from the perimeter dike along most of the perimeter. Summation of openings across cracks on the eastern side of the island indicates bayward lateral spreading of about 0.3 m. Movement across some ground cracks appears to have continued after the earthquake. Cracks caused by a small slump in the paved dike road (west side) in front of residence 1307 were marked by an unknown person with painted lines along with the amount of crack opening on November 13, 1989. On November 16, 1989, lengths were remeasured by U.S. Geological Survey personnel with a ruler, and vertical offset was documented with a level and ruler: |

| Line | Direction | Length (mm) Nov 13 | Length (mm) Nov 16 | Vertical Offset (mm) Nov 16 |
|---|---|---|---|---|
| B | N. 72° E. | 32 | 38 | 0 |
| C | N. 65° E. | 32 | 38 | 3 |
| D | N. 64° E. | 25 | 32 | 0 |
| E | N. 70° E. | 25 | 32 | 13 |
| F | ? | 19 | 25 | 0–10 |
| G | ? | ? | 4 | 0 |

Ground settlement, both differential settlement adjacent to buildings and associated with lateral spreading and regional settlement, was widespread. Differential settlements were as large as 150 mm. Approximately 100 to 150 mm of differential settlement occurred adjacent to pile-supported Buildings 2 and 3 on the south side of the island and around the old pile foundation of the Tower of the Sun on Fourth Avenue. Comparison of preearthquake and postearthquake surveys indi-

cated that regional ground settlements ranged from 50 to 150 mm.

Earthquake damage to most affected buildings was limited to minor cracks or differential settlements. Several buildings were more significantly damaged (Buildings 7, 107, and 461 and residential units 1211, 1218, 1233, 1235, and 1237, pl. 3). Buildings that were most heavily damaged were generally located near the perimeter dike and in areas of significant ground distress, primarily lateral spreading. Underground utilities were significantly damaged by lateral spreading and settlement. A total of 44 utility-line breaks were reported, consisting of 28 freshwater-line breaks, 10 sewage-line breaks, and 6 gasline breaks: (Bennett, this chapter; Power and others, this chapter; Lee and Prasaker, 1969; Egan and Wang, 1991).

4 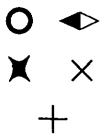

Marina District, San Francisco. Much of the district originally was a natural cove that was filled piecemeal from local sources from 1857 to 1912; the largest fill was hydraulically emplaced in the central part of the cove from offshore sources. Liquefaction and associated deformation were limited to, but widespread in, these fills. Sand boils erupted through streets and sidewalks, in garages and backyards and on Marina Green. Some sand boils erupted along Marina Boulevard between Divisadero and Scott Streets at the edges of buildings that settled differentially. Most sand boils consisted of fine ($D_{50} \approx 0.168$ mm) gray sand that originated from the hydraulic fill, but sand boils on Marina Green consisted of medium ($D_{50} \approx 0.235$ mm) brown sand that originated from dune sand used as fill.

Two types of settlement occurred in the Marina District: (1) regional settlement over a large area that required a precise survey to detect, and (2) local differential settlement at well-defined locations. On the basis of precise surveys conducted in 1961 and 1974 and a postearthquake survey in 1989, regional settlement in the area of the hydraulic fill was found to be almost 9 times greater for the interval 1974–89 than for the interval 1961–74. Most of the 1974–89 regional settlement was inferred to be caused by earthquake-induced compaction from liquefaction. Between 1974 and 1989, settlement within the hydraulic fill ranged from 38 to 143 mm and averaged 96 mm. Conspicuous examples of differential settlement associated with engineered structures within the area underlain by hydraulic fill were common but were not restricted to this area. At the St. Francis Yacht Club, as much as 200 mm of differential settlement occurred at the boundary between pile-supported and spread-footing foundations on land-tipped fill (a land-tipped fill is fill placed by mechanical means from land, as opposed to a hydraulically placed fill; the latter involves excavation, transport, and emplacement using flowing water). Building supports in several garages, in the area underlain by hydraulic fill, punched through the concrete and settled as much as 120 mm. Sewer-access structures showed as much as 75 mm of differential settlement at Jefferson and Broderick Streets. Differential settlement of 150 mm occurred at the 2.4-m-diameter storm-drain outfall at the Marina seawall. The grassy area of Marina Green above and adjacent to this outfall displayed approximately 60 mm of differential settlement. The south-side curb of Marina Boulevard showed 70 mm of differential settlement where the outfall passes underneath the curb. The outfall, which also passes under other houses on Cervantes and Beach Streets, showed approximately 70 mm of differential settlement where the outfall passes beneath them. On Marina Boulevard, between Scott and Broderick Streets, settlement of 20 to 150 mm occurred along the front and sides of some houses. On Webster Street, between Jefferson and North Point Streets, settlement of 40 to 50 mm occurred at many house/sidewalk boundaries. The west curb along Webster Street, near Jefferson Street, settled 100 mm and was level with the street. A complex pattern of settlement and lateral spreading occurred on North Point Street, between Fillmore and Webster Streets where at least 75 mm of settlement and 50 mm of lateral spreading occurred. The only settlement reported in 1906 was at Buchanan and North Point Streets (Youd and Hoose, 1978, loc. 223).

Horizontal ground deformation was common in, but not limited to, the area underlain by hydraulic fill. Evidence of horizontal displacement included buckled sidewalks, curbs thrust over streets, open cracks, and shear zones. Axes of buckled sidewalks were oriented both north-south and east-west. At the intersection of Mallorca and Alhambra Streets, the corners of all four curbs were thrust out over the street. Cumulative northward displacement across cracks at the St. Francis

Yacht Club totaled 0.6 m. Horizontal displacement of 175 mm, measured over 30 m, occurred at Winfield Scott School. The north-south and east-west sets of cracks in the schoolyard coincide with the boundary between the hydraulic fill and the older fills. The overall pattern or orientation of cracks in the Marina District showed no uniform trend. A fissure was reported in the beach at the end of Webster Street from the 1868 earthquake on the Hayward fault (Youd and Hoose, 1978, loc. no. 223).

Buried pipelines were extensively damaged. There was a close correspondence between the settlement and the pattern of pipeline damage; damage was concentrated in, but not limited to, the area of hydraulic fill: (Bennett, 1990; Benuska, 1990; Çelebi, 1990; Chieruzzi and Lew, 1990; O'Rourke and others, 1991, 1992; Bardet and others, 1992; Bonilla, 1992; Harris and Egan, 1992; Taylor, and others, 1992).

5 

Pier 45, San Francisco. Liquefaction-induced settlement and cracking of the pavement occurred at the entrance to the pier. Liquefaction-induced damage caused partial or complete closure of several warehouses on the pier (Seed, and others, 1990).

6 

The Embarcadero (north of the Ferry Building), San Francisco. Liquefaction was relatively minor in severity and did not appear to encompass the entire area of artificial fill. Most evidence of liquefaction consisted of relatively minor settlement and (or) cracking of pavements, although sand boils erupted in several places, including two sites on the west side of the Embarcadero: (1) beneath the former elevated-highway offramp between Washington and Clay Streets and (2) between Broadway and Vallejo Streets. Settlements of the extreme edge of the coastal fill at the ends of the pile-supported piers along the waterfront ranged from about 25 mm at several piers to 125–150 mm near Piers 15 and 17 (O'Rourke and others, 1990; Seed and others, 1990).

Foot of Market Street, San Francisco. Differential settlements and lateral displacements were observed along the Embarcadero from Howard Street to just north of the Ferry Building. Settlement of approximately 0.3 m was observed immediately north of the intersection of Market Street and the Embarcadero. Sand boils were observed along the Embarcadero between the Ferry Building and Pier 1 on the west side of the Embarcadero across from the Ferry Building. A conspicuous crack with as much as 100 mm of vertical offset occurred immediately north of the intersection of Market Street and the Embarcadero; the crack extended about 60 m northeastward from the intersection. A conspicuous 25-mm-wide crack opened beneath the Embarcadero Skyway, running parallel to the seawall for the full distance between Howard and Mission Streets; the crack indicated lateral displacement toward the bay at a distance of about 20 m behind the seawall. Differential settlements of 25 to 100 mm occurred adjacent to the pile-supported columns of the skyway (O'Rourke, and others, 1990).

7 

South of Market Street and north of Interstate Highway 80, San Francisco. Sand boils were observed along the curb and building lines in various places on Sixth, Seventh, Natoma, Russ, Moss, and Clara Streets. From Mission to Folsom Streets, 10- to 30-mm-wide cracks were observed down the centerline of Seventh Street, with differential settlement to the east and west of the cracks. Compression ridges in the form of buckled street pavements and sidewalks were observed along Russ Street, approximately 30 to 60 m north of Folsom Street. Differential settlement of about 0.3 m was observed at the southeast corner of Natoma and Seventh Streets, with settlement and severe deformation of the two- and three-story timber-frame buildings at this location. Sand flowed into the basement of a building at the corner of Howard and Seventh Streets, filling it to a depth of approximately 0.6 m. Differential settlements and cracks were apparent on Sixth Street, between Folsom and Harrison Streets. Sand boils and differential settlement damaged a structure on Sixth Street south of Howard Street. The basement of the building filled with sand, and sufficient structural damage occurred as a result of differential settlements that the building was condemned. The basement of a building one block farther north also had considerable sand intrusions; foundation settlements resulted in sufficient damage that this structure was condemned as well. Approximately 14 $m^3$ of sand erupted into the basement of a pile-supported building at 1077 Howard Street (grain-size characteristics: $D_{50}$ = 0.220 mm; $D_{60}/D_{10}$=

1.6) in an area where large settlements had occurred during earthquakes in both 1865 and 1906 (Youd and Hoose (1978, loc. 212). At the U.S. Court of Appeals and Post Office at Seventh and Mission Streets, approximately 100 mm of settlement of the lawn and sidewalk areas occurred adjacent to the south side of the building. This building straddles the original bay shoreline, and the southern part of the building extends into the reclaimed area. This building also was shaken by the 1906 earthquake. Conspicuous liquefaction-related ground-failure effects in 1906 were described in this area (Youd and Hoose, 1978, loc. 210). A 300-mm-diameter cast-iron water main of the Auxiliary Water Supply System, operated by the San Francisco Fire Department, ruptured on Seventh Street, between Mission and Howard Streets, in an area of liquefaction and differential movements. A hydrant branch at Sixth Street, between Howard and Folsom Streets, broke when it settled over a pile-supported sewer.

Sand boils erupted in the street near a crack at Sixth and Tehama Streets near an area noted for settlement during the 1906 earthquake (Youd and Hoose, 1978, loc. 209). The crack was 60 m long and opened 90 mm, with the west side down.

On Harriet Street, between Howard and Folsom Streets, a 4-in.-diameter pipe was broken, with water coming to the surface on October 18, 1989. On Seventh Street at Howard Street, a 50-m-long crack, opened 70 mm at the surface, and at least 0.3 m deep, was observed near settlement noted in 1906 (Youd and Hoose, 1978, loc. 212): (O'Rourke and others, 1990; Seed and others, 1990).

8 

South of Market Street and south of Interstate Highway 80, San Francisco. Approximately 0.3 m of differential settlement and sand boils were observed beneath Interstate Highway 280 near the intersection of Sixth, Bluxome, and Townsend Streets. At the intersection of Sixth Street with Bluxome and Townsend Streets substantial differential settlement occurred. Beneath the west curb-line of Sixth Street at this location, there is a 2-m-diameter concrete sewer supported on piles. The ground settled sharply adjacent to each side of this sewer, with settlements of roughly 0.4 to 0.5 m at the northeast corner of Sixth and Townsend Streets relative to the sewer centerline. Local differential settlement of about 150 mm was observed adjacent to the building at the northeast corner of Sixth and Townsend Streets. Differential settlements of 150 to 250 mm were observed adjacent to pile-supported columns of the California Interstate Highway 280 ramp at this location. Abrupt settlement with a maximum vertical offset of 200 mm was measured to the west of the pile-supported sewer beneath the California Interstate Highway 280 ramp. Modern differential settlements were apparent along the north side of Townsend Street for a distance of about one block to the east and west of its intersection with Sixth Street. Sand boils were observed beneath the California Interstate Highway 280 ramp. No sand boils or differential settlements were observed in the vicinity of the railyard immediately south of Townsend Street. Hydrant elbow breaks occurred at Sixth and Bluxome streets, and at Fifth Street, between Harrison and Bryant Streets; the second break has been attributed to settlement of the hydrant branch, which crossed over a pile-supported sewer that did not settle. Brown sand erupted under the freeway on Fifth Street, possibly owing to the broken water pipe; a large crack was noted in the median of Fifth Street adjacent to the vented sand.

At 1200 Seventh Street, between Irwin and Hubbell Streets, sidewalks settled approximately 25 mm with respect to the building; the curb was fractured (P.D. Spudich, November 6, 1989).

At 160-180 Hubbell Street, sidewalk settlements ranged from 37 to 65 mm opposite the Glidden Paint facility. Across the street from this facility, settlements damaged a brick structure and caused curb separations of less than 6 mm (P.D. Spudich, November 6, 1989; O'Rourke and others, 1990; Seed and others, 1990).

9 

Dore Street, San Francisco. About 0.3 m of settlement was observed in a parking lot off Dore Street approximately 30 m north of its intersection with Bryant Street, where substantial settlement and lateral spreading occurred in the 1906 earthquake (Youd and Hoose, 1978, loc. 214). About 100 mm of settlement in the sidewalk adjacent to the building occurred on the northeast

corner of Dore and Bryant Streets, and the structure settled differentially. The sidewalk along Bryant Street adjacent to the building was buckled, and a water service pipe had been ruptured (O'Rourke, and others, 1990).

10 Mission Creek District, San Francisco. East of Mission and Capp Streets, liquefaction occurred in the same places where it had been observed after the 1906 earthquake. The most conspicuous damage caused by liquefaction occurred as differential settlement, racking, and tilting of Victorian two- to four-story timber-frame buildings on South Van Ness Avenue and Shotwell and Folsom Streets between 17th and 18th Streets. Sand boils erupted on Shotwell Street between 17th and 18th Streets in immediate area of settlement and lateral spreading observed in 1906 earthquake (Youd and Hoose, 1978, loc. 215). Sand erupted from joints in sidewalks, next to foundations, and into basements. Sand erupted in the alleyway between 352 and 358 Shotwell Street and into basement of 364 Shotwell Street; sand (grain-size characteristics: $D_{50}$= 0.212 mm; $D_{60}/D_{10}$ = 1.5) erupted from a sidewalk joint in front of the lot next to 328 Shotwell Street; sand ($D_{50}$ = 0.221 mm; $D_{60}/D_{10}$ = 0.5) erupted from a sidewalk joint in front of 342 Shotwell Street; and sand ($D_{50}$= 0.224 mm; $D_{60}/D_{10}$ = 1.7) erupted from a sidewalk area at 2055 Folsom Street. No sand was seen on the 400 block of Shotwell Street. The most severe damage was observed at the middle west side of Shotwell Street, where maximum building settlements of about 0.2 to 0.4 m occurred. Differential settlement and conspicuous cracks were observed along 14th Street between Folsom and Harrison Street. Differential settlements at 2- to 4-story Victorian timber-frame buildings were observed on the north side of 15th Street about 30 m west of Folsom Street in an area where sand boils were apparent along the curbline. Occupants of these structures reported that settlement continued for as long as 4 days after the earthquake.

On 17th Street, between Shotwell and Folsom Streets, a 30-m-long crack was observed in the street median, open 20 mm, with north side down 10 mm. Sidewalk damage was noted on the north side of the same street; asphalt adjacent to the curb was thrust up northward over the rest of the sidewalk. On the west side of Folsom Street, between 16th and 17th Streets, the concrete sidewalk was shattered. A 50-m-long crack, open 40 mm, was observed in the median of South Van Ness Avenue between 17th and 18th Streets (O'Rourke and others, 1990; Seed and others, 1990).

11 Mission Creek District, San Francisco. The area west of Mission Street apparently was unaffected by liquefaction, even though lateral spreading and settlement of 1.5 to 2.0 m were observed at Valencia and Guerrero Streets in the 1906 earthquake (Youd and Hoose, 1978, loc. 216, 217; O'Rourke, et al., 1990).

12 Sunset District, San Francisco. No ground effects were seen near 47th and Kirkham Streets where sand boils and lateral spreading were observed in the 1906 earthquake (Youd and Hoose, 1978, loc. 247).

13 Islais Creek Channel, San Francisco. Scattered evidence of minor settlements was observed in the vicinity of the channel and in the northwestern part of Hunter's Point, causing minor pavement cracking.

14 Pier 80, San Francisco. Ground distress in this area was minimal and took the form of slight ground settlement and cracking. No damage to pile-supported structures, such as the wharves and storage sheds, was reported (Dames & Moore, 1990).

15 Hunters Point Naval Station, San Francisco. Liquefaction occurred in loose sandy fill placed within sheet piles that form the pier area. Settlements of as much as 150 mm occurred in the pier fill, and the outlines of the sheet-pile cells could be seen. A large sinkhole also occurred at this site, and silt boils covered an area of approximately 19 m. No apparent damage to the walls of the sheet-pile cell or to structures or other facilities occurred at this site (approximate location from Seed and others, 1990).

16 ○ Hunters Point, San Francisco. Two sand boils erupted on I Street, between J and Manseu Streets (grain-size characteristics: sample at Universal Transverse Mercator grid, zone 10: 555,681 m east, 4,174,700 m $D_{50}$ = 0.200 mm and $D_{60}/D_{10}$=2.7); sample at 555,695 m east, 4,174,659 m north had a $D_{50}$ = 0.196 mm and $D_{60}/D_{10}$=2.3; (R.D. Brown and W.P. Irwin, October 20, 1989).

17 ○ □ San Francisco International Airport. Sand boils erupted on undeveloped land at the bayshore immediately north of the airport. No evidence of liquefaction was observed near the airport facilities (approximate location from Seed and others, 1990).

18 □ Pacifica. The west side of Laguna Salada was examined because of sand deposits known to exist there and because postearthquake aerial photographs showed possible liquefaction deposits at a dike that parallels the seashore. The suspect deposits were beach sand, deposited by storm waves, across which the dike was rebuilt. No sand blows or evidence of ground failure were found on or near the dike (M.G. Bonilla, October 27, 1989).

19 ○ Brewer Island, Foster City; 2 km west-northwest of the San Mateo Bridge approach at Little Coyote Point. Sand boils and ground cracks followed the north shore of the island for about 100 m in an area north of the manmade levee system that protects Foster City from high tides These liquefaction effects extended inland about 25 m south of the shore. Isolated sand boils and aligned and overlapping sand boils erupted along linear, 10- to 30-mm-wide, extension cracks. Diameters of individual sand boils ranged from 0.5 to 2 m. The sand boils were composed of gray, fine to very fine sand and silt, but a few vents also discharged yellowish-brown (oxidized?) sand and silt before finally venting gray sediment (grain-size characteristics: sample at Universal Transverse Mercator grid, zone 10: 563,230 m east, 4,158,736 m north, $D_{50}$ = 0.066 mm and $D_{60}/D_{10}$ = 4.2, and sample at 563,266 m east, 4,158,724 m north, $D_{50}$ = 0.061 mm and $D_{60}/D_{10}$ = 3.2; (R.D. Brown and W.P. Irwin, October 20, 1989).

20 ⧓ × ▬ + Foster City. A 150-m-long crack formed in the parking lot of the shopping center southeast of the intersection of Edgewater and Beach Park Boulevards. The crack extended generally north-south, parallel to and about 40 to 50 m west of a waterway. The crack was about 1 or 2 mm wide and had no vertical displacement. No bank failures were visible at two places where the edges of the waterway were accessible. At the south end of the parking lot and approximately in line with the crack, a water pipe broke near its connection with the water main; the plumber in charge of repairs said that such breaks are common without earthquakes. A tentlike buckle occurred in the sidewalk on the south side of Port Royal Avenue, 0.3 km west of its intersection with the eastern part of Rockharbor Lane. A few minor cracks were visible in the bottom of an adjacent shallow concrete-lined pond, but no new cracks were visible in the street or adjacent sidewalk, and the curbs were not out of alignment. Metal plates at ground level near the buckle indicate some type of underground structure is adjacent to the buckle. Differential movement between the ground and the structure may explain the sidewalk buckle. Brick walks were deformed on both the northwest and southeast entrance areas of Metro Tower, a 22-story pile-supported building near the intersection of Metro Center Boulevard and Promendal Lane. The principal displacement of the bricks was downward, on sides away from the building, about 20 mm. The disturbances occurred at construction joints. The apparent cause was minor settlement and horizontal shifting of the ground under the walks in relation to the broad brick-paved area near the building (M.G. Bonilla, October 19 and 23, 1989).

21 ○ Foster City. Sand boils were observed and photographed on a beach at the south edge of Foster City. These sand boils were removed by tidal action during the first few days after the earthquake (approximate location from Seed and others, 1990).

22 ○ Redwood City. Several sand boils were observed at an undeveloped site on the shoreline of San Francisco Bay just south of Redwood City, approximately 2.4 km north of the Dumbarton Bridge earthquake (approximate location from Seed and others, 1990).

23 ◭ East Palo Alto. Water level, in a well monitoring an aquifer 45 m deep, rose 0.5 m between

measurements taken the morning of October 17, 1989, and the following week (P. Rey, oral commun., October 26, 1989).

24 □ Baylands Park, East Embarcadero Road, Palo Alto. Earthen dikes in this area were examined but no earthquake-related cracks were observed. No cracks or sand boils were visible along the boardwalk leading northeastward from the Palo Alto Baylands Interpretive Center, about 350 m northeast of the Palo Alto Yacht Club, and the observation platform at the end of the boardwalk was undamaged. The boat ramp about 0.4 km southeast of the Interpretive Center has a concrete floor and sloping concrete walls, as much as 1.5 m high. No new cracks formed in the concrete, but minor spalling occurred at one old crack (M.G. Bonilla, October 22, 1989).

25 □ Shoreline Park, Mountain View. No new cracks or earthquake damage were observed in the earthen dike that leads northeastward from the Bayshore Freeway along the northwest side of Charleston Slough. Slopes of dike 1.6 km northeast of the freeway are 11° on the northeast side and 8° on the southwest side; an 8° slope is typical of most of the dike (M.G. Bonilla, October 22, 1989).

26 ◀▶ O Half Moon Bay. Sand boils and lateral spreading occurred as a result of liquefaction at the edges of impounded lagoons at the mouth of streams, inboard of the surf zone. Ground cracking and sand boils were observed in this vicinity in 1906 (Youd and Hoose, 1978, loc. 109; Seed and others, 1990).

27 ◀▶ O San Gregorio State Beach. Sand boils and lateral spreading occurred as a result of liquefaction at the edges of impounded lagoons at the mouth of streams, inboard of the surf zone. Openings across cracks ranged from 15 to 20 mm and were plumbed to a depth of 50 mm (D.M. Peterson, October 19, 1989). Ground cracking and sand boils were observed in this vicinity in 1906 (Youd and Hoose, 1978, loc. 93; Seed and others, 1990).

28 ◀▶ O Pomponio State Beach. Sand boils and lateral spreading occurred as a result of liquefaction at the edges of impounded lagoons at the mouth of streams, inboard of the surf zone (approximate location from Seed and others, 1990).

29 ◀▶ O Gazos Beach. Sand boils and lateral spreading occurred as a result of liquefaction at the edges of impounded lagoons at the mouth of streams, inboard of the surf zone (approximate location from Seed and others, 1990).

30 ◀▶ O Big Basin Redwoods State Beach. Sand boils and lateral spreading occurred as a result of liquefaction at the edges of impounded lagoons at the mouth of streams, inboard of the surf zone (approximate location from Seed and others, 1990).

31 ◀▶ O ⧓ ⧔ Port of Richmond. Liquefaction occurred in hydraulic fill in an open-space area at the end of Harbor Way Road. Four large sand boils and a dozen smaller boils and vents discharged fine sand and silty sand at this site. In addition, minor settlements of approximately 20 to 80 mm and lateral movements of similar magnitude occurred at the edge of the harbor adjacent to a small pile-supported dock at the Tweed Towing/Maas Boats facility.

32 ◀▶ O Berkeley Marina. A single sand boil erupted on the northeast side of the marina immediately south of the municipal waste landfill, along with minor lateral spreading. During the 1906 earthquake, the lower alluvial flats of Berkeley were reported to have been "seriously disturbed" (Youd and Hoose, 1978, loc. 176).

33 ◀▶ O ⧓ × Berkeley. Minor lateral spreading and settlement occurred along Interstate Highway 80, south of the University Avenue exit from Interstate Highway 80 and the adjacent frontage road west of the highway. Between the Ashby Avenue and Powell Street exits, the observed lateral spreading resulted in pavement cracking oriented parallel to the shoreline; these cracks were typically less than 30 mm wide and 20 to 50 m long.

34 ○ ◀▷ + ×

Emeryville. Sand erupted into a ground level parking lot beneath the Watergate Apartments near the west end of Powell Street on the Watergate peninsula fill. Lateral spreading of several centimeters resulted in the dislocation of a water pipe and minor pavement cracking at the west end of the peninsula fill near the Emeryville Marina.

35 □

Emeryville. No ground failure or settlement was observed in the area immediately adjacent to the East Bay Park Condominium complex, a 30-story residential structure and 4-story garage structure. The site was improved from a medium-dense to an extremely dense condition by vibrocompaction probing (see Mitchell and Wentz, this chapter).

36 ◀▷ ○ ⧓ ×

Emeryville-Oakland. Interstate Highway 80 between the Powell Street exit and San Francisco Bay Bridge mole. Lateral spreading and settlement caused extensive pavement damage to the freeway road surface. Pavement cracking was oriented parallel to the shoreline, with a total lateral movement of 30 to 120 mm across the freeway. Several cracks were more than 50 m long. Sand and water issued to the surface through pavement cracks.

37 ◀▷ ○ ⧓ ⧖ × +

San Francisco-Oakland Bay Bridge mole (peninsula-approach fill), immediately south of Emeryville. Settlements of as much as 40 mm occurred over most of the peninsula fill, resulting in an uneven, wavy pavement surface. Lateral spreading produced numerous fissures in the road pavement parallel to the shoreline. Many of these pavement cracks were of considerable length (more than 100 m long), and open fissures 30 to 100 mm wide were common. Many of these fissures discharged fine sand and silty sand. Numerous additional sand boils erupted along the median strip of the roadway and off the shoulders of the roadway in undeveloped land at the bay's edge. Liquefaction-induced settlement of the pavement adjacent to the Toll Plaza administration and maintenance buildings resulted in the loss of some buried utilities entering the building. Settlements of the fill supporting the approach to the Bay Bridge, the California Interstate Highway 580 eastbound onramp, and the West Grand Avenue onramp structures were severe, resulting in pavement settlement and open fissures of as much as approximately 0.3 m wide at the soil-structure interface. The approach fill also settled below the bridge- and ramp-road level by as much a 0.5 m. Liquefaction was also observed adjacent to the piers of elevated freeway-distribution structures.

38 ◀▷ ○ ⧓ ⧖ × +

Port of Oakland, The Seventh Street Marine Container Terminal and Matson Terminal. Liquefaction of hydraulic fill resulted in settlement, lateral spreading, and cracking of the pavement over large areas of the Seventh Street Marine Container Terminal. Maximum settlements of the paved container yards inboard of the wharves were about 0.3 m. Several large cranes that operate along the edges of the fill traverse laterally along the wharves on crane tracks. The inboard rails for these cranes were supported on the fill throughout much of this terminal. As a result, differential settlements of the pavement and soil below the inboard rail rendered several loading cranes inoperable after the earthquake. The tops of several batter piles supporting the wharves at the Seventh Street Marine Container Terminal were damaged. Damage to the batter piles at the tops of the inboard two rows of piles consisted primarily of tensile failures. At the southwest end of the Seventh Street Marine Container Terminal, liquefaction caused considerable damage and landsliding at the now-closed Portview Park. Lateral spreading and failure of the southern perimeter dike wall occurred with lateral movements toward the bay of several meters. Numerous sand boils erupted on the park grounds.

39 ◀▷ ○ ⧓ × ⧖

Alameda Naval Air Station. Liquefaction occurred over a large area. Numerous large sand boils, settlement, and lateral spreading occurred at the west end of the station along the airfield's two runways and two taxiways, making them inoperable after the earthquake. Damage to pavements consisted of heaving, settlement, and minor lateral spreading, resulting in separation at joints. Maximum crack and joint openings were approximately 100 mm. Vertical offsets across joints and cracks ranged from 0 to approximately 50 mm.

40 ◀▷ +

Oakland. At Union and Adeline Streets, between Third and Fifth Streets, numerous cast-iron

main-pipeline breaks were reported. During the 1906 earthquake, a 24-in.-diameter riveted pipe was pulled apart 130 mm and displaced 200 mm laterally by settlement near this site (Youd and Hoose, 1978, loc. 176).

41A,B — Port of Oakland, Charles P. Howard (site 41A), and American Presidents Line (APL) (site 41B) Terminals. Liquefaction of the hydraulic fill caused appreciable settlements over large areas at both the Howard and APL Terminals, with maximum settlements of 300 mm. Pavement was cracked at the edges of the wharves and in the inboard container yards, with limited lateral spreading; however, no damage was reported to the dikes or pile-supported wharves. Several pipeline breaks also occurred in the yards of the Howard and APL Terminals. During the 1868 Hayward Earthquake, "portions of the wharves were carried away (into the Inner Harbor)" near this site (Wood, 1883, p. 665; Youd and Hoose, 1978, loc. 176).

42 — Mariner Square, Alameda. Seven pipeline breaks were reported in a one-block area around the square. Pipeline ruptures occurred in 1.5-in.-diameter service lines and several 6-in.-diameter mains. During the 1906 earthquake, settlement of more than 1 m occurred near this site (Youd and Hoose, 1978, loc. 173).

43 — Oakland. Settlement and several sand boils were observed along Lake Merritt Channel Park and Peralta Park, adjacent to the Laney College campus. Ground settlement resulted in the rupture of 6- ,12-, and 36-in.-diameter main pipelines. During the 1906 earthquake, damage to the Lake Merritt Dam, including foundation cracking, was reported at this site, as well as the rupture of a 24-in.-diameter main. A "37.5-inch" main, which may be the same main or a predecessor to the 36-in.-diameter main that ruptured in 1989, was slightly deformed in the 1906 earthquake but did not fail. Lateral spreading apparently occurred on the western bank of Lake Merritt during the 1906 event, but this bank was not distressed during the 1989 earthquake (Youd and Hoose, 1978, loc. 175).

44 — Alameda. Several small sand boils were observed at Robert W. Crown Memorial State Beach.

45 — Alameda. Liquefaction occurred along the west coast of the island, south and east of Robert W. Crown Memorial State Beach, as evidenced by sand boils, minor settlement, and minor lateral spreading. Ground deformation here caused minor cracking of pavements and separation of curbstones. Ground movement and softening in the area resulted in approximately two dozen residential pipeline ruptures. Pipeline ruptures occurred on nearly every street west of Otis Drive between Willow Street and Crown Park.

46 — Bay Farm Island, Alameda. Liquefaction in the form of sand boils, surface cracking, and pavement buckling occurred in an undeveloped, artificially filled site on the south side of a slough behind the improved west perimeter dike, northwest of the intersection of Aughinbaugh Lane and Mecartney Road. Numerous sand boils were observed at this site. During the 1906 earthquake, numerous "crevices and cracks" were reported on Bay Farm Island (Youd and Hoose, 1978, loc. 174).

47 — Bay Farm Island, Alameda. No liquefaction was observed in the fill in the perimeter sand dike of Harbor Bay Island Development, which was densified by deep dynamic compaction (see Mitchell and Wentz, this volume).

48 — Bay Farm Island, Alameda. Numerous sand boils and fissures were observed for 0.8 km along South Loop Road and Harbor Bay Parkway. Minor pavement cracks disrupted the street surface and parking lots, and several pipeline breaks were reported. In one place, a concrete storm drain rose approximately 150 mm out of the liquefied ground because of buoyancy.

49 — Oakland International Airport. Liquefaction caused considerable damage to the main jet runway, No. 11-29. Damage was principally located on the northwesternmost 900 m of the 3,000-m-long main runway and included sand boils, extensive runway-pavement cracking, and lateral spread-

ing. In addition, the adjacent taxiway pavement was heavily damaged. Cracks in the main runway and adjacent taxiway were as much as 300 mm wide, with vertical offsets of as much as 150 mm. Settlement and lateral spreading also occurred along the west perimeter dike in several places. The maximum observed levee settlement of the perimeter dike was about 0.5 to 0.7 m, and lateral deformations were similar in magnitude. Liquefaction-induced ground deformations also damaged an undeveloped area of fill to the north and west of the main runway.

50 

Oakland International Airport. Liquefaction occurred at the main terminal buildings and taxiways at the south end of the airport. Pavement settlement of as much as 80 mm adjacent to the two main terminal buildings was observed. A below-ground tramway, which allows for service vehicles carrying passengers' luggage to enter the main terminal buildings, filled to a depth of approximately 2 m with sand and water. Water-valve damage and a pipeline break were reported on Sally Ride Road on the airport grounds.

51A 

Dumbarton Point. Ground cracks formed over a distance of 76 m in the fill embankment of the Southern Pacific Railroad. Cracks paralleled the embankment and extended from 12 m southwestward to 64 m northeastward of the wood retaining wall that is the east end of the railroad bridge crossing of San Francisco Bay. On the southwest side of this wall, cracks extended southwestward from both ends of the retaining wall and passed along the alignment of the bridge piers to the edge of the fill. Fill on the southwest side and abutting the retaining wall settled differentially 0.1 m. On the northeast side of the retaining wall, a single crack was observed in the crown of the embankment; maximum horizontal separation was 150 mm, and maximum open depth was 1.9 m. Vertical offset of as great as 100 mm, downthrown to the southeast, was locally observed along the crown of the embankment. No sand boils were observed either in the embankment or in the adjacent undisturbed marsh (T.L. Holzer, December 18, 1989).

51B 

Alviso. Earthquake-related settlement occurred in the approach fills of the Gold Street bridge across the Guadalupe River. Dikes in the northwest part of Alviso showed no earthquake-related cracks. The slope of the dike on Alviso Slough northwest of the Alviso marina is 36° on the northeast side, where it has riprap of broken concrete; the other (channel) side is less steep and has no riprap (M.G. Bonilla, October 22, 1989).

51C 

Coyote Creek, San Jose/Milpitas. Ground and low-altitude aerial reconnaissance from the shoreline of the bay to California Highway 237 revealed no ground evidence of liquefaction or ground failure (J.A. Egan, October 18, 1989; T.L. Holzer, October 21, 1989) where conspicuous effects were observed in the 1868 and 1906 earthquakes (Youd and Hoose, 1978, loc. 149). The nonliquefaction behavior at this site was assessed by Egan and others (1992).

51D 

Guadalupe River, San Jose. Evidence of possible soil liquefaction was observed at an electrical-power station near the Guadalupe River, approximately 1 km north of San Jose Municipal Airport. Minor settlement of a tower foundation at this site suggested liquefaction-related ground softening; no significant damage resulted (Seed and others, 1990).

51E 

San Jose International Airport. Evidence of probable liquefaction was observed on the east bank of the Guadalupe River, across the river from the southeast corner of San Jose Municipal Airport. Minor lateral spreading and settlement caused minor cracking in the pavement of the airport frontage road at this site. No damage to airport lands or facilities was observed (Seed and others, 1990).

52 

Downtown Santa Cruz. Numerous sand boils were observed within developed neighborhoods south of Spruce Street along Pacific Avenue and Front Street. A large cluster of sand boils erupted in a paved parking area at the southeast corner of Front and Spruce Streets. A linear trail of sand boils was noted along the west curb of Front Street, approximately 30 m north of its intersection with Pacific Avenue, extending for approximately 10 m. Scattered sand boils were observed within the front and rear parking lots of an automobile dealership on the west side of Pacific Avenue at its intersection with Front Street. Specific locations of these sand boils are shown on

the map by Hryciw and others (this chapter, fig. 2), and photographs and additional details of these features were presented by Kropp and Thomas (1991). Sand boils erupted in the downtown Santa Cruz area in the 1906 earthquake (Youd and Hoose, 1978, loc. 44).

Buckled sidewalks were observed along Pacific Avenue, Front Street, and adjacent streets in the downtown area. In many places, buckling resulted in heaving of the sidewalk approximately 100 to 200 mm above its original position. A compressional humplike feature, approximately 50 mm high, appeared across Pacific Avenue just south of Laurel Street. Specific locations of many of these buckled sidewalks are shown on the map by Hryciw and others (this chapter, fig. 2) while more detailed discussions of these features are presented by Kropp and Thomas (1991).

Cracks in the street appeared throughout the downtown area, in addition to enlargement of areas that appeared to have previously been cracked. Along Center Street, between Walnut Avenue and Elm Street, a series of east-west cracks appeared at a relatively even spacing of approximately 7 to 10 m; these cracks typically were approximately 20 to 30 mm wide. In addition, a linear crack appeared in Pacific Avenue extending from approximately Washington Street to Front Street, a distance of more than 500 m. Specific locations of these street cracks are shown on the map by Hryciw and others, (this chapter, fig. 2) and photographs and additional details of these features were presented by Kropp and Thomas (1991). Fissures were reported in the downtown area during the 1906 earthquake (Youd and Hoose, 1978, loc. 44).

A waterline was ruptured below the sidewalk along the south side of Lincoln Avenue, just east of Center Street. The sidewalk was also badly cracked in this area, apparently as a result of earthquake-related ground failure.

53 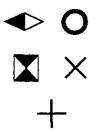

San Lorenzo River, Santa Cruz. Widespread lateral spreading occurred along the banks of the San Lorenzo River from the Water Street bridge to the mouth of the river. Scarps created by the lateral spreading commonly were more than 10 m long. Scarps approximately 200 to 300 mm high were noted within 2 days after the earthquake; approximately 10 days later, the height of these scarps had enlarged to approximately 300- to 500-mm. Specific locations of these failures are shown on the map by Hryciw and others (this chapter, fig.2), and photographs and additional details of these features were presented by Kropp and Thomas (1991). Similar failures were reported in the area during the 1906 earthquake (Youd and Hoose, 1978, loc. 43).

San Lorenzo River, Santa Cruz. An extensive complex of sand boils was observed along the river at the margins of its banks. Specific clusters were observed adjacent to the Soquel Avenue bridge, along the east bank just south of the Broadway bridge, and along the south bank just east of the Riverside Avenue bridge. In addition, sand boils erupted within various parking areas, tennis courts, and other improved areas immediately adjacent to the top of the riverbanks. Specific locations of these sand boils are shown on the map by Hryciw and others (this chapter, fig. 2), and photographs and additional details of these features were presented by Kropp and Thomas (1991). Sand boils were also reported in this area in the 1906 earthquake (Youd and Hoose, 1978, loc. 43).

Buckled roadways were observed along the top of the banks of the San Lorenzo River at the east abutment of the Soquel Avenue bridge and along East Cliff Drive, just south of Jessie Street.

Numerous areas of cracked pavement were observed in paved parking lots, tennis courts, roadways, and bicycle paths, which extend along the top of, or immediately adjacent to, the top of the riverbanks. Cracks typically extended at least several meters and commonly were approximately 30 to 50 mm wide. Specific locations of these cracks are shown on the map by Hryciw and others (this chapter, fig. 2), and photographs and additional details of these features were presented by Kropp and Thomas (1991).

An approximately 0.3-m-diameter cast-iron sewerline ruptured on the north side of the west abutment of the Broadway bridge. Extensive lateral spreading was observed in this area.

54 ◀▶ Moran Lake, Santa Cruz. Cracks formed in fill on East Cliff Drive immediately adjacent to the lake; fill apparently was spreading toward the lagoon. Possible liquefaction and lateral spreading were also observed along the east side of the lagoon, with approximately 150 to 300 mm of extension toward the lagoon (J.C. Tinsley, October 28, 1989).

55 ◀▶ Hazel Dell Road, from Simas Lake to its junction with Mount Madonna Road. A lateral spread damaged a 0.5-km-long section of Hazel Dell Road near the southeastern margin of Simas Lake. The roadbase is approximately 2 m above the marshy ground to the southwest. At the time of observation, the road had been regraded to allow traffic to pass, but the roadway remained uneven, reflecting the original displacement of the main scarp of this lateral spread. Other fissures were observed off the roadway in the area (G.F. Wieczorek, October 29, 1989).

56 □ Upper Corralitos Creek. No evidence of liquefaction was observed; a few soil blocks along streambanks had tumbled into the channel. The channel of the creek was dry. (See discussion of the absence of liquefaction-related ground failure in Corralitos Creek drainage by Dupré and Tinsley (this chapter).

57 □ Scurich Ranch (U.S. Geological Survey special studies site SCR). No liquefaction was noted in the earthquake by the owner or by a field party on October 23, 1989.

58 □ Watsonville Municipal Airport (U.S. Geological Survey special studies site WAT). No liquefaction was observed at the terminal and runways/taxiways; the site is underlain by Pleistocene fluvial deposits.

59 ◀▶ Carlton Road, northeast of Kelly Lake (U.S. Geological Survey special studies site KET). Lateral spreading occurred in roadfill and in thin Holocene alluvial-fan deposits where an unnamed drainage crosses Carlton Road in a corrugated-pipe culvert feeding Kelly Lake. Natural drainage was diverted for a short distance parallel to Carlton Road for agricultural development and road construction. Maximum downslope displacement of about 150 mm to the southwest was noted on the basis of offsets in the painted centerline strip of Carlton Road and deviated fence line on the Kett Ranch property that flanks the southwest side of road. Observed depth to shallow ground water was 0.7 m; shallow ground water was fed by irrigation water from field located north of Carlton Road (S.D. Ellen, M.J. Rymer, and J.C. Tinsley, October 22, 1989).

60 ✖ Carlton Road, north of Tynan Lake. Fill settled on both sides of a culvert situated beneath Carlton Road, where an unnamed creek feeding Tynan Lake crosses Carlton Road. No sand appeared to have been vented (J.C. Tinsley, October 22, 1989).

61 + ▬ Holohan Road, west of California State Highway 152. A ruptured natural-gas pipeline and ground cracking were observed where the Kelly Lake drainage crosses Holohan Road within unit Qyf of Dupré and Tinsley (1980) (City of Watsonville, Public Works Department, oral commun., 1989).

62 × ◀▶ + College Road area, north of Salsipuedes (Corralitos) Creek, between California Highway 152 (East Lake Drive) and Cutter Avenue. About 1 km north of Watsonville, a 0.6-km-long zone of cracks and fissures, which nearly paralleled Salsipuedes Creek, cracked water pipes and damaged structures along College Road. The most severe structural damage associated with these cracks was within a small business center on the southwest corner of the intersection of California Highway 152 and College/Holohan Road. A series of ground cracks, each with 20 to 30 mm of extensional opening, trended across the parking lot from a bridge over Salsipuedes Creek toward the corners of the buildings. Several ground cracks extended through the structures. Although no sand boils were observed, lateral spreading toward the drainage from College Lake into Salsipuedes Creek appears to have occurred. Cracks on the opposite (east) side of this drainage exhibited 200 to 250 mm of extension in a direction consistent with lateral spreading toward this drainage. The cracks passed beneath buildings at 22 College Road. Four other cracks paralleled the first; one crossed College Road perpendicularly, but exhibited negligible displacement. On the south side of the bridge, a discontinuous set of cracks passed along the manmade levee on

the south side of Salsipuedes Creek for approximately 90 m, individually showing as much as 50 mm of extensional opening toward the creek. Many of the homes between 48 and 106 College Road had ground cracks and broken water-pipe connections in their front yards, at a distance of least 50 m from the creek. In the backyard of 52 College Road, a series of cracks had a total cumulative extension of about 100 to 150 mm. These cracks mostly paralleled Salsipuedes Creek, suggesting lateral spreading toward the creek (G.F. Wieczorek, October 19, 1989).

63  San Felipe Lake. No sand boils or evidence of ground failure were noted; the lake was dry at the time of the earthquake (S.D. Ellen and J.C. Tinsley, October 24, 1989).

64  Bolsa Road. Lateral spreading and graben formation, with extruded sand filling the graben, were observed about 6 km north of Hollister, north of Bolsa Road. The failure developed in Holocene floodplain deposits (J. Tonascia, October, 1989).

65  Pajaro River and lower part of Carnadero Creek, northeast of Sargent. No ground failure was observed on either side of the Pajaro River from U.S. Highway 101 to California Highway 25 (S.D. Ellen and J.C. Tinsley, October 24, 1989).

66  Sargent. Sand boils and minor lateral spreading damaged a service road near the sugarbeet loading facility between the Southern Pacific Railroad tracks and U.S. Highway 101 at Sargent, about 1/2 km south of where the Pajaro River flows beneath the highway. Settlement of some segments of pavement summed to less than 100 mm; horizontal displacements of pavement were less than 100 mm. Ground cracking and settlement were reported in the area in 1906 (Youd and Hoose, 1978, loc. 33).

67  Betabel Road area, 2.01 km south of Sargent on U.S. Highway 101. Lateral spreading occurred in Holocene alluvium along the east bank of the Pajaro River at its confluence with an unnamed tributary drainage from the Lomerias Muertas. Displacements disturbed trees and produced extensional cracking and a graben 0.6 m deep. Extensional cracking of the ground surface was observed for about 50 m on either side of the tributary drainage (Chuck Snyder, pers. commun, summer, 1990; J. C. Tinsley, September 14, 1990).

68  Confluence of the Pajaro and San Benito Rivers. Minor lateral spreading, possibly merely ground cracking, occurred in a recent terrace deposit of the Pajaro River west of and near the confluence of the Pajaro and the San Benito Rivers. No liquefaction was noted near the U.S. Highway 101 bridge over the San Benito River dry (J.C. Tinsley and S.D. Ellen, October 24, 1989).

69  San Juan Bautista area, irrigation ditch about 1 km north of San Juan Bautista. No liquefaction was observed; the ditch was dry (J.C. Tinsley and S.D. Ellen, October 24, 1989).

70  San Benito River, 1 km north of Lucy Brown Road. No liquefaction or ground cracking was observed; the river channel was dry (J.C. Tinsley and S.D. Ellen, October 24, 1989).

71  San Benito River near Lucy Brown Road. No liquefaction or ground cracking was observed. The river channel was dry (J.C. Tinsley and S.D. Ellen, October 24, 1989).

72  San Juan Creek at the California Highway 156 bridge. No liquefaction or ground-failure-related damage to the bridge was observed; standing water was present locally in the creek bed (J.C. Tinsley and S.D. Ellen, October 24, 1989).

73A,B  Chittenden Pass. An isolated sand boil consisting of fine sand was observed in the modern channel of the Pajaro River at a point located 0.1 km upstream from the California Highway 129 bridge at site 73A. No damage was noted to any civil works. An isolated sand boil composed of medium sand was observed in the modern channel of the Pajaro River at site 73B. No damage to the Carpenter Road Bridge or to the Southern Pacific Railroad bridge located 3.5 km upstream from the town of Aromas, California, was observed. Settlement of 0.6 to 1.2 m was reported near

here in 1906 (Youd and Hoose, 1978, locs. 29 and 30; S.D. Ellen, October, 1989).

74 Soda Lake. Sand boils and ground cracks formed on Soda Lake, a tailings settlement basin, during the main shock of the earthquake on October 17, 1989; additional sand boils formed during the aftershocks of April 18, 1990 ($M_b$ = 5.5), and March 23, 1991 ($M_b$ = 4.6) (Sims and Garvin, this chapter).

75 Mattos Gulch at the Pajaro River near the mouth of Chittenden Pass. An isolated, 0.5-m-wide sand boil, was observed in an active channel-bar deposit opposite the mouth of Mattos Gulch, within unit Qyf of Dupré and Tinsley (1980).

76 1 km west of Murphy Crossing (Murphy Road), north side of the Pajaro River. Linear fractures bounded a graben and settled ground above channel deposits within unit Qyf of Dupré and Tinsley (1980). The relation of the graben to liquefaction is uncertain. Sand boils were not associated with the fractures. A few scattered small sand boils erupted adjacent to the manmade levee of Pajaro River. Some damaged irrigation pipelines noted (W. R Dupré, October, 1989).

77 North side of the Pajaro River, 0.75 km south of Johnston Corner. Three clusters of small sand boils were observed outside the manmade levee of the Pajaro River within unit Qyf of Dupré and Tinsley (1980); ground cracking and differential settlement cracked the levee. No significant lateral displacement was noted on either side of the manmade levee. The sand boils were less than 1 m in diameter; one set clustered along a fissure about 5 m long. Six small sand boils, less than 2 to 3 m in diameter, erupted in channel deposits within unit Qyf of Dupré and Tinsley (1980), along the Santa Cruz County-Monterey County line.

78 South side of the Pajaro River, 1.25 km south of Johnston Corner. Six sand boils erupted in a point-bar deposit within unit Qyf of Dupré and Tinsley (1980). The sand boils were 5 m across, elongated to 30 m along crop furrows. Minor lateral spreading and settlement were noted at a manmade levee (W.R. Dupré, October, 1989).

79 North side of the Pajaro River, 3.75 km east of the Main Street bridge, Watsonville. Lateral spreading, 40 m in length, was manifest as two extensional fissures, about 2 m apart, that diverged westward and were open to 1.6 m depth: the northern fissure trended azimuth 252° and showed a maximum component of horizontal slip amounting to 160 mm along azimuth 176°; the southern fissure trended azimuth 278° and showed a horizontal slip of 140 mm along azimuth 229°. The cumulative horizontal component of displacement was about 300 mm; the distance from the headscarp of the lateral spread to the north bank of the channel of the Pajaro River was about 15 m. The failure occurred in Holocene channel deposits or point-bar deposits within unit Qyf of Dupré and Tinsley (1980). Depth to ground water at the head of the ground-failure was 5.5 m (J.C. Tinsley and W.R. Dupré, October 26, 1989).

80 South side of the Pajaro River, 3.75 km east of the Main Street bridge, Watsonville. Numerous aligned sand boils and lateral spreads occurred in an area underlain by point-bar deposits within unit Qyf of Dupré and Tinsley (1980). The zone of failure extended from the river to a point about 125 m east of the manmade levee. About 200 to 300 m south of the point where the county line crosses the east levee, inward-facing scarps, less than 80 to 150 mm high and probably caused by differential settlement of the levee into a liquefied substrate, damaged the levee. Individual sand boils were aligned along 10-m-long fissures in an elongate array of vents 200 to 220 m southwest of, and extended subparallel to, the Santa Cruz County-Monterey County line, where the line describes a polygonal loop extending about 1 km southwestward, away from the modern channel of the Pajaro River. The county line generally follows the Pajaro River; this departure from the river reflects the position of a former channel of the Pajaro River that influenced the original survey of the county line (J.C. Tinsley and W.R. Dupré, October 26, 1989).

81 North side of the Pajaro River, 3.25 km east of the Main Street bridge, Watsonville. A lateral spread, 60 m long, occurred on the channel side of the manmade levee, along three extensional

fissures trending azimuth 285-300°, in a point-bar deposit within unit Qyf of Dupré and Tinsley (1980). Cumulative horizontal extension perpendicular to the headscarp fracture was 190 mm, with extension distributed incrementally as follows: 120 mm at the headscarp, plus an additional 30 and 40 mm developed on the two remaining fissures. The distance from the headscarp of the failure to the free face represented by the Pajaro River channel was about 50 m.

82 ◀▷ O

North side of Pajaro River, 2.5 km northeast of the Main Street bridge, Watsonville (U.S. Geological Survey special studies site MRR). Minor lateral spreading possibly occurred in channel or point-bar deposits within unit Qyf of Dupré and Tinsley (1980); the failure was wholly contained on the river channel's side of the flood-control levee. Evidence for displacement was obscured by off-road vehicle tracks, but measurable displacements summed to less than 200 mm; the greatest lateral displacements were restricted to within 15 m of a terraced free face, 3.6 m high (Pajaro River channel). Depth to ground water was 4.6 m on October 26, 1989. At least six sand boils erupted in an orchard northeast of this site (W.R. Dupré and J.C. Tinsley, October 26, 1989).

83 ◀▷ O
⧓

South side of the Pajaro River, 2.5 km northeast of the Main Street bridge, Watsonville (U.S. Geological Survey special studies site RAD). Sand boils, lateral spreading, and differential settlement of the southern manmade levee occurred in point-bar deposits within unit Qyf of Dupré and Tinsley (1980). Isolated sand boils erupted along fissures within 90 m of the levee and 150 m of the modern channel. These sand boils were less than 5 m across, a few were elongated to more than 100 m where sand and water flowed down plowed furrows (W.R. Dupré and J.C. Tinsley, October 26, 1989).

84 ◀▷ O

North side of the Pajaro River, 2.0 km northeast of the Main Street bridge, Watsonville (U.S. Geological Survey special studies site SIL). Lateral spreading and sand boils were observed in channel and point-bar deposits within unit Qyf of Dupré and Tinsley (1980). The lateral spread was wholly contained between manmade levees, but the sand boils occurred on both sides of the north levee (W.R. Dupré and J.C. Tinsley, October 26, 1989).

85 ◀▷ O

Confluence of Salsipuedes Creek (lower reach of Corralitos Creek) and the Pajaro River (U.S. Geological Survey special studies site FAR; also see Holzer and others, 1994). Lateral spreading and sand boils occurred in point-bar and channel deposits. The manmade levee was displaced horizontally 190 mm to the south (towards Pajaro River), where the margin of a channel complex intersects the north levee of Salsipuedes Creek. This stratigraphically controlled limit to the distribution of ground failure and sand boils corresponds to the contact between units Qyf and Qof of Dupré and Tinsley (1980). Extensive lateral spreading occurred parallel to the Pajaro River channel in an orchard located between the manmade levee and the channel; aggregate horizontal ground displacements amounting to 0.24, 0.82, and 0.50 m were measured, respectively, along three traverses; each traverse was normal to the extensional fissures produced by lateral spreading and to east-trending margin of the Pajaro River channel 50 m to the south. Depth to ground water was not measured directly at this site, but directly across the river at site no. 86, ground water was 4.6 m subsurface, and so, depth to ground water is believed to be similar at site 85.

California Highway 129-Corralitos (Salsipuedes) Creek bridge, Watsonville. Possible liquefaction and lateral spreading induced settlement of about 0.25 m in the east abutment and about 0.02 m in the west approach to the bridge. Extensional cracking in a parking lot north of California Highway 129 and east of the channel suggests lateral spreading occurred from the parking lot towards the creek channel. No sand boils were observed, but some recent grading had been completed at the time of observation (J.C. Tinsley, October 22, 1989; Buckle, 1990, p. 185).

86 ◀▷ O
+ ⧓
⧓

Pajaro, east of Main Street and north of San Juan Road (U.S. Geological Survey special studies site CMF; also see Holzer and others, 1994). Lateral spreading, differential settlement, and numerous large sand boils occurred in point-bar and channel deposits within unit Qyf of Dupré and Tinsley (1980). This ground failure, which mirrors the failure on the north side of the river at loc.

87, is the longest continuous failure zone associated with a lateral spread mapped by the U.S. Geological Survey during postearthquake investigations. The head scarp extended continuously for nearly 1.7 km and was visible as ground cracking, differential settlement, and graben formed in response to extensional displacements; graben locally contained vented sand. The failure extended from a point about 50 m west of the south abutment of the Main Street bridge, through the southern bridge-abutment area and the intersection of San Juan Road with Main Street, through parts of the town of Pajaro north of San Juan Road and through agricultural land, back to the Pajaro River. From the Main Street bridge eastward for 0.8 km, the outer boundary of the ground failure followed the contact between units Qyf and Qof of Dupré and Tinsley (1980). As many as 25 sand boils — some quite large, with vents approaching 2 m in diameter and throats 3 m deep — erupted at several points within this ground failure. The color of the erupted sand deposits suggested that at least two different subsurface units were involved in the liquefaction. Structures and civil works damaged by horizontal and vertical ground displacements in result of this ground failure included more than 12 residences and businesses within the town of Pajaro, the Pajaro River manmade levee, the Main Street-Porter Drive (Monterey County Route G12) bridge abutment, irrigation pipelines, and gradients of cultivated fields. Displacements were recorded by detailed profiling in the easternmost 15 per cent of the area involved in the failure, in an agricultural area where exposures were excellent. Lateral displacements were bimodal, amounting to about 120 mm across the headscarp zone, and including an additional 0.35 to 0.45 m near the Pajaro levee as much as 150 m distant. Depth to groundwater was 4.6 m on October 27, 1989. Lateral spreading and ground settlement were reported in the area in 1906 (Youd and Hoose, 1978, loc. 25); (Clint Miller, October 17, 1989; W.R. Dupré and J.C. Tinsley, October 22, 1989).

87 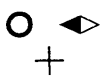 Watsonville, along the north side of the Pajaro River. Abundant lateral spreading and sand boils occurred along the northern margin of the Pajaro River between Salsipuedes Creek and the Main Street Bridge, within corporate limits of Watsonville. The lateral spreading along this reach of the Pajaro River occurred within unit Qyf of Dupré and Tinsley (1980), generally less than 15 m north of the base of the northern manmade levee, between the river channel and Front Street. A few sand boils may have erupted through unit Qof of Dupré and Tinsley along the east side of Front Street. Structures affected by liquefaction-related ground failure were chiefly those located closest to the levee, west of Marchant Street, and south of Front Street. A linear array of sand boils erupted diagonally from fissures and isolated vents from the southeast corner of Linear Park toward the intersection of Union and Front Streets. Erupted sand domed but did not rupture the asphalt pavement of Front Street opposite Linear Park. Liquefaction on Front Street caused reversal of a sewer grade and caused the vitrified-clay pipe to pull apart at its joints. The exposed portion of a 36-in. diameter welded steel, cement-mortar-lined outfall developed two leaks (joint separation) where it crossed a low-lying area of unstable soil (Benuska, 1990, p. 263). In 1906, conspicuous ground failures characterized this area, notably in Pajaro at the south-abutment area of the Main Street bridge at the foot of Marchant Street (Youd and Hoose, 1978, locs. 25, 30). Lateral spread ground failures left grabens, scarps, and settlement on both sides of the Pajaro River (Youd and Hoose, 1978, figs. 13 and 14; J.C. Tinsley and W.R. Dupré, October 25, 1989).

88  Main Street bridge over the Pajaro River, Watsonville. Lateral spreading damaged both bridge abutments; the north pier was cracked and tilted from plumb as its base migrated toward the channel of the Pajaro River. The bridge did not collapse but had to be reinforced by braces bolted through the cracked pier. Liquefaction caused differential settlements of several centimeters within the Main Street-Front Street intersection and lateral spreading toward the river on the east and west sides of Main Street. Liquefaction-related damage to structures, streets, and adjacent parking lots was generally limited to a zone between Front Street on the north and the Pajaro River's channel on the south and between the Main Street bridge on the east and the Southern Pacific Railroad bridge on the west. A road bridge at this site was damaged by lateral spreading in 1906 (Youd and Hoose, 1978, loc. 25; J.C. Tinsley, W.R. Dupré, and T.L. Holzer, several visits during October through December, 1989).

89 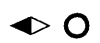 Southern Pacific Railroad bridge across the Pajaro River, Watsonville/Pajaro (U.S. Geological

Survey special studies sites SPR and GRA). Lateral spreading on the Monterey County (south) side of the river, within unit Qyf of Dupré and Tinsley (1980) shoved the bridge deck from the south at least 90 mm toward the north abutment, buckling a steel mesh walkway and causing the ends of longitudinal timbers to overlap within the zone of compensation near the north abutment. South of the Pajaro River thalweg, the southernmost concrete pier supporting the bridge was shattered. Differential settlement of 50 to 80 mm occurred across a lateral spread passing beneath the south portion of the bridge. The zone of lateral spreading that damaged the railroad bridge extended eastward, south of the manmade levee, around and through a machinery-storage yard and office buildings located between the manmade levee and San Juan Road, west of Porter Drive, in the town of Pajaro. This bridge also was damaged by lateral spreading in 1906 (Youd and Hoose, 1978, loc. 25; J.B. Berrill, October 20, 1989; J.C. Tinsley and T.L. Holzer, October–December, 1989).

90 

Watsonville, north of the Pajaro River and 0.5 km west of the Main Street bridge. Differential settlement and possible lateral spreading along the north bank of the Pajaro River damaged a maintenance facility and garage belonging to the Santa Cruz County Mass Transit System. The building was constructed across the contact between units Qyf and Qof of Dupré and Tinsley (1980); lateral spreading and settlement occurred within unit Qyf and was localized along the contact between units Qyf and Qof, cracking the slab foundation of the building and producing mainly about 50–100 mm of settlement, south side down.

91 

Near Watsonville, 0.5 to 0.75 km west of the Main Street bridge, south of the Pajaro River. Lateral spreading and sand boils caused differential settlement of cultivated fields south of the Pajaro River and west of the Southern Pacific Railroad right-of-way, within unit Qyf of Dupré and Tinsley (1980). These ground failures are a westward continuation of the failure at site 89, because the zone of settlement extends westward of the Southern Pacific Railroad right-of-way (J.C. Tinsley and W.R. Dupré, October 25, 1989).

92 

Near Watsonville, 1.0 km west of the Main Street bridge, north of the Pajaro River. Sand boils erupted north of the manmade levee in a cultivated field within unit Qyf of Dupré and Tinsley (1980); (J.C. Tinsley and W.R. Dupré, October 25, 1989).

93 

Near Watsonville, 1.5 km west of the Main Street bridge, north of the Pajaro River. Sand boils erupted from 20 to 300 m north of the manmade levee in a cultivated field in channel deposits within unit Qyf of Dupré and Tinsley (1980). Those sand boils farthest from the river integrated their vents along two northwest-trending subparallel fissures. No lateral spreading was noted (J.C. Tinsley, October 25, 1989).

94 

Pajaro River, 1.5 km upstream from the California Highway 1 bridge. Lateral spreading was noted, and sand erupted from fissures, near the base of the manmade levee south of river. Slight damage to this levee was caused chiefly by settlement (J.C. Tinsley, October 25, 1989).

95 

California Highway 1 bridge at Struve Slough. Structural failure and partial collapse of two 244-m-long bridges carrying the northbound and southbound lanes of California Highway 1 across the slough occurred at this site. Although no sand boils were observed, as much as 0.5 m of settlement of the soil relative to the columns occurred, and as much as 0.35 m of space was observed between the soil and the base of the column. Benuska (1990) attributed the bridge failure to shear failure at the tops of the supporting piles and gross relative movement of the bridge superstructure (J.B. Berrill, W.R. Dupré and J.C. Tinsley, October, 1989).

96 

Watsonville Wastewater Treatment Facility (U.S. Geological Survey special studies site WST). No ground failure was observed. Site had been improved prior to construction by compacting the soil and constructing a gravel mat at the surface prior to constructing the facility (David Koch, October, 1989).

97 

Pajaro River, 1.2 km west of California Highway 1. Differential settlements and cracking of the

manmade levee south of the river opposite the Watsonville Wastewater Treatment facility probably were caused by a liquefied substrate; no sand boils were observed (J.C. Tinsley, October 28, 1989).

98 

Pajaro River, Thurwachter Road and Thurwachter Road bridge. Lateral spreading occurred along the north bank in channel deposits within unit Qyf of Dupré and Tinsley (1980). The failure, which was between the manmade levee and the modern river channel, was mapped as four extensional cracks and a graben. The cracks trended subparallel to the riverbank for about 70 m, leading eastward from where Thurwachter Road formerly crossed the Pajaro River (a new bridge has somewhat altered the approach area). A measured profile oriented normal to the fractures and the bank of the Pajaro River channel indicated 1.11 m of cumulative lateral displacement summed across the zone of ground failure. Settlements of as much as 0.60 m were observed along the graben. Sand boils, less than 2 m in diameter, erupted along fractures, within the graben, and on relatively undeformed flood-plain areas. Depth to ground water was about 1.8 m on January 23, 1990. Lateral spreading was observed in a former orchard west of McGowan Road and south of the river in 1906 (Youd and Hoose, 1978, loc. 22; J.C. Tinsley and W.R. Dupré, October 26, 1989).

Thurwachter Road bridge (U.S. Geological Survey special studies site MCG). Lateral spreading on the south bank of the Pajaro River occurred entirely between the manmade levee and the modern river channel and displaced the base of a pier of the Thurwachter Road bridge about 0.70 m toward the Pajaro River channel. Displacement was estimated from the tilt of a bridge pier in a photograph by J. Tinsley (October 26, 1989). Depth to ground water was estimated to be less than 2 m. The distance from the head scarp to the free face represented by the Pajaro River channel was about 12 m.

99 

Pajaro River, airport for radio-controlled model aircraft (U.S. Geological Survey special studies site AIR). Lateral spreading and sand boils formed extensional fractures and grabens parallel to the north bank of the Pajaro River and severely damaged the runway and taxiways of the facility. The visual effect of the ground failure was enhanced, owing to the thin asphalt paving of the taxiways and runway. Liquefaction effects occurred entirely between the north manmade levee, which was constructed on unit Qof of Dupré and Tinsley (1980), and the north bank of the river. The levee was not involved in this failure. Cumulative horizontal displacements amounted to 0.99 m; vertical displacements of as much as 1.2 m were measured along two profiles trending normal to the fractures and to the riverbank. Depth to ground water was 1.9 m on November 2, 1989. The distance from the headscarp to the free face represented by the Pajaro River channel was about 35 m. (J.C. Tinsley, S.D. Ellen, and W.R. Dupré, October 20–26, 1989).

100 

Watsonville Slough, 1 km inland from the coastline. An extensional fissure containing extruded sand occurred adjacent to slough.

101 

Pajaro River valley, 2.4 km north of the mouth of the Pajaro River. Sand erupted around the casing of a water well, with attendant settlement of the ground adjacent to the well (E.L. Harp and G.F. Wieczorek, October, 1989).

102 

Pajaro River, 2.3 km upstream from Monterey Bay. Small sand boils erupted, and differential settlement cracked the south (Monterey County) flood-control levee of the Pajaro River, about 3 km upstream from the mouth. Liquefaction was in unit Qyf of Dupré and Tinsley (1980); (S.D. Ellen, E.L. Harp, R.C. Wilson, and J.C. Tinsley, October, 1989).

103 

Pajaro River, 2.3 km upstream from Monterey Bay. Sand boils and lateral spreading extensively damaged the north (Santa Cruz County) manmade levee from about 1.5 km to about 3 km above the mouth of the Pajaro River. Fractures occurred in the levee to depth of as much as 1.5 m, and multiple sets of inward-facing scarps occurred up to 0.3 m high in levee materials, indicated that the levee sank differentially into a liquefied substrate; extension was toward the Pajaro River channel. Between sites 99 and 103, dozens of sand boils with diameters less than 0.5 m in diam-

eter erupted between the levees and the river channel.

104 ◀▶ ○ ✖ ×

Pajaro River, 1.0 km upstream from Monterey Bay. Sand boils and lateral spreading extensively damaged the south (Monterey County) manmade levee from 1 to about 2.75 km above the mouth of the Pajaro River. Fractures, as much as 1.5 m deep, and sets of inward-facing scarps up to 0.3 m high indicated that the levee sank differentially into a liquefied substrate. Spreading is geomorphically associated with point-bar deposits of the Pajaro River. This area included the former grade of the Pajaro Valley Consolidated Railroad, which was displaced 1.2 m by the 1906 earthquake (Youd and Hoose, 1978, loc. 16). Displacements in 1989 were not profiled but exceeded 1 m along the point-bar between the levee and the thalweg. Depth to ground water was less than 1 m in this tidewater reach of the Pajaro River.

105 □

Pajaro Dunes at Pajaro Circle (U.S. Geological Survey special studies site PD2a). No liquefaction was observed at the edge of the eolian dunes at Plover Circle parking lot (W.R. Dupré, October, 1989).

106 ✖ ○

Pajaro River, 1.0 km upstream from Monterey Bay. Less than 0.3 m of settlement, accompanied by sand boils, occurred at the base of the north manmade levee of the Pajaro River, the downstream limit of major liquefaction-related damage to the levee north of the river.

107 ○

Lower part of Watsonville Slough. Isolated small sand boils erupted near the edge of the marsh along Watsonville Slough.

108 ◀▶ ○

Pajaro River, 0.4 km upstream from Monterey Bay. Lateral spreading and sand boils occurred near the mouth of the Pajaro River and in the backbeach area south of the Pajaro River. No damage to structures was noted. See Benuska, 1990, fig. 4.32.

109 ◀▶ ○ ×

Pajaro Dunes, mouth of the Pajaro River (U.S. Geological Survey special studies site PD1). Liquefaction produced lateral spreading and sand boils at the southeast tip of Pajaro Dunes, locally known as Pelican Point, at the confluence of Watsonville Slough and the Pajaro River. Lateral spreading caused structural damage to two residences constructed on 11-m wide woodpile foundations, and deformed a retaining wall and its tiebacks as much as 0.35 m. Paved parking lots were damaged by extruded sand and extensional cracking. Residential construction is built on dune sands that had migrated onto estuarine or fluvial sand; liquefaction occurred within the estuarine- or fluvial-sand unit and not within the dune sand (W.R. Dupré, October, 1989; Haro, Kasunich and Associates, written commun., 1990). No liquefaction was reported along the tennis court access road at Pajaro Dunes (U.S. Geological Survey special studies site PD2b). The strata beneath this site were found to be clay-rich and not susceptible to liquefaction (Bennett and Tinsley, 1995, p. 211–214).

110 ○

Mouth of the Pajaro River. A few small sand boils erupted on the south shore of the Pajaro River near its mouth.

111 ○

Zmudowski Beach State Park, 1 km south of the Pajaro River. Sand boils and minor ground cracking occurred along the former (post-1854) course of the Pajaro River (Dupré and Tinsley, this chapter). Surface deformation and venting of water occurred in the area in 1906 (Youd and Hoose, 1978, loc. 20).

112 ◀▶ ○

Zmudowski Beach State Park parking lot, 1.9 km south of the Pajaro River. Sand erupted from fissures and isolated sand boils; lateral spreading produced 250 mm horizontal displacement in the northwestern part of the parking lot across eight east-trending fractures. Underlying deposits include post-1854 strata of the Pajaro River (Dupré and Tinsley, this chapter). Surface deformation and vented water occurred in the area during the 1906 earthquake (Youd and Hoose, 1978, loc. 20).

113 ◀▶

Elkhorn Road at Elkhorn Slough. A small lateral spread affected fill of Elkhorn Road where it

crosses Elkhorn Slough, about 150 m west of the junction with Hall Road (John Kingsley, October, 1989).

114 Strawberry Canyon Road where it crosses the lower reach of Strawberry Canyon at its confluence with Swiss Canyon. Lateral spreading with a displacement of less than 100 mm occurred in basin deposits within unit Qb of Dupré and Tinsley (1980) that underlie the roadfill. A few tens of meters away, where Elkhorn Road crosses the confluence of Elkhorn Slough with Strawberry Canyon and Swiss Canyon, a second lateral spread and ground settlement produced lateral and vertical displacements of about 50 mm and cracked roadfill and pavement that overlie the basin deposits.

115 Pacific Coast, 2.5 km south of the mouth of the Pajaro River. Small sand boils erupted along the pre-1854 course of the Pajaro River near the margin of a dune field.

116 Moss Landing State Beach Road. Sand boils and lateral spreading heavily damaged the road, including the causeway where it crosses from Pauls Island to the Moss Beach spit at Bennett Slough. The fill of the causeway slumped about 1.5 m, and the roadway was damaged from the causeway to the point where the road turns south parallel to the coastline. Lateral spreading also caused extensional fissures within the eastern margin of the belt of coastal dunes. Along and east of the (southerly) bend in the road about 1/2 km west of California Highway 1, at least five extensional fractures caused by lateral spreading showed total cumulative horizontal displacements of at least 300 mm between the eastern limit of the dunes and the existing estuary north of the beach access road. Sites 116 through 123 correspond to Youd and Hoose's (1978) localities 19 and 20, where extensive liquefaction was observed in 1906 (W.R. Dupré and J.C. Tinsley, October 27,1989).

117 Moss Beach spit, north of the Moss Landing Marina and its nautical access to Monterey Bay. Lateral spreading caused as much as 200 mm of horizontal extension and 0.1 to 0.5 m of vertical displacement across fractures; both horizontal and vertical displacements increased southeastward. These ground failures were best expressed in the paved area of the parking lot near the tip of Moss Beach spit (Greene and others, 1991). The depth to the water table at this site is controlled by sea level and is generally less than 3 m (J.C. Tinsley and W.R. Dupré, October 27, 1989).

118 North margin of Elkhorn Slough. Slumping of an earthen dike was noted along the north bank of the slough between the slough and the salt ponds.

119 Moss Landing spit, south of the Moss Landing harbor access (road access via Sandholt Way); (U.S. Geological Survey special studies site ML1). Liquefaction caused lateral spreading, sand boils, and differential settlement intermittently along the north half of Moss Landing spit. Effects included arcuate extensional cracks rimming the northeast end of the spit, tilting of fuel storage tanks at the fuel depot (Tuttle and others, 1990), lateral spreading between the fuel tanks and the dock at Moss Landing harbor, and eastward lateral spreading along northeast-southwest-trending cracks in the equipment yard of the Pacific Diesel Co. Numerous other cracks trending both subparallel and transverse to the general north-southward trend of the spit were also visible in 1:6000-scale aerial and ground photography taken shortly after the earthquake. Numerous sewerlines and water mains were ruptured. See Greene and others, (1991) and Mejia (this chapter) for more complete discussions of offshore and onshore effects of the earthquake near the Moss Landing spit (J.C. Tinsley and W.R. Dupré, October 26, 1989).

120 California Highway 1 bridge, Elkhorn Slough. Settlement possibly related to liquefaction damaged the approaches to the bridge.

121 Moss Landing Harbor District office building and parking lot. Lateral spreading of about 0.15 m produced zones of ground cracking parallel to the shoreline and differential settlements as much as 0.3 m within the office parking lot. The area was mapped by Dupré and Tinsley (1980) as

underlain by fill, and liquefaction presumably occurred within the fill. Photographs of and descriptions of the damage at this site are included in the article by Mejia (this chapter). Ground cracking without venting of sand was noted along the northern access road to the spit, near the junction with California Highway 1 (J.C. Tinsley and W.R. Dupré, October 26, 1989).

122 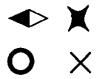

Moss Landing Marine Laboratories (MLML), California State University system (U.S. Geological Survey special studies site ML2). The buildings were destroyed by about 1.3 m of lateral spreading that occurred beneath the facility and literally tore the facility apart. Structural deformation indicated that the ground beneath the southwestern part of the main building spread oceanward; extensional cracking beneath the central part of this building and cracks along the east side of the property indicated that lateral spreading also occurred toward the harbor. Grabens and sinuous cracks extended southward along the spit from the buildings for a distance of about 150 m. Ground water is approximately at sea level, approximately 3 m subsurface. Observations of dock piers and submerged vegetation suggest about 0.3 m of settlement near the harbor at the northeast corner of the laboratory property along Sandholt Way. A resurvey of four of five U.S. Coast and Geodetic Survey bench marks was conducted by the U.S. Geological Survey in 1990; the fifth monument was not recovered. Comparison with preearthquake data indicated that about 0.42 m of settlement occurred along Sandholt Way near the northeast corner of the marine laboratory property, relative to a presumably locally stable bench mark located on Pleistocene marine-terrace deposits near California Highway 1. See also Greene and others, (1991) and Mejia (this chapter).

123 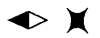

Moss Landing access, southern route. Differential settlement and some lateral spreading damaged the southernmost part of the Moss Beach parking lot near the west abutment of the bridge across the Old Salinas River to Moss Landing spit. This ground failure occurred in channel-fill deposits within unit Qcf of Dupré and Tinsley (1980); Mejia (this chapter).

124 

East of the Old Salinas River, 0.1 km northwest of Tembladero Slough. Differential settlement and a few small sand boils occurred in channel-fill deposits of the Old Salinas River within unit Qcf of Dupré and Tinsley (1980).

125 

West of the Old Salinas River, opposite the mouth of Tembladero Slough. Sand boils erupted near an area of differential settlement of about 0.2 m across fissures intersecting the southern approach to a farm-access bridge across the Old Salinas River. The sand boils erupted in channel-fill deposits within unit Qcf of Dupré and Tinsley (1980) along the southwest bank of the Old Salinas River; the sand boils were less than 1 m in diameter. Minor lateral spreading was noted along extensional fissures trending parallel to the Old Salinas River channel at points north and south of the farm-access bridge.

126 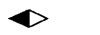

Old Salinas River, 0.2 km upstream from the mouth of Tembladero Slough. Lateral spreading was observed, with 150 to 200 mm of horizontal displacement. The failure occurred in Holocene flood-plain deposits within unit Qof of Dupré and Tinsley (1980) of the old Salinas River. Lateral displacements were reported in the area during the 1906 earthquake (Youd and Hoose, 1978, loc. 16).

127 

Old Salinas River, 1.0 km south of Tembladero Slough (U.S. Geological Survey special studies site SCA). Lateral spreading and sand boils occurred in point-bar deposits of a former meander, along both banks of the Old Salinas River. The deposits include both channel-fill deposits and Holocene flood-plain deposits (units Qcf and Qof, respectively, of Dupré and Tinsley, 1980). On the southwest side of the river, lateral displacements of as much as 0.6 m and averaging 0.45 m accumulated across three fissures as far as 150 m westward from the channel. Vertical components of displacement amounted to several centimeters, but releveling of the field was required to reestablish drainage. Landowners indicated that the area also liquefied and failed in the 1906 earthquake, a report confirmed by trenching operations (John D. Sims, oral commun., 1991). Depth to ground water was about 0.5 to 1.3 m, depending upon topographic position relative to the Old Salinas River (James Scattini, Robert Scattini, and J.C. Tinsley, October, 1989; 1990).

128 ◀▶ O

Old Salinas River, 1 km east of the coastline, at the east end of a large meander. Sand boils erupted from fissures that followed the point-bar in a former meander west of the channel of the Old Salinas River in channel-fill deposits within unit Qcf of Dupré and Tinsley (1980). East of the Old Salinas River channel, overbank facies composing unit Qof of Dupré and Tinsley (1980) did not fail by liquefaction in 1989. The amount of horizontal displacement of the lateral spreading was not measured in the field; estimated magnitudes of horizontal displacement probably about 0.3 m, on the basis of the appearance of the failures on aerial photographs, in comparison with the appearance of similar failures inspected in the field and found to have displacements of about 0.3 m. Depth to ground water is less than 1.5 m at the time of observations (W.R. Dupré and J.C. Tinsley, October 30, 1989).

129 □

Castroville. Liquefaction was not observed on the Pleistocene river terrace within unit Qan of Dupré and Tinsley, 1980) on which the town of Castroville is built. Liquefaction was absent in 1906 as well (Youd and Hoose, 1978, loc. 17).

130 ◀▶ O
×

Old Salinas River, 1.0 km north of Mulligan Hill. Lateral spreading and sand boils occurred east of the Old Salinas River in point-bar deposits within unit Qcf of Dupré and Tinsley (1980). Extension cracks were observable in fields and in field access roads as far as 100 m from the channel. Liquefaction and ground fissures were described in the area in 1906 and at loc. 131 (Youd and Hoose, 1978, location no. 16).

131 ◀▶ O
×

Old Salinas River, 0.3 km north of Mulligan Hill. Lateral spreading and sand boils occurred in point-bar deposits on both sides of the Old Salinas River channel, within 1/2 km of the mouth of the modern channel, within unit Qcf of Dupré and Tinsley (1980). Extension cracks occurred in field and in field access roads as far as 80 m from the channel. Liquefaction and ground fissures were described in the area in 1906 (Youd and Hoose, 1978, location no. 16).

132 ◀▶ O
⧓ ×

Mouth of the Salinas River, north side. Lateral spreading occurred in backbeach deposits at and north of the mouth of the Salinas River. The zone of failure was about 1 km long and as much as 50 m wide; spreading was indicated by conspicuous extensional fissures, erupted sand, and sets of grabens trending subparallel to the coastline. The spreading vector was apparently eastward, toward brackish lagoons that are former channels, now partly filled with fluvial, marine, and eolian sand. Horizontal displacement exceeded 0.5 m; vertical displacement approached 1 m, but precise measurements commonly were impossible, owing to the slumped, loose eolian sand mantling the scarps. Lateral spreading developed only where a nearby lagoon provided a free face. Depth to ground water was 1 m or less, depending on elevation above the water level in the lagoons at the time of observations (W.R. Dupré and J.C. Tinsley, October 30, 1989).

133 ◀▶ O

Mouth of the Salinas River, south side. A lobate lateral spread and numerous sand boils characterized fluvial and beach-sand deposits at the southern margin of the mouth of the Salinas River. Amounts of displacement were not measured but at the headscarp appeared to amount to 2 to 3 m. This lateral spread was the only 1989 ground failure in the Monterey Bay region observed to have zones of shear failure preserved along its lateral margins, as well as along the headscarp. Spreading was toward the lagoon (eastward); the slumped sand mass was visible in aerial photographs inland of the barrier bar where it extended beneath the shallow waters of the estuary.

134 ◀▶ O

Salinas River, 3 km upstream from Monterey Bay. Lateral spreading accompanied by sand boils occurred in point-bar deposits of meanders of the former Salinas River, within units Qof and Qyf of Dupré and Tinsley (1980). Sand-boil vents merged with fissures that parallel the accretionary fabric of the point-bar facies. Spreading was generally northward, toward the former channel of the river. About 0.55 m of horizontal displacement was measured across the failure zone.

135 ◀▶ O

Salinas River, 1.8 to 2.2 km upstream from Monterey Bay at the northwestern junction of the modern Salinas River with a former meander (U.S. Geological Survey special studies site SEA). Lateral spreading accompanied by sand boils occurred in channel and point-bar deposits within

units Qof and Qyf of Dupré and Tinsley (1980). Isolated sand boils northwest of the site, outside the channel deposits but within overbank deposits, oozed water for 3 weeks after the earthquake. Measured horizontal displacements on the lateral spread 1/4 km upstream of the junction of the modern and former channels of the Salinas River ranged from 230 mm along a field-access road to more than 0.71 m at the point of maximum displacement. Spreading was toward the Salinas River, the channel of which is filled by soft estuarine mud and compressible peat. Depth to ground water was about 1.95 m on November 9, 1989. Lateral spreading was observed almost continuously from here nearly to the California Highway 1 bridge; ground failures expressed by grabens and extensional fissures trended parallel to the Salinas River and spread toward the river (see sites 136, 137). Youd and Hoose (1978, locs. 10, 13, 15) compiled many descriptions of extensive lateral spreading, settlement, and sand boils caused by the 1906 earthquake along this reach of the Salinas River (J.C. Tinsley, S.D. Ellen, J.B. Berrill, and W.R. Dupré, October 19, 1989).

136 

Salinas River, 2.3 km upstream from Monterey Bay. Lateral spreading accompanied by sand boils occurred along the Salinas River in channel and point-bar deposits within units Qof and Qyf of Dupré and Tinsley (1980), (J.C. Tinsley and J.B. Berrill, October 19, 1989).

137 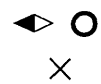

Salinas River, 2.6 to 2.8 km upstream from Monterey Bay meander (U.S. Geological Survey special studies site LEN). Lateral spreading and sand boils developed at the southwest end of a field northwest of and adjacent to California Highway 1, with extensional cracking causing damage to field gradients and to farm-access roads. Horizontal displacement along the toe of this failure reached approximately 2 m, an unusually large amount of displacement probably due to the proximity to a deep water-filled channel of the Salinas River in young flood-plain deposits within unit Qyf of Dupré and Tinsley (1980). Excluding the mobile toe of the failure, horizontal displacement ranged from 0.15 to 0.23 m. This zone of lateral spreading extended nearly to California Highway 1 but apparently did not damage the bridges (see also loc. 139). The areas along and on either side of California Highway 1, including the nearby railroad bridge, were extensively damaged by lateral spreading in 1906 (Youd and Hoose, 1978, loc. 12).

138 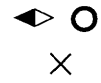

Heliport, 0.5 km west of the Nashua Road-California Highway 1 interchange. Lateral spreading and sand boils damaged fields and the access road at Gomes Brothers heliport. Extruded sand and water buried the parking area of the airport. Dozens of sand boils, short fissures, and shallow closed depressions formed near the helipad and adjacent parking lots and damaged several buildings and an irrigation-pump installation. Sand filled a corner of one building to a depth of 0.45 to 0.60 m. Differential settlement of the ground around one building constructed above an underground gasoline storage facility was several centimeters. Eyewitnesses reported water spurting to a height of 0.45 m from sandboil vents 15 minutes after the earthquake shaking stopped (G.F. Wieczorek, October 20, 1989). Horizontal displacements on extensional fractures of lateral spreads averaged 150 mm and ranged from 100 to 210 mm. Depth to ground water was about 0.45 m on October 19, 1989. The surface of the ground above the former channel of the Salinas River was covered by dozens of sand boils ranging from 1 m to greater than 10 m in diameter. Nearby fields also settled and accumulated extruded sand; fields required grading to restore drainage and irrigation gradients before being put back into full production. Liquefaction also occurred in the area in 1906 (Youd and Hoose, 1978, loc. 15).

139 

Salinas River at California Highway 1 bridge and vicinity. Liquefaction damaged water wells near California Highway 1 and caused settlement damage to the fill along the shoulders of the highway where it crosses an abandoned meander of the Salinas River within unit Qyf of Dupré and Tinsley (1980). The highway pavement was undamaged. Lateral spreading at the north bank of the Salinas River damaged the railroad bridge. Damage to the bridges from permanent ground deformation, probably lateral spreading, was reported in 1906 (Youd and Hoose, 1978, loc. 13); (J.C. Tinsley, W.R. Dupré, and J. Martin, October, 1989).

140 

Salinas River, 3.5 km upstream from Monterey Bay (U.S. Geological Survey special studies site JRR). Sand boils and lateral spreading damaged irrigation gradients of fields and caused crack-

ing and differential settling of flood-control levees southwest of the Salinas River in a reach situated within about 2 km south of the California Highway 1 bridge at Neponset. Liquefaction occurred in young floodplain deposits within unit Qyf of Dupré and Tinsley (1980). The most conspicuous lateral spreading was associated with the north perimeter of a prominent northeastward-projecting point-bar of the Salinas River, chiefly between the manmade levee and the present Salinas River channel, where minimum horizontal displacement was 0.64 m and was directed to the north toward the channel. Depth to ground water was at 2.03 m on December 14, 1989. Sand boils and differential settlement damaged fields bounded by this meander loop located east of Neponset; liquefaction-related damage, including settlement of the ground and vented sand, was concentrated along a former channel of the Salinas River that courses through the agricultural tract. Parts of these fields were leveled several days after the earthquake and again within 90 days after the earthquake; as much as 0.38 m of additional soil was required to be added to attain the required grade. The area continued to settle for several months, and a second episode of grading was required. These settlements apparently were associated not with lateral spreading but with areas of observed sand-boil activity in an area underlain by a former channel of the Salinas River.

141  Salinas River, 4 to 4.5 km upstream from Monterey Bay. Sand boils erupted adjacent to the manmade levee underlain by a modern point-bar deposit of the Salinas River. Differential settlement and possible lateral spreading damaged the nearby flood-control levee. Sand boils, 3 m in diameter, extended as far as 60 m along furrows of cultivated ground (J.C. Tinsley, October 19, 1989).

142  Salinas River, 1.0 km south-southeast of the California Highway 1 bridge. Six small sand boils erupted on the Jefferson Ranch along the southwestern margin of the modern flood plain of the river. Minimal grading was required to restore field gradient.

143  Salinas River, 1.0 km south-southeast of the California Highway 1 bridge (opposite site 141). Minor lateral spreading and small sand boils occurred north of the river within 30 m of the modern channel.

144  Salinas River, 4 km west-southwest of Cooper. Minor lateral spreading and cracking of a point-bar deposit and farm service roads were observed adjacent to the modern channel of the Salinas River.

145  Salinas River, 3.5 km west-southwest of Cooper (U.S. Geological Survey special studies site TAN). Lateral spreading was indicated by eight subparallel, arcuate, extension cracks that were concave toward the Salinas River and extended as far as 100 m away from the east margin of the active channel. Horizontal displacement was not measured directly but inferred from aerial photographs to be about 0.15 to 0.30 m. No sand boils were observed; farm service roads were cracked where intersected by these fractures.

146  Alisal Slough, 1.3 km south-southeast east of Cooper (U.S. Geological Survey special studies site MAR). Liquefaction was not observed in a prominent meander loop of the slough, a former channel of the Salinas River about 1 km northwest of the Graves School site along California State Highway 183 between Salinas and Castroville (Norman Martella and J.C. Tinsley, October 18–19, 1989).

147  Salinas River, 3.3 km west-southwest of Cooper. An isolated sand boil, less than 0.5 m diameter, erupted in a field about 130 m north of the north manmade levee of river. The area is underlain by young flood-plain deposits (unit Qyf of Dupré and Tinsley, 1980).

148  Salinas River at the Blanco Road bridge. Lateral spreading produced grabens, extension fractures, ground settlement, and a few small sand boils within a recent point-bar deposit on the south side of river. The curved bridge's piers, deck, and approaches were slightly damaged. Cumulative horizontal displacements amounted to approximately 0.40 m. Depth to ground water

was approximately 0.45 m on October 19, 1989 (J.C. Tinsley and J.B. Berrill, October 19, 1989).

149 Salinas River, 5.5 km south of Cooper. Sand boils erupted west of Davis Road in young floodplain deposits within unit Qyf of Dupré and Tinsley (1980) on which settling ponds of a wastewater treatment facility are built. No significant damage to earthworks was noted. The sand boils, which were less than 2 m in diameter, were accompanied by less than 30 mm of ground settlement (J.C. Tinsley and J.B. Berrill, October 19, 1989).

150 Salinas River at Davis Road, 3 km southwest of Salinas. Lateral spreading produced a graben, extension fractures, ground settlement, and two small sand boils that erupted in fill where Davis Road crosses the Salinas River; displacements extended into adjacent recent fluvial deposits. Ground failure occurred in channel and point-bar deposits within unit Qyf of Dupré and Tinsley (1980) and extended beyond the roadfill for approximately 100 m south of Davis Road along the south bank of the river. Horizontal displacements amounted to about 250 mm chiefly along azimuth N. 70° E. towards the Salinas River channel. The headscarp of the lateral spread, which was about 40 m west of the channel, was accompanied by sand boils of pebbly medium and fine sand. Depth to ground water near the headscarp was 0.43 m (G.F. Wieczorek, USGS, October 20, 1989). This site, the most southerly documented occurrence of lateral spreading in natural deposits, is about 44 km south of epicenter (J.B. Berrill, J.C. Tinsley, October 19, 1989).

151 Salinas River, 2 km downstream from the California Highway 68 bridge. An isolated sand boil erupted in a fine-grained sandbar in the active channel of the Salinas River. No damage to any civil works was noted. This sand boil was the most southerly documented occurrence of liquefaction caused by the earthquake.

152 Salinas River at the California Highway 68 bridge (U.S. Geological Survey special studies site SRB). No evidence of liquefaction or ground failure was observed on either side of the Salinas River after the earthquake. A lateral spread displaced the north pier of the Monterey County highway bridge approximately 2 m in 1906 (Youd and Hoose, 1978, loc. 12); (J.C. Tinsley, S.D. Ellen, and W.R. Dupré, October 19, and October 25, 1989).

153 Salinas River at Old Hilltown. No liquefaction or ground failure noted on either side of the Salinas River. Liquefaction and lateral spreading were observed near Hilltown west of the Spreckles Sugar Processing Plant in 1906 (Youd and Hoose, 1978, location no. 12); (J.C. Tinsley, S.D. Ellen, and W.R. Dupré, October 19 and October 22, 1989).

154 Spreckles Sugar Processing Plant. No liquefaction was noted on either side of the Salinas River. The Spreckles Sugar Processing Plant showed no liquefaction-related ground failure. Minor cracks, 0.5 to 2 mm wide, were noted in two levees confining the aeration ponds, but no leakage was observed on October 22, 1989. The area was extensively damaged in 1906 (Youd and Hoose, 1978, loc. 11); (J.C. Tinsley, October 19 and 22, 1989).

155 Salinas River, 3.5 km west of Spence. No liquefaction was noted in a modern point-bar deposit of the Salinas River. The area was extensively fissured and replete with many sand boils and much ground settlement following the 1906 earthquake (Youd and Hoose, 1978, loc. 12).

156 Chualar Road bridge over the Salinas River. No liquefaction was noted within or adjacent to the river's dry bed on October 19, 1989. Extensive recent activity by pocket gophers who had burrowed into a modern channel bar of the Salinas River suggest that ground shaking collapsed burrows or shook loose much sediment and necessitated housecleaning within the gopher colony at this site. Sand craters (sand boils) were noted in river bottoms west of Chualar in 1906 (Youd and Hoose, 1978, loc. 10); (J.C. Tinsley, October 19, 1989).

157 Seaside. Slumping was noted in fill at northwest corner of the southeast segment of Laguna del Rey. This ground failure, if caused by liquefaction, would be the most distant such failure recognized south of the epicenter (R. Barminski, Personal communication, 1989).

158 ☐ Mouth of the Carmel River. No evidence of liquefaction was observed in recent spits, beach areas, and river bars was observed (S.D. Ellen and J.C. Tinsley, October 24, 1989).

159 ☐ Carmel River at the California Highway 1 bridge. No liquefaction was observed; the river channel was dry; no distress occurred to the bridge deck, rails, abutments, or piers (S.D. Ellen and J.C. Tinsley, October 24, 1989).

160 ☐ Carmel River at the Schulte Road bridge, 7.5 km upstream from California Highway 1. No evidence of liquefaction was observed. Slight spalling of concrete was noted along the west aspect of the south abutment of the bridge (S.D. Ellen and J.C. Tinsley, October 24, 1989).

161 ☐ Carmel Valley. No liquefaction effects were observed from Buckeye Canyon Overlook (S.D. Ellen and J.C. Tinsley, October 24, 1989).

162 ☐ Upper Carmel Valley, 2.5 km upstream from Buckeye Canyon. No liquefaction was noted near a private bridge crossing the Carmel River (S.D. Ellen and J.C. Tinsley, October 24, 1989).

163 ☐ Carmel River at the bridge crossing opposite Miramonte Road, 2.5 km upstream from Buckeye Canyon. No liquefaction was noted. Water was present in the river channel below the bridge; no distress was noted to the steel bridge, its abutments, or its piers or footings (S.D. Ellen and J.C. Tinsley, October 24, 1989).

## REFERENCES CITED


Astaneh, Abolhassan, Bertero, V.V., Bolt, B.A., Mahin, S.A., Moehle, J.P., and Seed, R.B., 1989, Preliminary report on the seismological and engineering aspects of the October 17, 1989 Santa Cruz (Loma Prieta) earthquake: Berkeley, University of California, Earthquake Engineering Research Center Report UCB/EERC-89/14, 51 p.

Bardet, J.P., Kapuskar, M., Martin, G.R., and Proubet Jean, 1992, Site response analyses, *in* O'Rourke, T.D., ed., The Loma Prieta, California, earthquake of October 17, 1989—Marina District: U.S. Geological Survey Professional Paper 1551-F, p. F85–F140.

Bennett, M.J., 1990, Ground deformation and liquefaction of soil in the Marina District, chap. D *of* Holzer, T.L., and O'Rourke, T.D., eds., Effects of the Loma Prieta earthquake on the Marina District, San Francisco, California: U.S. Geological Survey Open-File Report 90-253, p. D1–D36.

Bennett, Michael J. and Tinsley, John. C., III, 1995, Geotechnical data from surface and subsurface samples outside of and within liquefaction-related ground failures caused by the October 17, 1989, Loma Prieta earthquake, Santa Cruz and Monterey Counties, California: U.S. Geological Survey Open-File Report 95-663, 358 p.

Bonilla, M.G., 1992, Geologic and historical factors affecting earthquake damage, *in* O'Rourke, T.D., ed., The Loma Prieta, California, earthquake of October 17, 1989 Marina District: U.S. Geological Survey Professional Paper 1551-F, p. F7–F34.

Benuska, Lee, ed., 1990, Loma Prieta Earthquake Reconnaissance Report: Earthquake Spectra, v. 6, supp. 90-01, 448 p.

Çelebi, Mehmet, 1990, Types of structural damage, chap. B *of* Holzer, T.L., and O'Rourke, T.D., eds., Effects of the Loma Prieta earthquake on the Marina District, San Francisco, California: U.S. Geological Survey Open-File Report 90-253, p. B1–B6.

Dupré, W.R. and Tinsley, J.C., 1980, Maps showing geology and liquefaction potential of northern Monterey and southern Santa Cruz counties, California: U.S. Geological Survey Miscellaneous Field Studies Map MF-1199, scale 1:62,500, 2 sheets.

Egan, J.A., and Wang, Z.-L., 1991, Liquefaction-related ground deformation and effects on facilities at Treasure Island, San Francisco, during the 17 October 1989 Loma Prieta earthquake, *in* O'Rourke, T.D., and Hamada, M., eds., Japan-U.S. Workshop on Earthquake Resistant Design of Lifeline Facilities and Countermeasures for Soil Liquefaction, 3rd, San Francisco, 1991, Proceedings: Buffalo, N.Y., National Center for Earthquake Engineering Research Technical Report NCEER-91-0001, p. 57–76.

Egan, J.A., Youngs, R.R., and Power, M.S., 1992, Assessment of nonliquefaction along Coyote Creek during the 1989 Loma Prieta earthquake: final technical report to U.S. Geological Survey, National Earthquake Hazards Reduction Program, award 14-08-0001-G1859, 18 p., 14 figs., 2 apps.

Greene, H.G, Gardner-Taggart, Joan, Ledbetter, M.T., Barminski, Robert, Chase, T.E., Hicks, K.R., and Baxter, Charles, 1991, Offshore and onshore liquefaction at Moss Landing spit, central California—results of the October 17, 1989, Loma Prieta earthquake: Geology, v. 19, no. 9, p. 945–949.

Harris, S.K., and Egan, J.A., 1992, Effects of ground conditions on the damage to four-story corner apartment buildings, *in* O'Rourke, T.D., ed., The Loma Prieta, California, earthquake of October 17, 1989—Marina District: U.S. Geological Survey Professional Paper 1551-F, p. F181–F194.

Holzer, T.L., Tinsley, J.C., III, Bennett, M.J., and Mueller, C.S., 1994, Observed and predicted ground deformation—Miller Farm lateral spread, Watsonville, California: Buffalo, N.Y., National Center for Earthquake Engineering Research Technical Report NCEER-94-0026, p. 79–99.

Kropp, Alan and Thomas, Michael, 1991, Ground Failure in downtown Santa Cruz, *in* Baldwin, J.E., Jr., and Sitar, Nicholas, eds., Loma Prieta earthquake, engineering geologic perspectives: Association of Engineering Geologists Special Publication 1, p. 61–74.

Lee, C.H., and Praszker, Michael, 1969, Bay Mud developments and related structural foundations, *in* Goldman, H.B., ed., Geologic and engineering aspects of San Francisco Bay fill: California Division of Mines and Geology Special Report 97, p. 41–85.

O'Rourke, T.D., Pease, J.W., and Stewart, H.E., 1992, Lifeline performance and ground deformation during the earthquake, *in* O'Rourke, T.D., ed., The Loma Prieta, California, earthquake of October 17, 1989—Marina District: U.S. Geological Survey Professional Paper 1551-F, p. F155–F180.

O'Rourke, T.D., Stewart, H.E., Blackburn, F.T., and Dickerman, T.S., 1990, Geotechnical and lifeline aspects of the October 17, 1989 Loma Prieta earthquake in San Francisco: Buffalo, N.Y., National Center for Earthquake Engineering Research Technical Report NCEER 90-0001, p. 2-1 through 2-9.

O'Rourke, T.D., Gowdy, T.E., Stewart, H.E., and Pease, J.W., 1991, Lifeline performance and ground deformation in the Marina during 1989 Loma Prieta earthquake, *in* O'Rourke, T.D. and Hamada, M., eds., Japan-U.S. Workshop on Earthquake Resistant Design of Lifeline Facilities and Countermeasures for Soil Liquefaction, 3rd, San Francisco, 1991, Proceedings: Buffalo, N.Y., National Center for Earthquake Engineering Research Technical Report NCEER-91-0001, p. 129–146.

Seed, R.B., Dickenson, S.E., Riemer, M.F., Bray, J.D., Sitar, Nicholas, Mitchell, J.K., Idriss, I.M., Kayen, R.E., Kropp, Alan, Harder, L.F., and Power, M.S., 1990, Preliminary report on the principal geotechnical aspects of the October 17, 1989 Loma Prieta earthquake; Berkeley, University of California, Earthquake Engineering Research Center Report UCB/EERC 90/05, 137 p.

Taylor, H.T., Cameron, J.T., Vahdani, S., and Yap, H., 1992, Behavior of the seawalls and shoreline during the earthquake, *in* O'Rourke, T.D., ed., The Loma Prieta, California, earthquake of October 17, 1989—Marina District: U.S. Geological Survey Professional Paper 1551-F, p. F141–F154.

Tuttle, Martitia, Cowie, Patience, Tinsley, J.C., III, Bennett, M.J., and Berrill, John, 1990, Liquefaction and foundation failure of Chevron oil and gasoline tanks at Moss Landing, California: Geophysical Research Letters, v. 17, no. 10, p. 1797–1800.

Wood, M.W., 1883, History of Alameda County: Oakland, Calif., M.W. Wood, 665 p.

Youd, T.L., and Hoose, S.N., 1978, Historic ground failures in northern California triggered by earthquakes: U.S. Geological Survey Professional Paper 993, 177 p.

☆ U.S. GOVERNMENT PRINTING OFFICE: 1998 - 673-048 / 20100 REGION NO. 8

# SELECTED SERIES OF U.S. GEOLOGICAL SURVEY PUBLICATIONS

## Periodicals

**Earthquakes & Volcanoes** (issued bimonthly).
**Preliminary Determination of Epicenters** (issued monthly).

## Technical Books and Reports

**Professional Papers** are mainly comprehensive scientific reports of wide and lasting interest and importance to professional scientists and engineers. Included are reports on the results of resource studies and of topographic, hydrologic, and geologic investigations. They also include collections of related papers addressing different aspects of a single scientific topic.

**Bulletins** contain significant data and interpretations that are of lasting scientific interest but are generally more limited in scope or geographic coverage than Professional Papers. They include the results of resource studies and of geologic and topographic investigations; as well as collections of short papers related to a specific topic.

**Water-Supply Papers** are comprehensive reports that present significant interpretive results of hydrologic investigations of wide interest to professional geologists, hydrologists, and engineers. The series covers investigations in all phases of hydrology, including hydrology, availability of water, quality of water, and use of water.

**Circulars** present administrative information or important scientific information of wide popular interest in a format designed for distribution at no cost to the public. Information is usually of short-term interest.

**Water-Resources Investigations Reports** are papers of an interpretive nature made available to the public outside the formal USGS publications series. Copies are reproduced on request unlike formal USGS publications, and they are also available for public inspection at depositories indicated in USGS catalogs.

**Open-File Reports** include unpublished manuscript reports, maps, and other material that are made available for public consultation at depositories. They are a nonpermanent form of publication that may be cited in other publications as sources of information.

## Maps

**Geologic Quadrangle Maps** are multicolor geologic maps on topographic bases in 7 1/2- or 15-minute quadrangle formats (scales mainly 1:24,000 or 1:62,500) showing bedrock, surficial, or engineering geology. Maps generally include brief texts; some maps include structure and columnar sections only.

**Geophysical Investigations Maps** are on topographic or planimetric bases at various scales, they show results of surveys using geophysical techniques, such as gravity, magnetic, seismic, or radioactivity, which reflect subsurface structures that are of economic or geologic significance. Many maps include correlations with the geology.

**Miscellaneous Investigations Series Maps** are on planimetric or topographic bases of regular and irregular areas at various scales; they present a wide variety of format and subject matter. The series also includes 7 1/2-minute quadrangle photogeologic maps on planimetric bases which show geology as interpreted from aerial photographs. The series also includes maps of Mars and the Moon.

**Coal Investigations Maps** are geologic maps on topographic or planimetric bases at various scales showing bedrock or surficial geology, stratigraphy, and structural relations in certain coal-resource areas.

**Oil and Gas Investigations Charts** show stratigraphic information for certain oil and gas fields and other areas having petroleum potential.

**Miscellaneous Field Studies Maps** are multicolor or black-and-white maps on topographic or planimetric bases on quadrangle or irregular areas at various scales. Pre-1971 maps show bedrock geology in relation to specific mining or mineral-deposit problems; post-1971 maps are primarily black-and-white maps on various subjects such as environmental studies or wilderness mineral investigations.

**Hydrologic Investigations Atlases** are multicolored or black-and-white maps on topographic or planimetric bases presenting a wide range of geohydrologic data of both regular and irregular areas; the principal scale is 1:24,000, and regional studies are at 1:250,000 scale or smaller.

## Catalogs

Permanent catalogs, as well as some others, giving comprehensive listings of U.S. Geological Survey publications are available under the conditions indicated below from USGS Map Distribution, Box 25286, Building 810, Denver Federal Center, Denver, CO 80225. (See latest Price and Availability List.)

**"Publications of the Geological Survey, 1879-1961"** may be purchased by mail and over the counter in paperback book form and as a set microfiche.

**"Publications of the Geological Survey, 1962-1970"** may be purchased by mail and over the counter in paperback book form and as a set of microfiche.

**"Publications of the U.S. Geological Survey, 1971-1981"** may be purchased by mail and over the counter in paperback book form (two volumes, publications listing and index) and as a set of microfiche.

**Supplements** for 1982, 1983, 1984, 1985, 1986, and for subsequent years since the last permanent catalog may be purchased by mail and over the counter in paperback book form.

**State catalogs**, "List of U.S. Geological Survey Geologic and Water-Supply Reports and Maps For (State)," may be purchased by mail and over the counter in paperback booklet form only.

**"Price and Availability List of U.S. Geological Survey Publications,"** issued annually, is available free of charge in paperback booklet form only.

**Selected copies of a monthly catalog** "New Publications of the U.S. Geological Survey" is available free of charge by mail or may be obtained over the counter in paperback booklet form only. Those wishing a free subscription to the monthly catalog "New Publications of the U.S. Geological Survey" should write to the U.S. Geological Survey, 582 National Center, Reston, VA 22092.

**Note.**–Prices of Government publications listed in older catalogs, announcements, and publications may be incorrect. Therefore, the prices charged may differ from the prices in catalogs, announcements, and publications.